

A Robust Design of a Renewable European Energy System Encompassing a Hydrogen Infrastructure

Dilara Gülçin Çağlayan

Energie & Umwelt / Energy & Environment

Band / Volume 523

ISBN 978-3-95806-516-1

Forschungszentrum Jülich GmbH
Institut für Energie- und Klimaforschung
Techno-ökonomische Systemanalyse (IEK-3)

A Robust Design of a Renewable European Energy System Encompassing a Hydrogen Infrastructure

Dilara Gülçin Çağlayan

Schriften des Forschungszentrums Jülich
Reihe Energie & Umwelt / Energy & Environment

Band / Volume 523

ISSN 1866-1793

ISBN 978-3-95806-516-1

Bibliografische Information der Deutschen Nationalbibliothek.
Die Deutsche Nationalbibliothek verzeichnet diese Publikation in der
Deutschen Nationalbibliografie; detaillierte Bibliografische Daten
sind im Internet über <http://dnb.d-nb.de> abrufbar.

Herausgeber
und Vertrieb: Forschungszentrum Jülich GmbH
 Zentralbibliothek, Verlag
 52425 Jülich
 Tel.: +49 2461 61-5368
 Fax: +49 2461 61-6103
 zb-publikation@fz-juelich.de
 www.fz-juelich.de/zb

Umschlaggestaltung: Grafische Medien, Forschungszentrum Jülich GmbH

Druck: Grafische Medien, Forschungszentrum Jülich GmbH

Copyright: Forschungszentrum Jülich 2020

Schriften des Forschungszentrums Jülich
Reihe Energie & Umwelt / Energy & Environment, Band / Volume 523

D 82 (Diss. RWTH Aachen University, 2020)

ISSN 1866-1793
ISBN 978-3-95806-516-1

Vollständig frei verfügbar über das Publikationsportal des Forschungszentrums Jülich (JuSER)
unter www.fz-juelich.de/zb/openaccess.



This is an Open Access publication distributed under the terms of the [Creative Commons Attribution License 4.0](https://creativecommons.org/licenses/by/4.0/), which permits unrestricted use, distribution, and reproduction in any medium, provided the original work is properly cited.

Abstract

The role of variable renewable energy sources (VRES) in future energy systems is evident when the latest trends in the global installed capacities are examined. Nevertheless, the intermittency of these technologies remains an obstacle to the high penetration of VRES technologies. To address this, hydrogen is often proposed as an alternative chemical energy carrier in the energy system design to provide flexibility in the system. Although hydrogen is taken into account in many studies which optimize future energy system design, seasonal storage and international hydrogen transmission have not been investigated in any study at a European scale. Thus, an 100% renewable European energy system with hydrogen infrastructure shall be performed in this thesis.

For such an analysis, in-depth assessments of offshore wind energy and the underground hydrogen storage in the salt formations across Europe are necessary due to the lack of consistent data across Europe. Evaluation of offshore wind energy is conducted for different turbine designs derived from cost optimal analysis. When cost-optimal turbine designs are used across Europe, the estimated average levelized cost of electricity (LCOE) is found at $7 \text{ €}_{\text{ct}} \text{ kWh}^{-1}$, which is 1.0 to $3.5 \text{ €}_{\text{ct}} \text{ kWh}^{-1}$ cheaper than if uniformly applied single turbine design were used; in which case the lowest average cost value attainable is $8 \text{ €}_{\text{ct}} \text{ kWh}^{-1}$. Optimal turbine designs result in a capacity and generation potential of 8.6 TW and 39.9 PWh . The investigation on the storage potential of salt caverns across Europe reveals that a total capacity of $84.8 \text{ PWh}_{\text{H}_2}$ is possible when both onshore and offshore locations are deployed. Consideration of onshore locations only results in a capacity of $23.2 \text{ PWh}_{\text{H}_2}$, nearly 32% of which is located within a distance of 50 km from shore.

Before designing the final energy system, the major operational assumptions were analyzed; such as the number of typical days, the number of groups for VRES technologies, and how results change with respect to the selected weather year. Additionally, the novel categorizing of each VRES technology by cost percentile provides a higher fidelity to the ultimate design; yet the change is insignificant after 60 groups per technology. Even still, when the system is designed for individual years between 1980 and 2017, significant variations in optimal system configurations are observed. Therefore, a novel iterative approach is proposed to obtain a robust energy system design across all weather years. A value-of-analysis is also performed to investigate the impact of individual technologies, wherein the largest impactor is observed to be wind energy; which, if excluded, could increase total system costs by 56.2%. The second most impactful technologies are found to be trading between countries and the electricity grid.

In the end, a European energy system design is proposed consisting of 842 GW onshore, 78 GW offshore wind energy, as well as 654 GW photovoltaics. Additionally, 154 GW of biomass combined heat and power plants and 203 GW of hydropower are also utilized. The proposed system has total storage capacities of 130 TWh , 562 GWh and 587 GWh for salt caverns, vessels and lithium-ion batteries, respectively. Total curtailment is estimated as 441 TWh a^{-1} .

Kurzfassung

Die Rolle der variablen erneuerbaren Energiequellen (VRES) in zukünftigen Energiesystemen wird deutlich, wenn man die neuesten Trends bei den weltweit installierten Kapazitäten untersucht. Dennoch bleibt die Intermittenz dieser Technologien ein Hindernis für die hohe Verbreitung der VRES-Technologien. Um dies zu beheben, wird Wasserstoff oft als alternativer chemischer Energieträger im Energiesystemdesign vorgeschlagen, um Flexibilität im System zu gewährleisten. Obwohl Wasserstoff in vielen Studien berücksichtigt wird, die das Design zukünftiger Energiesysteme optimieren, sind die saisonale Speicherung und die internationale Wasserstoffübertragung in keiner Studie auf europäischer Ebene untersucht worden. Daher soll in dieser Arbeit ein zu 100 % erneuerbares europäisches Energiesystem mit Wasserstoffinfrastruktur durchgeführt werden.

Für eine solche Analyse sind eingehende Bewertungen der Offshore-Windenergie sowie der unterirdischen Wasserstoffspeicherung in den Salzformationen in ganz Europa erforderlich, da es an einheitlichen Daten für ganz Europa mangelt. Eine Bewertung der Offshore-Windenergie wird für verschiedene Turbinenkonzepte durchgeführt, die aus einer kostenoptimalen Analyse abgeleitet werden. Wenn kostenoptimale Turbinenkonstruktionen in ganz Europa verwendet werden, liegen die geschätzten durchschnittlichen nivellierten Stromkosten (LCOE) bei $7 \text{ €}_{\text{ct}} \text{ kWh}^{-1}$, was $1,0$ bis $3,5 \text{ €}_{\text{ct}} \text{ kWh}^{-1}$ günstiger ist als bei einer einheitlich angewandten Einzel-Turbinenkonstruktion; in diesem Fall liegt der niedrigste erreichbare durchschnittliche Kostenwert bei $8 \text{ €}_{\text{ct}} \text{ kWh}^{-1}$. Optimale Turbinenauslegungen führen zu einem Leistungs- und Erzeugungspotenzial von $8,6 \text{ TW}$ und $39,9 \text{ PWh}$. Die Untersuchung des Speicherpotenzials von Salzkavernen in ganz Europa zeigt, dass eine Gesamtkapazität von $84,8 \text{ PWh}_{\text{H}_2}$ sowohl an Land als auch auf See möglich ist. Die Berücksichtigung von Onshore-Lagen führt nur zu einer Kapazität von $23,2 \text{ PWh}_{\text{H}_2}$, von denen sich fast 32% in einer Entfernung von 50 km vom Ufer befinden.

Vor dem Entwurf des endgültigen Energiesystems wurden die wichtigsten betrieblichen Annahmen analysiert, wie z.B. die Anzahl der typischen Tage, die Anzahl der Gruppen für VRES-Technologien und die Veränderung der Ergebnisse in Bezug auf das ausgewählte Wetterjahr. Zusätzlich bietet die neuartige Kategorisierung jeder VRES-Technologie nach Kostenperzentil eine höhere Treue zum ultimativen Design; die Änderung ist jedoch nach 60 Gruppen pro Technologie unbedeutend. Auch wenn das System für einzelne Jahre zwischen 1980 und 2017 ausgelegt ist, sind große Unterschiede in der optimalen Systemkonfiguration zu beobachten. Daher wird ein neuartiger iterativer Ansatz vorgeschlagen, um ein robustes Energiesystemdesign über alle Wetterjahre hinweg zu erhalten. Ein Analysewert wird auch durchgeführt, um die Auswirkungen einzelner Technologien zu untersuchen, wobei der größte Impaktor die Windenergie ist, die, wenn sie nicht berücksichtigt wird, die Gesamtsystemkosten um 56,2% erhöhen könnte. Die zweitwirksamsten Technologien sind der Handel zwischen Ländern und dem Stromnetz.

Am Ende wird ein europäisches Energiesystemdesign vorgeschlagen, das aus 842 GW Onshore-, 78 GW Offshore-Windenergie und 654 GW Photovoltaik besteht. Zusätzlich werden 154 GW Biomasse-Heizkraftwerke und 203 GW Wasserkraft genutzt. Das vorgeschlagene System verfügt über Gesamtspeicherkapazitäten von 130 TWh davon, 562 GWh und 587 GWh für Salzkavernen, Behälter sowie 587 GWh und Lithium-Ionen-Batterien. Die Gesamtkürzung wird auf 441 TWh a^{-1} geschätzt.

Acknowledgments

I would like to express my gratitude to Prof. Dr. Detlef Stolten for enabling me to conduct my doctoral studies in IEK-3 by providing the funding and the infrastructure necessary for my research. Additionally, I would like to communicate my gratitude to all my superiors in the hierarchy chain of IEK-3 for the general supervision they have provided. Beyond anything else, this supervision model has strengthened my self-sufficiency, as I was told in the beginning.

I would like to present my deepest gratitude to Assoc. Prof. Dr. Yilser Devrim and Prof. Dr. Inci Eroglu for introducing the topic of hydrogen energy and endorsing me to commence my career on this topic. Their long-lasting support has always been a motivation source to pursue my career on the topic of hydrogen.

I would like to communicate my utmost appreciation for the motivational support of my dearest friends currently distributed all around the world, yet being as close as a phone call. Our conversations have always given me comfort, highlighting the importance of friends who listen and understand. For sure, growing and experiencing life together has played a significant role in this, and I really appreciate that we have been through these major steps together.

Everyone who has touched my life since my first day in Germany, I would like to express my deepest gratitude for your support and contributions. Adapting to a new culture and abiding the new lifestyle has become easier with my friends/colleagues from FZJ as well as those “coolkidz” in Jülich. Especially, I am indebted to David Severin Ryberg (Seviii) not only for the endless fruitful discussions about every single idea but also for his irreplaceable friendship. Utilization of the tools he developed has enhanced my research significantly, thankfully he has a function for everything ☺. Being the unofficial supervisor of each other, our contributions are embedded in every single section written in our theses.

Last but not least, I would like to express my deepest gratitude to my family but in Turkish. *“Alışlagelmişin dışında evladınızı binlerce kilometre uzağa tek başına göndermenin sizin için ne kadar zor olduğunu biliyorum. Bu önemli kararımda beni desteklemenizin ne kadar anlam ifade ettiğini anlatmam mümkün değil. Bu tezi acısıyla tatlısıyla kendi kaderimin mimarı olmamı sağlayan aileme ama en çok da ponçik babannem Döndü Çağlayan’a adamak isterim...”*

“Faber est suae quisque fortunae”

To those who are the artisans of their own fortune...

Table of Contents

Abstract	i
Kurzfassung	iii
Acknowledgments	v
Table of Contents	vii
List of Figures	xi
List of Tables	xvii
Nomenclature	xxi
1 Introduction	1
1.1 Motivation	2
1.2 Research Question	3
1.3 Structure	4
2 Background	7
2.1 Techno-economic Potential of Offshore Wind Energy	7
2.1.1 Fundamental Principles of Wind Energy	7
2.1.2 Offshore Wind Energy	9
2.1.3 Literature Analysis on Offshore Wind Energy Modeling	11
2.2 Hydrogen Storage in Salt Caverns	15
2.2.1 Fundamental Principles of Underground Storage Technologies	15
2.2.2 Underground Storage of Hydrogen	16
2.2.3 Literature Review of Hydrogen Storage in Salt Cavern	17
2.3 Energy System Modeling	17
2.3.1 Existing Studies on the European Energy System	18
2.3.2 Weather Years Used in the Literature	22
2.3.3 Technical and Economic Parameters of Technologies Considered in 100% Renewable Energy Systems Design	23
2.4 Summary	28
3 Methodology	31
3.1 Technical Potential of Offshore Wind Energy across Europe	31

3.1.1	Ocean Eligibility and Turbine Placement	31
3.1.2	Turbine Simulation	32
3.1.3	Cost Estimation	34
3.1.4	Optimal Turbine Design.....	38
3.1.5	Clustering Optimal Turbine Designs	39
3.2	Technical Potential of Salt Caverns across Europe	40
3.2.1	Land Eligibility	41
3.2.2	Salt Cavern Design	43
3.2.3	Calculation of Cavern Capacity	44
3.3	Model Aggregation Toolset for Energy Systems (MATES)	47
3.3.1	Electricity Generation via VRES	48
3.3.2	Electricity Demand	52
3.3.3	Hydrogen Demand for Passenger Vehicles.....	52
3.3.4	Hydrogen Pipeline.....	53
3.3.5	Salt Caverns.....	54
3.3.6	Additional Features of the Model Chain.....	54
3.4	Scenario Definition for the Design of a 100% Renewable European Energy System... 55	
3.4.1	Definition of the Region	56
3.4.2	Demand Sectors	57
3.4.3	Source Technologies.....	58
3.4.4	Storage Technologies	63
3.4.5	Conversion Technologies	65
3.4.6	Transmission Technologies.....	66
3.5	Discussion on the Impact on Time Series Aggregation.....	69
3.6	Robust Energy System Design over 38 Weather Years.....	71
3.7	Summary.....	72
4	Estimated Potentials for Offshore Wind Energy and Salt Cavern Storage	75
4.1	Techno-economic Potential of Offshore Wind Energy in Europe	75
4.1.1	Optimal Turbine Design.....	75
4.1.2	Literature Comparison and Application of Different Single Turbine Designs	79

4.1.3	Clustered Optimal Turbine Designs	84
4.2	Technical Potential of Salt Cavern for Hydrogen Storage	87
4.2.1	European Salt Basins Suitable for Underground Hydrogen Storage	87
4.2.2	Eligibility Assessment and Cavern Placement	89
4.2.3	Distribution of Volumetric Energy Density across Europe	90
4.2.4	National Storage Potential	92
4.3	Summary	94
5	Sensitivities in the 100% Renewable European Energy System Design	97
5.1	Impact of Number of Typical Days	98
5.2	Impact of Grouping VRES Sources	103
5.3	Impact of Weather Years	107
5.3.1	Variation in the Optimal Capacity of VRES at National Level	110
5.3.2	Variation in the Optimal Capacity of Conversion Technologies at National Level	112
5.3.3	Variation in the Optimal Capacity of Storage Technologies at National Level	115
5.3.4	Variation in the Hydrogen Pipeline Connections	117
5.4	Value-of-Analysis of Technologies Considered in the Design	119
5.4.1	Value of Wind Energy and PV Energy in the System	123
5.4.2	Value of Connection between Countries	125
5.4.3	Value of Individual VRES Generation Technologies	127
5.4.4	Value of Individual Transmission Technologies	131
5.5	Sensitivity Analyses	133
5.5.1	Pipeline Cost	134
5.5.2	Electrolyzer Cost	135
5.5.3	Impact of Hydrogen Demand Market Penetration	136
5.6	Summary	138
6	Design of European Energy System Based on 100% Renewable Energy	141
6.1	Overall European Energy System Design	141
6.1.1	Conversion Technologies	144
6.1.2	Storage Technologies	147
6.2	Different Regional Behaviors in the Operation of Technologies	150

6.3	Curtailment and Efficiency Losses in the System	153
6.4	Roles of Countries in the Future Energy System	157
6.5	Comparison of the Designed System against Literature	163
6.5.1	Comparison of VRES Capacities and Electricity Generation	163
6.5.2	Comparison of Annual Curtailment	166
6.5.3	Comparison of Storage Capacities	168
6.6	Discussion and Evaluation of the Methodology in Present Work	169
6.7	Summary	171
7	Summary	173
7.1	Scope and Objective	173
7.2	Techno-Economic Potential of Offshore Wind Energy	173
7.3	Technical Potential of Salt Caverns for Hydrogen Storage	174
7.4	Sensitivities of 100% Renewable Energy System Design	174
7.5	Design of European Energy System Based on 100% Renewable Energy	176
7.6	Conclusion	177
8	References	179
A.	APPENDICES	195
A.1.	Population Density	195
A.2.	Maximum Capacities Defined in the Scenario (VRES technologies are aggregated).	196
A.3.	Model Runs Performed in Section 5	199
A.4.	National Capacity Distribution by Model Run	202
A.5.	System Design with Different Market Penetration Values of Hydrogen Demand	288
A.6.	Top-down Spatial Redistribution of VRES Technologies	299
A.7.	Variation in Total Annual Cost by Iterations	301
A.8.	Regional Capacities of System Design Proposed in Section 6	303
A.9.	Average Losses in the System Design Proposed in Section 6	309

List of Figures

Figure 1-1 Historical greenhouse gas emissions in EU-28 and Iceland with reduction targets in 2050 with respect to the levels in 1990. (LULUCF: Land use, land-use change, and forestry).....	1
Figure 1-2 Overview of the structure of the thesis broken down to chapters with their main aspects.	4
Figure 2-1 Representation of a power curve estimated by the synthetic power curve method by Ryberg et al. [39] (Exemplary turbine capacity and rotor diameter are chosen as 8.0 MW and 164 m similar to the design of Vestas V164-8.0 MW [41]).	9
Figure 2-2 Cumulative installed capacity of offshore wind energy across the world. Adapted from [48].	9
Figure 2-3 Representation of offshore wind turbine foundation types. Adapted from [58].	11
Figure 2-4 Distribution of the specific investment cost for generation technologies in 2050 [64], [133], [143], [161]–[173].	25
Figure 2-5 Distribution of the specific investment cost for conversion technologies in 2050 [13], [14], [167], [168], [170], [177]–[184], [187], [188].	27
Figure 3-1 Representation of workflow used in offshore turbine simulations.	33
Figure 3-2 Representation of raw power curve, power curve with only convolution and power curve with convolution and losses.	34
Figure 3-3 Cost break-down for offshore wind turbines fixed-bottom (left) and floating (right). Adapted from NREL [56].	35
Figure 3-4 Variation of specific cost with respect to the capacity, rotor diameter, hub height, water depth, and distance to shore. Derived by the models described in [54]–[56].	37
Figure 3-5 Distribution of future turbine design parameters by the expert opinions. Adapted from Wisser et al. [93].	39
Figure 3-6 Overall workflow used in the optimal turbine design analysis.	39
Figure 3-7 Algorithm applied to cluster the optimal turbine designs.	40
Figure 3-8 Concept of potential with different potential types. Adapted from [47], published in [192].	41
Figure 3-9. A simplified representation of an exemplary cavern and estimated pressure limits as a function of depth, which is adapted from Stolzenburg et al. [187] (Calculation of pressure is explained in Section 3.2.3).	44
Figure 3-10. Comparison of reported and calculated storage capacities of natural gas salt caverns (Reported values are extracted from the existing natural gas storage facilities in Europe [96]). .	46

Figure 3-11 Structure of Model Aggregation Toolset for Energy Systems	48
Figure 3-12 Distribution of onshore turbine locations in North Rhine-Westphalia, Germany, with corresponding generation time series (weather year: 2015) different groups which are classified by an equal division of percentiles of the turbine's LCOE. (upper) for single grouping and (lower) 4 turbine groups.	50
Figure 3-13 Representation of grouping as an example in North Rhine-Westphalia, in which 3 groups of onshore wind turbines are categorized by LCOE.	51
Figure 3-14 Representative workflow for onshore wind turbines and electricity generation in Juelich, Germany.	52
Figure 3-15 Representation of technologies and their interactions within a region in the energy system.	55
Figure 3-16 Regions used in the analysis. Adapted from [141].	56
Figure 3-17 Distribution of hydrogen demand and electricity demand across regions.	58
Figure 3-18 LCOE of onshore, offshore, rooftop PV, open-field PV with tracking and open-field PV without tracking for single grouping of technologies with a weather year 2015.	62
Figure 3-19 Maximum storage potential for salt caverns, reservoir and PHS storage in regions.	64
Figure 3-20 Left: HVAC and HVDC connections between regions and their corresponding line capacities. Right: all possible hydrogen pipeline connections between regions.	67
Figure 3-21 Comparison of different assumptions in the pipeline investment cost as a function of capacity. Contains data from Mischner [189].	68
Figure 3-22 (Upper) Percent error caused by time series aggregation with 30 typical days, (Bottom) Capacity factor time series of onshore wind energy in "32_de" for the weather year 2015.	69
Figure 3-23 Distribution of absolute error estimated for 30 typical days for onshore wind energy in "32_de" for the weather year 2015.	70
Figure 3-24 (Upper) Percent error caused by time series aggregation with 30 typical days, (Bottom) Capacity factor time series of openfield PV in "32_de" for the weather year 2015.	70
Figure 3-25 Algorithm used in the enhanced energy system design to ensure the security of supply.	72
Figure 4-1. Specifications of resulting turbine design across European maritime boundaries, a) capacity, (b) hub height, (c) foundation, (d) FLH with optimal design [60].	78
Figure 4-2. Comparison of LCOE calculated by this approach with the literature. Left: LCOE estimations in the literature changing by year, right: the relative occurrence of the LCOE for single turbine design and optimal turbine design in the context of 2050 [60].	80

Figure 4-3 LCOE distribution of individual single turbine designs [60].	81
Figure 4-4 Comparison of full load hour distribution of selected turbines [60].	83
Figure 4-5 (a) Distribution of cost-optimal turbine capacities across European Maritime Boundaries without eligibility constraints. The change in LCOE of top 100 turbines with respect to LCOE of optimal turbine design as a result of the optimization with respect to their design parameters for (b) Location A and for (c) Location B.	84
Figure 4-6 Distribution of different turbine designs across Europe for exemplary LCOE thresholds as 1% (left) and 0.5% (left). In the legend: upper values are for turbine capacity in MW; lower values are for rotor diameter in m.	86
Figure 4-7. Map of European salt deposits and salt structures as a result of suitability assessment for underground hydrogen storage (1. Alsace Basin; 2. Bresse Basin; 3. Greoux Basin; 4. Valence Basin; 5. Lower Rhine Basin; 6. Hessen Werra Basin; 7. Sub-Hercynian Basin; 8. Lausitz Basin; 9. Leba Salt; 10. Fore-Sudetic Monocline; 11. Carpathian Foredeep; 12. Lublin Trough; 13. Ocenele Mari; 14. Cardona Saline Formation; 15. Pripyat Basin; 16. Cheshire Basin; 17. UK Permian Zechstein Basin; 18. Larnie Salt Field; 19. Wessex Basin). Previously published in Caglayan et al. [192].	89
Figure 4-8. Land eligibility results with an exemplary representation of cavern placement in central Germany (extent of exemplary placement: 51.9°-52.0° N, 10.0°-10.1° E). Previously published in Caglayan et al. [192].	90
Figure 4-9. Distribution of potential salt cavern sites across Europe with their corresponding energy densities (cavern storage potential divided by the volume). Previously published in Caglayan et al. [192].	92
Figure 4-10. Total cavern storage potential in European countries classified as onshore, offshore and within 50 km of the coast. Previously published in Caglayan et al. [192].	94
Figure 5-1 Overview of exploratory design analyses in Section 5.	98
Figure 5-2 Variation of solution time by the number of typical days (Calculations for the case without time series aggregation is performed in a different computer).	99
Figure 5-3 Variation of total annual cost with respect to the number of typical days.	100
Figure 5-4 Capacity distributions of generation technologies and hydrogen pipeline for different number of typical days (5, 10 and 30) and without time series aggregation.	102
Figure 5-5 Optimal European capacities and corresponding total annual cost with respect to a different number of groups.	104
Figure 5-6 National optimal capacities broken down to onshore wind energy, offshore wind energy, open-field PV with and open-field PV without tracking for different number of groups of all technologies.	106

Figure 5-7 Variation of total annual cost with respect to the weather year used in the simulation.	109
Figure 5-8 Boxplot of the optimal capacity of VRES technologies obtained for different weather years at a national level.	112
Figure 5-9 Boxplot of the optimal capacity of conversion technologies obtained for different weather years at a national level.	114
Figure 5-10 Boxplot of the optimal capacity of storage technologies obtained for different weather years at a national level.	117
Figure 5-11 Average optimal capacities for salt caverns and pipeline with pipeline repetitions as a result of optimization performed for 38 years (between 1980 and 2017).	119
Figure 5-12 Optimal design of the reference scenario used in the value-of-analysis. Weather year is chosen as 2015, 60 groups per VRES technologies and 30 typical days.	121
Figure 5-13 Variation in the total annual cost of the system with respect to individual technologies prohibited.	123
Figure 5-14 Spatial distribution of generation technologies when wind (right) or PV (left) technologies are prohibited.	125
Figure 5-15 Spatial distribution of generation technologies when transmission technologies between countries are prohibited.	127
Figure 5-16 Spatial distribution of generation technologies for different scenarios with individual generation technologies prohibited.	130
Figure 5-17 Spatial distribution of generation technologies for different scenarios with individual transmission technologies prohibited.	133
Figure 5-18 Variation of total annual cost and increase in the total annual cost per additional hydrogen with respect to the market penetration of hydrogen demand for passenger vehicles.	137
Figure 5-19 Capacity distribution of generation technologies as well as hydrogen pipeline as a result of energy system design without hydrogen demand.	138
Figure 6-1 Proposed 100% renewable European energy system design with ensured security of supply over 38 weather years investigated.	143
Figure 6-2 Proposed capacities for electrolyzer (left) and reelectrification (right) technologies in the 100% renewable European energy system.	145
Figure 6-3 Variations in conversion technology the full load hours for the proposed system design across input weather years.	146

Figure 6-4 Proposed capacities for storage technologies in the 100% renewable European energy system.....	148
Figure 6-5 Hourly time series for the state of charge of salt caverns, pumped hydro storage and hydro reservoirs for individual years (between 1980 and 2017). Red line is the average time series of all years at each hour.	150
Figure 6-6 Operation of technologies for different commodities in “52_it” for the 2 nd week of July (upper) electricity, (lower) hydrogen. 2015 is used as the weather year.....	151
Figure 6-7 Operation of technologies for different commodities in “90_uk” for the 2 nd week of July (upper) electricity, (lower) hydrogen. 2015 is used as the weather year.....	152
Figure 6-8 Operation of technologies for different commodities in “80_no” for the 2 nd week of July (upper) electricity, (lower) hydrogen. 2015 is used as the weather year.....	153
Figure 6-9 Distribution of the average for the proposed system design.....	155
Figure 6-10 Losses caused by conversion technologies as well as lithium-ion batteries.	157
Figure 6-11 Net energy flow between regions for (left) electricity (right) hydrogen.	159
Figure 6-12 Net transport of electricity versus hydrogen, with electricity generation and total demand within the regions indicated as the marker size and colors, respectively.	161
Figure 6-13 Geospatial distribution of the net hydrogen transport across regions with proposed pipeline connections.	162
Figure 6-14 Comparison of VRES capacity distribution for regions defined by Cebulla et al. [146].	164
Figure 6-15 Comparison of total capacity distribution and generation for (left) Europe, (right) regions defined by Cebulla et al. [146]. Note that the capacities present work on the right is calculated according to the region definition.	166
Figure 6-16 Comparison of Ryberg [37], Syranidou [136] and present work.	167
Figure 6-17 Comparison of storage ratio estimated by literature sources as cited in Blanco and Faaij [94].	169
Figure A-1 Population density distribution used in the regionalization. (Left) Number of people per km ² , (Right) Total number of people in each region	195
Figure A-2 System design at 0% market penetration	288
Figure A-3 System design at 10% market penetration	289
Figure A-4 System design at 20% market penetration	290
Figure A-5 System design at 30% market penetration	291
Figure A-6 System design at 40% market penetration	292

Figure A-7 System design at 50% market penetration	293
Figure A-8 System design at 60% market penetration	294
Figure A-9 System design at 70% market penetration	295
Figure A-10 System design at 80% market penetration	296
Figure A-11 System design at 90% market penetration	297
Figure A-12 System design at 100% market penetration	298
Figure A-13 Top-down spatial distribution of wind energy based on the regional capacities reported in Table A-89 (Resulting system design presented in Chapter 6).....	299
Figure A-14 Top-down spatial distribution of open-field PV based on the regional capacities reported in Table A-89 (Resulting system design presented in Chapter 6)	300
Figure A-15 Total annual cost distribution as a boxplot between Iteration 0 and Iteration 5	302

List of Tables

Table 2-1 Studies investigating offshore wind energy potential across Europe or the World. ECMWF: European Centre for Medium-Range Weather Forecasts; NCEP: National Centers for Environmental Prediction; MERRA-2: Modern-Era Retrospective analysis for Research and Applications-version 2; ERA-Interim: European Reanalysis Interim.	12
Table 2-2 Summary of the studies investigating at least European energy system.....	18
Table 3-1. Constraints used in the ocean eligibility analysis	32
Table 3-2 Constraints used in the land eligibility analysis for salt cavern construction	42
Table 3-3 Techno-economic parameters of generation technologies considered in the analysis.	60
Table 3-4 Techno-economic parameters of storage technologies considered in the analysis. ...	65
Table 3-5 Techno-economic parameters of conversion technologies considered in the analysis.	66
Table 4-1 Comparison of results of different single turbine characteristics [60].....	82
Table 4-2 Number of turbine designs with respect to the LCOE threshold and parameters considered in turbine design.....	85
Table 5-1 Total annual cost with respect to assumed pipeline cost with a percent deviation....	134
Table 5-2 Resulting parameters of 300 € kW ⁻¹ electrolyzer cost and reference case (the weather year 2015, 60 groups per VRES technology).....	135
Table A-1. Maximum Capacities of Technologies Defined in the Optimization.....	196
Table A-2. Definition of model runs performed in Section 5 with corresponding model run ID .	199
Table A-3. Capacity distribution for Model Run 1 (5 Typical Days)	202
Table A-4. Capacity distribution for Model Run 2 (10 Typical Days)	203
Table A-5. Capacity distribution for Model Run 3 (15 Typical Days)	204
Table A-6. Capacity distribution for Model Run 4 (20 Typical Days)	205
Table A-7. Capacity distribution for Model Run 5 (30 Typical Days)	206
Table A-8. Capacity distribution for Model Run 6 (45 Typical Days)	207
Table A-9. Capacity distribution for Model Run 7 (60 Typical Days)	208
Table A-10. Capacity distribution for Model Run 8 (90 Typical Days)	209
Table A-11. Capacity distribution for Model Run 9 (Without time series aggregation)	210
Table A-12. Capacity distribution for Model Run 10 (2 Groups per VRES technology)	211

Table A-13. Capacity distribution for Model Run 11 (3 Groups per VRES technology)	212
Table A-14. Capacity distribution for Model Run 12 (4 Groups per VRES technology)	213
Table A-15. Capacity distribution for Model Run 13 (5 Groups per VRES technology)	214
Table A-16. Capacity distribution for Model Run 14 (6 Groups per VRES technology)	215
Table A-17. Capacity distribution for Model Run 15 (10 Groups per VRES technology)	216
Table A-18. Capacity distribution for Model Run 16 (10 Groups per VRES technology)	217
Table A-19. Capacity distribution for Model Run 17 (12 Groups per VRES technology)	218
Table A-20. Capacity distribution for Model Run 18 (15 Groups per VRES technology)	219
Table A-21. Capacity distribution for Model Run 19 (20 Groups per VRES technology)	220
Table A-22. Capacity distribution for Model Run 20 (30 Groups per VRES technology)	221
Table A-23. Capacity distribution for Model Run 21 (60 Groups per VRES technology)	222
Table A-24. Capacity distribution for Model Run 22 (72 Groups per VRES technology)	223
Table A-25. Capacity distribution for Model Run 23 (90 Groups per VRES technology)	224
Table A-26. Capacity distribution for Model Run 24 (Value of onshore wind energy)	225
Table A-27. Capacity distribution for Model Run 25 (Value of offshore wind energy)	226
Table A-28. Capacity distribution for Model Run 26 (Value of PV without tracking)	227
Table A-29. Capacity distribution for Model Run 27 (Value of PV with tracking)	228
Table A-30. Capacity distribution for Model Run 28 (Value of Hydro Run-of-river).....	229
Table A-31. Capacity distribution for Model Run 29 (Value of Rooftop PV).....	230
Table A-32. Capacity distribution for Model Run 30 (Value of Pumped Hydro Storage).....	231
Table A-33. Capacity distribution for Model Run 31 (Value of Hydro Reservoir)	232
Table A-34. Capacity distribution for Model Run 32 (Value of Biomass)	233
Table A-35. Capacity distribution for Model Run 33 (Value of SOFC).....	234
Table A-36. Capacity distribution for Model Run 34 (Value of PEMFC)	235
Table A-37. Capacity distribution for Model Run 35 (Value of H ₂ OCGT).....	236
Table A-38. Capacity distribution for Model Run 36 (Value of H ₂ CCGT).....	237
Table A-39. Capacity distribution for Model Run 37 (Value of Salt Cavern)	238
Table A-40. Capacity distribution for Model Run 38 (Value of Vessel)	239
Table A-41. Capacity distribution for Model Run 39 (Value of Lithium-ion Battery)	240
Table A-42. Capacity distribution for Model Run 40 (Value of Pipeline)	241

Table A-43. Capacity distribution for Model Run 41 (Value of HVAC Connections)	242
Table A-44. Capacity distribution for Model Run 42 (Value of HVDC Connections)	243
Table A-45. Capacity distribution for Model Run 43 (Value of Wind Energy)	244
Table A-46. Capacity distribution for Model Run 44 (Value of Solar Energy)	245
Table A-47. Capacity distribution for Model Run 45 (Weather Year 1980)	246
Table A-48. Capacity distribution for Model Run 45 (Weather Year 1981)	247
Table A-49. Capacity distribution for Model Run 47 (Weather Year 1982)	248
Table A-50. Capacity distribution for Model Run 48 (Weather Year 1983)	249
Table A-51. Capacity distribution for Model Run 49 (Weather Year 1984)	250
Table A-52. Capacity distribution for Model Run 50 (Weather Year 1985)	251
Table A-53. Capacity distribution for Model Run 51 (Weather Year 1986)	252
Table A-54. Capacity distribution for Model Run 52 (Weather Year 1987)	253
Table A-55. Capacity distribution for Model Run 53 (Weather Year 1988)	254
Table A-56. Capacity distribution for Model Run 54 (Weather Year 1989)	255
Table A-57. Capacity distribution for Model Run 55 (Weather Year 1990)	256
Table A-58. Capacity distribution for Model Run 56 (Weather Year 1991)	257
Table A-59. Capacity distribution for Model Run 57 (Weather Year 1992)	258
Table A-60. Capacity distribution for Model Run 58 (Weather Year 1993)	259
Table A-61. Capacity distribution for Model Run 59 (Weather Year 1994)	260
Table A-62. Capacity distribution for Model Run 60 (Weather Year 1995)	261
Table A-63. Capacity distribution for Model Run 61 (Weather Year 1996)	262
Table A-64. Capacity distribution for Model Run 62 (Weather Year 1997)	263
Table A-65. Capacity distribution for Model Run 63 (Weather Year 1998)	264
Table A-66. Capacity distribution for Model Run 64 (Weather Year 1999)	265
Table A-67. Capacity distribution for Model Run 65 (Weather Year 2000)	266
Table A-68. Capacity distribution for Model Run 66 (Weather Year 2001)	267
Table A-69. Capacity distribution for Model Run 67 (Weather Year 2002)	268
Table A-70. Capacity distribution for Model Run 68 (Weather Year 2003)	269
Table A-71. Capacity distribution for Model Run 69 (Weather Year 2004)	270
Table A-72. Capacity distribution for Model Run 70 (Weather Year 2005)	271

Table A-73. Capacity distribution for Model Run 71 (Weather Year 2006)	272
Table A-74. Capacity distribution for Model Run 72 (Weather Year 2007)	273
Table A-75. Capacity distribution for Model Run 73 (Weather Year 2008)	274
Table A-76. Capacity distribution for Model Run 74 (Weather Year 2009)	275
Table A-77. Capacity distribution for Model Run 75 (Weather Year 2010)	276
Table A-78. Capacity distribution for Model Run 76 (Weather Year 2011)	277
Table A-79. Capacity distribution for Model Run 77 (Weather Year 2012)	278
Table A-80. Capacity distribution for Model Run 78 (Weather Year 2013)	279
Table A-81. Capacity distribution for Model Run 79 (Weather Year 2014)	280
Table A-82. Capacity distribution for Model Run 80 (Weather Year 2015)	281
Table A-83. Capacity distribution for Model Run 81 (Weather Year 2016)	282
Table A-84. Capacity distribution for Model Run 82 (Weather Year 2017)	283
Table A-85. Capacity distribution for "Value of Country Connection"	284
Table A-86. Capacity distribution for "Pipeline Investment Cost 145 € kW ⁻¹ m ⁻¹ "	285
Table A-87. Capacity distribution for "Pipeline Investment Cost 225 € kW ⁻¹ m ⁻¹ "	286
Table A-88. Capacity distribution for "Electrolyzer Investment Cost 300 € kW ⁻¹ "	287
Table A-89. Proposed Capacities of Generation and Conversion Technologies in Section 6...	303
Table A-90. Proposed Capacities of Storage Technologies in Section 6.....	306
Table A-91. Average Losses in the System Proposed in Section 6.....	309

Nomenclature

GHG	Greenhouse gases
CHP	Combined Heat and Power
CLC	Corine Land Cover
CSP	Concentrated solar power
ECMWF	European Centre for Medium-Range Weather Forecasts
ENTSO-E	European Network of Transmission System Operators for Electricity
ERA-Interim	European Reanalysis Interim
EU	European Union
FINE	Framework for Integrated Energy System Assessment
FLH	Full load hours
geokit	Geospatial toolkit for Python
GIE	Gas Infrastructure Europe
GLAES	Geospatial Land Availability for Energy Systems
GWA	Global Wind Atlas
HVAC	High voltage alternating current
HVDC	High voltage direct current
IEC	International Electrotechnical Commission
JRC	Joint Research Centre
LCOE	Levelized cost of electricity
LHV	Lower heating value
LULUCF	Land use, land-use change, and forestry
MATES	Model Aggregation Toolset for Energy Systems Modern-Era Retrospective analysis for Research and Applications- version 2
MERRA-2	
NCEP	National Centers for Environmental Prediction
NREL	National Renewable Energy Laboratory
PEM	Polymer Electrolyte Membrane
PV	Photovoltaics
SOFC	Solid oxide fuel cells
TAC	Total annual cost
TSA	Time Series Aggregation
TYNDP	Ten Year Network Development Plan
VRES	Variable renewable energy sources

1 Introduction

The average surface temperature of the Earth has increased by 1 °C globally compared to the values in 1880, which raises concerns regarding global warming [1], [2]. A broader concept in addition to global warming is climate change, which involves the consequences of global warming such as increases in sea level and forest fires [3]. Greenhouse gases (GHG) ensnare some of the heat reaching Earth’s surface via solar radiation, contributing to global warming [4]. At the end of 2015 (December 12th, 2015), the Paris Agreement was ratified to set ambitious reduction targets to mitigate climate change. The main objective is to maintain the increase in temperature below 2 °C [5]. Individual countries are encouraged to develop their contributions and assist developing countries to address their respective contributions [5]. The European Union (EU) has set a target of the GHG emissions reduction by 85 to 90% of the levels in 1990 until 2050 [6]. Figure 1-1 involves the historical values for the GHG emissions in EU-28 and Iceland as well as a linear projection to the target in 2050, where the total reduction is reported as 23% by 2017. Nearly 75% of GHG emissions are caused by carbon dioxide (CO₂), which has been reduced by approximately 22% since 1990 [4]. Industries such as electricity/heat generation, manufacturing, residential, steel, cement and petroleum refineries decreased the CO₂ emissions at different degrees, whereas an increase of nearly 170 Mt CO_{2,eq} is observed between 1990 and 2017 for road transport sector [4].

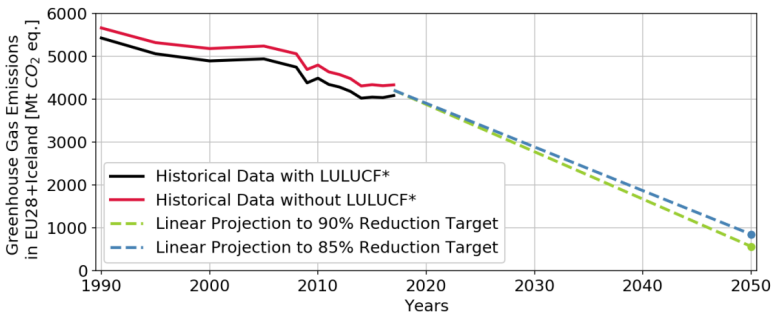


Figure 1-1 Historical greenhouse gas emissions in EU-28 and Iceland with reduction targets in 2050 with respect to the levels in 1990. (LULUCF: Land use, land-use change, and forestry)
Adapted from [4].

In order to decarbonize the European energy system, there is an increasing trend in the shares of renewable energy, especially wind and solar power. An increase in the globally installed capacity of renewables between 2010 and 2018 is reported as 1127 GW, nearly 74% of which comprises wind and solar energy [7]. However, despite the increase in the share of these technologies, which will be referred to variable renewable energy sources (VRES), the issue of intermittency persists as the main obstacle for high shares of VRES in the energy systems [8]. This can be addressed

by introducing chemical energy carriers that can be produced at the peak power generation periods, and later utilized for grid balancing or as a feedstock in the other processes. This process consists of the production of chemical energy carriers at periods when the electricity generation is higher than the demand is called "Power to gas" [9]. Owing to its high energy density, relatively lower storage cost, and carbon-free nature, hydrogen is a promising alternative chemical energy carrier. Electrolyzers can be used in the production of hydrogen by splitting the water molecules into hydrogen and oxygen. In addition, being a chemical energy carrier, hydrogen can be used as feedstock in many industries such as ammonia and polymer production, hydrotreatment, or hydrocracking processes in the refineries [10]. Furthermore, it can be utilized as a fuel in the transport sector in fuel cell electric vehicles [9]. By this, hydrogen enables many sector coupling options when it is used in different sectors [11].

1.1 Motivation

Introducing hydrogen in the energy systems design has been conducted by several studies at different scales. For instance, the German energy system is modeled by considering hydrogen as an alternative energy carrier for different scenarios [11]–[14]. Similar analyses are conducted for different European countries such as France [15] and Italy [16]. Hydrogen has also been considered in the European energy systems design [17], [18]. Nevertheless, although it is included in the future energy systems, the transmission of hydrogen is not taken into account in any of the studies at a European scale. Trading between countries and the cost of hydrogen when it is produced at cheap locations are assessed by some studies [19], yet the use of a deterministic approach finding the minimum cost is still missing. When the whole system is not optimized but simulated based on a capacity scenario definition, the cost of that system is overestimated. Moreover, which regions play an essential role in the energy systems design cannot be identified with scenario-based simulations, since the roles of the countries are already defined by the scenario scope. As a result, the cost optimization of the overall system helps the identification of the regions with cheap commodity production.

In addition to the lack of hydrogen transmission in energy systems design, there are several aspects that are not taken into account. For instance, up to now, most of the European system designs are conducted by assuming each country as one node, sometimes even aggregation of some countries as one node. In this way, the trading and infrastructure design cannot be modeled in detail. Moreover, larger regional definition (spatially aggregated regions) decreases the accuracy in the modeling of VRES technologies due to their locational dependency. The time series of these technologies alter with respect to weather phenomena (i.e., wind speeds, solar irradiance, and cloud coverage) and terrain (i.e., surface roughness and shading). Furthermore, either a representative location or average of all possible locations is defined in the energy system model, which has a strong possibility of over- or underestimating the capacities (cf. Section 3.3.1).

Finally, all the studies designing a future energy system either considers one representative year¹ or a few years in order to model the VRES generation time series [13], [20]–[31]. Whether or not the selected year provides a robust system design is investigated in detail in almost none of the literature sources.

Taking into account all the aforementioned aspects lacking in the system design, existing studies on the European energy system analyses with hydrogen infrastructure do not cover the details of a realistic system design. Due to the missing technologies (seasonal storage or transmission) or oversimplification in the modeling, the existing designs do not reflect all the aspects of a future energy system design. Therefore, a detailed European energy system design based on 100% renewables with hydrogen infrastructure is necessary in order to be able to understand if such a system can be cost-competitive or not. While designing such a system, future projections of technologies through techno-economic parameters, high accuracy of VRES technology modeling, and consideration of different weather years in order to cover the weather uncertainty in 2050 will be taken into account.

All in all, it can be said that the unique selling point of this study comes from many aspects taken into account. First of all, covering Europe and dividing it into 96 regions is one of the strengths in this analysis using the local definition with high spatial resolution. With this spatial resolution, a detailed infrastructure can be attained. Furthermore, modeling VRES technologies by grouping them within each region increases the accuracy of the model while maintaining the locational information of wind and PV parks. Detailed modeling of salt caverns at a European scale improves the approach in terms of seasonal storage of hydrogen. Moreover, taking 38 weather years into account and proposing a system design that can ensure the security of supply across all weather years improves the robustness of the proposed design and the results. By taking the aforementioned aspects into account, the existing research gap in the literature is aimed to be closed by this thesis.

1.2 Research Question

In order to address the issues as mentioned earlier, a thesis that derives 100% renewable European energy system design in the context of 2050 has been developed. Within the context of this project, the techno-economic potential of European offshore wind energy and technical storage potential of salt caverns for hydrogen storage are also determined due to the lack of a consistent and reproducible dataset for these technologies across Europe. By using the results derived from these analyses, the design of the European energy system is conducted with a high spatial and temporal resolution.

¹ Even some weeks representing the whole year can be considered.

The major research question to be answered in this thesis is “What is the design of a future 100% renewable European energy system with hydrogen infrastructure?”. In order to answer this major research question, several subquestions listed below are raised and addressed within the scope of this study:

- How can offshore wind power be harnessed effectively?
- What is the storage potential of salt caverns? Where can these salt caverns be located?
- What amount of spatial and temporal details should be considered to represent the system in a stable manner?

1.3 Structure

This thesis contains the methodology to answer the research questions addressed in Section 1.2 as well as the results obtained by applying the tools explained in the methodology. Therefore, a structure illustrated in Figure 1-2 is applied within the context of this work.

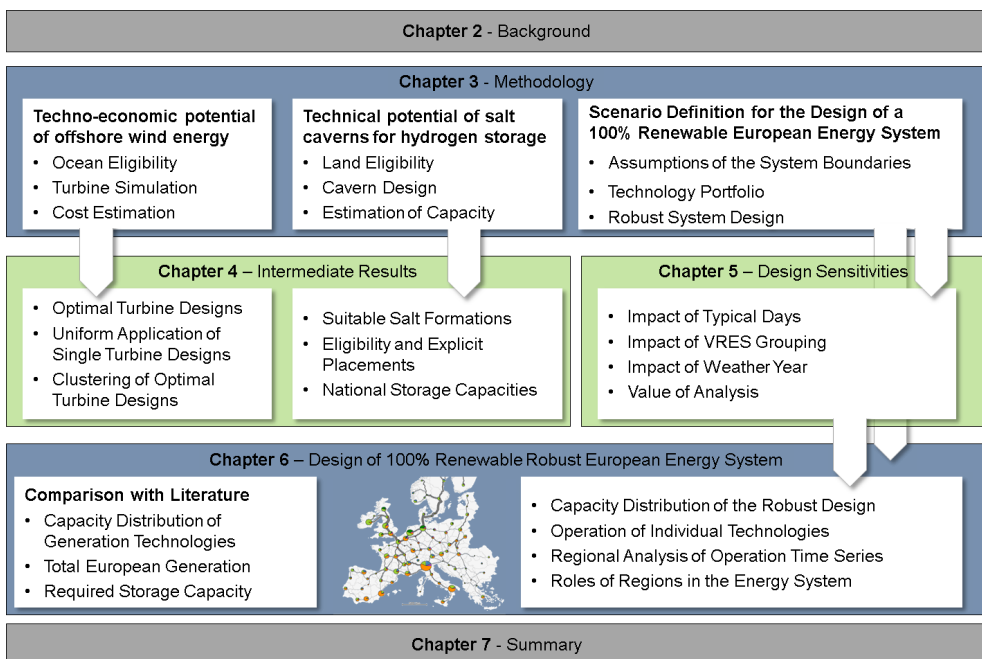


Figure 1-2 Overview of the structure of the thesis broken down to chapters with their main aspects.

The background related to the fundamentals of technologies, as well as previous analyses conducted regarding those technologies, is provided in Section 2. The content in this chapter can be classified into three groups as seen in the figure. Firstly, the fundamentals of wind energy are introduced, which is then followed by the literature review on the offshore wind energy potential. A detailed explanation of the strengths and weaknesses of the existing studies are discussed. Secondly, underground storage in salt caverns is discussed, and a literature review is also provided for this topic. Finally, the European energy system analyses found in the literature are briefly explained to give an insight into the existing energy system designs. Furthermore, the issue of the use of one or a few weather years while designing a VRES based energy system design is raised. Finally, individual technologies in such energy systems are discussed by providing the technical and economic aspects of individual technologies.

All of the tools derived in this thesis are included in Section 0, classifying these tools into three groups. Firstly, offshore wind energy-related tools are discussed by breaking them down into three main analyses: ocean eligibility, turbine simulation, and cost estimation. A combination of these three aspects results in the techno-economic potential of offshore wind energy for any given region and turbine design definition. Secondly, the method used to derive the technical potential of salt caverns is explained by including land eligibility analysis on the ground level (at the surface) of salt formations, cavern designs used in this work, and how the storage capacity is estimated for different cavern depths. Thirdly, an explanation of the model chain² developed within the context of the thesis is described. The definition of the scenario boundaries, technologies, and assumed techno-economic parameters are provided to clarify the input parameters used in the model.

Section 4 involves the intermediate results³, which include the results of offshore wind energy and salt cavern analyses. Cost-optimal turbine designs and uniformly applied single turbine definitions are compared to show the importance of optimal turbine designs. Afterward, the optimal wind turbines are clustered to decrease the number of designs within a levelized cost of electricity (LCOE) tolerance. In addition to the offshore wind energy, suitable salt formations used in the assessment of the technical potential of salt caverns for hydrogen storage are provided⁴. Eligibility analysis of these salt formations and the precise cavern placements are shown. Finally, storage capacities for different cases are investigated at a national level.

The sensitivities proposed before designing the energy system are analyzed in Section 5. The first sensitivity analysis is conducted on the impact of typical days, which is used to reduce temporal resolution as well as the memory requirement of the problem. By using the number of typical days estimated in this analysis, the impact of grouping VRES technologies is performed to determine

² Model Aggregation Toolset for Energy Systems (MATES) (cf. Section 3.3)

³ "Intermediate results" indicate all the analyses conducted before the energy system design. Therefore, it refers to the analyses performed in order to prepare the techno-economic input parameters of the optimization.

⁴ The method used for determination of suitable salt formations across Europe is explained in detail by Weber [112], which is a Masters project under supervision of this doctoral project.

the number of groups providing high fidelity in the energy system design. Following this, the energy system design is conducted by using different weather years to show the variations in the results, which prove the fact that the system is not robust when a single year is used. Finally, by using a reference scenario design, the value-of-analysis is performed to estimate the importance of individual technologies (as well as some combinations of these technologies). Some of the technologies are proven to be insignificant in the energy system design; thus, they are not considered in future analyses.

The proposed methodology in Section 3.6 to attain a robust system design, ensuring the security of supply is employed to design the energy system. The results of the robust design, which do not contain any generation lulls is explained in Section 6. The capacity distribution and operation of individual technologies are addressed for each region. Exemplary operation time series is shown for both electricity and hydrogen flow in two regions with different behaviors. Afterward, some roles are assigned in the system through the net transport of commodities. Following this, the resulting system design is compared against literature.

Finally, the critical aspects within the context of this work are addressed in Section 7. These aspects consist of the main findings of the intermediate results, proposed energy system design as well as the main sensitives observed in the energy system design.

2 Background

This chapter consists of the background information on offshore wind energy, hydrogen storage in salt caverns, and energy system design. The first two topics are addressed in order to fill the gap in the scenario design, which could not be covered with consistent datasets by the literature. Moreover, relevant literature sources have been briefly discussed concerning these concepts in order to provide insight into the existing methods and missing pieces in these tools. Therefore, analyses that model offshore wind energy to estimate the techno-economic potential of a study region are explained in Section 2.1. Before discussing the existing tools and methods, critical concepts of offshore wind energy are shortly explained. Following this, background information and a literature review on underground hydrogen storage are provided in Section 2.2. In spite of the lack of European scale analysis, existing assessments at national levels are provided. Finally, studies conducted on 100% renewable energy system design are discussed. While choosing the analyses to be listed, only studies with a regional definition larger than or equal to Europe are discussed. Besides, the weather years selected by each study are listed along with the expressed reasoning, if possible.

2.1 Techno-economic Potential of Offshore Wind Energy

In this section, a brief explanation of the fundamentals of wind energy will be provided in Section 2.1.1. Following this, offshore wind energy and especially turbine foundation types will be explained, since the terminology will be then used in the assessment of Europe's techno-economic potential of offshore wind energy in Section 3.1. Following this, a literature review on the modeling of offshore wind energy in a larger regional scope will be provided, which serves as a backbone for the methodologies developed in this thesis. This review will be focused on different aspects of offshore wind energy modeling, such as ocean eligibility assessment, and the estimation of capacity and generation potentials. Finally, a brief discussion of the strengths and weaknesses of existing methodologies is included in Section 2.1.3.3.

2.1.1 Fundamental Principles of Wind Energy

Wind turbines are devices that can convert the kinetic energy of wind into electrical energy. The raw power available to the wind turbine estimated from its kinetic energy, which is a function of its wind speed affected by topography and season, can be represented by using Equation 1 [32].

$$P_{wind} = 1/2 \rho_{air} A_{swept} v^3 = \pi/8 \rho_{air} D_{rotor}^2 v^3 \quad \text{Equation 1}$$

P_{wind} stands for power in the wind, ρ_{air} for air density, A_{swept} for the swept area, v for wind speed, and D_{rotor} for the rotor diameter. As it can be seen from Equation 9, wind power is directly proportional to the cubic wind speed and the square of the rotor diameter. Therefore, doubling

wind speed results in an eightfold increase in wind power. Nevertheless, according to Betz Law, the conversion of wind power into electrical power by wind turbines is limited by a maximum theoretical efficiency of 59.3% [33].

In this thesis, upwind, horizontal axis, pitch regulated wind turbines with three rotor blades will be focused due to the wind industry's recent convergence on this design [34]. Details of turbine components will not be explained in this thesis since the topic is already covered extensively in many literature sources [35]–[37]. Manwell et al. [35], for example, explain the fundamentals of wind energy including different turbine types and their components in detail.

The International Electrotechnical Commission (IEC) has set the standards for the definition of a turbine's power curve, which is a graph indicating expected power output at different wind speeds [38]. To predict how a wind turbine generates electricity in response to wind speed, the turbine's power curve can be of use. Power curves are often provided by the turbine's manufacturer and specify either total generation or energy efficiency as a function of wind speed, which is given in the context of 10-minute averaged measurements and at standard air density [38]. Figure 2-1 shows the representation of a power curve for an exemplary turbine design with capacity and a rotor diameter of 8.0 MW and 164 m, respectively [39], [40]. As seen in the figure, a turbine will begin generating electricity once the cut-in wind speed is reached, at which point the torque imparted onto the rotors by incident wind overcomes internal friction within the turbine's nacelle. The wind turbine rapidly increases its generation up until the rated wind speed, shown in the figure at 13 m s^{-1} , after which the turbine's pitch regulation system is activated to prevent damage to turbine components by preventing further increases in generation. This system works by longitudinally-rotating the turbine's rotors to change the incident wind's angle of attack. Once the angle of attack reaches 90° , the incident wind will cease imparting a torque unto the wind turbine's rotors and electricity generation will drop to zero; this is referred to as the cut-out wind speed. Note that the control of the pitch and yaw systems, which determines which direction the turbine should face, are inexact processes which can lead to suboptimal generation and increased wear when not properly aligned.

If two turbines of differing designs are exposed to the same wind speeds, two good indicators of how the generation from these turbines should compare to one another are the hub height and the specific power⁵. Due to wind shear, wind speeds at higher altitudes are often faster than wind speeds nearer to the surface. Therefore, even when accounting for the slight reduction in air density, taller turbines are exposed to a larger pool of energy and thus will perform at higher full load hours. Secondly, turbines with lower specific power (which can be found from the ratio between a turbine's capacity and its swept area) often correlate to a power curve with lower-rated wind speed. Because of this, turbines with lower specific power will respond to low wind speeds better than those with a higher specific power while, for higher wind speeds, both would operate

⁵ The specific power of a turbine is calculated from the ratio of the turbine's capacity to its swept area

at the rated capacity. Therefore, low specific power turbines should also perform at higher full load hours. Because of these two dynamics, it is therefore clear to see why the wind industry is progressing towards turbines with taller hub heights and larger rotor diameters.

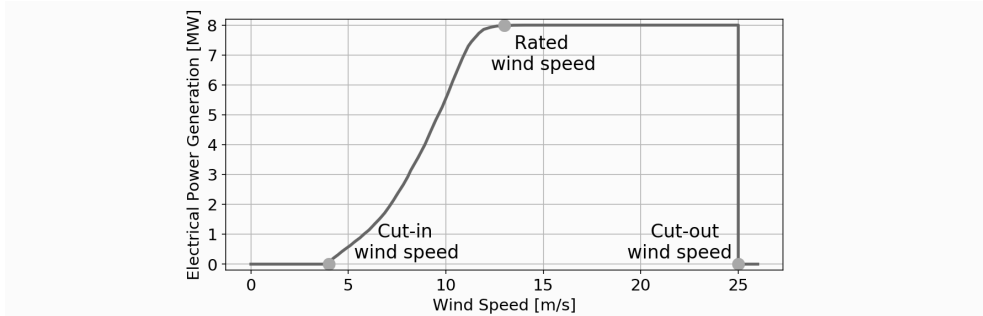


Figure 2-1 Representation of a power curve estimated by the synthetic power curve method by Ryberg et al. [39] (Exemplary turbine capacity and rotor diameter are chosen as 8.0 MW and 164 m similar to the design of Vestas V164-8.0 MW [41]).

2.1.2 Offshore Wind Energy

In the last decade, offshore wind energy has grown significantly, which can be seen from the installed capacity of offshore wind energy for the European (disaggregated into countries), Asian and American continents shown in Figure 2-2. This growing interest can be attributed to the availability of area for larger wind farms, generally higher wind speeds compared to onshore locations, lower intrinsic turbulence intensity and less wind shear [35]. Moreover, with decreasing turbine cost and higher performance, LCOE of offshore wind energy decreases to $10 \text{ €}_{\text{ct}} \text{ kWh}^{-1}$ according to the projections by 2050 [42]–[47]. Conversely, higher project costs, low accessibility for operation and maintenance activities along with additional requirements for corrosion prevention are often discussed disadvantages of this technology [35].

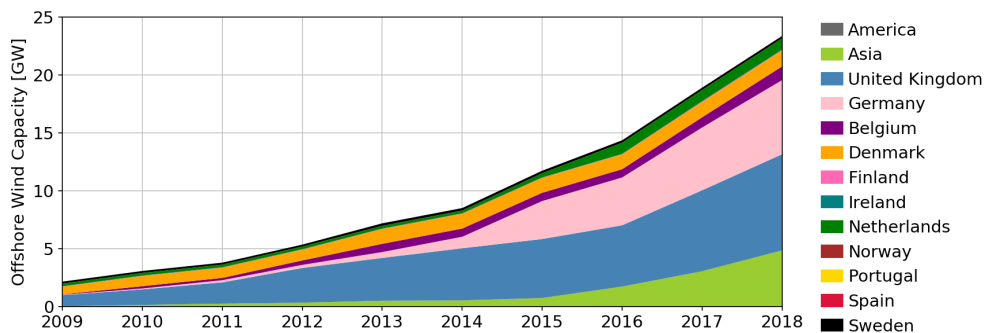


Figure 2-2 Cumulative installed capacity of offshore wind energy across the world. Adapted from [48].

Compared to onshore wind energy, offshore wind turbine designs have higher capacity and larger rotor diameter. For instance, the highest wind turbine capacity at the time of this thesis belongs to the General Electric (GE) Haliade-X [49] with the capacity and rotor diameter of 12 MW and 220 m, respectively. In terms of capacity, this turbine is followed by Vestas V164-10 MW [50] with 10 MW capacity and 164 m rotor diameter. In the life cycle analysis conducted by Bonou et al. [51], larger wind turbines having direct-drive generators are stated to perform better compared to the small ones. Moreover, the greenhouse gas emissions of offshore wind turbines are found to be lower than that of fossil fuels and conventional power plants [52], [53].

As the name indicates, fixed-bottom foundations are connected to the seabed directly with the pile/piles, whereas floating turbines are anchored to the seabed via mooring. Typical fixed-bottom foundation types are monopile, gravity, tripod, and jacket. Only monopile, jacket, spar, and semisubmersible foundation types as shown in Figure 2-3 are considered in this analysis. The reason behind this is the cost models used in the assessment of the techno-economic potential of offshore wind energy. These cost models and cost-breakdowns suggested by NREL [54]–[57] are the most up-to-date source taking into account many aspects such as distance to shore, water depth and so on. The details of these cost models will be discussed in Section 3.1.3.

In the figure, three fixed-bottom foundation types are shown: gravity-based, monopile, and jacket. Gravity foundation is used for fixed-bottom offshore wind turbines with a water depth of 30 m, which has a precast concrete on the sand or stone [58]. Thus, the gravity supports the structure, yet investigation of the seabed is crucial for this foundation type [58]. As it is seen from the figure, a monopile foundation consists of a large steel tube embedded into the seabed. Generally, there is no requirement for seabed preparation; however, drilling might be necessary in the cases when the seabed is hard soil or rock [35]. Nevertheless, this foundation type is stated to be the most economical for European seabed conditions [59]. Furthermore, the maximum water depth for monopile foundations is suggested as 100 m by Maness et al. [54]. A jacket foundation involves a truss-like lattice structure generally with four legs and is more suitable in relatively deeper water compared to monopile [35], [54]. The maximum depth for a jacket foundation is also suggested as 100 m [54].

In Figure 2-3, three foundations used in the deeper water are also shown, these are tension-leg platform, semisubmersible, and spar foundations. Tension-leg platform is a floating foundation, which is moored by tendons at each corner of the platform [58]. These tendons are connected between the anchors on the seabed and the bottom of the platform under high tension [58]. A spar foundation is a floating structure consisting of a single long tube with a thrust system [35], [54], [60]. The structural stability of a spar foundation is ensured by the weight of the rotor-nacelle assembly and truss loads [35]. It is connected to the seabed via mooring and anchors, and the suggested water depth range for this foundation is between 100 and 1000 m [54]. Finally, semisubmersible foundations involve three steel/concrete buoyant with a truss system, and their installation is comparably simpler than the spar foundation [35]. The suggested water depth is

slightly different from spar with a range of 20 to 1000 m. Although floating foundations are relatively newer, the first spar and semisubmersible foundations have been operated since 2009 and 2011, respectively [61]. Demonstrations for spar and semisubmersible foundations can be found in Norway, Portugal and, most recently, Japan [61].

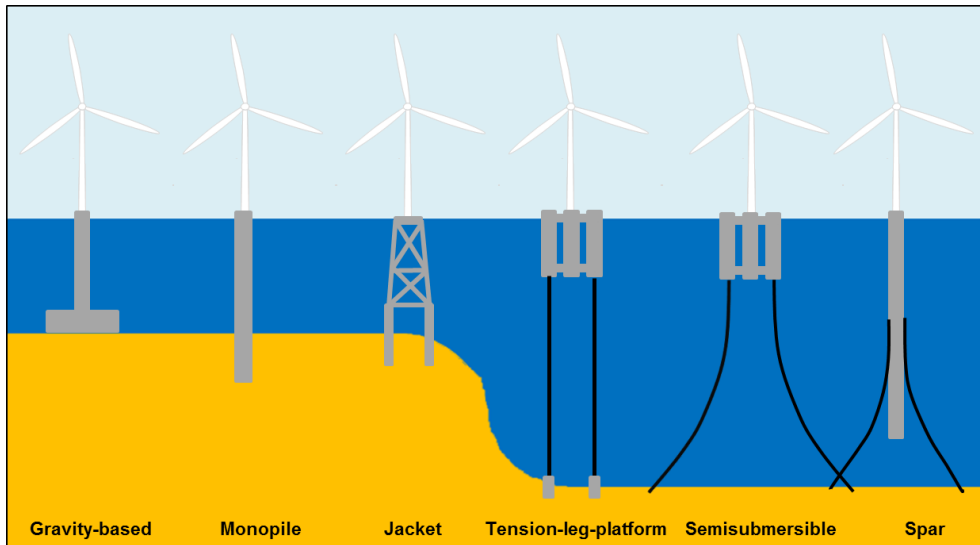


Figure 2-3 Representation of offshore wind turbine foundation types. Adapted from [58].

2.1.3 Literature Analysis on Offshore Wind Energy Modeling

Several studies with different regional scopes have determined offshore wind energy potentials. Generally, the methodology consists of three main steps: determination of available areas, derivation of technical capacity by a power factor applied in the available areas, and estimation of electricity generation. Nevertheless, there are often differences in the level of detail of an analysis, which is applied to a smaller versus a larger regional scope. For example, a national or subnational analysis might consider many other criteria and assumptions derived from the national regulations. However, on continental scales, consideration of country-specific legislation or targets might be challenging due to data availability. Therefore, within the scope of this analysis, only studies deriving the European or global offshore potential are taken into account, since analyses with smaller regional definitions might differ due to the level of detail available in their analysis. WindEurope [62] can be considered as an exceptional study, which does not perform analysis across Europe but only focusing on the North Sea, Baltic Sea and the Atlantic Ocean between France to the northern United Kingdom. The reason for including this study is their consideration of future-oriented turbine design and large coverage of Europe (only excluding the Mediterranean Sea and southern part of the Atlantic Ocean).

2.1.3.1 Eligibility Assessment and Determination of Capacity Potential

The total available offshore area within the region of interest is analyzed in all of the studies shown in Table 2-1; nevertheless, the difference in the results of available areas is a result of the data and assumptions employed in each study. In addition to the eligibility analyses performed by EEA [63] and Zappa and van den Broek [64], suitability factors for each criterion are also considered. In both of these analyses, the protected areas are taken into account in the assessment of the suitable area. However, while EEA [63] assume the deepest permissible water depth to be 50 m (only for fixed-bottom structures), Zappa and van den Broek [64] allow areas with a water depth of 1000 m (for both fixed-bottom and floating turbines). In addition to the water depth constraint, the maximum distance from the shore is set to 185 km by Arent et al. [65] and 370 km by Bosch et al. [66]. Although floating wind turbines with a maximum depth of 1000 m are taken into account by Wind Europe [62], the maximum distance is not used as an exclusion constraint. Subsea cables are also excluded by Bosch et al. [66] and Wind Europe [62]; the latter also excludes sea ice, shipping lanes, and wind speed thresholds.

Table 2-1 Studies investigating offshore wind energy potential across Europe or the World. ECMWF: European Centre for Medium-Range Weather Forecasts; NCEP: National Centers for Environmental Prediction; MERRA-2: Modern-Era Retrospective analysis for Research and Applications-version 2; ERA-Interim: European Reanalysis Interim.

	EEA [63]	Arent et al. [65]	Wind Europe ⁶ [62]	Bosch et al. [66]	Zappa and van den Broek [64]
Context	Europe	Global	Partly Europe	Global	Europe
Weather data	ECMWF	NCEP & ECMWF	NCEP	MERRA-2	ERA-Interim
Wind speed temporal resolution	Average	Weibull distribution	Rayleigh distribution	Aggregated time series sliced into 32 bins	3-hourly time series
Floating considered	No	Yes	Yes	Yes	Yes
European Capacity [TW]	0.82	10.49	3.0	26.9	5.9

Once the available area is estimated within a region, then the capacity potential can be derived either by explicitly placing the wind turbines with a separation distance or use of a uniform power density factor that stands for the area required for a certain turbine capacity. In all of the analyses shown in Table 2-1, a power density factor is used to determine the generation capacity potential

⁶ Only the North Sea, Baltic Sea and Atlantic Ocean from France to the Northern UK are considered in the analysis.

within the eligible areas. This power density factor is a function of turbine design and separation distance. Similar to the variations in the turbine designs, the power density factor used in the estimation of capacity potential differs between 5 and 6 MW km⁻² in each study. Exceptionally, the power density factor assumed by EEA [63] is 15 MW km⁻².

While EEA [63] and Wind Europe [62] consider a single turbine design for each scenario, Arent et al. [65], Bosch et al. [66] and Zappa and van den Broek [64] take into account different turbine designs capacities which differ between 1.5 and 8.0 MW. In terms of the specific power of the turbines employed in these analyses, the highest value (400 W m⁻²) is observed for the turbine design used by Bosch et al. [66] for a turbine capacity of 5 MW. The specific power of 368 W m⁻² is used for both scenarios by Wind Europe [62] with different turbine capacities (13 MW and 15 MW). The rotor diameter of the turbine used by Arent et al. [65] is not explicitly provided, yet the capacity of the turbine design is given as 3.5 MW. The turbine design used by EEA [63] has a capacity of 10.0 MW with a rotor diameter of 150 m and a hub height of 120 m. On the other hand, Wind Europe [62] assesses two scenarios, which are referred to as the 'baseline' and 'upside' scenarios. In the baseline scenario, a turbine design with a capacity of 13.0 MW, 212 m rotor diameter, and 128 m hub height is assumed, whereas these values are 15.0 MW, 228 m, and 136 m in the upside scenario. It must be noted that the specific power of both turbine designs employed by Wind Europe [62] are the same with a value of 368 W m⁻².

2.1.3.2 Estimation of Generation Potential

Similar to the estimation of capacity potential and eligible area, data, and methods used in the derivation of generation potential differ among these studies. For instance, full load hours (FLH) are estimated by EEA [63] by using an empirical equation based on average wind speeds, which are obtained from European Centre for Medium-Range Weather Forecasts (ECMWF). Arent et al. [65] calculated FLHs using a power curve represented for an IEC I class 3.5 MW wind turbine and Weibull distribution of wind speeds, which are derived from the National Centers for Environmental Prediction (NCEP) Reanalysis and ECMWF data. This dataset has also been employed by Wind Europe [62], where a Rayleigh distribution of wind speed is used, yet the simulation algorithm is not explicitly discussed in the report. Zappa and van den Broek [64] employed the 3-hourly resolved European Reanalysis Interim (ERA-Interim) dataset in their analysis. The same analysis uses a power curve convolution as it is explained by Staffel et al. [67] and Ryberg et al. [39] besides a holistic loss factor of 13%. A finer temporal resolution is used by Bosch et al. [66], where the Modern-Era Retrospective analysis for Research and Applications-version 2 (MERRA-2) dataset with hourly resolution is chosen [68]. In their assessment, 35 years of weather data are extracted and averaged into one single annual time series. Afterwards, 32 consecutive bins are used for further complexity reduction. The wind simulation algorithm which is employed by Bosch et al. [66], was developed by Staffel et al. [67] in the context of onshore wind turbines. Similar to Zappa and van den Broek [64], power curve convolution is taken into account to enhance the estimations besides the correction factors which are unique to each country. In all previously mentioned

studies, the estimated FLHs in the region are multiplied by the power density factor in order to calculate the annual generation within that region.

2.1.3.3 Discussion of Existing Tools for Techno-Economic Potential Assessment of Offshore Wind Energy

Several studies investigate the technical or techno-economic potential of offshore wind energy across Europe. Nevertheless, some aspects of their methodology require further improvement. The most important aspect is the requirement for higher spatial and temporal resolution of the weather data due to the intermittency of these technologies. As the temporal resolution becomes coarser (i.e., 3-hourly [64] or annually [66] aggregated values), the accuracy of predicted generation decreases due to the non-linear relation between wind speeds and generation as well as the volatility of these data. In addition to the temporal resolution, the importance of spatial resolution is evident due to the importance of prime locations' identification. The use of a power density factor instead of explicitly placed turbine designs also causes inaccuracies in the determination of capacity and generation potentials in smaller regions. Although the existing analyses do not focus on regional definitions smaller than the national level, subnational regions might play an important role in the energy system design (further discussion will be in Section 3.3.1), which is generally performed by spatial aggregation of the explicit locations [69]–[71]. Nevertheless, high temporal and spatial resolution for the potential of offshore wind energy is required by the detailed analysis of the energy system [72]. Furthermore, for scenarios involving future energy systems, future-oriented turbine designs should be used instead of the contemporary ones. Moreover, consideration of multiple turbine designs is necessary in order to utilize the available energy within a region in the most efficient way. For instance, use of a strong wind turbine (suitable for higher wind speed locations) across Europe would result in an underestimation of the potential as it is already explained by the author [60], since the locations with lower wind speeds would not be utilized as in the case of a weak wind turbine (suitable for lower wind speed locations). Thus, different designs for the corresponding turbine classes should be considered, as in the study published by Bosch et al. [66]. Explicit placement of turbine locations, which incorporates the geographical context of the region, improves a potential analysis, instead of using power density factors [62]–[66]. Finally, with the increasing trends in the rotor diameter and capacity [73], future-oriented turbine designs should be incorporated in the energy system, which has been missing in the literature and causing uncertainties because of the predictive nature.

In order to fill this gap in the literature, within the context of this study, an analysis is performed by Caglayan et al. [60]. In order to assess the eligible areas and determine the explicit wind turbine placements across European Maritime Boundaries [74], Geospatial Land Availability for Energy Systems (GLAES), developed by Ryberg et al. [75], [76], based on the methodology suggested by Robinus et al. [11], [12] is used. Many criteria, such as water depth [77], shore distance [78], subsea cables, and pipelines [79]–[81], protected areas [82] and shipping routes [83] are included

in the ocean eligibility assessment. The buffer distances and criteria to be considered are determined as a result of a literature review [62]–[66], [84], [85]. Explicit turbine placement is conducted following similar distances [86]. In order to address the temporal resolution, MERRA-2 [68] is used as the weather dataset, and it is scaled by the average wind speeds in Global Wind Atlas (GWA) [87]. Following this, these wind speed values at 50 m height are projected to the hub height by using a logarithmic profile, which is a function of roughness length. In order to determine the roughness length at each location, Corine Land Cover (CLC) dataset [88] is used to get the terrain information at that location; and roughness length is estimated following the suggestions of Silva et al. [89]. Finally, the onshore wind simulation algorithm developed by Ryberg et al. [39] is slightly modified for offshore wind. For instance, excluding scaling by GWA is not conducted, since it is not available for the large distances from shore (30 km). Constant roughness length of 0.0002 m is used [90], [91]. Besides the investment cost and generation of the turbines, LCOE is calculated by using interest rate and lifetime [92]. This developed methodology is applied for many turbine designs with capacity, rotor diameter and hub height constraints obtained from Wisser et al. [93]. By using these tools (both for onshore and offshore), explicit turbine placements, hourly generation time series from 1980 until the time of writing and use of future turbine designs are included in this study, which are the main strengths of this thesis compared to the other literature sources (c.f. Section 2.3.1).

2.2 Hydrogen Storage in Salt Caverns

Increasing shares of VRES technologies in the energy mix has the disadvantage of fluctuations and uncertainty [94]. This intermittency can be overcome in several ways, such as increasing the generation or storage capacities as well as introducing a dispatchable back-up generation technology. Among the mechanical storage options, pumped-hydro storage can be considered as the largest scale storage, which generally has storage times up to one week [94], [95].

2.2.1 Fundamental Principles of Underground Storage Technologies

There are mainly three underground storage technologies used for natural gas storage: depleted oil/gas fields, aquifers, and salt caverns. The use of these technologies for hydrogen storage will be briefly discussed in Section 2.2.2. Depleted oil/gas fields are the most commonly used technology for natural gas storage with 65% of the working gas capacity of natural gas storage across Europe [96]. As it is indicated in the name, these sites are previously used for oil/gas extraction, resulting in some amount of residual hydrocarbons from the previous extraction. This issue with the leftover hydrocarbons will be mentioned in Section 2.2.2 in order to discuss the suitability of this technology for hydrogen storage. Similar to depleted oil/gas fields, aquifers are underground formations filled with water or brine. Finally, salt caverns are the storage technologies constructed in the salt formations.

Underground formations have been used to store natural gas since the 1950s [96]. The Beynes site (located in France) where natural gas is stored in an aquifer has been operated since 1956 [96]. The Cortemaggiore facility with natural gas storage in depleted oil fields has been operating since 1964 [96]. Finally, natural gas is stored in salt caverns since 1970 in the Tersanne/Hauterives and Brugggraf-Bernsdorf facilities located in France and Germany, respectively. This knowledge obtained from natural gas storage can be utilized in the hydrogen storage owing to the similarities in the cavern design as well as the operation. The difference between hydrogen and natural gas is mainly observed in the non-salt material such as access wells, cavern head, and components used in transmission since embrittlement of steel material due to hydrogen absorption might result in cracks (leakage) [97].

2.2.2 Underground Storage of Hydrogen

Hydrogen can be stored in the depleted oil and gas reservoirs, aquifers and salt caverns. The use of depleted oil and gas reservoirs decreases the efforts required for mineral exploration since the site is already known due to previous use for the production of oil/gas. Cushion gas requirement for such facilities is approximately 50%. Moreover, stored gas needs to be purified and controlled due to the impurities caused by oil/gas as well as minerals and bacteria. Different than depleted oil/gas fields, aquifers do not have the disadvantage of previously-stored oil/gas and contamination caused by these hydrocarbons, yet gas contamination in aquifers might occur because of sulfate-reducing bacteria. Moreover, the cushion gas requirement for aquifers is higher than the one of depleted oil/gas fields with evident gas leakage. Finally, hydrogen storage in salt caverns is considered as the most promising option among the ones as mentioned earlier due to several reasons. First of all, the cushion gas requirement for salt cavern is nearly 30%, and the flexible operation can be attained with high injection and withdrawal rates [98], [99]. Furthermore, leakage in the salt caverns is not pronounced owing to the low permeability of rock salt, inert nature of which also prevents gas contamination [94], [97], [100]–[103].

Underground storage of hydrogen has been operated in the United Kingdom and the United States for decades. For instance, in the United Kingdom, three salt caverns with a total storage volume (cavern volume) of 210,000 m³ were constructed at a depth around 400 m during the 1970s, and total working gas capacity is reported as 30 GWh in these elliptically shaped caverns [104]. Clemens Dome in the United States has been operated since 1983, with a total storage volume of 580,000 m³ at a depth around 930 m [104]. The reported capacity of Clemens Dome is nearly 100 GWh [104], which is mainly because of the high share of cushion gas (approximately 53%). Similar to Clemens Dome, Moss Bluff is located in the United States. It has been operated since 2007 with a working gas capacity of 148 GWh, corresponding to a total storage volume of 566,000 m³ at a reference depth of 820 m [104]. Moreover, a cavern with a total storage volume of nearly 900,000 m³ at a reference depth of 1300 m has been constructed in Spindletop (the United States) [104].

2.2.3 Literature Review of Hydrogen Storage in Salt Cavern

Several studies have investigated hydrogen storage in underground formations. For Poland, suitable hydrogen storage locations among deeply seated aquifers, depleted oil and gas reservoirs, and salt caverns are analyzed by Tarkowski [105] to estimate the storage potential. Furthermore, geological investigation of the salt formations in Poland is conducted by Czapowski and Bukowski [106]. Moreover, Tarkowski and Czapowski [107] performed an analysis to determine potential hydrogen storage sites focusing on salt domes within the context of Poland, and only seven domes are claimed to be promising among 27 domes investigated. Another similar analysis is performed by Lordache et al. [108] in the context of Romania; nevertheless, storage potentials are not explicitly discussed in spite of the investigation performed on four cavern sites. While investigating the role of hydrogen in a scenario analysis for Germany, Michalski et al. [14] employed the existing data for natural gas and liquid storage facilities. The total storage capacity in northern North-Rhine Westfalia, northwestern Germany, and central Germany is estimated to be nearly 26.5 TWh. Within the future context (2050), the HyUnder study [109] reports the total number of caverns for Germany, the Netherlands, Spain, the United Kingdom and Romania as 74, 43, 24, 21 and 1, respectively. For this analysis, a standard salt cavern design with 500,000 m³ volume and 133 GWh storage capacity is used [109]. A similar analysis is performed to estimate the storage potential for compressed air energy storage in a case study for Cheshire Basin (the United Kingdom) [110]. According to this study, when a cavern height of 100 m is used to be consistent with the other storage facilities, there are 1600 possible cavern placements between depth of 500 and 1500 m [110]. A smaller regional context is used by Fichtner [111] to derive the hydrogen storage potential of salt caverns in Lower Saxony, Germany. The results of this study shows nearly 2300 cavern sites that can be located in the region. Despite the existing literature sources reporting values at a smaller regional scope (at most five countries), technical storage potential across Europe has not been reported, yet.

As discussed in Section 2.2.3, there are several studies with different methodologies to investigate the potential of hydrogen storage in salt caverns in smaller regional contexts. However, a consistent and uniformly applied methodology across Europe is necessary to identify the potential locations in the energy system design. Therefore, a master's project was supervised within the context of this thesis in order to analyze the salt geology across Europe and derive potentials for hydrogen storage. The thesis of this master's project was submitted to RWTH Aachen University by Nikolaus Weber [112], and some portions will be included in this thesis. In the context of the master's project, a literature review is conducted by using several sources [113]–[129], and suitable salt formations for hydrogen storage are identified.

2.3 Energy System Modeling

In this section, the existing studies on the European energy system will be discussed by means of their approach. While discussing the methodologies of these studies, mainly the technologies

considered in the analyses, as well as the weather years considered, are focused in order to examine the robustness of the system designs proposed. As discussed by Caglayan et al. [130], several analyses not only at the European level but also at the national levels are exemplified in order to pinpoint the issue caused by the use of single weather year in a future energy system scenario.

2.3.1 Existing Studies on the European Energy System

In this section, energy system analyses on a regional scope larger than Europe have been explained thoroughly in terms of their methodology as well as the key results. While selecting the studies to be included in this section, two criteria are used: large regional scope (at least Europe) and 100% renewable energy systems. Therefore, many other studies [92], [131]–[138] investigating large shares of technologies like fossil fuels, nuclear power and so on are not included in the following discussion, since their methodologies are considered to be out of the scope of this project. Nevertheless, despite the differences in the technology portfolios, the overall capacity and generation results of these studies are compared against the results presented in this thesis in Section 6.5.1. The studies considered in this section are given in Table 2-2.

Table 2-2 Summary of the studies investigating at least European energy system

	Regional Scope	Hydrogen considered	Notes
E-Highway [139]–[141]	Europe	No	Partly optimization
Aboumahboub et al. [142]	Global	No	Lack of explanation for VRES inputs
Siala and Mahfouz [25]	Europe	No	Only second weeks of January, April, July, and October representing the whole year
Zappa et al. [20]	Europe	No	The first week of each month representing the whole year
Bussar et al. [143]	Europe	Yes	No hydrogen pipeline
Steinke et al. [18]	Europe	Partly	Consideration of hydrogen storage in one scenario
Schlott et al. [144]	Europe	Yes	No hydrogen pipeline

E-Highway project [139] involves five scenarios defined with respect to different sociotechnical assumptions to reduce carbon dioxide emissions by at least 80% (in reference to the values of 1990) in the context of 2050. For this purpose, a top-down approach is employed by using a multi-level approach in which the system is analyzed, starting with a coarser spatial resolution (nearly 7 regions) towards smaller clusters (106 regions). Among these 5 scenarios, the “100% RES” scenario is focused within the scope of this thesis since it has the highest shares of renewables among the other scenarios with a negative attitude towards nuclear energy. Moreover, partial

electrification of heat demand and high penetration of battery-electric and plug-in hybrid vehicles are also considered. Three different electricity demand (determined by using historical demand time series between 2010 and 2012) and 11 generation time series for renewable technologies are derived [139]. A random selection of the demand and generation time series results in thousands of combinations, which are simulated by a Monte-Carlo based simulation tool [139]. As a result of these analyses, suggested capacities for onshore, offshore and PV technologies across Europe are 760, 115 and 662 GW, respectively. It must be noted that only the North Sea is investigated for offshore wind energy. In addition, two biomass classes with a total capacity of 184 GW and concentrated solar power with 29 GW are used to supply an overall demand of 4277 TWh.

Aboumahboub et al. [142] models the global electricity sector based on a setup with 100% renewable energy by using an optimization model with an objective function of minimization of the total system cost. For this purpose, solar and wind energy potentials and hourly capacity factor time series are determined, yet the methodology of the latter is not explained. Claiming transmission and storage as critical technologies, three scenarios are defined: considering both interconnections of supply area and storage, excluding only storage and excluding both interconnection and storage. As a result of the optimization, overall European capacity is found between 6 TW and 6.7 TW, a large share of which is mainly wind energy [142]. However, the capacity for PV energy is nearly 500 GW corresponding nearly 10% of the total capacity.

Siala and Mahfouz [25] investigated the impact of the regional definition on a European scale by using a linear optimization model. Different definitions like administrative boundaries, wind, or solar potentials are used for regionalization; nevertheless, 2015 was decided to be used as weather year for different scenarios [25]. As a simplification, only the second weeks of January, April, July, and October are assumed to be representative for all year. Comparing the results of optimization for each region definition against the generation and capacity values from ENTSO-E for 2015 reveals that overprediction in the nuclear power and underprediction in the lignite are observed in the optimization [25]. Moreover, nearly no curtailment is observed in any of the model results [25].

For example, Zappa et al. [20] performed an analysis across Europe to investigate whether or not a 100% renewable energy system is feasible without consideration of hydrogen as an energy carrier. For this purpose, ERA-Interim weather data for the weather year 2010 is used noting the importance of the consideration of different weather years [20]. Moreover, instead of optimizing the consecutive time series, optimization is performed only by using individual monthly load duration curves for 12 time slices [20]. Following this, hourly data is used for unit commitment and economic dispatch simulations, yet only the first week of each month with 2 hours of time limitation is solved [20]. The study reveals that with the assumption of no expansion of CSP, hydropower and geothermal, a 100% renewable energy system is not feasible without the use of biomass [20]. Among all the scenarios, maximum capacities for onshore wind and PV technologies are estimated as 543 GW and 895 GW, respectively [20]. The total annual cost of the base scenario

is estimated as 560 Billion € a⁻¹, and in most of the scenarios, the value does not change significantly [20].

Another European analysis is performed by Bussar et al. [17], [143], [145] by dividing Europe into 21 regions and optimized with hourly time series of generation technologies and load in the context of 2050. Nevertheless, the selected weather year used in their optimization and generation of the time series is not explained explicitly in any of the studies. Wind and PV systems are considered as generation technologies; hydrogen storage, battery, and pumped hydro as storage technologies; and HVDC is considered as transmission technologies. In all the studies conducted, wind to solar ratio based on installed power is assumed to be 40/60. In addition, electrolyzers, types of which are not specified, and combined cyclic gas turbines are used for hydrogen production and reelectrification. In the analysis with a demand of 4122 TWh a⁻¹, the reported storage capacity is 248 TWh, 99% of which belongs to hydrogen storage systems. When the demand is assumed at 6250 TWh a⁻¹, the results of their base scenario reveals that the total capacities of wind and PV are 1850 GW and 2785 GW, respectively. The storage capacity of hydrogen is estimated as 800 TWh [17], [143]. Optimal electrolyzer capacity is calculated as 900 GW, and the combined cyclic turbine capacity is 550 GW.

Cebulla et al. [146] applied the REMix optimization model [147] to determine the mix of VRES technologies and electrical energy storage in Europe in 2050. Similar to this work, Cebulla et al. [146] aimed for a fully renewable system that is primarily reliant on solar and wind. Furthermore, the following storage technologies are considered: hydrogen salt caverns, lithium-ion batteries, pumped hydro storage, compressed air, and redox-flow batteries. Their analysis comprises northern, western, and southern Europe, which is subdivided into 29 regions in total, most of which are equal to national borders except for Germany which is split into 20 regions. Ultimately Cebulla et al. [146] find an optimal design across Europe, which requires total electrical energy storage of 30 TWh and 206 GW of generation capacity. Following their primary analysis, Cebulla et al. [146] go on to evaluate numerous sensitivity optimizations that cover: use of multiple weather years, differing techno-economic assumptions, as well as constraints based on generation shares and total emissions.

Child et al. [148] also investigate the least-cost configuration of a 100% RES Europe in 2050. As with Cebulla et al. [146], multiple generation options are allowed, including the common VRES technologies (onshore and offshore wind, as well as open-field and rooftop PV) and most conventional technologies as well. Furthermore, the following storage options are allowed as well: batteries, pumped hydro, compressed air energy storage, thermal energy storage, and natural gas storage. Child et al. [148] consider all of Europe in their analysis, including the Balkan and Baltic states, Turkey, Ukraine, and Iceland, with each country, and in some cases groups of countries, representing a single node. Using a myopic optimization evaluated in 5-year steps between 2015 and 2015, Child et al. [148] finally conclude that a 100% RES system is not only possible in Europe, yet could supply electricity at 74% the LCOE seen today. Furthermore, they find that nearly 220

TWh of energy storage will need to be required; the vast majority of which is dedicated to methane [148].

Comparison of grid versus storage (as pumped hydro storage, batteries, and hydrogen storage) for 100% renewable energy system with 65:35 wind to PV ratio is conducted by Steinke et al. [18] across Europe by using optimization. A weather model data is used for 8 year period similar to Heide et al. [24], yet the methodology remains unclear. According to their results, Steinke et al. [18] claim a back-up generation of 40% of the demand without grid and storage for wind and solar energy-based system, whereas this value decreases to 20% with an ideal grid. Moreover, in their model, only one storage technology at a time is considered to decrease the complexity [18]; which simplifies the problem significantly. With such a simplification, combination of these storage technologies are not captured, and the conclusion is made by using the storage technologies with different behavior. Thus, the nature of these storage technologies such as daily or seasonal storage, as well as the injection rate of the storage technologies is not captured in the system design.

Schlott et al. [144] analyzed the influence of climate change by using a linear optimization model (PyPSA) until 2100 by taking hydrogen into account in a highly renewable-based system. For this purpose, years between 1970 and 2100 are classified into four periods, each of which consists of 6-8 yearly model runs with each run having a temporal resolution of 3 hours. According to their results from the first time period (1970-2005), northern and northwestern Europe has high wind capacity with a strong transmission grid, whereas the south and southeastern Europe has high PV capacities with relatively weaker grid [144]. In the last time period (2070-2100), onshore wind and PV capacities are estimated as 669.4 GW and 119.4 GW, respectively. Offshore wind energy is claimed not to be cost-competitive within the scenario definition [144]. The mean of the total annual cost of the system for the first time period is estimated as 135.5 Billion € a⁻¹, whereas this value increases to 141.2 Billion € a⁻¹ in the last period [144].

In spite of the existence of several studies on the European Scale within the context of 2050, the approaches employed in each study do not fully cover all the aspects in a future energy system. First of all, none of the aforementioned studies considers the future-oriented technologies (especially wind turbines and PV panels). Neglecting the developments in certain technologies might result in overprediction of the system capacities. Secondly, almost all of these studies consider either a single year or even representative weeks of a year; which does not guarantee the security of supply. As it is previously discussed by Caglayan et al. [130] and Pfenninger [149], multiple weather years should be considered in the design of a future energy system due to the variations with respect to the selected weather year. This issue will be discussed further in Section 2.3.2. Consideration of hydrogen as an alternative energy carrier and how the future energy system is affected by it is also missing in many studies [20], [25], [139], [142]. Furthermore, among the ones taking hydrogen into account, none of the studies include pipeline transport between regions. Additionally, hydrogen storage is considered by Bussar et al. [143], although the

technology is not explicitly communicated (whether it is salt caverns, vessels or pipe storage). All in all, a systematic analysis of the European energy system with consideration of hydrogen is not available in the literature.

2.3.2 Weather Years Used in the Literature

There are several analyses investigating energy systems in a large regional definition as well as the national energy systems analysis. Nevertheless, most of these studies propose an energy system design in the context of 2050, yet only one weather year is used. Some of them consider various weather years with a simplification of time series, such as averaging the hourly or three-hourly time series to monthly time series. In this section, the studies available in the literature are discussed independent of their regional context. Nevertheless, the results of these analyses are not focused on the discussion since it would be out of the scope of the presented section.

The European analysis conducted by Heide et al. [24], [26] takes into account 8 years between 2000 and 2007 by averaging it monthly over these 96 months. This methodology is adopted by other studies, too [144], [150]. Robinius et al. [12] analyzed German power and transport sectors by using a Weibull distribution of measured wind speed data between 1981 and 2000. In an optimal design and operation of a wind-hydrogen-electricity network, Samsatli et al. [31] use the weather data of 2014 in their spatio-temporal optimization model. The analysis is performed in Great Britain, and it is mainly for supplying hydrogen demand for transport [31]. The techno-economic analysis of underground storage of hydrogen in France to supply the demand of the transport sector is conducted by Duigou et al. [21] by using the weather year 2005. Wind-based energy system to supply the hydrogen demand for the transport sector, as well as the industry in Germany, is investigated by Welder et al. [13] by using the weather year 2012. For this purpose, a spatio-temporal optimization model is employed by using the framework "Framework for Integrated Energy System Assessment-FINE" [151] and Gurobi [152] as the solver of the optimization problem.

As it is mentioned in the previous section, Siala and Mahfouz [25] used 2015 for their analysis of the impact of regions across Europe. Zappa et al. [20] pinpoint the importance of the selection of weather in the energy system design, yet only 2010 is chosen as a low generation year (conservative assumption) due to the computational limitations.

The issue of selection of weather years in the energy system is dealt similarly for non-European countries. For instance, in northeastern Asia, the weather year of 2005 is used by Bogdanov et al. [22] for their analysis of electricity, gas, and heat supply chain. The same dataset used by Bogdanov et al. [22] is adopted by Gulagi et al. [23] in the context of India as well as South Asian Association for Regional Cooperation; furthermore, in this analysis, it is claimed that the installed capacities of renewables would not be affected by the weather year. Elliston et al. [30] chose 2010 for the scenarios with 100% renewable electricity conducted for Australia. The electricity sector

with large shares of renewables (90-99.9% renewables) is analyzed by Budischak et al. [28] by using the weather years between 1999 and 2002 in the context of the eastern United States. Similarly, high shares of renewables are modeled by using 2004 as the weather year by Fripp [153] for California.

Finally, the influence of different weather years in the system design is analyzed by Pfenninger [149] for Great Britain in the analysis of the reduction of VRES time series resolution as well as the inter-annual variability by using weather years between 1990 and 2014. Which reduction technique and system boundaries are used in the impact of weather year analysis remain unclear. However, the study is only limited to a small regional definition: Great Britain, not capturing the variations in the time series within a larger scope. Caglayan et al. [130] investigated the impact of weather year in an exemplary wind-to-hydrogen system to supply the hydrogen demand of passenger cars in 7 European countries (Germany, Netherlands, Belgium, Luxemburg, France, Switzerland and Italy). Nevertheless, neither by Pfenninger [149] or Caglayan et al. [130] applies a further analysis to attain a robust system design.

When the studies are analyzed, it is seen that the weather year is generally chosen with respect to data availability or the average/representative weather years. However, as it is investigated by Caglayan et al. [130], for a large regional scope, the weather year cannot be generalized as good or bad due to the variations in the weather phenomena and generation. The existing analyses on this topic lack either the larger regional scope or consideration of extensive alternative energy carriers which might compensate these fluctuations in the time series effectively. Furthermore, some analyses do not mention the weather year or the weather data source explicitly [154]–[160].

Although deterministic models (i.e., optimization problems) attain the best alternative (generally the lowest system cost) amongst many others, the security of supply at any time within the system is questionable. In other words, a methodology to attain a robust system design is lacking in the literature among the energy system designs by optimization. Therefore, the importance of this issue will be addressed by showing variations in the results among 38 years in Section 5.3. Afterward, proposing a methodology and system design that can supply the demand at any time within these weather years will be included in Section 3.6 and Section 6.

2.3.3 Technical and Economic Parameters of Technologies Considered in 100% Renewable Energy Systems Design

In this section, the literature analysis on the technical and economic parameters for technologies will be discussed. Only the values within the context of 2050 are extracted from several sources to verify the techno-economic parameter assumptions that are explained in Section 3.4. These parameters are discussed under four sections regarding the main class where individual technologies belong to: generation, conversion, transmission and storage technologies. The assumptions made in Section 3.4 are based on the literature review given in this section.

2.3.3.1 Generation Technologies

A literature review on the technical and economic parameters is performed for each generation technology in the context of 2050, and resulting specific investment cost distribution for individual generation technologies considered in this analysis are shown in Figure 2-4 [64], [133], [143], [161]–[173]. The range in the distribution of onshore wind turbines, open-field PV, and rooftop PV vary by 1000 € kW⁻¹, whereas it increases to 4000 € kW⁻¹ for offshore wind energy and 6200 € kW⁻¹ for run-of-river (also called as run-off river).

Cost estimations for onshore wind turbines vary between 660 and 1630 € kW⁻¹. Both scenarios available in “Energy [R]evolution” conducted by Greenpeace [169] have the lowest projections with values of nearly 670 € kW⁻¹, whereas the highest cost projection is reported by the scenario-based cost trajectories published by Joint Research Centre (JRC) [167]. As it is seen in Figure 2-4, the median of onshore cost estimates is nearly 1100 € kW⁻¹, which is assumed by the baseline onshore turbine cost. It must be noted that this value also corresponds to the reference specific investment cost of onshore wind turbines estimated for 2050 by JRC [168].

In the case of offshore wind energy, there is a wide range of cost estimations, which is mainly because of the strong dependence of the specific investment cost of offshore wind turbines on the site location. In their report, Schröder et al. [162] distinguish turbines close to shore and far from shore with cost values of 1800 € kW⁻¹ and 4000 € kW⁻¹ (for 2010), respectively. In many sources, investment costs of offshore wind turbines are differentiated by their foundation type, distance to shore and water depth. For example, Tsiropoulos et al. [167] classify offshore wind turbines into three classes, which are monopile medium distance to shore, jacket medium distance to shore, and floating long distance to shore. Moreover, several cost values as a function of global growth scenario and learning rates are derived for each of these classes. The minimum cost value estimated in that report is nearly 1300 € kW⁻¹ (monopile, medium distance to shore), whereas the maximum value is reported as 4850 € kW⁻¹ (floating, far from shore). Unlike the studies classifying foundation types or distance to shore, several studies project one cost value in 2050. An example of these studies, conducted by Greenpeace [169] reports the lowest cost as 980 € kW⁻¹. Two outliers can be seen for offshore projections within the range of 4000 to 5000 € kW⁻¹. Both of these values are reported by Tsiropoulos et al. [167], and they are within the floating turbine class with a longer distance to shore.

In spite of the narrow range by many studies, open-field PV projections have several outliers. This wide range in the cost estimations for PV systems can be understood by the differences in the designs. Although it is not distinguished by many studies, the specific investment costs of open-field PV with and without tracking vary. For instance, specific investment costs of the reference scenario for open-field PV with and without tracking are estimated as 710 € kW⁻¹ and 520 € kW⁻¹ by Carlsson et al. [168]. Besides, the lowest and highest cost values estimated for open-field PV

are 230 € kW^{-1} [171] and 1700 € kW^{-1} [166], respectively. Similar to open-field PV, the specific investment cost of rooftop PV varies between 350 € kW^{-1} [167] and 1400 € kW^{-1} [172], [173].

Run-of-river experiences the largest variation in investment cost which ranges between 1800 € kW^{-1} and 8180 € kW^{-1} . As might be expected, the run-of-river plant cost is strongly dependent on the location. It must be noted that the repowering of existing run-of-river plants is not included in this plot. It is seen that reference cost projections by JRC [168] are very similar to the mean and median values shown in Figure 2-4. In order to have consistency in the assumptions, the investment costs of generation technologies in this study are taken from JRC [168].

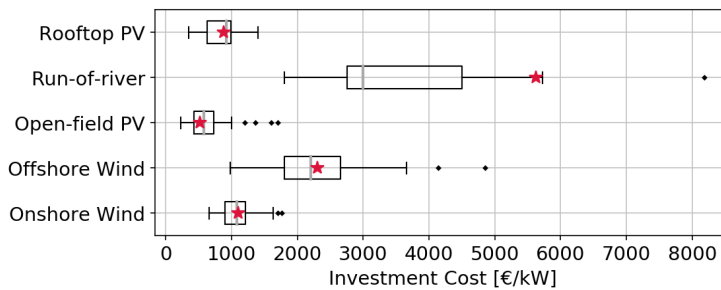


Figure 2-4 Distribution of the specific investment cost for generation technologies in 2050 [64], [133], [143], [161]–[173].

2.3.3.2 Conversion Technologies

Conversion technologies can be classified into two groups within the context of power-to-hydrogen: hydrogen production and reelectrification technologies. Different energy sources such as electrical, thermal, photonic and biochemical can be used in hydrogen production [174]. Within the context of “Power-to-gas”, electricity is used to split water into hydrogen and oxygen [9]. Currently, three electrolyzer technologies exist in the literature: alkaline electrolysis, polymer electrolyte membrane (PEM) electrolysis, and solid oxide electrolysis. A comparison of the technical and economic parameters is performed by many studies [9], [174]–[176]. Compared to alkaline and PEM electrolyzers, solid oxide electrolyzers have high operation temperatures (600–1000 °C), and still in the research and development phase [176]. Moreover, flexible operation with a solid oxide fuel cell is a challenging topic due to the thermal stress of the ceramics [9]. Due to the aforementioned reasons, solid oxide electrolyzers are not considered in this analysis. Currently, alkaline electrolyzers are the cheapest ones with a longer lifetime than PEM electrolyzers. Both alkaline and PEM electrolyzers have high hydrogen purity and fast response time (cold start-up of PEM electrolyzers are up to 15 minutes, whereas it is nearly 20 minutes for alkaline electrolyzers) [174], [176]. Alkaline electrolyzers have the disadvantage of a hazardous electrolyte, and PEM electrolyzers contain the precious metals [176]. All in all, considering

aforementioned aspects of different electrolyzers, only the PEM electrolyzer is chosen to be included in the analysis.

Variation in the investment cost of conversion components is shown in Figure 2-5. In addition to the PEM electrolyzer, a “Low Temperature Electrolyzer” is included in the figure because of the lack of clarification in the literature. Some studies [177]–[182] do not distinguish alkaline and PEM electrolyzers, instead the term “Low Temperature Electrolysis” is used. Therefore, this classification is involved in the literature review for the sake of improving cost estimations. The range is observed between 350 and 767 € kW⁻¹ for PEM electrolyzers [13], [14], [176], [183], [184], and 200 and 761 € kW⁻¹ for low temperature electrolyzers in general [177]–[182]⁷. Unlike electrolyzers, there are insignificant variations in the investment cost of hydrogen combined cycle turbines, open-cycle turbines, and gas engines; which can be explained by how mature these technologies are.

In addition, a variation of 1500 € kW⁻¹ is observed for biomass combined heat power plants. Combined heat and power (CHP) plant for biomass has a spread between 2140 € kW⁻¹ [169] and 3400 € kW⁻¹ [167]. Nevertheless, the type of biomass might differ in these cost estimations. In this work, the type of biomass and technical potential are not derived as detailed as wind or solar energy due to a lack of consistent European data. Instead, a simpler approach is employed; which assumes the biomass potentials provided by Bruninx et al. [139] in the context of the “100% RES” scenario of the E-Highway project (cf. Section. 3.4.3). Therefore, a detailed analysis of biomass is not involved in this work. By means of biomass fuel cost, a literature review is conducted [139], [185], [186]. However, biomass fuel cost is assumed to be the same as the value of E-Highway study [139] since the capacities and techno-economic parameters of biomass CHP plant are obtained from the same source.

PEM fuel cells experience large ranges for the investment cost. This range is significantly dominated by the values projected by Carlsson et al. [168] since their values are in the range of 8000 € kW⁻¹. Nevertheless, it must be noted that these higher values might not take mass production into account. Moreover, there is not many studies on the cost projection of PEM fuel cells compared to other conversion technologies shown in the figure. For solid oxide fuel cells (SOFC), the variation in the investment costs projected to 2050 is not wide, like in the case of PEM fuel cells. Finally, reelectrification technologies for hydrogen besides fuel cells have a narrow cost range [14], [183], [187], [188], since the gas engines and turbines are already mature technologies.

⁷ All economic parameters are extracted within the context of year 2050.

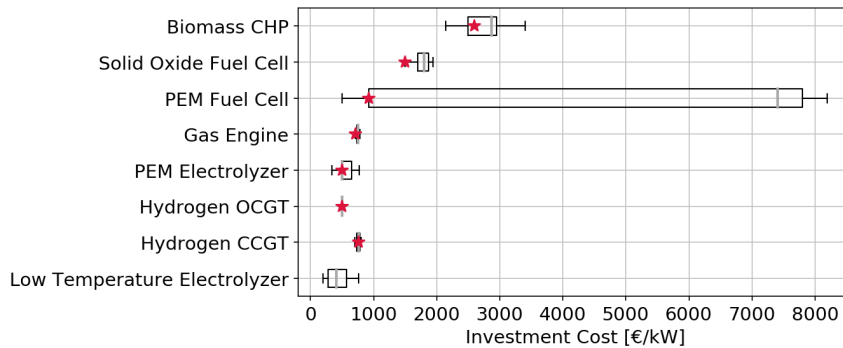


Figure 2-5 Distribution of the specific investment cost for conversion technologies in 2050 [13], [14], [167], [168], [170], [177]–[184], [187], [188].

2.3.3.3 Transmission Technologies

There are several pathways in terms of hydrogen transmission technologies. Pathways, including gaseous hydrogen transport via trucks or trailers, use of liquefied organic hydrogen carrier, gaseous, or liquid hydrogen transport via trailers and pipeline transport are investigated by Reuß et al. [184]. According to Reuß et al. [184], pipelines are found to be the cost optimal technologies for higher amounts of hydrogen transport over large distances. Therefore, taking into account the distances between countries, only pipeline transport will be focused on the transmission of hydrogen within the scope of this analysis. For pipeline transport, cost parameters as a function of pipeline diameter are performed by Mitschner [189]. This relation is shown in Equation 2. $pipeCost$ stands for investment cost of the pipeline in € m^{-1} and D represents the pipeline diameter in m.

$$pipeCost = 292.152 \times \exp(1.6 \times D) \quad \text{Equation 2}$$

In terms of high voltage alternating current (HVAC) and high voltage direct current cables (HVDC), investment costs are not introduced in the model. This is because of not allowing the HVAC and HVDC connection expansions. Therefore, the line capacities are obtained for the connections given in the E-Highway project, which makes use of the Ten Year Network Development Plan [190].

2.3.3.4 Storage Technologies

Storage technologies can be classified into four groups: hydrogen storage in salt caverns, lithium-ion batteries, pumped-hydro storage, and hydro reservoirs. Compressed air energy storage is not included in this analysis, since future deployment of this technology is stated to be unlikely by Stemmer [135] as a result of an analysis comparing of different storage technologies. All these

storage technologies listed above have a different role in the energy system. As briefly discussed in Section 2.2, salt caverns are used for seasonal storage of hydrogen. Compared to previously mentioned storage technologies, the storage capacity of salt caverns can be 10-20 times higher than that of hydro storage technologies (pumped-hydro storage and hydro reservoirs). Despite its advantages, the use of salt caverns in energy system analysis is not as common as other storage technologies. Not considering hydrogen as an alternative energy carrier in the system and lack of an extensive analysis of the storage potential of salt caverns can be the main reasons for not taking salt caverns into account in the energy system design. Some studies [13], [14] considered salt caverns in their analysis, yet the regional scope is generally limited to Germany. Focusing on the cost parameters provided in these studies reveals that the investment cost for salt caverns varies between 0.280 and 0.520 € kWh^{-1} [13], [14], [187].

As an alternative to the cavern storage, gaseous hydrogen storage in vessels is also considered as a storage technology as well. Therefore, techno-economic parameters assumed by Reuß et al. [184] are assumed to in this analysis. Following the assumptions by Reuß et al. [184], the gaseous hydrogen storage is assumed to be operated between 15 to 250 bar pressure with no losses. Moreover, the investment cost of such a system is stated as 500 $\text{€ kg}_{\text{H}_2}^{-1}$, translating into 15 $\text{€ kWh}_{\text{H}_2}^{-1}$ based on the lower heating value of hydrogen, by Reuß et al. [184], yet it is possible to have an investment cost of 250 $\text{€ kg}_{\text{H}_2}^{-1}$, translating into 7.5 $\text{€ kWh}_{\text{H}_2}^{-1}$, with detailed cost calculations for components as it is explained by Welder et al. [13].

Cost projections for hydropower and dam are reported by several studies [162], [167], [168], it must be highlighted that these studies reported power based investment costs for hydropower. Investment costs range from 1000 to 3500 € kW^{-1} , it must be noted that in spite of being a mature technology, the cost of hydropower plants depends on the location. Therefore, this variation is mainly caused by the high-cost and low-cost projections caused by the location of the plant. The average cost value derived from these individual sources amounts to 2200 € kW^{-1} , which is also the reference cost value given by Carlsson et al. [168].

Finally, lithium-ion batteries can be used primarily in compensating the diurnal variations caused by discrepancies between generation and demand. These variations are generally observed in the locations with high penetration of solar energy (photovoltaics (PV) and concentrated solar power (CSP)). The lower and upper values of the investment cost of lithium-ion batteries are found as 112 and 245.5 € kWh^{-1} within the scope of year 2050 [168], [191].

2.4 Summary

In this section, the fundamentals of three main components, which are offshore wind energy, salt caverns for hydrogen storage, and European energy system design, are covered. In addition, existing studies related to the modeling of these components as well as the assumptions made in these analyses are indicated briefly.

Firstly, the fundamentals of wind energy, including the turbine characteristics, trends regarding offshore wind energy, different foundation types covered in this thesis and modeling of the techno-economic potential of offshore wind energy are provided. By turbine characteristics, the key aspect of specific power density is described, and its relation to the turbine power curve is explained briefly. Following this, a description of four different foundation types, which are monopile, jacket, semisubmersible, and spar, is provided. The reason to consider these foundation types, which are the only ones taken into account in the detailed cost model employed in this analysis, is clarified. Finally, different studies deriving the techno-economic potential of offshore wind energy across Europe are discussed with their assumptions and differences in their approach. Consideration of multiple turbine designs covering different wind characteristics, lack of future-oriented turbine designs, and approximating the potential by power density factors are the main weaknesses of these studies. Taking the best aspects of these individual approaches, a methodology is developed for this work, which is provided in the next chapter.

Secondly, salt cavern storage is explained by providing background information on the existing hydrogen storage facilities. Furthermore, different underground storage technologies are briefly explained. Afterward, the existing literature sources deriving capacity potentials are discussed: however, only a few studies limited to a smaller regional scope are provided due to the lack of approaches and analyses in the literature.

As the main component of this thesis, analyses on the energy system design at the European scale are provided with their main assumption. These studies are classified into two groups with respect to the consideration of hydrogen. Nevertheless, in order to provide an insight about the approaches regarding the energy system design at a European level, these analyses which do not consider hydrogen are also provided within the scope of the literature review. Following this, one of the strengths of the presented work, which is the consideration of different weather years, is discussed by providing the weather years, and the reasoning to choose that specific weather year (if possible) is supplied.

Finally, an extensive literature review is conducted for techno-economic parameters of the technologies considered in the energy systems design. For this purpose, technologies are classified into four groups following the structure in the modeling, these groups are as follows: generation, storage, conversion, and transmission technologies. Each of these groups is analyzed by means of the techno-economic parameters of individual technologies.

3 Methodology

As it is previously mentioned, this thesis is composed of three main topics: the techno-economic potential of offshore wind energy, the techno-economic potential of salt caverns for hydrogen storage, and the design of hydrogen pipeline in 100% renewable European energy system. The analyses on the techno-economic potentials are conducted in order to fill the existing gap in the literature, derive a consistent European dataset so that these technologies are included in the energy system design. Several sources analyze the potential of offshore wind energy across Europe, as it is discussed in Section 2.1. A methodology consisting of the best aspects of the literature is developed to derive the techno-economic potential of described turbine designs. Following this, the most appropriate turbine designs at each location are determined by optimization with discretization. Each component in the assessment of offshore wind energy is explained in Section 3.1. Following this, the technical potential of salt caverns for hydrogen storage is determined. How the technical potential is derived for salt cavern storage is explained in Section 3.2. Following this, the model chain developed within this project in order to conduct an energy system design is briefly explained with its features in Section 3.3. Finally, a general definition of the scenario, its boundaries, and main assumptions are provided in Section 3.4. It is then followed by the discussion of time series aggregation as one of the main assumptions; and the methodology on how to attain a system design that can withstand across several weather years.

3.1 Technical Potential of Offshore Wind Energy across Europe

In order to assess the offshore wind energy potential for any region definition, three fundamental issues should be addressed: determination of eligible areas, evaluation of turbine performance and estimation of cost. These issues can be evaluated independently and combined in the end. By doing so, the turbine performance results can be used in the future for different ocean eligibility scenarios to maintain a general use for the optimal turbine designs by adapting the eligibility constraints if needed. The overall method, in which the three fundamental issues are combined, is used for different scenarios in order to compare several single turbine designs and the optimal turbine design. In the following sections, the methodology used in each fundamental piece in the determination of offshore wind energy potential will be explained.

3.1.1 Ocean Eligibility and Turbine Placement

Eligible areas for offshore wind energy are determined by using an open-source model: GLAES (cf. Section 2.1.3.3). Depending on the user's need, GLAES can apply exclusion or inclusion constraints from any geospatial datasets within a given regional definition and spatial resolution. In this analysis, the entire European offshore region is processed at a resolution of 100 m x 100 m to determine the technically available area for offshore wind energy in European Maritime Boundaries [74]. For this purpose, constraints listed in Table 3-1 are applied in succession,

resulting in the exclusion of all ineligible offshore areas. These exclusions are determined based on a review of previous analyses that have investigated ocean eligibility in various contexts (cf. [62]–[66], [84], [85]).

Table 3-1. Constraints used in the ocean eligibility analysis

Constraint	Excludes		Data Source
Water Depth	above	1000 m	[77]
Distance to Shore	below	15000 m	[78]
Protected Areas	below	3000 m	[82]
Bird Protected Areas	below	5000 m	[82]
Shipping Routes	below	3000 m	[83]
Natural Gas Pipelines	below	500 m	[81]
Cable Lines	below	500 m	[79], [80]

After ocean eligibility assessment, turbines can be located in the potential locations by using the item distribution feature of GLAES [75] with a separation distance. The separation distance in this analysis is assumed to be 10 times the rotor diameter in the predominant wind speed direction and 4 times the rotor diameter in the transversal direction [86]. Since the separation distance is a function of rotor diameter, the total number of turbines distributed in the eligible areas for different scenarios vary depending on the value of their rotor diameter. For optimal turbine design scenario, the placement is performed by extracting the rotor diameter of individual turbines, whereas a constant rotor diameter of the corresponding turbine is assumed for single turbine definition scenarios.

3.1.2 Turbine Simulation

A turbine simulation scheme, which was developed primarily for onshore wind energy by Ryberg et al. [39] is employed and adapted to the offshore wind energy context. The algorithm used in the offshore workflow can be seen in Figure 3-1. As is seen in Figure 3-1, there are three input parameters required for this workflow: the turbine location in terms of latitude and longitude, weather data source, and turbine design parameters (capacity, rotor diameter, and hub height). Once these input parameters are defined, weather data is extracted around the location. Wind speeds at the location are calculated by using bilinear interpolation, which interpolates the extracted closest weather data to the turbine location. These wind speeds available in the weather data are at an altitude of 50 m.

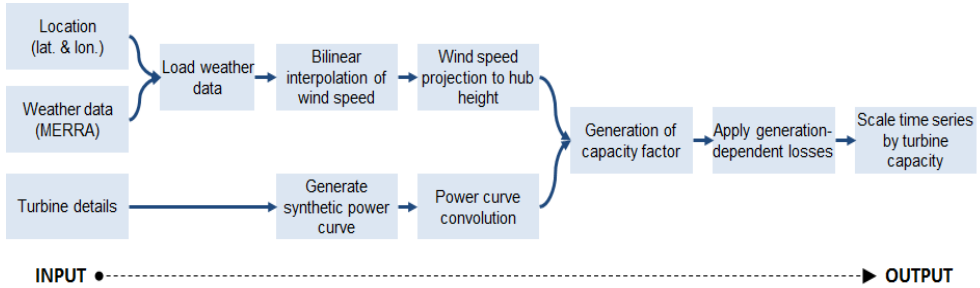


Figure 3-1 Representation of workflow used in offshore turbine simulations.

Following this, interpolated wind speed at an altitude of 50 m is projected to the hub height by using a logarithmic wind profile with a constant roughness factor of 0.0002 m [90], [91]. Equation 3 shows the vertical wind speed projection. v stands for wind speed, h for height, z for roughness length. Subscript *hubHeight* indicates the values at hub height, and *reference* for the values at a reference altitude.

$$v_{hubHeight} = v_{reference} \frac{\ln(h_{hubHeight}/z)}{\ln(h_{reference}/z)} \quad \text{Equation 3}$$

Afterward, the wind speed time series at hub height is used in the convoluted power curve to obtain the normalized generation time series (generation values vary between 0.0 and 1.0 kW kW⁻¹). After the application of generation-dependent losses, time series data is scaled by the turbine capacity. A representative power curve is shown in Figure 3-2 for three different cases: raw power curve, power curve with the only convolution, and power curve with convolution and generation-dependent loss. Only a slight difference between raw power curve and power curve with convolution at the low wind speeds (mainly before cut-in wind speed) can be seen, especially a smooth transition around the cut-out wind speed is observed due to the convolution. However, after the application of a generation-dependent loss factor on the convoluted curve, the deviation from the raw power curve is more pronounced especially after cut-in and cut-out wind speeds. Moreover, it is not possible to achieve a capacity factor of 1.0 kW kW⁻¹ because of the consideration of losses, as seen in the figure. In other words, generation-dependent losses have a minimum holistic loss of 3%.

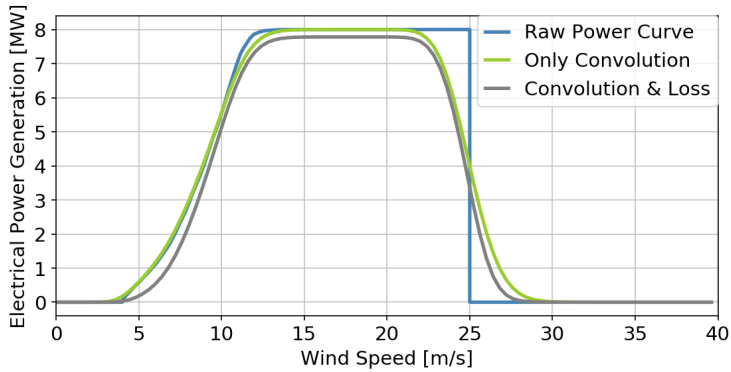


Figure 3-2 Representation of raw power curve, power curve with only convolution and power curve with convolution and losses.

3.1.3 Cost Estimation

According to the cost breakdown by the National Renewable Energy Laboratory (NREL), turbine costs can be categorized into three groups: turbine capital cost, the balance of system cost, and financial cost [56]. Each of these components varies with respect to the turbine design as well as the location-specific parameters such as water depth and distance to shore. These variations and their impact on the turbine cost can be explained by a cost model, relating turbine cost with the turbine design characteristics and the location-specific parameters. In this analysis, the most recent and detailed cost models developed by NREL is employed to calculate turbine capital cost ([55], [57]) and offshore balance of system [54]. Estimation of turbine capital cost depends on the total turbine mass in the turbine capital cost model, which was developed in 2006, and updated in 2010. Ultimately, the turbine capital cost model is a non-linear function of three fundamental characteristics, namely: turbine capacity, hub height, and rotor diameter. It must be noted that the offshore balance of system cost model from NREL was developed based on the European offshore wind data [54] due to the lack of data in the United States regarding offshore wind energy. The total turbine mass is expressed by using these characteristics in the calculation of turbine capital cost. In addition to these characteristics, distance to shore, water depth and foundation type are taken into account in the offshore balance of system cost model, which was developed in 2017. Although there are more than four foundation types, only monopile, jacket, semi-submersible, and spar are considered in the cost model. Other foundation types such as gravity-based, tripile, tripod or tension-leg platform are not taken into account in this analysis since the contribution of each in the balance of system cost model remains as unknown. Finally, financial costs, as the third component in a turbine cost, are considered by their share in the cost breakdown, which is shown in Figure 3-3.

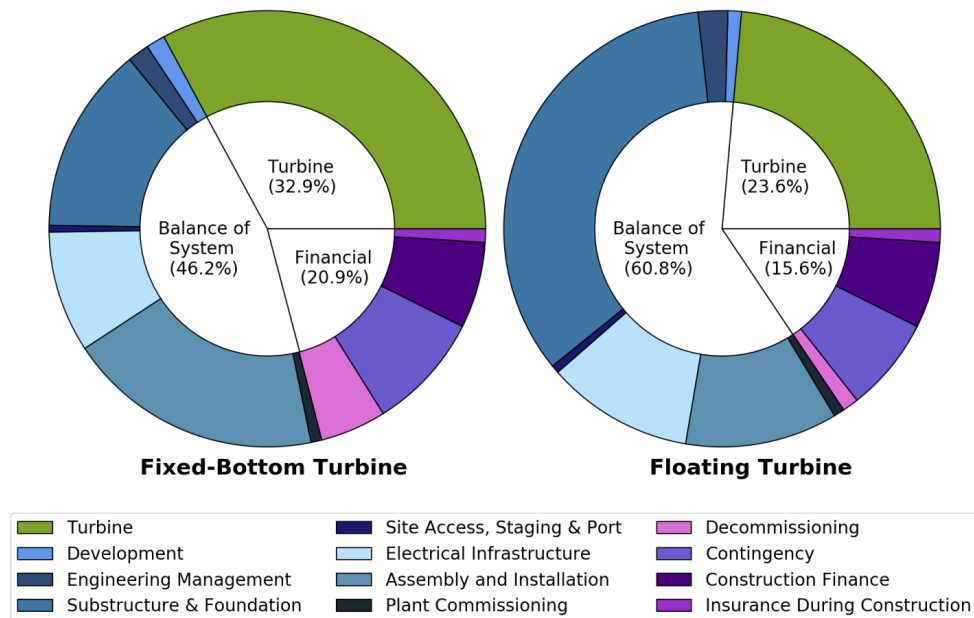


Figure 3-3 Cost break-down for offshore wind turbines fixed-bottom (left) and floating (right). Adapted from NREL [56].

Both turbine capital cost model and balance of system cost model were designed to turbine costs at the time of their inception, meaning that they are not directly applicable to future applications such as in 2050. In order to adjust the models to future applications, the final cost is calculated by scaling NREL's turbine capital cost, the balance of system cost and financial cost models by using baseline turbine assumptions of future design and cost parameters. Therefore, they are adapted to a future turbine design concept by scaling their cost while sensitivities of the cost model are maintained. This scaling of cost component is performed by using three equations shown below. TCC' stands for turbine capital cost of the evaluated turbine, BOS' for the balance of system cost of the evaluated turbine, θ_{TCC} and θ_{BOS} for shares of turbine capital cost and balance of system cost, respectively. Moreover, c , h , r , d , s and f represent capacity, hub height, rotor diameter, water depth, shore distance and foundation type of the turbine, and the cost is the final cost estimation. Subscript b indicates the assumed values of the baseline turbine. As previously mentioned, financial costs are assumed to be proportional to the summation of turbine capital and balance of system costs, which can be seen in Equation 5. Considering the cost breakdown published by NREL as shown in Figure 3-3, θ_{TCC} and θ_{BOS} are assumed as 0.329 and 0.462 for fixed-bottom foundations versus 0.236 and 0.608 for floating foundations [56].

$$TCC' = \frac{cost_b * \theta_{TCC} * TCC(c, h, r)}{TCC(c_b, h_b, r_b)} \quad \text{Equation 4}$$

$$BOS' = \frac{cost_b * \theta_{BOS} * BOS(c, h, r, d, s, f)}{BOS(c_b, h_b, r_b, d_b, s_b, f_b)} \quad \text{Equation 5}$$

$$cost = TCC' + BOS' + \left[\frac{(1 - \theta_{TCC} - \theta_{BOS})}{\theta_{TCC} + \theta_{BOS}} * (TCC' + BOS') \right] \quad \text{Equation 6}$$

The definition of a baseline turbine with a cost value assigned from a literature review maintains the sensitivities of the turbine cost to turbine design characteristics as well as the location-specific parameters. For example, a turbine with a capacity of 6 MW, rotor diameter of 154 m, the hub height of 90 m, shore distance of 40 km and water depth of 25 m with a monopile foundation was introduced as a baseline turbine by Maness et al. [54] in their sensitivity analysis. This definition is employed at the initial stage of optimal turbine design since a typical turbine design could not be decided beforehand. However, in the final cost and potential estimation with optimal turbine designs, a new turbine design will be defined by the results of optimal turbine analysis, which has a capacity of 9.4 MW, a rotor diameter of 210 m, hub height of 135 m, shore distance of 60 km and water depth of 40 m with monopile foundation.

Figure 3-4 illustrates the sensitivity of specific investment cost with respect to percent change in the input parameters of the cost model such as capacity, rotor diameter, hub height, water depth, and distance to shore. Reference values are chosen as 6 MW for capacity, 154 m for rotor diameter, 90 m for hub height, 40 km for shore distance, 25 m as water depth for fixed bottom wind turbines (monopile and jacket) and, 500 m as water depth for floating turbines (semisubmersible and spar) as used by Maness et al. [54]. The turbine cost is a strong function of capacity since many cost components both in the turbine capital cost, and the balance of system cost are expressed in terms of capacity such as structure and foundation cost. The total investment cost of the turbine increases with increasing capacity; nevertheless, the specific investment cost of a wind turbine (total investment cost divided by the turbine capacity) decreases. This decrease in the specific investment cost indicates that the rate of increase in the total investment cost is lower than the rate of increase in the capacity, causing a decrease in the specific investment cost. An increasing trend in the specific investment cost of the jacket foundation with respect to capacity is seen after 25% variation; it might be because of the empirical equation expressed as a function of the logarithm of the capacity with a base of 10 to estimate the jacket transition piece mass. Rotor diameter has a significant impact on the specific investment cost; however, unlike capacity, an increase in the rotor diameter increases the specific investment cost mainly affecting the turbine capital cost and electrical infrastructure. As it is expected, higher rotor diameter increases total turbine mass, which explains its impact on the turbine capital cost. Moreover, the cable length is expressed as a function of rotor diameter in the balance of system, which illustrates the relationship between these two parameters. Compared to capacity and rotor diameter, hub height

and water depth do not have a high impact on the specific investment cost of floating foundation; nevertheless, a slight increase can be observed. Nevertheless, a strong correlation of these parameters is seen for fixed-bottom foundations, especially the impact of hub height for monopile foundation. Unlike floating foundations, fixed-bottom foundations are directly connected to the sea bed. Therefore, the total length of the turbine tower increases with increasing sea depth or hub height. The non-linear relation in the case of the monopile foundation for hub height is resulted from the fact that hub height is also factored in the monopile mass in the balance of system. Finally, distance to shore has a significant linear relation with the specific investment cost due to the electrical infrastructure costs in the balance of system, since individual turbines are connected to the grid at the nearest coast. This can be considered as a weakness in the current model; however, without optimal turbine design, it is not possible to cluster individual wind parks and factor the wind park connection costs instead of individual wind turbines.

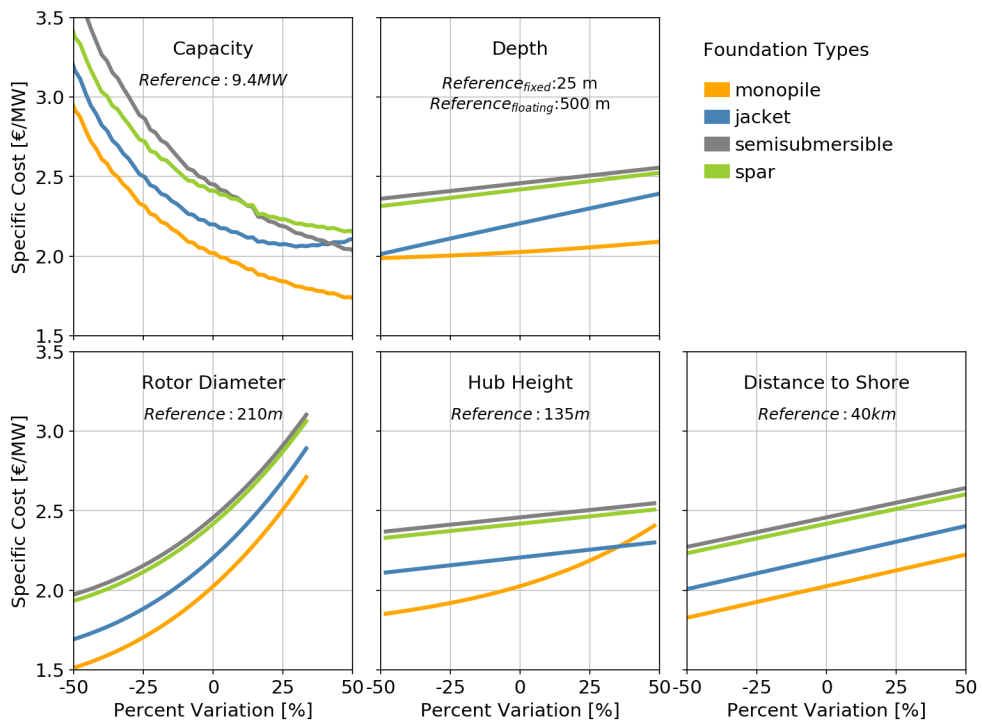


Figure 3-4 Variation of specific cost with respect to the capacity, rotor diameter, hub height, water depth, and distance to shore. Derived by the models described in [54]–[56].

While comparing different turbine designs, the total energy generation is also taken into account besides the total cost, since the turbine design influences both. Thus, LCOE is chosen for comparison, which can be calculated by using Equation 7. $specificCost_{turbine}$ stands for specific cost of turbine in € kW^{-1} , $FLH_{average}$ for average FLH, r for interest rate, n for economic lifetime of

the wind turbine and $\theta_{operating}$ for specific operating cost. In the LCOE calculation, an economic lifetime of 25 years [92], a specific operating cost of 2% and an interest rate of 8% [92] are assumed.

$$LCOE = \frac{specificCost_{turbine}}{FLH_{average}} \left[\frac{r}{1-(1+r)^{-n}} + \theta_{operating} \right] \quad \text{Equation 7}$$

3.1.4 Optimal Turbine Design

As discussed in Section 2.1.1, turbine design parameters have a significant impact on performance. Over-engineering the wind turbine design at a location can be avoided following the suggestions of IEC, which defines different wind turbine classes according to the average wind speed at hub height and turbulence intensity the turbine can withstand. In many analyses, a single turbine definition is uniformly applied to determine the overall generation and the capacity potential in a specified region, as it is discussed in Section 2.1.3. However, such an approach may over- or underestimate the potential, if there is no in-depth comparison of different designs. For instance, the use of a high wind speed class wind turbine across Europe would cause underestimation of generation potential in the Mediterranean Sea and the Adriatic Sea due to the lower average wind speed at these locations compared to the North Sea or Baltic Sea. A comparison in which different single turbine definition is applied uniformly across Europe will be further discussed in Section 4.1.2 in order to observe the impact of these parameters.

An analysis that involves optimization of turbine designs at each location by minimizing LCOE is performed across European Maritime Boundaries without considering ocean eligibility constraints so that the analysis can be combined with different eligibility scenarios instead of optimizing the locations again. For this purpose, different turbine designs are simulated for each location and the resulting total generation value and cost of the turbine design are used in the calculation of LCOE for each possible foundation type. Figure 3-5 shows the industry expert opinions about the future distribution of turbine parameters according to a survey reported by Wiser et al. [93]. The upper and lower boundaries for turbine design parameters are assumed to be within the range suggested by Wiser et al. [93]. Therefore, capacity, hub height, rotor diameter, and specific capacity ranges are defined as 3-20 MW, 80-200 m, 80-280 m and 220-550 W m⁻², respectively. In addition to these constraints, a minimum distance between blade-tip and sea-level is set to 30 m. In case of violating this constraint, the turbine design is disqualified. Due to non-linearities in the cost model and also in the simulation scheme, a discretization of turbine characteristics is performed to avoid intractability issues. As a result of the discretization, the increments for capacity, hub height, and specific power are assumed to be 0.2 MW, 2 m and 5 W m⁻², respectively. Moreover, water depth limitations are applied to foundation types. Fixed-bottom foundations, monopile and jacket, are only allowed to be built between 0 to 100 m water depth, whereas this range is assumed to be 20-1000 m for semisubmersible, and 100-1000 m for spar [54].

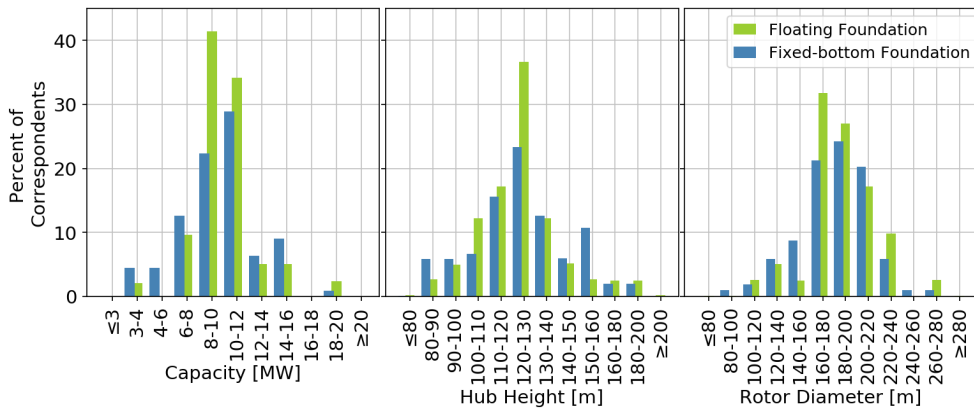


Figure 3-5 Distribution of future turbine design parameters by the expert opinions. Adapted from Wisser et al. [93].

The overall workflow followed in the analysis of optimal turbine design is illustrated in Figure 3-6. In terms of location, 5 km grid is created across European Maritime Boundaries [74]. As it is mentioned earlier, for all possible turbine designs within the predefined range, simulation is performed between weather years 1980 and 2017 in order to calculate the average capacity factor. Following this, LCOE is calculated by combining average capacity factors and the corresponding turbine design's cost. Finally, by comparing all LCOE values with turbine designs, the one with minimum LCOE is determined. In addition, the top 100 turbines with the lowest LCOE are stored for further investigations of different designs at each location.



Figure 3-6 Overall workflow used in the optimal turbine design analysis.

3.1.5 Clustering Optimal Turbine Designs

Optimal turbine designs explained in Section 3.1.4 have a large variety of turbine designs⁸. Hence, the question arises: What is the minimum number of turbine designs for all locations within a predefined LCOE threshold? In order to be able to answer this question, all turbine designs having

⁸ 92 different turbine designs are observed when optimal turbine designs are analyzed in terms of their capacity and rotor diameter as turbine characteristics. Addition of hub height increases the number of different turbine designs to 181. Furthermore, in total 202 designs have to be used if capacity, rotor diameter, hub height and foundation are used as indication of turbine characteristics.

an LCOE between the minimum and 101% of the minimum LCOE are saved for each location, while analyzing the optimal turbine design. The different turbine designs are examined to cluster and find the lowest number of turbine designs which is applicable everywhere across Europe. For this purpose, three LCOE thresholds (1%, 0.5% and 0.01%) are introduced in order to get the corresponding turbine designs within the limits of LCOE values (minimum and the threshold as maximum). Nevertheless, one last question remains unclear: What are the properties determining turbine designs? Tower height, as well as the foundation, can be considered location-specific parameters. For example, a turbine with specific capacity and rotor diameter would have different tower heights because of the water depth, since it is highly related to the hub height and water depth. Moreover, the foundation has also the same feature; it is decided based on the parameters related to certain locations where the wind turbine is planned to be built. In order to avoid this confusion with the definition of turbine designs, three different property sets are defined in order to identify turbine designs: “capacity and rotor diameter”, “capacity, rotor diameter, and hub height” and “capacity, rotor diameter, hub height, and foundation”. Finally, the algorithm shown in Figure 3-7 is applied for all 9 cases (3 LCOE thresholds and 3 turbine parameter sets).

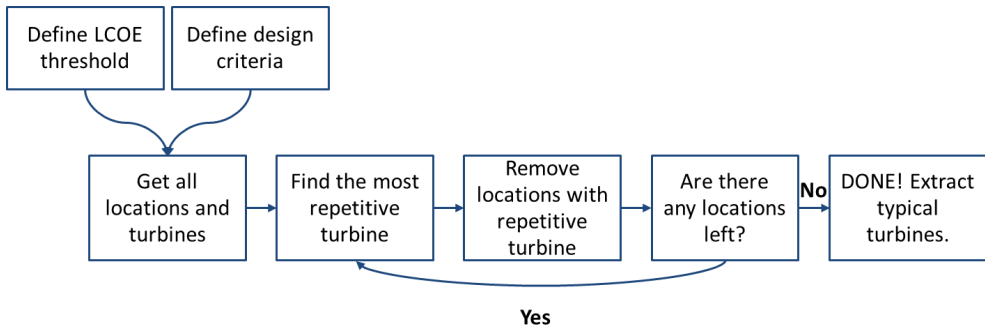


Figure 3-7 Algorithm applied to cluster the optimal turbine designs.

3.2 Technical Potential of Salt Caverns across Europe

It must be noted that the content of Section 3.2 is published in the “International Journal of Hydrogen Energy” by Caglayan et al. [192]. Determination of technical potential for salt caverns requires detailed analysis of the geology of salt formations. Once the vector files of salt structures, which are suitable for hydrogen storage are available, the eligibility of the structure is estimated as it is presented in Section 3.2.1. Both bedded salt layers and salt domes are considered in this analysis. By using two different cavern designs for these two distinct salt formations, the distribution of these caverns is performed across eligible areas. Following this, the technical potential of salt caverns for hydrogen storage is estimated by using these locations and calculating the storage potential under thermodynamic considerations.

Figure 3-8 shows the concept of potential including different types. Within the context of this work, theoretical potential includes the total hydrogen storage capacity of all possible salt caverns, whereas technical potential takes into account the limitations (i.e., cushion gas). Economic and ecological potentials consider corresponding criteria which might be derived from a scenario. Finally, the realizable potential is the combination of technical, ecological and economic criteria with additional considerations (i.e., social acceptance). It must be noted that the potential values derived in this work cannot be utilized fully; moreover, to what extent it should be deployed can be determined as a result of the energy system design. In other words, the technical potential of salt caverns is different from the realizable potential.

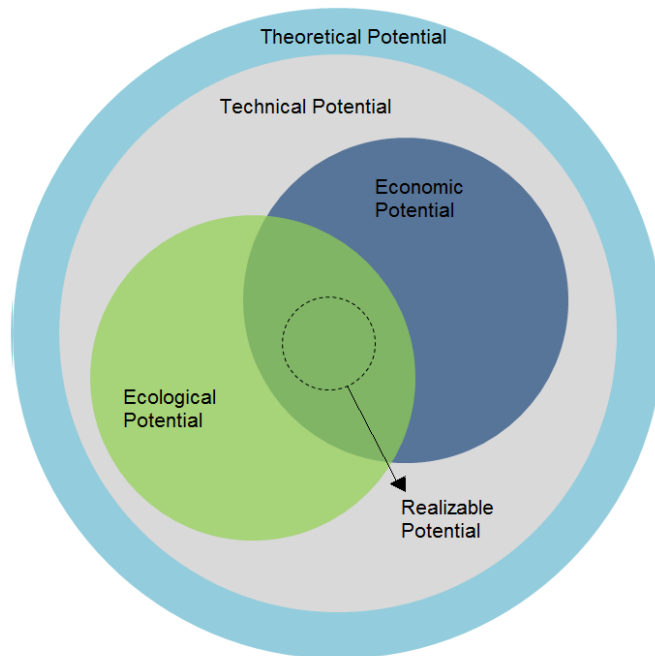


Figure 3-8 Concept of potential with different potential types. Adapted from [47], published in [192].

3.2.1 Land Eligibility

A salt cavern, the bottom tip of which is located approximately 2,000 m below ground, affects an area of 13 km² considering an angle of 35° – 45° between the bottom of the cavern and surface. These areas are mainly affected because of cavern closure happening due to salt inflow into the cavern due to increasing pressure difference with a depth between gas in the cavern and lithostatic pressure exerted on the cavern. Creep closure of a cavern caused by these pressure differences results in refilling the space by overburden rock; in other words, the volume loss of the cavern is

compensated by the surrounding rock. This takes place within an upwardly rising cone and ultimately leads to a subsidence funnel at the surface. Therefore, eligible areas for salt deposits have been investigated in order to determine the storage potential of salt caverns. For this purpose, an open-source model, Geospatial Land Availability for Energy Systems (GLAES), developed by Ryberg et al. [75], is employed as the tool for land availability analysis. By using GLAES, exclusion constraints have been applied to the areas under which the salt deposit exists. A resolution of 100 m is used for the eligibility assessment since it is the lowest resolution in the data used for the analysis (Prior Datasets). Following this, the exclusion constraints shown in Table 3-2 have been applied with the buffer distances defined as a result of a literature analysis for underground storage and compressed air energy storage. The use of studies focusing on compressed air energy storage is mainly because of the lack of data for such an assessment on the salt caverns for hydrogen storage. Therefore, assuming similar behavior, analyses on the compressed air energy storage is also involved in the literature review, which is then used to determine the criteria and exclusion constraints.

Table 3-2 Constraints used in the land eligibility analysis for salt cavern construction

Criteria	Excludes	Source
Urban areas	below 2,500 m	[75]
Rural areas	below 2,000 m	[75]
Major fault zones	below 200 m	[193]
Natural protected areas, water bodies	below 200 m	[75]
Railway, major roads and gas pipelines	below 200 m	[75], [81]
Geological correction factor (distance from salt edge):		
- Bedded salt	below 2,000 m	Own data
- Salt domes	500 m	

A detailed outline of a salt structure is not possible to obtain without extensive seismic, well drilling or further geological investigations. Therefore, a buffer distance of 500 m for salt domes and 2000 m for bedded salt deposits are applied from the edge of each salt formation to ensure salt cavern construction in more pure-salt locations [2]. This exclusion is mainly performed in order to increase the likelihood of having an appropriate salt structure at the cavern location, yet it can be considered as a safety buffer from the edges. Although it is not shown in Table 3-2, the proximity to the coast, the distance from the coast, plays a major role in the brine disposal. Concerning the high salt content of the brine during the cavern construction process, the brine solution cannot be disposed in a river or a lake due to environmental concerns.

3.2.2 Salt Cavern Design

The design of a salt cavern highly depends on the salt deposit to be considered; nevertheless, there are some factors that should be taken into account in order to maintain a stable operation. Figure 3-9 illustrates a representation of a salt cavern with related terms as well as the pressure limitations as a function of depth. For geomechanical safety of caverns, thicknesses of salt layers above and under the cavern are defined as hanging wall and foot wall, respectively; and they are shown in Figure 3-9. The minimum thickness of these layers for a safe operation is expressed as a function of cavern diameter. For example, the minimum thickness of the hanging wall is suggested as 75% of cavern diameter, whereas this value is 20% of the cavern diameter for the foot wall [194].

Ozarslan [97] stated that capsule-shaped salt caverns are more stable with decreased stress risk in comparison to a cavern with an elliptical or cylindrical shape under 1200 m depth and 270 bar lithostatic pressure. Therefore, the capsule shape is chosen to be used in the calculation of cavern volume as well as the determination of the appropriate construction and operation of the caverns. For bedded salt deposits, a cavern volume of 500,000 m³ is applied with a diameter of 84 m and cavern height of 120 m; whereas 750,000 m³ for cavern volume, 58 m diameter and 300 m for height are assumed for caverns in salt domes. Suitability of the salt formations is conducted by assuming a minimum salt thickness of 200 m⁹ for bedded salt layers. Therefore, following the suggestions for foot wall and hanging wall thicknesses, maximum height is determined for salt caverns that are planned to be placed in the bedded salt layers. In other words, the caverns designed for bedded deposits have a limitation in their height due to the salt layer thickness, which causes the larger cavern diameter in comparison to the ones designed for salt domes.

⁹ This value is calculated by using the cavern height and minimum salt thickness for the foot-wall and hanging-wall (cf. Figure 3-9).

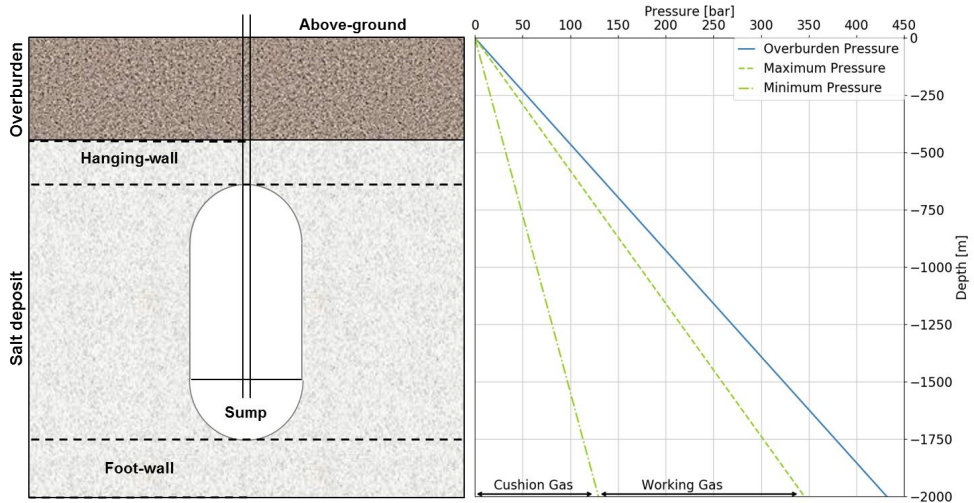


Figure 3-9. A simplified representation of an exemplary cavern and estimated pressure limits as a function of depth, which is adapted from Stolzenburg et al. [187] (Calculation of pressure is explained in Section 3.2.3).

3.2.3 Calculation of Cavern Capacity

The average operation temperature of hydrogen over the depth of the salt cavern is assumed to be the same as the temperature of the surrounding salt rock. However, the temperature in a sedimentary basin varies with respect to the depth by a gradient of 25 K km^{-1} until approximately 5 km depth. Because of their respective height, the variation in the temperature results in a difference of 3 K between the top and the bottom of a small cavern and 7.5 K for a large salt cavern. Therefore, the average temperature of the gas is calculated by using Equation 8, assuming a surface temperature of 288 K (15 °C). $T_{average}$ stands for average gas temperature in K, $depth$ in m, $cavernHeight$ for height of the cavern in m, which are 120 m and 300 m for bedded and domal-salt caverns, respectively.

$$T_{average} = 288 + 0.025 * (depth - cavernHeight/2) \quad \text{Equation 8}$$

Salt caverns are exposed to lithostatic pressure (sometimes referred to as overburden pressure). This pressure can be calculated by Equation 9, which is a function of rock density (ρ_{rock}) in kg m^{-3} , gravitational acceleration (g , assumed as 9.81 m s^{-2}), $depth$ and $cavern height$ in m. $depth$ shown both in Equation 8 and Equation 9 are in reference to the bottom tip of the salt cavern, nevertheless, it is scaled to the center of cavern by subtracting the half of cavern height in order to estimate the average pressure, that is between the lithostatic pressures at top and bottom tips of the cavern.

$$P_{overburden} = \rho_{rock} * g * (depth - cavernHeight) \quad \text{Equation 9}$$

Due to concerns about geotechnical safety, maximum and minimum gas operation pressures are limited to 80% and 24% of lithostatic pressure. Exceeding the maximum gas operation pressure may result in salt rock fractures because of the high pressure exerted on the cavern walls [109], and low pressure limitation is for maintaining gas injection and withdrawal as well as the stability of the cavern [195]. Since empirical operating pressure values for hydrogen storage in salt caverns are not accessible, pressure ranges are largely derived from natural gas storage experiences [109]. These upper and lower limits for gas operation pressure are used in the density calculation at the corresponding pressure level, which is shown in Equation 10. Density of the gas (ρ) in kg m^{-3} is decided by using real gas law, in which compressibility factor (Z), pressure (P) in Pa, molar mass of the species (M) in kg mol^{-1} , universal gas constant (R), which is equal to $8.314 \text{ J K}^{-1} \text{ mol}^{-1}$ and temperature (T) in K are used. The compressibility factor is calculated by a Python Module called CoolProp [196], which is a C++ library involving equations of state and fluid properties for many species. It has a fully-featured Python wrapper enabling utilization in the Python environment.

$$\rho_{H_2} = \frac{P * M}{Z * R * T} \quad \text{Equation 10}$$

Minimum and maximum limits for density are used in the calculation of the mass of working gas, shown in Equation 11. $m_{workingGas}$ stands for mass of working gas in kg, ρ for density in kg m^{-3} , V_{cavern} for cavern volume in m^3 , and finally θ_{safety} for safety factor which is assumed 70%, which accounts for the loss of storage capacity to the sump and the brine at the bottom of the cavern as well as unplanned construction circumstances during the leaching of the cavern. Subscripts minimum and maximum are calculated at the corresponding pressure limit.

$$m_{workingGas} = (\rho_{H_2,maximum} - \rho_{H_2,minimum}) * V_{cavern} * \theta_{safety} \quad \text{Equation 11}$$

Finally, storage capacity of a salt cavern is determined by using the lower heating value and mass of working gas calculated by specifications of the cavern and location, which is shown in Equation 12. $cavernCapacity$ is calculated in GWh, and lower heating value of the gas (LHV) is defined in GWh kg^{-1} .

$$cavernCapacity = m_{workingGas} * LHV_{gas} \quad \text{Equation 12}$$

Due to the lack of data, validation of the methodology for salt cavern capacity by using hydrogen is not possible. Nevertheless, technical storage potential can be estimated for any species if the composition of the gas is known. Therefore, a validation is performed by using a dataset ("Gas

Infrastructure Europe” - GIE) compiled from natural gas storage sites in operation [96]. This dataset has 94 cavern sites for natural gas storage in salt caverns across Europe. However, when caverns without available information on depth, cavern volume, or capacity are excluded, only 40 sites remain. Since the composition of natural gas varies and is not reported for each cavern site, a sample composition of natural gas is assumed as 94% methane (CH_4), 4% ethane (C_2H_6), and 2% propane (C_3H_8) [197]. The volume and depth of the salt caverns obtained from the dataset are used for storage capacity calculation. A comparison of capacities given in the dataset and calculated by the current approach is shown in Figure 3-10. In some cases, there are two capacity values connected with a line, which is calculated by a depth range given in the dataset. Therefore, the actual total capacity of the cavern site is supposed to be between these maximum and minimum capacities. The gray line in the figure indicates a 100% match between reported and calculated values, and as further a point is from this gray line means a higher error in the estimation of the capacity. As it is seen from the figure, in general, there is a good agreement in most of the results. Deviations in the estimations may be caused by several factors, such as different compositions for natural gas, different operation pressure limits especially for cushion gas, geological conditions altering temperature and pressure environments. Besides slight deviations from the gray line, there are large differences in the estimated and reported capacities for two cavern sites (the Etrez site in France and the Nüstermoor L-Gas site in Germany). More detailed data for the two cavern sites do not exist on the website of the operators; thus, they are just assumed as outliers.

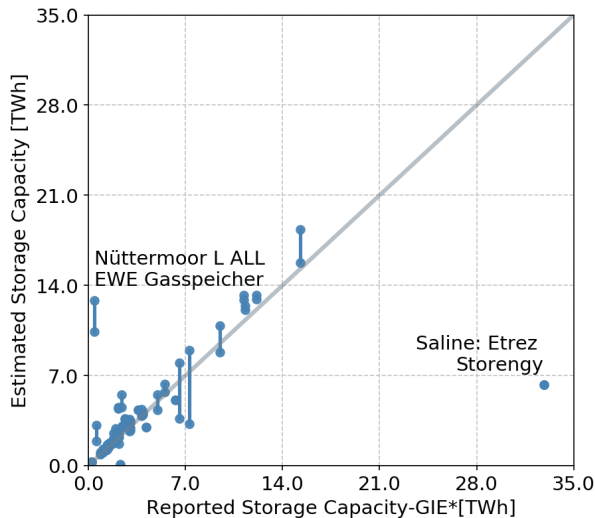


Figure 3-10. Comparison of reported and calculated storage capacities of natural gas salt caverns (Reported values are extracted from the existing natural gas storage facilities in Europe [96]).

3.3 Model Aggregation Toolset for Energy Systems (MATES)

Energy system design by using the optimization framework FINE (Framework for Integrated Energy System Assessment) requires input parameters with a specific format [151]. Preparation of these parameters by manual effort (such as defining it in MS Excel or as CSV files) in the appropriate format for different regions, scenarios and technologies can be time-consuming. Furthermore, there is a high risk of error that is caused by changes in the data (changing a value in an MS Excel or CSV files). Moreover, it makes the version control of the input/output of energy system design harder. For instance, finding which input parameters are used for a specific energy system design is not that straightforward when all the files are saved separately. Therefore, a python module has been developed in order to make the input preparation and optimization formulation fully automatized. This model chain combines the internal models (such as FINE, GLAES, geokit, TSA¹⁰) with the required input format of the corresponding module and designs the energy system.

The structure of the model chain can be seen in Figure 3-11. There are three main components in this tool: “Input Generator”, “Optimization Manager” and “Output Manager”. “Input Generator” is used to prepare the energy system inputs in the format required by FINE (optimization framework used in the energy system design), such as techno-economic parameters of VRES, hydrogen pipelines, determination of hydrogen demand for passenger vehicles and so on. Moreover, when components of the energy system model are completed it creates a file (netCDF4 format), including all required input parameters. The features available in “Input Generator” are explained in the following sections. “Optimization Manager” is used to unpack the input parameters and passes them to the open-source optimization framework (FINE), an open-source package developed in Python 3.6 as the programming language. This framework is a spatio-temporal optimization explained by Welder et al. [13], [151], and it optimizes the energy system with an objective function of minimization of total annual cost (TAC). Pyomo [198] and Gurobi [152] are used as the optimization modeling language and solver for the optimization problem. A Pyomo model is initialized as the energy system model instance, and input parameters for the related technologies are added consecutively to this model instance. In the “Optimization Manager”, this process of adding technologies consecutively by manual effort is automatized; and technologies with their parameters are extracted from the input file and passed to the model instance. After solving the created model, the results of the optimal energy system design are extracted and saved onto the input file, which enables user to keep track of input parameters for a specific energy system design. Finally, “Output Manager” can be used to format the output parameters in a user-

¹⁰ FINE: “Framework for Integrated Energy System Assessment”, GLAES: “Geospatial Land Availability for Energy Systems”, geokit: “Geospatial toolkit for Python”, TSA: “Time Series Aggregation”

friendly format, mainly tables and enable user plot the operation time series, residual load within a region as well as GIS¹¹ plots, which include region geometries.

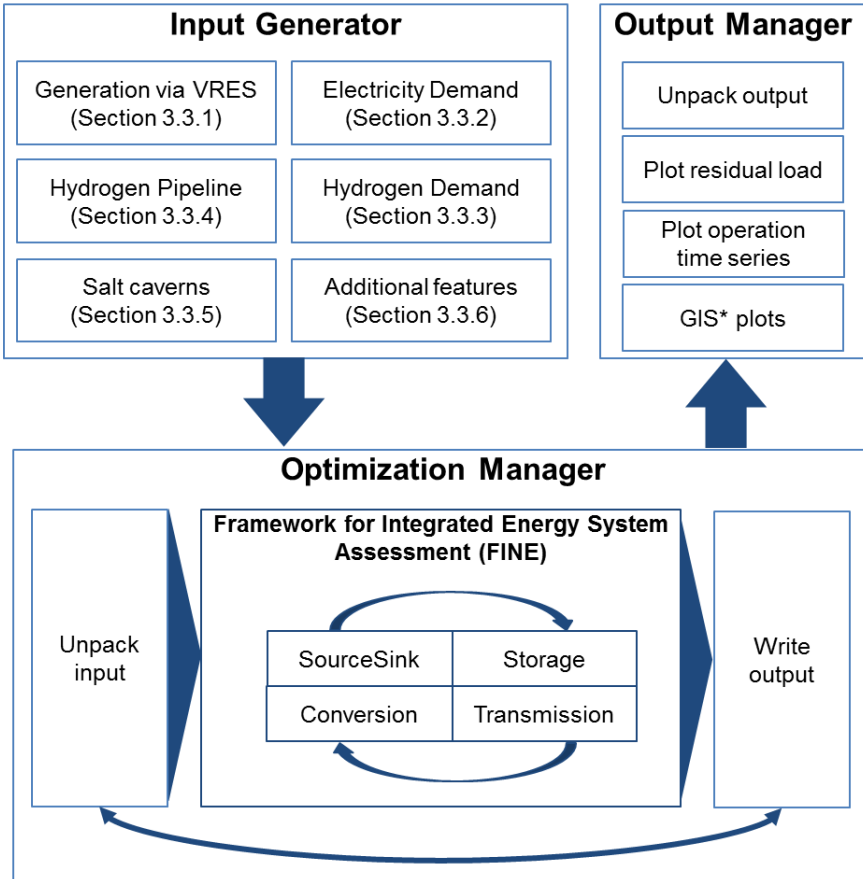


Figure 3-11 Structure of Model Aggregation Toolset for Energy Systems.

3.3.1 Electricity Generation via VRES

Similar methodologies are employed in the simulation of variable renewable energy sources, including onshore and offshore wind, open field PV with and without tracking as well as roof-top PV. As mentioned earlier, for the simulation workflows, a global weather climate dataset published by NASA called Modern-Era Retrospective analysis for Research and Applications-version 2 (MERRA-2) is chosen [68]. The spatial resolution of MERRA-2 dataset is 0.625° by 0.5° (nearly 60 km). Although the spatial resolution is coarser compared to other weather datasets (i.e.,

¹¹ GIS: Geographic Information System

European Centre for Medium-Range Weather Forecasts, National Centers for Environmental Prediction), the MERRA-2 dataset has a wide coverage of many weather years across world with hourly resolution. These periods cover between 1980 and 2018, enabling an analysis of 38 weather years by the time of the analyses conducted in this thesis.

Once the eligibility analysis is performed, and placements of the technologies (individual wind turbines or PV panels) are prepared, the simulation can be performed. Due to the computational limitations of optimization problems, it is not possible to define individual generation time series for each location within a region. Therefore, all the locations within the region are simulated for individual VRES technologies. Afterward, a normalized generation time series of these locations are calculated and defined as a single technology in the model. This normalized generation is obtained by calculating the total generation of all the locations by summing them, and then dividing it by the total capacity within the region (summation of the capacities of individual placements). This generation time series is then scaled in the optimization problem by the optimum capacity that is installed in the region. It must be noted that optimum capacity is limited by the maximum capacity of that technology that can be installed within the region. Under- or overprediction of the generation time series by the scaling with optimal capacities is evident. However, the definition of individual turbine designs is not possible in an optimization problem, since additional technologies increase the complexity of the problem resulting in higher solution time. Therefore, by increasing the number of groups, higher fidelity can be attained within a reasonable solution time.

Grouping of placements:

As it is discussed earlier, the number of regions and technologies considered in the energy system design is limited due to the tractability issues of optimization problems. Simplification of the system while maintaining the detailed modeling is possible by grouping the VRES placements by a criterion. By doing so, spatial resolution can be increased while keeping the number of regions constant. The definition of several groups of technologies instead of averaging enhances the accuracy of the technologies by a drastic increase in the modeling details. In other words, having different groups provides higher spatial resolution without increasing the complexity of the model with a higher number of regions. It must be noted that a generation technology for VRES in the energy system model is defined by a generation time series and maximum capacity to be installed within a region; thus, each group is defined as an independent technology.

As an example, Figure 3-12 shows the turbine locations in North Rhine-Westphalia, Germany, and their corresponding generation time series in 2015 in order to emphasize the impact of grouping on the generation time series. It is seen that the peak power is not attained most of the times in the upper figure since the average time series is affected by turbines with low generation. As a result, the utilization of high generation locations is not possible when a single time series is used in the model. The lower figure shows the same time period in the same region when only 4 turbine groups are defined by their average LCOE. As it is seen from the generation time series, the time

series shown in purple covers the peak power generation time periods better than single generation time series, whereas the time series shown in blue represents the low generation locations. Although the overall behavior is still not fully captured, the technology can be modeled in a more realistic way with a higher number of groups (the ideal modeling occurs when the number of groups is equal to the number of turbines in that region).

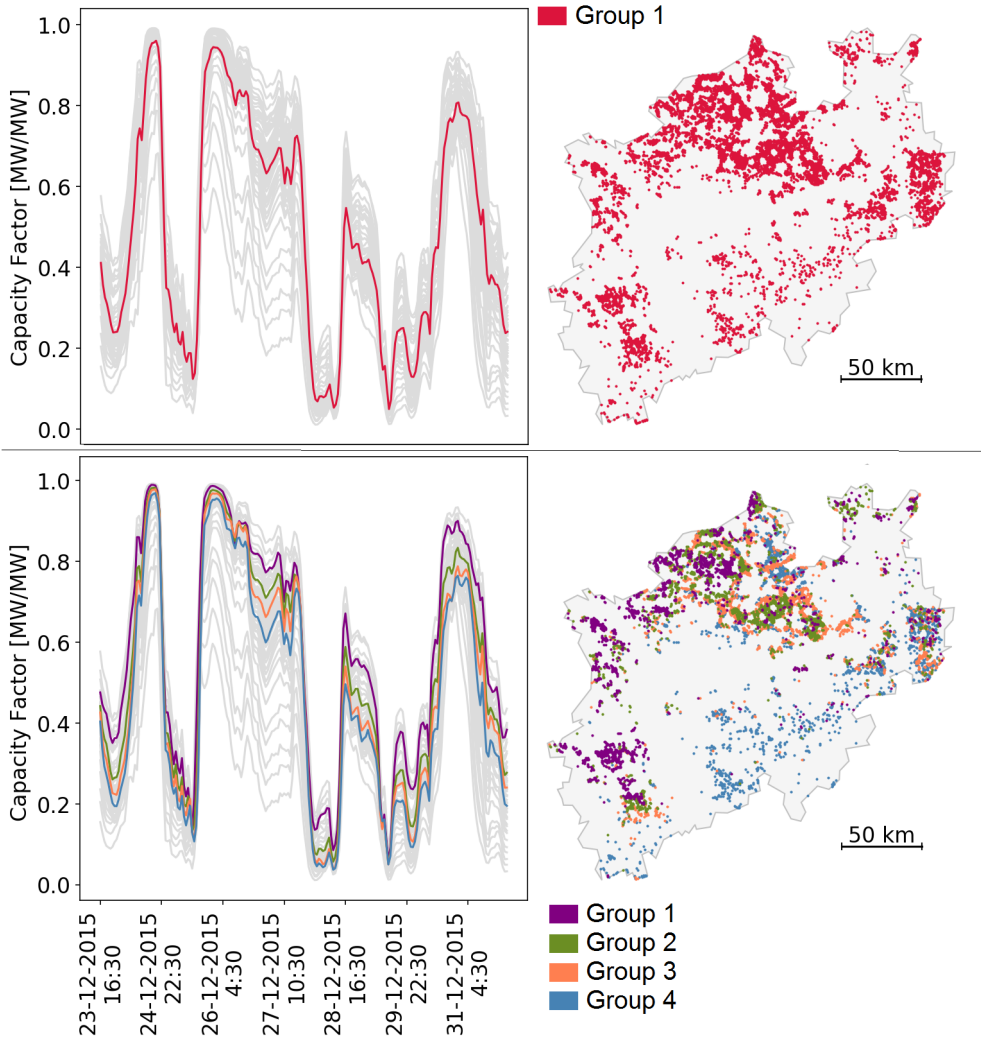


Figure 3-12 Distribution of onshore turbine locations in North Rhine-Westphalia, Germany, with corresponding generation time series (weather year: 2015) different groups which are classified by an equal division of percentiles of the turbine's LCOE. (upper) for single grouping and (lower) 4 turbine groups.

Grouping can be performed by using different criteria defined at each location. Average wind speed, solar irradiance, location of items or combination of multiple criteria can be used in the grouping of these technologies. In this analysis, the average LCOE of individual placements is used as a criterion to group the placements by equally distributed percentiles since LCOE is a common criterion amongst wind turbines and PV panels. Figure 3-13 illustrates the method used for grouping. First, the criterion that is used for grouping is sorted by their values independent from the location. Following this, as it is seen in the cumulative density function, equally separated classes are formed. For instance, the use of locations having values between 0th and 50th percentile and 50th to 100th percentiles results in the definition of equally separated 2 groups. The specific example shown in the figure has 3 groups, which are separated between 0th to 33rd percentiles, 33rd to 67th percentiles and 67th to 100th percentiles shown as “Group 1”, “Group 2” and “Group 3”, respectively. Therefore, the locations are categorized with respect to the thresholds shown as orange lines in the plot. These groups are then simulated and defined in the optimization model as three independent generation technologies¹².

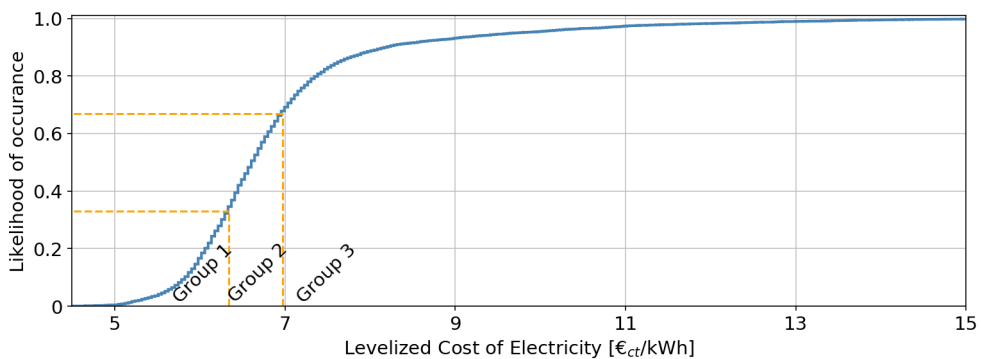


Figure 3-13 Representation of grouping as an example in North Rhine-Westphalia, in which 3 groups of onshore wind turbines are categorized by LCOE¹³.

The application of the aforementioned method to categorize different groups for a technology is conducted for wind turbines and PV panels. In order to give insight into the overall method of how these things are combined, an exemplary region is defined. Figure 3-14 shows an application of workflow to obtain the maximum capacity and generation time series for onshore wind energy in Juelich with 3 groups. Having region geometry as input, uniform eligibility constraints are applied with different sets of constraints, which are derived from a literature review. Following this, the placement algorithm is performed across eligible locations by using separation distances, and then they can be grouped by a criterion. Finally, individual placements in each group are simulated for

¹² The actual analysis on the impact of grouping consists of 90 groups for each VRES technology. (cf. Section 5.2)

¹³ The small increments on the figure are caused by the histogram bin widths chosen; however, as the bin width decreases the line gets smoother.

a specified weather year, and the total generation time series of all turbines is normalized by the maximum capacity in that region.

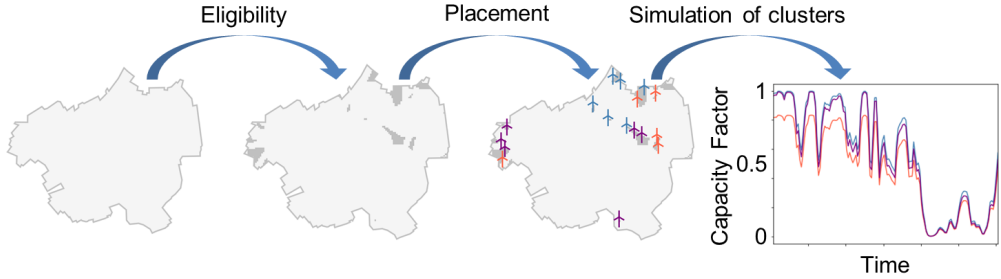


Figure 3-14 Representative workflow for onshore wind turbines and electricity generation in Juelich, Germany.

3.3.2 Electricity Demand

Electricity demand in Europe is implemented by including the demand time series estimated by Syranidou [136] that employs the methodology suggested by E-Highway [139]. These time series data include electricity demand with electrified heat demand and transport demand for battery electric vehicles and plug-in hybrid electric vehicles. The transport demand is excluded from the overall demand so that hydrogen demand for passenger vehicles can be taken into account.

The demand time series for a region smaller than a country can be scaled by using population density distribution [199]. Different parameters such as gross domestic product, average temperature, global horizontal irradiance or wind speed within the region. Nevertheless, despite the comparison of different parameter combinations, the population is chosen also following the suggestions in the literature by Syranidou [136]. The estimation of demand time series for a given regional definition is conducted by using Equation 13 shown below [136].

$$ElectricityDemand = \frac{Population_{region}}{Population_{country}} \times Demand_{country} \quad \text{Equation 13}$$

3.3.3 Hydrogen Demand for Passenger Vehicles

The approach to determine the hydrogen demand for passenger vehicles is suggested by Robinius et al. [11], calculating yearly demand for a region by using Equation 14. *totalCars* for the total number of passenger vehicles within the region, *ADD* for annual driving distance of these passenger cars in km, *fuelConsumption* for fuel consumption of fuel cell electric vehicles in kg H₂ km⁻¹ and *MP* for market penetration.

$$Demand_{H_2} = totalCars * ADD * fuelConsumption * MP \quad \text{Equation 14}$$

Fuel consumption of fuel cell electric vehicles is assumed as $0.0071 \text{ kg H}_2 \text{ km}^{-1}$ [9]. The total number of cars and annual driving distance for each country are obtained from E-Highway [139] since consistent data is available for all countries investigated in this analysis. For 75% market penetration of fuel cell electric vehicles, hydrogen demand in Germany is reported as 2.93 million tons H_2 per year by Robinius et al. [11]. When the data for the total number of cars and annual driving distance are taken from the E-Highway study [139], this demand is calculated by 2.71 million tons H_2 per year. This difference of nearly 7% is mainly caused by dataset, which includes the total number of cars and annual driving distance. Robinius et al. [11] used 2015 values for the total number of cars and annual driving distance, whereas in E-Highway study [139] annual driving distance in 2050 is assumed to be the same as 2010. In addition, car ownership (cars per capita) is projected to 2050 by using the relation between gross domestic product and car ownership rate between the years 2003 and 2010. Finally, the population of Germany is assumed as 81 million by Robinius et al. [11], whereas it is reported as 70 million by E-Highway [139]. All in all, taking into account the difference of data sources used in the calculation of hydrogen demand, a 7% variation in the results is found to be reasonable. Therefore, the dataset used by E-Highway is employed in the rest of this study, with 75% market penetration of fuel cell electric vehicles.

After calculating the overall yearly hydrogen demand for a region, it is spatially distributed by population density, which is also used to determine the demand center by a weighted centroid. By distributing the hydrogen demand, the spatial resolution is decreased to 100 m by 100 m from the size of the region geometry. Following this, the yearly demand is projected onto an hourly demand profile of a reference fueling station.

3.3.4 Hydrogen Pipeline

A combination of railways, highways and primary roads and existing natural gas pipelines results in all possible connections between regions. In order to decrease the computational time, these connections for all European countries are calculated and saved as a vector file. When demand centroids of all regions are defined, all possible connections around these centroids are extracted from the precalculated vector file, and then pipeline routes are determined by using these connections according to the specified algorithm. This algorithm can be the shortest distance between each centroid, or a weighting factor can be defined for a chosen pipeline. Nevertheless, different routing options are still possible within the model chain. For example, use of the existing pipeline routes, Euclidian distance with a detour factor or combination of railways and road is still possible once the vector or raster files are defined in this feature.

3.3.5 Salt Caverns

A vector file of salt caverns for hydrogen storage is created by using the method explained in Section 3.2. This vector file consists of point geometries of possible cavern centroids with corresponding gas storage capacity in GWh, average temperature of salt structure around cavern in °C, mass of required cushion gas (hydrogen) in kg, cavern depth in reference to the ground level, energy density in kWh m⁻³, maximum and minimum cavern operation pressure in Pa. Given the region geometry, it is possible to extract the maximum hydrogen storage potential within the region. In addition to the maximum storage potential, techno-economic parameters of salt caverns are also defined in this feature.

3.3.6 Additional Features of the Model Chain

Before building the energy system design, the definition of different technologies as a source, sink, storage, transmission or conversion components is possible in the model chain besides the technologies which are already implemented. With this feature, users can change the scenario and include additional components in the energy system. For example, including the natural gas purchase in the energy system design is possible by defining as a general source component with corresponding techno-economic parameters. However, the main disadvantage of using this feature is that the input parameters have to be defined manually by the user.

All the technologies added as components of the energy system design are saved as input parameters in a netCDF4 file. As it is mentioned in Section 3.3, there are four main classes required by the optimization framework (FINE): “SourceSink”, “Storage”, “Conversion” and “Transmission”. These classes are used as a reference in the format of the netCDF4 file and further broken down into the groups: “Source”, “Sink”, “Storage”, “Conversion”, “Transmission” and “Linear optimal power flow”. These groups in the netCDF4 file are passed to the optimization framework automatically once the optimization manager of the model chain is used. It builds the optimization problem of the energy system design and optimizes the system. Finally, outputs of the energy system design are saved onto the same netCDF4 so that the inputs and corresponding results are stored in the same file.

There is not a user-friendly way to extract the content of a netCDF4 file. Unlike MS Excel or CSV files, netCDF4 file cannot be viewed directly by opening the file. Therefore, the output manager has been developed under the same model chain. The output manager unpacks the netCDF4 file and formats it according to the user’s requirement. For instance, the operation time series of all components in the energy system design can be extracted and plotted. Moreover, optimum installed capacities and the total annual cost of components can also be extracted.

3.4 Scenario Definition for the Design of a 100% Renewable European Energy System

The technologies and their interactions with corresponding commodities within a region are shown in Figure 3-15. Four different commodities (hydrogen, water, electricity, and biomass) are included in the system when all generation and demand technologies shown in the figure are taken into account. There are two different demand types defined in the energy system: electricity demand and hydrogen demand. For generation technologies, 6 main renewable energy sources are used with electricity as a commodity. In addition, biomass fuel can be purchased and used in a combined heat and power (CHP) to produce electricity. Modeling hydropower could be performed by using electricity as a commodity; however, the current version of the optimization framework is not capable of defining inflow for the reservoir or pumped hydro storage technologies. Definition of inflow as a free generation technology violates capacity limitations of these technologies, yet a free charging of storage technologies is not possible since it is not implemented in the framework. Therefore, hydropower is modeled by using water as a commodity. Besides hydropower as a storage technology, lithium-ion batteries, gas vessels, and salt caverns are considered. 7 conversion technologies are defined; 5 of these technologies can be used in the conversion of hydrogen into electricity. Finally, there are three different transmission technologies that enable the interactions between regions via hydrogen or electricity. Maximum capacities defined in the optimization are provided in Appendix A.2.

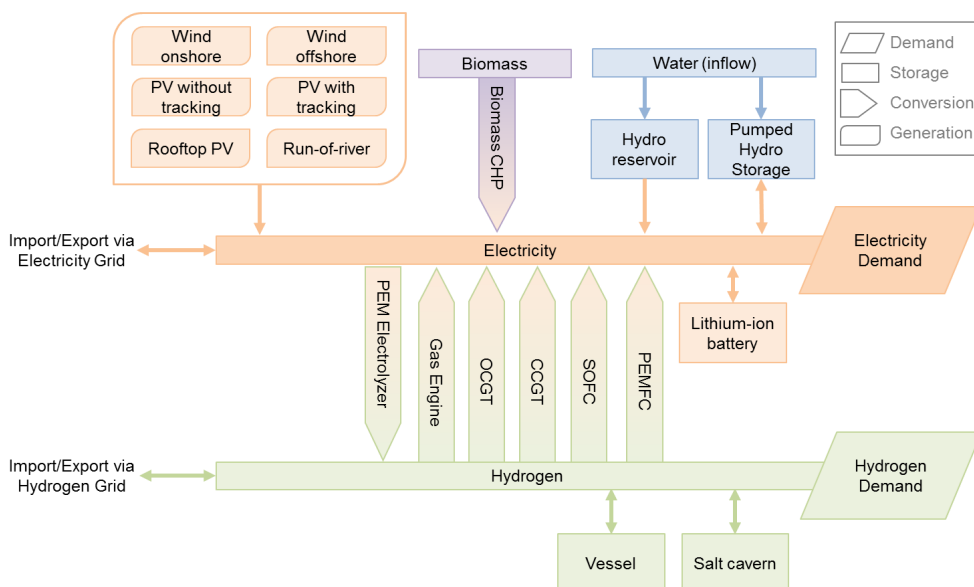


Figure 3-15 Representation of technologies and their interactions within a region in the energy system.

3.4.1 Definition of the Region

Several criteria are taken into account in the determination of regions by E-Highway: highlighting the main energy flows, size of the region, a limited number of regions and respecting national boundaries due to policies as well as the high interest in the national-level results. Following this, the results are consulted through ENTSO-E [140]. In order to be able to compare the results of this analysis by the E-Highway study [141] as well as a previous analysis performed by Ryberg [37], region definition of E-Highway study is used in the scenario. It must be noted that European countries are assumed to operate under island mode due to the lack of time series data of imports and exports between European regions and African regions. Therefore, resulting 96 regions used in the E-Highway study and this thesis are shown in Figure 3-16.

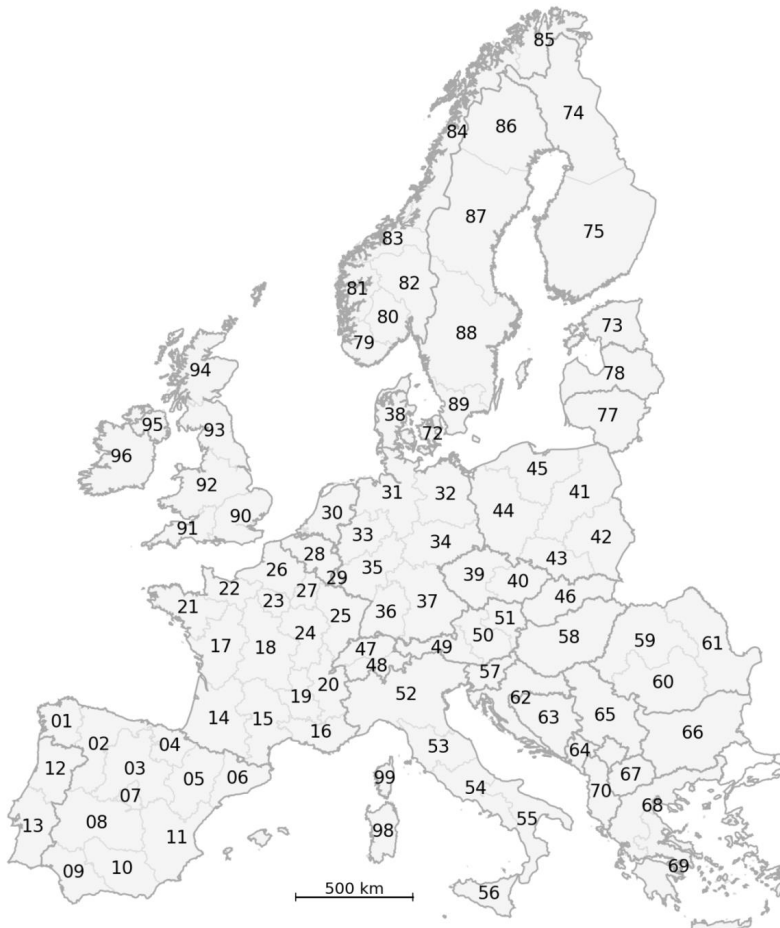


Figure 3-16 Regions used in the analysis. Adapted from [141].

3.4.2 Demand Sectors

Electricity demand and hydrogen demand are considered as the components of the demand sectors. Electricity demand data for the year 2050 are obtained from the “100% RES” Scenario of E-Highway study [139], which is recreated and discussed in detail by Syranidou [136]. Increases in the efficiency, electrified heat demand of the residential sector, the industry and electric vehicles (battery electric vehicles and plug-in hybrid electric vehicles) and network losses are included in this electricity demand. However, within the scope of this analysis, the electricity demand required by the transport sector (electric vehicles) is excluded in order to observe the role of fuel cell electric vehicles. Comparison of battery electric vehicles and fuel cell electric vehicles is not performed due to the differences in the methodology used in the calculation of demand time series. In order to determine the hydrogen demand for passenger vehicles, 75% market penetration of fuel cell electric vehicles is assumed following the assumption of Robinius et al. [12]. Nevertheless, a sensitivity analysis of market penetration is also conducted to observe the impact on the system design. Estimation of demand time series and centroids is explained in Section 3.3.3.

Figure 3-17 displays the distribution of electricity and hydrogen demands in each region. Overall hydrogen demand across all regions is around 692 TWh, corresponding to 20.8 million tons H₂ per year. Among the regions investigated, the highest hydrogen demand, which is around 1.44 million tons H₂ per year, is observed in “90_uk” which is the region including London. Similarly, the highest demand at the country scale is also observed in the United Kingdom with a value of 3.89 million tons H₂ per year due to the combination of their high population and annual driving distance. It is then followed by France, Italy and Germany with 3.21, 2.98 and 2.71 million tons H₂ per year, respectively. The overall electricity demand across Europe is approximately 3740 TWh. At a regional scale, the highest demand belongs to “52_it” involving Milan. The highest electricity demand at a country level is in France with 576.28 TWh; which is followed by Germany, Spain, Italy and the United Kingdom with values of 575.72, 441.02, 380.05 and 356.61 TWh, respectively.

The population density distributions used in the estimation of both hydrogen and electricity demands are provided in Appendix A.1. For the sake of clarity, the raw population density with a spatial resolution of 100 m and the aggregated population for each region are provided. In order to derive these values, population projections of the E-Highway study [141] are employed.

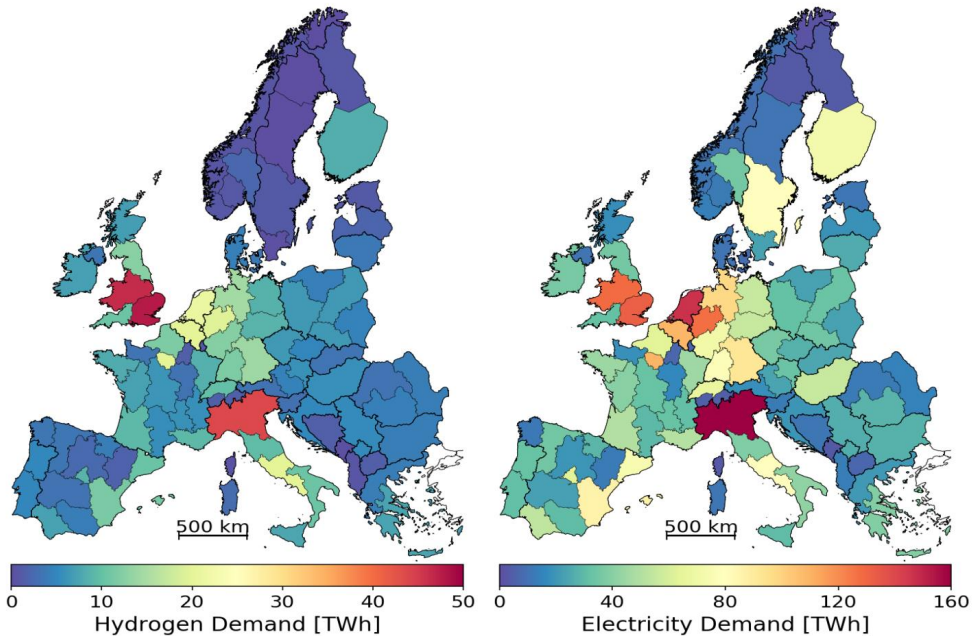


Figure 3-17 Distribution of hydrogen demand and electricity demand across regions.

3.4.3 Source Technologies

Simulations of VRES technologies are conducted by using a Python module called “RESKit” [39], [200] developed by Ryberg [37]. The offshore wind energy simulation algorithm explained in Section 3.1.2 is also incorporated this module within the context of this thesis. As a result, RESKit involves simulation workflows for onshore and offshore wind energies as well as open-field and rooftop PV systems. The detailed explanation of onshore wind and solar energy simulations can be found in the doctoral thesis of Ryberg [37]; therefore, in this thesis, the simulation workflows of these three technologies are not explained in detail.

Onshore wind energy: Uniform land eligibility constraints for the distribution of onshore wind turbines are performed by using the criteria suggested by Ryberg et al. [39], [76]. Afterward, turbines are placed with a separation distance of 8 and 4 times rotor diameter (8 for wind speed direction and 4 for the transversal direction) by using the placement algorithm in GLAES [75]. In terms of turbine design, future-oriented turbine designs are used as it is discussed by Ryberg et al. [39] since the scenario is defined in the context of 2050. Calculation of individual investment cost by cost model and their hourly simulations with corresponding weather year is performed by using the same methodology as Ryberg et al. [39].

Offshore wind energy: Application of the constraints for ocean eligibility and turbine placement is explained in Section 3.1.1. Since the scenario is defined for future energy system design (in the context of 2050), offshore wind energy simulations are also performed by using future-oriented optimal turbine designs, and it is explained in Section 3.1.4. Moreover, the investment cost of turbines at each location with different water depth, distance to shore and turbine design are calculated by the cost model expressed in Section 3.1.3.

Open-field PV: Same land eligibility constraints are used both for open-field PV with and without tracking [37]. Following this, simulation locations are determined with a separation distance of 1000 m; however, it must be noted that the overall technical potential is determined by using an open-field coverage of $20 \text{ m}^2 \text{ kWp}^{-1}$ [37]. As it is suggested by Ryberg [37], Winaico WSx-240P6 [201] is used as a module. Finally, all locations are simulated for open-field PV with single-axis tracking and for the same PV module without tracking by using the relevant algorithm described by Ryberg [37]. Both technologies are defined as individual technologies in the energy system model; however, the overall technical potential is assumed to be the same for both of them. In other words, the summation of installed capacities of open-field PV with tracking and without tracking cannot exceed the maximum allowable capacity; however, share of capacity of each technology may vary in each region. Due to the lack of data in global solar atlas beyond 60° latitude [202], this technology is excluded in most of the regions in Norway, Sweden, and Finland, which is also assumed by Ryberg [37].

Rooftop PV: Available rooftop area based on population distribution is used in order to determine the overall rooftop PV potential in each region [37]. Rooftop coverage of $6.67 \text{ m}_{\text{rooftop}}^2 \text{ kWp}^{-1}$ is assumed; moreover, as the module “LG 360Q1C-A5” is used in the simulations of rooftop PV [37]. It must be noted that north facing roofs are excluded by assuming coverage of $6.67 \text{ m}_{\text{rooftop}}^2 \text{ kWp}^{-1}$ instead of $3.33 \text{ m}_{\text{rooftop}}^2 \text{ kWp}^{-1}$, following the suggestion by Ryberg [37]. Due to the aforementioned reason about global solar atlas, this technology is excluded in most of the regions in Norway, Sweden, and Finland.

Run-of-river: The locations and time series for run-of-river, data for the year 2015 are used. Considering the high deployment of hydropower across the world (including Europe) [203], no expansion in the capacity is allowed besides the values in 2015. Moreover, within the time constraints of the project, it is not possible to model run-of-river in detail since it is highly dependent on the location. Therefore, historical generation time series and capacity values for each region suggested by Syranidou [136] are used in this analysis.

Biomass fuel: Modeling of biomass with technical potential and composition of biomass components (i.e., straw, wood chips, wood pellets... etc.) in each region could improve the system design; however, a less detailed approach is chosen due to lack of a consistent dataset for whole Europe. Biomass is modeled as a commodity that can be purchased and converted into electricity by CHP. In the E-highway study [139], two different cost values are assumed for Biomass1 (mainly

domestic and agricultural waste and forest residues) and Biomass2 (dedicated energy crops and biomass imports) of with cost values of $1.0 \text{ €}_{\text{ct}} \text{ kWh}^{-1}$ and $2.0 \text{ €}_{\text{ct}} \text{ kWh}^{-1}$, respectively. Nevertheless, the summation of both capacities is used as a single biomass component with higher cost value to maintain a conservative assumption, since the potential values in each region for latter biomass type are not provided explicitly. In addition to the cost values provided by E-Highway [139], Duić et al. [185] investigated the analysis of the biomass fuel prices in Europe for 2015, 2030, and 2050 for straws, wood chips, and wood pellets. The average biomass price in 2050 is reported as $3.5 \text{ €}_{\text{ct}} \text{ kWh}^{-1}$; for straw, wood chips and wood pellet prices of $3.0 \text{ €}_{\text{ct}} \text{ kWh}^{-1}$, $3.4 \text{ €}_{\text{ct}} \text{ kWh}^{-1}$ and $4.0 \text{ €}_{\text{ct}} \text{ kWh}^{-1}$, respectively. In addition, assuming 10% water content in wood pellets and 35% for wood chips, Oeko-Institut [186] estimated an average cost of $5.0 \text{ €}_{\text{ct}} \text{ kWh}^{-1}$ and $3.0 \text{ €}_{\text{ct}} \text{ kWh}^{-1}$ for wood pellets and wood chips for the year 2015. With an inflation rate of 3% per year until 2050, these cost values increase to $14.1 \text{ €}_{\text{ct}} \text{ kWh}^{-1}$ and $8.4 \text{ €}_{\text{ct}} \text{ kWh}^{-1}$, respectively. Although the cost values are similar in 2015, values as a result of the projection to 2050 vary significantly, especially the ones suggested by Oeko-Institut [186], which might be caused by the assumption in the inflation rate.

Taking into account all the literature values, the resulting economic parameters are determined and presented in Table 3-3. It must be noted that the specific investment cost of onshore and offshore wind turbines given in Table 3-3 are for reference turbine designs. The average specific investment cost for each region for these technologies is calculated by using cost models explained in Section 3.1.3 as also by Ryberg et al. [39].

Table 3-3 Techno-economic parameters of generation technologies considered in the analysis.

	Economic Lifetime [a]	Investment [€ kW ⁻¹]	Fix O&M [% CapEx]	Variable O&M [€ MWh ⁻¹]	Source
Onshore wind turbine ¹⁴	20	1100	2.0	0	[39]
Offshore wind turbine ¹⁵	25	2300	2.0	0	[60]
Open-field PV with tracking	25	710	1.5	0	[168]
Open-field PV without tracking	25	520	1.7	0	[168]
Rooftop PV	25	880	2.0	0	[168]
Run-of-river	60	0 (5620) ¹⁶	1.5	5.0	[168]

¹⁴ Onshore wind turbine values correspond to a reference turbine (capacity: 4 MW, rotor diameter: 136 m, hub height 100 m) [39]

¹⁵ Offshore wind turbine values correspond to a reference turbine (capacity: 9.4 MW, rotor diameter: 210 m, hub height 135 m, distance to shore: 60 km, water depth: 40 m, foundation: monopile) [60]

¹⁶ Due to the assumption of existing run-of-river plants (2015 data) is employed, investment cost is not defined for this technology. However, investment cost is assumed as 5620 € kW^{-1} in the calculation of O&M costs.

When the cost values and generation time series defined for each region are used to calculate LCOE of corresponding technologies, the distribution shown in Figure 3-18 is obtained. In terms of onshore wind energy, it is seen that Ireland has the lowest LCOE. Generally, the regions in the south have higher LCOE values. A similar trend can be observed in offshore wind energy except for Greece, which is caused by the higher full load hours around the Aegean Sea (when compared with the Mediterranean Sea). Moreover, a wide range is observed in the offshore LCOE between 4.6 and 15.6 €_{ct} kWh⁻¹.

Unlike wind energy, open-field PV both with and without tracking has less variation between regions. The main variation in the LCOE is observed between northern and southern regions, as is expected. A comparison of open-field PV technologies reveals a slight difference in the LCOE when the tracking system is used. Although the specific investment cost of the one with the tracking system is higher, it has a higher generation early in the morning and late in the afternoon resulting in slightly higher FLH. The difference is pronounced more in the northern regions, especially the United Kingdom and Ireland.

The comparison of all PV technologies, which include rooftop PV, open-field PV with tracking, and open-field PV without tracking systems, is seen from Figure 3-18. The average LCOE for rooftop PV systems is higher compared to the open-field PV systems with a difference of nearly 4 €_{ct} kWh⁻¹. This can be explained by the higher investment cost of rooftop PV systems as discussed earlier (cf. Section 2.3.3.1). On one hand, the specific investment costs of open-field PV with and without tracking systems vary between 520 to 710 € kW⁻¹, whereas for rooftop PV, this value increases to 880 € kW⁻¹. On the other hand, the full load hours do not differ significantly. As a result, higher average LCOE is attained for rooftop PV.

Despite the higher investment cost, rooftop PV systems have several advantages. The use of electricity generated via rooftop PV systems has been more beneficial instead of feeding the electricity into the grid owing to the discrepancy between PV feed-in tariffs and electricity price from the grid [204]. A combination of the rooftop PV system with storage increases the self-consumption while decreasing the grid-dependency. Nevertheless, within the scope of this thesis, the distribution grid and behavior in the residential sector are not taken into account. Therefore, the optimization problem is not able to take into account these aspects (i.e., self-sufficient and lower grid dependency). Due to the nature of the optimization with the objective of cost minimization, the cheapest electricity generation method is generally preferred. In other words, open-field PV and rooftop PV systems are modeled in the same way independent from the consumer behavior; thus, rooftop PV technologies are not involved in the optimal solutions due to lower investment cost of the open-field PV systems (cf. Table 3-3).

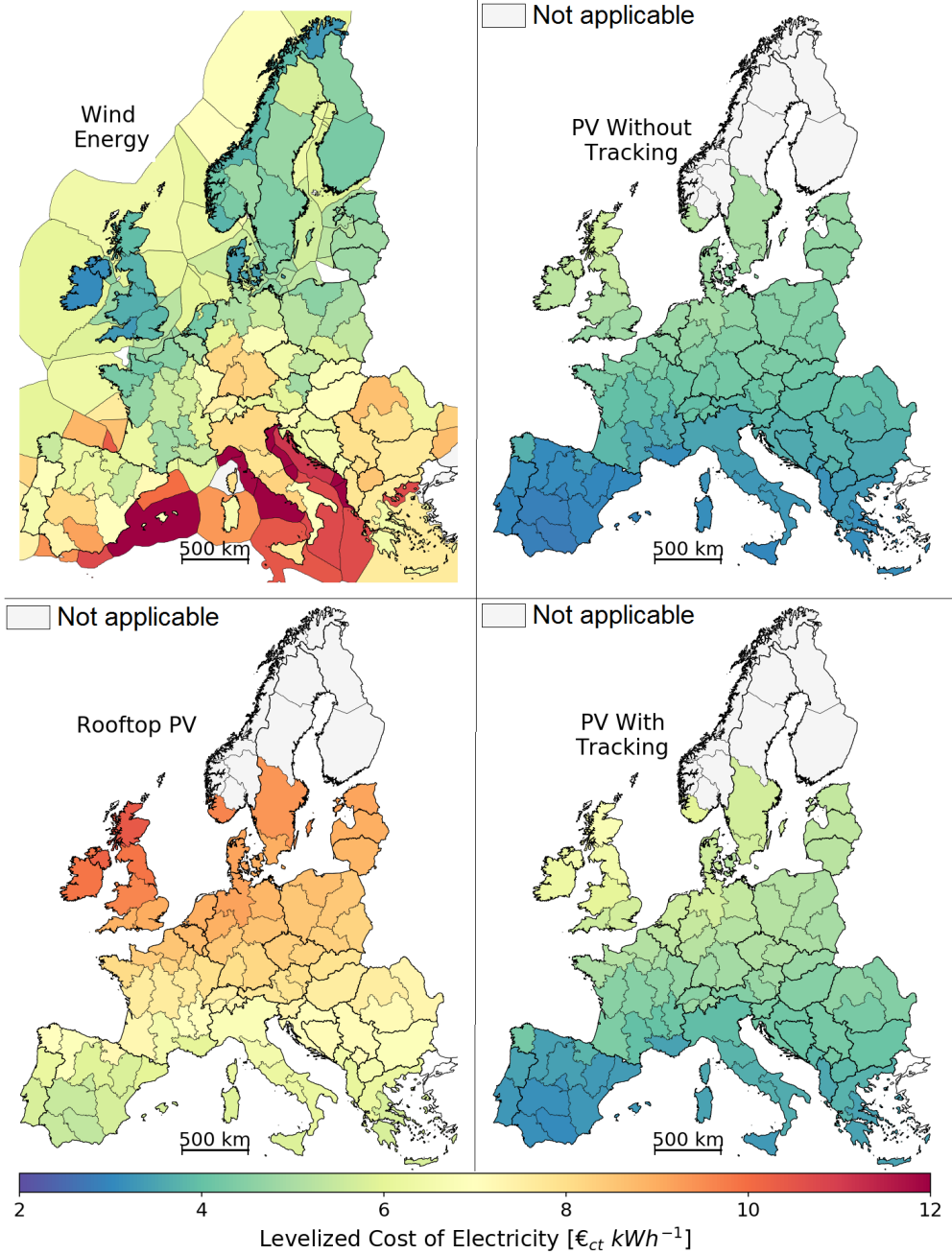


Figure 3-18 LCOE of onshore, offshore, rooftop PV, open-field PV with tracking and open-field PV without tracking for single grouping of technologies with a weather year 2015.

3.4.4 Storage Technologies

Salt caverns and gas vessels are included in order to store hydrogen. For electricity storage, lithium-ion batteries are considered, since they are found to be the dominant daily storage options among several other storage options [135]. In addition, pumped-hydro storage (PHS) and reservoir storage are taken into account. The maximum storage potential of the salt cavern is calculated by using the methodology explained in Section 3.2. For PHS and reservoir storage, storage and plant capacities in terms of GWh and GW are obtained for the year 2015 similar to run-of-river. These capacities are defined as fixed capacities, and further expansion is not allowed in the energy system since the determination of potential locations for these technologies and also inflow requires a more detailed analysis with appropriate data, which is not possible to implement within the time constraints of this analysis. Inflow time series are obtained from Syranidou [136] for the year 2015. A maximum storage capacity for vessels or lithium-ion battery is not defined in the system since they can be scaled depending on the demand for these technologies.

Figure 3-19 shows the shares and distribution of maximum storage potential of salt caverns, PHS, and reservoir storage. It is seen that the storage potential of salt caverns are orders of magnitude higher than that of PHS or reservoir storages. The highest storage potential for salt caverns is observed in two regions in northern Germany, with an approximate value of 8.9 PWh. These regions are followed by regions in Poland 7.1 PWh. These values are caused by the high storage potential of salt caverns built-in salt domes, which are located mainly in these regions. The highest storage potential for PHS and reservoir storage are observed in Norway and Sweden with values of 80 and 30 TWh, respectively. All in all, it is seen from the figure that almost all the regions have either salt cavern storage or hydro storage (PHS and reservoir storage).

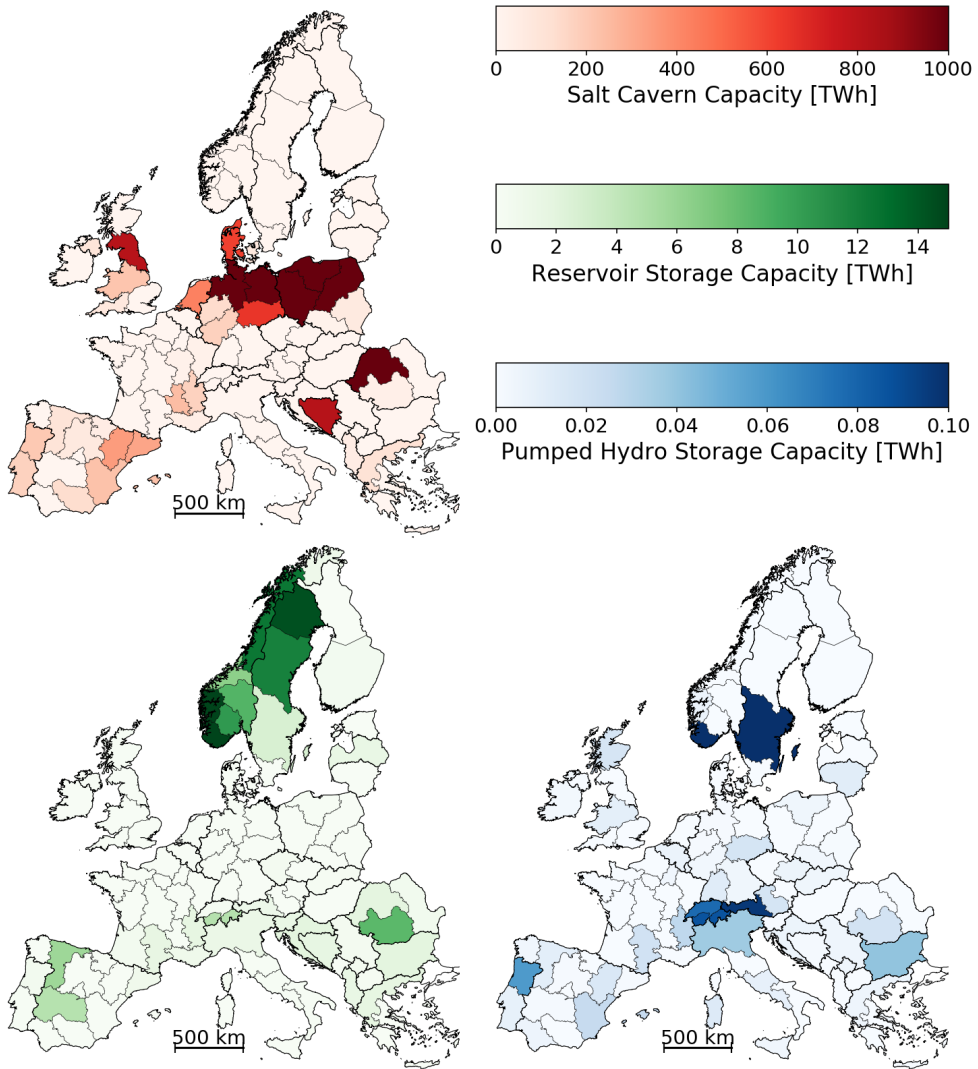


Figure 3-19 Maximum storage potential for salt caverns, reservoir and PHS storage in regions.

Parameters for storage technologies used in the analysis are listed in Table 3-4. It must be noted that the investment cost of PHS and reservoir storage is not defined in the energy system model; however, for the calculation of fixed O&M, a specific investment cost of 2200 € kW⁻¹ is assumed [168]. Moreover, the investment cost of the salt cavern is calculated by a reference salt cavern capacity of 133 GWh, the investment cost of which is assumed to be approximately 48 million € [184].

Table 3-4 Techno-economic parameters of storage technologies considered in the analysis.

	Economic Lifetime [a]	Investment [€ kWh ⁻¹]	Fixed O&M [% CapEx]	Variable O&M [€/MWh]	Source
PHS & reservoir storage	60	0 ¹⁷	1.0	3	[168]
Salt cavern	30	0.362	2.0	0	[187]
Lithium-ion battery	22	151	1.0	0	[191]
Vessel	20	7.5	2.0	0	[13], [184]

3.4.5 Conversion Technologies

Several conversion technologies are employed in the analysis in order to compare their performance by efficiency and cost. Polymer electrolyte membrane electrolyzer (PEMEL) is used for the production of hydrogen from electricity, due to their development in terms of performance as well as the decrease in the investment cost [175]. In terms of re-electrification, all the technologies used by Welder et al. [188] considered to be able to compare the efficiency and cost of individual technologies, which include polymer electrolyte membrane fuel cells (PEMFC), solid oxide fuel cell (SOFC), hydrogen open cycle gas turbine (OCGT), hydrogen combined cycle gas turbine (CCGT) and hydrogen gas engine. The techno-economic parameters of the conversion technologies are given in Table 3-5. Although the efficiencies of PEMFC and SOFC are higher, their costs are also higher than the ones of OCGT, CCGT, and gas engines. Finally, biomass combined heat and power (CHP) is also considered for the conversion of biomass fuel into electricity. The maximum capacity for this technology is introduced due to the capacity limitations of biomass. For this purpose, the biomass capacity values are given in the “100% RES” scenario, and techno-economic parameters have been defined by using the values used by the E-Highway study [139] in order to have consistent modeling of biomass in terms of techno-economic parameters of biomass CHP.

¹⁷ Due to the use of existing PHS and reservoir storages, investment costs of these technologies are not defined, yet for the calculation of O&M costs a value of 2200 € kW⁻¹ is assumed as an average investment cost.

Table 3-5 Techno-economic parameters of conversion technologies considered in the analysis¹⁸.

	Economic Lifetime [a]	Efficiency [%]	Investment [€ kW ⁻¹]	Fixed O&M [€ kW ⁻¹ a ⁻¹]	Variable O&M [€ MWh ⁻¹]	Source
PEMEL	10	70	500	3% of CapEx	0	[184]
PEMFC	10	51	923	0	7.5	[187]
SOFC	10	70	1500	2.0	0	[187]
H ₂ Gas Engine	20	48.5	715	4.0	7.0	[187]
H ₂ OCGT	25	40	504	5.0	7.5	[187]
H ₂ CCGT	25	60	760	11.0	2.4	[187]
Biomass CHP	30	38	2600	2.5% of CapEx	0	[172]

3.4.6 Transmission Technologies

Electricity can be transported via the electrical grid which includes high-voltage alternating-current (HVAC) and high-voltage direct-current (HVDC) lines. In this analysis, HVAC and HVDC line capacities within the context of 2050 are obtained from the E-Highway study. The simplified equivalent grid for HVAC and HVDC lines can be seen in Figure 3-20 with their corresponding capacities. Moreover, further expansion of the grid is not allowed. It must be noted that grid topography data for the year 2050 does not exist yet; nevertheless, consideration of existing lines with addition to the expansions suggested by the “Ten Year Network Development Plan” (TYNDP) [190] is a common method applied by studies developed for future applications [136], [139]. The Equivalent Impedances and the Power Transfer Distribution Factor (PTDF) methods are compared on an exemplary case in their analysis [140], and the Equivalent Impedances method is employed for grid reduction by E-Highway study.

In terms of hydrogen transportation between regions, only pipelines are considered as transmission technologies, since pipelines are found to be the cheapest transportation method in large scale transportation between long distances [184]. Injection of hydrogen to the natural gas grid is not considered, since hydrogen injection to the existing natural grid is not considered as a business case [9]. Routing of these pipelines between centroids of the regions is performed by using the methodology explained in Section 3.3.4. Existing natural gas pipelines [81], railways,

¹⁸ PEMEL: Polymer Electrolyte Membrane Electrolyzer, PEMFC: Polymer Electrolyte Membrane Fuel Cell, SOFC: Solid Oxide Fuel Cell, H₂ OCGT: Hydrogen Open Cycle Gas Turbine, H₂ CCGT: Hydrogen Combined Cycle Gas Turbine, Biomass CHP: Biomass Combined Heat Plant

highways and primary roads are considered by using Prior datasets of GLAES [75]. After combining these connections, the shortest connection between each region is estimated. Results including all possible connections between regions are shown in Figure 3-20. It must be noted that the connection between the United Kingdom and Norway results from the shape of natural gas pipelines between those regions in the North Sea. Being the only possible solution to the lack of railways and roads on the North Sea, these connections are found to be the shortest ones. Finally, the distances between regions are calculated by using these routes in order to determine the cost of the pipelines which is a function of both capacity and the length of the connection.

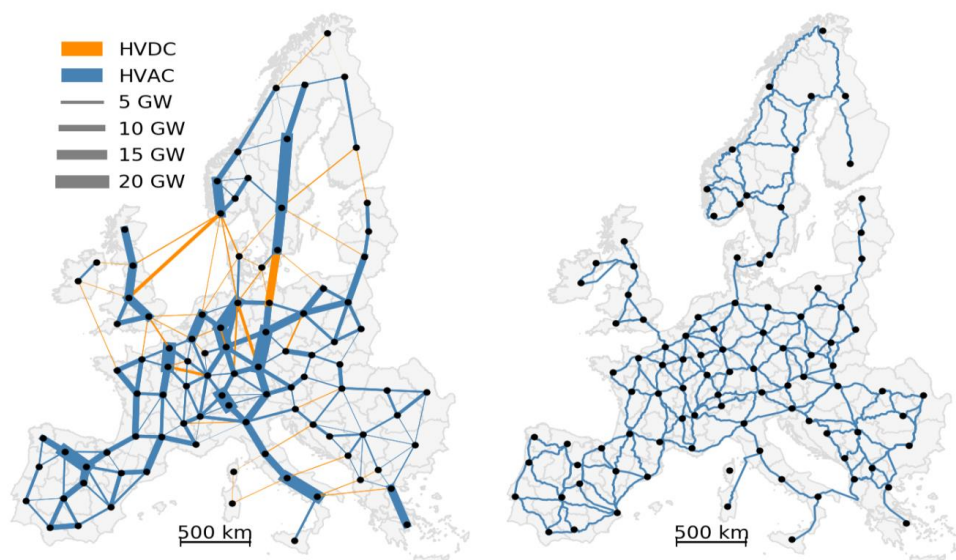


Figure 3-20 Left: HVAC and HVDC connections between regions and their corresponding line capacities. Right: all possible hydrogen pipeline connections between regions.

As previously discussed, Mischner [189] estimates the pipeline cost per unit capacity and distance as a function of the pipeline diameter, which can be seen in Figure 3-21. Green points on the figure show the cost of the pipeline estimated by Mischner [189]. However, it is required to be linearized due to the intractability problems of the optimization. Blue lines in Figure 3-21 show the linear fit to the cost values suggested by Mischner [189]. However, the definition of 333.8 €/m as a cost component causes an energy system model to become a mixed-integer linear program, which takes longer to solve the optimization problem. Therefore, the total linearization of pipeline cost is estimated by fitting the orange line shown in the same figure, which underestimates the pipeline cost at low capacities and overestimates at high capacities. As a conservative approach, such a cost is defined for the pipelines instead of totally underestimating the cost at all capacities. By doing so, energy system is totally modeled as a linear program, which can be considered as a

reasonable simplification. In the end, assumed pipeline cost is $185 \text{ € kW}^{-1} \text{ km}^{-1}$ with an economic lifetime of 40 years. Conversion of hydrogen mass flow into energy flow (from kg to kW) is explained in the coming paragraph. Both operation and maintenance costs are defined to be $1 \text{ € kW}^{-1} \text{ km}^{-1} \text{ a}^{-1}$. However, in order to observe the variations with respect to the assumed pipeline cost, a sensitivity analysis is performed (three scenarios with cost values of $145 \text{ € kW}^{-1} \text{ km}^{-1} \text{ a}^{-1}$, $185 \text{ € kW}^{-1} \text{ km}^{-1} \text{ a}^{-1}$ and $225 \text{ € kW}^{-1} \text{ km}^{-1} \text{ a}^{-1}$). The result of this sensitivity analysis is presented in Section 5.5.1.

The conversion of pipeline diameter into capacity is performed by assuming an average gas flow of 15 m s^{-1} with a density of 5.7 kg m^{-3} . Following this, the mass flow rate of hydrogen within the pipe is estimated by using Equation 15 for different pipeline diameters ranging between 0 to 1.4 m, which is the largest diameter used for natural gas transport. Where \dot{M}_{H_2} is the mass flow of hydrogen in kg s^{-1} , v is the velocity in m s^{-1} and D is the pipeline diameter in m.

$$\dot{M}_{H_2} = v \cdot \frac{\pi D^2}{4} \quad \text{Equation 15}$$

Following this, capacity is estimated by multiplication of mass flow rate by a lower heating value, which is assumed as 33.3 kWh kg^{-1} of hydrogen [196].

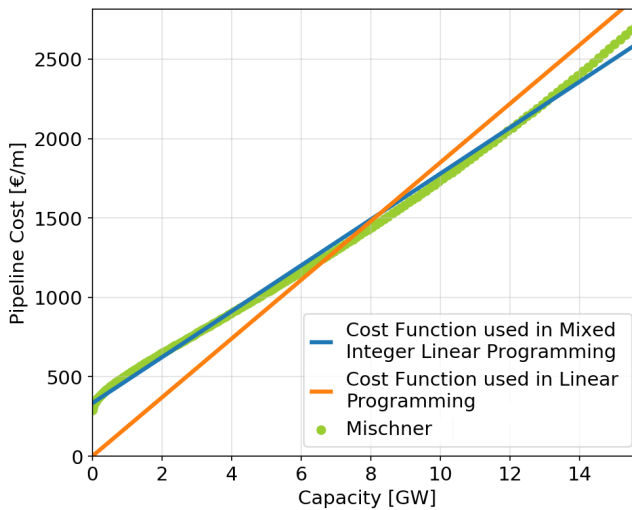


Figure 3-21 Comparison of different assumptions in the pipeline investment cost as a function of capacity. Contains data from Mischner [189].

3.5 Discussion on the Impact on Time Series Aggregation

In order to observe the impact of time series aggregation on the optimization, a sensitivity analysis is performed (c.f. Section 5.1). However, the test runs with a higher number of VRES groups revealed the limitation of memory. As a result, the sensitivity analyses presented in Section 5 are performed by using 30 typical days. Nevertheless, especially the final results on the proposed design unveil the deviations caused by time series aggregation. In order to investigate it further in detail, exemplary regions and technologies are chosen and shown in this section. Figure 3-22 shows the percent error estimated by 30 typical days as well as the hourly generation time series for onshore wind energy in “32_de”. The percentage deviation of hourly time series estimated via time series aggregation is limited between $\pm 150\%$, yet larger values are also observed. For example, the high generation period seen on the 248th day of the year is underestimated with time series generation. An overview of this figure reveals that the overestimation generally expands over a day.

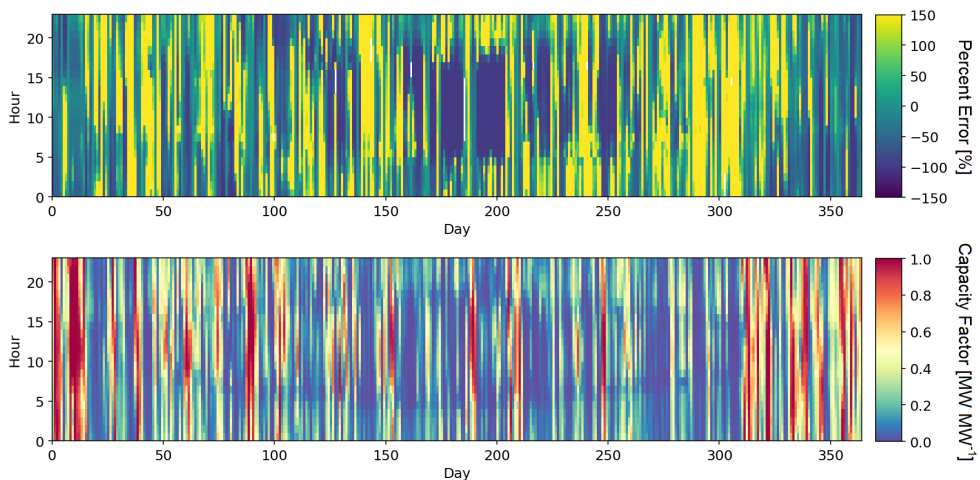


Figure 3-22 (Upper) Percent error caused by time series aggregation with 30 typical days, (Bottom) Capacity factor time series of onshore wind energy in “32_de” for the weather year 2015.

Figure 3-23 is another representation of the error shown in Figure 3-22 for northeastern Germany. For this purpose, the percent error is multiplied by the capacity factor at each time step to estimate the absolute error. Following this, the absolute error is sorted by their values and plotted in order to observe the amount of over- and underestimations. Due to the limitations discussed earlier, the use of 30 typical days is not representative of all regions and technologies. Nevertheless, nearly a homogenous distribution is seen with underestimation in half the year and overestimation in the other half.

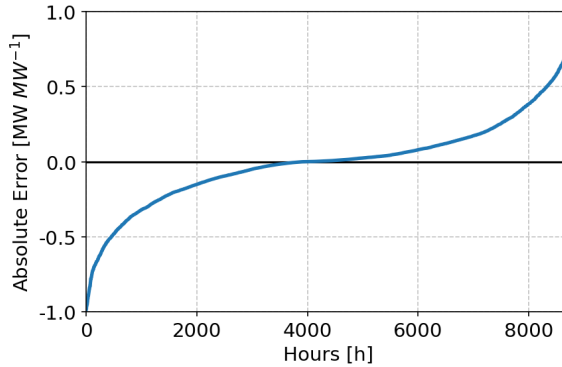


Figure 3-23 Distribution of absolute error¹⁹ estimated for 30 typical days for onshore wind energy in “32_de” for the weather year 2015

In the case of open-field PV with tracking, the behavior is slightly different. There are some days that the generation is overestimated for an entire day. Late January (20th day) can be an example since not only some hours, but an overestimation of 150% is observed for all hours. Moreover, an underestimation of nearly 50% is also observed mainly around February-March (around 50th day of the year). In addition to errors observed for all days, the highest underestimation is observed in early mornings and late evenings.

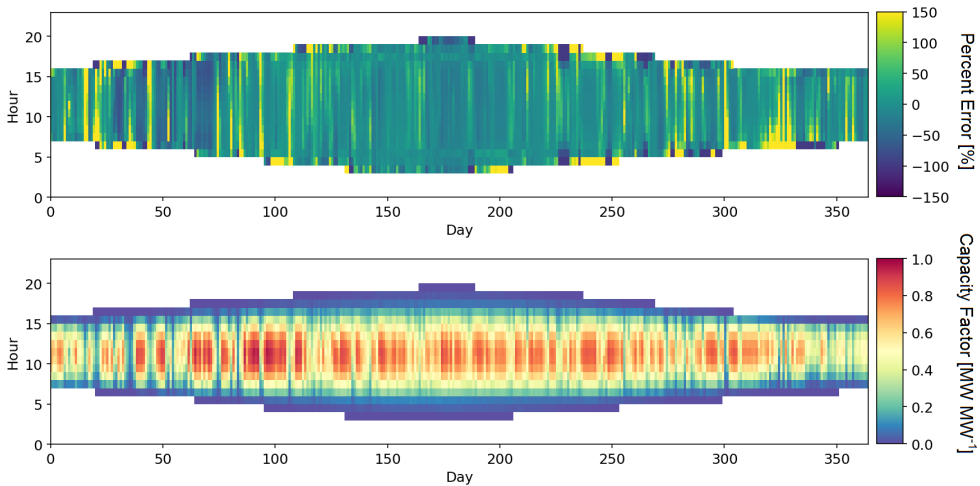


Figure 3-24 (Upper) Percent error caused by time series aggregation with 30 typical days, (Bottom) Capacity factor time series of openfield PV in “32_de” for the weather year 2015.

¹⁹ Absolute error is calculated by taking the difference between hourly capacity factor time series data estimated by time series aggregation and actual data used. In other words, positive absolute error indicate overestimation by time series aggregation, while negative means underestimation.

3.6 Robust Energy System Design over 38 Weather Years

In order to obtain a robust system design, an iterative approach is taken in this analysis. According to this approach, the averages of optimal capacities across 38 weather years presented in Section 5.3 are calculated. Afterward, these average capacities are defined as the minimum capacity to be installed in the system allowing the optimizer to choose only capacity values higher than the averages. Moreover, the maximum capacities for each technology are changed to the maximum values estimated in Section 5.3, since the optimal solution would not require capacities more than previously determined maximum optimal capacities. In order to clarify the method, an example for the Netherlands is further explained for salt caverns. As it is presented in Section 5.3 and shown in Figure 5-10, there is a large variation in the optimal storage capacities of salt caverns in the Netherlands. The minimum, average and maximum storage capacities for salt caverns in the Netherlands are estimated as 1711, 10484 and 31816 GWh, respectively. Thus, the minimum capacity for salt caverns in the Netherlands is set to 10484 GWh, while the maximum capacity is also changed to the 31816 GWh (the maximum value amongst all weather years). This procedure is applied to all technologies except run-of-river, pumped hydro storage, hydro reservoirs, HVAC and HVDC cables, since their capacities have not been optimized but fixed in the beginning (c.f. Section 3.4). An additional consideration is taken into account for hydrogen pipelines by defining the minimum and maximum capacities only for the connections repeating 50% of the weather years, since the others occasionally appear, meaning that those connections are not crucial for the system design. Once all the minimum and maximum capacities are changed for the corresponding technology, each weather year is optimized. This whole process, from the calculation of minimum and maximum capacities, changing the input files, and optimizing every weather year with the new capacity values, is considered as iteration. In total, only three iterations are performed, since the variation in the results has become insignificant. In other words, the total annual cost and average capacities have a narrow range except for the extreme weather years. In these years, the optimal capacities of individual technologies have been increased to some extent to be able to supply the demand.

After attaining a plateau in terms of capacities, the average capacities are fixed for all technologies except biomass CHP plants. Therefore, biomass is assumed to be the back-up generator owing to its dispatchable nature at this stage. Moreover, after this point, time series aggregation is not needed, because capacity optimization is not performed anymore. Therefore, one more iteration round is conducted with fixed capacities of all technologies except biomass CHP plants and without time series aggregation so that the extreme time periods which cannot be covered by time series aggregation are eliminated. The primary purpose of this step is to determine the amount of biomass CHP plants that should be installed so that the security of supply is ensured among all the weather years.

Finally, the final system design is obtained by extracting the maximum capacities of biomass CHP plants among all weather years. All in all, the capacities determined as a result of the iterations,

maximum required biomass capacities determined without time series aggregation results in the final system design, which can be considered as the most robust design with slightly higher total annual cost to ensure the security of supply. The final energy system design by using the method explained in this section will be discussed in Section 6.

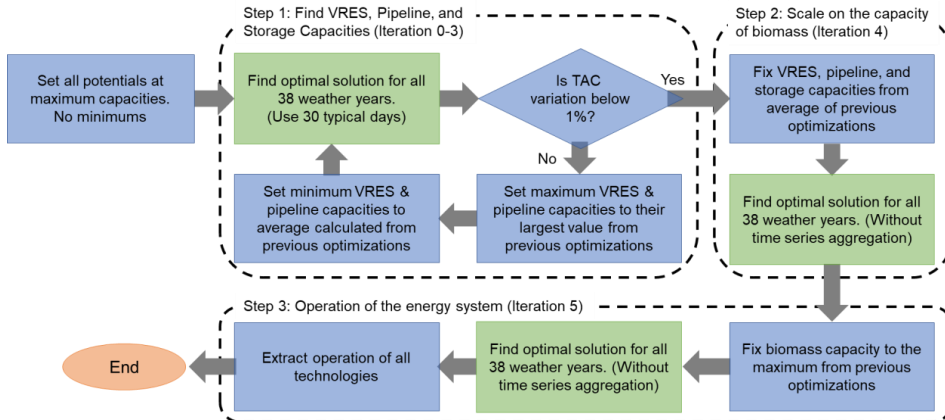


Figure 3-25 Algorithm used in the enhanced energy system design to ensure the security of supply.

3.7 Summary

In this section, the methodologies employed to derive the techno-economic potential of offshore wind energy and technical potential of salt caverns across Europe are explained. In addition, the model chain developed to combine the existing frameworks with its additional features are briefly provided. Definition of a 100% renewable energy system scenario across Europe with the scenario boundaries and assumptions are also explained.

The techno-economic potential of offshore wind energy is derived by using three fundamental analyses: ocean eligibility, turbine simulation, and cost estimation. Constraints of ocean eligibility and how they are applied within the context of this work are briefly explained in Section 3.1.1. For this analysis, both fixed-bottom and floating wind turbines are taken into account with a maximum water depth of 1000 m. Following this, the offshore simulation algorithm is briefly explained. As the third component, how the existing cost models are put together and scaled to the future-oriented turbine designs are clarified. Finally, how these individual components are put together to derive capacity and generation potentials in the case of optimal and uniformly applied single turbine designs is illustrated.

Following the methodology used in the derivation of the technical potential for salt caverns is explained in Section 3.2. Application of land eligibility on the salt formations and design of salt

cavern geometries are discussed thoroughly in this section. Finally, the salt caverns distributed over available salt formations with their corresponding cavern volume are used to calculate individual cavern storage capacities, which are also a function of the cavern depth.

A model chain called “Model Aggregation Toolset for Energy Systems (MATES)” is developed in order to combine the existing toolsets and automatize the workflow of building an energy system model as much as possible. Moreover, additional features such as netCDF4 files for input and output of the optimization model are included in MATES to be able to store inputs and outputs together. A base scenario definition is proposed in Section 3.4. In this definition, the technology portfolio, as well as the techno-economic parameters assumed within the context of this work, is explained. Four different commodities (electricity, hydrogen, water, and biomass) are taken into account with several source, sink, conversion, storage, and transmission technologies.

The validity of “Time Series Aggregation” within the scope of this work has been discussed since it is used in the exploratory sensitivity analyses of energy system design. Although the overall error is relatively small, days with under- or overestimation are observed for specific technologies. Finally, a method to develop a robust energy system design is proposed in order to ensure the security of supply among 38 weather years considered in this analysis. For this purpose, the optimal results of the energy system design of individual years are used in order to calculate the mean and maximum capacities for each technology and the region. Then, an iterative approach is employed to derive a robust system design that can withstand.

4 Estimated Potentials for Offshore Wind Energy and Salt Cavern Storage

The input parameters are crucial while building a 100% renewable energy-based European energy system model since the design might alter by different assumptions. The techno-economic data required for the model are obtained from the existing model chain and data (described in Section 3.4) except the two technologies: offshore wind energy and salt caverns. As it is explained in Section 3.1 and Section 3.2, a detailed analysis is performed for these two technologies in order to obtain a consistent dataset taking into account the future energy system design (especially wind turbine design). Therefore, intermediate results referred in this section involve the results of proposed methodologies explained in Section 3.1 and Section 3.2. These results consist of the techno-economic potential of offshore wind energy and the technical potential of salt caverns across Europe.

4.1 Techno-economic Potential of Offshore Wind Energy in Europe

The techno-economic potential of offshore wind energy changes with the scenario definition as well as the boundaries defined in the assessment. Therefore, this section involves several results of the techno-economic potential of offshore wind energy based on different turbine definitions in order to compare different potential scenarios. Section 4.1.1 includes the results of optimal turbine designs obtained by the method explained in Section 3.1.4; moreover, it is available as a journal article published by Caglayan et al. [60] in “Applied Energy”. Following this, potential results estimated by uniformly applied single turbine designs are compared in Section 4.1.2. Finally, optimal turbine designs are clustered in order to have similar turbine designs which can be used in the design of wind parks and so on. A different number of clusters and their impact on the potential have been analyzed and presented in Section 4.1.3.

4.1.1 Optimal Turbine Design

This section shows the specifications of cost-optimal turbine designs across Europe. Independent of the ocean eligibility assessment, the analysis remains general and applicable to other eligibility scenarios. However, the discussion of these results will mainly focus on suitable locations within the constraint scenario outlined. As previously mentioned, the region of interest comprises European maritime boundaries excluding Iceland. Therefore, the areas belonging to northern African countries such as Morocco and Tunisia are not presented here. The content discussed in this section is directly taken from the aforementioned article published by Caglayan et al. [60].

Figure 4-1 displays the resulting turbine design characteristics, including capacity (a), hub height (b), foundation type (c) and the corresponding FLH (d). Focusing first on the capacity distribution reveals that a large variety of capacities result from cost optimality. Turbines with lower

capacities are preferred in areas with low sea depth and low wind speed, which can often be found closer to shore. Although lower capacities are primarily installed in near-shore areas, there are some exceptions, such as near to the Dogger Bank area in the North Sea, where relatively low capacities are found despite being far from shore. This observation supports the trend of lower capacity turbines installed in regions with relatively low wind speeds. This can be explained by the low-cost sensitivity of the selected increments in capacity in that area. Where high wind speeds are found, the maximum capacity observed in this analysis occurs around the northern UK, Ireland and southern France. In general, the designed capacities in the deep-sea regions are approximately 16 MW, whereas this value decreases to 10 MW in the near-shore North Sea region with low sea depth.

Like capacity distribution, there is some similarity in lower hub heights of between 130-140 m in the near-shore North Sea and Northern Adriatic Sea, as is shown in Figure 4-1(b). Likewise, in deeper waters, and especially in the Mediterranean Sea and Bay of Biscay, hub heights are in the range of 160-170 m. The maximum hub height of 200 m can mainly be observed in the Mediterranean Sea, where a floating foundation is necessary. The vast majority of locations attaining a 200 m hub height are excluded due to water depth, however. In general, as the distance from shore increases, hub height always increases with reference to the respective magnitude at the coast due to increasing water depth. The abrupt variation in the middle of the North Sea is one exception to this, however. This variation in hub height, as well as capacity, is mainly due to the hub height discretization, resulting in cascading design changes in the other parameters. A more in-depth investigation, which will be presented in Section 4.1.3, reveals that despite this discrete design step, there is only a negligible change in the final LCOE of 0.02% with finer discrete design steps. Compared with a previous analysis of onshore wind energy, hub height design is seemingly the opposite of the onshore turbine design trend predicted by Ryberg et al. [39] where, as a rule, capacity increases, and hub height decreases, along with increasing average wind speed. In this case, the rise in hub heights while moving away from the shore corresponds to increasing wind speed. This effect is caused by the balance of system cost model functions, where the cost is not as sensitive to hub height compared to the other parameters, such as distance to shore or water depth. Therefore, high hub heights in deep-sea regions are preferred in order to access higher FLH and offset the increase in investment costs. High hub heights are not seen only to the deep sea, however, as it can be seen that higher hub heights and lower capacities are chosen for locations near to shore and with lower wind speeds.

The distribution of foundation types is shown in Figure 4-1(c). The jacket is not chosen except in a few regions that are extremely close to shore, whereas in near-shore regions it is predominantly monopile. Spar, in particular, is chosen when close to shore and with water depths greater than 100 m, as is seen in the areas surrounding Italy and much of Spain. Depending slightly on the distance to shore, there is a distinct transition between a monopile and semisubmersible foundation around 50 m in water depth. This is notable because it is within the range where all foundation options except spar are possible, and yet the jacket foundation is still not selected. In

their report, Maness et al. [54] state that monopile is economically preferred between 0-40 m water depth, after which jacket should become the most economical option. Nevertheless, this is not observed here, which may be caused by the difference in the U.S. versus European deployment. Besides economic considerations, the mitigation potential for greenhouse gas emissions can affect decisions on turbine design, too, when considering a life-cycle perspective. Considering the life cycle greenhouse gas emissions of wind turbines performed by Wang et al. [52], the intensity of a coal plant is 3 times higher than onshore turbines and 2 times higher than offshore wind turbines (higher intensity of offshore wind turbines is caused by the fixed floating platform in the sea). Moreover, a similar analysis is performed by Huang et al. [53] on the life cycle assessment and net energy analysis of offshore wind turbines. Huang states that offshore wind energy is acknowledged with the recycling of waste materials and a reduction in the material amount [53]. Finally, Bonou et al. [51] estimated greenhouse gas emissions of offshore wind energy as 11 g CO₂-eq. kWh⁻¹. Moreover, bigger turbines with direct-drive generators are found to have better performance compared to the small and geared turbines [51].

Figure 4-1(d) shows the distribution of FLH in the region of interest ranging between 2000-6000 h a⁻¹. Despite the wide range observed across Europe, there is a clear difference between regions. For example, the values of FLH in the North Sea and Northwestern British Isles attain 5000-6000 h a⁻¹. On the other hand, FLHs are generally below 4500 h a⁻¹ in the Adriatic Sea, with some even lower than 3500 h a⁻¹. Independent of the average FLH in a region, there is always an increase in the FLH as the distance from the shore increases. In the very near shore cases, this can be caused by the chance arrangement of the MERRA-2 grid cells that are oriented directly over the coastline. Complex micro-scale climactic interactions caused by the terrain are not well reflected within the single MERRA-2 cell due to its low resolution, and because of this, inconsistent design behavior is possible. This is especially noticeable in western Portugal and southwestern France. In spite of this behavior, these areas are excluded due to the distance to shore constraint and do not affect the final results that are presented in this analysis.

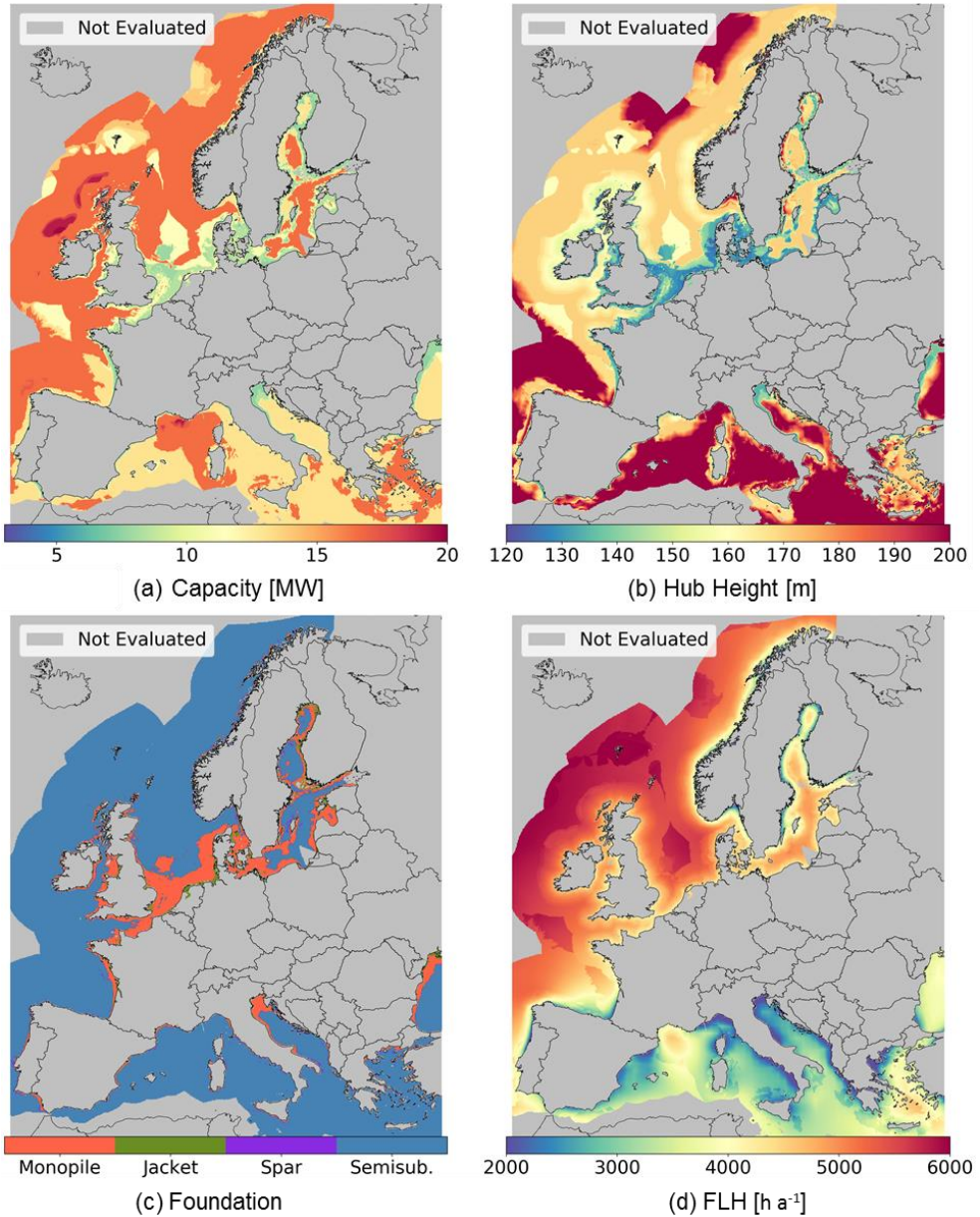


Figure 4-1. Specifications of resulting turbine design across European maritime boundaries, a) capacity, (b) hub height, (c) foundation, (d) FLH with optimal design [60].

4.1.2 Literature Comparison and Application of Different Single Turbine Designs

In order to have a comparison of own results and values reported in the literature, the overall methodology is applied by using characteristics of a single turbine available in the literature. The turbine used in the single turbine design scenario has a capacity of 13 MW with a 212 m rotor diameter and 128 m hub height, corresponding to the baseline scenario of Wind Europe [62]. Placement of this turbine is performed across all eligible areas, totaling 956,000 potential locations, each of which was simulated between weather years 1980 and 2017 to calculate the average capacity factor for each location. The total capacity, generation, and average FLH across all locations are 12.4 TW, 43.65 PWh and 3500 h a^{-1} , respectively. Afterward, by using the constant turbine specifications in addition to depth and shore distance values specific to each location, the turbine cost is calculated. LCOE is then calculated based on the cost, as well as the average FLH. Figure 4-2 compares LCOE estimates available in the literature to the distribution of results observed in this scenario and the optimal turbine design. Although the analysis is performed in the context year 2050, LCOE enhancements over time are shown so that the importance of future turbine designs can be recognized.

A few studies have cost projections through 2050 and predict values of between 4-12 $\text{€}_{\text{ct}} \text{ kWh}^{-1}$ ([44], [93], [131], [168], [170]); however, they are generally performed by using an average capacity factor and cost for the single turbine design across Europe. In addition to the projections in 2050, two reports published by Kost et al. [43] and Hobohm et al. [42] provide LCOE estimations for Germany through 2035 and 2023, respectively. Hernandez et al. [45] estimate LCOE for fixed-bottom wind turbines, only considering deep water and up to 50 km distance from shore for 2025 and 2030. European Wind Energy Association (EWEA) [46] reported a decrease in LCOE down to 9 $\text{€}_{\text{ct}} \text{ kWh}^{-1}$ by 2030. Moreover, IRENA [73] published a cost estimation for offshore wind energy in 2020 in accordance with global trends and outlooks. When the method explained in Section 2 is employed, the results with a single turbine design show a wide range across Europe concerning the distribution to all eligible locations. Nevertheless, 75% of turbines with single turbine design are in the range of 4-12 $\text{€}_{\text{ct}} \text{ kWh}^{-1}$, which shows good agreement with the LCOE values determined in the literature. Ultimately, in this scenario, the average LCOE of all turbines that can be placed within the eligible area is found to be 10.3 $\text{€}_{\text{ct}} \text{ kWh}^{-1}$, whereas the median is 9.2 $\text{€}_{\text{ct}} \text{ kWh}^{-1}$.

Despite of the high LCOE values observed in single turbine analysis shown as a long tail in Figure 4-2, there is a good agreement between the presented results and literature values. It must be noted that most of these values are estimated by using a reference capacity or wind park instead of the distribution obtained as a result of a technical potential analyses. Therefore, focusing on the high relative occurrence observed between 5 and 15 $\text{€}_{\text{ct}} \text{ kWh}^{-1}$ reveals that there are many locations within the cost range estimated by a few studies in the literature.

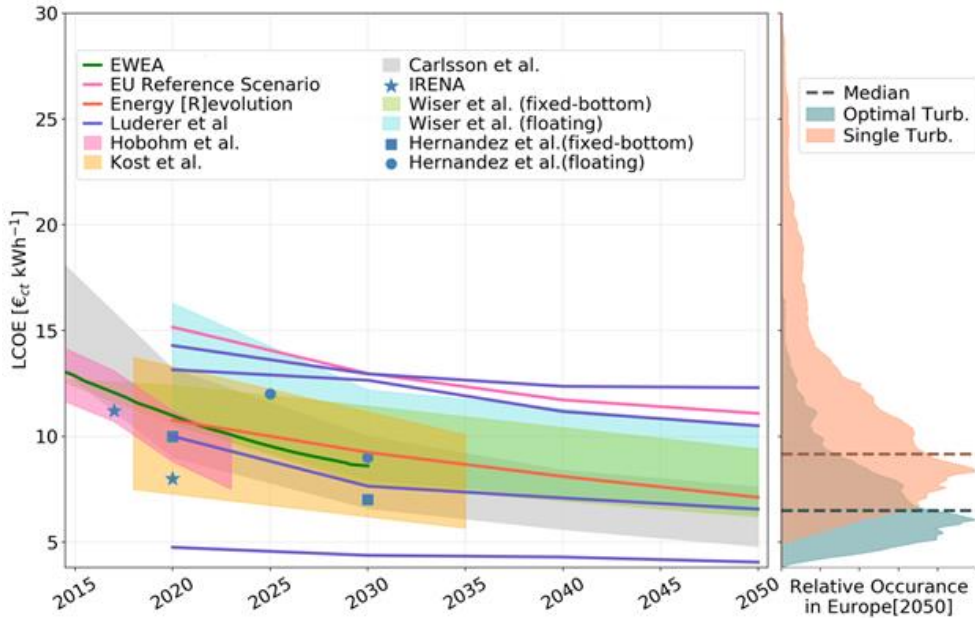


Figure 4-2. Comparison of LCOE calculated by this approach with the literature. Left: LCOE estimations in the literature changing by year, right: the relative occurrence of the LCOE for single turbine design²⁰ and optimal turbine design in the context of 2050 [60].

The selection of a single turbine design and applying it over Europe can be misleading since assuming an inappropriate turbine definition could result in misinterpretation of the results. In a large regional scope, using turbines suitable for strong wind speeds at weak wind speed location or vice versa overestimates or underestimates the potential. In order to observe this effect (change in the results with a single turbine definition uniformly applied across Europe), several single turbine designs found in the literature are used in the estimation of potential. These exemplary turbine designs are used by Bosch et al. [66] and WindEurope [4] in their “Baseline” and “Upside” scenarios. Moreover, the largest offshore turbines produced by Vestas [41] (by the time this analysis is performed) as well as a future-oriented design which will be produced by General Electric (GE) [49] are also included in this comparison. Specifications in terms of capacity, rotor diameter, and hub height can be found in Table 4-1. As it is seen in the case of optimal turbine designs and uniformly applied single turbine designs, the generation potential for a region (in this specific example, it is Europe) can be significantly higher with a detailed investigation of appropriate turbine designs.

The power curves of these turbines are estimated by using the synthetic power curve method suggested by Ryberg et al. [39]. Figure 4-3 shows a comparison of these single turbine designs

²⁰ A single turbine has a capacity of 13 MW with a 212 m rotor diameter and 128 m hub height [62].

as well as the optimal turbine designs by the distribution of LCOE at each location. It reveals that the lowest LCOE values are attained via optimal turbine designs. Optimal designs are then followed by GE Haliade-X and the turbine design used in the Upside Scenario of WindEurope [4]. The differences in the turbine designs are more pronounced especially in the low LCOE regions as well as high LCOE regions. For example, a more appropriate turbine design in cheap locations can decrease the LCOE as it is observed in the range of 3-7 $\text{€}_{\text{ct}} \text{kWh}^{-1}$ and 10-20 $\text{€}_{\text{ct}} \text{kWh}^{-1}$. Especially the minimum LCOE values observed for each turbine shows that the cost can be decreased by introducing a more suitable turbine in a location. The extent of this decrease is; nevertheless, highly dependent on the location since increases in the average generation and the turbine cost are not of the same degree all the time. Therefore, it can be said that for a larger context a detailed analysis should be performed to choose a suitable turbine design for areas with different wind regimes. Nevertheless, only looking at the LCOE of individual turbine design is not sufficient to conclude this comparison, since spatial distribution, especially in terms of full load hours, might assist understanding the locations with over- or underestimation.

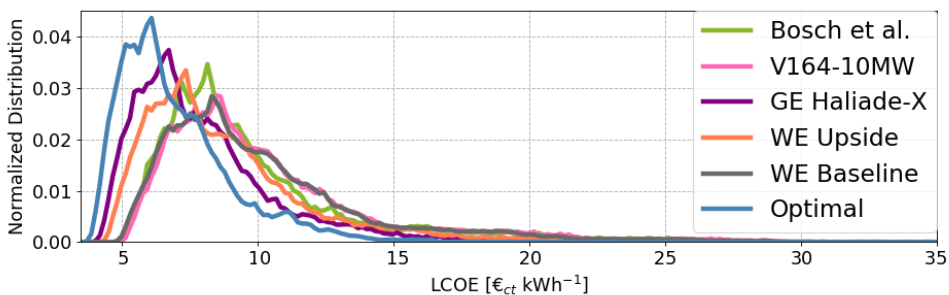


Figure 4-3 LCOE distribution of individual single turbine designs [60].

The results are further analyzed by comparing their different aspects, as listed in Table 4-1. In addition to the capacity, hub height, and rotor diameter of each turbine, specific capacities are also listed. It must be noted that the specific capacity of turbines can be used as an indication for power curves, meaning that low specific capacity turbines have lower-rated wind speed hence higher generation between cut-in wind speed and rated wind speed compared to the high specific capacity turbines. It is seen that the current turbine design (Vestas V164-10MW [41]) has the highest specific capacity, the lowest is observed for GE Haliade-X 12MW [49] turbine when optimal turbines are not taken into account. In the case of optimal turbines, the lowest value for specific capacity can be 220 W m^2 which is seen at some locations. When the total number of turbines placed by using their respective rotor diameter, substantial variation in the results can be seen. For example, 2.6 million turbines are placed for the turbine design of Bosch et al. [66] owing to its small rotor diameter, which is 126 m. Only 20% of that number of turbines is used in the placement of optimal turbines. Knowing that the number of turbines placed across eligible areas is only a function of their rotor diameters, such a significant deviation in the numbers is expected. The total

capacity potential for each turbine design has the same trend as the number of turbines since they are highly tied to each other (total capacity is the summation of turbine nameplate capacities). When total generation potential is focused, it is seen that the total generation is approximately 54 PWh for Vestas V164-10MW. The generation via optimal turbines and GE Haliade-X 12MW is nearly 20% less than the potential of Vestas turbine (V-164 10 MW). However, the average LCOE and total investment costs show that these turbines have the lowest cost. Therefore, neither capacity nor generation potential can be used as the only criterion for comparison despite of the strong correlation. While estimating the potential for offshore wind energy, location-specific turbine designs and their cost must be taken into account. As it is seen in the case of optimal turbine designs and uniformly applied single turbine designs, the generation potential for a region (in this specific example it is Europe) can be significantly higher with detailed investigation of appropriate turbine designs.

Table 4-1 Comparison of results of different single turbine characteristics [60]

	Optimal designs	Bosch et al. [66]	Vestas V164-10MW [41]	GE Haliade-X 12MW [49]	Wind Europe Baseline [62]	Wind Europe Upside [62]
Capacity [MW]	3-20	5	10	12	13	15
Rotor Diameter [m]	80-280	126	164	220	212	228
Hub height [m]	80 – 200	100	140	150	128	136
Specific Capacity [$W m^{-2}$]	220-550	401	474	316	368	368
Number of turbines	590,000	2,630,700	1,579,000	894,000	956,000	832,000
Total Capacity [TW]	8.6	13.15	15.78	8.94	12.4	12.48
Mean FLH [$h a^{-1}$]	4660	3640	3440	4280	3500	3790
Total Generation [PWh]	39.86	47.87	54.33	38.28	43.65	47.3
Total investment [10^{12} €]	23.85	38.43	45.73	30.57	36.18	35.82
Average LCOE [$€_{ct} kWh^{-1}$]	7.02	10.03	10.51	8.03	10.30	8.86

Figure 4-4 shows the full load hour distribution of selected turbines placed in the eligible locations across Europe. Similar to previous discussions, it is evident that full load hours are enhanced with optimal turbine designs. Although the full load hours increase at all the locations by introducing the optimal turbine designs, in certain areas, this increase is more pronounced. For example,

despite the similarities between GE Haliade-X 12MW and optimal designs observed in the near-shore North Sea areas, in the middle of the North Sea, at least 1500 h a^{-1} of an increase is observed. Another example is the increase observed in the Adriatic Sea, which also has a value of at least 1500 h a^{-1} . By looking at these distributions, it can be said that the turbine designs shown in this figure are not representative of the locations in the Mediterranean Sea. Amongst these turbines, GE Haliade-X 12MW has the closest full load hours in comparison to the optimal designs. However, full load hours can be further enhanced by using a different turbine design.

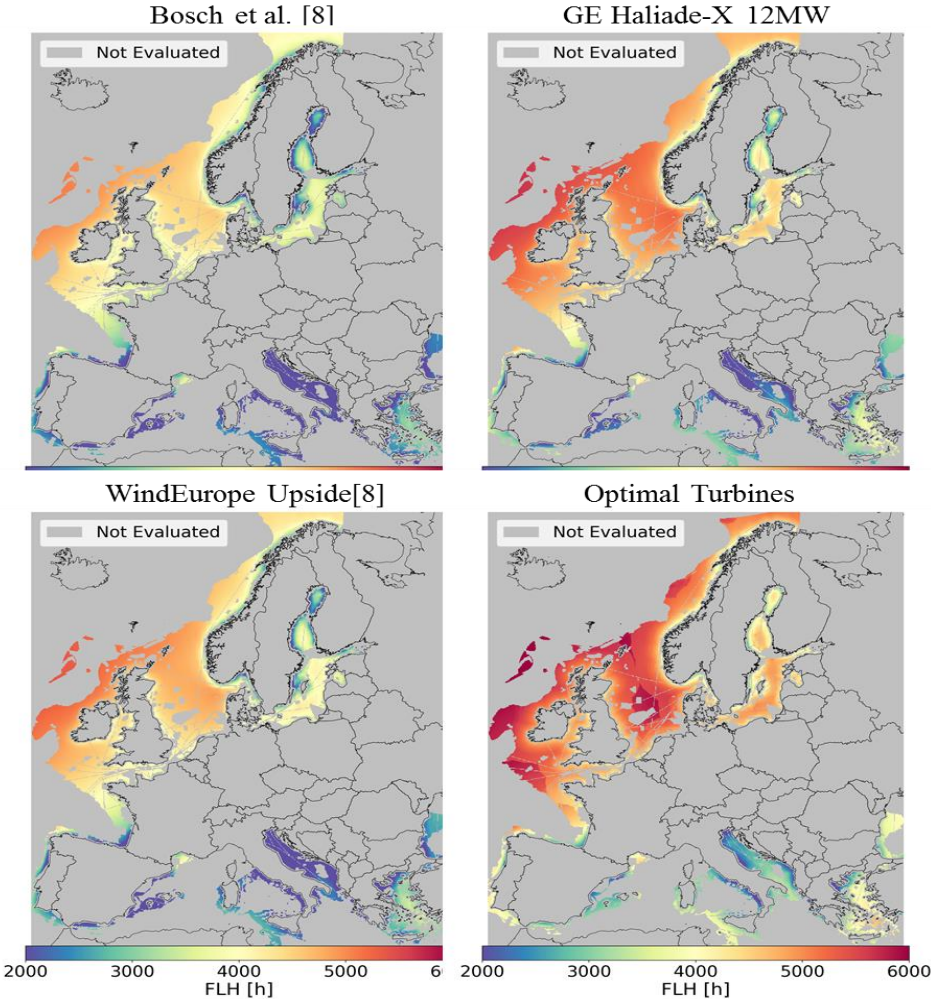


Figure 4-4 Comparison of full load hour distribution of selected turbines [60].

4.1.3 Clustered Optimal Turbine Designs

Once the distributions are obtained via optimal turbine design, as discussed in the previous section, it is seen that there are several different turbine types across Europe. For example, when capacity and rotor diameter are considered as criteria, 92 different turbine types are found as optimal designs across Europe. When hub height is added as an additional criterion for turbine design definition, this number increases to 181. Furthermore, consideration of foundation results in 202 different types that should be installed across Europe in order to have the cheapest electricity generation. Thus, as a result of the variation observed in the optimal turbine designs, the question arises: Is it possible to decrease the number of turbine types within an economic limitation? In order to answer this question, different turbine parameters and their corresponding LCOE are saved for all locations in addition to the optimal turbine designs. Figure 4-5 shows the exemplary distribution of the top 100 lowest LCOE turbine designs at two locations in the North Sea. These locations are the adjacent locations where a switch in the turbine design occurs. As it is seen from the figure, the increase in the LCOE is at most 0.2% when a different turbine definition is used among these 100 turbine designs.

Focusing on the turbine designs reveals that there are variations in all parameters such as capacity, rotor diameter, and hub height. Nevertheless, it is evident that for a specific rotor diameter and a capacity chosen in the figure, there are several hub heights with a slight change in the LCOE, which is expected due to the fact that dependency of turbine cost on hub height is not as strong as the cost on rotor diameter or capacity (cf. Figure 3-4). Therefore, the lowest LCOE in these exemplary locations are observed at the shortest possible hub height, which is generally limited by the difference between hub height and rotor radius cannot be below 30 m.

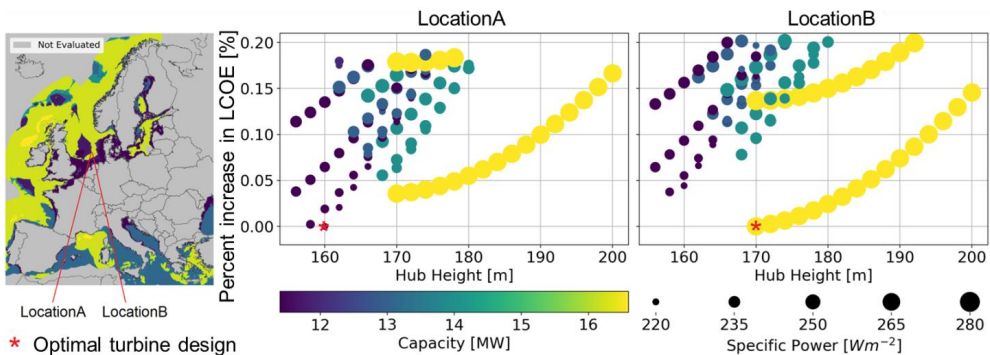


Figure 4-5 (a) Distribution of cost-optimal turbine capacities across European Maritime Boundaries without eligibility constraints. The change in LCOE of top 100 turbines with respect to LCOE of optimal turbine design as a result of the optimization with respect to their design parameters for (b) Location A and for (c) Location B.

The number of turbine designs clustered following for each LCOE threshold and parameters considered in turbine design is obtained by applying the methodology explained in Section 3.1.5, and the resulting numbers for turbine types are shown in Table 4-2. The minimum number of turbine designs is found as 7 for 1% LCOE threshold for only capacity and rotor diameter as turbine design parameters, whereas it reaches 45 designs for 0.1% LCOE threshold and consideration of hub height and foundation besides capacity and rotor diameter. Higher LCOE threshold results in fewer turbine designs as it is expected. Therefore, for all parameter sets for turbine designs, there is an increase in the number of turbine types with decreasing LCOE threshold as cost tolerance. In the case of parameter sets, it is seen that adding hub height or foundation as design parameters to the capacity and rotor diameter does not increase the numbers significantly. Especially in the case of a 1% LCOE threshold, for example, each criterion increases the number by one.

Table 4-2 Number of turbine designs with respect to the LCOE threshold and parameters considered in turbine design

		Cap. - Rotor diam.	Cap. - Rotor diam. - Hub height	Cap. - Rotor diam. - Hub height – Found.
LCOE Thresholds	1%	7	8	9
	0.5%	13	14	18
	0.1%	34	38	45

The sample distribution of turbine types with design parameters of capacity and rotor diameter for 1% and 0.5% LCOE thresholds are shown in Figure 4-6 for the sake of simplicity owing to a fewer number of turbine designs in these cases. Focusing on the 1% threshold with a fewer number of variation reveals that the turbine design with capacity and rotor diameter of 16.6 MW and 279 m is chosen in the majority of locations. Nevertheless, a different turbine design with capacity and rotor diameter of 11.4 MW and 256 m is chosen in the center of the North Sea to maintain a lower LCOE. The selection of a lower specific capacity increases the average generation and compensates for the higher investment cost due to the larger distance to shore (electrical infrastructure is affected). Unlike at the center of the North Sea, a smaller rotor diameter is chosen for the same capacity (11.4 MW) as the one observed in the center of the North Sea.

When these two distributions are compared against each other, many similarities can be observed. For example, the turbines chosen in the majority of the North Sea do not alter except for the locations closer to shore and center. The same turbine design is used in the eastern Aegean Sea, too. In the areas closer to shore, there are several different turbine designs in the 0.5% LCOE threshold case; nevertheless, generally, 11 MW turbines with rotor diameters around 200 m are chosen in these areas. Similar to the North Sea, the same turbine designs are also observed in the English Channel as well as the Celtic Sea.

Alterations in the turbine designs at specific locations are also evident, especially in the Mediterranean Sea. For instance, the design observed in the Northern Baltic Sea and Northern Black Sea for 1% LCOE threshold (8.4 MW turbine with 218 m rotor diameter) alters in the 0.5% LCOE threshold with a drastic increase in the capacity (19.8 MW turbine with 268 m rotor diameter). Lower LCOE can be attained either by a powerful (low specific capacity resulting in higher generation) or a cheaper turbine design. Therefore, the use of both turbine designs results in low LCOE in different ways.

All in all, a general trend in the clustering can be noticed in large areas. Nevertheless, which LCOE threshold to use and how many turbine designs to consider remain unknown since the selection of these parameters might affect the overall energy system design. It can be said that the variety can be decreased by increasing the tolerance for minimum LCOE as it is expected. However, optimal turbine designs do not differ significantly in small regions such as wind parks or national offshore zones. Therefore, the clustering of optimal turbine designs is not applied in the energy system design in order not to have biased results obtained by a particular set of criteria (both threshold and turbine definition).

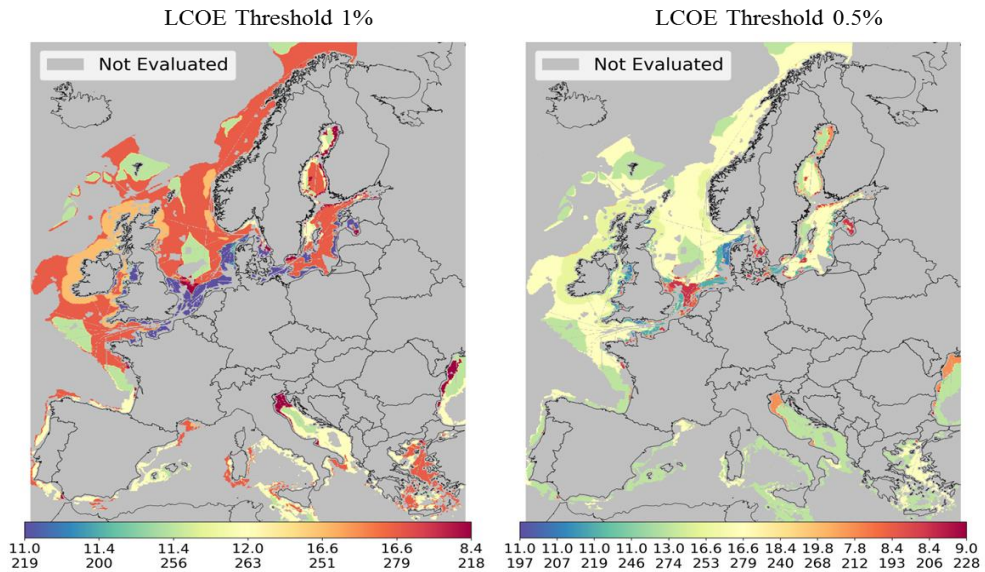


Figure 4-6 Distribution of different turbine designs across Europe for exemplary LCOE thresholds as 1% (left) and 0.5% (left). In the legend: upper values are for turbine capacity in MW; lower values are for rotor diameter in m.

4.2 Technical Potential of Salt Cavern for Hydrogen Storage

The technical potential of salt caverns is estimated by applying the methodology explained in Section 3.2. It must be noted that the results presented in this section are obtained in a Master's project under the supervision of this work, which is submitted by Nikolaus Weber to RWTH Aachen University [112]. After an initial suitability assessment on the salt formations, a geospatial eligibility analysis is performed on the suitable salt formations with uniform constraints. Following this, the distribution of salt caverns across eligible salt formations is performed. Finally, the storage capacity of each cavern is estimated as explained in Section 3.2.3. The results presented in this section involve suitable European salt formations for hydrogen storage, eligibility assessment performed on these suitable formations and distribution of cavern energy density over these eligible areas. Finally, national storage potentials are presented for three different definitions, which are "only onshore", "only offshore" and "only onshore with 50 km distance from shore", in order to gain an insight about the overall storage potentials in different countries and the variation in these potentials when a constraint is introduced from distance to shore. The content presented in this section is also published by Caglayan et al. [192].

4.2.1 European Salt Basins Suitable for Underground Hydrogen Storage

As a result of the assessment, suitable salt structures, as well as suitable bedded salt deposits, are shown in Figure 4-7, with the respective salt basins denoted. The assumption was made that all encountered salt bodies that are not identified as bedded salt deposits were to be classified as salt structures (encompassing salt domes, salt pillows, salt walls, etc.). As a geological suitability assessment would require individual evaluation for a vast number of salt structures distributed all over Europe, the assumption was made that all salt structures were to be suitable for underground hydrogen storage instead of excluding all from the potential analysis from the very beginning. Therefore, the geological suitability assessment is exclusively applied to bedded salt deposits and briefly discussed in the following. Bedded salt deposits that do not fulfill the thickness and chemical requirements for underground hydrogen storage construction, or for which no reliable information concerning geological properties could be found, were dismissed and not considered in the further process of the potential analysis. A minimum salt thickness of 200 m and a range of minimum to a maximum depth of 500 m to 2,000 m were selected as being suitable for salt cavern construction.

Within the framework of this analysis, assumptions of highly idealized salt deposits can be made; however, this does not necessarily correspond to the actual shape and conformity of the salt formations in reality. Bedded salts are assumed to be perfectly layered with equal thickness and equal depth ranges spanning the entire geographical extent of the salt deposit. The geometrical shape of the salt structures was assumed to be positioned upright as cylindrical shaped bodies without any inclination or tectonically-induced modifications of the salt.

Due to the geological formation conditions of the salt structures, which always originate from bedded salt deposits, all regions with a high abundance of salt structures often also correlate with

the presence of remnant bedded salt deposits, forming base salt. In these cases, salt structures are favored over bedded salt deposits, due to their higher storage capacity and the unfavorable thickness of the remaining bedded salt deposits for cavern construction.

The Tertiary (Cenozoic) sub-basins (1-4) in France contain thick evaporite sequences reaching up to 1,800 m, with overall low sulfate concentrations in thick salt layers.[114] The thickness of the Mesozoic salt deposits in Northwestern France shows high insoluble content within the salt formation (such as anhydrite/clay interbeds or gypsum). This is in contrast to the aforementioned Tertiary deposits, and which rules out the suitability of these Mesozoic deposits for cavern construction. In Italy, Tertiary salt deposits in the Crotone Basin of Calabria and Western Sicily are also not suitable due to high insoluble content, as well as the lower thickness of the salt layer.[114], [127] In Spain, Mesozoic evaporite deposits cover large areas of the subsurface and extend from the Betic Cordillera over the Iberian Range to the northern coast of Spain, up to the Bay of Biscay; however, top salt exceeds depths of 2,000 m. Tertiary evaporitic formations are present in the Ebro, Duero and Tagus Basin. These halite beds have a considerable thickness but show highly folded facies and high amounts of anhydrite and gypsum concentration.[120] The Cardona Saline Formation (14) is included in this analysis, as the thickness of salt in some areas is proven to attain approximately 300 m at reasonable depths of below 2,000 m for cavern construction.[120]

Major periods of salt deposition in central Europe took place during the Paleozoic (Permian) and Mesozoic eras. The European Permian Basin (EPB) of central Europe belongs to the largest sedimentary paleobasins of the world and contains a considerable amount of bedded salt deposits and diapiric salt structures, reaching from the eastern United Kingdom up to the North Sea, the Netherlands, Denmark and Northern Germany, down to the central basins of Poland.[106], [115], [121], [125], [126], [128], [205] At the margin of the EPB, bedded Zechstein salt deposits are thinned out and buried at depths shallower than 2,000 m. These deposits are found on the east coast of the UK (17), western, eastern and central Germany (5-8) and as far south as Upper Silesia in Poland (8-12).

Outside of the EPB, Mesozoic salt, which formed during the early Triassic period, can be found in northwestern England, Northern Ireland and southern Germany. The Cheshire Basin, amongst other Triassic basins in the UK, shows promise for salt cavern construction, as it fulfills ideal geological prerequisites, such as depth and thickness (16, 18, 19).[121], [126]

Amongst the youngest salt deposits in the central and eastern European region are the Badenian Tertiary deposits, reaching from the Carpathian Foredeep in southern Poland to the Transylvanian Basin in Romania. Apart from the Ocele Mari salt deposit (13), where salt lies at depths of 650 m and can attain a thickness of 500 m, the Tertiary salt deposits do not qualify for cavern construction, as the salt strata is highly folded and imbricated, or is not favored over the presence of salt structures.[117], [129] Ukraine and Belarus (15) are excluded from this analysis due to the lack of data for urban and rural areas necessary for the following surface eligibility assessment [123], [124].

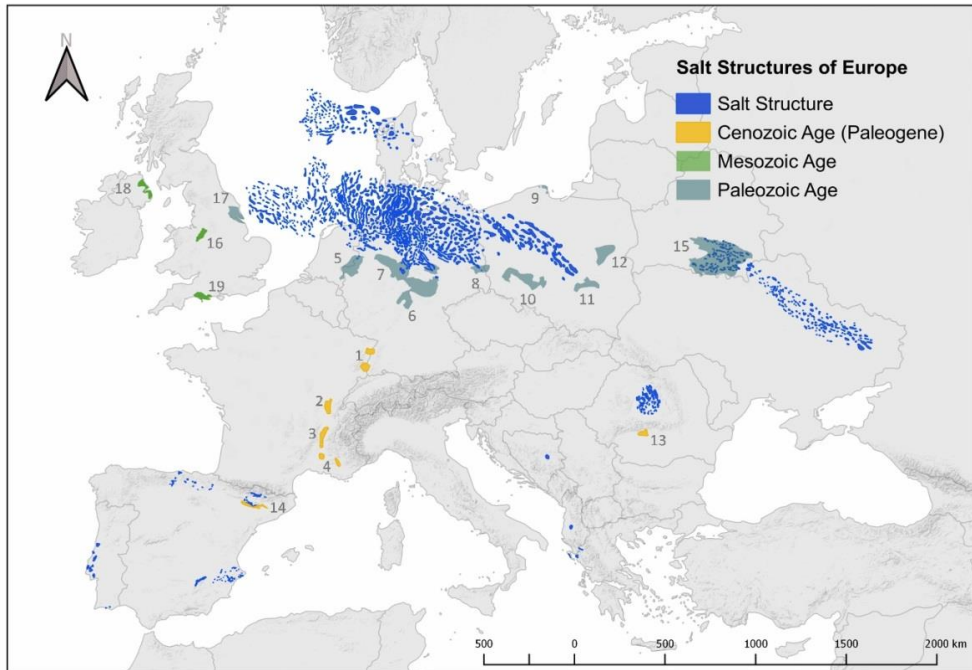


Figure 4-7. Map of European salt deposits and salt structures as a result of suitability assessment for underground hydrogen storage (1. Alsace Basin; 2. Bresse Basin; 3. Greoux Basin; 4. Valence Basin; 5. Lower Rhine Basin; 6. Hessen Werra Basin; 7. Sub-Hercynian Basin; 8. Lausitz Basin; 9. Leba Salt; 10. Fore-Sudetic Monocline; 11. Carpathian Foredeep; 12. Lublin Trough; 13. Ocnele Mari; 14. Cardona Saline Formation; 15. Pripyat Basin; 16. Cheshire Basin; 17. UK Permian Zechstein Basin; 18. Larne Salt Field; 19. Wessex Basin).²¹ Previously published in Caglayan et al. [192].

4.2.2 Eligibility Assessment and Cavern Placement

The application of the eligibility constraints and item placement algorithm, as shown in Section 3.2.1, produces possible cavern locations. Figure 4-8 illustrates the results of a land eligibility assessment applied to the salt formations. Additionally, an exemplary representation of a salt cavern distribution field across different types of salt structures is shown for an area in central Germany. This area consists of both salt domes and bedded salt deposits. As part of the methodology, in a case where there is an overlap between salt domes and bedded salt deposits, the overlapping area is processed following the designs for salt domes (large cavern size). The larger and smaller salt caverns represent different volumes of caverns, with 750,000 m³ and

²¹ A detailed list of publications containing geological maps that were used for the visualization and digitization of the layered and domal salt bodies can be found in Weber [112]. The suitable salt formations were determined by the literature review.[113]–[119], [122]–[129]

500,000 m³ placed in salt domes and bedded salt deposits, respectively. As mentioned earlier, the separation distance of smaller and larger caverns are different due to different diameters used in the cavern design. It must be noted that these cavern placements are used in order to calculate the technical potential for hydrogen storage²². In other words, these cavern placements correspond to all possible locations where a salt cavern can be built, yet the extent to which these locations should be utilized is not within the scope of this study. The results of these placements can be further used in the design of energy systems, as well as in analyses taking social acceptance into consideration in the related area.

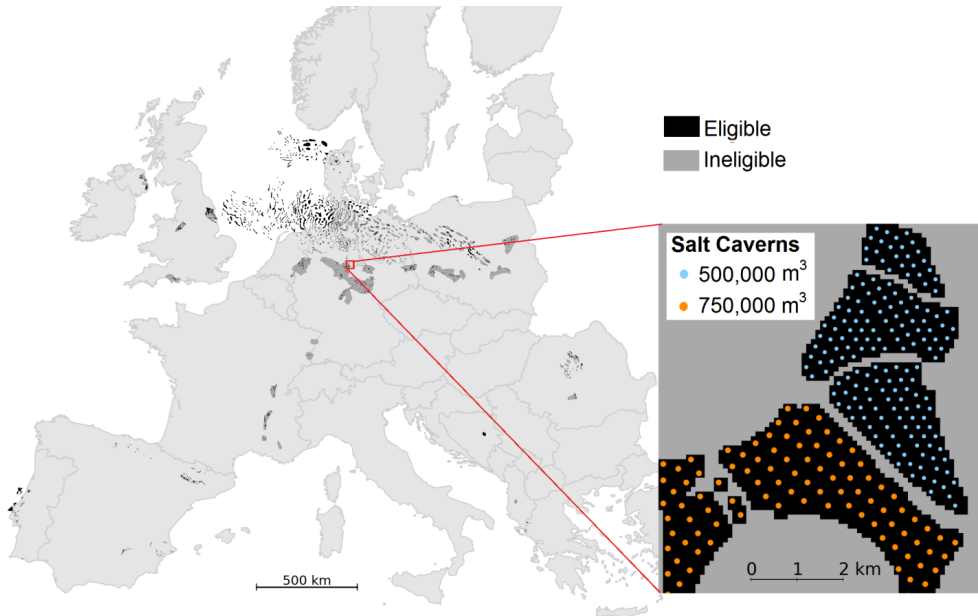


Figure 4-8. Land eligibility results with an exemplary representation of cavern placement in central Germany (extent of exemplary placement: 51.9°-52.0° N, 10.0°-10.1° E). Previously published in Caglayan et al. [192].

4.2.3 Distribution of Volumetric Energy Density across Europe

By using individual cavern placement depths, the storage capacity of each cavern is calculated on the basis of properties such as cavern volume and temperature (cf. Section 3.2.3). However, the direct comparison of storage capacities can be misleading because of two cavern designs having different volumes. Instead, the energy density, which is calculated as a cavern's storage potential divided by its volume, is employed for comparison. The energy density distribution of the potential hydrogen salt cavern locations across Europe is shown in Figure 4-9. The energy density of

²² Social, economic and environmental concerns are not taken into account in the estimation of hydrogen storage potential.

caverns in salt domes does not vary (whether northern Germany, Portugal or southern Spain, etc.), which is due to the assumption of the same placement depths and cavern design applied to all caverns. Nevertheless, variation in the energy density of salt caverns placed in the bedded salt deposits is evident owing to different depths possessing specific thermodynamic and storage conditions. The energy density of all salt caverns varies between 214 and 458 kWh_{H₂} m⁻³. Examining the distribution of the volumetric energy density, the lowest energy density is estimated in the Cheshire Basin (the United Kingdom) and Ocnele Mari (Romania) due to salt lying in shallow geological environments. The maximum depth in the Cheshire Basin and Ocnele Mari are approximately 700 m and 650 m, respectively; whereas the assumed maximum depth for salt caverns in the domal salt is 1,400 m. Given that the amount of working gas increases as a function of depth, these results are thought to be consistent. When energy density is translated into storage capacity (by multiplying the energy density by the cavern volume), the capacity of salt caverns in domal salt structures is estimated to be nearly 210 GWh_{H₂}, whereas it varies between 65 and 160 GWh_{H₂} for the caverns placed in bedded salt deposits. As is discussed in Section 3.2.2, the depth of the salt structure determines the maximum and minimum operating pressures, which are then used in estimating the amount of working gas. Deeper salt structures can accommodate an increase in the amount of working gas (storage capacity), which can also be seen in Figure 3-9. A deeper look at the energy densities reveals that having a suitable salt formation is not enough to determine the storage potential. In addition to the quantity, in terms of salt caverns placed in eligible and suitable salt areas, the depth of the salt structure, thermodynamic gas storage behavior and cavern design are required to estimate a well-founded storage capacity. As can be seen in the United Kingdom, for example, different characteristics can be observed even on a national scale due to different salt depths and, consequently, different geomechanical and thermodynamic storage conditions.

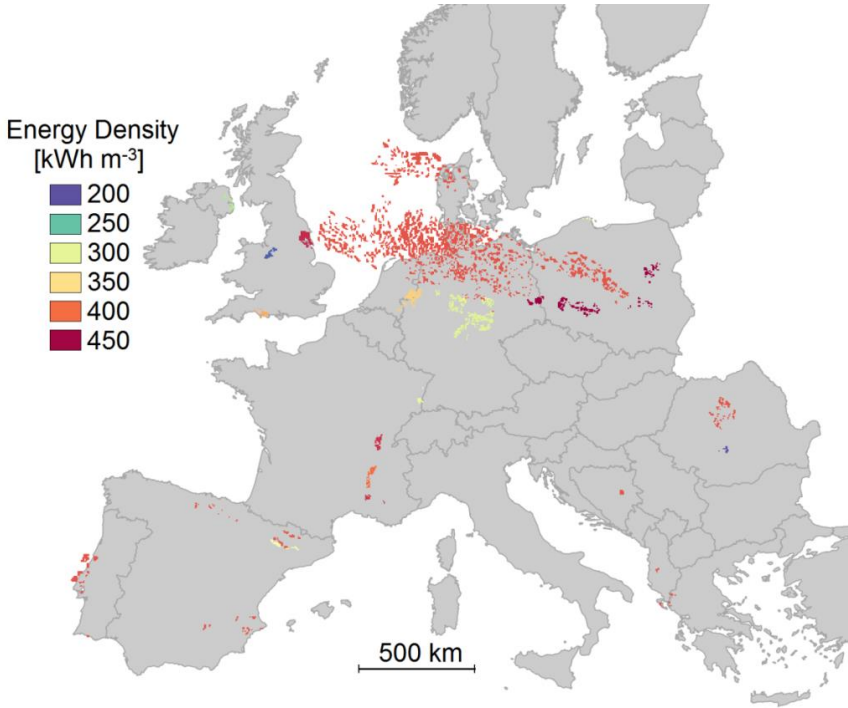


Figure 4-9. Distribution of potential salt cavern sites across Europe with their corresponding energy densities (cavern storage potential divided by the volume). Previously published in Caglayan et al. [192].

4.2.4 National Storage Potential

Overall national storage capacities are shown in Figure 4-10, with three classifications: onshore, onshore constrained and offshore. The countries are sorted by their total storage potential. Cavern capacities labeled as “Offshore” stand for caverns placed in salt domes under the North Sea, whereas the “Onshore” ones refer to the remaining caverns located on land (after the application of eligibility constraints). Finally, as an additional constraint, a maximum distance of 50 km from shore has been included in the calculation of the storage potential of onshore salt caverns, and defined as “Constrained”. This constraint is added in order to take into account the economic and environmental constraints regarding brine solution disposal during cavern construction, as disposing of the solution in lakes and rivers is not possible due to its high salt content.

Overall, the storage potential considering offshore and onshore salt caverns constitutes 84.8 PWh_{H₂}, 42% of which belongs to Germany. This is followed by the Netherlands and the United Kingdom, with 10.4 and 9.0 PWh_{H₂}, respectively. Most of the countries have both onshore and

offshore salt caverns options, the exception being Norway, which only has offshore salt cavern potential.

When offshore salt caverns are excluded, Germany has the largest storage potential of the countries considered in this analysis, constituting 41% of the total. Overall, European storage potential for salt caverns located in onshore areas is estimated to be 23.2 PWh_{H2}, 19.0 PWh_{H2} of which is located in salt domes. Due to the lack of data on the potential analysis of European salt caverns, the results presented are compared against pumped hydropower potential. Gimeno-Gutiérrez and Lacal-Aránegui report that the storage potentials of pumped hydropower to be 0.054 and 0.123 PWh (two different topologies) with a regional definition slightly different from that presented here.[203] In their report, the Netherlands and Denmark are not included, yet Turkey and Iceland are. The highest potential is observed in Germany (9.45 PWh_{H2}), followed by Poland and Spain (7.24 PWh_{H2} and 1.26 PWh_{H2}). These three countries account for 77% of the total onshore storage potential. Despite the widespread bedded-salt deposits seen in France, the onshore storage potential is estimated at 510 TWh_{H2}, which is only 2% of the overall storage potential. This is mainly because the salt deposits are mostly located around densely populated areas. Limited areas for cavern construction can especially be seen in northern Alsace and all the salt basins of the Rhone valley in southern France.

Hydrogen storage potential in Lower Saxony, a German state, is estimated to be nearly 390 TWh_{H2} (2320 potential caverns sites) by Fichtner [111]. The assessment by Fichtner [111] is performed with an average gas density of 10 kg_{H2} m⁻³ and assumes a cavern size of 500,000 m³, separated by a distance of 280 m. Moreover, the use of a cavern safety factor (30%), geological uncertainty factor (50%) and a factor for urban and rural area exclusion (23%) significantly decreases the estimated capacity. In addition, protected areas are excluded from the potential cavern sites. In the presented work, geological uncertainty and urban and rural exclusion factors are not used; instead, an extensive land eligibility analysis is performed to take the settlement areas into account. Moreover, the salt structures in Lower Saxony are mostly salt domes, with an assumed cavern size of 750,000 m³. Considering these differences in the assumptions (especially the geological uncertainty factor), a calculated estimate difference of 880 TWh_{H2} is regarded as acceptable.

Proximity to the coast is considered to obtain up to approximately 50 km in order to still economical in terms of brine disposal [111], [205]. This constraint is assumed to be a socio-economic factor rather than a technical one; thus, it is not applied in the eligibility analysis, after which the technical potential of salt caverns will be determined. Nevertheless, it is noted in order to observe the variation in the storage potential with respect to the proximity to the coast. In the “constrained” case, a maximum distance of 50 km for cavern construction is defined as incorporating the economic and ecological disposal of brine in the sea, resulting from cavern leaching. Even though the storage capacity is decreased to a total of 7.3 PWh_{H2}, Germany has the largest share, corresponding to 60%. Furthermore, some of the countries, such as the United Kingdom, Denmark, Greece and Portugal retain all their storage potential owing to the proximity of their

suitable salt formations to the shore. In contrast, the storage potential in Poland decreases by 98% with this constraint, as most of its salt structures are located in the center of the country. There is no storage potential in France, Bosnia or Romania in the constrained scenario. The minimum distances between the shore and salt caverns in Bosnia and Romania are estimated to be 140 km and 340 km, respectively. In France, the closest cavern is approximately 65 km from the shore. When the overall technical potential of salt caverns is considered, it is evident that there is abundant storage potential available across Europe.

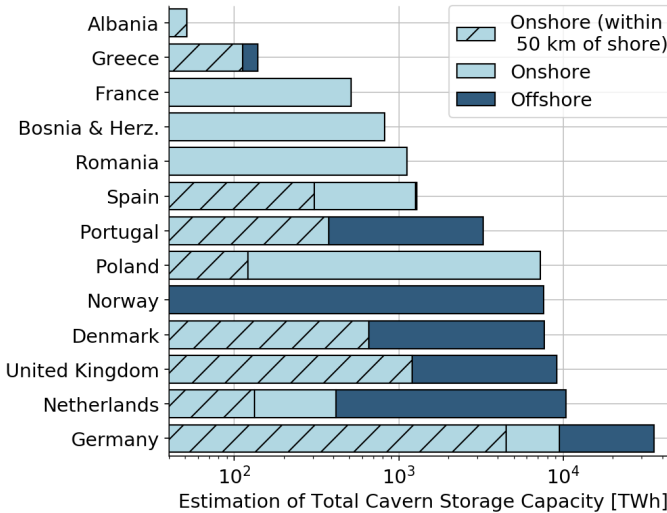


Figure 4-10. Total cavern storage potential in European countries classified as onshore, offshore and within 50 km of the coast. Previously published in Caglayan et al. [192].

4.3 Summary

The techno-economic potential of offshore wind energy is conducted not only for the optimal turbine designs with minimal LCOE but also for several single turbine designs uniformly applied across Europe. Results reveal that the use of optimal turbine designs across Europe has a capacity and generation potentials of 8.6 TW and 39.9 PWh. When the overall technical potential is deployed, the average LCOE is estimated as 7 €_{ct} kWh⁻¹. Application of the single turbine designs in the existing European studies, as well as the current largest turbine design (Vestas V-164 10 MW) and a future oriented turbine design which will be produced by General Electric (GW Haliade-X 12 MW), is also conducted within this project to compare the optimal turbines with these definitions. According to this analysis, the optimal designs have the cheapest average LCOE, and it is followed by GE Haliade-X 12 MW with a value of 8 €_{ct} kWh⁻¹. It is seen that the LCOE at high potential locations can attain nearly 4 €_{ct} kWh⁻¹; whereas, 3.6 €_{ct} kWh⁻¹ can be achieved with

optimal turbines. In addition to the comparison of different turbines, a clustering method is applied to the optimal turbine designs in order to decrease the number of designs required across Europe. For this purpose, different LCOE thresholds as cost tolerance and different parameters are defined for the turbine design definition. Results reveal that the number of 202 different turbine designs in the optimal case might decrease to 9 if an LCOE tolerance of 1% is assumed. As it is expected, this value increases when the LCOE threshold decreases (0.1% has 45 different turbine designs). Nevertheless, optimal turbine designs are decided to be employed in the energy system design, since the selection of LCOE threshold and turbine design parameters is vague and might affect the system design.

Estimation of the technical potential of salt caverns is performed on the bedded salt formations and salt domes across Europe. In order to take into account the above-ground, land eligibility is applied to the salt formations based on a literature review (mainly conducted for CAES storage). Individual storage potential for each potential cavern placement is determined by using the depth and cavern volumes; furthermore, a conservative safety factor of 70% is used to consider uncertainties. In the analysis, both onshore and offshore locations are analyzed. The total technical potential for hydrogen storage both for onshore and offshore locations across Europe is estimated at 84.8 PWh. When only onshore locations are taken into account, 23.2 PWh of storage potential is estimated. The highest national storage potential across onshore locations is observed in Germany with a value of 9.4 PWh, which decreases to 4.4 PWh if at most 50 km distance to shore is assumed for the salt caverns due to environmental and economic considerations. With this limitation of 50 km, the storage potential of certain countries such as Bosnia and Herzegovina, France and Romania is eliminated. However, neither offshore potentials nor 50 km constraint storage potentials are considered in the energy system design due to the lack of cost data for offshore salt caverns in the literature.

5 Sensitivities in the 100% Renewable European Energy System Design

Several aspects must be taken into account in the optimization of the European energy system, primarily when it is based on 100% renewable energy sources. Oversimplification of the parameters in the problem definition might result in under- or overestimation of the overall system cost. For this purpose, essential parameters in the problem definition are investigated in detail in order to find the most realistic and appropriate scenario definition within the boundaries of the optimization approach. The individual model runs and how each sensitivity analysis is compared are illustrated in Figure 5-1.

Several model runs are planned to estimate the most robust system design with few changes in each approach. Despite the common knowledge on a higher number of typical days increase in the solution time, the impact of the number of typical days is analyzed within the context of this analysis. This analysis is performed by using the reference scenario definition explained in Section 3.4. The outcome of this analysis represents the system with a plausible deviation from the results with the full time series. It must be noted that the sensitivity analyses which are aimed to be included in this project require the least number of typical days so that the solution time and memory use of individual problems is decreased as much as possible. Therefore, the impact of typical days on the system design is analyzed and discussed in Section 5.1.

Following this, the impact of the number of groups for each VRES technology, the method of which is explained in Section 3.3.1, is examined by using the number of typical days determined in the previous analysis. After estimating the most appropriate value in terms of the number of groups for each VRES technology, that number is used in the following analyses, including the impact of weather year, the value-of-analysis as well as the final design of the system. The results of the impact of group numbers on the design are examined and discussed in Section 5.3.

Finally, the value of system components is estimated by a similar approach used by Samsatli et al. [31] and Welder et al. [13]. For this purpose, the system is optimized by excluding each component from the problem definition individually by using the scenario for the weather year 2015 with 60 VRES groups per technology and 30 typical days in the optimization. The results of the value-of-analysis are presented in Section 5.4, and then used in order to eliminate the technologies which are not crucial in the energy system design in the iterations for final system design which is presented in Section 6. In addition to the value-of-analysis, the impacts of pipeline and electrolyzer costs, as well as the market penetration of hydrogen demand, are analyzed and discussed in Section 5.5.

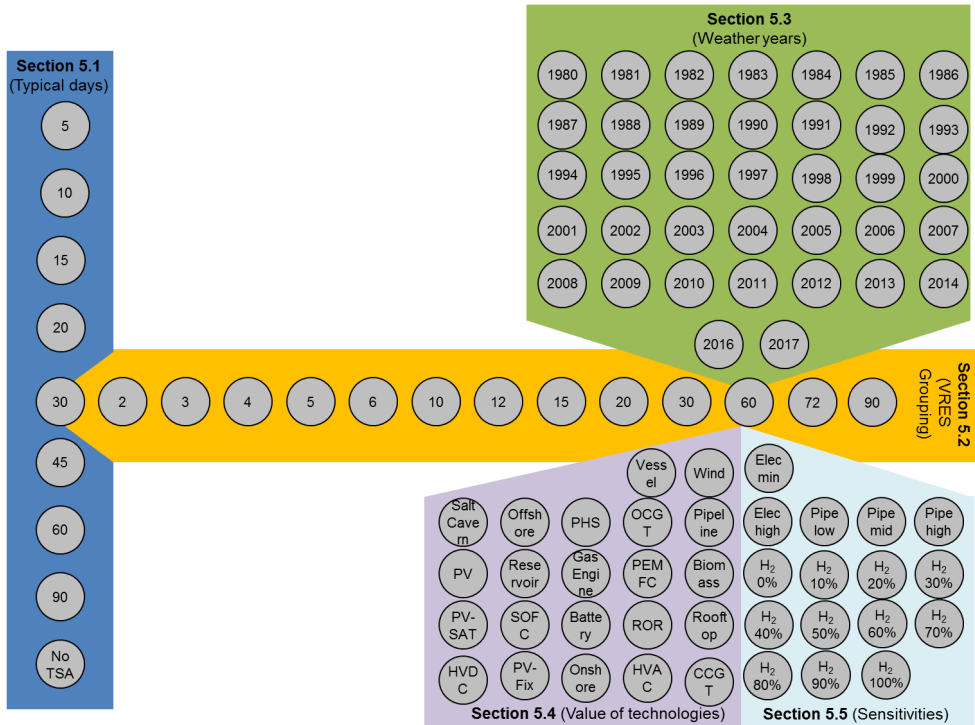


Figure 5-1 Overview of exploratory design analyses in Section 5²³.

5.1 Impact of Number of Typical Days

Solution time is a challenging issue due to the nature of optimization problems since the problem can easily become intractable with increasing complexity. Time series aggregation is a useful tool to decrease problem complexity to attain reasonable solution time and memory. However, which number to assume as typical periods remains unclear since it might vary due to the differences in the region of interest as well as the technology portfolio considered in the analysis. Therefore, an analysis of the effect of typical days on the base scenario (one group per VRES technology) is performed by changing only the number of typical days. For this purpose; 5, 10, 15, 20, 30, 45, 60 and 90 typical days are used to represent a wide range of days, and the results are analyzed by means of solution time as well as the variation in the overall total annual cost of the system, which is broken down to technology level. This analysis is performed in the work computer, which has 32 GB RAM with Intel Core i7-6700 processors with 3.40 GHz frequency with 8 threads since other computations running in the same device might affect the solution time of the optimization. Thus,

²³ When individual solution times of the calculations shown in the figure are summed, it corresponds to 4313 h (180 days) of calculation. When all these calculations assumed independent from each other (in real life they are not independent), and perfectly parallelized across 6 compute nodes, it corresponds to 210 hours of calculation.

a dedicated computer (work computer) is employed for this analysis in order to minimize the deviations in the solution time caused by other calculations taking place on the same computer. The maximum number for typical days that can be attained in the work computer is estimated as 90 due to memory limitations; thus, calculations and results of solution time are presented until that limit. The variation of solution time with respect to the number typical days is shown in Figure 5-2, which also shows the solution time of the problem without time series aggregation calculated in a different computer (Workstation in IEK3, which has 500 GB RAM with 2 Intel Xeon Platinum 8176 processors with 2.10 GHz frequency and 112 threads). Nevertheless, it must be noted that the value of solution time without time series aggregation should not be compared with the others (until 90 typical days) since the solution time depends on the computer specifications. Looking at the figure reveals that the solution time is significantly affected by the number of typical days, as it is expected. For example, model run with 15 typical days takes nearly 1.5 hours whereas it increases to 2.5 hours when 20 typical days are assumed. Surprisingly solution time with 30 typical days takes longer than the expected value, which is between 2.5 and 4.5 hours as solution time with 20 and 45 typical days, respectively. This might be caused by the other processes/tasks running in the computer at the same time with the calculations, affecting the solution time of the model runs with 30 typical days. Nevertheless, the exponential relationship between the number of typical days and the solution time can be seen despite the irregular behavior observed at 30 typical days.

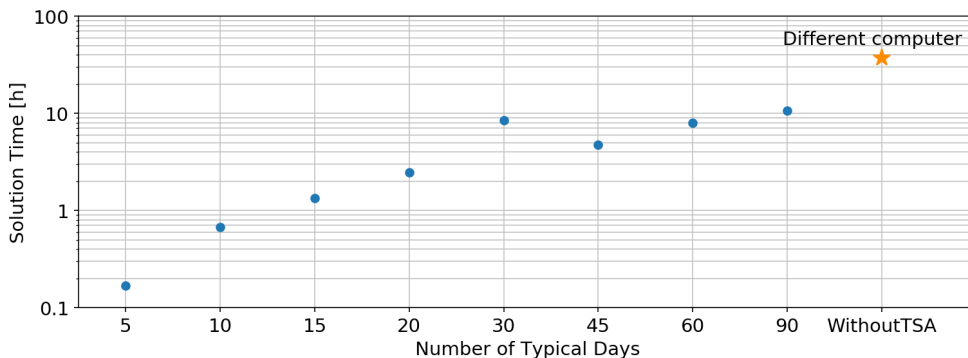


Figure 5-2 Variation of solution time by the number of typical days (Calculations for the case without time series aggregation is performed in a different computer).

Considering the intermittency observed in the VRES generation time series, a few typical days might not be sufficient to represent all time steps. This issue is more pronounced in a large regional context (such as Europe) since the individual time series are significantly affected by the local weather phenomenon. Therefore, aggregation of these time series plays an essential role in the optimization problem. Optimization input in terms of time series alters with the use of a different number of typical days, causing variations in the resulting system design. Thus, not only the solution time with respect to the number of typical days but also these variations in the system

design have to be investigated. For this purpose, total annual costs with shares of technologies, as well as its normalized value (normalization is performed by using the result of optimization without time series aggregation as reference) are shown in Figure 5-3. An increasing trend in the total annual cost is seen as the number of typical days increases, and the system cost is underestimated below 30 typical days. Especially the variations in the cost of onshore and offshore wind turbines, salt caverns and electrolyzer between the results between 5 and 30 typical days can be seen clearly. When fewer typical days are used like in the case of 5 typical days, the aggregated time series data are not able to represent the actual data, especially on such a large scale with 96 regions and many technologies (cf. Section 3.5). Therefore, the use of fewer typical periods causes time series to have similar profiles (with fluctuations) when they are normalized. Due to these similarities in the time series data, the requirement for storage technologies, for example, will not be as high as the cases with more fluctuations. Specifically, in the case of 5 and 10 typical days, the total annual cost is underestimated by nearly 15%. Lower optimal capacities of some technologies (biomass, salt caverns, electrolyzer... etc.) compared to the results without time series aggregation are apparent. However, despite the variations observed between 5 and 30 typical days, the cost of components does not change significantly above 30 typical days. As a result, considering the solution time and the variations in the system design, the number of typical days that is used in the rest of this report is assumed to be 30.

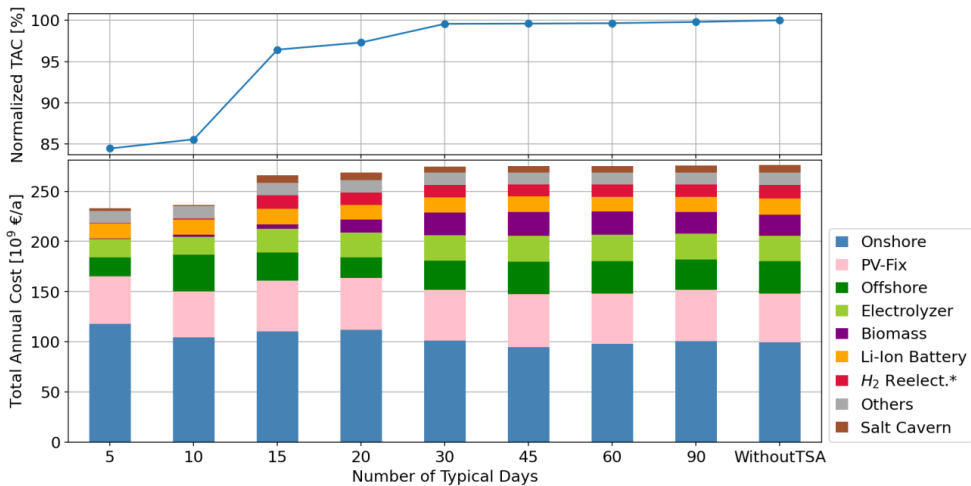


Figure 5-3 Variation of total annual cost with respect to the number of typical days.

Focusing on the shares of technologies in the total annual cost might be misleading since the distribution might vary. Therefore, resulting in capacity distributions of 5, 10, 30 typical days as well as without time series aggregation is shown in Figure 5-4. Focusing on the pipeline capacities reveals that the pipeline design alters significantly with respect to the number of typical days. These variations are more apparent especially in the Nordic countries as well as the regions in

Spain and Portugal. For instance, southern Portugal (“13_pt”) is connected to any regions when time series aggregation is used, as it is seen in the lower right figure. Nevertheless, this region is connected to “08_es” in the case of 5 typical days and “09_es” in the case of 10 typical days. Furthermore, a significant amount of underprediction of pipeline capacities in the United Kingdom is also evident when 5 or 10 typical days are used.

Not only the pipeline connections but also the optimal capacities of individual technologies vary in many regions. Offshore wind energy observed in southern Sweden (“89_se”) is observed in all cases except 5 typical days. Similarly, a switch between onshore and offshore wind energies is observed in many other regions such as northwestern Germany (“31_de”), northeastern Poland (“45_pl”), and northwestern Spain (“01_es”). As previously mentioned, this switch observed between technologies occurs due to the lack of representation of the time series data with few numbers of typical days. For instance, when 5 typical days are used, all time series data for 96 regions, more than 10 technologies (nearly 960 combinations having 8760 time steps per each combination) is represented by 5 normalized 24-hourly profiles, where these typical profiles are ordered by closest estimate to the actual profile (a region can experience same typical day profile multiple times for representing a year). Finally, these ordered normalized time series data are scaled according to the overall generation of each combination. Therefore, if a region experiences the same amount of overestimation and underestimation, it will not be scaled well since the summation of these estimations will be compensated by one another. All in all, a higher number of typical days would decrease the errors in the time series data; nevertheless, the drawbacks of a higher number of typical days are the significantly higher solution time and high memory requirement while solving the problem.

Despite the variations in the pipeline design as well as the optimal capacity of generation technologies in some regions, the optimal system design and the total annual cost do not change significantly after 30 typical days. Therefore, future analyses presented in this work will be performed by using 30 typical days. It must be noted that the application of time series aggregation can overcome not only the simplification in terms of temporal resolution but also the decrease in the memory requirement of the problem. Although memory does not become an obstacle in this analysis with a single group for each VRES technology as it is in this analysis, it is a limiting factor when the number of groups increases for technology (this issue will be addressed in Section 5.2). Despite high memory available in the IEK-3 Cluster (where all the following calculations are performed), then parallelization of the optimization problems will remain as an obstacle since memory requirement is scaled linearly with the number of problems.

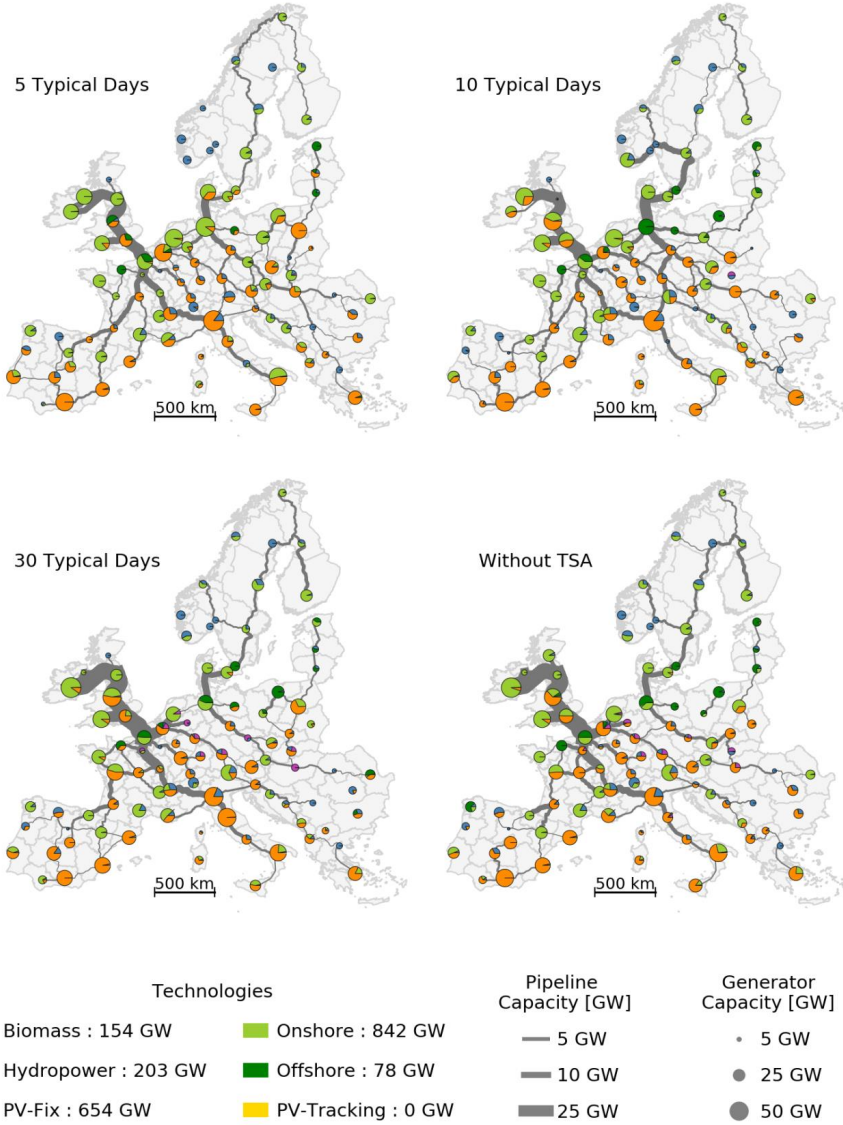


Figure 5-4 Capacity distributions of generation technologies and hydrogen pipeline for different number of typical days (5, 10 and 30) and without time series aggregation.

5.2 Impact of Grouping VRES Sources

In order not to repeat the simulation of all turbine placements across Europe for VRES technologies, simulation is performed for all weather years between 1980 and 2017 only once by creating 360 groups in each region as a result of the percentile distribution of LCOE values of corresponding technologies (cf. Section 3.3.1). These technologies considered in the grouping are onshore wind energy, offshore wind energy, open-field PV with tracking, and open-field PV without tracking. The reason to choose 360 groups is the ability to create various combinations for the analysis owing to many divisors of 360 without repeating the simulations for each number of groups. By using these divisors, several different groups can be designed. For each model run, the number of groups in each region and each VRES technology is assumed to be the same. For instance, having 60 groups indicates that there are 60 onshore wind technologies, 60 offshore wind technologies, 60 open-field PV technologies with and without tracking, corresponding in a total of 240 VRES technologies considered across all regions. The number of groups for each VRES technology is kept constant in order to avoid bias towards technology. For example, in case of keeping all technologies with a single group except onshore wind energy influences the optimizer in favor of onshore wind energy technologies, since high potential locations would be preferred compared to the competitive technologies (which are compensated and averaged because of single technology definition as discussed in Section 3.3.1) due to lower fidelity of other technologies.

The maximum number of groups is defined as 90 instead of 360 because of two reasons: less significant variations after 90 groups and a drastic increase in the solution time. Although the solution times in VRES grouping analysis are not comparable with each other because of the calculations performed in the same compute node, they will be mentioned in order to give an insight into the increase. The solution times of the problems with 60, 72 and 90 VRES groups are 28.6 hours, 85.6 hours and 163.4 hours (nearly 7 days), respectively. After observing these solution times, the problem with 120 VRES groups is canceled after 8 days of calculation.

Figure 5-5 shows the optimal European capacities of VRES technologies and total annual cost with respect to the different number of groups defined in each independent calculation. Focusing on the optimal capacities, a decreasing trend in the installed capacities of VRES technologies is evident especially between 1 and 10 groups. This might be explained by the averaging of time series as shown in Figure 3-12, which is an exemplary representation of onshore wind turbines. Nevertheless, the same behavior is also observed in offshore wind turbines and PV panels. The optimal capacity increases with a lower number of groups in order to supply the demand by the smoother generation time series. The smoother time series are not capable of covering the peak generation periods and have lower generation due to the averaging. This is avoided by introducing as many groups as possible so that mainly peak generation time periods are not compensated by the locations with low generation. Therefore, the optimizer chooses to install VRES technologies starting from these groups with high generation locations, and in the cases where the capacity in

that group is not enough, the following groups with relatively lower generation locations are chosen. All in all, optimal capacity remains more or less the same after a certain number of groups, which is nearly 10 groups in this case.

When the total annual cost is analyzed for a different number of groups, it is seen that biomass is chosen especially in the case of a single and two groups. As the number of groups increases, the share of biomass in the total annual cost decreases, because locations generating electricity cheaper than biomass emerged owing to the higher fidelity of the grouping. Therefore, these cost-competitive locations are utilized in the optimization instead of biomass; this issue will be discussed further in detail in the discussion of Figure 5-6, since this behavior can be observed better at a national scale instead of the cumulative variations. Similar to the optimal European capacities, variation in the total annual cost decreases with a higher number of groups. Nevertheless, slight changes in the shares of on-/offshore wind turbines and open-field PV systems without tracking are still observed. Hence, the optimal capacity distribution should be investigated in order to understand these slight variations and make sure that system design does not change drastically.

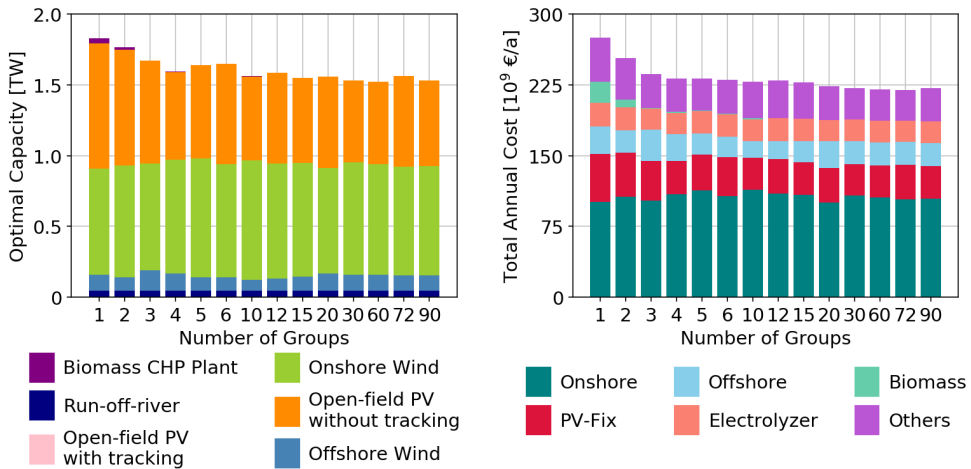


Figure 5-5 Optimal European capacities and corresponding total annual cost with respect to a different number of groups.

In order to decide on the number of groups, regional capacities and whether or not they change within the regions should be investigated. Although the results do not vary significantly in the European scale as discussed earlier, regional capacities might alter with respect to a different number of groups. Therefore, optimal national capacities of VRES technologies are shown in Figure 5-6 in order to observe the results summed over all regions and check if the capacities vary with respect to a number of groups. It must be noted that although open-field PV with tracking is

introduced in the plot, it is not chosen by the optimizer mainly because of its higher cost compared to the one without tracking (cf. Table 3-3).

As it is discussed briefly in the optimal European capacities, an increase in the number of groups results in a decrease in the overall installed capacity. For example, the use of 3 VRES groups instead of a single group decreases the optimal capacity in Ireland from 98 GW to 22 GW, which is caused by the competitiveness of the technologies in surrounding regions due to grouping. Introducing more groups unveils the high generation locations in these neighboring regions, which becomes cost-competitive with the cheap onshore locations observed in Ireland. In this specific example, Denmark experiences a decrease in the optimal capacity by 15 GW between single and 3 VRES groups. Similar behavior but the opposite trend can be observed in Hungary and Slovenia for open-field PV without tracking and Norway, Netherlands, and Lithuania for onshore wind energy. By unveiling these high generation locations, the capacity distribution changes such as the relationship between northern and southern Greece. With more VRES groups, the optimal capacity of onshore wind energy increases in northern Greece, which then affects the optimal capacity of open-field PV without tracking in southern Greece. In other words, high potential onshore wind locations in northern Greece, which are exposed by using higher number of groups, are more favorable to the energy system than some of the PV locations in southern Greece. This is mainly caused by the use of an optimization model to design the energy system, since it seeks to reduce the total annual cost.

In the United Kingdom and the Netherlands, offshore wind energy becomes cost-competitive owing to the impact of grouping. This cost-competitiveness results from variation in the investment cost of wind turbines within the region rather than the significant increase in the generation of offshore wind turbines. Since the maritime boundaries of these two countries have large area extending long distances from shore (c.f. Figure 3-4), the expensive wind turbines increase the average of the investment cost of offshore wind energy in these regions. Especially in the countries with a large area extending far from shore, the investment cost can attain to 4000 € kW⁻¹ because of the electrical infrastructure cost of the turbines dominating the overall cost. For example, the average specific investment cost for offshore wind turbines in the Netherlands is 2800 € kW⁻¹ for the overall capacity of 149.7 GW, 42.3 GW of which has an average cost of 2060 € kW⁻¹ because of closer distance to shore. Therefore, with the introduction of 3 groups, the specific investment cost is decreased by nearly 30% as well as the maximum allowable capacity. In the case of Belgium, since the maritime area is small, the maximum available capacity of offshore wind energy in that country is utilized in all different group scenarios due to the low average specific investment cost (nearly 2000 € kW⁻¹). In some regions such as Poland and Estonia, a switch between onshore and offshore wind energy is evident. This is caused by the impact of grouping and change in the specific investment costs of onshore and offshore wind energies. In such regions, these two technologies might become cost-competitive, and slight changes in their cost or generation might cause switching the optimal capacity of individual technologies.

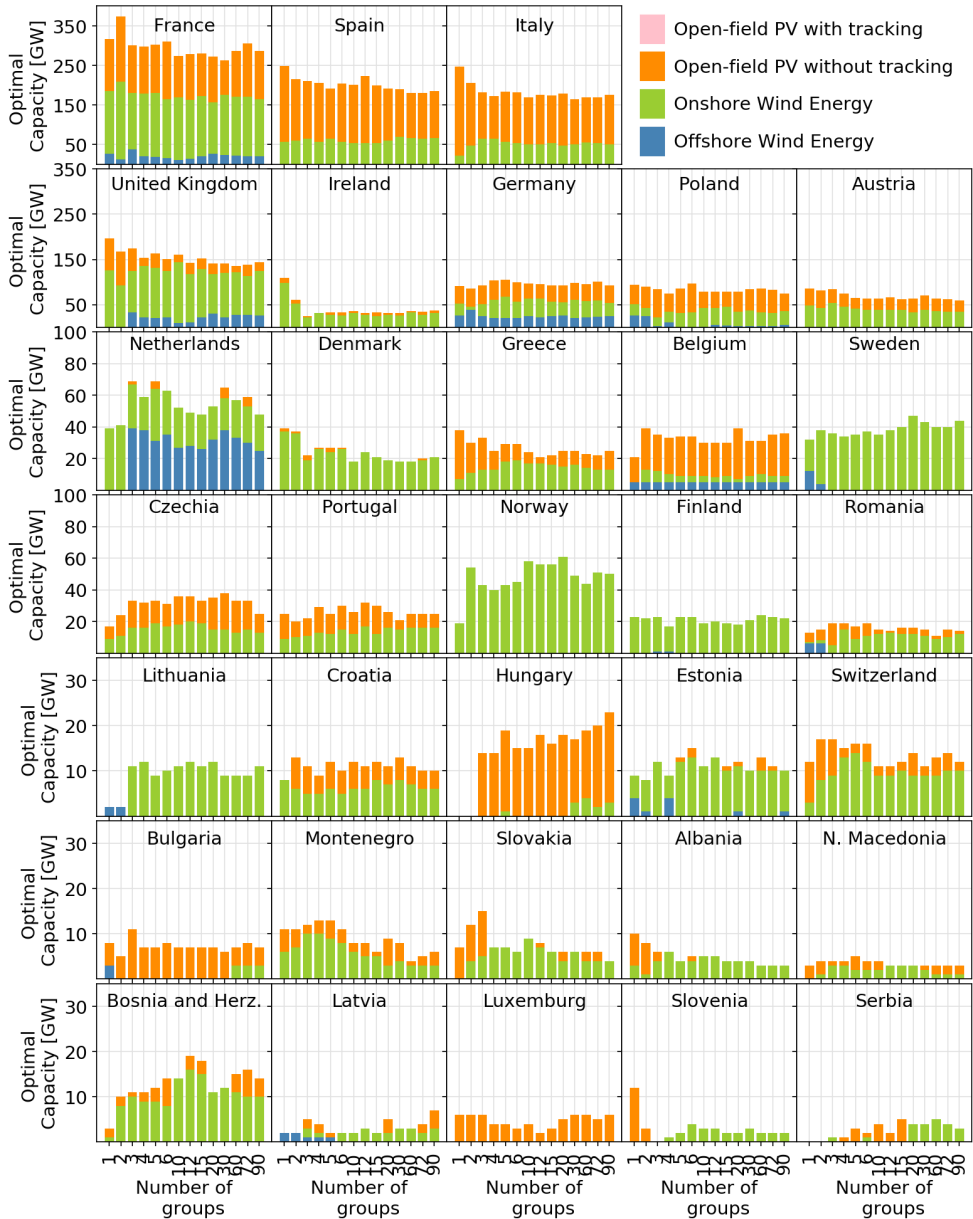


Figure 5-6 National optimal capacities broken down to onshore wind energy, offshore wind energy, open-field PV with and open-field PV without tracking for different number of groups of all technologies.

It must be noted that the weather year 2015 is used in this analysis, while grouping is performed by using average wind speeds of the global wind atlas. Moreover, the spatial distribution of the placements within a region is not taken into account. With the percentile division of technologies as a simple approach, extreme weather phenomena taking place in a specific year or small variations caused by different turbine designs are not captured in all details. Nevertheless, it is shown that consideration of this method enhances the problem definition. All in all, despite the variations in the optimal capacities and penny switch between technologies due to similar cost and generation values, there are minor changes in the overall system design after 60 VRES groups especially in the countries with high optimal capacities. Taking into account the computational time and these slight variations, the number of groups that will be used in the design is determined as 60 for each VRES technology due to the substantial increase²⁴ in the solution time of the problem as it is previously mentioned.

5.3 Impact of Weather Years

Simulation of VRES technologies using MERRA-2 weather data requires a historical year to be specified, yet which year to use in the design of a future energy system remains unclear. Therefore, the use of different weather years for VRES simulations and their impact on the future energy system design should be performed as it is previously mentioned by Caglayan et al. [130]. For this analysis, all the input parameters in the energy system are kept constant except hourly generation time series defined for onshore wind energy, offshore wind energy, open-field PV with tracking, open-field PV without tracking, and rooftop PV. Variation in the inflow time series for hydropower (run-of-river, pumped hydro storage and hydro reservoirs) is also expected with respect to the weather year; however, it is not taken into account due to the lack of data and a methodology to derive related time series for these technologies within the time limit of this project. The resulting energy system designs are compared by means of optimal capacity of individual technologies as well as the total annual cost. This comparison is conducted for overall designs independent from region definition in addition to the in-depth analysis of regional capacities. For visualization and simplicity of data presentation, regional results are aggregated at the national level.

Change in the total annual cost with respect to the weather year used in the VRES simulations is shown in Figure 5-7 with the individual contribution of components in the total annual cost. It is seen that VRES technologies constitute at least 68% of the total annual cost in all of the weather years. Specifically, onshore wind turbines have a minimum share of 43%; the share this value increases to 51% when onshore and offshore turbines' are combined. It must be noted that the significant share of VRES in the total annual cost is caused by the green-field assumption, which neglects the current installed capacities of all generation technologies. Consideration of existing

²⁴ Solution times for 60, 72 and 90 groups are estimated as 28.6 h, 85.7 h and 163.4 h, respectively. However, it must be noted that they might be affected by the other calculations taking place in the same compute note. Therefore, they are included to provide a better understanding of the limitations.

wind turbines and PV parks in the system might change the cost breakdown since the optimal capacity of additional wind turbines, or PV technologies would not be as high as the values obtained as a result of the green-field scenario. In addition to the generation technologies including VRES technologies as well as biomass and run-of-river, the share of the remaining technologies varies between 18 and 26%, nearly 50% of which is constituted by electrolyzers. Moreover, it is seen that the hydrogen pipeline cost only takes up to 1.3% of the total annual cost. This indicates that the construction and design of hydrogen transmission pipelines are not of a major obstacle in terms of cost, although routing and consideration of pressure drop remain as the main concern in the design of the infrastructure.

The total annual cost is the highest with a value of 238 Billion € a⁻¹ when 1982 is used as the weather year, whereas the lowest value (205 Billion € a⁻¹) is obtained for the weather year 1988. Average of all years is estimated as 222 Billion € a⁻¹, and the median of these 38 model runs is found as 220 Billion € a⁻¹. In the study conducted by Caglayan et al. [130], the cheapest and the most expensive system designs are obtained for weather years 1998 and 2006, respectively. In this analysis, which includes PV technologies, as well as hydropower and biomass, the cheapest and the most expensive system designs, are obtained for weather years 1988 and 1982, respectively. Nevertheless, 1998 is observed as the third cheapest, and 2006 is the third most expensive system designs. These deviations result from the consideration of additional generation technologies, which compensates the intermittency of wind energy to some extent. Despite the slight variations in the orders of the cheapest and most expensive system designs in both studies, significant variations in the total annual cost are still observed even in two consecutive years, such as the results of 1997 and 1998. Therefore, it can be said that the energy system design still alters even with the consideration of PV, biomass, run-of-river technologies as well as pumped hydro storage, hydro reservoir, lithium-ion batteries, and electricity transmission networks.

In order to understand these variations in the total annual cost, optimal VRES capacities are analyzed for all regions. A direct proportionality between optimal VRES capacities and the total annual cost is not observed. For example, the highest total annual cost is observed in 1982 in this analysis; despite the optimal VRES capacities in this year are nearly the same as the average over all years. Another example could be a comparison between the results of 1982 and 1983 revealing approximately 23 Billion € a⁻¹ variation in the total annual costs. Optimal capacities for onshore wind energy and open-field PV in these years vary by 20 GW (1983 has lower capacities in both cases), and offshore capacity varies only by 1.6 GW. Despite similar VRES capacities in both years, higher electrolyzer capacities are required due to the fluctuations in the VRES generation time series. The optimal capacities for electrolyzer are estimated as 268 and 238 GW in 1982 and 1983, respectively. Thus, in this specific example, an increase in the total annual is caused mainly because of the cumulative increase in the optimal capacities of individual technologies.

A different example of comparison could be 2005 and 2006, with a difference of 26 Billion € a⁻¹ in the total annual costs. Despite the higher total annual cost observed in 2006, optimal onshore capacity in 2005 and 2006 are estimated as 806 and 763 GW, respectively. This lower optimal capacity in onshore wind energy is compensated by offshore wind energy to some extent by installing 92 GW in 2006, which is 15 GW higher than the value estimated in 2005. Moreover, a variation of 135 GW in the optimal capacities of open-field PV is observed. In spite of all these variations, the contribution of VRES technologies differs only by 4 Billion € a⁻¹ in these years. Remaining 22 Billion € a⁻¹ is mainly observed in storage and conversion technologies, especially lithium-ion batteries, and salt caverns contribute to 50% of this discrepancy. The rest is mainly the electrolyzer and technologies used in the re-electrification of hydrogen. Moreover, the use of biomass and higher utilization of hydrogen is also observed in 2006. This is caused by the high intermittency observed in this year compared to 2005. A comparison of the optimal parameters for electrolyzer reveals a decrease of 400 h a⁻¹ in the full load hours and an increase of 30 GW in the optimal capacity.

All in all, despite the significant variations in the total annual cost, observed between 205 and 238 Billion € a⁻¹, a generalization and correlation of variation by the optimal capacities of individual technologies cannot be derived. In some cases, a slight increase in the optimal capacities of individual technologies and their cumulative sum causes an increase in the total annual cost. In other examples, irregular distribution in the optimal capacities (both increase and decrease in the optimal capacity of individual technologies) and high intermittency observed in VRES generations in that specific year results in these variations. Nevertheless, it is evident that the system design chosen in any specific year is not robust. In other words, the selection of the optimal results of one weather year is not sufficient in terms of security of supply.

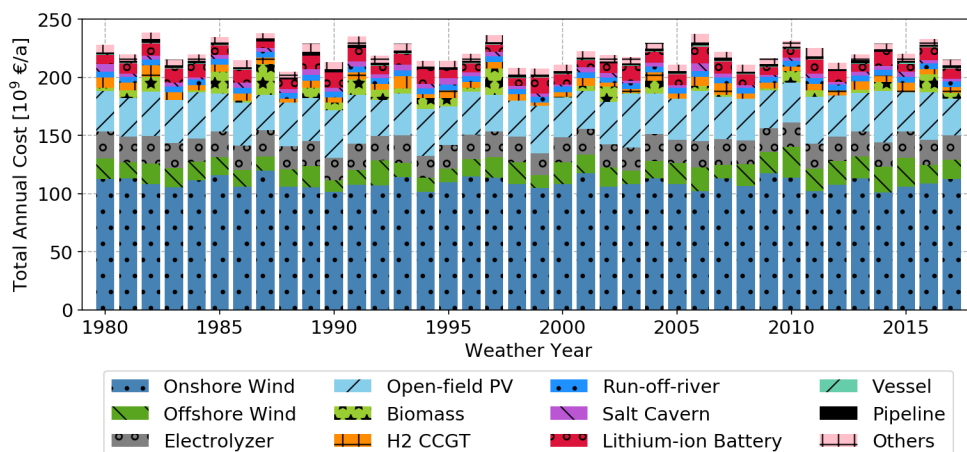


Figure 5-7 Variation of total annual cost with respect to the weather year used in the simulation.

5.3.1 Variation in the Optimal Capacity of VRES at National Level

In the previous section, the overall results independent from each region in terms of total annual cost and optimal capacities of VRES technologies are investigated in order to have an insight into the variation. However, aggregated values are not sufficient to understand the variations system. Therefore, optimal VRES capacities are analyzed in detail by checking the deviations in the system design at a national level. Although there are 96 regions in the scenario definition, results here are presented and discussed at a national level for the sake of succinct explanation. Nevertheless, national optimal capacity results for each region, year and technology can be found in Appendix A.4. Figure 5-8 shows the distribution of optimal VRES capacities as a boxplot, which is plotted as a statistical distribution independent from the order of years when these capacities are observed. The red lines represent the median of optimal capacities for a specific country, whereas black markers stand for the outliers in the distribution. Rooftop PV is not shown since the optimizer does not choose this technology because of its relatively higher cost (cf. Figure 3-18).

Optimal onshore capacity across Europe varies between 750 and 890 GW, and these differences are more pronounced in certain countries. Optimal capacities in many countries do not alter significantly. For instance, variations in the optimal onshore capacities in 25% of the countries are estimated at less than 5 GW. In countries like Spain, the United Kingdom, France, Ireland, Poland, Italy, Norway and Germany, these differences are greater than 35 GW. However, the only absolute magnitude in the lower and upper optimal capacities is not sufficient. When percent variations in the results are analyzed, the difference in France corresponds to nearly 15% variation when the average optimal onshore capacity is taken into account. This value increases to 30% for the United Kingdom, 50% for Germany.

Compared to onshore wind energy, optimal offshore capacities are significantly low, yet they are still noticeable in certain countries. Especially Germany, France, the Netherlands, Poland and the United Kingdom experience deviations ranging between 15 and 40 GW. Although the magnitude of deviations in Belgium is smaller, the percent utilization with respect to maximum potential has a wide range. In 2017, the offshore wind in Belgium is not utilized at all, whereas in years like 1981, 1998, and 2015 the optimal offshore capacity in Belgium is estimated as 4.72 GW, which is its maximum allowable capacity. In the United Kingdom, as an outlier, the maximum optimal offshore capacity is observed in 2010 with a value of 41 GW (which is nearly 2% of the maximum allowable offshore capacity). Besides this extreme value, the highest capacity is estimated as 31 GW for 2006, and the lowest value is found to be 3.1 GW. When the optimal offshore capacities in France are investigated, 27.3 and 29.5 GW capacities are calculated for 2013 and 1983, respectively. However, in some years, such as 1993, 1994 and 2007, offshore wind energy in France is not utilized at all. Such behavior in offshore wind energy can be explained by the switch occurring between onshore and offshore wind energies in several regions. Due to certain weather phenomena happening at the onshore locations, occasionally, generation via onshore wind turbines might be relatively cheaper compared to the ones at offshore locations. Moreover,

variations in the optimal capacities can also be caused by the variations in the wind speeds or generation time series at an hourly level. When the time series have low generation periods, higher optimal capacities of generation technologies are required in order to decrease the lulls and supply the demand, especially in these low generation periods.

Focusing on the open-field PV with and without tracking reveals that open-field PV without tracking is more favorable in almost all countries and years, owing to its lower specific investment cost. Slightly higher generation early in the morning and late afternoon is observed in the open-field PV with tracking does not provide a significant advantage for this technology by making it more favorable despite its relatively higher investment cost. The optimal open-field PV without tracking varies between 529 to 811 GW, whereas this variation is in between 0 to 5.15 GW for the ones with tracking, which experiences an optimal capacity higher than 1 GW only in 8 years among 38 years considered in this analysis. This can be explained by the use of open-field PV systems to compensate for the fluctuations occurring in the generation time series of wind energy. Therefore, the slightly higher generation observed with a tracking system is not necessary while compensating for the intermittency of on-/offshore wind energy. In cases where it is chosen by the optimizer, open-field PV with tracking systems are able to supply the demand better than the ones without tracking owing to these higher generation locations. However, since this does not occur very often with high optimal capacities, consideration of open-field PV with tracking might not be necessary since it further increases the complexity of the problem. When open-field PV systems without tracking are analyzed, high optimal capacities with average values greater than 100 GW in Spain, France, and Italy are observed. However, the differences in the optimal capacities in these three countries are approximately 90 GW. Similar to the behavior observed in the distribution of optimal wind energy capacities, these differences are less pronounced in the countries having lower optimal capacities. It is seen that PV technologies are chosen in countries such as Poland and the United Kingdom despite their relatively low full load hours compared to countries such as Greece, Albania, and Portugal. This can be explained by the combination of wind energy and PV systems as hybrid systems result in shorter lulls and they generally compensate each other's low generation periods. This phenomenon is explained by Ryberg [37] while comparing the lull periods in different locational contexts for wind and PV technologies. Ryberg states that the probability of observing a lull period decreases when hybrid systems are used [37]. Therefore, the installation of some amount of open-field PV without tracking in regions such as the United Kingdom and Poland is observed in order to decrease the lulls and fluctuations in the generation time series.

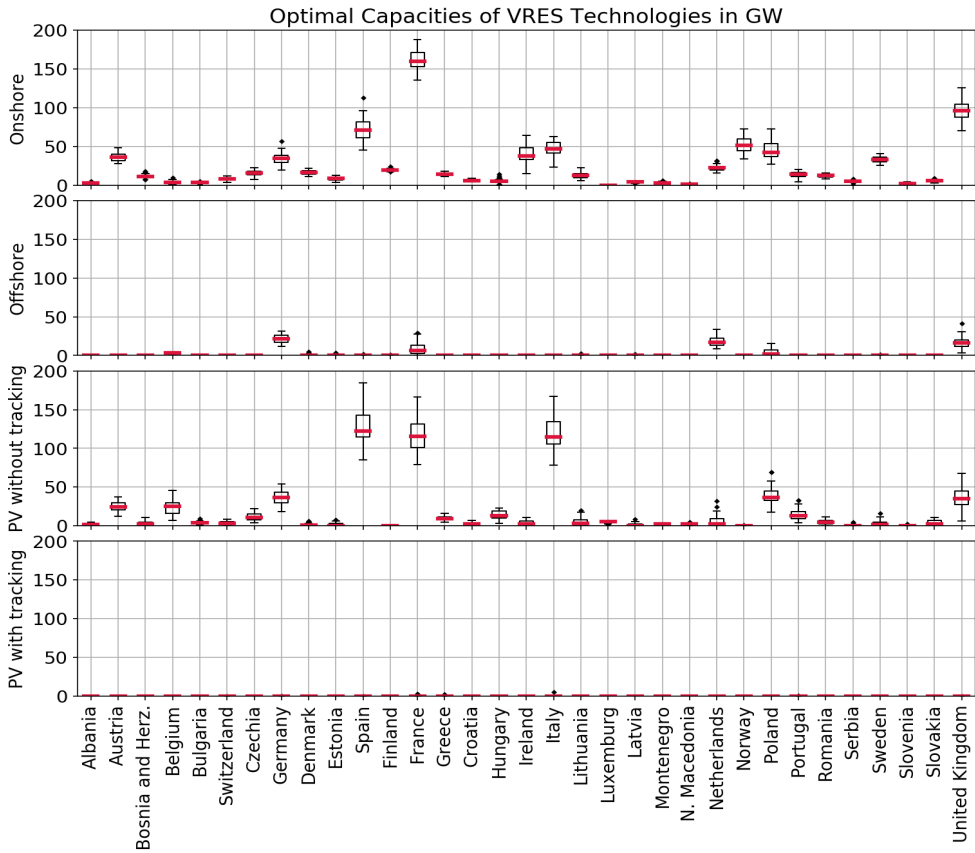


Figure 5-8 Boxplot of the optimal capacity of VRES technologies obtained for different weather years at a national level.

5.3.2 Variation in the Optimal Capacity of Conversion Technologies at National Level

In addition to the optimal capacities of VRES technologies, optimal capacities of conversion technologies are also investigated in a similar way, as presented in Section 5.3.1. Resulting distributions for four conversion technologies chosen as a result of the optimization are shown in Figure 5-9. Although 5 different conversion technologies are defined for the conversion of hydrogen into electricity, only two of them (H₂ CCGT and H₂ OCGT) are chosen to be installed by the optimizer. This is mainly because of the high investment costs of PEMFC and SOFC, and low efficiency of H₂ gas engine compared to the other technologies. Therefore, optimal capacities for PEMFC, SOFC, and H₂ gas engine are not shown in the figure, since the optimal values are always zero for all regions and years.

Focusing on biomass CHP plants reveals that in half of the years, biomass CHP plants are not installed in any region. These variations with respect to the weather year in which biomass CHP plants are utilized can also be seen in Figure 5-7. Although 50% of the years do not experience the utilization of biomass, countries such as Germany, Belgium, France, and the Netherlands have an average optimal capacity larger than 1 GW. When the maximum capacities for each country are investigated, it is seen that most of the countries experience their maximum in 1987. For this specific year, optimal capacities in Germany, France, and the United Kingdom are estimated as 25, 13 and 7 GW, respectively. Despite the variations observed in these countries, in Belgium, for example, the maximum allowable capacity for biomass CHP plants (4.75 GW) is found to be optimal in 55% of the years. On the other hand, biomass CHP plants in this region are not utilized at all in half of the remaining years. It needs to be considered that biomass is used as a back-up generation in the countries having high optimal capacities of wind and open-field PV technologies within the context of this system design.

When the distributions of optimal electrolyzer capacities are investigated, wide ranges are seen in the countries with high generation capacities. Spain, France, Ireland, Norway, and the United Kingdom have the highest average among all the countries. Therefore, it can be said that the electricity generated via wind and PV technologies in these countries is utilized in hydrogen production via electrolyzer (the roles of countries and distribution of the technologies will be further discussed in Section 6.1 and Section 6.4). Among these countries with high capacities, Germany has different behavior in spite of the high optimal capacities observed for onshore, offshore and open-field PV without tracking. Only in three years (2008, 2011, and 2014) electrolyzer capacities of 1.2 to 2.8 GW are estimated to be optimal, and in the remaining 35 years, they are not installed at all. This is also related to the high biomass CHP plant capacity observed in Germany, showing the use of all electricity generated in that country to supply the country's demand. Austria experiences similar optimal VRES capacities compared to Germany, yet the behavior is different in terms of the electrolyzer. While Germany uses its generation capacities to supply its demand, Austria produces hydrogen with a wide range for the optimal electrolyzer capacities (an average of 8.4 GW). Thus, this difference is caused by the role of Austria as a hydrogen exporter to northern Italy.

Finally, hydrogen OCGT and hydrogen CCGT technologies are competitive due to their efficiencies, specific investment costs and variable operation cost. Although hydrogen OCGT is cheaper in terms of specific investment costs, its operation cost is higher than the hydrogen CCGT (cf. Table 3-5). Although hydrogen CCGT is widely chosen with relatively higher optimal capacities compared to hydrogen OCGT, in certain countries, the latter is preferred, too. For instance, a maximum capacity of nearly 25 GW is attained for hydrogen OCGT in Spain, France, the Netherlands, and the United Kingdom, even though these values are taken into account as outliers in the figure. However, these outliers are observed in both technologies and many countries. This is mainly because of the fluctuations in the generation time series and requirement for higher capacity for re-electrification technologies in order to supply the demand by utilizing the hydrogens

for electricity generation at low generation periods. Therefore, experiencing these outliers in almost all countries and both re-electrification technologies can be explained by these extreme periods, at which lulls are observed. The widest range in hydrogen CCGT is observed in Germany, whereas France and the United Kingdom have similar ranges for hydrogen OCGT. When the outliers in hydrogen OCGT are investigated per country, these maximum capacities are observed in the years where system cost is above average. For example, the Netherlands and the United Kingdom experience the highest optimal capacity in 2006, yet for France and Spain, these years are 1989 and 1991, respectively. Thus, it can be said that the use of hydrogen as a back-up generator is more pronounced in these extreme years (outliers) with more fluctuations.

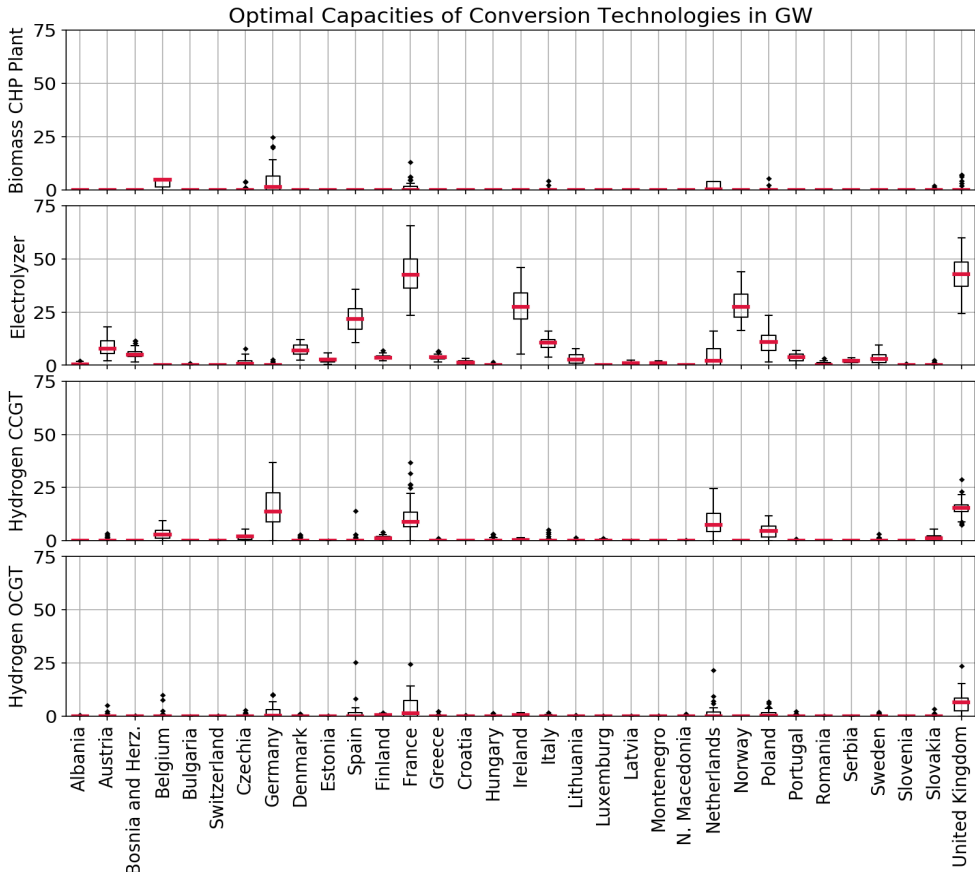


Figure 5-9 Boxplot of the optimal capacity of conversion technologies obtained for different weather years at a national level.

5.3.3 Variation in the Optimal Capacity of Storage Technologies at National Level

Distribution of the optimal capacities for storage technologies is shown in Figure 5-10 as boxplots. Pumped hydro storage and hydro reservoirs are considered as a storage technology with fix capacity values without allowing expansion; thus, they are not shown in the figure. Comparison of the storage capacities of salt caverns, lithium-ion batteries, and vessels reveals that there is a significant difference in the order of magnitude of the optimal capacities between salt caverns and the others. This is mainly because of the role of the salt caverns in an energy system since they are considered as seasonal storage technologies. Unlike salt caverns, lithium-ion batteries are generally used in the intra-day storage requiring less capacity in comparison to them. Finally, vessels have less capacity owing to their high specific investment cost compared to salt caverns. Nevertheless, vessels are preferred in certain regions because of different reasons.

Focusing on salt caverns shows that in all the countries where salt caverns are available, at least one cavern is installed in most of the years. Exceptions are observed in Albania: for instance, the use of a salt cavern is not required in 1998, which has one of the lowest total annual costs. Moreover, in the same country, storage capacities in 2000, 2005, 2008 and 2013 are estimated at less than 60 GWh²⁵. These effects are seen because of the linearization of the optimization problem; nevertheless, it must be noted that the construction of smaller salt caverns is also possible by decreasing the volume. Besides Albania, the requirement for salt caverns in Bosnia and Herzegovina, Greece, Portugal, and Romania are not as significant as the other countries such as Germany, France, and the United Kingdom. The highest average storage potentials are observed in Germany, France, and the United Kingdom with values of 15, 16 and 23 TWh, respectively. The minimum storage potential in these countries is estimated at around 5 TWh. The highest optimal capacities in the United Kingdom shown as outliers are observed in 1980 and 2006 as 43 and 49 TWh, respectively. For France, it is 1989, and for Spain, these outliers are observed in 1980, 1989, 1991 and 2007. Finally, the behavior observed in optimal electrolyzer capacity in Germany can be explained by looking at the optimal storage capacity of salt caverns in this country. The high potential of salt caverns in Germany is used for hydrogen storage in order to use it in the re-electrification in addition to the biomass CHP plants for the same purpose: lull periods. Therefore, although hydrogen is not produced in Germany, the utilization of large storage capacities for this energy carrier is observed.

Unsurprisingly, the significantly high storage potential of lithium-ion batteries is observed in countries with high open-field PV penetration (France, Spain, and Italy). As it is expected, this technology is mainly used in order to compensate for the fluctuations of PV generation time series caused by day and night within a day. When the storage capacities and optimal open-field PV capacities are investigated together in general, a correlation between these two technologies can be seen easily. Despite slight variations, the order of the years in both technologies is found to be

²⁵ A 500,000 m³ salt cavern has a storage potential of nearly 130 GWh.

similar when they are sorted by the capacities. For instance, Italy experiences the highest storage potential in 1989, where also the highest open-field PV capacity is observed. Similarly, the highest capacities in both technologies are observed in 2006 for Spain and France.

Finally, similar behavior is also seen in vessels, which is installed in locations with high electricity generation. Nevertheless, it must be noted that this technology is generally preferred in the regions where salt caverns are not available. For example, nearly 300 GWh of vessel capacity in the United Kingdom is observed in the region "90_uk", which involves London as a high demand center and does not have any potential for salt caverns. Moreover, vessels are also preferred in certain regions, and especially when the discharge rate of salt caverns becomes limiting at specific time periods, and additional hydrogen is required. Therefore, vessels become necessary at low electricity generation time periods and limited hydrogen supply from the salt caverns due to limited withdrawal rate. These lower and upper bounds of optimal vessel storage capacities shown in Figure 5-10 represent the extreme time periods, when there is no requirement for vessel storage (lower bound), or there is a relatively high demand (upper bound) due to the lack of demand-supply. Finally, unlike the countries experiencing a wide range in the optimal capacities, Italy and Austria experience a narrow range despite the outliers observed in these regions. Similarly to the previous discussion, these narrow ranges can be explained by the lack of salt cavern storage in these countries and requiring some amount of hydrogen storage to be used as a backup generator. Although there are many outliers especially in Italy representing the extreme weather years for the regions, the variation in the storage capacity for the vessels in Italy is calculated as 120 GWh.

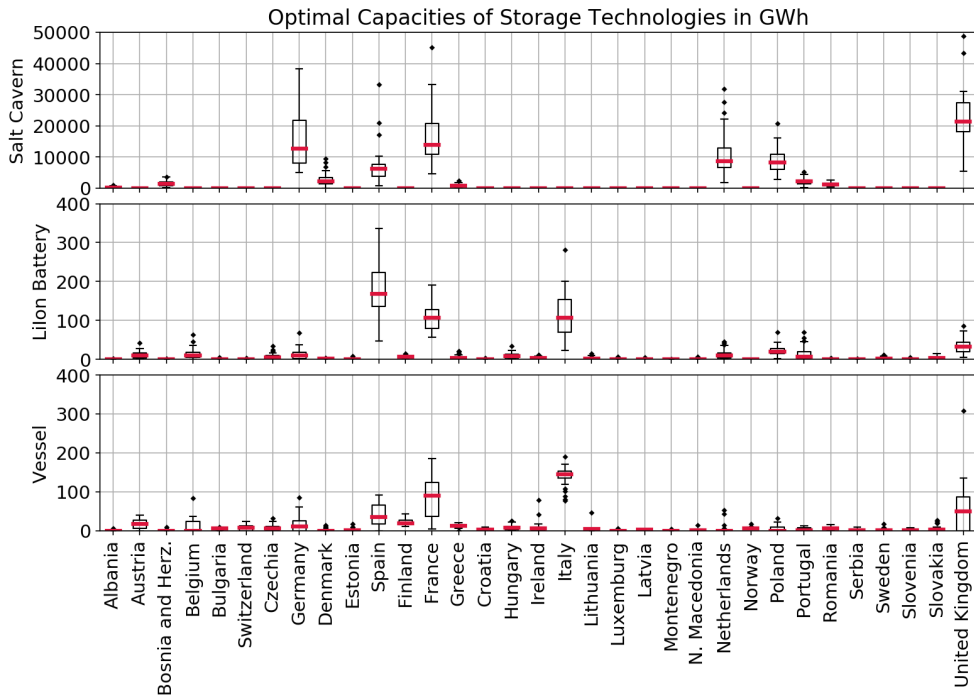


Figure 5-10 Boxplot of the optimal capacity of storage technologies obtained for different weather years at a national level.

5.3.4 Variation in the Hydrogen Pipeline Connections

Optimal hydrogen pipeline capacities as a result of optimization for each weather year have been analyzed. Before the analysis of variations in the pipeline capacities, repetition of pipeline connections has been investigated, since most of the connections are not built in every weather year. In order to obtain these results, optimal capacities between regions are extracted for each weather year used in this analysis. Then a value of “1” is attained to the connection if the optimal capacity higher than 0.5 GW (nearly 0.15 m in diameter as the smallest diameter in the natural gas transmission network), if the connection is not built or have a capacity less than 0.5 GW the value is set to “0”. In the end, these connections are summed in order to visualize how many times each of them is chosen by the optimizer. Following this, the pipeline capacities are extracted from the results of each year. In order to calculate the average pipeline capacity of a connection between two regions, only the years where it is built is considered with their corresponding capacities. Finally, in order to investigate whether or not there is a correlation between pipelines and salt caverns, the average storage capacity of salt caverns are also taken into account. The combination of average pipeline capacities, salt cavern storage capacities, as well as the repetition of the pipeline connections between regions are shown in Figure 5-11.

Some of the pipeline connections are built in 80% of the model runs, such as the ones within the United Kingdom and also then ones within Ireland. Similar to this, the regions within Italy are also repeatedly connected. It is also seen that many connections are built at least 90% of the cases (among 38 model runs). For example, the connections built between northern and southern Germany are evident, which is similar to the findings of Robinius et al. [12] and Welder et al. [13]. Only one region in Switzerland ("48_ch") is not connected via hydrogen pipeline in any of the years investigated, which is mainly because of the low demand as well as high flexibility in the operation (both electricity and hydrogen). Moreover, electrical infrastructure and electricity generation via VRES sources are found to be sufficient to supply the demand in this region. Furthermore, the extreme periods where lulls occur can be compensated by the comparably high pumped hydro storage in this region. When the pipeline repetition is combined with the regions with salt cavern capacities, a pipeline corridor can be seen passing through the regions having a potential for salt cavern storage except for the Nordic countries and Italy. In the case of the Nordic countries, two storage technologies (pumped hydro storage and hydro reservoir) can substitute the salt caverns, and enable supply of hydrogen from these regions. Italy experiences a perpetual pipeline design due to the cheap hydrogen produced in the northern countries as well as the stored hydrogen transported over southeastern France, in spite of the lack of salt caverns. In other words, installation of vessels in Italian regions is found cost-optimal with the consideration of pumped hydro storage and hydro reservoir technologies (as their capacity is taken from 2015 values) compared to producing the hydrogen in Italy. When individual capacities of pipeline connections are analyzed, large capacities are observed between Sweden and Denmark as well as the United Kingdom and France. Both Nordic countries and the United Kingdom export large amounts of hydrogen to the continental Europe owing to lower production costs in these regions. Moreover, the connections between France and Italy have also an average capacity of nearly 10 GW. Besides these connections, average pipeline capacities are below 5 GW.

All in all, as it is also found in the exemplary scenario for the use of different weather years to supply the hydrogen demand for passenger vehicles conducted by Caglayan et al. [130], variations in the connections are apparent between years. Therefore, consideration of additional technologies, especially PV and biomass, as well as the high electricity and hydrogen demands, does not compensate for the variations between different weather years. Nevertheless, a perpetual pipeline design is generally observed in the results of different weather years in spite of the occasionally built connections. Most of the frequently built pipeline connections are observed around the regions having salt cavern potential. Exceptionally, pumped hydro storage and hydro reservoirs can be used as a substitute for salt caverns in the Nordic countries. The perpetual pipeline connections can further be used to design a robust system, which is feasible for all weather years. Nevertheless, variations in the capacities should be investigated in addition to the repetition of the connections, since these two aspects of pipelines are independent of each other.

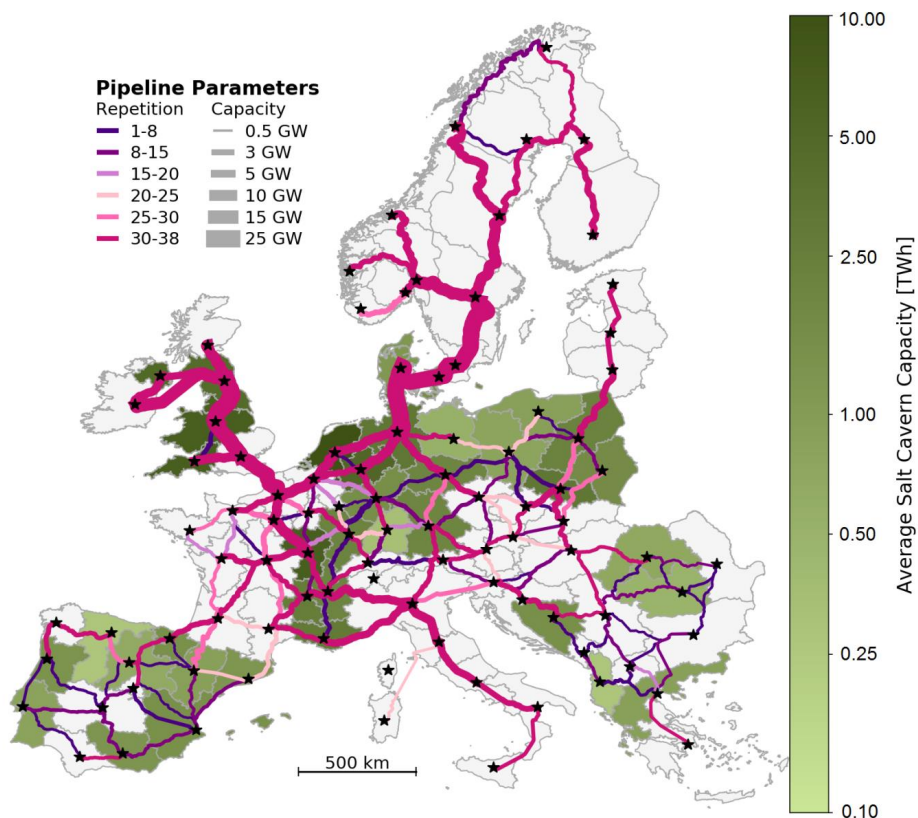


Figure 5-11 Average optimal capacities for salt caverns and pipeline with pipeline repetitions as a result of optimization performed for 38 years (between 1980 and 2017).

5.4 Value-of-Analysis of Technologies Considered in the Design

Each technology defined in the model has a role and a value in the overall energy system. In order to estimate how important these individual technologies are, a value-of-analysis is performed by defining a reference scenario (c.f. Figure 5-1) following the same method performed by Samsatli et al. [31] and Welder et al. [13]. In this method, individual technologies are prohibited one by one from the reference scenario. In that way, the increase in the total annual cost of the system can be used as an indication of the value of a technology. For example, the importance of the technology becomes apparent when the total annual cost of the system increases drastically, whereas insignificant changes in the cost indicate that the technology does not have a crucial role in the overall system, and another technology can substitute it with a slight change in the system cost.

In order to perform this analysis, all the technologies defined in Section 3.4 are excluded one by one from the reference scenario definition, which is chosen as the scenario with the weather year 2015 and 60 groups per VRES technology (c.f. Figure 5-1). The only technology that is not excluded in this analysis is the PEM electrolyzer since it is the only technology used in hydrogen production. The optimization problem would not be feasible without the electrolyzer due to the lack of technology supplying hydrogen demand. The reason for choosing this scenario is to be able to compare the value of individual technologies with the optimal results that are closest to the final system design. Since the final system is obtained as a result of iterations to provide the most robust design, it overpredicts the capacities of technologies installed in each region in order to supply the demand even in the extreme time periods observed in any year within the time frame, which is between 1980 and 2017 (security of supply). Therefore, this overprediction includes back-up generation in these regions; the values of individual technologies might be misleading owing to the higher capacity and cost assumed in the reference scenario. Moreover, among all the weather years considered in the analysis, 2015 is the only year used in the determination of inflows of pumped hydro storage as well as hydro reservoirs. Therefore, due to the lack of data, the use of this year with 60 VRES groups gives to most realistic scenario definition among all the others.

The reference scenario has a total annual cost of 220 Billion € a⁻¹, shares of individual technologies can be seen in Figure 5-7 (the weather year 2015). Overall, VRES capacity installed in this scenario is estimated as 1480 GW, 785 and 110 GW of which belong to onshore and offshore wind energies. Furthermore, only 0.6 GW biomass CHP plants are installed, which is mainly in Germany. The optimal capacities of generation technologies and the pipeline design of the reference scenario are given in Figure 5-12. As it is seen from the figure, there is a large pipeline connection between Sweden, Denmark, and Germany providing hydrogen to continental Europe, which is already discussed in Section 5.3.4. Similarly, large pipeline capacity between the United Kingdom and continental Europe is evident. Offshore wind energy is chosen to be installed in the United Kingdom, Netherlands, Germany, Belgium, and northern France, yet onshore wind energy is installed almost in all the regions with capacities reaching 33 GW. Moreover, utilization of open-field PV without tracking, especially in southern regions, is evident; nevertheless, it is also found to be optimal to have some amount of PV in Poland and the United Kingdom, mainly because of its ability to compensate fluctuations in the generation via wind energy.

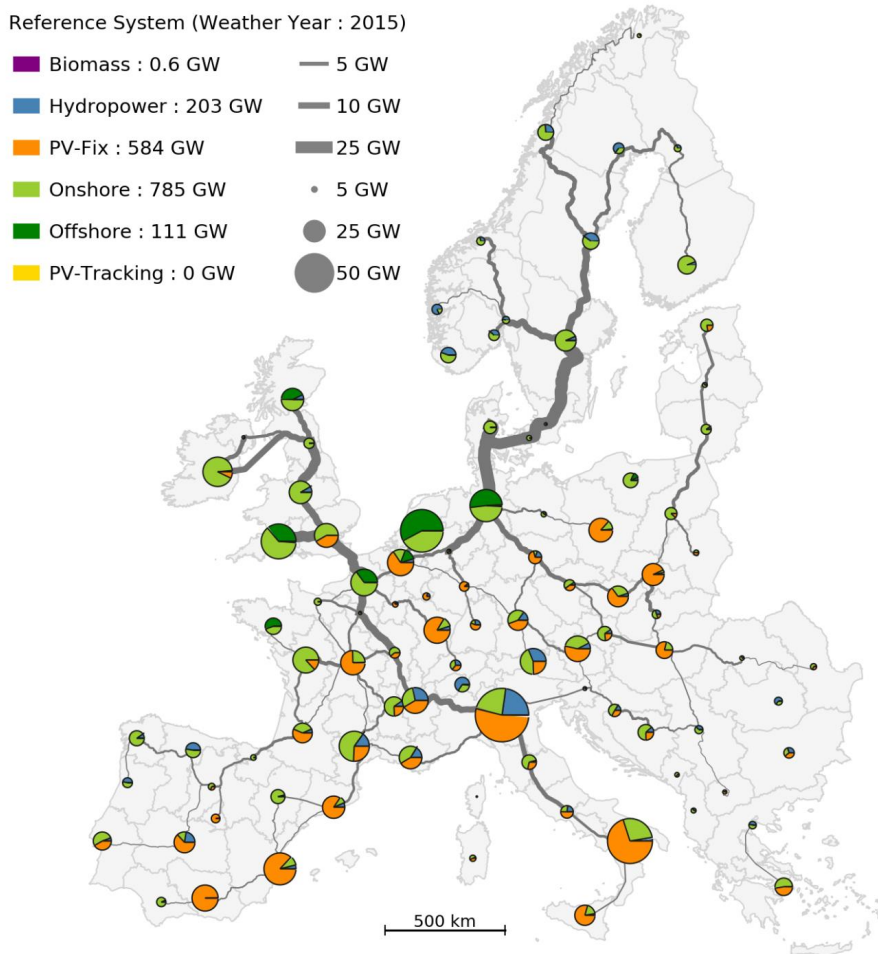


Figure 5-12 Optimal design of the reference scenario used in the value-of-analysis. Weather year is chosen as 2015, 60 groups per VRES technologies and 30 typical days.

Variations in the total annual cost corresponding to the scenario where individual technologies (wind and solar energies are also considered together) are prohibited in the system are shown in Figure 5-13 in order to compare the value of individual technologies. It is seen that the combination of onshore and offshore wind energies plays the most significant role in the system with an increase of 56.2% in case of their absence. Following this, the connections between countries, in which the interaction of countries is prohibited, has an increase of 43.4% with respect to the reference system. It is then followed by HVAC connections and onshore wind energy only with 31.2% and 22.3% increase, respectively. In the case of prohibiting onshore turbines, a drastic increase in the share of offshore wind turbines is evident. In addition, in these three cases, a

drastic increase in biomass is also apparent. Nevertheless, the corresponding system design due to absence of these technologies will be discussed in Section 5.4.1, Section 5.4.4, Section 5.4.3 and Section 5.4.4 considering the other technologies within the same component class (open-field PV and offshore wind energy in generation technologies, pipelines and HVDC cables in transmission technologies).

Hydro reservoirs have an impact of 12.1% on the total annual cost when they are removed from the system design. From the cost components, an increase in generation technologies such as onshore and offshore wind, as well as the open-field PV, is evident when the hydro reservoir is forbidden in the system. Optimal capacities for onshore, offshore and open-field PV without tracking are increased by 20.4, 4.6 and 186.5 GW, respectively. It is more pronounced in "86_se", a region located in Sweden with an increase of 15.2 GW in the optimal capacity of onshore wind energy due to the absence of 5.8 GW withdrawal capacity of reservoirs located in that region. In addition to the increase in the overall capacities of generation technologies, higher utilization of pumped hydro storage systems are also observed based on the increase in their cost-share due to the variable operation cost of this technology.

Following these technologies, salt caverns have a considerable impact on the system design due to their role as seasonal storage. The specific investment cost of salt caverns is lower than that of vessels by a factor of 20. Therefore, when the salt caverns are not allowed to be built, use of biomass as a dispatchable generation technology to compensate intermittency of VRES technologies rather than utilization of vessels (to the similar storage capacity of salt caverns in the reference scenario) is preferred. In addition, the shares of electrolyzer and hydrogen CCGT technologies decrease, since the system relies more on biomass and produces hydrogen only to supply the hydrogen demand. Therefore, the behavior observed in the reference system regarding reelectrification and higher hydrogen production as a backup during lull periods is changed when salt caverns are prohibited in the system.

Many technologies increase the total annual cost of the system by 1 to 4% when they are prohibited, yet their absence can be compensated in different ways. For instance, not allowing run-of-river technology increases the total annual cost by 3.5%, yet higher capacities of VRES technologies can substitute the absence of run-of-river. In the case of pumped hydro storage, higher reliance on hydrogen and lithium-ion batteries is sufficient to place this technology. Finally, the use of hydrogen and biomass can substitute the lack of lithium-ion batteries with a 2.8% increase in the total annual cost.

Technologies, which are not chosen by the optimizer because of their high costs, can be seen from the figure with no change in the total annual cost. Hydrogen gas engines, PEMFC, SOFC, and rooftop PV can be considered among these technologies. As it is expected, they do not play a crucial role in the system design within the scope of the scenario definition. In this specific year, biomass also seems to have an insignificant impact on the system. Nevertheless, biomass is

considered as a backup generator in the extreme years where lulls are observed as it is briefly discussed in Section 5.3.2. Therefore, it must be reminded that the value-of-analysis presented here is limited by the scenario definition and the values of individual technologies might change when a different weather year is used.

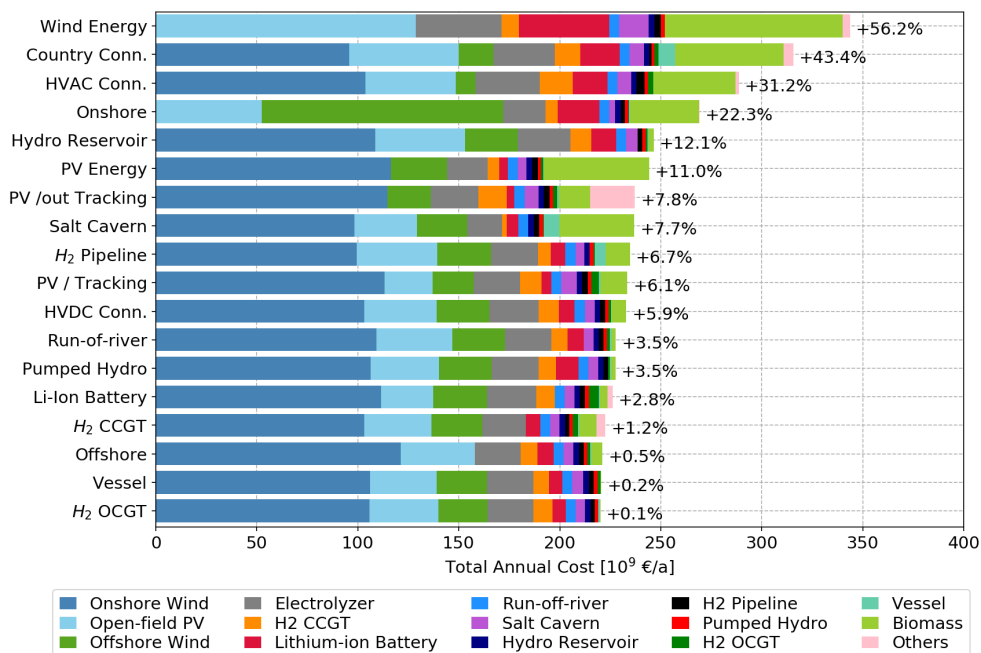


Figure 5-13 Variation in the total annual cost of the system with respect to individual technologies prohibited.

5.4.1 Value of Wind Energy and PV Energy in the System

As VRES technologies, wind and PV energies play significant roles in the 100% renewable energy system, which can be seen in Figure 5-13. Although onshore and offshore wind technologies can be considered separately, a scenario where both of them are prohibited is investigated in order to observe the value of wind energy in the energy system. Furthermore, a similar approach is applied to PV technologies, which include open-field PV with tracking and without tracking as well as rooftop PV. The resulting system designs for these scenarios are shown in Figure 5-14.

When both onshore and offshore wind technologies are prohibited, the system mainly relies on open-field PV as well as biomass. It is seen that pipeline connections play a crucial role in the system; nevertheless, the roles of countries in terms of import and export change. Opposite to the reference scenario in which the hydrogen is provided by the Nordic countries as well as the United Kingdom, hydrogen is transported from south to north (especially from Spain and France to the

United Kingdom as well as central Europe) when the system is dominated by PV technologies. The estimated optimal capacity for open-field PV is nearly 2275 GW, which corresponds to an increase of approximately 290% compared to the reference scenario. In other words, the absence of 895 GW of wind energy, 110 GW of which is offshore wind, is compensated by nearly 1700 GW PV and also 150 GW of biomass CHP plants. Although the vast majority of open-field PV systems are without tracking, "09_es" experiences nearly 40 GW of open-field PV with tracking. This is mainly caused by the slight difference in the generation time series of that technology, which is found to be more beneficial to supply the demand despite its relatively more expensive cost. Moreover, a significant increase in the utilization of vessels and lithium-ion batteries, as well as salt caverns, is observed in the system. The optimal storage capacity of vessels in the reference scenario is estimated as 670 GWh, whereas this value increases to 9200 GWh due to the absence of wind energy in the system. The higher storage capacity of vessels is mainly observed in the regions where salt caverns are not available. The drastic increase in the capacity of lithium-ion battery (3 folds of the reference scenario) can be explained by the diurnal dependence of PV technologies. Although it is not as pronounced as batteries and vessels, the storage capacity of salt caverns increases by a factor of 1.5 (120 TWh in the reference scenario).

The influence of prohibiting PV energy in the system increases the total annual cost by 11%. A similar system design compared to the reference scenario can be attained with higher capacities of onshore and offshore, which are 80 GW and 8 GW, respectively. Although PV is not complementary to wind energy, the combination of these two technologies decreases the fluctuations and storage needs to some extent [37], [94]. However, the fluctuations in the generation time series of wind energy can also be compensated by biomass. In this case, a total increase of 87 GW in the biomass CHP plant capacity is observed. It must be noted that in the reference scenario, biomass is not chosen due to the abundance of VRES technologies for a comparably cheaper cost. Therefore, it can be said that the absence of PV energy results in reliance on biomass. This dependency is especially observed in the southern and in central Europe. In most of the regions, there is still some onshore wind energy potential cheaper than biomass. However, this is not observed in Paris, Rhineland-Palatinate & Hesse and North-Rhine Westphalia. The pipeline connections and their capacities do not change significantly.

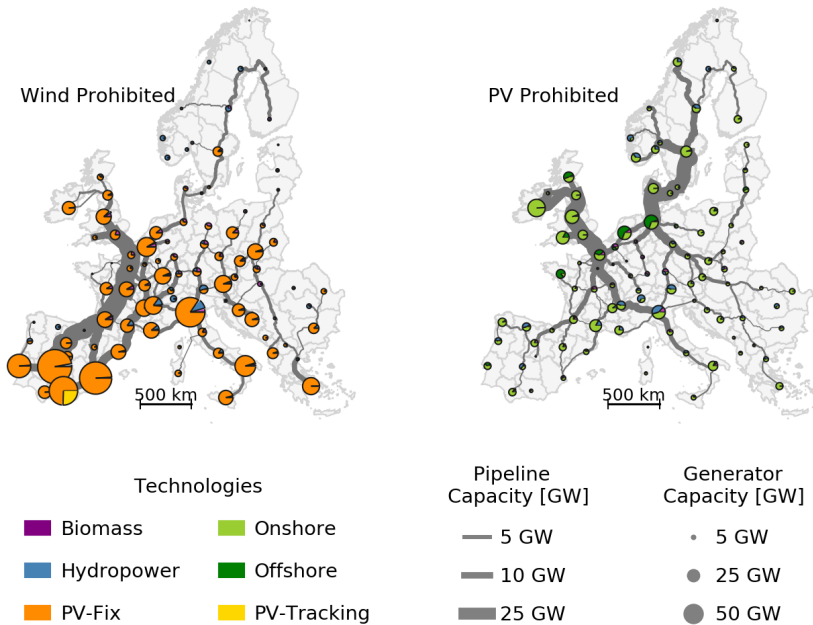


Figure 5-14 Spatial distribution of generation technologies when wind (right) or PV (left) technologies are prohibited.

5.4.2 Value of Connection between Countries

The second-highest impact is observed for the connections between countries. In this scenario, HVAC, HVDC and pipeline connections between countries are prohibited to analyze the importance of trading between countries. Therefore, the change in the transmission network causes in total 43.4% increase in the total annual cost of the system. The optimal capacities of onshore, offshore and open-field PV without tracking are estimated as 707 GW, 73 GW and 938 GW, respectively. Compared to the reference scenario, the optimal capacity for onshore and offshore wind decreases nearly by 80 GW and 40 GW, respectively. On the other hand, an increase in the optimal capacity of open-field PV without tracking is estimated at approximately 350 GW. As is expected, the prohibition of transmission technologies between countries disables importing hydrogen, which is produced via cheap generation technologies. Thus, the excess capacities of these cheap generation technologies are not needed anymore. Onshore wind energy in the Nordic countries, as well as offshore wind energy in the Netherlands, both onshore and offshore wind energy in the United Kingdom, can be some examples for these cheap technologies and locations, where hydrogen is produced.

The resulting system design is shown in Figure 5-15. Optimal pipeline capacities are lower than the reference scenario owing to the additional constraint in the presented scenario, yet three

pipeline connections are apparent: London, Paris, and North-Rhine Westphalia. Due to the limited potentials as well as lack of possibility of cheaper electricity generation and hydrogen production in the neighboring regions, aforementioned regions import hydrogen by utilization of large capacity pipelines. It must be noted that the main reason for the large pipeline capacity in Paris and London is the lack of salt caverns, which enables the seasonal storage of hydrogen at a relatively cheaper cost. Therefore, London and Paris import hydrogen from “91_uk” and “24_fr”, which have large salt cavern utilization. Similar behavior can be observed in Madrid as well as the southeastern region in Spain (“09_es”). When Germany is focused, two distinct pipeline connections from north to south can be seen in the figure. A brief discussion on the pipeline connections between northern and southern Germany is already included in Section 5.3.4. Unlike the reference scenario, demand in eastern Germany is not provided by a pipeline connection from northwestern Germany. This is because cheap hydrogen produced in the Nordic countries cannot be imported due to the prohibition of the connections. Therefore, low demand observed in eastern Germany can be supplied by northeastern Germany. At this point, the question of “Why is demand in eastern Germany not provided by the hydrogen pipeline from western Germany?” might arise, since the optimizer starts choosing the cheapest technology first, and then recursively adds the second, third... etc. cheapest technologies... In the case of northern Germany, the specific investment cost of offshore wind energy increases with increasing capacity. Therefore, additional capacities in the North Sea besides 30 GW (already chosen) might be more expensive than the locations in the Baltic Sea, meaning that relatively lower full load hours in the Baltic Sea still has lower cost than the more expensive locations in the North Sea. As a result, offshore locations closer to the shore in both regions are utilized in addition to the high potential onshore wind energy, and eastern and western German regions are connected via two distinct pipeline connections.

Although this analysis in which interactions of countries are prohibited shows the value of these connections, there is only a little likelihood of such a scenario, especially for the electricity transmission network. This is mainly because most of the HVAC and HVDC cables already exist today or planned to be expanded in the next decade (c.f. assumption about transmission grid, Section 3.4.6). Hence, system design based on this assumption would not be meaningful despite the scientific value of the analysis presenting a possible scenario.

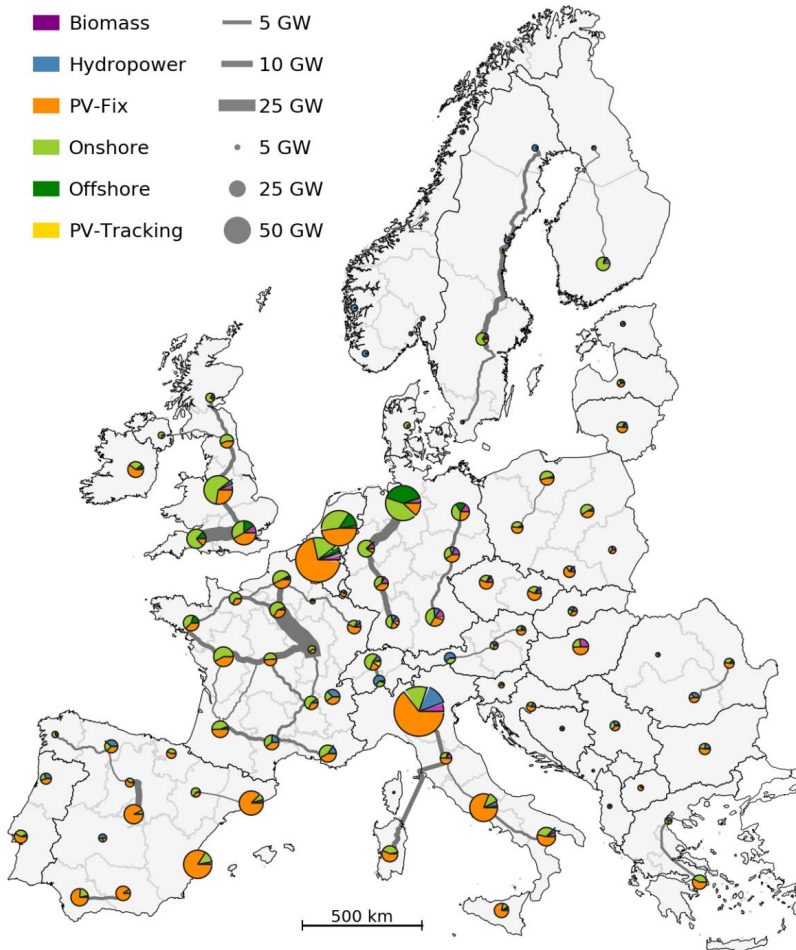


Figure 5-15 Spatial distribution of generation technologies when transmission technologies between countries are prohibited.

5.4.3 Value of Individual VRES Generation Technologies

The variations in the total annual cost are used as an indication for the value of corresponding technology within the context of the defined scenario. Although some conclusions can be drawn from the result of the overall system, investigation of capacity distributions is required in order to analyze how the design differs in response to the lack of each technology. Hence, in order to investigate the differences, system designs are presented in Figure 5-16 for the cases where onshore wind, offshore wind, open-field PV with tracking, open-field PV without tracking are prohibited. By doing so, whether or not the system design alters and if it alters which technology substitutes the prohibited one can be analyzed further in detail.

As the third-highest increase in the total annual cost following HVAC transmission lines, onshore wind energy plays an important role in the system. When it is absent, offshore wind energy in the north and open-field PV without tracking in the south are mainly used as a substitute. Concerning optimal capacities for VRES technologies, 785 GW of onshore wind, 111 GW offshore wind, and 584 GW open-field PV without tracking estimated in the reference scenario are substituted by 528 GW and 913 GW of offshore wind and open-field PV without tracking, respectively. The capacity of pipeline connections between the United Kingdom and continental Europe increases drastically, which is caused by the comparably cheap electricity generation via offshore wind turbines. Moreover, many connections between Norway and Sweden disappear, which causes Norway operating nearly isolated (island operation) and supplying its demand only by hydropower (which includes run-of-river, hydro reservoir and pumped hydro storage). Unlike many other countries having a shore in the North Sea, offshore wind turbines are not preferred in Norway because of their high investment cost caused by high water depth in that area. Biomass is preferred as a substitute in central Europe, especially in southern Germany. While the optimal capacity for biomass CHP plants is nearly 0.6 GW across Europe in the reference scenario, this value increases to 60 GW when onshore wind energy is prohibited.

Prohibition of offshore wind energy results in an increase of 0.5% in the total annual cost. In nearly all regions, offshore wind energy is substituted by onshore wind energy. Nevertheless, in order to compensate for the intermittency of onshore wind energy as it is briefly discussed in Section 5.3.1, open-field PV without tracking is also added in some regions, especially in the United Kingdom and Ireland. The optimal capacities for onshore and open-field PV without tracking increase to 903 and 637 GW, respectively. Optimal biomass CHP plant capacity also increases to 10 GW, half of which is installed only in Germany. Unlike the value of onshore wind energy, pipeline connections do not change drastically in the offshore case. Nevertheless, the capacity varies slightly and additional connections, especially in Spain and Portugal, are observed.

In the reference system, the preference of open-field PV systems without tracking is evident; the reasons behind this preference are also discussed briefly in Section 5.3.1. When this technology is not allowed, the resulting system design shown in the figure is obtained. As it is expected, the substitute for this technology is open-field PV with tracking system. However, there are many differences in terms of optimal capacities compared to the reference scenario. For instance, large optimal capacities observed in Italy and southern Spain and France in the reference scenario are not seen with tracking systems. Instead, slightly higher capacities for onshore wind turbines are preferred in these regions. The optimal capacity of open-field PV without tracking (584 GW) decreases to 284 GW with tracking system. Furthermore, an additional 28 GW of biomass and 70 GW of onshore wind energy are also added to the reference optimal capacities. This is mainly due to relatively higher specific investment cost of tracking system (720 € kW^{-1}) compared to 520 € kW^{-1} . It can be said that higher specific investment cost results in a shift towards onshore wind energy having cost-competitive locations. Thus, utilization of these cost-competitive onshore locations is preferred by the optimizer, since the objective function is the minimization of the total annual cost.

Furthermore, an increase in the capacities of pipeline connections around the United Kingdom and Denmark is also evident, indicating that hydrogen produced in these regions is transported to continental Europe to supply the demand.

Although it is not chosen by the optimizer, prohibiting open-field PV with tracking changes the system design by 6.1%. Although open-field PV without tracking is preferred in the reference scenario in central Europe, especially in southern Germany, biomass takes it over when tracking systems are prohibited. This unexpected result is mainly caused by the simplification in the temporal resolution, in other words, time series aggregation. Concerning solution time and memory limitations, time series aggregation is used to create 30 typical days to decrease the complexity of the problem (cf. Section 3.5). The impact of this assumption is investigated in Section 5.1. In the time series aggregation, typical periods are created by the weights of the data. Therefore, the elimination of 60 technologies (with time series for each region) in the optimization while prohibiting open-field PV without tracking decreases the weight of the PV profiles in the time series aggregation. As a result, although excluding this technology does not influence the system design, it affects the time series data given as an input to the optimization problem. Fewer PV profiles result in less variation in the PV profiles and high fidelity in the other time series data, which causes slightly more fluctuations compared to the reference time series; thus, requiring more back-up generation such as biomass. Hence, 24 GW of biomass CHP plants is found to be optimal when the tracking systems are prohibited.

All in all, despite the simplification in the time series data, variations in the system design are evident in every case where a generation technology is prohibited. The absence of a specific technology does not violate the constraint of supplying the demand at any time, yet prohibiting each technology increases the total annual cost to some extent. Although offshore wind energy seems to have the lowest value among the other generation technologies discussed in this section, it must be noted that the public acceptance factor is not taken into account in this analysis. Consideration of public acceptance uniformly or even regionally might change the values of these technologies significantly.

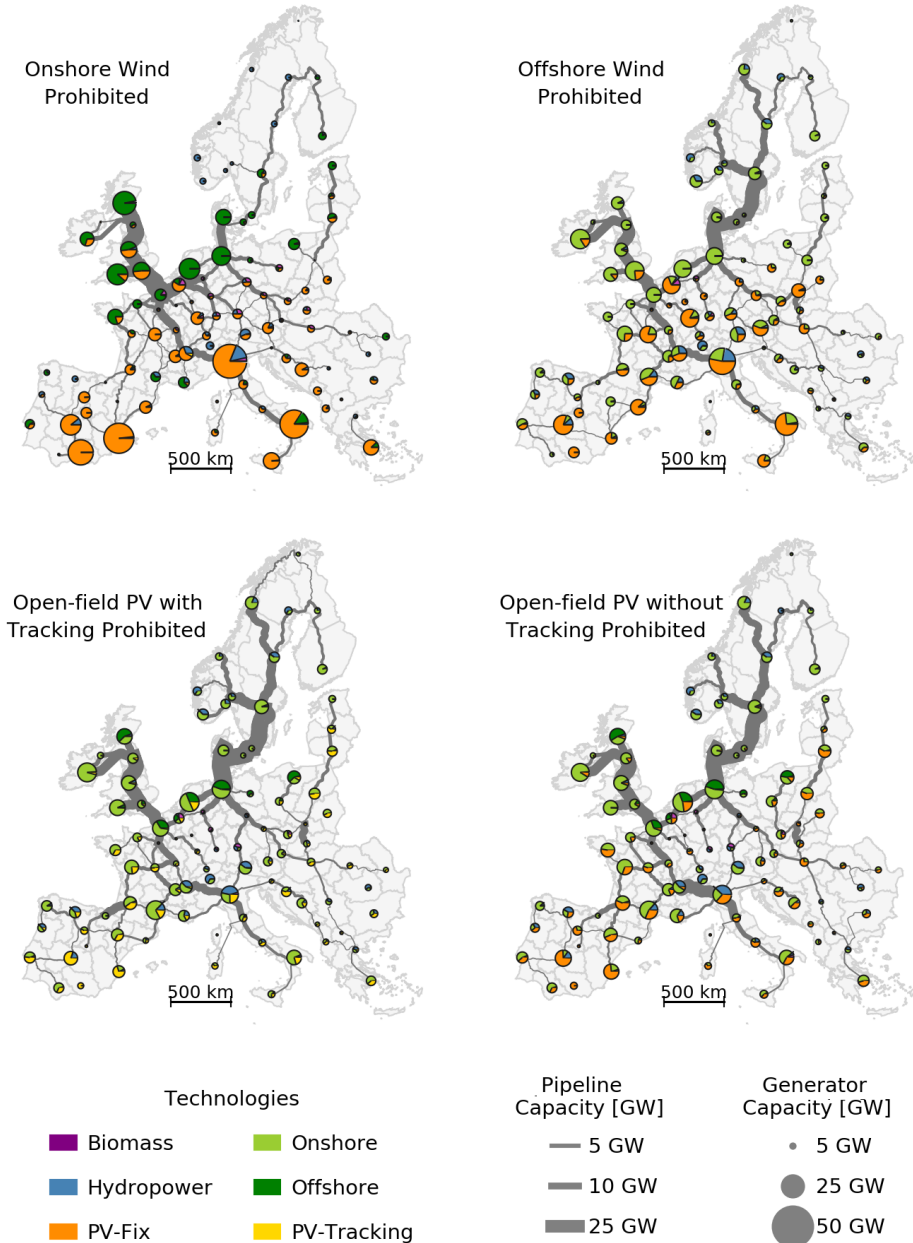


Figure 5-16 Spatial distribution of generation technologies for different scenarios with individual generation technologies prohibited.

5.4.4 Value of Individual Transmission Technologies

The variations in the system design by means of optimal capacity of generation technologies as well as capacities of hydrogen pipelines for the value-of-analysis performed for transmission technologies are shown in Figure 5-17. When HVAC cables, HVDC cables, or hydrogen pipelines are prohibited, the total annual cost of the system increases at different levels proving the importance of transmission technologies.

The highest impact is observed in the case of HVAC cables with an increase of 31% in the total annual cost, as it might be already expected. Connecting many regions with comparably higher capacities (especially with the HVDC cables), HVAC cables enable many regions to import electricity instead of generating at a higher cost. Analyzing the results presented in the previous sections (c.f. Section 5.2 and Section 5.3) reveals that electricity generation in the cheap locations and use of transmission technologies is found cost-optimal rather than having decentralized generation having distributed technologies over all regions. Taking into account the objective function (minimization of the total annual cost) and assumption of a perfect European electricity market, prohibiting this technology causes many regions to supply the electricity demand by their own resources, which might cause an increase in the system cost. In order to decrease this impact, higher utilization of biomass and hydrogen can be observed. The utilization of biomass can be seen especially in southern Germany and northeastern continental Europe. In the case of higher hydrogen utilization, an increase in the pipeline capacities between the United Kingdom and continental Europe as well as Sweden and continental Europe are more pronounced. Nevertheless, since most of the HVAC connections have already been built and would not be removed, such an increase in the cost remains an analysis reminding the importance of these connections.

Prohibiting HVDC cables causes an increase of 5.9% in the total annual cost, which is mainly resulted from higher capacities of hydrogen CCGT, electrolyzer, and biomass with respective increases of 16, 21, and 12 GW. Although the biomass CHP plant capacity does not change in some regions, few regions experience higher capacities. The highest increase in the biomass CHP plant capacity is observed in northeastern Germany ("32_de") with a value of 4.0 GW, which is then followed by regions in western Germany ("35_de" and "33_de") with values of 3.0 and 2.0 GW, respectively. Due to cheaper electricity generation in Sweden compared to "32_de", the electricity is imported from Sweden via the previously mentioned HVDC connection. Therefore, "32_de" relies on biomass utilization to compensate for the lack of this connection. Another country affected by prohibited HVDC connections is the United Kingdom. Especially the region including London "90_uk" experiences an increase in onshore, offshore, and open-field PV without tracking as 5.0, 2.0 and 2.0, respectively; which is caused by prohibiting the HVDC connections from the Netherlands, Belgium, and France. All in all, the increase in the total annual cost and optimal capacities are observed when HVDC connections are prohibited, yet these variations are not as pronounced as in the case of HVAC cables.

The resulting system design with the absence of hydrogen pipelines is shown in Figure 5-12. The increase in the total annual cost of the system is estimated at 6.7%. Slight increases in the optimal VRES capacities are observed to substitute this technology. The decrease in the hydrogen CCGT reveals that instead of using hydrogen as a back-up source, share in the biomass increases. Moreover, large variations in the storage capacity of salt caverns, as well as vessels, are observed. The regions with large pipeline connections in the reference scenario experience a drastic decrease in their salt cavern storage capacities. For instance, a decrease of 8.6 TWh in “24_fr” and 7.3 TWh in “33_de” is observed in the salt cavern storage capacity. Hydrogen produced in the Nordic countries is distributed to continental Europe over “33_de”, and from the United Kingdom towards Italian regions over “24_fr”. Therefore, prohibiting the pipeline connections decreases the required storage capacities in these regions. In terms of higher storage capacities, “92_uk” experiences a 9.0 TWh increase in its salt cavern storage capacity, which is then followed by “31_de”, “35_de” and “32_de” with values of 5.7, 2.0 and 1.7 TWh, respectively. In these regions, electricity imported via HVDC and HVAC connections is used in the production of hydrogen within the region to supply their demand. Therefore, still the cheaper locations are utilized both for hydrogen and electricity, yet the transmission connections have changed. It is seen that although pipeline connections are not allowed, cheaper electricity is still utilized in the hydrogen production in the system. However, this production takes place in each region locally instead of connecting them via large pipelines, yet this is limited by the capacities of electricity transmission technologies. Lower capacities in Ireland and the Nordic countries can be a good example of this limit, which restricts the capacities of these cheap electricity locations.

All in all, all transmission technologies considered in this analysis play a crucial role in the system. Concerning HVAC and HVDC connections, they have a large impact on the system design (especially HVAC), yet their absence can be compensated by increasing the capacities of other technologies (such as VRES technologies) in each region. This can be used as an implication of all regions having the capability to supply their demand, yet perfect European energy market would decrease the cost of the system by at least 6.7%. Moreover, most of the HVAC and HVDC connections already exist today, and their removal is not very likely in the future. Therefore, the value and essential roles of these technologies have been investigated and shown despite the unlikelihood of this scenario. In terms of hydrogen pipelines, alterations in the system design are more apparent, yet its role in the energy system design is also shown with an increase of 6.7% in the total annual cost.

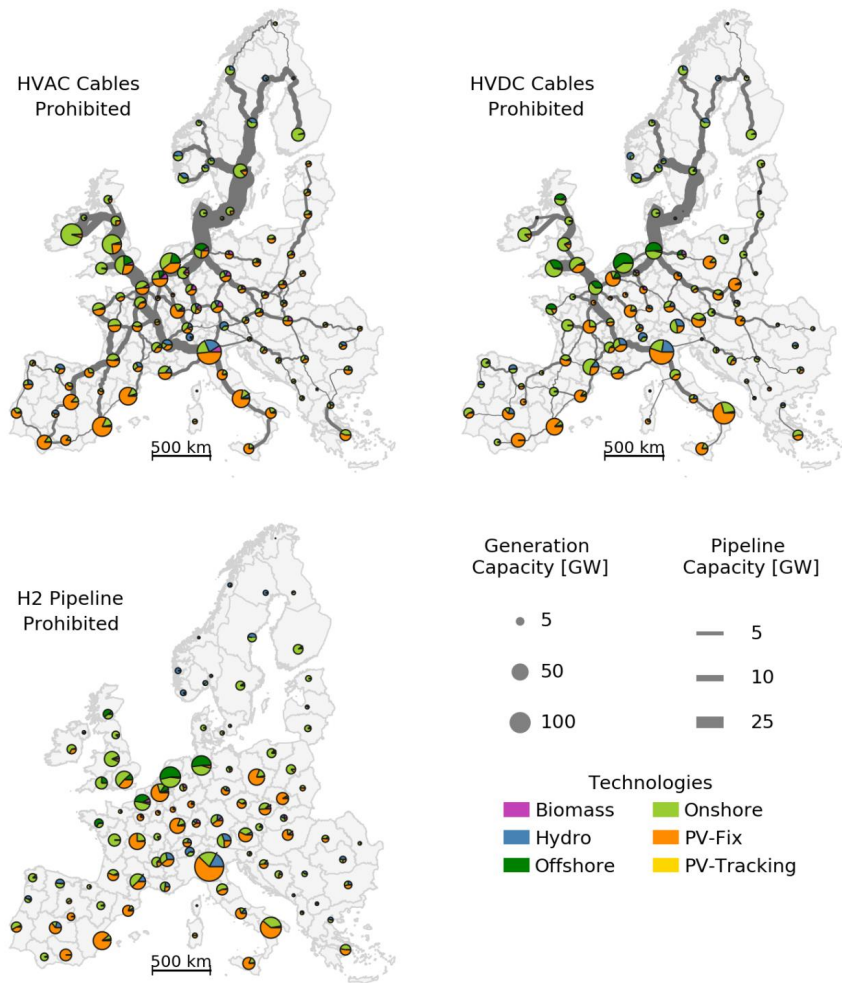


Figure 5-17 Spatial distribution of generation technologies for different scenarios with individual transmission technologies prohibited.

5.5 Sensitivity Analyses

In order to observe variations in the system design regarding the cost assumptions made for pipeline and electrolyzer, additional analyses are performed. For this purpose, whether or not the system design alters in response to different specific investment costs for pipeline or electrolyzer is investigated. In the case of a pipeline, a lower and an upper specific investment cost values are chosen based on the estimations performed on the linearization of pipeline cost, which is

expressed as an exponential relation claimed by Mischner [189]. Since the cost is over- and underestimated at certain capacities, as shown in Figure 3-21 (underestimation below 8 GW, overestimation above 8 GW), a lower cost value of pipelines estimated without a fixed investment cost and a higher cost which is well above these estimations are performed. The results of this analysis are discussed in Section 5.5.1. Following this, an additional analysis is performed on the cost of PEM electrolyzers in order to observe the impacts on the system design by a further decrease in the projected specific investment cost. Thus, cost value of 300 € kW⁻¹ is assumed for the PEM electrolyzers, and variations are presented in Section 5.5.2.

5.5.1 Pipeline Cost

Due to the linearization of the problem, a linear pipeline cost is assumed to be 185 € kW⁻¹ m⁻¹ as it is previously discussed in Section 3.4.6. As it is seen from Figure 3-21, pipeline cost is over- and underestimated at different capacity values due to the linearization of cost. Therefore, a sensitivity analysis of the pipeline cost is performed in order to investigate the variations in the system design as well as the total annual cost. For this purpose, two additional values for an investment cost of pipelines are used in addition to the value assumed in the reference case: 185 € kW⁻¹ m⁻¹ (the weather year 2015, 60 groups per VRES technology). The lower investment cost value is defined as 145 € kW⁻¹ m⁻¹ since that value corresponds to the variable investment cost estimated in a problem definition for mixed-integer linear optimization with a fix investment cost of 334 € kW⁻¹. As the upper boundary, a value of 225 € kW⁻¹ m⁻¹ is chosen since their average (lower and upper costs) results in the cost assumed in the reference problem. The total annual costs of these three problems with the cost values are given in Table 5-1. As it is seen from the table, the total annual cost of the system changes by 0.2% in both cases. Unsurprisingly, the lower investment cost of pipelines results in a lower total annual cost.

Table 5-1 Total annual cost with respect to assumed pipeline cost with a percent deviation

	Pipeline Cost [€ kW ⁻¹ m ⁻¹]		
	145	185	225
Total annual cost [10 ⁹ € a ⁻¹]	219.6	220.0	220.4
Percent deviation	-0.2%	-	+0.2%

In addition to the comparison of the total annual cost, installed capacities of technologies are analyzed. The capacity of pipelines between Sweden, Denmark, and Germany as well as the United Kingdom and continental Europe decrease by 1 GW between high investment cost and reference cases as well as reference and low investment cost cases. As might be expected, the installed capacity of pipeline increases with decreasing cost, so that hydrogen produced via very cheap electricity is transported to supply the demand. Moreover, the overall capacity for generation

technologies varies by 0.2% in both cases. Hence, considering the small deviation obtained as a result of two extreme cases, it can be said that the assumption of $185 \text{ € kW}^{-1} \text{ m}^{-1}$ is acceptable, and does not change the system design significantly.

5.5.2 Electrolyzer Cost

The specific investment cost of the PEM electrolyzer in all model runs is assumed as 500 € kW^{-1} as it is discussed in Section 3.4.5. However, taking into account the electrolyzer cost contributing 10% in the total annual cost of the green-field system design discussed as a reference case, an analysis of the cost of electrolyzer is performed by assuming a specific investment cost of 300 € kW^{-1} . Corresponding results for two different cases are shown in Table 5-2. It is evident that with lower specific investment costs of electrolyzer lower total annual cost can be achieved (4.5% decrease compared to the reference case). Share of electrolyzer in the total annual cost also decreases, as it might be expected as a result of the lower cost assumption. Despite this decrease in the total annual cost, an increase in the overall optimal capacity for electrolyzers is observed almost in all regions to produce more hydrogen at the peak generation periods. Nevertheless, the downside of higher electrolyzer capacity is also seen with average full load hours given that are analyzed as shown in the table. Average electrolyzer full load hours decrease is nearly 500 MWh MW^{-1} with large variations in each region. For example, the “86_se” region located in Sweden experiences a decrease of nearly 2000 MWh MW^{-1} ; it is then followed by “99_fr” and “56_it” with 1500 and 1000 MWh MW^{-1} , respectively. Nearly 60% of the regions experience a decrease of less than 500 MWh MW^{-1} in the electrolyzer full load hours. Higher electrolyzer capacity also impacts the optimal capacity of VRES technologies as it is seen in the table. Although the variation is only by 1%, the decrease in the optimal capacity of VRES technologies is apparent. These variations in the optimal capacities impact the operation of the technologies by means of hourly variations in the system parameters; nevertheless, a reverse proportionality between the optimal capacity of electrolyzer and VRES technologies is evident.

Table 5-2 Resulting parameters of 300 € kW^{-1} electrolyzer cost and reference case (the weather year 2015, 60 groups per VRES technology)

	Electrolyzer Investment Cost	
	300 € kW^{-1}	500 € kW^{-1}
Total annual cost [Billion € a^{-1}]	210.3	220.0
Share of electrolyzers in TAC	7.4%	10.3%
Optimal capacity of electrolyzers [GW]	292.5	254.0
Average full load hours of electrolyzers [MWh MW^{-1}]	3860	4320
Optimal capacity of VRES technologies [GW]	1464	1480

All in all, it can be said that a 60% decrease in the specific investment cost of the electrolyzer does not influence the system design significantly in terms of optimal capacities of technologies and how they are distributed. As it is discussed, the optimal electrolyzer capacities increase in order to attain higher hydrogen production at peak power generation periods despite the decrease in the electrolyzer full load hours. However, the optimal capacity of VRES technologies decreases, since 40 GW higher electrolyzer capacity can compensate for the variations in the hourly operation resulted from a capacity decrease of 15 GW in VRES technologies. Therefore, it can be said that a further decrease in the specific cost of the electrolyzer does not influence the system design significantly from the energy system design point of view. As it is expected, the overall cost of the system decreases, yet only slight variations in the system design are observed.

5.5.3 Impact of Hydrogen Demand Market Penetration

In order to analyze the impact of hydrogen demand included in the system, a sensitivity analysis is performed on the market penetration of hydrogen demand for passenger vehicles. For this purpose, different market penetration values between 0% to 100% are assumed with an increment of 10%, and the system is optimized for each value. The total annual cost of the system for each case is calculated and shown in Figure 5-18. Additionally, the increase in the total annual cost per additional hydrogen in the system is also illustrated in the figure. As it is expected, the total annual cost of the system increases with increasing market penetration because of the higher overall demand. In order to provide the demand both by means of electricity and hydrogen, higher capacities are installed especially for generation technologies, specifically onshore wind energy. Moreover, increasing electrolyzer costs are also evident since more hydrogen has to be produced to supply the hydrogen demand. Although the increase in the total annual cost per additional hydrogen demand in the system does not correspond to the cost of hydrogen, yet it can provide an indication of the higher cost per unit amount of hydrogen. It must be noted that this estimation assumes free-use of all facilities estimated in the case without hydrogen demand.

The increase in the total annual cost per unit hydrogen at low market penetration values is lower than the ones at high market penetration. This can be explained by the system boundaries and volatility of the generation technologies. The existence of surplus energy in a 100% renewable energy system with high shares of renewables is inevitable; therefore, hydrogen demand can be supplied by utilizing the surplus with additional generation technologies at low market penetration. Nevertheless, as the hydrogen demand increases, additional components, which can be considered as the dedicated components for hydrogen production, are necessary to supply the demand.

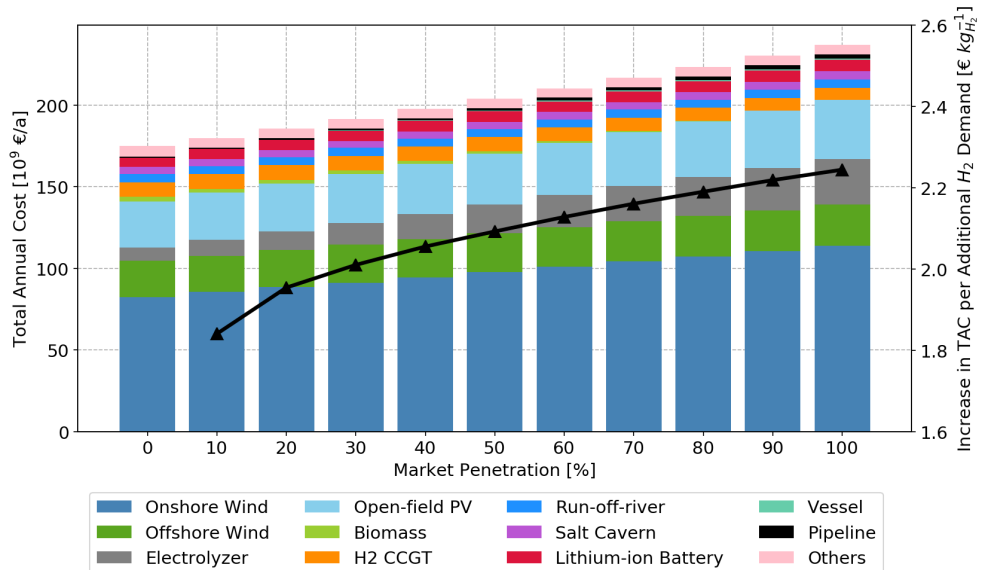


Figure 5-18 Variation of total annual cost and increase in the total annual cost per additional hydrogen with respect to the market penetration of hydrogen demand for passenger vehicles.

In order to provide insight into the system design with an extreme case that has no hydrogen demand at all, capacity distribution of generation technologies and pipeline connections are shown in Figure 5-19. Interestingly, the existence of hydrogen pipelines indicates that the use of hydrogen in the system as flexibility is still cost-optimal, although there is not an explicit hydrogen demand. Thus, it can be said that even if hydrogen is not supplied as a fuel in this sensitivity, it is produced and then used in reelectrification technologies to generate electricity.

For this purpose, the cheap electricity generation locations are used to produce hydrogen, which is distributed to the other regions where electricity cost is higher. The most apparent pipeline connection is seen between “23_fr” (Paris) and “24_fr” with a capacity of 15 GW. This can be explained by the high electricity demand requiring reelectrification in “23_fr”. Nevertheless, the lack of salt caverns in the region results in a pipeline connection between the closest region having some potential for hydrogen storage in salt caverns. Similar plots for different market penetration values are provided in Appendix A.5.

0% Market Penetration (Weather Year : 2015)

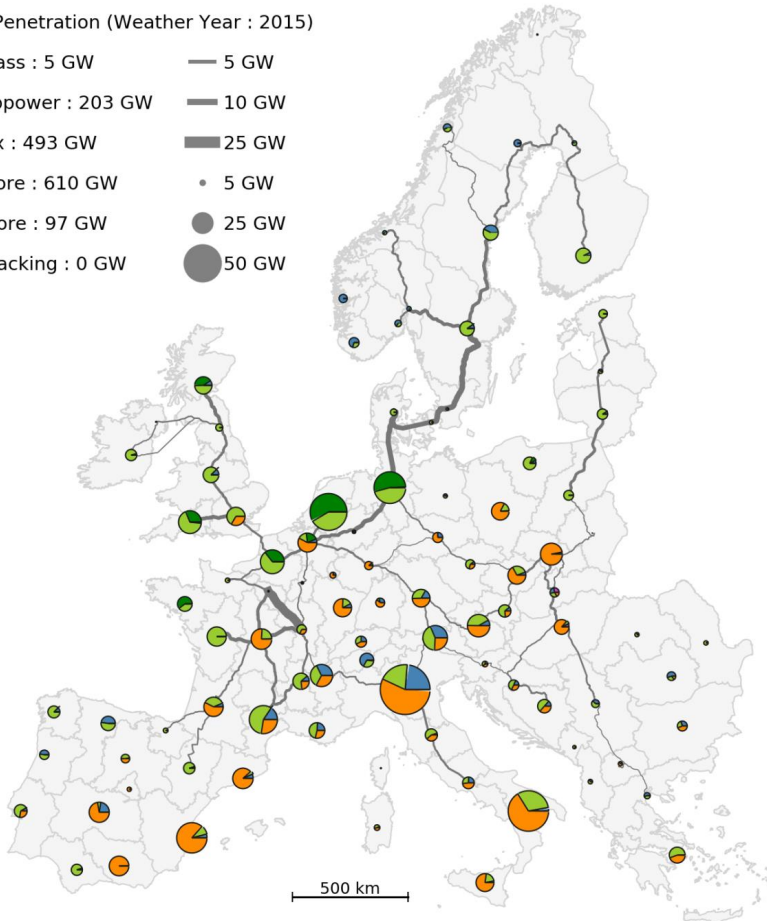


Figure 5-19 Capacity distribution of generation technologies as well as hydrogen pipeline as a result of energy system design without hydrogen demand.

5.6 Summary

In this section, the main assumptions in the energy system model are investigated. These assumptions include the number of typical days, groups per VRES technology and selection of the weather year. Moreover, the value of technologies and sensitivity of pipeline and electrolyzer costs are addressed.

The impact of typical days used in the analysis reveals that the use of a few typical days cannot represent the yearly time series. This misrepresentation underestimates the total annual cost of

the system. Nevertheless, within the regional scope of this project use of 30 typical days is found to be sufficient to decrease the temporal resolution and memory requirement.

When the impact of VRES technologies grouping is examined, a decrease in the total annual cost is seen with an increasing number of groups in each region. This expected result is caused by cheap electricity generation locations unveiled in each region. In general, higher utilization of offshore wind energy in larger areas is observed, since the investment cost of certain portion becomes cost-competitive with the other technologies within that region. Furthermore, the requirement for biomass CHP plants decreases with an increasing number of groups. Although the higher fidelity is attained with more groups, solution time increases drastically; thus, the use of 60 VRES groups for each technology is found to be reasonable.

The impact of weather year used in the energy system is analyzed by varying the generation time series of VRES technologies between 1980 and 2017. In spite of the technology portfolio and consideration of biomass as a dispatchable source, significant variations in the system design are observed. These deviations are persistent even in consecutive years. The variations are mainly observed in the regions where large capacities are deployed, such as open-field PV in France and Italy.

The values of individual technologies, as well as combination of some (i.e. onshore and offshore wind energies), are investigated by using a reference scenario of the optimal system design. The value-of-analysis is not conducted in the final energy system design proposed in this work since that design would include higher capacities due to ensuring the security of supply across all weather years. Therefore, the value-of-analysis with a non-optimal system design would be misleading. The highest value belongs to wind energy, which is then followed by the connection of countries (transmission network) and HVAC cables. On the other hand, technologies such as PEM fuel cell, solid oxide fuel cell, gas engine, and rooftop PV do not have any impact on the cost since they are not utilized because of their higher investment costs.

Variations of the cost of hydrogen pipeline and electrolyzer reveal that the costs of these technologies do not have a significant impact on the system design. Considering the fact that pipeline cost does not have a high share, nearly a 27% variation in the investment cost of pipeline causes a 0.2% variation in the total annual cost of the system with respect to the reference scenario. In the case of electrolyzers, lower electrolyzer cost increases the installed capacity of electrolyzers to some extent despite the decrease in their average full load hours. Additionally, a sensitivity analysis is conducted on the market penetration of fuel cell electric vehicles. For this purpose, both the total annual cost breakdown and the increase in the total annual cost with additional hydrogen demand are analyzed. Results show that even without hydrogen demand defined in the system, the use of hydrogen is evident especially as a backup generation system via reelectrification.

6 Design of European Energy System Based on 100% Renewable Energy

Sensitivities of the optimization model for a 100% renewable energy system are explained in Section 5. Especially, significant variations in the system design are observed both in the results illustrated in Section 5.3 and a similar analysis conducted by Caglayan et al. [130]. Independent from the technology portfolio used in the system as well as consideration of different demand sectors (electricity and hydrogen demands), system design is highly sensitive to the weather year assumed in the generation time series. Therefore, proposing a system design based on a single weather year is not sufficient in terms of the robustness of the system design ensuring the security of supply. Moreover, defining a worst-case scenario, that consists of the maximum optimal capacities of all technologies among all weather years, causes overengineering the design. As a result, an improvement in the methodology of the energy system design is sought, the method of which is explained in Section 3.5. Following the enhanced methodology, the system design obtained as a result of the iterative approach will be presented in Section 6.1, which includes the distribution of the optimal capacities of technologies. Moreover, the operation of the energy system is discussed in Section 6.2 and Section 6.3. Different roles of individual regions in the energy system are identified and discussed in Section 6.4. Finally, the proposed system design is compared against studies in the literature, which are briefly explained in Section 2.3.1.

6.1 Overall European Energy System Design

Once the enhanced method is applied over the system design iteratively based on the optimal designs of individual weather years (c.f. Section 5.3), a plateau²⁶ is attained after 3 iterations. After achieving stable results for almost all years (except the extreme weather years shown as outliers), biomass is chosen as a backup generation in order to ensure the security of supply for all these years without exception owing to its dispatchable nature. Time series aggregation is not needed after this point since the capacities of all technologies except biomass is set to the average of the ones obtained in the last iteration. Therefore, all weather years are optimized only to determine the necessary biomass CHP plant capacities without time series aggregation. Following this, the maximum capacities among all these weather years are used as the final biomass capacity. Finally, operation of the technologies is optimized as the last iteration over all weather years in order to obtain the average results (especially for curtailment and generation) that are presented in this section.

Figure 6-1 illustrates the energy system design obtained as a result of this iterative approach, which ensures the security of supply with decreasing the possible overengineering of the system components. The proposed system design involves 154 GW of biomass CHP plants, 203 GW

²⁶ The variations in the optimal capacities and total annual cost of individual years do not change significantly. For instance, total annual cost of the system between second and third iterations vary by nearly 1%.

hydropower plants (including run-of-river, reservoir and pumped storage), 654 GW open-field PV without tracking, 842 GW of onshore wind energy and 78 GW of offshore wind energy.

A comparison between proposed capacities and average capacity values²⁷ obtained as a result of the analysis on different weather years (cf. Section 5.3) reveals that these two capacity values are very similar, especially in Spain and France. For example, Spain experiences higher onshore and open-field PV without tracking capacities by 6% and 1%, respectively. However, it also has an additional 17 GW of a biomass CHP plant in addition to the VRES generation technologies. France can be considered as another example with an increase of 4% in the onshore, offshore and open-field PV with tracking capacities. The most substantial deviation in VRES technologies with respect to the averages of the results presented in Section 5.3 is observed in Slovenia with a 65% increase in the open-field PV without tracking. Slovenia is followed by Ireland, Switzerland, and Latvia for the same technology. However, it must be noted that relatively lower capacities in these countries (between 0.3 to 4 GW) is the main reason behind this significant deviation. Nevertheless, it can be said that the average capacities over all weather years are sufficient to supply a large portion of the demand.

In addition to the VRES technologies, a drastic increase in the biomass CHP plants is observed. However, this increase is expected because of the optimization of all time steps without time series aggregation (cf. Section 3.5) and also the assigned role for biomass as back-up generation technology. The impact of time series aggregation on the generation profiles is already discussed in Section 3.5; moreover, the variation in the system design is addressed in Section 5.1, revealing the biomass capacity expansion for higher typical periods. All time series, including the extreme periods (i.e., peak generation or demand periods), are smoothed by the use of 30 typical days. As a result, these unveiled extreme periods which were not covered in the previous analyses require higher capacity for biomass CHP plant, since it is the only technology allowed for capacity expansion.

All in all, the total capacities proposed for each technology is similar to the average values obtained in the analysis on the impact of weather year (cf. Section 5.3) with slight variations. These variations are more pronounced for biomass CHP plants since time series aggregation is eliminated in the final system optimization. This puts the importance of biomass insight, showing the role of this technology as a back-up generator in the extreme periods.

²⁷ The mean values are calculated by using the optimal capacities of 38 weather years presented in Section 5.3.

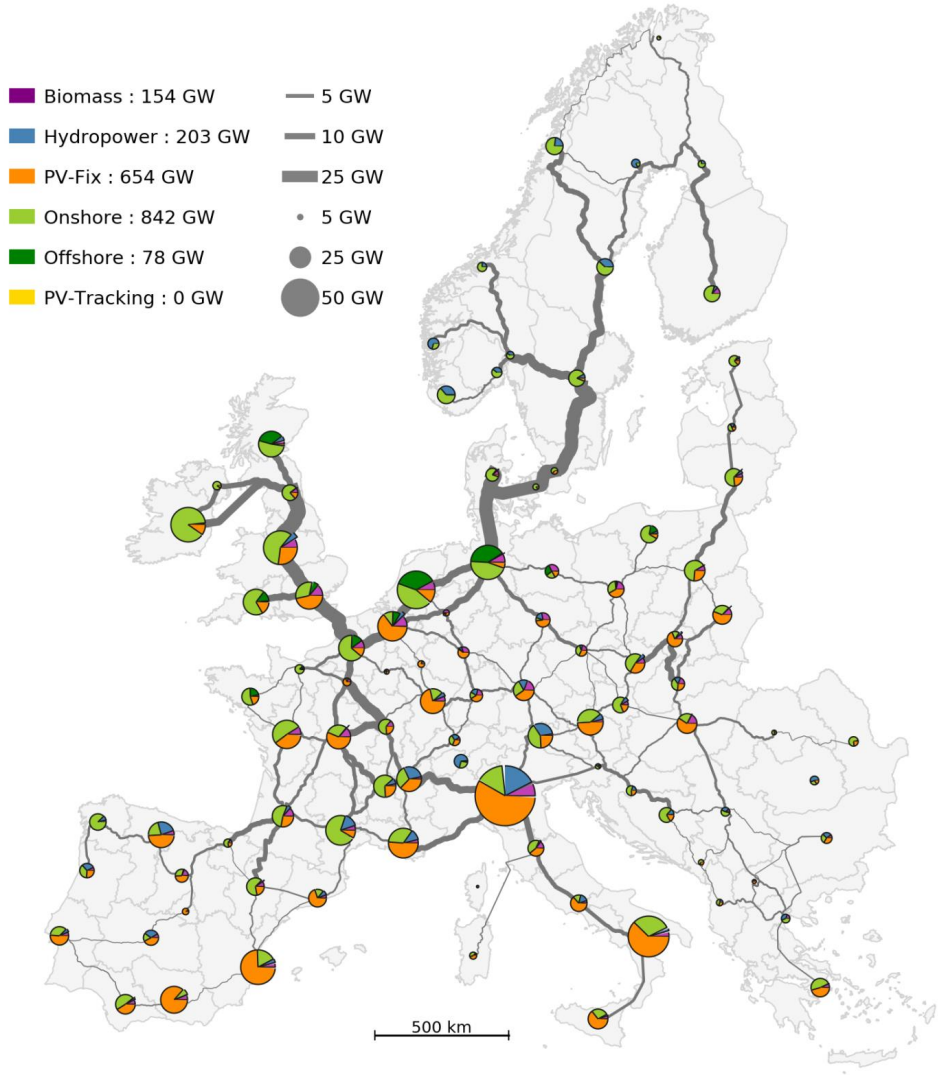


Figure 6-1 Proposed 100% renewable European energy system design with ensured security of supply over 38 weather years investigated.

6.1.1 Conversion Technologies

The proposed capacities of conversion technologies are not included in order to keep Figure 6-1 simpler. Nevertheless, in order to understand the system entirely, the distribution of electrolyzer and reelectrification technologies must be taken into account. Therefore, the proposed capacities for the conversion technologies are shown in Figure 6-2. In order to provide a succinct discussion, capacities of hydrogen OCGT and CCGT technologies are aggregated and shown as reelectrification technologies. However, the detailed capacities are provided in Appendix E.

Total electrolyzer capacity is estimated as 258 GW across Europe. When the results of these conversion technologies are analyzed at a national level, the highest electrolyzer capacity is observed in France (nearly 47.5 GW), which is then followed by the United Kingdom, Norway and Ireland with capacities of 45, 30 and 28 GW, respectively. Once more, hydrogen is mainly produced in these regions. Conversely, the utilization of electrolyzer in countries such as Belgium, Luxemburg and Switzerland is not preferred by the optimizer.

As it is expected, the electrolyzer capacities are high in the regions with higher generation capacities. Hydrogen is produced in the regions where cheap electricity generation is possible, and it is transported to the other regions owing to the low cost of hydrogen pipelines compared to the wind turbines and PV modules. Thus, it can be said that the critical aspect of the hydrogen infrastructure is the cost of electricity since the transportation cost does not play a significant role in the system (nearly 1.3%).

Focusing on the reelectrification technologies reveals that northwestern Germany, Netherlands, and the southern United Kingdom highly rely on hydrogen. On the other hand, nearly no reelectrification technologies are preferred to be installed in the Balkans, Norway, and nearly all Sweden, southern Italy, and Switzerland. Investigation of the results at the national level reveals that the highest proposed capacity is observed in the United Kingdom with a value of 28.5 GW (10 GW of which belongs to hydrogen OCGT). It is followed by Germany and France with capacity values of 27.3 and 26.1 GW, respectively. Nearly 30% of the countries experience capacities less than 500 MW. It can be said that the direct use of electricity is more favorable than the use of conversion technologies because of the losses while generating electricity. Nevertheless, reelectrification of hydrogen comes to the play in the cases where maximum biomass capacity is utilized, and there is still a need for a flexible generation. For instance, in the Netherlands, northwestern Germany and "92_uk" all of biomass CHP plant capacity is utilized.

When the capacity distributions of the reelectrification technologies are analyzed, a switch between two technologies (hydrogen OCGT and CCGT) is observed. The reason behind this switch is caused by the operation cost of these technologies. Hydrogen OCGT has an investment cost of 500 € kW⁻¹ with 40% efficiency, whereas hydrogen CCGT has 760 € kW⁻¹ and 60%

efficiency. The variable operation cost of OCGT is 7.5 € MWh^{-1} , and CCGT is 2.4 € MWh^{-1} . The full load hours of these technologies will be compared in the following paragraph.

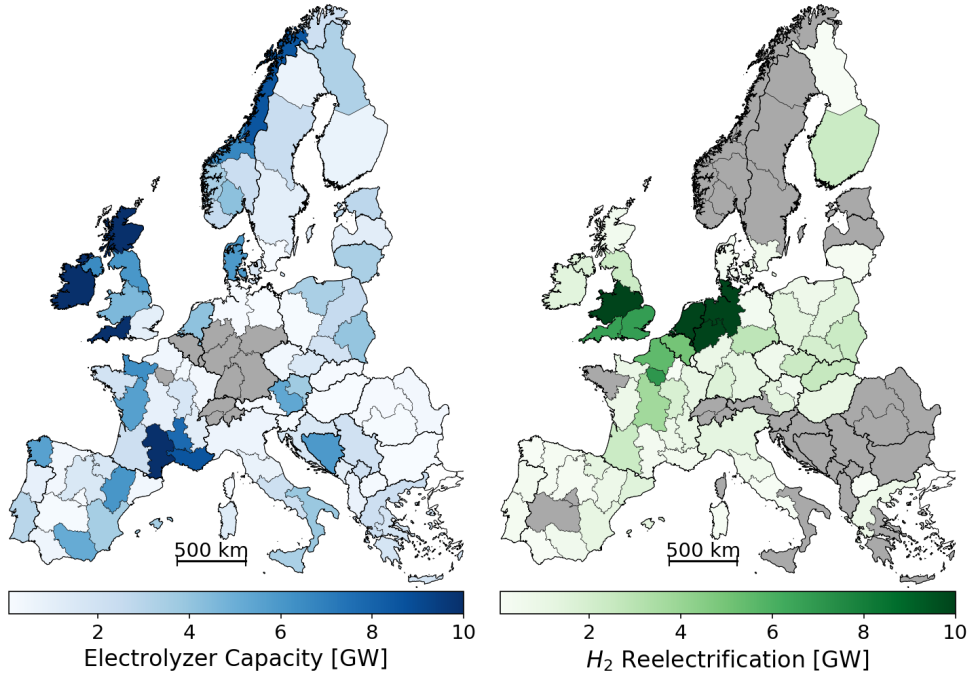


Figure 6-2 Proposed capacities for electrolyzer (left) and reelectrification (right) technologies in the 100% renewable European energy system.

As it is mentioned earlier, although the capacity variables are kept constant across all weather years, system operation is optimized for each year in order to be able to compare the results and ensure the security of supply. Thus, the average full load hours of individual technologies at a national level are estimated for all weather years individually. Resulting distribution for the conversion technologies, including electrolyzer, hydrogen OCGT, hydrogen CCGT, and biomass CHP plants, are shown in Figure 6-3. Despite slightly overengineering the system design to prevent lulls, full load hours of electrolyzers are still above 2700 h a^{-1} . The maximum electrolyzer full load hours is observed in Norway with a value of nearly 8300 h a^{-1} . In the Nordic countries, the full load hours are generally higher than the rest, because of the flexible electricity generation (high hydropower capacities, cf. Figure 3-19). A steady operation with high full load hours can be attained since the intermittency is compensated by the high capacity hydropower available in these regions.

Focusing on the hydrogen reelectrification technologies reveals that there is an apparent difference in the full load hours of hydrogen OCGT and CCGT technologies as it is previously

mentioned. Full load hours higher than 340 h a⁻¹ are not observed for hydrogen OCGT technologies because of its higher operational cost (7.5 € MWh⁻¹). On the other hand, hydrogen CCGG plants experience a maximum of 2000 h a⁻¹ full load hours in Belgium.

Finally, focusing on the biomass CHP plants reveals the large variation especially in Belgium, the Netherlands, and the United Kingdom. In some years, the full load hours of biomass CHP plants in these countries might attain 2000, whereas the average is around 100 h a⁻¹. This can be interpreted to understand the role of biomass in the energy system as the back-up generation. In other words, it can be said that the higher biomass capacities observed in the proposed system design are not to cover many time periods and maintain a steady generation, but to cover the periods where demand cannot be supplied.

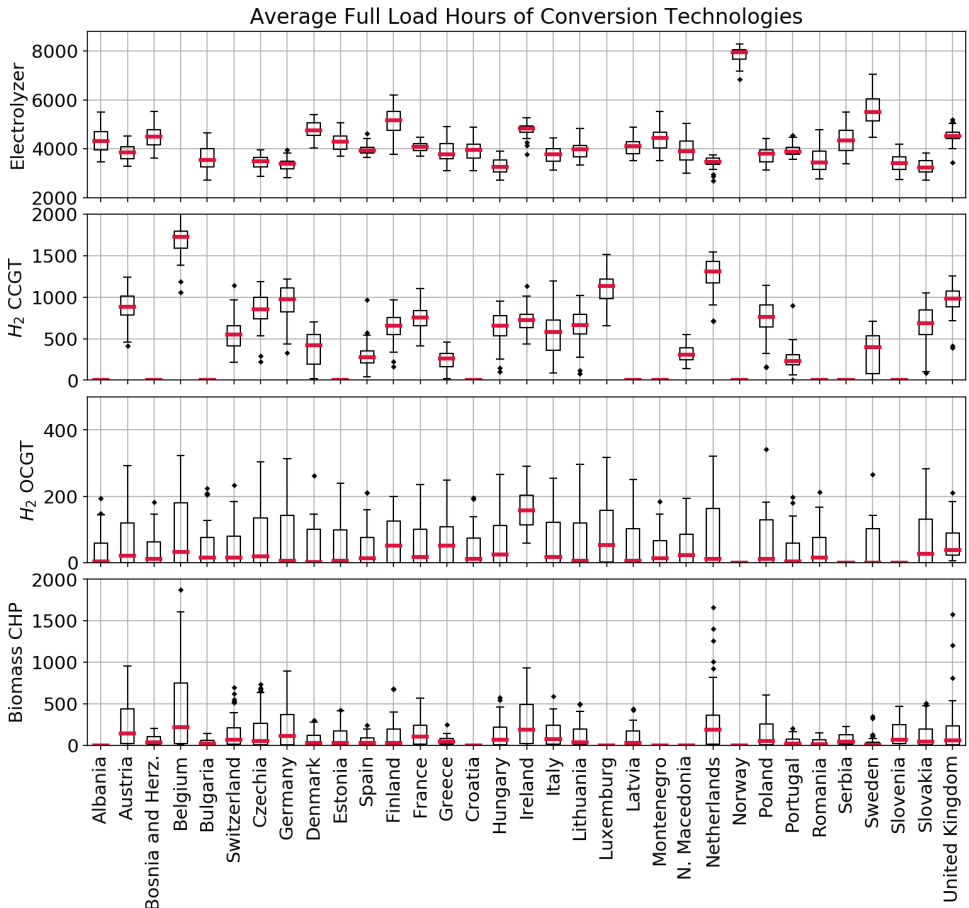


Figure 6-3 Variations in conversion technology the full load hours for the proposed system design across input weather years.

6.1.2 Storage Technologies

The proposed storage capacities are shown separately in Figure 6-4. Note that the storage capacities of pumped hydro storage and hydro reservoirs are not included in this figure since their capacities are not optimized and already shown in Figure 3-19. When the storage capacities of salt caverns are focused, it is seen that some portion of the potential is utilized in all regions where it is available. The proposed storage capacity in the energy system is estimated at 129.6 TWh, which is approximately 0.6% of the technical storage potential of hydrogen in salt caverns across Europe (cf. Section 4.2). Investigation of the capacity values at a national level shows that the United Kingdom has approximately 31 TWh of storage, which is only 2.5% of the technical storage potential. It is then followed by France with a capacity of 24.5 TWh and Germany with 23.3 TWh. These storage capacities in France and Germany correspond to 4.8% and 0.2% of the technical storage potentials of these countries, respectively. The high storage capacity in the United Kingdom is utilized owing to the massive hydrogen production taking place both in the United Kingdom and also in Ireland. Similarly, cavern utilization in the Netherlands and northwestern German regions (“31_de” and “33_de”) are significantly higher than the other regions such as the ones in Spain, Portugal and so on. The main reason behind higher utilization in these regions is similar to the ones in the United Kingdom: hydrogen transported from the Nordic countries. Therefore, large amounts of hydrogen are stored and distributed generally in the regions with high salt cavern availability and proximity to the production sites. Different behavior is observed with the deployment of large salt cavern capacity in “24_fr” because of the neighboring high demand region: “23_fr”.

In spite of its higher investment cost compared to salt caverns, the utilization of vessels in all regions can be seen in Figure 6-4. In total, 562 GWh of storage capacity for vessels is proposed. Looking at the results at a national level reveals that the highest vessel storage capacity is observed in Italy, France, and the United Kingdom with values of 141.5, 101.4 and 61.4 GWh, respectively. The lowest capacity is estimated in Albania as 0.3 GWh. The storage capacities in the region with salt cavern availability are generally less than 1 GWh; however, in the other regions such as “52_it” or “90_uk” (regions with the highest demand and no salt caverns) experience a storage potential of 30-50 GWh. Southern Finland (“75_fi”) has a vessel storage potential of 21.1 GWh, which is relatively high compared to its neighboring regions. This can be explained by the lack of other storage technologies in Finland compared to Sweden and Norway, which have high pumped storage (both reservoir and pumped hydro storage, cf. Figure 3-19). Having the second highest investment cost, vessels are not needed in northern continental Europe because of its high salt cavern storage potential.

Lithium-ion batteries are also required in the system, especially to compensate for the fluctuations caused by PV technologies (i.e., diurnal behavior). Nevertheless, it must be noted that lithium-ion batteries have a significantly high specific investment cost and limited cycle time compared to the other storage technologies considered in the system. The overall utilization of lithium-ion batteries

in the system is nearly 590 GWh, approximately 70% of which are utilized in Spain, Italy, and France. The highest regional capacities are observed in “55_it”, “10_es,” and “11_es” with values of 54.4, 54.1 and 40.3 GWh, respectively. In terms of national capacities, Spain, Italy, and France have 180.2, 117.9 and 110.0 GWh, respectively. Norway does not require any lithium-ion battery owing to its hydropower capacity. Moreover, 40% of the countries experience a lithium-ion battery capacity of less than 1 GWh.

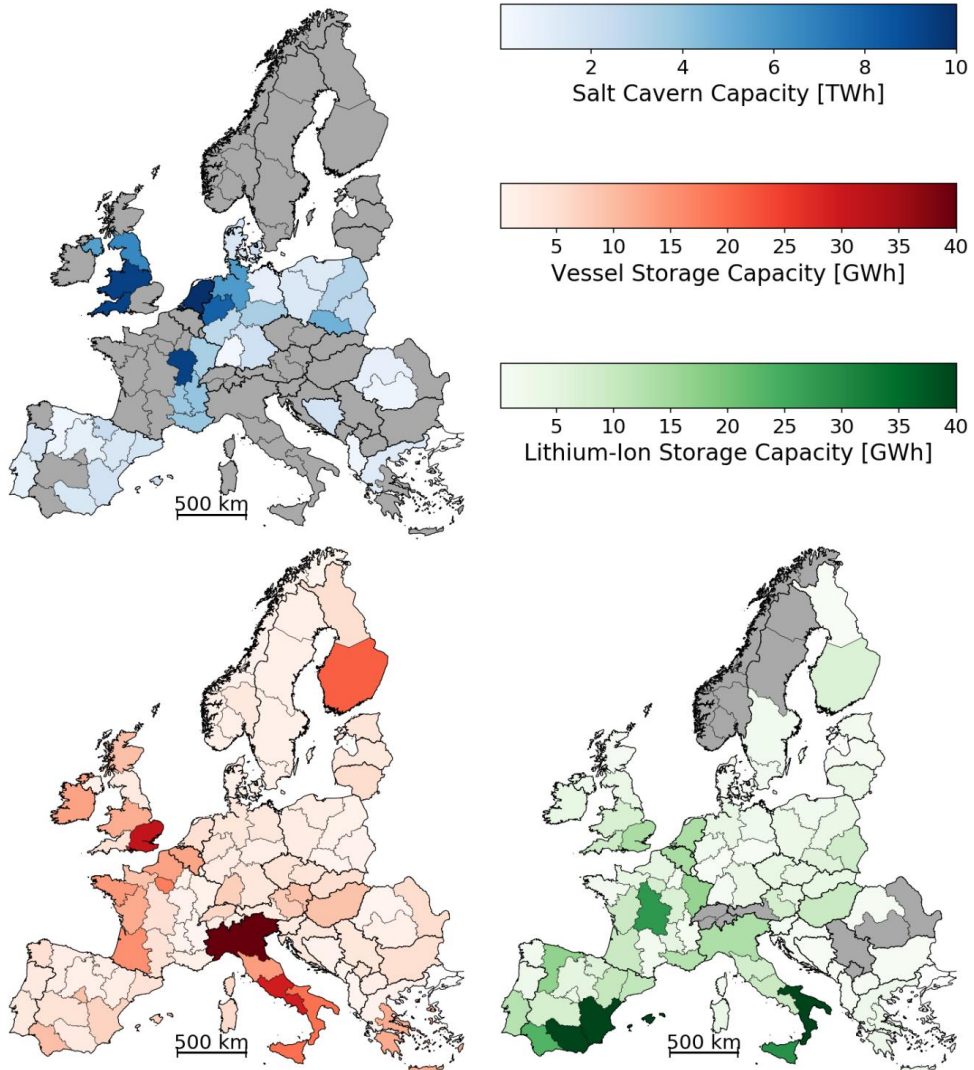


Figure 6-4 Proposed capacities for storage technologies in the 100% renewable European energy system.

The role of lithium-ion battery as a short-term (intraday) storage technology is evident. In addition, the energy system requires seasonal storage technologies in order to compensate for the variations in the generation. Many studies in the literature use only hydropower for large scale storage, and some of the studies take salt cavern storage into account, yet only with the hydrogen produced within that region (without hydrogen transmission). However, the storage capacity of hydropower is smaller than that of salt caverns (cf. Section 2.2). In addition to pumped storage and reservoirs, salt caverns and vessels are also taken into account in the presented system design in order to ensure the seasonal storage hydrogen. The aggregated state of charge time series for these large-scale storage technologies is illustrated as individual gray lines in Figure 6-5, each gray line representing the state of charge profile of a weather year. It must be noted that as an assumption, the initial and final state of charges is assumed to be the same.

Focusing on salt caverns reveals that the minimum value for the state of charge in the caverns is 33%, which corresponds to the minimum amount of gas required for operation (cushion gas). The role of salt caverns as a seasonal storage technology can be seen from Figure 6-5, which contains generally a smooth state of charge profiles with similar trends over all weather years shown. As it is seen from the figure, there is a decreasing trend in the state of charge until mid-February, which then gradually increases until November. From these profiles, it can be inferred that the discharge of hydrogen mainly occurs between November and mid-February.

The smooth profile observed in the salt caverns is not seen in the case of pumped hydro storage. A large variation in the state of charge within short periods (even daily) is evident with a lot of fluctuations. Therefore, it can be said that in addition to the seasonal storage, pumped hydro is also used mainly for flexible electricity generation. Especially, when combined with other technologies, this technology can provide flexibility in the system operation. Owing to the massive capacities in Norway and Sweden, the role of pumped storage can be understood in the production of hydrogen. This technology is utilized in order to attain higher electrolyzer full load hours and provide a steady hydrogen production. A detailed discussion of this behavior is included in Section 6.2 by using an exemplary region ("80_no").

Hydro reservoirs are the technologies that provide flexibility like pumped storage with a difference: no ability to charge the reservoir. In other words, this technology has only the possibility to discharge when required, and the only way to increase the state of charge of a reservoir is the water inflow. Therefore, looking at the time series data emphasizes this increase in the state of charge especially in spring. The major portion of the reservoir capacities is located in the Nordic countries (70% of the storage capacity is located in Norway, Sweden, and Finland). Compared to the salt cavern and pumped storage profiles, hydro reservoirs have a smoother time series, which does not differ significantly with respect to the individual weather years. It must be noted that water inflows are not modeled for different weather years due to the lack of data, which can be considered as the weakness of hydropower modeling. Nevertheless, the time periods where

discharge is taking place do not alter significantly. Among the large-scale storage technologies, the least amount of fluctuations is observed for this technology.

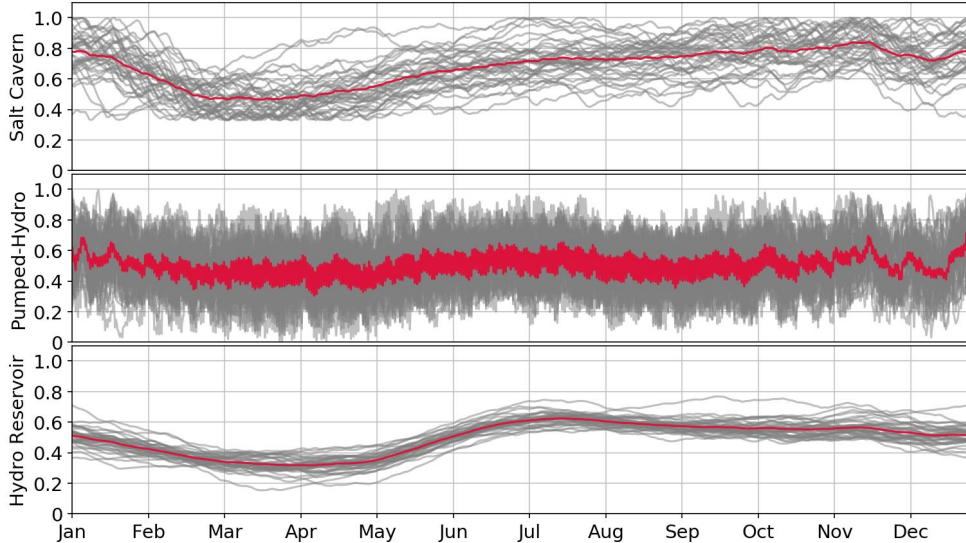


Figure 6-5 Hourly time series for the state of charge of salt caverns, pumped hydro storage and hydro reservoirs for individual years (between 1980 and 2017). Red line is the average time series of all years at each hour.

6.2 Different Regional Behaviors in the Operation of Technologies

The results of the optimization model include the hourly operation of individual technologies for each region. For instance, Figure 6-6 illustrates an exemplary operation time series for northern Italy ("52_it", the region covering Milan). The dashed lines showed both in upper and lower figures stand for the demand profiles, whereas the solid line is the overall consumption of the corresponding commodity. The difference between the overall consumption and demand profile gives the total profile, which is shown as negative. For instance, electrolyzer operation can be considered within the overall consumption in the electricity balance, since it consumes electricity. All in all, it can be said that if there is a technology consuming electricity or hydrogen they are shown in the negative axis of both upper and lower figures. Moreover, operations including charging a battery or pumped hydro storage, exporting electricity, use of electrolyzer can be considered as the sinks for electricity, whereas reelectrification paths and charging salt caverns or vessels are the sinks in the hydrogen circle. Therefore, they are also shown in the negative axes of the plots.

The region ("52_it) showed in this figure has an important role owing to its high demand as well as the high capacity share of solar energy. Nearly 60% of the total generation capacity in this

region belongs to open-field PV without tracking (51.4 GW proposed capacity). As it is expected, during the day time demand is supplied via open-field PV, and the large portion of the remaining electricity is exported. Curtailment is observed around peak generation time periods, and sometimes nearly 30% of the overall generated power is curtailed. In spite of the lower full load hours of onshore wind energy compared to the high potential regions such as Ireland, 13.2 GW is installed in this region. Thus, the fluctuations in the PV energy are compensated to some extent. Although there is no potential for salt caverns, pumped hydro storage can be used for flexible operation, besides hydrogen storage in the vessels. At this point, the role of hydropower can be seen in the figure with discharging it overnight and charging during the daytime. Focusing on the lithium-ion battery reveals its role in the system, compensating the diurnal variation in the energy generation. The battery is discharged at night to supply the demand (no generation of PV); it is charged back during the day. When hydrogen is focused, it is seen that the major portion of the demand is supplied by importing hydrogen via pipelines. Besides, a small portion of electricity is also converted into hydrogen in this region by using electrolyzers. Finally, the utilization of vessels is evident despite its relatively higher costs. However, since there is no potential in terms of salt caverns storage in Italy, vessels are used to supply the hydrogen demand, especially at the peak demand periods. When the demand is low, the imported hydrogen is injected back to the vessels. All in all, it can be said that northern Italy seems like a net hydrogen importer providing nearly all its hydrogen demand via pipelines.

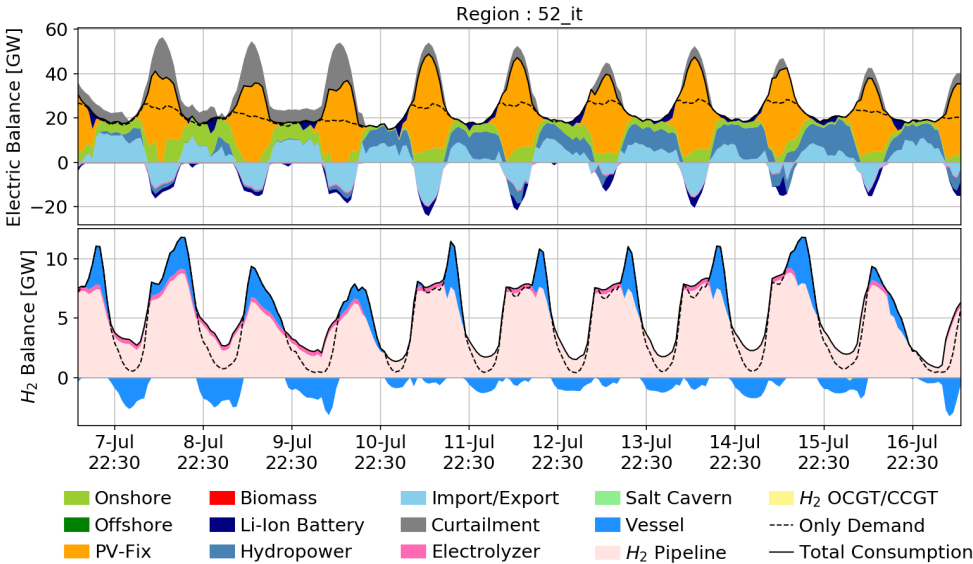


Figure 6-6 Operation of technologies for different commodities in “52_it” for the 2nd week of July (upper) electricity, (lower) hydrogen. 2015 is used as the weather year.

Similar to “52_it” as a large demand center, operation in the region involving London (“90_uk”) is illustrated in Figure 6-7 for the same time period as “52_it”. The dissimilarity in the profiles is apparent in terms of the technologies’ shares. While open-field PV without tracking is the dominant technology in Italy, the United Kingdom experiences large shares of onshore wind energy in the energy mix. Besides the onshore wind energy, a small portion of offshore wind energy is also utilized in this region with a capacity value of 2.7 GW. Although this share is comparably lower with respect to the other regions in the United Kingdom, still it is higher than in Italy. Another aspect that is different in this region is the use of reelectrification technologies. An example of this case is seen around July 15th. The demand which cannot be supplied due to the lack of wind and PV energies at that time period is supplied by the reelectrification of hydrogen. In terms of hydrogen flow in this region, a large dependency on the neighboring regions is observed. As it is seen from the lower figure, a significant portion of the hydrogen demand is supplied by the imports via hydrogen pipelines. Nevertheless, the utilization of electrolyzers with a small penetration is also apparent.

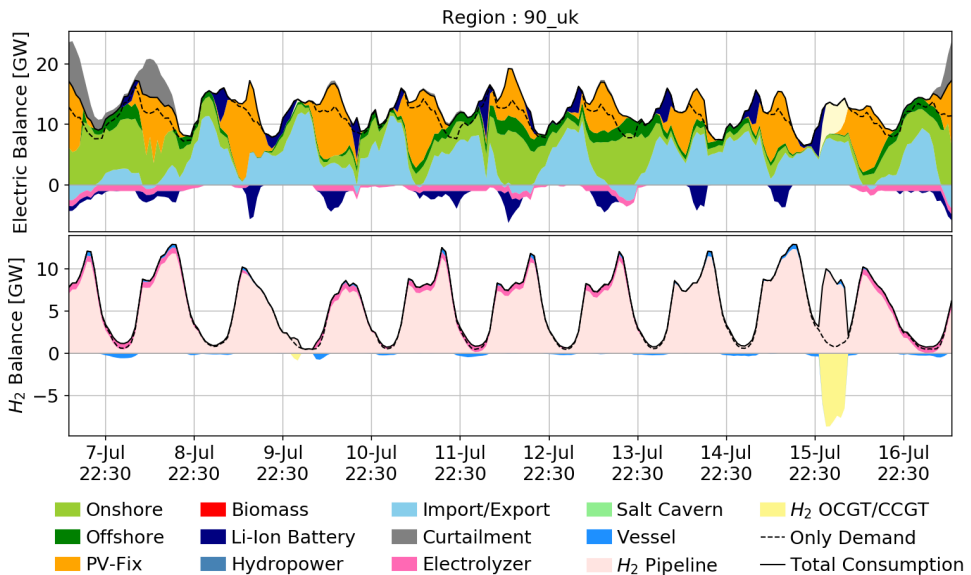


Figure 6-7 Operation of technologies for different commodities in “90_uk” for the 2nd week of July (upper) electricity, (lower) hydrogen. 2015 is used as the weather year.

Different behavior in terms of operation time series is observed and shown in Figure 6-8 for in “80_no”. In terms of generation technologies, only 6.7 GW of onshore wind energy and 0.5 GW run-of-river plant are proposed. Despite low hydrogen and electricity demand observed in this region, a large utilization of the hydropower and onshore wind energy is seen in this region in order to produce hydrogen via electrolyzer (4.2 GW of capacity). As it is seen, almost all produced hydrogen is exported via pipeline, since the demand is insignificant compared to the electrolyzer

capacities. Therefore, it can be said that this region is highly hydrogen exporter, yet this issue will be discussed in Section 6.4. An interesting behavior can be seen in this region in terms of electricity imports. Although electricity can be produced at a cheap price by using onshore wind turbines, still some portion of electricity is utilized to maintain high electrolyzer full load hours. However, at this point the question might arise: Why does the region have higher generation technologies? This is mainly because of the availability of electricity in the neighboring regions, which can be utilized already. Nevertheless, in the case of higher generation capacities, the curtailment might increase due to the excess electricity that cannot be utilized in the electrolyzers. In spite of the flexibility due to the hydropower capacities in this region, still, a small portion of curtailment is observed.

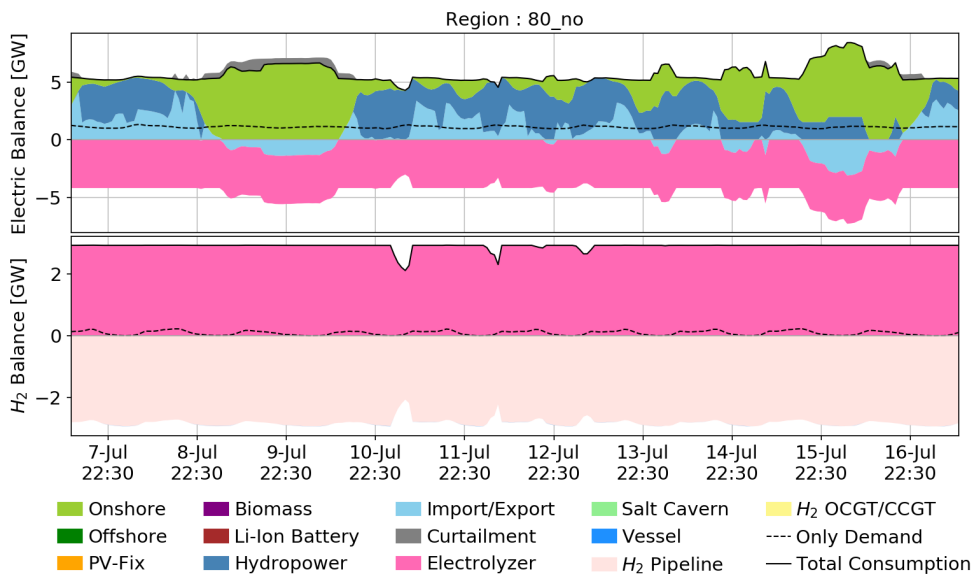


Figure 6-8 Operation of technologies for different commodities in “80_no” for the 2nd week of July (upper) electricity, (lower) hydrogen. 2015 is used as the weather year.

6.3 Curtailment and Efficiency Losses in the System

Curtailing some portion of the energy is inevitable in a highly VRES energy system, as it is also seen in the operation of exemplary regions shown in Figure 6-6 and Figure 6-8. Therefore, the average curtailment in each region is illustrated in Figure 6-9. The energy curtailed in all regions not only belongs to on/offshore wind energy and PV but also run-of-river, pumped storage, and reservoirs. The average of European curtailment across all years is nearly 441 TWh a⁻¹, which corresponds to nearly 13% of the electricity demand and 10% of the average electricity generation. In terms of the absolute value, “52_it” has the highest amount of curtailment, which is approximately 14 TWh a⁻¹. It is then followed by Ireland (“96_it”) and southeastern France (“16_fr”)

with values of 11 TWh a⁻¹ and 10 TWh a⁻¹, respectively. The high curtailment in “52_it” is expected because of the high share of open-field PV, onshore, and run-of-river in its capacity mix (51.4 GW, 13.2 GW and 7.6 GW, respectively). Although there is 6.75 GW of biomass CHP plant, which is the maximum capacity defined for this region, and maximum withdrawal rate of 5.5 GW and 3.7 GW for pumped storage and hydro reservoir, still nearly 12 TWh of energy is curtailed. It is noticed that the optimizer does not choose to install electrolyzer to produce hydrogen with the energy, which is actually curtailed in “52_it”. This can be explained by the full load hours of the electrolyzers. Since the large portion of electricity is generated by PV, the electricity is generally curtailed at the peak generation time periods. Installing electrolyzer is not worthwhile since the electrolyzer full load hours would be too low (Expected value is nearly 1000-1500 h a⁻¹). Having the second-highest amount of curtailment in Ireland is expected because almost all electricity is generated via onshore wind capacity (nearly 90%). 40.7 GW of onshore and 4.5 GW of open-field PV without tracking cannot be compensated by 0.25 GW biomass CHP plants, which is again the maximum capacity defined in this region. Finally, “16_fr” experiences the third-largest curtailment with the corresponding capacity values: 13.0 GW of onshore, 19.8 GW of open-field PV without tracking, and 2.0 GW of run-of-river. Furthermore, biomass CHP plant capacity is the maximum potential defined for this region with a value of 1.5 GW.

Despite the insight gained by absolute amounts of the curtailment, a direct comparison cannot be made without knowing how much electricity is generated. In other words, analyzing the curtailment without the total generation might be misleading. Therefore, the ratio of curtailed energy to total generation is also shown in Figure 6-9. It can be seen that the regions with the highest absolute curtailment values have nearly 5 to 10% of their total generation curtailed. Nevertheless, nearly 40% of the generation is curtailed in “99_fr,”; which is followed by “86_se” and “27_fr” with 33% curtailment in both regions. However, it must be noted that the average generation in these regions is at most 6 TWh a⁻¹.

All in all, neither absolute values of curtailment nor the percentage can be analyzed without considering the other since both quantities depend on the total generation significantly. Therefore, high curtailment observed in the regions becomes reasonable once curtailed energy is related to the total generation. Furthermore, there is barely electricity generation in the regions with a high curtailment ratio, causing the ratio to be unreasonably high. Once the total amount of curtailment and generation values across Europe are taken into account, the overall curtailment is found to be approximately 9%.

Analysis of the curtailment at a national level shows that France, Spain, and Italy have curtailment of 82, 49 and 38 TWh a⁻¹, respectively. As it can be inferred, these countries have the highest open-field PV penetration in their energy mix, causing more fluctuations in the generation profile. The United Kingdom and Germany follow these countries with the values of 35 and 23 TWh a⁻¹. When the curtailment is investigated with respect to the total generation within the region, three

countries with the highest values have nearly 9% of their generated electricity curtailed. For the United Kingdom and Germany, this value decreases to 7%.

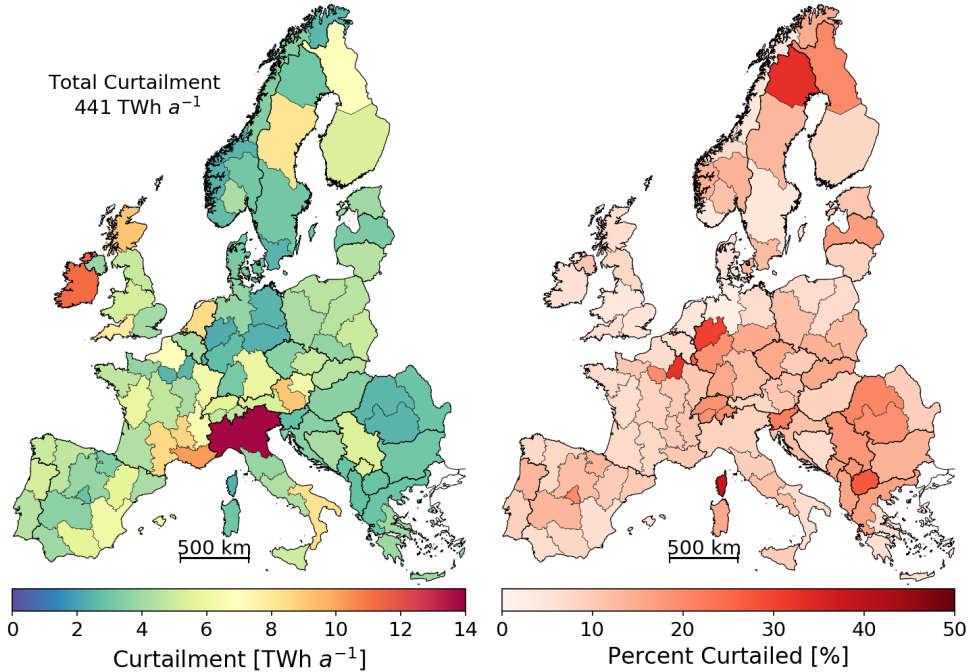


Figure 6-9 Distribution of the average for the proposed system design.

In addition to the curtailment, electrical losses are another reason for energy dissipation (in terms of electrical energy). Therefore, total losses caused by technologies (hydrogen OCGT, CCGT, electrolyzer, biomass CHP plant, and lithium-ion batteries) are shown in Figure 6-10. The total amount of energy dissipation by these losses is 491 TWh a⁻¹, 74% of which is caused by the electrolyzers. This is mainly caused by direct use of electricity to supply the demand, while electrolyzers have to be utilized in order to meet the hydrogen demand. The contribution of biomass CHP plants is estimated at 9%, whereas the losses caused by reelectrification of hydrogen and operation of lithium-ion batteries contribute to 5% and 12%, respectively. Lithium-ion batteries have a major role in the compensation of diurnal fluctuations generally in PV-dominated regions, especially in the locations without pumped hydro storage. Therefore, there is a large portion of energy dissipation due to the high utilization of the batteries at these locations. The high share of losses caused by biomass can be explained by CHP plant efficiency, which is assumed to be 38%. A significant portion of the energy is lost during electricity generation via biomass; nevertheless, the contribution is limited to 9% owing to lower utilization of biomass compared to the other generation technologies. Finally, it is seen that reelectrification technologies

have a share of 5% in the overall losses, meaning that the losses caused by the utilization of hydrogen are not pronounced as much as the other conversion technologies. In spite of having low efficiencies (c.f. Table 3-5), the contribution does not exceed 5% due to the low utilization of hydrogen.

Discussion of the losses caused by different technologies will be conducted at the national level since there are four main groups requiring analysis (electrolyzer, hydrogen reelectrification, biomass CHP and lithium-ion batteries). Average losses for each region and technology are provided in the Appendix E.

The most considerable amount of losses at the regional level is observed in Ireland with a value of 41 TWh a⁻¹, which is mainly because of the large amounts of hydrogen production by electrolyzers. Ireland is followed by several regions in the United Kingdom, aggregation of the regional capacities in the United Kingdom results in 79 TWh a⁻¹. Moreover, Norway also experiences losses as much as the United Kingdom with a value of 70 TWh a⁻¹ in total. Owing to the cheap electricity generation via wind turbines in these regions, a significant amount of energy is used for hydrogen production. In other words, the losses experienced by these countries are largely caused by electrolyzers, since hydrogen demand across Europe is largely supplied by these countries (detailed explanation regarding the roles of countries in the future energy system is discussed in Section 6.4).

The second highest losses are observed for lithium-ion batteries, capacity distribution of which is discussed in Section 6.1.2. The losses in Spain, Italy, and France are estimated as 7.5, 4.9 and 4.4 TWh a⁻¹, respectively. The losses in these countries can be explained by the high share of especially open-field PV without tracking in the system, requiring a storage technology that can compensate the diurnal profile. Note that diurnal profile compensation is not the only role of lithium-ion batteries in the energy system. Fluctuations caused by any VRES sources require batteries to some extent, as it is seen in the example of Ireland and Sweden.

Concerning the contribution of the losses caused by biomass CHP plants, Germany has the highest contribution with 10.7 TWh a⁻¹. Due to cheaper locations for electricity generation and hydrogen production, Germany imports both electricity, and hydrogen from the neighboring regions. Nevertheless, a large share of its electricity is also generated by the biomass CHP plants. Germany is followed by France and the United Kingdom with 7.7 and 4.2 TWh a⁻¹, respectively. It must be noted that the efficiency of biomass CHP plant plays an important role in these losses since it is assumed to be 38%. In other words, 62% of the energy dissipates (as losses) during electricity generation periods.

Finally, hydrogen reelectrification technologies (namely OCGT and CCGT) are aggregated together. The variation between these two technologies mainly occurs due to the difference in their operation cost. The same order in the countries for biomass CHP losses is seen for reelectrification

losses, but with higher values. Highest losses are observed in Germany, the United Kingdom, and France with values of 14.5, 12.9 and 9.8 TWh a⁻¹, respectively. It must be noted that the highest utilization is observed in the countries with high storage capacities for salt caverns. When the regions are analyzed specifically for reelectrification, it is seen that regions with high electricity and hydrogen demands benefit from hydrogen reelectrification the most.

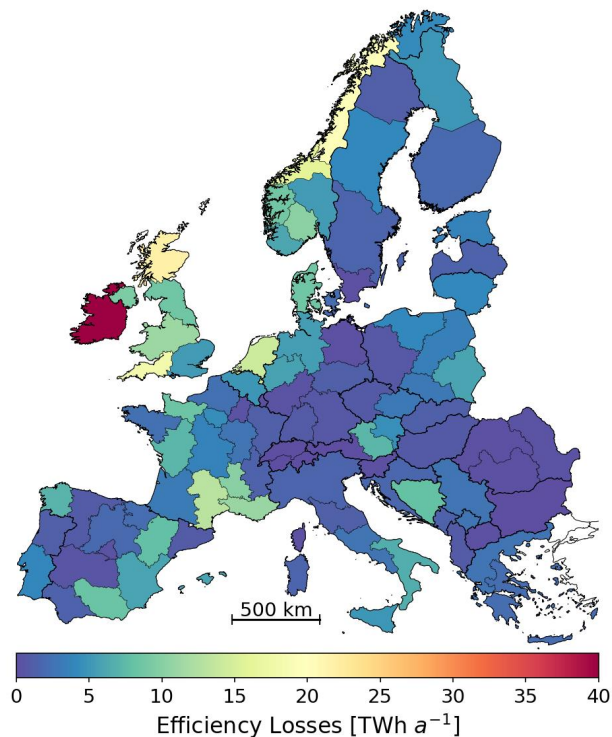


Figure 6-10 Losses caused by conversion technologies as well as lithium-ion batteries.

6.4 Roles of Countries in the Future Energy System

When the system design shown in Figure 6-1 is investigated, the capacity distribution of generation technologies can be seen as well as pipeline connections between regions. Nevertheless, whether or not the region imports hydrogen cannot be understood by only looking at the pipeline capacity, which connects two regions. To understand the dynamics between regions, the net hydrogen and electricity transport and its direction have to be derived, which is shown in Figure 6-11 with the flow direction. Electricity transport is estimated both for HVDC and HVAC cables, and hydrogen pipelines are used for net hydrogen transport. Owing to the high spatial resolution flows in the figure are not very easy to follow. Nevertheless, the main reason to include these plots is to provide

an insight into the dynamics between the regions instead of discussing each connection one by one.

Focusing on electricity transport unveils the electricity flow towards continental Europe in several directions. Denmark, Germany, the Netherlands and the United Kingdom import electricity from Norway owing to the locations with cheaper electricity generation. Electricity transport is evident not only from Norway but also from Finland and Sweden. However, an interesting flow in terms of electricity is seen in Norway towards “83_no” and “84_no”. In spite of their low electricity and hydrogen demand, these regions import electricity in order to produce hydrogen. This can be explained by the full load hours of the electrolyzers, which causes these two regions to import electricity in order to maintain certain full load hours and produce more hydrogen (cf. Figure 6-2). Moreover, it is seen that Ireland and the United Kingdom supply electricity in western European countries such as France, Belgium, and the Netherlands. This is mainly because of the nature of the optimization while finding the lowest possible solution for the total annual cost. As it is discussed previously, cheap electricity generation and transporting it are preferred compared to the utilization of relatively more expensive locations. Unlike the flow from the Nordic countries and from the United Kingdom and Ireland, there is not a clear pattern within continental Europe in terms of electricity transport. Nevertheless, the roles of certain locations are evident. For instance, southern France (“15_fr”) and northwestern Germany (“31_de”) export electricity to the neighboring regions. In addition, northwestern Germany also exports electricity to southern Germany via HVDC cables. Furthermore, regions like “33_de” (North-Rhine Westphalia), “23_fr” (Paris) and “07_es” (Madrid) import electricity from almost all the neighboring regions.

Flows shown for hydrogen are relatively more succinct with a pattern that can be followed easily. Similar behavior seen in the electricity flow from Nordic countries and the United Kingdom to continental Europe is observed for hydrogen flow, too. Focusing on hydrogen transport in the Nordic countries, it is seen that the amount of hydrogen transport increases from the north towards south, which shows the accumulation of individual regions contribution transported towards continental Europe. Once the hydrogen pipeline reaches to northwestern Germany (“31_de”), it is then distributed to the neighboring regions within continental Europe. Similarly, there is a large hydrogen transport from the United Kingdom towards “26_fr”. Northern Italy is also interesting because of the hydrogen transported from France and Slovenia, yet exported to Austria. This is mainly because of the excess amount of hydrogen production in the peak power generation periods via PV. Moreover, hydrogen export from Austria to southern Germany also indicates that Austria might act as a conduit in hydrogen transport towards southern Germany. However, this issue will be addressed in the next paragraph, while attaining roles to the regions. Finally, also the hydrogen import from both northern and southern Italy is seen in the case of central Italian regions.

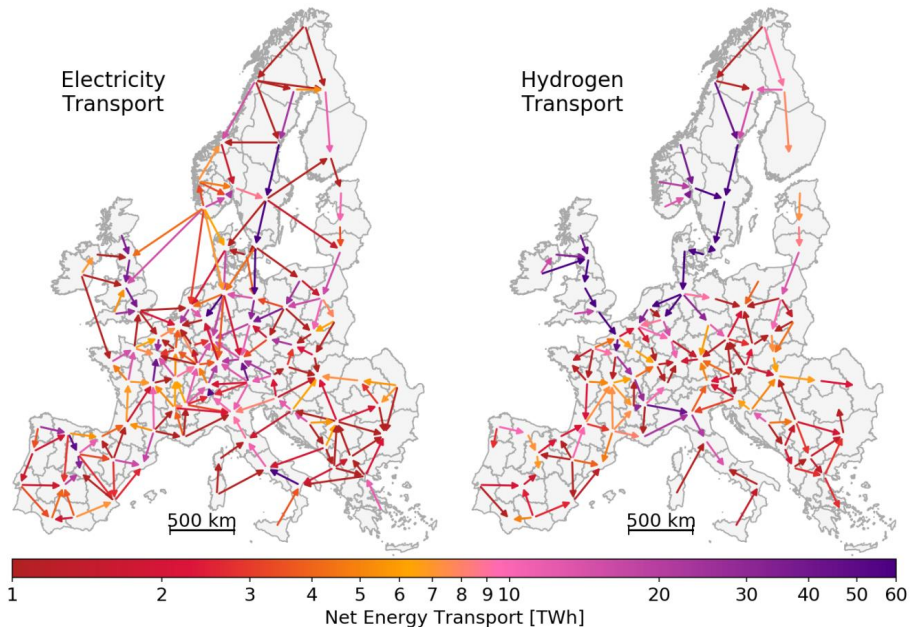


Figure 6-11 Net energy flow between regions for (left) electricity (right) hydrogen.

By looking at Figure 6-11, indicating the amount of transported hydrogen and electricity, regions and some roles can be identified. However, additional dimensions in regards to the total generation and consumption in each region would improve the discussion of hydrogen and electricity transport. Therefore, removing the geospatial aspects and aggregating total imports and exports in each region result in Figure 6-12. Furthermore, the figure also involves the total demand and electricity generation in the corresponding region. These results can be analyzed by classifying them into 4 groups as it is also shown in the figure.

Both hydrogen and electricity exporters: The regions in the upper right of the figure belong to this group. As the name indicates, both commodities are exported to the neighboring regions. Ireland has the highest export of hydrogen and electricity with values of 85 TWh a⁻¹ and 95 TWh a⁻¹, respectively. Following Ireland, “94_uk”, “84_no” and “15_fr” are the regions with high export.

Both hydrogen and electricity importers: Regions importing both commodities and shown in the lower left of the figure belong to this group. For instance, “92_uk”, “90_uk”, “33_de”, “23_fr” and “52_it” are the regions with the highest import of electricity and hydrogen. Among these regions, “90_uk” including London, “92_uk” including Liverpool and Manchester, and “52_it” including Milan have high demand but also the high generation to supply the demand. Nevertheless, after the utilization of the good locations for electricity generation, the remaining areas in these regions cannot compete with the neighboring regions in terms of electricity

generation cost. Therefore, some portion of the demand is supplied by the generation within these regions, and the remaining is imported. A different dynamic is observed in the regions “33_de” (North Rheine Westphalia) and “23_fr” (Paris). Unlike aforementioned regions with high imports yet still utilizing the local sources, “33_de” and “23_fr” mainly supply their demand by importing electricity from almost all of their neighboring regions.

Hydrogen importer – electricity exporter: This category is located on the upper left part of the figure. As it is seen, there are not many regions importing hydrogen but exporting electricity. The most apparent region is northwestern Germany (“31_de”). This region exports approximately 50 TWh a⁻¹ electricity to the neighboring regions and it imports almost 30 TWh a⁻¹ of hydrogen. Although electricity transport is limited by the capacities of HVAC and HVDC cables connecting regions, the maximum capacity defined for hydrogen pipelines is not a limiting factor due to relatively lower capacity requirements. Hydrogen demand in many regions is supplied by the cheapest electricity generation locations, in this specific region, it is imported from the Nordic countries. However, as the distance increases from these cheap locations (making electricity transport harder due to the cable capacities), utilization of the local sources becomes necessary. As a result, in “31_de”, for example, utilization of both onshore and offshore wind energy is seen due to its relatively cheaper electricity generation compared to the other locations in northern continental Europe. All in all, this region imports the hydrogen produced in the north while exporting electricity that is generated by the utilization of the local sources.

Hydrogen exporter – electricity importer: This is the group seen on the lower right. As it is seen there are not many regions in this category. Nevertheless, “81_no” and “82_no” can be used as an example of this category. What happens in these regions is as follows: import electricity to maintain reasonable full load hours for the electrolyzer, and then export the hydrogen produced via imported electricity. In other words, the imported electricity is not used to supply the electricity demand in these regions but to maintain electrolyzer full load hours and produce hydrogen.

The number of groups categorizing these regions can be increased further. Nevertheless, general behavior can be inferred from these four categories. What is not included and cannot be interpreted from Figure 6-12 is the conduit type of region. In other words, the regions nearly no net hydrogen transport, but a large pipeline passing through. The role of these regions is to connect hydrogen sources and sinks, although the regions are not adjacent to one another. In order to investigate this behavior, an additional dimension of pipeline capacities has to be added to the plot, which is not possible in Figure 6-12 for the sake of a succinct discussion.

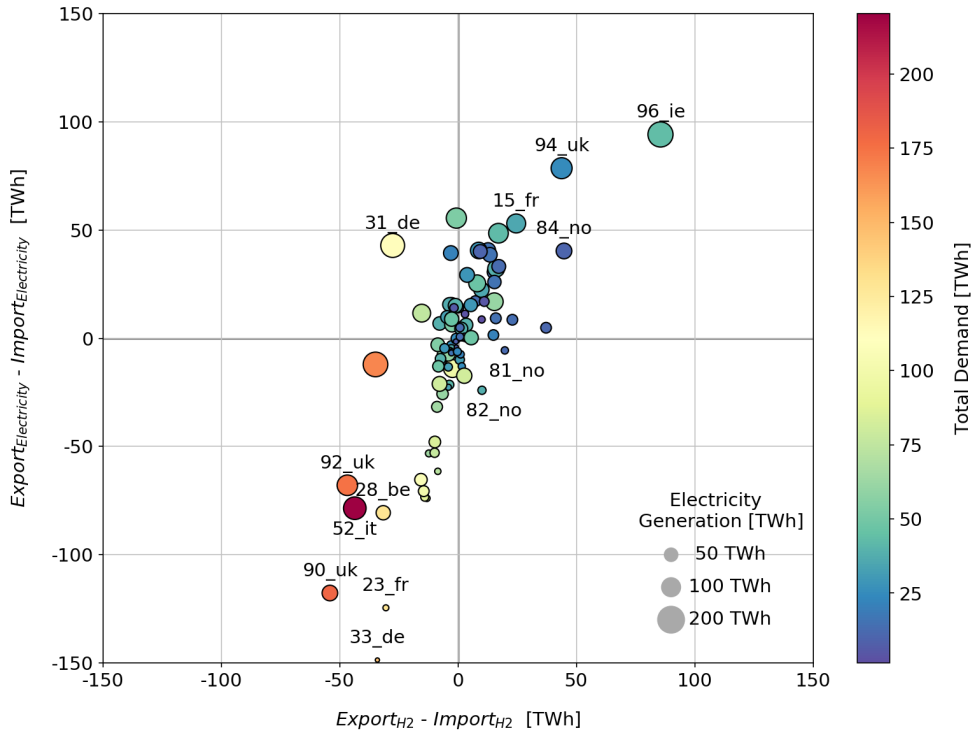


Figure 6-12 Net transport of electricity versus hydrogen, with electricity generation and total demand within the regions indicated as the marker size and colors, respectively.

As it is previously mentioned, the net importer or exporter regions can be identified by looking at Figure 6-12. However, another role a region might take in terms of hydrogen can be a conduit. Identification of these regions can be conducted by looking at the pipeline capacities and whether or not the region imports hydrogen. Thus, the distribution of net hydrogen transport and proposed pipeline connections are shown in Figure 6-13. Net hydrogen transport indicates the quantity of hydrogen transport in addition to the direction of this transport via the sign. In other words, if the value is positive, there is hydrogen leaving the region (hydrogen export) and vice versa. For the sake of simplicity, region borders are not shown in the figure, yet it can be understood by the color transition. Looking at the Nordic countries, larger pipeline capacities towards continental Europe are observed. Gathering the hydrogen produced in all regions except "75_fi" (southern Finland), a large pipeline passes through southern Sweden ("88_se" and "89_se"), which do not export hydrogen significantly. Then the connection passes by regions in Denmark with a slight increase in their capacities. Therefore, these regions do not benefit from the large hydrogen pipelines connecting them, yet acting like a conduit allowing the hydrogen transport to the non-neighboring regions. Northern United Kingdom experience the same behavior, especially "93_uk" collects all pipeline connections from the neighboring regions and transmits some portion to "92_uk" and also

a large portion to the continental Europe over “90_uk”. The hydrogen produced both in the United Kingdom and Ireland is transported to continental Europe via the connection between “90_uk” and “26_fr”. After that, it is distributed to the neighboring regions.

The importance of conduit regions cannot be identified in this analysis due to the perfect European market assumption made in the beginning. However, it must be noted that prohibiting any of these connections would change the proposed energy system design. For instance, in case of a public acceptance issue raised by Denmark would disconnect the Nordic regions and continental Europe. Another reason for prohibiting these connections can be political reasons. Therefore, despite the high generation potential and cheaper hydrogen production compared to continental Europe, a more decentralized design would be required in such a case. Moreover, this would result in a change in the roles of countries as hydrogen importers or exporters, since a new balance in the system has to be attained. All in all, it is worthwhile to emphasize the importance of these conduit regions in the energy system design.

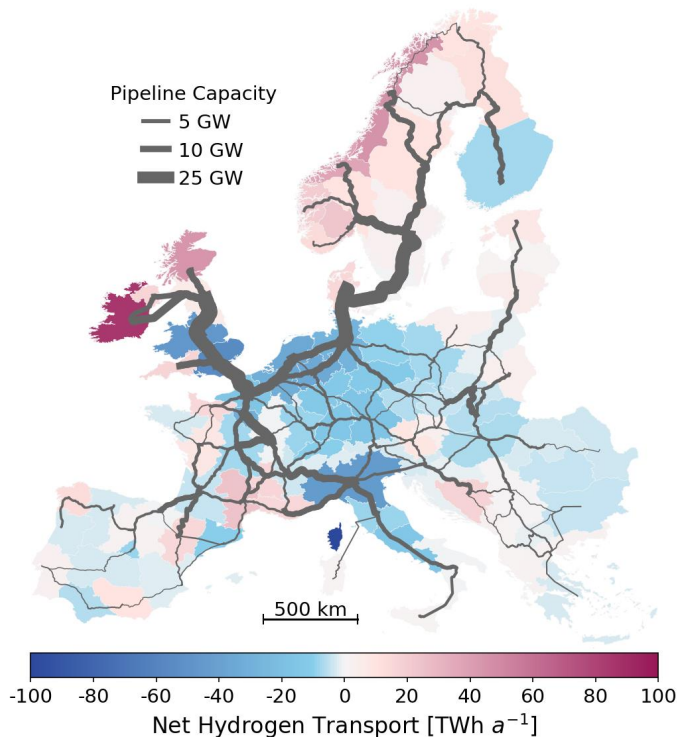


Figure 6-13 Geospatial distribution of the net hydrogen transport across regions with proposed pipeline connections.

6.5 Comparison of the Designed System against Literature

In the view of comparing the design results against literature, several studies are chosen with respect to their area of application and consideration of VRES technologies. Nevertheless, most of these studies do not provide all the results such as capacity distribution, total generation, curtailment and so on. Therefore, the discussion is divided into three sections, which are classified according to the VRES capacity and generation, annual curtailment and storage capacities. For each section, the data which could be extracted from the sources are discussed in detail in terms of the discrepancy and the reasons. In Section 6.5.1, VRES capacities and electricity generation results are compared at a regional level as well as the European level. Afterward, the average annual curtailment values estimated by several studies are discussed in the context of Europe as well as Germany in Section 6.5.2. Finally, the required capacity for storage technologies is examined and presented in Section 6.5.3.

6.5.1 Comparison of VRES Capacities and Electricity Generation

Capacity distribution of the VRES technologies is conducted in several studies [20], [92], [131]–[134], [141], yet the results are not provided with respect to the spatial resolution considered. Therefore, discussion of the capacity distribution is conducted considering only two literature sources providing these values explicitly. The spatial resolution of this work is determined with reference to the E-Highway study [141], yet the results published by Cebulla et al. [146] include aggregation of some countries. Thus, the literature comparison is performed by aggregating the values to the lowest spatial resolution, which is the region definition by Cebulla et al. [146]. The resulting comparison of VRES capacity distribution is shown in Figure 6-14.

It can be seen that onshore capacities in all regions except “Poland-Czechia-Slovakia” and Germany is higher than that reported by Cebulla et al. [146] and the E-Highway study [141]. Moreover, offshore capacities estimated by Cebulla et al. [146] is always higher than the presented work, except the region of “Poland-Czechia-Slovakia”. It must be noted that the average full load hours in this study is higher owing to the future-oriented turbine designs. This is more pronounced especially in the regions with relatively lower wind speeds and full load hours. Therefore, in general, lower capacities can be understood by a better generation. Furthermore, the regions with relatively lower potential in terms of generation are enhanced by the future-oriented turbine designs, which enables these locations to deploy more VRES technologies to supply their demand.

There are significant variations in the capacities of some regions. For instance, in the United Kingdom and Ireland, capacity estimated by Cebulla et al. [146] is nearly 60% of the capacities estimated in this study and also by E-Highway. Moreover, offshore wind energy in these regions is not preferred as much in this analysis. In the presented work, these locations have the role of exporter owing to their cheap electricity generation potential; moreover, they produce a large

portion of hydrogen and export it to Europe. Thus, a higher capacity compared to Cebulla et al. [146] can be expected. Nevertheless, comparison with the E-Highway results reveals that the share of onshore wind energy is slightly higher than the offshore in the same region. It must be noted that this is an effect of the turbine designs; in other words, enhanced generation both in the onshore and offshore wind energies. The enhancement in the onshore is more pronounced, causing it to be chosen more compared to the offshore. Similar behavior can be seen in “Norway-Sweden-Finland”, too. Better turbine designs and cheap electricity generation make these regions install onshore wind turbines. Regions such as France, “Spain-Portugal” and “Austria-Switzerland” experience higher capacities either in onshore wind energy or PV, because of the enhancements as well as the flexibility gained by the introduction of hydrogen in the system. Therefore, especially in the southern regions, high utilization of PV is observed owing to the electrolyzers and power-to-hydrogen option in operation. Finally, a large discrepancy in the capacities in Germany is observed. It must be noted that Germany behaves as a net importer of electricity and hydrogen because of high potential regions with cheap electricity generation surrounding the country. Since the methodology consists of optimization with an objective function of minimization of the cost, importing the commodities (electricity and hydrogen) from the neighboring countries is found more cost-effective for Germany.

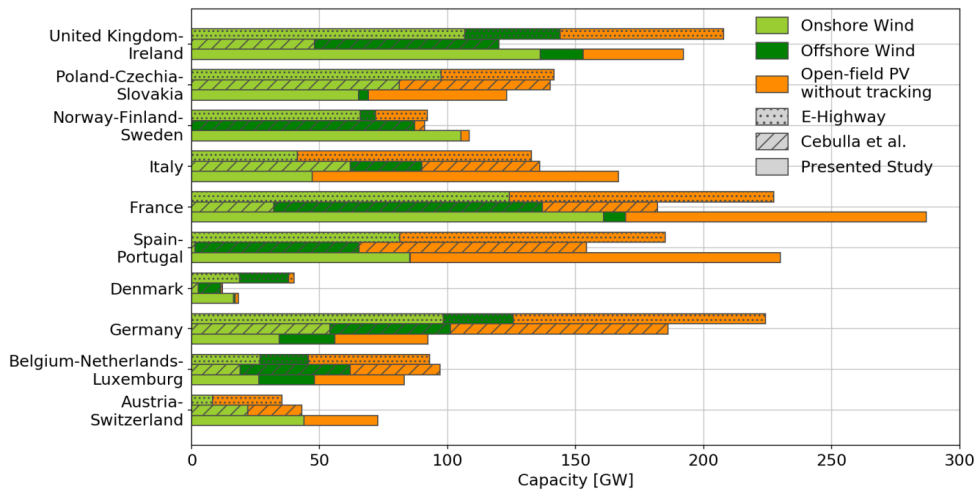


Figure 6-14 Comparison of VRES capacity distribution for regions defined by Cebulla et al. [146].

In addition to the regionally resolved capacity distributions reported by Cebulla et al. [146] and the E-Highway study [141], many studies demonstrate the overall European capacity. The comparison of the energy mix suggested by these studies with respect to the present work is shown in Figure 6-15. It must be noted that the figure on the right is separated from the remaining due to the different regional definitions suggested by Cebulla et al. [146] (cf. Figure 6-14). Therefore, for that comparison, only the capacity values within the corresponding region definition are extracted and

shown as “Present Work*^o”. Another remark regarding the capacity mix is the fact that some of these studies include fossil fuels and its derivatives, nuclear power, and geothermal energy. Thus, onshore and offshore wind energy, open-field PV, biomass and hydropower are shown explicitly as the only comparable technologies. Remaining technologies such as hydrogen CCGT, nuclear, geothermal energy and so on are aggregated and demonstrated in the category shown as “Others”.

Focusing on the left-hand side of the figure reveals that the proposed capacity is within the upper and lower limits of literature estimations. EU Reference Scenario [131], as well as the 7th scenario from Zappa et al. [17], has the lowest capacity values, nearly 500 GW deviating from the results presented in this work. In the energy mix of the “Reference Scenario” [131], utilization of 270 GW of natural gas, 50 GW of coal and 90 GW of nuclear power is observed. In the case of Zappa et al. [20], nearly 470 GW of gas utilization is reported. Therefore, the lower capacity estimates can be expected considering these dispatchable power sources. Focusing on the capacity mixes reported by Zappa et al. [20] (2nd, 4th and 6th scenarios) and “Energy [R]evolution 5th edition”, a large discrepancy can be seen in comparison to the presented work. While 2nd scenario of Zappa et al. [20] and “Energy [R]evolution 5th edition” can be explained by the high demand and generation considered (both assumes a demand of 6020 TWh a⁻¹); the overestimation of 4th and 6th scenarios are caused by high capacities assumed for biomass. The results of the present work are closely in line with the E-Highway “100% RES” scenario [141], Roadmap 2050 [92], Zappa et al. [20] (1st and 5th scenarios), as well as Re-thinking 2050 [134]. However, a slight deviation from the results of Re-thinking 2050 [134] is observed, yet the reason behind the lower capacity estimate is the consideration of nearly 75 GW of geothermal energy in the energy mix.

Sensitivity analyses conducted by Cebulla et al. [146] and different values for the capacity mix are shown on the right-hand side of Figure 6-15. It must be noted that the electricity generation is not reported in their report; thus, it is not shown in the results of Cebulla et al. [146]. As previously mentioned, the regional definition of Cebulla et al. [146] differs from the present work. Therefore, the results shown as “Present study*^o” include only the capacity values for the countries defined by Cebulla et al. [146]. The proposed capacities are higher than all the capacity mixes shown in the plot. There are two main reasons behind this: consideration of hydrogen demand in addition to the electricity demand and the roles of countries within the region of interest. Firstly, the hydrogen demand increases the electricity demand by nearly 600 TWh a⁻¹, which requires hydrogen production by electrolyzers with an efficiency of 70%. Therefore, even with the best-case scenario and an additional electricity generation of 850 TWh a⁻¹ is required. In addition, the countries excluded by Cebulla et al. [146] are net electricity and hydrogen importers, meaning that the capacity is shown on the right-hand side of the plot also covers most of the electricity and hydrogen demand of other regions by exports.

All in all, in spite of some discrepancies caused by different assumptions, technology portfolios or region definitions, the capacity results estimated in this work are in line with the values reported in

the literature. Moreover, a close agreement with the results of the E-Highway study [141] is also attained, although different VRES generation workflows are used in addition to the introduction of hydrogen in the system.

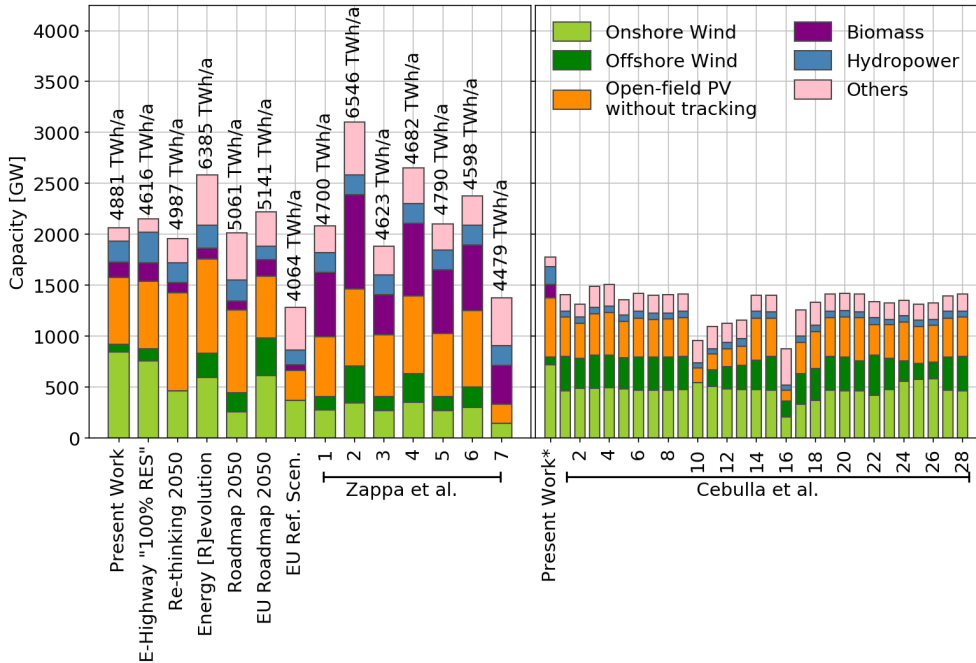


Figure 6-15 Comparison of total capacity distribution and generation for (left) Europe, (right) regions defined by Cebulla et al. [146]. Note that the capacities present work on the right is calculated according to the region definition.

6.5.2 Comparison of Annual Curtailment

Depending on the context and scenario, curtailment varies significantly. In this section, curtailments available in the literature are compared against the average annual curtailment. Zappa et al. [20] stated that considering the worst year (2010), optimizing the system and VRES sites prevent curtailment. Moreover, system balance via dispatchable sources is found to be more cost-effective than increasing the VRES capacities to cover the demand [20].

In the presented study, annual curtailment for Europe is estimated as 441 TWh a⁻¹ when the proposed system design assumed over 38 weather years. Figure 6-16 shows a comparison of Ryberg [37], Syranidou [136] and present work. In the doctoral thesis of Ryberg [37], annual curtailment is reported as 1067 TWh a⁻¹ in the analysis conducted to determine generation lulls by using nearly 185 scenarios with different weather years. The discrepancy between the results is significantly high with a value of 620 TWh a⁻¹. The main reason for the high curtailment reported

by Ryberg [37] is the difference in the methodology used since Ryberg [37] only optimizes the operation of technologies with fix capacities. Moreover, while capacity values are obtained from the E-Highway study [141], Ryberg [37] uses a future-oriented technology definition with higher full load hours. When the same scenario of E-Highway study (“100% RES”) is analyzed by Syranidou [136], the average curtailment is reported approximately 770 TWh a^{-1} , decreasing nearly by 100 TWh a^{-1} with a flexible operation (flexible dispatch). Although similar workflows are used by Syranidou [136] and Ryberg [37], values for curtailment differ because of the nearly 185 scenarios with different weather years employed by Ryberg [37]. As a result, since the capacities are not optimized with respect to the generation time series, system design presented by Ryberg [37] and Syranidou [136] is overengineered. In addition to the capacity scaling, consideration of hydrogen provides flexibility in the operation of technologies; which also decreases the curtailment.

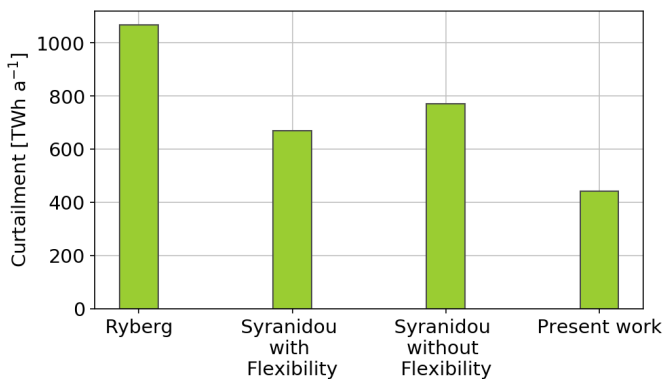


Figure 6-16 Comparison of Ryberg [37], Syranidou [136] and present work.

Cebulla et al. [146] performed nearly 30 sensitivity analyses and reported the total annual curtailment for the region of their interest. According to their results, annual curtailment across Europe varies between 450 to 1250 TWh a^{-1} . Among the reported curtailments, the lowest is observed when there is no constraint enforcing 80% VRES technologies and low carbon dioxide certificate prices. Then the second lowest value is stated as 690 TWh a^{-1} , which is obtained for a copper-plate energy system (no grid limitation). Hydrogen pipeline transport can be considered the main difference between the presented study and Cebulla et al. [146], which enables a more flexible operation.

Michalski et al. [14] declare annual curtailment of Germany for 11 scenarios, consisting of a combination of whether the reconversion is local or central, consideration of hydrogen in the mobility sector, dispatchable power generation and storage size. The results reveal that the annual curtailment, estimated as 55.7 TWh a^{-1} , can decrease down to 0.4 TWh a^{-1} with increasing

dispatchable power generation. In the presented analysis, the average annual curtailment in Germany is calculated as 22.8 TWh a⁻¹. Focusing on the scenarios with hydrogen use in the mobility sector with central reelectrification, the curtailment range narrows down to 0.4 to 10 TWh a⁻¹ in the analysis reported by Michalski et al. [14]. An overestimation of 100% can be seen in the results presented in this report. However, it must be noted that the reported value of 22.8 TWh a⁻¹ might decrease further if the energy system is optimized by using time series from a single weather year²⁸. Taking into account 38 weather years ensuring the security of supply overestimates the VRES capacity, which increases the curtailment. Therefore, this deviation in the results can be expected due to the different methods employed in both analyses.

6.5.3 Comparison of Storage Capacities

Another method to compare the results against literature is the storage ratio, which enables comparing slightly different regional context independent from assumed demand value. Only the studies, consisting of 100% renewable energy systems are included in this comparison, since decreasing VRES penetration would require less storage as it is discussed in detail by Blanco and Faaij [94]. The sources are chosen with respect to their regional definition (at least Europe) independent from the intended time context of the scenario. For instance, Bussar et al. [17], [145] assume a total demand of 4122 and 6250 TWh a⁻¹ in the context of 2050, respectively. Moreover, not only Europe but also the Middle East and North Africa are covered in the regional definition of these studies. Another study by Bogdanov et al. [29] adds Eurasia to the previously defined region; furthermore, a total demand of 10576 TWh a⁻¹ is estimated including the gas and desalination demands besides the electricity demand. Thus, in order to normalize these values and to be able to compare the results, the definition of storage ratio is used. The corresponding storage ratio found in the literature is demonstrated in Figure 6-17.

The storage ratios estimated by Bussar et al. [17], [145], Heide et al. [24], and Thien et al. [138] are higher than the present work. The results obtained by Aboumahboub et al. [142], Rasmussen et al. [137], Steinke et al. [18] and Cebulla et al. [146] are approximately 1%, which is below the estimated value in this analysis. Finally, the storage ratios found by Bogdanov et al. [29] and Child et al. [148] are closely in the with the value estimated in this work. It must be noted that the storage technologies considered in these systems vary significantly. For instance, Steinke et al. [18] compare different storage technologies, which are pumped hydro storage, batteries and hydrogen storage, independent from each other. On the other hand, Bussar et al. [17], [143], [145] model these technologies together in the energy system. Another example of how different storage technologies are modeled is Aboumahboub et al. [142] that do not differentiate any storage technology explicitly.

²⁸ Michalski et al. [14] consider 2006 as the weather year in their analysis.

Bussar et al. [17], [143], [145] modeled Europe, Middle East, and North Africa regions by using mainly wind and PV energy. In the analysis having nearly 6% storage ratio, a constraint of self-sufficient regions with possible power balance, whereas, in the second analysis with nearly 13%, 80% of the demand has to be supplied by local sources. Nevertheless, neither a discussion nor reasoning is provided for the high storage capacities. Similarly, Heide et al. [24] perform a European analysis with wind and PV systems and states a storage requirement between 400 to 480 TWh without explicit reasoning. Therefore, the storage ratios reported by Bussar et al. [17], [143], [145] and Heide et al. [24] could not be analyzed further due to the lack of explanation in their system.

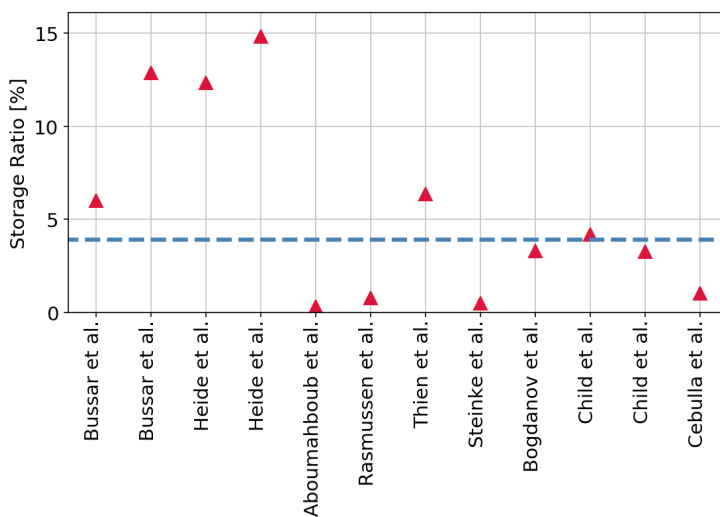


Figure 6-17 Comparison of storage ratio²⁹ estimated by literature sources as cited in Blanco and Faaij [94].

6.6 Discussion and Evaluation of the Methodology in Present Work

It is seen that the proposed system design is in line with the ones available in the literature. Therefore, it can be said that the approach and model are validated. In this section, an overall discussion of the weaknesses and strengths of the method will be discussed.

The presented approach has many aspects that can be considered as strengths compared to the analyses in the literature. Firstly, the hourly resolution of this analysis is one of the most important strengths when the volatility of VRES technologies is taken into account. Although time series aggregation is applied in some parts of the analysis, the final design is conducted with full-time

²⁹ Storage ratio is estimated by dividing the total storage capacity by the total annual demand.

series involving the extreme periods. Moreover, the importance of this aspect is emphasized also in the discussion of the final design.

Another aspect of this presented approach is the high spatial resolution, which involves 96 regions across Europe. Considering the existing literature sources designing the future European energy system by optimization, the number of regions is limited such as one node per country. It must be noted that the level of detail increases with the higher number of regions, especially in terms of infrastructure modeling.

In addition to the higher spatial resolution, a further increase in the spatial resolution of VRES technologies is conducted by creating different VRES groups as technologies (cf. Section 3.3.1). By doing so, wind parks and solar parks are modeled by creating 5760 groups across Europe. Therefore, the drawbacks of averaging or misrepresentation of time series by wrong location selection are eliminated. All possible locations across Europe are defined in the optimization, which then determines the most suitable ones among all of them.

Finally, the most important strength of the presented analysis is the consideration of different weather years (between 1980 and 2017), which covers many different weather phenomena. It must be noted that the robustness of the system design increases when all these years are taken into account. The assumption while conducting this analysis is all the extreme periods within these 38 years cover the behavior of the weather in 2050.

In addition to the strengths listed above, there are several assumptions simplifying the problem. For instance, assuming the same inflow time series for hydropower might cause small deviations in the results. Owing to the difference in the order of magnitude of hydropower capacities and the maximum inflow, the results are expected to deviate insignificantly. Nevertheless, it must be noted that the consideration of dry and wet years would enhance the approach.

Secondly, the partly green-field assumption³⁰, which neglects the existing capacities of technologies especially fossil-fueled, nuclear, and biomass power plants, can be considered as a simplification, too. Additionally, reassignment of existing pipelines is not taken into account. By doing so, the cost is overestimated, since the energy system will not be constructed within a year and some portion of the existing power plant capacities will remain.

Another weakness of this approach is the lack of detail in the hydrogen pipeline modeling. Neither the pressure drop along the pipeline nor the number of compressor stations with their respective locations are taken into account in this work. Especially for long distances as well as the mountainous areas such as the Alps, pressure drop might be an important issue that has to be considered. Nevertheless, it must be noted that pressure drop estimations in the pipelines cannot

³⁰ Existing HVAC and HVDC cables as well as hydropower plants including pumped hydro storage, hydro reservoirs and run-of-river are taken into account.

be considered in the optimization without simplification since the estimation involves highly non-linear equations³¹.

Lastly, detailed modeling of biomass power would enhance the problem, since the cost varies for different biomass feedstocks such as straw, wood pellets and wood chips [185]. Biomass is not differentiated in the presented approach. Thus, as a conservative approach, the expensive biomass cost is obtained from the E-Highway study [141], since the technical potentials for two biomass sources are not explicitly available. However, it must be noted that the derivation of the technical potential of different biomass components across Europe requires a detailed analysis, which cannot be conducted within the timeframe and scope of this work.

6.7 Summary

In this section, this proposed system is explained in detail in terms of the capacities, aggregated operational parameters, hourly operation, and net transport of commodities between regions. Moreover, the results are compared against literature at a different level of detail.

The proposed European energy system consists of 842 GW of onshore wind energy, 78 GW of offshore wind energy, and 654 GW of open-field PV without tracking in terms of VRES technologies. Biomass CHP plants with a total capacity of 154 GW are utilized in addition to the assumed total capacity of 203 GW for hydropower plants, which involve pumped hydro storage, reservoirs, and run-of-river.

In terms of conversion technologies, electrolyzer, hydrogen OCGT, and hydrogen CCGT plants are installed with the proposed capacities of 258 GW, 40 GW and 94 GW, respectively. Almost all the regions have some amount of electrolyzer capacities except, "23_fr" (Paris), Belgium, Luxemburg, Switzerland, and southern Germany. Reelectrification of hydrogen is not preferred in many regions such as the Balkans, Norway, Sweden, and Switzerland. The regional full load hours of an electrolyzer, hydrogen OCGT, and hydrogen CCGT vary between 2500 to 8300 h a⁻¹, 0 to 350 h a⁻¹ and 0 to 2000 h a⁻¹, respectively. The difference between OCGT and CCGT full load hours comes from the different variable operation costs assumed for these technologies (cf. Section 3.4.5).

Storage capacities considered in this analysis play an important role in the system. Proposed capacities for salt caverns, vessels, and lithium-ion batteries are 130 TWh, 562 GWh, and 587 GWh, respectively. Considering these values, it is seen that salt caverns have a high storage capacity, yet this capacity only corresponds to 0.6% of the technical storage potential of salt caverns.

³¹ For instance the Bernoulli equation, which can be used in the estimation of pressure drop in the pipelines, involves the kinetic energy of the fluid even when the fluid is assumed to be incompressible (as the simplest approach) [32].

On average, 441 TWh a⁻¹ of energy is curtailed in the system, which corresponds to 10% of the electricity generation. When the losses caused by electrolyzers, reelectrification technologies, biomass CHP plants, and lithium-ion batteries are taken into account, it is seen that nearly 490 TWh a⁻¹ of energy dissipates during the operation of these technologies.

When different roles are defined, it is seen that the Nordic countries, as well as Ireland and the United Kingdom, are mainly exporters in terms of hydrogen and electricity owing to the cheap electricity generation at these locations. In addition to these regions, northwestern Germany and southern France are also considered as exporters. As it is expected, large demand centers such as regions containing London, Paris, and Milan are net electricity and hydrogen importers.

Finally, the system design is compared against several literature sources by means of curtailment, capacity distribution, and total capacities. It can be said that the proposed system design is in line with the existing sources.

7 Summary

In this section, a summary of the scope of the thesis, main assumptions in the methodology, key aspects of intermediate results, sensitivities of the energy system design and main findings of the proposed European system design is provided. Finally, the main conclusions are drawn from the analyses conducted within the scope of this work.

7.1 Scope and Objective

Despite the increase in the global capacities of wind and solar energy, their intermittency remains a major hurdle to address in decarbonizing the energy system. In this regard, chemical energy carriers, especially hydrogen, are considered as a solution to tackle this issue by producing it at the peak power generation periods. Future energy system design with consideration of hydrogen has been conducted at different regional fidelity. Many of these analyses are performed at a national level, and the ones modeled at a European scale do not consider the hydrogen transmission technology or seasonal storage of hydrogen. Moreover, the analyses at the European level model the system by assuming each country as one node and using a single year (at most few years) to represent the future context. The existing gap is filled by answering the research question “What is the design of a future 100% renewable European energy system with hydrogen infrastructure?”. While answering the main question, potential analyses on offshore wind energy and salt cavern storage are conducted across Europe.

7.2 Techno-Economic Potential of Offshore Wind Energy

The best aspects of existing studies on the assessment of techno-economic potential are combined to create the methodology to be used in this work. 31.5% of European maritime boundaries (1,650,000 km²) found to be eligible for offshore wind energy. The turbine designs resulting in the lowest LCOE across eligible locations are estimated among all possible turbine designs with a capacity range of 3-20 MW and a maximum rotor diameter and hub height of 280 m and 200 m, respectively. Use of these optimal turbine designs results in a capacity potential of 8.6 TW with average full load hours of 4660 h a⁻¹.

Comparison of optimal turbine designs and uniformly applied single turbine designs reveals that the average LCOE of optimal turbine designs are nearly 7 €_{ct} kWh⁻¹, whereas it increases to 10.5 €_{ct} kWh⁻¹ for the turbine design giving the highest capacity potential. In other words, although the total capacity decreases when the optimal turbine designs are used, the average LCOE in the optimal case decreases by approximately 30%. Therefore, from the economic point of view, optimal turbine designs are more beneficial due to the better utilization of resources with lower investment costs.

Finally, a method to cluster these turbine designs within an LCOE tolerance is defined. When the LCOE tolerance is set to 0.1% higher than that of optimal designs, 45 distinct turbine designs are required. Using a threshold of 1% gives a result of 9 different turbine designs. Nevertheless, which threshold or characteristics to use manipulates the turbine designs. Therefore, clustered designs are not used in the energy system design.

7.3 Technical Potential of Salt Caverns for Hydrogen Storage

Underground storage technologies have been operated successfully for decades. Compared to aquifers and depleted oil/gas fields, salt caverns are the most promising ones due to the low cushion gas requirement, flexible operation, and low permeability of the salt, the inert behavior of which prevents contamination [94], [97], [100]–[103]. Furthermore, hydrogen storage in salt caverns has been operated for decades in the United Kingdom and also in the United States.

In the present work, a Master's project was supervised to derive suitable salt formations as well as the storage capacities. Therefore, the detailed analysis of the technical potential of salt caverns can be found in the thesis of Weber [112]. A land eligibility analysis on the areas above the suitable salt formations consisting of salt domes and bedded salt is conducted. A larger cavern (750,000 m³) is used in the salt domes, whereas a small design (500,000 m³) is utilized in the bedded salt formations. Finally, by using the maximum and minimum pressure levels as well as the temperature, the amount of working gas is derived by thermodynamic assessment.

Three scenarios are defined to determine the storage capacity across Europe. Both onshore and offshore locations, only onshore locations and finally onshore locations within the 50 km distance from shore. The results show that the total potential covering both onshore and offshore locations correspond to 84.8 PWh_{H₂}, 27% of this capacity belongs to the onshore locations. A maximum distance of 50 km from the shore results in a storage capacity of 7.3 PWh_{H₂} among these onshore locations. In all cases, the largest capacity is observed in Germany. The constraint of 50 km distance results in no storage potential in France, Bosnia, and Romania. The shortest distance in Bosnia and Romania are calculated as 140 km and 340 km, respectively. In the case of France, the distance between the shore and the closest cavern is only 65 km.

7.4 Sensitivities of 100% Renewable Energy System Design

A simple definition for the system boundaries, including the region definition and technology portfolio is provided in Section 3.4. The analysis is conducted for Europe, which is broken down into 96 regions following the boundaries suggested by the E-Highway study [141]. The maximum capacities for onshore, offshore wind energy as well as open-field PV and rooftop PV are obtained by following similar workflows with slight differences. However, due to the lack of consistent data to derive biomass potential at a European level, maximum capacities for biomass CHP plants are obtained from E-Highway study [141], since the same regional scope is assumed. Before the

system design, some of the key parameters, which might have an important role in the energy system, have to be defined. Therefore, analyses on several aspects of the energy system design are performed.

While decreasing the temporal complexity of the problem by time series aggregation, it is seen that the time series data is not represented well when a few number of typical days are assumed (i.e., 5 to 20 typical days). The cost and capacities are underestimated until 30 typical days. Nevertheless, it is seen that the results do not change significantly after 30 days. Therefore, 30 typical days are decided to be used in the other sensitivity analyses in the present work.

Following this, the impact of VRES groups is examined by using equally separated percentiles of LCOE values obtained from individual placements. As one of the strengths of the present work, increasing groups are found to be more accurate in terms of capturing the time series with peak generation periods. A higher number of groups decreases the system cost; since the cheaper electricity generation locations are distinguished. Moreover, these locations also become cost-competitive with the biomass. Despite the higher accuracy and fidelity attained with more VRES groups, the number of groups is decided to be 60 for the rest of the analyses due to the increase in the solution time.

Additionally, the selection of the weather year and its importance has been analyzed by changing the weather data for VRES simulations between 1980 and 2017. Despite the availability of dispatchable electricity generation, a large variation in the designs of different weather years is observed. These variations are more pronounced in the regions with large penetration of wind and solar energies (i.e., open-field PV without tracking in France or Spain).

Using the weather year 2015 as the reference scenario, a value-of-analysis is conducted by prohibiting individual technologies. Among all the scenarios, it is seen that the value of wind energy is the largest, which is followed by trading between countries and HVAC connections. Increases in the total annual cost for these scenarios are estimated at 56.2%, 43.4%, and 31.2%, respectively. Furthermore, the increase in the total annual cost when the lithium-ion battery, offshore wind energy, vessels, and biomass are prohibited individually is less than 1%. A sensitivity analysis is performed on the cost of the electrolyzer and hydrogen pipeline. Assumption of 300 € kW⁻¹ for electrolyzer cost causes higher electrolyzer capacities with less full load hours. However, the variation in the system design is insignificant. Similarly, when the investment cost of pipelines is changed by nearly 27%, it is seen that the system design does not change. The variation in the total annual cost is only 0.2% in both cases (lower pipeline cost results in lower total annual cost). Finally, increasing market penetration for fuel cell electric vehicles is investigated between 0% to 100%. Results show that hydrogen is still utilized in the system even without an explicitly defined hydrogen demand so that it can be utilized in reelectrification technologies to generate electricity as a backup generator. Moreover, the total annual cost per unit hydrogen is lower when the market penetration is low since the existing system is used to

produce hydrogen, meaning that the surplus energy is more utilized at low penetration scenarios. However, as the additional demand requires higher capacities for electrolyzer and VRES technologies, the increase in the total annual cost per unit hydrogen is higher with increasing market penetration.

7.5 Design of European Energy System Based on 100% Renewable Energy

Application of the iterative approach suggested in Section 3.6 gives a robust system design that can ensure the security of supply among all the weather years considered in the present work. The proposed system involves 842 GW of onshore wind energy, 78 GW of offshore wind energy and 654 GW of open-field PV without tracking in terms of VRES technologies. Biomass CHP plants with a total capacity of 154 GW are utilized in addition to the assumed total capacity of 203 GW for hydropower plants, which involve pumped hydro storage, reservoirs, and run-of-river.

Besides the generation technologies, utilization of 258 GW electrolyzer, 40 GW, and 94 GW of hydrogen OCGT and CCGT technologies are proposed. It is seen that Paris, Belgium, Luxemburg, Switzerland, and southern Germany do not involve any electrolyzers; since they import hydrogen from the cheap hydrogen production regions. The full load hours of electrolyzer varies between 2500 to 8300 h a⁻¹, where the highest value is observed in Norway. When the regional capacities of hydrogen OCGT and CCGT are aggregated, it is seen that reelectrification technologies are not installed in the Balkans, Norway, Sweden, and Switzerland.

When storage technologies are examined, 130 TWh, 562 GWh and 587 GWh of storage capacities are observed for salt caverns, vessels and lithium-ion batteries, respectively. It must be noted that the deployed salt cavern capacity is nearly 0.6% of the technical potential of onshore locations. Large capacities of salt caverns are installed in northwestern Germany, the Netherlands, the United Kingdom, and central France. When the distribution of vessels is investigated, large deployment in the regions where salt caverns are not available is observed. Capacity distribution of lithium-ion batteries shows that southern regions with large open-field PV capacities experience large battery storage owing to their nature for compensating diurnal generation of PV.

Analysis of the net transport of electricity and hydrogen between regions shows that electricity and hydrogen are mainly transported from the Nordic countries as well as Ireland and the United Kingdom to continental Europe. It is seen that regions in these countries are generally net exporters for both hydrogen and electricity. Additionally, northwestern Germany and southern France are also exporters. Unsurprisingly, regions with large hydrogen and electricity demands are always net hydrogen and electricity importers.

Finally, a comparison of the proposed design with the literature shows that the results are in line with the previously reported ones. This comparison is performed for different aspects of the energy

system design. For instance, average curtailment (441 TWh a⁻¹) is compared against the reported values. It is seen that the estimated curtailment is within the minimum and maximum reported values, but closer to the lower boundary. This might be expected due to the flexibility obtained with the consideration of hydrogen in the system. When the total generation and capacity values are compared at different levels, it is seen that similar values are attained. All in all, it can be said that the model validation is conducted, and the results are in line with the literature.

7.6 Conclusion

The present work consists of three main topics, which are namely offshore wind energy, hydrogen storage in salt caverns, and 100% renewable European energy system design. A methodology is developed in order to attain a robust final energy system design in the context of 2050. Taking the key results into account, some key points must be emphasized.

Offshore wind energy:

- Optimal turbine design for offshore wind energy decreases the overall system cost, in addition to enhancing the generation potential. Therefore, low average LCOE can be attained by using the optimal designs.
- Uniform application of single turbine designs over a large regional scope, such as Europe, cannot utilize all the energy in the most efficient way. Therefore, over- or underengineering of the system is inevitable.

Underground Hydrogen Storage in Salt Caverns:

- Europe has a large storage potential in terms of hydrogen storage in salt caverns.
- This potential is mainly located at northern continental Europe, covering northern Germany. Analysis of the capacity at a national level reveals that 30% of the European countries have some potential for salt caverns.
- Considering the required storage capacities as a result of the optimization, less than 1% of the technical potential is utilized.

Energy System Design:

- The reduction of temporal resolution by time series aggregation might eliminate the extreme time periods.
- Grouping VRES technologies decreases the system cost by utilizing the cheaper electricity generation locations, which are unveiled by the grouping (cf. Figure 3-13)
- Selection of weather year plays a significant role in the energy system design, consideration of one weather year in the design is not sufficient
- Wind energy is a key technology in a 100% renewable energy system across Europe owing to the significant increase in the total annual cost when it is prohibited.

-
- The robust energy system design is based on imports from cheap electricity generation and hydrogen production locations. The transportation cost of hydrogen does not play an important role in the energy system design (approximately 1.3%)
 - Only wind or only PV regions do not exist; hybrid systems including both technologies provide a smoother generation profile.
 - The introduction of hydrogen in the energy system decreases the curtailment, as it is expected. Estimated curtailment with consideration of hydrogen is nearly 40% of the reported values. However, mainly conversion losses, as well as storage losses, compensate for the low curtailment, and the total energy dissipation in the system increases when both losses and curtailments are taken into account.
 - Due to the availability of cheap electricity generation, Ireland, the United Kingdom, Norway, and Sweden behave like a net exporter in the energy system.
 - Importance of regions from which a large pipeline passes through (conduit regions such as Denmark, northern France, southern United Kingdom) has to be emphasized once more since lack of these pipeline connections would change the system design significantly.

8 References

- [1] NASA Goddard Institute for Space Studies, “2019: GISS Surface Temperature Analysis (GISTEMP), version 4,” 2019. <https://data.giss.nasa.gov/gistemp/> (accessed Jun. 06, 2019).
- [2] N. J. L. Lenssen *et al.*, “Improvements in the GISTEMP Uncertainty Model,” *Journal of Geophysical Research: Atmospheres*, vol. 124, no. 12, pp. 6307–6326, Jun. 2019, doi: 10.1029/2018JD029522.
- [3] IPCC, *Global warming of 1.5°C. An IPCC Special Report on the impacts of global warming of 1.5°C above pre-industrial levels and related global greenhouse gas emission pathways, in the context of strengthening the global response to the threat of climate change.*, In Press., 2018.
- [4] European Environment Agency, “Annual European Union greenhouse gas inventory 1990–2017 and inventory report 2019,” Copenhagen, 2019. [Online]. Available: <https://www.eea.europa.eu/publications/european-union-greenhouse-gas-inventory-2019>.
- [5] United Nations, “Report of the Conference of the Parties, Addendum Part two: Action taken by the Conference at its twenty-first session,” 2016. [Online]. Available: <http://unfccc.int/resource/docs/2015/cop21/eng/10a01.pdf>.
- [6] European Commission, “Communication from the commission to the European Parliament, the Council, the European Economic and Social Committee and the Committee of the Region: A Roadmap for moving to a competitive low carbon economy in 2050,” 2011. [Online]. Available: <https://eur-lex.europa.eu/LexUriServ/LexUriServ.do?uri=COM:2011:0112:FIN:EN:PDF>.
- [7] IRENA, “Renewable Capacity Statistics 2019,” Abu Dhabi, 2019. [Online]. Available: <https://www.irena.org/publications/2019/Mar/Renewable-Capacity-Statistics-2019>.
- [8] M. H. Albadi and E. F. El-Saadany, “Overview of wind power intermittency impacts on power systems,” *Electric Power Systems Research*, vol. 80, no. 6, pp. 627–632, 2010.
- [9] S. Schiebahn, T. Grube, M. Robinius, V. Tietze, B. Kumar, and D. Stolten, “Power to gas: Technological overview, systems analysis and economic assessment for a case study in Germany,” *International Journal of Hydrogen Energy*, vol. 40, no. 12, pp. 4285–4294, Apr. 2015, doi: 10.1016/j.ijhydene.2015.01.123.
- [10] IRENA, “Hydrogen from renewable energy: Technology outlook for the energy transition,” Abu Dhabi, 2018. [Online]. Available: <https://www.irena.org/publications/2018/Sep/Hydrogen-from-renewable-power>.
- [11] M. Robinius *et al.*, “Linking the Power and Transport Sectors—Part 1: The Principle of Sector Coupling,” *Energies*, vol. 10, no. 7, p. 956, Jul. 2017, doi: 10.3390/en10070956.
- [12] M. Robinius *et al.*, “Linking the Power and Transport Sectors—Part 2: Modelling a Sector Coupling Scenario for Germany,” *Energies*, vol. 10, no. 7, p. 957, Jul. 2017, doi: 10.3390/en10070957.
- [13] L. Welder, D. S. Ryberg, L. Kotzur, T. Grube, M. Robinius, and D. Stolten, “Spatio-temporal

- optimization of a future energy system for power-to-hydrogen applications in Germany,” *Energy*, vol. 158, pp. 1130–1149, Sep. 2018, doi: 10.1016/j.energy.2018.05.059.
- [14] J. Michalski *et al.*, “Hydrogen generation by electrolysis and storage in salt caverns: Potentials, economics and systems aspects with regard to the German energy transition,” *International Journal of Hydrogen Energy*, vol. 42, no. 19, pp. 13427–13443, May 2017, doi: 10.1016/j.ijhydene.2017.02.102.
- [15] O. Tlili, C. Mansilla, D. Frimat, and Y. Perez, “Hydrogen market penetration feasibility assessment: Mobility and natural gas markets in the US, Europe, China and Japan,” *International Journal of Hydrogen Energy*, vol. 44, no. 31, pp. 16048–16068, Jun. 2019, doi: 10.1016/j.ijhydene.2019.04.226.
- [16] P. Colbertaldo, G. Guandalini, and S. Campanari, “Modelling the integrated power and transport energy system: The role of power-to-gas and hydrogen in long-term scenarios for Italy,” *Energy*, vol. 154, pp. 592–601, Jul. 2018, doi: 10.1016/j.energy.2018.04.089.
- [17] C. Bussar *et al.*, “Large-scale Integration of Renewable Energies and Impact on Storage Demand in a European Renewable Power System of 2050,” *Energy Procedia*, vol. 73, pp. 145–153, Jun. 2015, doi: 10.1016/j.egypro.2015.07.662.
- [18] F. Steinke, P. Wolfrum, and C. Hoffmann, “Grid vs. storage in a 100% renewable Europe,” *Renewable Energy*, vol. 50, pp. 826–832, Feb. 2013, doi: 10.1016/j.renene.2012.07.044.
- [19] P.-M. Heuser, D. S. Ryberg, T. Grube, M. Robinius, and D. Stolten, “Techno-economic analysis of a potential energy trading link between Patagonia and Japan based on CO₂ free hydrogen,” *International Journal of Hydrogen Energy*, vol. 44, no. 25, pp. 12733–12747, May 2019, doi: 10.1016/j.ijhydene.2018.12.156.
- [20] W. Zappa, M. Junginger, and M. van den Broek, “Is a 100% renewable European power system feasible by 2050?,” *Applied Energy*, vol. 233–234, pp. 1027–1050, Jan. 2019, doi: 10.1016/j.apenergy.2018.08.109.
- [21] A. Le Duigou *et al.*, “Hydrogen pathways in France: Results of the HyFrance3 Project,” *Energy Policy*, vol. 62, pp. 1562–1569, Nov. 2013, doi: 10.1016/j.enpol.2013.06.094.
- [22] D. Bogdanov and C. Breyer, “North-East Asian Super Grid for 100% renewable energy supply: Optimal mix of energy technologies for electricity, gas and heat supply options,” *Energy Conversion and Management*, vol. 112, pp. 176–190, Mar. 2016, doi: 10.1016/j.enconman.2016.01.019.
- [23] A. Gulagi, D. Bogdanov, and C. Breyer, “The role of storage technologies in energy transition pathways towards achieving a fully sustainable energy system for India,” *Journal of Energy Storage*, vol. 17, pp. 525–539, Jun. 2018, doi: 10.1016/j.est.2017.11.012.
- [24] D. Heide, L. von Bremen, M. Greiner, C. Hoffmann, M. Speckmann, and S. Bofinger, “Seasonal optimal mix of wind and solar power in a future, highly renewable Europe,” *Renewable Energy*, vol. 35, no. 11, pp. 2483–2489, Nov. 2010, doi: 10.1016/j.renene.2010.03.012.
- [25] K. Siala and M. Y. Mahfouz, “Impact of the choice of regions on energy system models,” *Energy Strategy Reviews*, vol. 25, pp. 75–85, Aug. 2019, doi: 10.1016/j.esr.2019.100362.

- [26] D. Heide, M. Greiner, L. von Bremen, and C. Hoffmann, "Reduced storage and balancing needs in a fully renewable European power system with excess wind and solar power generation," *Renewable Energy*, vol. 36, no. 9, pp. 2515–2523, Sep. 2011, doi: 10.1016/j.renene.2011.02.009.
- [27] S. Samsatli and N. J. Samsatli, "A general spatio-temporal model of energy systems with a detailed account of transport and storage," *Computers & Chemical Engineering*, vol. 80, pp. 155–176, Sep. 2015, doi: 10.1016/j.compchemeng.2015.05.019.
- [28] C. Budischak, D. Sewell, H. Thomson, L. Mach, D. E. Veron, and W. Kempton, "Cost-minimized combinations of wind power, solar power and electrochemical storage, powering the grid up to 99.9% of the time," *Journal of Power Sources*, vol. 225, pp. 60–74, Mar. 2013, doi: 10.1016/j.jpowsour.2012.09.054.
- [29] D. Bogdanov, O. Koskinen, A. Aghahosseini, and C. Breyer, "Integrated renewable energy based power system for Europe, Eurasia and MENA regions," in *2016 International Energy and Sustainability Conference (IESC)*, Jun. 2016, pp. 1–9, doi: 10.1109/IESC.2016.7569508.
- [30] B. Elliston, I. MacGill, and M. Diesendorf, "Least cost 100% renewable electricity scenarios in the Australian National Electricity Market," *Energy Policy*, vol. 59, pp. 270–282, Aug. 2013, doi: 10.1016/j.enpol.2013.03.038.
- [31] S. Samsatli, I. Staffell, and N. J. Samsatli, "Optimal design and operation of integrated wind-hydrogen-electricity networks for decarbonising the domestic transport sector in Great Britain," *International Journal of Hydrogen Energy*, vol. 41, no. 1, pp. 447–475, Jan. 2016, doi: 10.1016/j.ijhydene.2015.10.032.
- [32] R. B. Bird, W. E. Stewart, and E. N. Lightfoot, *Transport Phenomena*, 2nd Editio. Wiley, 2012.
- [33] A. Rauh and W. Seelert, "The Betz optimum efficiency for windmills," *Applied Energy*, 1984, doi: 10.1016/0306-2619(84)90037-0.
- [34] European Wind Energy Association (EWEA), "UpWind: Design limits and solutions for very large wind turbines," 2011. [Online]. Available: http://www.ewea.org/fileadmin/files/library/publications/reports/UpWind_Report.pdf.
- [35] J. F. Manwell, J. G. McGowan, and A. L. Rogers, *Wind Energy Explained: Theory, Design and Application*. Chichester, U.K.: Wiley, 2010.
- [36] T. Burton, N. Jenkins, D. Sharpe, and E. Bossanyi, *Wind Energy Handbook*. Chichester, UK: John Wiley & Sons, Ltd, 2011.
- [37] D. S. Ryberg, "Generation Lulls from the Future Potential of Wind and Solar Energy in Europe," RWTH Aachen University, 2019.
- [38] International Electrotechnical Commission (IEC), "61400-12-1: Wind turbines—Part 12-1: Power performance measurements of electricity producing wind turbines," Geneva, Switzerland, 2005. [Online]. Available: <https://webstore.iec.ch/publication/26603>.
- [39] D. S. Ryberg, D. G. Caglayan, S. Schmitt, J. Linßen, D. Stolten, and M. Robinus, "The future of European onshore wind energy potential: Detailed distribution and simulation of

- advanced turbine designs,” *Energy*, vol. 182, pp. 1222–1238, Sep. 2019, doi: 10.1016/j.energy.2019.06.052.
- [40] The Wind Power, “Wind turbines database,” 2016. https://www.thewindpower.net/store_manufacturer_turbine_en.php?id_type=4.
- [41] MHI Vestas Offshore Wind, “V164-8.0 MW® breaks world record for wind energy production.” <http://www.mhivestasoffshore.com/v164-8-0-mw-breaks-world-record-for-wind-energy-production/>.
- [42] J. Hobohm, L. Krampe, F. Peter, A. Gerken, P. Heinrich, and M. Richter, “Kostensenkungspotenziale der Offshore-Windenergie in Deutschland - Kurzfassung,” Berlin, 2013. [Online]. Available: https://www.prognos.com/uploads/tx_atwpubdb/130822_Prognos_Fichtner_Studie_Offshore-Wind_Lang_de.pdf.
- [43] C. Kost *et al.*, “Levelized Cost of Electricity - Renewable Energy Technologies,” 2013. [Online]. Available: https://www.ise.fraunhofer.de/content/dam/ise/en/documents/publications/studies/EN2018_Fraunhofer-ISE_LCOE_Renewable_Energy_Technologies.pdf.
- [44] G. Luderer *et al.*, “Assessment of wind and solar power in global low-carbon energy scenarios: An introduction,” *Energy Economics*, vol. 64, pp. 542–551, May 2017, doi: 10.1016/j.eneco.2017.03.027.
- [45] C. V. Hernández, T. Telsnig, and Anahí Villalba Pradas, “JRC Wind Energy Status Report 2016 Edition,” Luxemburg, 2017. doi: 10.2760/332535.
- [46] EWEA, “Offshore wind in Europe: Walking the tightrope to success,” 2015. [Online]. Available: <https://www.ewea.org/fileadmin/files/library/publications/reports/EY-Offshore-Wind-in-Europe.pdf>.
- [47] I. Lütkehus *et al.*, “Potenzial der Windenergie an Land: Studie zur Ermittlung des Bundesweiten Flächen-und Leistungspotenzials der Windenergienutzung an Land,” Dessau-Roßlau, 2013. doi: 004.
- [48] IRENA, “Renewable Capacity Statistics 2018,” Abu Dhabi, 2018.
- [49] GE Renewable Energy, “Haliade-X Offshore Wind Turbine Platform.” <https://www.ge.com/renewableenergy/wind-energy/offshore-wind/haliade-x-offshore-turbine>.
- [50] MHI Vestas Offshore Wind, “Vestas V164-10 MW.” <http://www.mhivestasoffshore.com/innovations/> (accessed Oct. 10, 2019).
- [51] A. Bonou, A. Laurent, and S. I. Olsen, “Life cycle assessment of onshore and offshore wind energy-from theory to application,” *Applied Energy*, vol. 180, pp. 327–337, Oct. 2016, doi: 10.1016/j.apenergy.2016.07.058.
- [52] S. Wang, S. Wang, and J. Liu, “Life-cycle green-house gas emissions of onshore and offshore wind turbines,” *Journal of Cleaner Production*, vol. 210, pp. 804–810, Feb. 2019, doi: 10.1016/j.jclepro.2018.11.031.

- [53] Y.-F. Huang, X.-J. Gan, and P.-T. Chiueh, "Life cycle assessment and net energy analysis of offshore wind power systems," *Renewable Energy*, vol. 102, pp. 98–106, Mar. 2017, doi: 10.1016/j.renene.2016.10.050.
- [54] M. Maness, B. Maples, and A. Smith, "NREL Offshore Balance-of System Model," Golden, 2017. [Online]. Available: <https://www.nrel.gov/docs/fy17osti/66874.pdf>.
- [55] L. Fingersh, M. Hand, and A. Laxson, "Wind Turbine Design Cost and Scaling Model," Golden, 2006. doi: 10.2172/897434.
- [56] T. J. Stehly, D. M. Heimiller, and G. N. Scott, "2016 Cost of Wind Energy Review," 2017. [Online]. Available: <https://www.nrel.gov/docs/fy18osti/70363.pdf>.
- [57] B. Maples, M. Hand, and W. Musial, "Comparative assessment of direct drive high temperature superconducting generators in multi-megawatt class wind turbines," Golden, 2010. [Online]. Available: <https://www.nrel.gov/docs/fy11osti/49086.pdf>.
- [58] S. Bhattacharya, *Design of Foundations for Offshore Wind Turbines*. John Wiley & Sons, 2019.
- [59] K.-Y. Oh, W. Nam, M. S. Ryu, J.-Y. Kim, and B. I. Epureanu, "A review of foundations of offshore wind energy converters: Current status and future perspectives," *Renewable and Sustainable Energy Reviews*, vol. 88, pp. 16–36, May 2018, doi: 10.1016/j.rser.2018.02.005.
- [60] D. G. Caglayan, D. S. Ryberg, H. Heinrichs, J. Linßen, D. Stolten, and M. Robinius, "The techno-economic potential of offshore wind energy with optimized future turbine designs in Europe," *Applied Energy*, vol. 255, p. 113794, Dec. 2019, doi: 10.1016/j.apenergy.2019.113794.
- [61] International Renewable Energy Agency, "Innovation Outlook: Offshore Wind," 2016. [Online]. Available: <https://www.irena.org/publications/2016/Oct/Innovation-Outlook-Offshore-Wind>.
- [62] G. Hundleby and K. Freeman, "Unleashing Europe's offshore wind potential- A new resource assessment," 2017. [Online]. Available: <https://windeurope.org/wp-content/uploads/files/about-wind/reports/Unleashing-Europes-offshore-wind-potential.pdf>.
- [63] European Environmental Agency, "Europe's Onshore and Offshore Wind Energy Potential: An Assessment of Environmental and Economic Constraints," Copenhagen, 2009. doi: 10.2800/11373.
- [64] W. Zappa and M. van den Broek, "Analysing the potential of integrating wind and solar power in Europe using spatial optimisation under various scenarios," *Renewable and Sustainable Energy Reviews*, vol. 94, pp. 1192–1216, Oct. 2018, doi: 10.1016/j.rser.2018.05.071.
- [65] D. Arent *et al.*, "Improved Offshore Wind Resource Assessment in Global Climate Stabilization Scenarios," Golden, 2012. [Online]. Available: <https://www.nrel.gov/docs/fy13osti/55049.pdf>.
- [66] J. Bosch, I. Staffell, and A. D. Hawkes, "Temporally explicit and spatially resolved global offshore wind energy potentials," *Energy*, vol. 163, pp. 766–781, Nov. 2018, doi:

- 10.1016/j.energy.2018.08.153.
- [67] I. Staffell and S. Pfenninger, "Using bias-corrected reanalysis to simulate current and future wind power output," *Energy*, vol. 114, pp. 1224–1239, Nov. 2016, doi: 10.1016/j.energy.2016.08.068.
- [68] M. M. Rienecker *et al.*, "MERRA: NASA's Modern-Era Retrospective Analysis for Research and Applications," *Journal of Climate*, vol. 24, no. 14, pp. 3624–3648, Jul. 2011, doi: 10.1175/JCLI-D-11-00015.1.
- [69] H. U. Heinrichs and P. Jochem, "Long-term impacts of battery electric vehicles on the German electricity system," *The European Physical Journal Special Topics*, vol. 225, no. 3, pp. 583–593, May 2016, doi: 10.1140/epjst/e2015-50115-x.
- [70] European Commission, "The JRC-EU-TIMES model - Assessing the long-term role of the SET Plan Energy technologies," 2013. doi: 10.2790/97596.
- [71] A. Dhakouani, F. Gardumi, E. Znouda, C. Bouden, and M. Howells, "Long-term optimisation model of the Tunisian power system," *Energy*, vol. 141, pp. 550–562, Dec. 2017, doi: 10.1016/j.energy.2017.09.093.
- [72] K. Syranidis, M. Robinius, and D. Stolten, "Control techniques and the modeling of electrical power flow across transmission networks," *Renewable and Sustainable Energy Reviews*, vol. 82, pp. 3452–3467, Feb. 2018, doi: 10.1016/j.rser.2017.10.110.
- [73] IRENA, "Renewable Power Generation Costs in 2017," Springer-Verlag, 2018. doi: 10.1007/SpringerReference_7300.
- [74] Flanders Marine Institute, "Maritime Boundaries Geodatabase, version 10." 2018, [Online]. Available: <http://www.marineregions.org/>.
- [75] D. S. Ryberg, Z. Tulemat, M. Robinius, and D. Stolten, "GLAES - Geospatial Land Availability for Energy Systems," 2017. <http://github.com/FZJ-IEK3-VSA/glaes>.
- [76] D. S. Ryberg, M. Robinius, and D. Stolten, "Evaluating Land Eligibility Constraints of Renewable Energy Sources in Europe," *Energies*, vol. 11, no. 5, p. 1246, May 2018, doi: 10.3390/en11051246.
- [77] British Oceanographic Data Centre, "The GEBCO Digital Atlas - 2014 Grid version 20141103." <http://www.gebco.net>.
- [78] Global Administrative Areas, "GADM database of Global Administrative Areas, version 2.0." 2012, [Online]. Available: www.gadm.org.
- [79] "EMODnet Human Activities, Cables, Actual Routes." 2015, [Online]. Available: <http://www.emodnet-humanactivities.eu>.
- [80] "EMODnet Human Activities: Telecom cables (schematic routes)." 2014, [Online]. Available: <http://www.emodnet-humanactivities.eu>.
- [81] WorldMap, "Natural Gas Pipelines in Europe, Asia, Africa & Middle East." https://worldmap.harvard.edu/data/geonode:natural_gas_pipelines_j96 (accessed Apr. 04, 2017).

- [82] UNEP-WCMC and IUCN., "Protected Planet: The World Database on Protected Areas (WDPA)." 2016, [Online]. Available: <https://www.protectedplanet.net/>.
- [83] B. Halpern *et al.*, "Cumulative human impacts: raw stressor data (2008 and 2013).," *KnB. Knowledge Network for Biocomplexity*, 2015, doi: 10.5063/F1S180FS.
- [84] L. Hong and B. Möller, "Offshore wind energy potential in China: Under technical, spatial and economic constraints," *Energy*, vol. 36, no. 7, pp. 4482–4491, Jul. 2011, doi: 10.1016/j.energy.2011.03.071.
- [85] S. Jay, "Planners to the rescue: Spatial planning facilitating the development of offshore wind energy," *Marine Pollution Bulletin*, vol. 60, no. 4, pp. 493–499, Apr. 2010, doi: 10.1016/j.marpolbul.2009.11.010.
- [86] L. Amaral and R. Castro, "Offshore wind farm layout optimization regarding wake effects and electrical losses," *Engineering Applications of Artificial Intelligence*, vol. 60, no. January, pp. 26–34, Apr. 2017, doi: 10.1016/j.engappai.2017.01.010.
- [87] Technical University of Denmark, "DTU Global Wind Atlas 1km resolution [Dataset]." 2015, [Online]. Available: <https://irena.masdar.ac.ae/gallery/#map/103>.
- [88] European Environmental Agency (EEA), "Corine Land Cover (CLC) 2012, Version 18.5.1 [Dataset]." 2012, [Online]. Available: <https://land.copernicus.eu/pan-european/corine-land-cover/clc-2012>.
- [89] J. Silva, C. Ribeiro, and R. Guedes, "Roughness Length Classification of Corine Land Cover Classes," 2000. <http://citeseerx.ist.psu.edu/viewdoc/download;jsessionid=5553BF237EA27088446BF89B39E2CA6E?doi=10.1.1.608.2707&rep=rep1&type=pdf> (accessed May 14, 2017).
- [90] N. G. Ejsing Jørgensen, Hans; Nielsen, Morten; Barthelmie, Rebecca Jane; Mortensen, "Modelling offshore wind resources and wind conditions," 2005, [Online]. Available: http://orbit.dtu.dk/files/107919793/Modelling_offshore_wind_resources_and_wind_conditions.pdf.
- [91] W. M. Drennan, P. K. Taylor, and M. J. Yelland, "Parameterizing the Sea Surface Roughness," *Journal of Physical Oceanography*, vol. 35, no. 5, pp. 835–848, May 2005, doi: 10.1175/JPO2704.1.
- [92] European Climate Foundation, "Roadmap 2050. A practical guide to a prosperous, low carbon Europe," 2010. doi: 10.2833/10759.
- [93] R. Wiser *et al.*, "Expert elicitation survey on future wind energy costs," *Nature Energy*, vol. 1, no. 10, p. 16135, Oct. 2016, doi: 10.1038/nenergy.2016.135.
- [94] H. Blanco and A. Faaij, "A review at the role of storage in energy systems with a focus on Power to Gas and long-term storage," *Renewable and Sustainable Energy Reviews*, vol. 81, pp. 1049–1086, Jan. 2018, doi: 10.1016/j.rser.2017.07.062.
- [95] J. P. Deane, B. P. Ó Gallachóir, and E. J. McKeogh, "Techno-economic review of existing and new pumped hydro energy storage plant," *Renewable and Sustainable Energy Reviews*, vol. 14, no. 4, pp. 1293–1302, May 2010, doi: 10.1016/j.rser.2009.11.015.

- [96] Gas Infrastructure Europe, "GIE Storage Map," *GIE Storage Map Dataset in Excel-Format*, 2016. <https://www.gie.eu/index.php/gie-publications/databases/storage-database> (accessed Jun. 11, 2017).
- [97] A. Ozarslan, "Large-scale hydrogen energy storage in salt caverns," *International Journal of Hydrogen Energy*, vol. 37, no. 19, pp. 14265–14277, Oct. 2012, doi: 10.1016/j.ijhydene.2012.07.111.
- [98] O. Kruck, F. Crotagino, R. Prelicz, and T. Rudolf, "HyUnder: Overview of all Known Underground Storage Technologies for Hydrogen," 2013. [Online]. Available: http://hyunder.eu/wp-content/uploads/2016/01/D3.1_Overview-of-all-known-underground-storage-technologies.pdf.
- [99] F. Crotagino, S. Donadei, U. Bünger, and L. H., "Large-Scale Hydrogen Underground Storage for Securing Future Energy Supplies: 18th World Hydrogen Energy Conference 2010 - WHEC 2010, May 16.-21. 2010, Essen," *Schriften des Forschungszentrums Jülich Reihe Energie & Umwelt*. Forschungszentrum IEF-3, Jülich, p. 506, 2010.
- [100] H. Landinger *et al.*, "HyUnder: Update of Benchmarking of large scale hydrogen underground storage with competing options," 2014. [Online]. Available: https://www.fch.europa.eu/sites/default/files/project_results_and_deliverables/D2.2_Benchmarking_of_large_scale_seasonal_hydrogen_underground_storage_with_competing_options_final.pdf.
- [101] T. F. Barron, "Regulatory, Technical Pressures Prompt More U.S. Salt-Cavern Gas Storage," *Oil & Gas Journal*, vol. 92, no. 37, 1994.
- [102] T. M. Letcher, *Storing energy: With special reference to renewable energy sources*. Amsterdam: Elsevier, 2016.
- [103] D. Stolten and B. Emonts, Eds., *Hydrogen Science and Engineering: Materials, Processes, Systems and Technology*, 2nd ed. Berlin: Wiley-VCH Verlag GmbH & Co. KGaA, 2016.
- [104] H. Landinger and F. Crotagino, "The role of large-scale hydrogen storage for future renewable energy utilisation," 2007, [Online]. Available: <https://www.netinform.de/GW/files/pdf/IRES-II.pdf>.
- [105] R. Tarkowski, "Perspectives of using the geological subsurface for hydrogen storage in Poland," *International Journal of Hydrogen Energy*, vol. 42, no. 1, pp. 347–355, Jan. 2017, doi: 10.1016/j.ijhydene.2016.10.136.
- [106] G. Czapowski and K. Bukowski, "Geology and resources of salt deposits in Poland: The state of the art," *Geological Quarterly*, vol. 54, no. 4, pp. 509–518, 2010, [Online]. Available: <http://internal-pdf/bkwa - Geol. Quart.pdf>.
- [107] R. Tarkowski and G. Czapowski, "Salt domes in Poland – Potential sites for hydrogen storage in caverns," *International Journal of Hydrogen Energy*, vol. 43, no. 46, pp. 21414–21427, Nov. 2018, doi: 10.1016/j.ijhydene.2018.09.212.
- [108] I. Iordache, D. Schitea, A. V Gheorghe, and M. Iordache, "Hydrogen underground storage in Romania, potential directions of development, stakeholders and general aspects," *International Journal of Hydrogen Energy*, vol. 39, no. 21, pp. 11071–11081, Jul. 2014, doi: 10.1016/j.ijhydene.2014.05.067.

- [109] J. Simón *et al.*, “HyUnder: Assessment of the Potential, the Actors and Relevant Business Cases for Large Scale and Long Term Storage of Renewable Electricity by Hydrogen Underground Storage in Europe,” 2014. [Online]. Available: http://hyunder.eu/wp-content/uploads/2016/01/D6.3_Joint-results-from-individual-case-studies.pdf.
- [110] D. Parkes, D. J. Evans, P. Williamson, and J. D. O. Williams, “Estimating available salt volume for potential CAES development: A case study using the Northwich Halite of the Cheshire Basin,” *Journal of Energy Storage*, vol. 18, pp. 50–61, Aug. 2018, doi: 10.1016/j.est.2018.04.019.
- [111] Fichtner, “Erstellung eines Entwicklungskonzeptes Energiespeicher in Niedersachsen,” 2014. [Online]. Available: <https://docplayer.org/5174810-Erstellung-eines-entwicklungskonzeptes-energiespeicher-in-niedersachsen.html>.
- [112] N. Weber, “Assessment of the Technical and Economic Potential of Salt Deposits for Hydrogen Storage,” RWTH Aachen University, 2018.
- [113] T. Velaj, “The structural style and hydrocarbon exploration of the subthrust in the Berati Anticlinal Belt, Albania,” *Journal of Petroleum Exploration and Production Technology*, vol. 5, no. 2, pp. 123–145, Jun. 2015, doi: 10.1007/s13202-015-0162-1.
- [114] A. Gillhaus, F. Crotogino, and S. Albes D. Leo v., “Compilation and Evaluation of Bedded Salt Deposits and Bedded Salt Cavern Characterisitcs Important to Successful Cavern Sealing and Abandonment,” *Solution Mining Research Insitute and KBB Underground Technologies GmbH*, vol. 2006, p. 257, 2006.
- [115] J. Ślizowski, L. Lankof, K. Urbańczyk, and K. Serbin, “Potential capacity of gas storage caverns in rock salt bedded deposits in Poland,” *Journal of Natural Gas Science and Engineering*, vol. 43, pp. 167–178, Jul. 2017, doi: 10.1016/j.jngse.2017.03.028.
- [116] F. C. Lopes, A. J. Pereira, and V. M. Mantas, “Mapping of salt structures and related fault lineaments based on remote-sensing and gravimetric data: The case of the Monte Real salt wall (onshore west-central Portugal),” *AAPG Bulletin*, vol. 96, no. 4, pp. 615–634, Apr. 2012, doi: 10.1306/08101111033.
- [117] C. Krézsek and A. W. Bally, “The Transylvanian Basin (Romania) and its relation to the Carpathian fold and thrust belt: Insights in gravitational salt tectonics,” *Marine and Petroleum Geology*, vol. 23, no. 4, pp. 405–442, May 2006, doi: 10.1016/j.marpetgeo.2006.03.003.
- [118] P. Fernandes, B. Rodrigues, M. Borges, V. Matos, and G. Clayton, “Organic maturation of the Algarve Basin (southern Portugal) and its bearing on thermal history and hydrocarbon exploration,” *Marine and Petroleum Geology*, vol. 46, pp. 210–233, Sep. 2013, doi: 10.1016/j.marpetgeo.2013.06.015.
- [119] J. I. Soto, J. F. Flinch, and G. Tari, *Permo-Triassic Salt Provinces of Europe, North Africa and the Atlantic Margins*, 1st ed. Elsevier, 2017.
- [120] F. Gutiérrez, J. M. Calaforra, F. Cardona, F. Ortí, J. J. Durán, and P. Garay, “Geological and environmental implications of the evaporite karst in Spain,” *Environmental Geology*, vol. 53, no. 5, pp. 951–965, Jan. 2008, doi: 10.1007/s00254-007-0721-y.
- [121] D. J. Evans and S. Holloway, “A review of onshore UK salt deposits and their potential for

- underground gas storage," *Geological Society, London, Special Publications*, vol. 313, no. 1, pp. 39–80, 2009, doi: 10.1144/SP313.5.
- [122] A. Gillhaus, "Underground Salt Deposits of Portugal and Spain - Geological Potential to Meet Future Demand for Natural Gas Storage?," *Solution Mining Research Institute*, p. 20, 2008, [Online]. Available: <http://internal-pdf//Gillhaus - Gillhaus Potential NG Caverns Iberia.pdf>.
- [123] M. D. Cocker, G. J. Orris, and P. Dunlap, "Geology and Undiscovered Resource Assessment of the Potash-Bearing Pripyat and Dnieper-Donets Basins, Belarus and Ukraine: Global Mineral Resource Assessment - Scientific Investigations Report 2010-5090-BB," *U.S. Geological Survey*, p. 130, 2010.
- [124] S. . Stovba and R. . Stephenson, "Style and timing of salt tectonics in the Dniepr-Donets Basin (Ukraine): implications for triggering and driving mechanisms of salt movement in sedimentary basins," *Marine and Petroleum Geology*, vol. 19, no. 10, pp. 1169–1189, Dec. 2002, doi: 10.1016/S0264-8172(03)00023-0.
- [125] Nordic CCS Competence Centre, "Geology and stratigraphy." <https://data.geus.dk/nordiccs/geology.xhtml#s2> (accessed Jun. 11, 2018).
- [126] H. Doornenbal, *Petroleum geological atlas of the southern Permian Basin Area*. Houten, the Netherlands: EAGE Publications BV, 2010.
- [127] A. Le Duigou, A.-G. Bader, J.-C. Lanoix, and L. Nadau, "Relevance and costs of large scale underground hydrogen storage in France," *International Journal of Hydrogen Energy*, vol. 42, no. 36, pp. 22987–23003, Sep. 2017, doi: 10.1016/j.ijhydene.2017.06.239.
- [128] Bundesanstalt für Geowissenschaften und Rohstoffe, "Geoviewer (InSpEE Salzstrukturen)." <https://geoviewer.bgr.de/mapapps/resources/apps/geoviewer/index.html?lang=de> (accessed Mar. 14, 2018).
- [129] K. Bukowski, "Salt Sources and Salt Springs in the Carpathian Zone: Explorations in salt archaeology in the Carpathian zone Chapter: Salt sources and salt springs in the Carpathian zone," *Archaeolingua*, p. 9, 2013, [Online]. Available: <http://internal-pdf//Rita - Harding.indb.pdf>.
- [130] D. G. Caglayan, H. U. Heinrichs, J. Linssen, M. Robinus, and D. Stolten, "Impact of different weather years on the design of hydrogen supply pathways for transport needs," *International Journal of Hydrogen Energy*, vol. 44, no. 47, pp. 25442–25456, Oct. 2019, doi: 10.1016/j.ijhydene.2019.08.032.
- [131] European Commission, "EU Reference Scenario 2016 - Energy, transport and GHG emissions - Trends to 2050," 2016. doi: 10.2833/001137.
- [132] European Commission, "Energy Roadmap 2050," 2012. doi: 10.2833/10759.
- [133] Greenpeace International, European Renewable Energy Council, and Global Wind Energy Council, "Energy [R]evolution - A Sustainable World Energy Outlook," 2012. [Online]. Available: https://www.greenpeace.de/sites/www.greenpeace.de/files/publications/greenpeace_energy-revolution_erneuerbare_2050_20150921.pdf.

- [134] European Renewable Energy Council (EREC), "Re-thinking 2050: a 100% renewable energy vision for the European Union," Brussels, 2010. [Online]. Available: <http://www.erec.org/media/publications/re-thinking-2050.html>.
- [135] S. Stemmer, "Modeling and Techno-Economic Analysis of Balancing and Storage Options in Energy Systems with a High Penetration of Renewable Energy," RWTH Aachen University, 2018.
- [136] C. Syranidou, "Investigation of the Integration of Renewable Energy Sources into the Future European Power System Using a Verified Dispatch Model with High Spatiotemporal Resolution," RWTH Aachen University, 2019.
- [137] M. G. Rasmussen, G. B. Andresen, and M. Greiner, "Storage and balancing synergies in a fully or highly renewable pan-European power system," *Energy Policy*, vol. 51, pp. 642–651, Dec. 2012, doi: 10.1016/j.enpol.2012.09.009.
- [138] T. Thien, M. Moos, R. Alvarez, H. Chen, Z. Cai, and M. Leuthold, "Storage demand in a 100% RES power system for Europe with different PV installation levels," 2013.
- [139] K. Bruninx *et al.*, "Modular Development Plan of the Pan-European Transmission System 2050 - D2.1: Data sets of scenarios for 2050," 2015. [Online]. Available: http://www.e-highway2050.eu/fileadmin/documents/Results/D2_1_Data_sets_of_scenarios_for_2050_20072015.pdf.
- [140] T. Anderski *et al.*, "Modular Development Plan of the Pan-European Transmission System 2050 - D2.2: European cluster model of the Pan-European transmission grid," 2014. [Online]. Available: http://www.e-highway2050.eu/fileadmin/documents/Results/D2_2_European_cluster_model_of_the_Pan-European_transmission_grid_20072015.pdf.
- [141] G. Sanchis, "Europe's future secure and sustainable electricity infrastructure: e-Highway2050 project results," 2015.
- [142] T. Aboumahboub, P. Tzscheuschler, and T. Hamacher, "Optimizing World-wide Utilization of Renewable Energy Sources in the Power Sector," *Renewable Energy and Power Quality Journal*, vol. 1, pp. 15–21, Apr. 2010, doi: 10.24084/repqj08.207.
- [143] C. Bussar *et al.*, "Large-scale integration of renewable energies and impact on storage demand in a European renewable power system of 2050—Sensitivity study," *Journal of Energy Storage*, vol. 6, pp. 1–10, May 2016, doi: 10.1016/j.est.2016.02.004.
- [144] M. Schlott, A. Kies, T. Brown, S. Schramm, and M. Greiner, "The impact of climate change on a cost-optimal highly renewable European electricity network," *Applied Energy*, vol. 230, pp. 1645–1659, Nov. 2018, doi: 10.1016/j.apenergy.2018.09.084.
- [145] C. Bussar *et al.*, "Optimal Allocation and Capacity of Energy Storage Systems in a Future European Power System with 100% Renewable Energy Generation," *Energy Procedia*, vol. 46, pp. 40–47, 2014, doi: 10.1016/j.egypro.2014.01.156.
- [146] F. Cebulla, T. Naegler, and M. Pohl, "Electrical energy storage in highly renewable European energy systems: capacity requirements, spatial distribution, and storage dispatch," *Journal of Energy Storage*, vol. 14, pp. 211–223, Dec. 2017, doi: 10.1016/j.est.2017.10.004.

- [147] H. C. Gils, Y. Scholz, T. Pregar, D. Luca de Tena, and D. Heide, "Integrated modelling of variable renewable energy-based power supply in Europe," *Energy*, vol. 123, pp. 173–188, Mar. 2017, doi: 10.1016/j.energy.2017.01.115.
- [148] M. Child, C. Breyer, D. Bogdanov, and H.-J. Fell, "The role of storage technologies for the transition to a 100% renewable energy system in Ukraine," *Energy Procedia*, vol. 135, pp. 410–423, Oct. 2017, doi: 10.1016/j.egypro.2017.09.513.
- [149] S. Pfenninger, "Dealing with multiple decades of hourly wind and PV time series in energy models: A comparison of methods to reduce time resolution and the planning implications of inter-annual variability," *Applied Energy*, vol. 197, pp. 1–13, Jul. 2017, doi: 10.1016/j.apenergy.2017.03.051.
- [150] R. A. Rodríguez, S. Becker, G. B. Andresen, D. Heide, and M. Greiner, "Transmission needs across a fully renewable European power system," *Renewable Energy*, vol. 63, pp. 467–476, Mar. 2014, doi: 10.1016/j.renene.2013.10.005.
- [151] L. Welder, H. Heinrichs, J. Linßen, M. Robinius, and D. Stolten, "Framework for Integrated Energy Systems Assessment (FINE)," 2018. <https://github.com/FZJ-IEK3-VSA/FINE>.
- [152] Gurobi Optimization, "Gurobi Optimizer Reference Manual, Version 5.0," www.gurobi.com. 2018, [Online]. Available: <http://www.gurobi.com>.
- [153] M. Frupp, "Switch: A Planning Tool for Power Systems with Large Shares of Intermittent Renewable Energy," *Environmental Science & Technology*, vol. 46, no. 11, pp. 6371–6378, Jun. 2012, doi: 10.1021/es204645c.
- [154] S. Ashok, "Optimised model for community-based hybrid energy system," *Renewable Energy*, vol. 32, no. 7, pp. 1155–1164, Jun. 2007, doi: 10.1016/j.renene.2006.04.008.
- [155] J. Jung and M. Villaran, "Optimal planning and design of hybrid renewable energy systems for microgrids," *Renewable and Sustainable Energy Reviews*, vol. 75, pp. 180–191, Aug. 2017, doi: 10.1016/j.rser.2016.10.061.
- [156] E. M. Nfah, J. M. Ngundam, and R. Tchinda, "Modelling of solar/diesel/battery hybrid power systems for far-north Cameroon," *Renewable Energy*, vol. 32, no. 5, pp. 832–844, Apr. 2007, doi: 10.1016/j.renene.2006.03.010.
- [157] H. Lund and B. V. Mathiesen, "Energy system analysis of 100% renewable energy systems—The case of Denmark in years 2030 and 2050," *Energy*, vol. 34, no. 5, pp. 524–531, May 2009, doi: 10.1016/j.energy.2008.04.003.
- [158] M. Haller, S. Ludig, and N. Bauer, "Decarbonization scenarios for the EU and MENA power system: Considering spatial distribution and short term dynamics of renewable generation," *Energy Policy*, vol. 47, pp. 282–290, Aug. 2012, doi: 10.1016/j.enpol.2012.04.069.
- [159] H. Dagdougui, A. Ouammi, and R. Sacile, "Modelling and control of hydrogen and energy flows in a network of green hydrogen refuelling stations powered by mixed renewable energy systems," *International Journal of Hydrogen Energy*, vol. 37, no. 6, pp. 5360–5371, Mar. 2012, doi: 10.1016/j.ijhydene.2011.07.096.
- [160] B. Pfluger and M. Wietschel, "Impact of renewable energies on conventional power generation technologies and infrastructures from a long-term least-cost perspective," in

- 2012 9th International Conference on the European Energy Market, May 2012, pp. 1–10, doi: 10.1109/EEM.2012.6254768.
- [161] Y. Scholz, “Möglichkeiten und Grenzen der Integration verschiedener regenerativer Energiequellen zu einer 100% regenerativen Stromversorgung der Bundesrepublik Deutschland bis zum Jahr 2050,” 2010. [Online]. Available: https://digital.zlb.de/viewer/rest/image/15488706/42_DZLR_Integration_Energiequellen_2050.pdf/full/max/0/42_DZLR_Integration_Energiequellen_2050.pdf.
- [162] A. Schröder, F. Kunz, J. Meiss, R. Mendelevitch, and C. von Hirschhausen, “Current and Prospective Costs of Electricity Generation until 2050,” Berlin, 2013. [Online]. Available: https://www.diw.de/documents/publikationen/73/diw_01.c.424566.de/diw_datadoc_2013-068.pdf.
- [163] Black & Veatch Corporation, “Cost report cost and performance data for power generation,” 2012. [Online]. Available: <https://www.bv.com/docs/reports-studies/nrel-cost-report.pdf>.
- [164] P. Nielsen *et al.*, “Vindmøllers Økonomi,” 2010. [Online]. Available: https://www.emd.dk/files/Vindmøllers_økonomi_EMD-Feb2010.pdf.
- [165] Desertec Industrial Initiative GmbH, “Desert Power - Perspectives on a Sustainable Power System for EUMENA,” Munich, 2012. [Online]. Available: http://www.desertec-uk.org.uk/reports/DII/DPP_2050_Study.pdf.
- [166] VGB Powertech, “Investment and Operation Cost Figures – Generation Portfolio,” Essen, 2012. [Online]. Available: https://www.vgb.org/vgbmultimedia/LCOE_Final_version_status_09_2012-p-5414.pdf.
- [167] I. Tsiropoulos, D. Tarvydas, and A. Zucker, “Cost development of low carbon energy technologies - Scenario-based cost trajectories to 2050,” Luxembourg, 2018. doi: 10.2760/490059.
- [168] S. J. Carlsson, M. del Mar Perez Fortes, G. de Marco, J. Giuntoli, M. Jakubcionis, A. Jäger-Waldau, R. Lacal-Arantequi and E. W. Lazarou, D. Magagna, C. Moles, B. Sigfusson, A. Spisto, M. Vallei, “ETRI 2014 - Energy Technology Reference Indicator projections for 2010-2050,” 2014. doi: 10.2790/057687.
- [169] S. Teske, T. Pregger, S. Simon, T. Naegler, W. Graus, and C. Lins, “Energy [R]evolution 2010—a sustainable world energy outlook,” *Energy Efficiency*, vol. 4, no. 3, pp. 409–433, Aug. 2011, doi: 10.1007/s12053-010-9098-y.
- [170] Greenpeace, “Energy [R]evolution - A sustainable World Energy Outlook 2015,” 2015.
- [171] C. Gerbaulet and C. Lorenz, “dynELMOD: A dynamic investment and dispatch model for the future European electricity market,” Berlin, 2017. [Online]. Available: <http://hdl.handle.net/10419/161634>.
- [172] I. Pineda and E. Peirano, “Modular Development Plan of the Pan-European Transmission System 2050 - D3.1 Technology Assessment from 2030 to 2050,” 2014.
- [173] C. Elberg, C. Growitsch, F. Höffler, J. Richter, and A. Wambach, “Untersuchungen zu einem zukunftsfaehigen Strommarktdesign,” Cologne, 2012. [Online]. Available: <https://www.bmw.de/Redaktion/DE/Publikationen/Energie/endbericht-untersuchungen-zu->

einem-zukunftsaehigen-strommarktdesign.pdf?__blob=publicationFile&v=7.

- [174] I. Dincer and C. Acar, "Review and evaluation of hydrogen production methods for better sustainability," *International Journal of Hydrogen Energy*, 2014, doi: 10.1016/j.ijhydene.2014.12.035.
- [175] S. M. Saba, M. Müller, M. Robinius, and D. Stolten, "The investment costs of electrolysis – A comparison of cost studies from the past 30 years," *International Journal of Hydrogen Energy*, vol. 43, no. 3, pp. 1209–1223, Jan. 2018, doi: 10.1016/j.ijhydene.2017.11.115.
- [176] Directorate-General for Energy (European Commission), "METIS Studies - The role and potential of Power-to-X in 2050," 2019. doi: 10.2833/459958.
- [177] Agora Verkehrswende, Agora Energiewende, and Frontier Economics, "The Future Cost of Electricity-Based Synthetic Fuels," 2018. [Online]. Available: https://www.agora-energiewende.de/fileadmin2/Projekte/2017/SynKost_2050/Agora_SynKost_Study_EN_W EB.pdf.
- [178] H.-M. Henning and A. Palzer, "Was kostet die Energiewende? Wege zur Transformation des deutschen Energiesystems bis 2050," Freiburg, 2015. [Online]. Available: [https://www.fraunhofer.de/content/dam/zv/de/Forschungsfelder/Energie-Rohstoffe/Fraunhofer-ISE_Transformation-Energiesystem-Deutschland_final_19_11\(1\).pdf](https://www.fraunhofer.de/content/dam/zv/de/Forschungsfelder/Energie-Rohstoffe/Fraunhofer-ISE_Transformation-Energiesystem-Deutschland_final_19_11(1).pdf).
- [179] P. Schmidt, W. Zittel, W. Weindorf, T. Rakasha, and D. Goericke, "Renewables in transport 2050 – Empowering a sustainable mobility future with zero emission fuels," 2016. doi: 10.1007/978-3-658-13255-2_15.
- [180] U. Caldera, S. Afanasyeva, D. Bogdanov, and C. Breyer, "Integration of reverse osmosis seawater desalination in the power sector, based on PV and wind energy, for the Kingdom of Saudi Arabia," 2016.
- [181] M. . Sterner, M. . Thema, F. . Eckert, T. . Lenck, and P. Götz, "Bedeutung und Notwendigkeit von Windgas für die Energiewende in Deutschland," 2015. [Online]. Available: <https://speicherinitiative.at/assets/Uploads/04-2015-FENES-EBP-GPE-Windgas-Studie.pdf>.
- [182] H. Hermann, L. Emele, and C. Loreck, "Prüfung der klimapolitischen Konsistenz und der Kosten von Methanisierungsstrategien," Berlin, 2014. [Online]. Available: <https://www.oeko.de/oekodoc/2005/2014-021-de.pdf>.
- [183] R. van Gerwen, M. Eijgelaar, and T. Bosma, "Hydrogen in the electricity value chain." DNV.GL, 2019, [Online]. Available: <https://www.dnvgl.com/publications/hydrogen-in-the-electricity-value-chain-141099>.
- [184] M. Reuß, T. Grube, M. Robinius, P. Preuster, P. Wasserscheid, and D. Stolten, "Seasonal storage and alternative carriers: A flexible hydrogen supply chain model," *Applied Energy*, vol. 200, pp. 290–302, Aug. 2017, doi: 10.1016/j.apenergy.2017.05.050.
- [185] N. Duić, N. Stefanic, Z. Lulic, G. Krajačić, T. Pukšec, and T. Novosel, "Heat Roadmap Europe: EU28 fuel prices for 2015,2030 and 2050," 2017. [Online]. Available: <https://heatroadmap.eu/wp-content/uploads/2018/12/D6.1-Future-fuel-price-review.pdf>.

- [186] M. Koch, K. Hennenberg, K. Hünecke, M. Haller, and T. Hesse, "Rolle der Bioenergie im Strom- und Wärmemarkt bis 2050 unter Einbeziehung des zukünftigen Gebäudebestandes," Freiburg, 2018. [Online]. Available: https://www.energetische-biomassenutzung.de/fileadmin/Steckbriefe/dokumente/03KB114_Bericht_Bio-Strom-Wärme.pdf.
- [187] K. Stolzenburg *et al.*, "Integration von Wind-Wasserstoff-Systemen in das Energiesystem: Abschlussbericht," Berlin, 2014. [Online]. Available: https://www.now-gmbh.de/content/1-aktuelles/1-presse/20140402-abschlussbericht-zur-integration-von-wind-wasserstoff-systemen-in-das-energiesystem-ist-veroeffentlicht/abschlussbericht_integratio_n_von_wind-wasserstoff-systemen_in_das_energiesystem.pdf.
- [188] L. Welder *et al.*, "Design and evaluation of hydrogen electricity reconversion pathways in national energy systems using spatially and temporally resolved energy system optimization," *International Journal of Hydrogen Energy*, vol. 44, no. 19, pp. 9594–9607, Apr. 2019, doi: 10.1016/j.ijhydene.2018.11.194.
- [189] J. Mischner, *Gas2Energy.net: systemplanerische Grundlagen der Gasversorgung*, 2., überar. München: DIV, Deutscher Industrieverlag, 2015.
- [190] ENTSO-E, "10-Year Network Development Plan 2012," 2012. [Online]. Available: https://eepublicdownloads.entsoe.eu/clean-documents/pre2015/SDC/TYNPD/2012/TYNPD_2012_report.pdf.
- [191] P. Elsner, M. Fishedick, and D. U. Sauer, "Energiespeicher Technologiesteckbrief zur Analyse „Flexibilitätskonzepte für die Stromversorgung 2050“,“ 2015.
- [192] D. G. Caglayan *et al.*, "Technical potential of salt caverns for hydrogen storage in Europe," *International Journal of Hydrogen Energy*, vol. 45, no. 11, pp. 6793–6805, Feb. 2020, doi: 10.1016/j.ijhydene.2019.12.161.
- [193] "European database of active faults and seismogenic SHARE." <http://www.share-eu.org/node/70> (accessed Oct. 10, 2018).
- [194] T. Wang, C. Yang, H. Ma, J. J. K. Daemen, and H. Wu, "Safety evaluation of gas storage caverns located close to a tectonic fault," *Journal of Natural Gas Science and Engineering*, vol. 23, no. Volume 21, Bundle 22, pp. 281–293, Mar. 2015, doi: 10.1016/j.jngse.2015.02.005.
- [195] Y. Wang, J. Kowal, M. Leuthold, and D. U. Sauer, "Storage System of Renewable Energy Generated Hydrogen for Chemical Industry," *Energy Procedia*, vol. 29, pp. 657–667, 2012, doi: 10.1016/j.egypro.2012.09.076.
- [196] I. H. Bell, J. Wronski, S. Quoilin, and V. Lemort, "Pure and Pseudo-pure Fluid Thermophysical Property Evaluation and the Open-Source Thermophysical Property Library CoolProp," *Industrial & Engineering Chemistry Research*, vol. 53, no. 6, pp. 2498–2508, Feb. 2014, doi: 10.1021/ie4033999.
- [197] Uniongas, "Chemical Composition of Natural Gas." <https://www.uniongas.com/about-us/about-natural-gas/chemical-composition-of-natural-gas> (accessed Sep. 09, 2018).
- [198] W. E. Hart, C. Laird, J.-P. Watson, and D. L. Woodruff, "Pyomo – Optimization Modeling in

-
- Python," *Advances in Modeling Agricultural Systems*, 2012, doi: 10.1007/978-1-4614-3226-5.
- [199] European Commission, Joint Research Centre, C. University, and C. for I. E. S. I. Network, "GHS population grid, derived from GPW4, multitemporal (1975, 1990, 2000, 2015)." 2015, [Online]. Available: http://data.jrc.ec.europa.eu/dataset/jrc-ghsl-ghs_pop_gpw4_globe_r2015a.
- [200] D. S. Ryberg, H. U. Heinrichs, M. Robinius, and D. Stolten, "RESKit - Renewable Energy Simulation toolkit for Python," 2019. <https://github.com/FZJ-IEK3-VSA/RESKit>.
- [201] G. S. California, "PV Module List - Full Data." 2018, [Online]. Available: http://www.gosolarcalifornia.ca.gov/equipment/pv_modules.php.
- [202] World Bank Group, "Global Solar Atlas [Dataset]." 2016, [Online]. Available: <https://globalsolaratlas.info/download>.
- [203] M. Gimeno-Gutiérrez and R. Lacal-Aránzategui, "Assessment of the European potential for pumped hydropower energy storage," 2013. doi: 10.2790/86815.
- [204] J. Weniger, T. Tjaden, and V. Quaschnig, "Sizing of residential PV battery systems," 2014, doi: 10.1016/j.egypro.2014.01.160.
- [205] C. Noack *et al.*, "Studie über die Planung einer Demonstrationsanlage zur Wasserstoff-Kraftstoffgewinnung durch Elektrolyse mit Zwischenspeicherung in Salzkavernen unter Druck: Ludwig Bölkow Systemtechnik GmbH (LBST), Fraunhofer Institut für Solare Energiesysteme (ISE), KBB," 2014. [Online]. Available: <https://docplayer.org/58727009-Studie-ueber-die-planung-einer-demonstrationsanlage-zur-wasserstoff-kraftstoffgewinnung-durch-elektrolyse-mit-zwischenspeicherung-in-salzkavernen.html>.

A. APPENDICES

A.1. Population Density

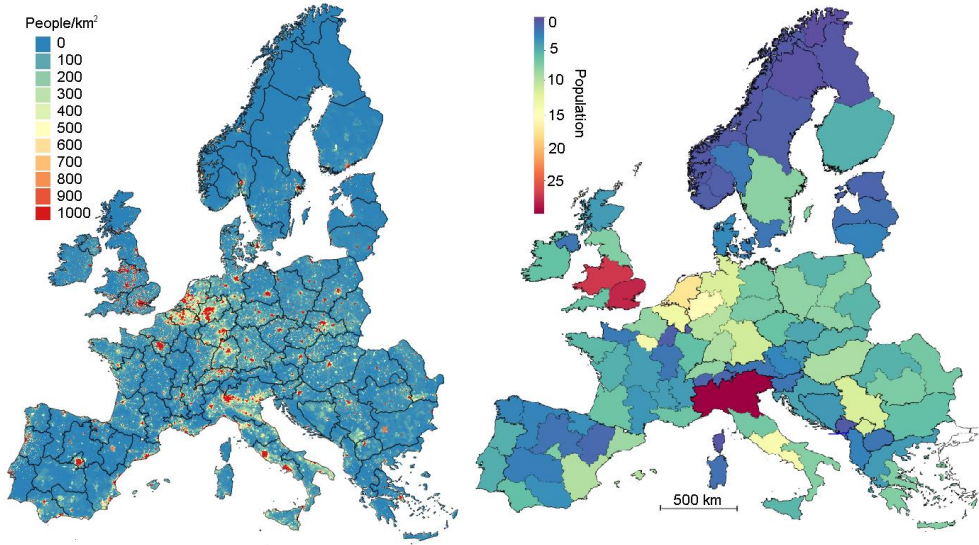


Figure A-1 Population density distribution used in the regionalization. (Left) Number of people per km², (Right) Total number of people in each region

A.2. Maximum Capacities Defined in the Scenario (VRES technologies are aggregated)

Table A-1. Maximum Capacities of Technologies Defined in the Optimization

	Maximum Capacity [GW]					Maximum Storage Capacity [GWh]		
	Rooftop PV	Biomass CHP	Onshore Wind	Offshore Wind	Open-field PV	Salt Cavern	Pumped Storage	Hydro Reservoir
01_es	4.4	0.8	122.8	43.8	370.9	0	3.5	0.0
02_es	3.7	1.8	172.6	14.4	366.8	105233	10.0	5760.0
03_es	2.4	2.8	248.1	0.0	282.6	73403	1.4	0.0
04_es	3.4	1.3	65.8	12.3	40.3	51750	0.0	0.0
05_es	1.7	2.0	170.8	0.0	299.8	346024	14.5	0.0
06_es	7.4	1.3	67.8	25.3	58.5	318177	1.5	807.4
07_es	5.4	0.3	13.2	0.0	34.1	0	0.0	0.0
08_es	3.4	1.5	223.9	0.0	661.3	0	1.9	4580.7
09_es	6.0	1.8	121.4	32.3	151.9	0	5.4	0.0
10_es	3.9	2.0	115.1	24.7	163.5	134248	0.0	0.0
11_es	9.2	2.0	215.2	96.3	444.0	228221	24.7	0.0
12_pt	7.7	1.3	120.2	38.5	430.5	204186	58.7	581.8
13_pt	6.3	1.5	162.9	74.7	486.8	172790	8.0	105.0
14_fr	8.5	3.5	236.4	53.0	415.5	0	0.0	552.9
15_fr	5.3	2.0	147.1	11.9	296.1	0	19.3	1605.6
16_fr	7.6	1.5	52.5	17.9	113.3	45941	0.0	906.8
17_fr	7.9	3.3	191.6	68.1	251.9	0	0.0	0.0
18_fr	6.5	4.0	226.4	0.0	186.9	0	0.0	70.3
19_fr	5.0	1.0	70.8	0.0	102.2	242728	0.0	140.6
20_fr	5.7	1.0	50.4	0.0	66.0	173665	27.2	1720.8
21_fr	8.2	0.8	155.3	303.9	349.2	0	0.0	0.0
22_fr	3.8	0.5	81.4	18.4	56.3	0	0.0	0.0
23_fr	10.2	1.5	21.2	0.0	8.8	0	0.0	0.0
24_fr	3.5	2.5	134.0	0.0	68.3	24542	0.0	0.0
25_fr	8.0	2.0	106.9	0.0	90.2	24079	0.0	0.0
26_fr	10.7	3.3	110.7	17.8	35.4	0	0.0	0.0
27_fr	1.5	1.3	47.7	0.0	18.0	0	3.6	0.0
28_be	16.3	4.8	19.3	4.7	93.5	0	6.2	13.8
29_lu	0.8	0.0	2.5	0.0	6.2	0	5.0	0.0
30_nl	22.4	4.0	78.3	149.7	201.6	425868	0.0	0.0
31_de	18.3	3.8	149.5	76.5	9.1	5387785	1.5	0.0

	Maximum Capacity [GW]					Maximum Storage Capacity [GWh]		
	Rooftop PV	Biomass CHP	Onshore Wind	Offshore Wind	Open-field PV	Salt Cavern	Pumped Storage	Hydro Reservoir
32_de	9.5	5.0	114.2	5.7	8.1	3544422	0.0	0.0
33_de	22.0	3.0	25.5	0.0	2.4	137863	1.4	0.4
34_de	12.4	4.5	79.3	0.0	9.9	646460	17.5	0.0
35_de	15.6	3.8	56.3	0.0	8.8	179298	3.1	0.5
36_de	14.2	3.0	52.7	0.0	5.8	323	11.7	0.0
37_de	18.5	4.8	140.3	0.0	10.4	2086	4.1	4.5
38_dk	5.1	2.5	121.1	218.3	18.7	609529	0.0	0.0
39_cz	8.6	2.8	114.1	0.0	73.0	0	0.2	441.9
40_cz	6.8	2.3	85.6	0.0	53.6	0	5.8	0.0
41_pl	11.6	2.5	202.0	0.0	209.1	1451254	0.0	8.2
42_pl	9.5	2.8	120.3	0.0	140.7	69190	0.8	3.2
43_pl	12.7	2.0	58.9	0.0	63.2	22314	3.1	27.3
44_pl	11.7	4.0	194.4	2.0	89.2	3584364	0.3	2.9
45_pl	7.5	3.0	168.9	88.7	74.6	2109328	4.1	77.5
46_sk	8.2	2.8	85.1	0.0	81.5	0	3.9	277.6
47_ch	9.0	1.0	37.9	0.0	8.1	0	77.4	349.8
48_ch	1.9	0.3	15.5	0.0	0.8	0	86.4	4681.4
49_at	3.4	0.8	37.3	0.0	8.8	0	96.6	1018.0
50_at	4.9	1.3	74.4	0.0	74.8	0	17.5	35.5
51_at	4.8	1.5	52.3	0.0	42.4	0	0.0	0.0
52_it	37.1	6.8	110.9	19.3	260.7	0	36.8	1328.3
53_it	8.6	2.8	106.2	42.5	107.2	0	0.0	71.1
54_it	15.3	1.0	68.4	83.3	173.3	0	8.3	75.7
55_it	9.5	2.5	144.5	142.6	188.5	0	0.0	172.2
56_it	5.9	1.3	82.9	144.1	75.2	0	3.7	0.0
57_si	3.5	0.8	30.1	0.0	60.1	0	0.5	1491.6
58_hu	13.8	7.3	267.5	0.0	200.6	0	0.0	48.3
59_ro	8.7	2.5	168.9	0.0	167.3	1083944	0.0	1921.0
60_ro	9.5	3.3	167.6	0.0	111.6	37078	18.6	8387.5
61_ro	10.1	3.5	226.9	96.3	81.6	0	0.0	604.8
62_hr	6.2	0.0	132.5	109.1	588.9	0	5.7	1955.8
63_ba	4.7	0.3	207.1	0.0	476.3	817397	1.6	1692.8
64_me	0.8	0.0	55.9	18.0	103.4	0	0.0	0.0
65_rs	11.7	1.0	297.0	0.0	671.4	0	4.3	424.6
66_bg	9.5	4.8	229.9	40.8	262.3	0	40.6	1964.2

	Maximum Capacity [GW]					Maximum Storage Capacity [GWh]		
	Rooftop PV	Biomass CHP	Onshore Wind	Offshore Wind	Open-field PV	Salt Cavern	Pumped Storage	Hydro Reservoir
67_mk	2.6	0.0	55.5	0.0	133.9	0	0.0	265.5
68_gr	5.1	2.0	123.0	51.2	254.1	112162	4.6	1753.4
69_gr	8.0	1.8	157.1	271.2	324.0	0	0.0	0.0
70_al	3.5	0.0	57.4	33.5	102.4	51317	0.0	1470.6
72_dk	3.2	1.3	29.7	45.4	2.5	72320	0.0	0.0
73_ee	1.7	1.0	178.4	86.1	206.5	0	0.0	0.0
74_fi	0.7	0.8	307.1	18.1	0.0	0	0.0	0.0
75_fi	6.2	3.0	768.5	176.0	0.5	0	0.0	519.0
77_it	3.4	1.8	263.1	18.2	451.4	0	11.1	23.5
78_lv	2.2	1.8	236.3	97.0	408.5	0	0.0	1472.0
79_no	1.0	0.3	89.9	451.6	21.3	0	385.5	17956.3
80_no	1.1	0.3	126.4	4.7	31.2	0	0.0	10383.7
81_no	1.2	0.0	53.9	319.2	3.0	0	6.1	22397.4
82_no	2.2	0.0	195.2	0.0	114.6	0	0.0	8711.0
83_no	0.9	0.0	82.5	274.9	0.0	0	0.0	6491.5
84_no	0.8	0.0	171.3	587.0	0.0	0	0.3	12520.2
85_no	0.1	0.0	46.1	321.8	0.0	0	0.0	961.0
86_se	0.4	0.8	209.7	16.9	0.0	0	0.0	14440.9
87_se	1.2	3.0	586.5	107.3	0.0	0	0.1	11894.0
88_se	8.2	1.3	623.1	235.3	118.5	0	158.6	2701.5
89_se	2.8	0.5	123.4	34.8	38.5	0	0.0	0.0
90_uk	24.6	4.8	97.5	82.7	18.8	0	0.0	0.0
91_uk	6.7	0.5	60.5	282.5	6.2	77056	0.0	0.0
92_uk	26.1	4.0	174.8	104.4	44.8	218466	9.7	0.0
93_uk	7.5	1.8	156.1	276.5	94.6	814618	0.0	0.0
94_uk	4.1	1.5	143.2	1212.4	69.3	0	16.9	143.7
95_uk	2.8	0.0	54.2	15.4	21.1	97024	0.0	0.0
96_ie	7.2	0.3	317.1	1138.9	124.7	0	2.5	0.0
98_it	2.2	0.5	88.0	70.4	194.0	0	13.0	46.1
99_fr	0.5	0.3	10.0	0.0	29.1	0	0.0	74.7

A.3. Model Runs Performed in Section 5

Table A-2. Definition of model runs performed in Section 5 with corresponding model run ID

	Model Run ID	Year	Onshore	Offshore	PV /out Tracking	PV / Tracking	Run-of-river	Rooftop PV	PHS	Reservoir	Biomass	SOFC	PEMFC	PEMEL	H2 OCGT	H2 CCGT	Salt Cavern	Vessel	Li-Ion Battery	Pipeline	HVAC	HVDC	Typical Days
Impact of Typical Days	1	2015	1	1	1	1	1	1	1	1	1	1	1	1	1	1	1	1	1	1	1	1	5
	2																						10
	3																						15
	4																						20
	5																						30
	6																						45
	7																						60
	8																						90
	9																						365
Impact of Grouping	10	2015	2	2	2	2	1	1	1	1	1	1	1	1	1	1	1	1	1	1	1	1	30
	11		3	3	3	3																	
	12		4	4	4	4																	
	13		5	5	5	5																	
	14		6	6	6	6																	
	15		8	8	8	8																	
	16		10	10	10	10																	
	17		12	12	12	12																	
	18		15	15	15	15																	
	19		18	18	18	18																	
	20		24	24	24	24																	
	21		30	30	30	30																	
	22		60	60	60	60																	
	22		72	72	72	72																	
23	90	90	90	90																			

A.4. National Capacity Distribution by Model Run

Table A-3. Capacity distribution for Model Run 1 (5 Typical Days)

Country	Onshore	Offshore	PV /out Tracking	PV / Tracking	Run-of-river	Rooftop PV	PHS	Reservoir	Biomass CHP	PEM Electrolyzer	H2 OCGT	H2 CCGT	Salt Cavern	Vessel	Li-ion Battery
AL	3.66	0	5.98	0	0.03	0	0	1471	0	0.59	0	0	103	0	7.81
AT	21.88	0	30.93	0	4.61	0	114.15	1054	0	3.35	0	0	0	0	10.12
BA	10.76	0	0.39	0	0.28	0	1.61	1693	0	0.91	0	0	1207	0	0
BE	9.34		55.22	0	0.08	0	6.18	13.82	0	6.21	0	0	0	0	52.47
BG	0	0	8.73	0	0.61	0	40.59	1964	0	0	0	0	0	5.75	3.4
CH	0	0	8.96	0	3.74	0	163.81	5031	0	0	0	0	0	0	0
CZ	18.55	0	28.08	0	0.41	0	5.99	442	0	0	0	0	0	0	29.23
DE	99.4	5.72	48.9	0	4.15	0	39.27	5.46	0	0	0	0	7453	0	88.32
DK	47.28	0	21.15	0	0	0	0	0	0	22.83	0	0	2559	0	4.24
EE	0	10.47	0	0	0	0	0	0	0	2.84	0	0	0	1.34	19.95
ES	51.93	0	163.14	0.23	2.27	0	63.06	11148	0	18.85	0	0	5189	5.57	239.57
FI	17.4	0	0	0	2.96	0	0	519	0	0.12	0	0	0	11.3	15.99
FR	138.17	28.04	60.2	0	6.56	0	50.15	5071	0	19.47	0	0	7071	16.57	19.17
GR	0	1.67	33.08	0	0.22	0	4.64	1753	0	4.4	0	0	318	11.62	52.47
HR	7.36	0	0	0	0.44	0	5.69	1955	0	0	0	0	0	0.01	0.04
HU	5.05	0	13.48	0	0.03	0	0	48.33	0	0	0	0	0	0.01	5.02
IE	46.41	0	0	0	0.12	0	2.54	0	0	27.94	0	0	0	0	0
IT	48.47	0	169.68	0	10.36	0	61.78	1693	0	12.25	0	0	0	118.68	163.91
LT	0	4.69	0	0	0	0	11.06	23.46	0	0	0	0	0	4.46	5.52
LU	0	0	1.21	0	0	0	5.04	0	0	0	0	0	0	0	0
LV	0	1.61	4.87	0	0.26	0	0	1472	0	0	0	0	0	2.47	1.84
ME	5.44	0	8.91	0	0	0	0	0	0	0.89	0	0	0	0	10.91
MK	0	0	3.83	0	0.29	0	0	265.54	0	0	0	0	0	1.3	0.41
NL	78.32	0	3.1	0	0	0	0	0	0	10.49	0	0	3667	0	6.67
NO	10.35	0	0	0	0.73	0	391.93	79421	0	5.49	0	0	0	7.38	0
PL	59.34	1.98	69.76	0	0.4	0	8.32	119.15	0	11.63	0	0	5125	0	91.54
PT	9.32	0	32.63	0	2.66	0	66.67	686.82	0	3.69	0	0	732	0	38.66
RO	14.27	0	8	0	0	0	18.55	10913	0	0.55	0	0	1060	3.88	0
RS	0	0	0	0	1.98	0	4.32	425	0	0	0	0	0	0	0
SE	33.44	0	3.48	0	1.88	0	158.68	29036	0	0	0	0	0	0.95	0
SI	0	0	2.57	0	0.19	0	0.54	1492	0	0	0	0	0	1.49	0.1
SK	12.38	0	0	0	1.1	0	3.94	278	0.99	0	0	0	0	0	3.16
UK	124.13	18.97	34.59	0	1.2		26.64	144	0	54.64	6.28	0	37791	0	48.74

Table A-4. Capacity distribution for Model Run 2 (10 Typical Days)

Country	Onshore	Offshore	PV /out	PV / Tracking	Run-of-river	Rooftop PV	PHS	Reservoir	Biomass CHP	PEM Electrolyzer	H2 OCGT	H2 CCGT	Salt Cavern	Vessel	Li-ion Battery
AL	3.04	0	0	7.58	0.03	0	0	1470.55	0	1.11	0	0	214.65	0.18	7.96
AT	36.91	0	0	22.81	4.61	0	114.15	1053.49	0	4.61	0	0	0	23.5	1.37
BA	8.84	0	0	3.82	0.28	0	1.61	1692.83	0	0	0	0	0.14	0.01	4.87
BE	0.66	4.72	0	21.57	0.08	0	6.18	13.82	0	0	0	0	0	15.6	7.19
BG	0	0	0	5.19	0.61	0	40.59	1964.22	0	0	0	0	0	5.43	0
CH	0	0	0	8.34	3.74	0	163.81	5031.16	0	0	0	0	0	14.24	0
CZ	18.2	0	0	24.36	0.41	0	5.99	441.86	0.35	3.06	0	0	0	17.81	31.08
DE	22.83	58.35	0	37.39	4.15	0	39.27	5.46	0	0	0	0	2672.69	55.09	14.51
DK	53.31	0	0	0.42	0	0	0	0	0	24.97	0	0	2208	0	0.09
EE	2.88	6.89	0	0	0	0	0	0	0	1.76	0	0	0	1.42	7.42
ES	36.21	0	0	195.06	2.27	0	63.06	11148.12	0	23.82	0	0	2220.95	68.31	326.26
FI	17.77	0	0	0	2.96	0	0	518.99	0	0.12	0.07	1.07	0	16.51	14
FR	155.67	27.75	0	73.47	6.56	0	50.15	5071.64	0	22.44	0	0	2918.84	115.82	69.45
GR	2.44	0	0	46.64	0.22	0	4.64	1753.4	0	7.99	0	0	314.34	24.51	96.93
HR	7.21	0	0	0	0.44	0	5.69	1955.8	0	0	0	0	0	5.21	2.82
HU	0	0	0	23.32	0.03	0	0	48.33	0	0	0	0	0	7.28	30.67
IE	10.62	0	0	8.27	0.12	0	2.54	0	0	3.72	0.48	0	0	8.76	2.97
IT	41.73	0	0	162.22	10.36	0	61.78	1693.37	0	10.82	0	0	0	148.57	147.84
LT	11.39	4.04	0	0	0	0	11.06	23.46	0	1.83	0	0	0	4.74	2.63
LU	0	0	0	2.69	0	0	5.04	0	0	0	0	0	0	1.47	0
LV	0.99	2.15	0	0	0.26	0	0	1472.02	0	0	0	0	0	2.61	2.54
ME	4.8	0	0	9.85	0	0	0	0	0	1.4	0	0	0	2.22	16.84
MK	0	0	0	4.2	0.29	0	0	265.54	0	0.38	0	0	0	0.14	0.36
NL	73.25	0	0	2.83	0	0	0	0	0	5.2	0	0	1352.73	0.02	43.74
NO	42.74	0	0	0	0.73	0	391.93	79421.13	0	16.67	0	0	0	7.15	0
PL	13.99	19.68	0	23.56	0.4	0	8.32	119.15	0	3.13	0	0	421.87	38.89	29.67
PT	12.35	0	0	8.25	2.66	0	66.67	686.82	0	0	0	0	514.16	0.16	0.02
RO	11.41	0	0	9.87	0	0	18.55	10913.39	0	0.18	0	0	15.94	16.21	0
RS	0	0	0	0	1.98	0	4.32	424.6	0	0	0	0	0	1.51	0
SE	18.13	8.26	0	0	1.88	0	158.68	29036.31	0	0	0	0	0	0.95	0
SI	0	0	0	0	0.19	0	0.54	1491.62	0	0	0	0	0	3.91	0
SK	0	0	0	0	1.1	0	3.94	277.62	2.75	0	0	0	0	4.81	0.12
UK	167.77	0	0	90.97	1.2	0	26.64	143.74	0	68.79	15.34	0.44	14295.49	67.17	78.75

Table A-5. Capacity distribution for Model Run 3 (15 Typical Days)

Country	Onshore	Offshore	PV /out	PV / Tracking	Run-of-river	Rooftop PV	PHS	Reservoir	Biomass CHP	PEM Electrolyzer	H2 OCGT	H2 CCGT	Salt Cavern	Vessel	Li-ion Battery
AL	1.03	0	0	10.16	0.03	0	0	1470.55	0	0	0	0	713.99	0.53	20.01
AT	53.31	0	0	43.13	4.61	0	114.15	1053.49	0	5.67	0	0	0	26.51	34.43
BA	0	0	0	4.07	0.28	0	1.61	1692.83	0	0	0	2.1	2939.07	0.81	0.01
BE	0	4.72	0	18.95	0.08	0	6.18	13.82	0.49	0	0	9.51	0	25.36	1.77
BG	0	1.19	0	4.25	0.61	0	40.59	1964.22	0	0	0	0	0	6.39	0.03
CH	15.53	0	0	8.96	3.74	0	163.81	5031.16	0	0	0	0	0	14.76	0
CZ	16.22	0	0	14.15	0.41	0	5.99	441.86	0	0	0	1.03	0	12.71	11.13
DE	20.92	33.08	0	41.55	4.15	0	39.27	5.46	3	0	8.55	40.6	41902.32	24.12	0.01
DK	50.92	0	0	2.45	0	0	0	0	0	30.9	0.19	0	9495.39	2.72	0.75
EE	8.22	1.25	0	0	0	0	0	0	0	2.59	0	0	0	1.89	0
ES	55.38	0	0	184.4	2.27	0	63.06	11148.12	0	16.63	0	0	4173.74	66.17	349.22
FI	22.78	0	0	0	2.96	0	0	518.99	0	2.89	0	1.9	0	18.26	9.38
FR	159.33	21.15	0	143.75	6.56	0	50.15	5071.64	0	47.2	10.8	25.13	33280.18	134.19	98.69
GR	13.05	0	0	21.78	0.22	0	4.64	1753.4	0	3.31	0	0	1265.19	12.36	40.2
HR	10.41	0	0	0	0.44	0	5.69	1955.8	0	0	0	0	0	0.08	0.53
HU	0	0	0	0.13	0.03	0	0	48.33	1.04	0	0	2.95	0	8.51	0
IE	67.01	0	0	10.12	0.12	0	2.54	0	0	54.95	0	0	0	9.32	13.71
IT	32.45	0	0	182.34	10.36	0	61.78	1693.37	0	9.45	0	0	0	144.3	266.56
LT	1.09	0	0	0	0	0	11.06	23.46	0	0	0	0	0	4.89	0.03
LU	0	0	0	6.22	0	0	5.04	0	0	0	0	0	0	1.31	0.15
LV	0	2.44	0	0	0.26	0	0	1472.02	0	0.07	0	0	0	3.31	0.14
ME	7.01	0	0	4.15	0	0	0	0	0	0	0	0	0	0.64	12.79
MK	0	0	0	3.68	0.29	0	0	265.54	0	0	0	0.72	0	0.42	2.62
NL	58.24	0	0	20.98	0	0	0	0	0	11.45	10.84	18.68	33713.23	18.76	10.99
NO	19.34	0	0	0	0.73	0	391.93	79421.13	0	6.27	0	0	0	7.85	0
PL	23.17	24.14	0	44.08	0.4	0	8.32	119.15	0	13.67	5.01	5.78	15866.55	18.54	17.35
PT	10.21	0	0	11.31	2.66	0	66.67	686.82	0	0.49	0	0	615.51	5.59	9.8
RO	8.42	1.94	0	7.38	0	0	18.55	10913.39	0	0	0	0.5	2296.55	9.94	0.03
RS	0	0	0	0	1.98	0	4.32	424.6	0	0	0	0	0	6.2	0
SE	14.37	14.1	0	0	1.88	0	158.68	29036.31	0	0	0	0	0	4.31	0.7
SI	0	0	0	9.52	0.19	0	0.54	1491.62	0	0	0	0.65	0	3.66	9.72
SK	5.84	0	0	7.15	1.1	0	3.94	277.62	2.75	0	0	2.56	0	3.64	0
UK	143.2	0	0	70.31	1.2	0	26.64	143.74	0	58.26	12.17	23.07	46794.11	102.4	33.6

Table A-6. Capacity distribution for Model Run 4 (20 Typical Days)

Country	Onshore	Offshore	PV /out	PV / Tracking	Run-of-river	Roof-top PV	PHS	Reservoir	Biomass CHP	PEM Electrolyzer	H2 OCGT	H2 CCGT	Salt Cavern	Vessel	Li-Ion Battery
AL	3.6	0	0	6.3	0.03	0	0	1470.55	0	0	0	0	267.34	0.05	9.44
AT	55.44	0	0	35.93	4.61	0	114.1	1053.49	0	6.33	0	0	0	23.01	17.36
BA	0.33	0	0	1.2	0.28	0	1.61	1692.83	0	0	0	2.16	2730.21	0.02	0
BE	0	4.72	0	25.62	0.08	0	6.18	13.82	3.58	0	0	6.39	0	25.27	2.56
BG	1.67	1.7	0	5.23	0.61	0	40.59	1964.22	0	0	0	0	0	5.7	0
CH	15.53	0	0	8.96	3.74	0	163.8	5031.16	0	0	0	0	0	13.63	0
CZ	14.36	0	0	15.87	0.41	0	5.99	441.86	2.04	0	0.01	1.73	0	10.97	3.38
DE	48.11	5.72	0	49.56	4.15	0	39.27	5.46	10.1	0	12.0	23.7	39250.8	11.78	1.5
DK	32.14	0	0	8.68	0	0	0	0	0	19.6	0.18	0	7014.59	0.01	0.12
EE	0.26	6.11	0	0	0	0	0	0	0	0.76	0	0	0	2.37	0
ES	56.32	0	0	175.1	2.27	0	63.06	11148.1	0	17.6	0	0	4640.78	53.12	312.4
FI	24.09	0	0	0	2.96	0	0	518.99	0	3.77	0.14	1.65	0	23.96	10
FR	159.6	22.7	0	130.7	6.56	0	50.15	5071.64	0	44.7	14.0	24.6	31319.6	134.7	75.74
GR	6.7	0	0	36.43	0.22	0	4.64	1753.4	0	6.2	0	0	1174.85	10.87	68.28
HR	10.04	0	0	0	0.44	0	5.69	1955.8	0	0	0	0.44	0	4.89	0
HU	1.06	0	0	0	0.03	0	0	48.33	2.5	0	0	1.88	0	12.54	0.01
IE	81.67	0	0	9.95	0.12	0	2.54	0	0	67.8	0.01	0.05	0	9.29	11.57
IT	43.32	0	0	185.1	10.3	0	61.78	1693.37	0	14.9	0	0.05	0	132.8	250.4
LT	0	5.93	0	0	0	0	11.06	23.46	0	0	0	0	0	4.66	1.2
LU	0	0	0	6.22	0	0	5.04	0	0	0	0	0	0	1.34	0.12
LV	0	2.16	0	0	0.26	0	0	1472.02	0	0.59	0	0	0	3.28	0.56
ME	6.62	0	0	3.34	0	0	0	0	0	0	0	0	0	0.45	18.95
MK	0	0	0	3.75	0.29	0	0	265.54	0	0	0	0.02	0	1.15	7.24
NL	63.32	0	0	14.76	0	0	0	0	0	18	20.0	9.08	34348.0	0.03	1.97
NO	14.6	0	0	0	0.73	0	391.9	79421.1	0	5.4	0	0	0	7.31	0
PL	15.96	23.3	0	44.4	0.4	0	8.32	119.15	0	10.5	3.9	8.69	17531.5	1.17	16.97
PT	9.6	0	0	18.81	2.66	0	66.67	686.82	0	1.76	0	0	555.76	7.56	26.3
RO	0	1.2	0	13.67	0	0	18.55	10913.3	0	0	0	0	1749.61	5.69	6.19
RS	0	0	0	0	1.98	0	4.32	424.6	0	0	0	0	0	4.73	0
SE	21.66	10.1	0	0	1.88	0	158.6	29036.3	0	0	0	0	0	1.99	2.09
SI	0	0	0	10.33	0.19	0	0.54	1491.62	0	0	0	0.1	0	3.27	7.92
SK	4.98	0	0	5.33	1.1	0	3.94	277.62	2.75	0	0	2.64	0	8.32	0.01
UK	137.9	0	0	77.21	1.2	0	26.64	143.74	0	59.0	12.0	23.3	48203.2	67.41	32.51

Table A-7. Capacity distribution for Model Run 5 (30 Typical Days)

Country	Onshore	Offshore	PV /out	PV / Tracking	Run-of-river	Rooftop PV	PHS	Reservoir	Biomass CHP	PEM Electrolyzer	H2 OCGT	H2 CCGT	Salt Cavern	Vessel	Li-ion Battery
AL	2.95	0	0	7.1	0.03	0	0	1470.55	0	0.1	0	0	201.77	0.09	15
AT	48.01	0	0	37.65	4.61	0	114.15	1053.49	0	5.83	0	0	0	18.67	19.89
BA	1.06	0	0	1.8	0.28	0	1.61	1692.83	0	0	0.36	0.39	1918.62	0.03	0
BE	0	4.72	0	16.15	0.08	0	6.18	13.82	4.75	0	0	5.25	0	25.93	3.11
BG	0	2.71	0	4.78	0.61	0	40.59	1964.22	0	0	0	0	0	5.12	0.33
CH	3.18	0	0	8.96	3.74	0	163.81	5031.16	0	0	0	0	0	14.85	0
CZ	8.68	0	0	8.12	0.41	0	5.99	441.86	3.2	0	0	0.69	0	13.37	0
DE	26.13	25.55	0	39.2	4.15	0	39.27	5.46	14.6	0	1.76	37.95	34376.03	26.72	5.05
DK	36.82	0	0	2.45	0	0	0	0	0	23.38	0	0.38	6769.03	1.7	3.5
EE	5.22	3.51	0	0	0	0	0	0	0	3.11	0	0	0	3.33	0.12
ES	55.54	0	0	191.82	2.27	0	63.06	11148.12	0	20.64	0.43	1.31	6842.95	52.22	346.41
FI	23.25	0	0	0	2.96	0	0	518.99	0	2.95	0	2.04	0	19.06	7.31
FR	159.23	25.89	0	131.71	6.56	0	50.15	5071.64	1.24	41.72	3	29.64	26257.3	141.1	75.43
GR	6.68	0	0	31.04	0.22	0	4.64	1753.4	0	5.54	0	0	1165.67	10.23	51.72
HR	7.53	0	0	0	0.44	0	5.69	1955.8	0	0	0	0	0	4.76	0
HU	0	0	0	0	0.03	0	0	48.33	5.15	0	0	0	0	7.27	0
IE	98.05	0	0	10.56	0.12	0	2.54	0	0	74.93	0.63	0	0	8.09	12.02
IT	22.09	0	0	224.88	10.36	0	61.78	1693.37	0	23.5	0	1.2	0	129.69	284.02
LT	0	2.06	0	0	0	0	11.06	23.46	0	0	0	0	0	4.91	0.05
LU	0	0	0	5.84	0	0	5.04	0	0	0	0	0	0	1.34	0.83
LV	0	2.18	0	0	0.26	0	0	1472.02	0	0	0	0	0	3.2	0.87
ME	5.65	0	0	4.9	0	0	0	0	0	0.1	0	0	0	0.44	11.3
MK	0.5	0	0	3.18	0.29	0	0	265.54	0	0	0	0	0	1.21	3.25
NL	39.04	0	0	0	0	0	0	0	4	0	0.52	19.21	18234.68	0.07	2.42
NO	18.94	0	0	0	0.73	0	391.93	79421.13	0	6.28	0	0	0	8.01	0
PL	25.32	25.82	0	42.78	0.4	0	8.32	119.15	0	15.03	0.97	12.96	14180.94	16.18	12.6
PT	9.24	0	0	15.78	2.66	0	66.67	686.82	0	1.33	0	0	708.54	5.66	24.99
RO	0.78	6.49	0	6.28	0	0	18.55	10913.39	0	0	0	0	1433.58	9.31	0.12
RS	0	0	0	0	1.98	0	4.32	424.6	0	0	0	0	0	6.3	0
SE	19.91	11.62	0	0	1.88	0	158.68	29036.31	0	0.91	0	0	0	1.99	6.47
SI	0	0	0	11.87	0.19	0	0.54	1491.62	0.09	0	0	0	0	3.14	10.35
SK	0	0	0	7.02	1.1	0	3.94	277.62	2.75	0	0	0.91	0	6.17	0
UK	125.77	0	0	70.27	1.2	0	26.64	143.74	0	55.28	8.96	25.99	43399.75	118.92	35.05

Table A-8. Capacity distribution for Model Run 6 (45 Typical Days)

Country	Onshore	Offshore	PV /out	PV / Tracking	Run-of-river	Rooftop PV	PHS	Reservoir	Biomass CHP	PEM Electrolyzer	H2 OCGT	H2 CCGT	Salt Cavern	Vessel	Li-Ion Battery
AL	2.01	0	0	8.26	0.03	0	0	1470.55	0	0.66	0	0	462.02	0.02	19.87
AT	44.69	0	0	40.87	4.61	0	114.1	1053.49	0	6.86	0	0	0	18.18	21.7
BA	0	0	0	2.52	0.28	0	1.61	1692.83	0	0	0.28	1.38	2731.65	0.01	0
BE	0	4.72	0	17.5	0.08	0	6.18	13.82	4.75	0	2.8	5.85	0	25.85	1.06
BG	0	2.89	0	5.45	0.61	0	40.59	1964.22	0	0	0	0	0	5.06	0.09
CH	7.98	0	0	8.96	3.74	0	163.8	5031.16	0	0	0	0	0	15.4	0
CZ	3.11	0	0	18.54	0.41	0	5.99	441.86	4.96	0	0	0.01	0	15.28	1.16
DE	23.97	25.9	0	34.86	4.15	0	39.27	5.46	13.3	0	1.79	37.2	34247.3	29.83	0.57
DK	35.56	0	0	8.36	0	0	0	0	0	22.8	0	0	6434.24	3.42	0.92
EE	7.92	0.36	0	0	0	0	0	0	0	2.37	0	0	0	1.88	0
ES	53.75	0	0	198.1	2.27	0	63.06	11148.1	0	22.2	0.67	0.68	6628.45	63.33	347.1
FI	22.64	0	0	0	2.96	0	0	518.99	0.13	3.07	0	1.95	0	19.79	10.54
FR	160.2	23.8	0	137.7	6.56	0	50.15	5071.64	1.92	46.0	1.16	27.2	24310.1	129.3	79.62
GR	8.09	0	0	29.77	0.22	0	4.64	1753.4	0	5.3	0	0	1086.6	10.42	46.75
HR	9.19	0	0	0	0.44	0	5.69	1955.8	0	0	0	0	0	4.94	0
HU	0	0	0	0	0.03	0	0	48.33	5.69	0	0	0	0	6.7	0
IE	68.53	0	0	5.44	0.12	0	2.54	0	0	60.1	1.31	0.24	0	13.06	4.92
IT	19.53	0	0	228.2	10.3	0	61.78	1693.37	0	23.8	0	1.47	0	130.0	310.5
LT	0	7.52	0	0	0	0	11.06	23.46	0	0.58	0	0	0	4.86	0.01
LU	0	0	0	6.22	0	0	5.04	0	0	0	0	0	0	1.33	0.01
LV	0	2.31	0	0	0.26	0	0	1472.02	0	0	0	0	0	3.2	0.01
ME	6.52	0	0	3.52	0	0	0	0	0	0.6	0	0	0	0.19	7.56
MK	0.17	0	0	2.81	0.29	0	0	265.54	0	0	0.4	0	0	0.96	3.05
NL	39.52	0	0	0	0	0	0	0	4	0.16	0.15	14.9	16051.8	0.1	1.1
NO	13.85	0	0	0	0.73	0	391.9	79421.1	0	3.54	0	0	0	7.81	0
PL	16.75	25.0	0	46.01	0.4	0	8.32	119.15	0	14.4	1.33	12.5	13974.5	16.97	12.09
PT	9.97	0	0	11.44	2.66	0	66.67	686.82	0	0.64	0	0	415.88	10.42	19.41
RO	2.51	4.32	0	9.25	0	0	18.55	10913.3	0	0	0	0	1388.43	9.81	0.85
RS	0	0	0	0	1.98	0	4.32	424.6	0	0	0	0	0	6.71	0
SE	13.95	15.1	0	0	1.88	0	158.6	29036.3	0	0.51	0	0	0	1.99	8.28
SI	0	0	0	8.09	0.19	0	0.54	1491.62	0	0	0	0	0	3.56	4.56
SK	0	0	0	2.85	1.1	0	3.94	277.62	2.75	0	0	0.36	0	4	0
UK	131.6	12.0	0	79.7	1.2	0	26.64	143.74	0	75.4	11.6	22.4	45277.4	121.0	40.28

Table A-9. Capacity distribution for Model Run 7 (60 Typical Days)

Country	Onshore	Offshore	PV /out	PV / Tracking	Run-of-river	Rooftop PV	PHS	Reservoir	Biomass CHP	PEM Electrolyzer	H2 OCGT	H2 CCGT	Salt Cavern	Vessel	Li-ion Battery
AL	2.14	0	0	8.11	0.03	0	0	1470.55	0	0.41	0	0	474.67	0.01	17.88
AT	47.05	0	0	36.69	4.61	0	114.1	1053.49	0	7.95	0	0	0	20.51	13.6
BA	0	0	0	2.93	0.28	0	1.61	1692.83	0	0	0.27	1.48	2891.87	0.01	0
BE	0	4.72	0	17.74	0.08	0	6.18	13.82	4.75	0	1.96	4.97	0	25.28	0.34
BG	2.53	1.08	0	6.86	0.61	0	40.59	1964.22	0	0	0	0	0	5.06	0.99
CH	11.35	0	0	8.96	3.74	0	163.8	5031.16	0	0	0	0	0	16.06	0
CZ	6.97	0	0	16.33	0.41	0	5.99	441.86	4	0	0	0.15	0	13.21	1.55
DE	25.59	24.7	0	34.85	4.15	0	39.27	5.46	13.7	0	1.93	43.2	39064.0	26.34	0.26
DK	37.81	0	0	2.45	0	0	0	0	0	23.9	0.12	0.03	6729.74	4.23	0.83
EE	6.16	2.16	0	0	0	0	0	0	0	2.36	0	0	0	1.99	0.11
ES	54.87	0	0	198.8	2.27	0	63.06	11148.1	0	21.0	0.5	0.02	5613.81	59.18	365.8
FI	21.57	0	0	0	2.96	0	0	518.99	0.43	2.67	0.1	1.86	0	19.85	8.03
FR	147.8	28.6	0	127.1	6.56	0	50.15	5071.64	2.9	46.3	1.37	26.4	25574.3	129.4	59.92
GR	9.07	0	0	28.03	0.22	0	4.64	1753.4	0	4.03	0	0	1056.85	10.59	45.49
HR	8.53	0	0	0.14	0.44	0	5.69	1955.8	0	0	0	0	0	1.9	0
HU	0	0	0	0	0.03	0	0	48.33	4.87	0	0	0.06	0	6.88	0
IE	80.74	0	0	0	0.12	0	2.54	0	0	67.5	1.43	0.26	0	11.82	4.73
IT	18.31	0	0	229.2	10.3	0	61.78	1693.37	0	23.4	0	1.06	0	130.0	310.1
LT	0	7.34	0	0	0	0	11.06	23.46	0	0.27	0	0	0	4.76	0
LU	0	0	0	6.22	0	0	5.04	0	0	0	0	0	0	1.32	0
LV	0	2.2	0	0	0.26	0	0	1472.02	0	0	0	0	0	3.04	0.42
ME	6.56	0	0	2.24	0	0	0	0	0	0.27	0	0	0	0.12	4.09
MK	0	0	0	2.68	0.29	0	0	265.54	0	0	0.27	0.12	0	0.41	2.42
NL	42.88	0	0	0	0	0	0	0	4	1.96	1.74	15.1	17419.5	0.03	0.38
NO	15.46	0	0	0	0.73	0	391.9	79421.1	0	4.02	0	0	0	8.21	0
PL	18.47	25.4	0	39.09	0.4	0	8.32	119.15	0	13.8	1.47	10.2	12679.7	18.53	10.64
PT	9.27	0	0	11.27	2.66	0	66.67	686.82	0	0.34	0	0	409.69	10.65	15.32
RO	3.38	5.11	0	8.74	0	0	18.55	10913.3	0	0	0	0	1442.49	9.16	0.18
RS	0	0	0	0	1.98	0	4.32	424.6	0	0	0	0	0	6.4	0
SE	20.59	11.3	0	0	1.88	0	158.6	29036.3	0	0.89	0	0	0	3.49	3.53
SI	0	0	0	6.71	0.19	0	0.54	1491.62	0	0	0	0.26	0	3	2.04
SK	0	0	0	5.43	1.1	0	3.94	277.62	2.75	0	0	1.29	0	4.09	0
UK	128.5	11.5	0	70.36	1.2	0	26.64	143.74	0	70.0	12.9	22.4	43998.4	104.2	36.53

Table A-10. Capacity distribution for Model Run 8 (90 Typical Days)

Country	Onshore	Offshore	PV /out	PV / Tracking	Run-of-river	Rooftop PV	PHS	Reservoir	Biomass CHP	PEM Electrolyzer	H2 OCGT	H2 CCGT	Salt Cavern	Vessel	Li-Ion Battery
AL	2.21	0	0	7.88	0.03	0	0	1470.55	0	0.12	0	0	205.48	0.01	13.67
AT	50.62	0	0	35.3	4.61	0	114.1	1053.49	0	9.09	0	0	0	25.44	14.97
BA	0	0	0	2.83	0.28	0	1.61	1692.83	0	0	0.65	1.32	2721.44	0	0
BE	0	4.72	0	24.14	0.08	0	6.18	13.82	4.75	0	0	4.21	0	25.81	1.24
BG	6.08	0	0	5.68	0.61	0	40.59	1964.22	0	0	0	0	0	5.03	0.58
CH	10.71	0	0	8.96	3.74	0	163.8	5031.16	0	0	0	0	0	14.09	0
CZ	11.44	0	0	13.27	0.41	0	5.99	441.86	2.67	0	0	1.41	0	12.06	1.82
DE	27.24	20.8	0	37.48	4.15	0	39.27	5.46	14.8	0	11.8	32.3	40378.7	16.67	0.87
DK	38.33	0	0	2.45	0	0	0	0	0	24.3	0.28	0	7398.95	0.05	1
EE	5.73	3.04	0	0	0	0	0	0	0	2.41	0	0	0	3.16	0
ES	55.69	0	0	200.6	2.27	0	63.06	11148.1	0	22.5	0.73	0	6132.56	67.83	369.5
FI	23.73	0	0	0	2.96	0	0	518.99	0.03	4.82	0.17	2.02	0	12.54	10.32
FR	146.4	31.2	0	119.0	6.56	0	50.15	5071.64	1.88	45.2	4.91	24.9	25489.6	136.1	60.76
GR	8.41	0	0	28.15	0.22	0	4.64	1753.4	0	3.48	0	0	1011.48	10.45	42.38
HR	8.91	0	0	1.53	0.44	0	5.69	1955.8	0	0	0	0	0	4.53	0
HU	0	0	0	0.69	0.03	0	0	48.33	3.49	0	0	0	0	7.5	0
IE	83.74	0	0	7.77	0.12	0	2.54	0	0	68.8	1.08	0.49	0	18.51	10.49
IT	16.55	0	0	228.6	10.3	0	61.78	1693.37	0.05	21.0	0	0.87	0	131.7	297.4
LT	0	6.02	0	0	0	0	11.06	23.46	0	0	0	0	0	3.72	0.9
LU	0	0	0	6.22	0	0	5.04	0	0	0	0	0	0	1.32	0
LV	0	2.03	0	0	0.26	0	0	1472.02	0	0	0	0	0	2.99	0.74
ME	7.08	0	0	2.12	0	0	0	0	0	0.54	0	0	0	0.11	5.28
MK	0	0	0	3.27	0.29	0	0	265.54	0	0	0	0	0	1.37	2.92
NL	47.47	0	0	0	0	0	0	0	4	6.43	9.22	12.3	24490	0.02	0
NO	19.92	0	0	0	0.73	0	391.9	79421.1	0	5.63	0	0	0	8.32	0
PL	23.73	24.1	0	45.31	0.4	0	8.32	119.15	0	14.9	3.84	10.5	16538.4	16.31	6.42
PT	8.57	0	0	12.63	2.66	0	66.67	686.82	0	0.79	0	0	449.79	9.06	16.83
RO	2.05	5.17	0	10.6	0	0	18.55	10913.3	0	0	0	0	1702.75	8.81	2.15
RS	0	0	0	0	1.98	0	4.32	424.6	0	0	0	0	0	6.01	0
SE	22.57	10.5	0	0	1.88	0	158.6	29036.3	0	0.17	0	0	0	7.26	1.69
SI	0	0	0	8.15	0.19	0	0.54	1491.62	0	0	0	0.01	0	3.3	7.93
SK	0	0	0	6.51	1.1	0	3.94	277.62	2.75	0	0	1.55	0	4.43	0
UK	118.4	9.72	0	63.8	1.2	0	26.64	143.74	0	61.4	11.3	23.7	43659.9	80.22	51

Table A-11. Capacity distribution for Model Run 9 (Without time series aggregation)

Country	Onshore	Offshore	PV /out	PV / Tracking	Run-of-river	Rooftop PV	PHS	Reservoir	Biomass CHP	PEM Electrolyzer	H2 OCGT	H2 CCGT	Salt Cavern	Vessel	Li-ion Battery
AL	0.44	0	0	9.1	0.03	0	0	1470.55	0	0.18	0	0	703.36	0.02	19.9
AT	56.17	0	0	30.6	4.61	0	114.1	1053.49	0	9.63	0.04	0.11	0	31.59	14.71
BA	0	0	0	4.44	0.28	0	1.61	1692.83	0	0	1.03	0.4	2775.89	0.01	0.75
BE	0	4.72	0	31.09	0.08	0	6.18	13.82	4.75	0	0	2.08	0	34.82	9.25
BG	0	0	0	8.48	0.61	0	40.59	1964.22	0	0	0	0	0	5.48	1.88
CH	4.48	0	0	8.96	3.74	0	163.8	5031.16	0	0	0	0	0	16.69	0
CZ	14.61	0	0	8.81	0.41	0	5.99	441.86	1.67	0	0.16	3.59	0	12.29	1.93
DE	14.98	29.2	0	37.39	4.15	0	39.27	5.46	14.2	0	18.8	30.8	50945.8	48.56	0.32
DK	31.98	0	0	1.21	0	0	0	0	0	19.7	0.21	0	5871.93	0.03	0.17
EE	0.65	7.22	0	0	0	0	0	0	0	2.24	0	0	0	3.27	0.03
ES	37.27	10.7	0	213.3	2.27	0	63.06	11148.1	0	28.0	1.36	0	8581.65	63.35	401.3
FI	21.17	0	0	0	2.96	0	0	518.99	0.38	3.44	0.09	2.6	0	35.64	7.08
FR	125.8	33.5	0	127.2	6.56	0	50.15	5071.64	1.36	37.6	17.8	25.8	33404.3	126	107.3
GR	8.91	0	0	29.32	0.22	0	4.64	1753.4	0	2.82	0	0	923.38	11.7	62.47
HR	10.3	0	0	0	0.44	0	5.69	1955.8	0	0	0	0	0	1.69	0.32
HU	0	0	0	10.62	0.03	0	0	48.33	3.42	0	0	0.27	0	6.42	0
IE	98.04	0	0	5.68	0.12	0	2.54	0	0	79.1	1.21	0.68	0	9.63	6.63
IT	26.46	0	0	180.1	10.3	0	61.78	1693.37	2.35	8.78	0	1.5	0	138.9	266.2
LT	2.1	5.73	0	0	0	0	11.06	23.46	0	0.19	0	0	0	4.61	0
LU	0	0	0	5.11	0	0	5.04	0	0	0	0	0	0	1.31	0
LV	0	1.99	0	0.22	0.26	0	0	1472.02	0	0.2	0	0	0	3.23	0.87
ME	7.13	0	0	2.99	0	0	0	0	0	0.65	0	0	0	0.12	4.32
MK	0	0	0	4.33	0.29	0	0	265.54	0	0	0.4	0.33	0	1.21	6.91
NL	53.36	0	0	1.52	0	0	0	0	2.31	10.1	4.94	18.2	23838.1	0.82	3.55
NO	24.05	0	0	0	0.73	0	391.9	79421.1	0	7.52	0	0	0	6.99	0
PL	22.03	19.5	0	33.51	0.4	0	8.32	119.15	0	9.74	0.49	10.2	13073.2	21.66	13.97
PT	9.8	0	0	9.77	2.66	0	66.67	686.82	0	1.07	0	0	431.76	10.33	11.24
RO	10.43	0	0	10.8	0	0	18.55	10913.3	0	0	1.57	1.16	4180.58	6.35	2.72
RS	0	0	0	0	1.98	0	4.32	424.6	0	0	0	0	0	8.07	0
SE	28.54	8.19	0	0	1.88	0	158.6	29036.3	0	1.18	0	0	0	4.59	0.25
SI	0	0	0	1.84	0.19	0	0.54	1491.62	0	0	0	0	0	4.73	2.87
SK	0	0	0	0.15	1.1	0	3.94	277.62	2.75	0	0	0.94	0	0.04	0
UK	128.2	4.06	0	67.65	1.2	0	26.64	143.74	0	62.0	14.6	21.3	41919.1	51.96	61.74

Table A-12. Capacity distribution for Model Run 10 (2 Groups per VRES technology)

Country	Onshore	Offshore	PV /out	PV / Tracking	Run-of-river	Rooftop PV	PHS	Reservoir	Biomass CHP	PEM Electrolyzer	H2 OCGT	H2 CCGT	Salt Cavern	Vessel	Li-ion Battery
AL	1.39	0	0	6.71	0.03	0	0	1470.55	0	0	0	0	97.43	0.02	14.17
AT	42.44	0	0	40.23	4.61	0	114.15	1053.49	0	8.12	0	0	0	20.63	20.63
BA	7.6	0	0	1.72	0.28	0	1.61	1692.83	0	0	0	0	859.05	0.03	6.09
BE	7.96	4.72	0	25.87	0.08	0	6.18	13.82	4.59	0	0	0	0	24.92	1.43
BG	0	0	0	5.26	0.61	0	40.59	1964.22	0	0	0	0	0	5.53	0
CH	7.82	0	0	8.96	3.74	0	163.81	5031.16	0	0	0	0	0	15.22	0
CZ	10.57	0	0	12.66	0.41	0	5.99	441.86	2.13	0	0.65	2.41	0	5.08	1.13
DE	7.66	38.34	0	39.14	4.15	0	39.27	5.46	5.59	0	34.31	16.64	47755.89	51.9	4.38
DK	36.16	0	0	1.27	0	0	0	0	0	21.9	0	0	6953.44	0.07	0.32
EE	7.24	1.06	0	0	0	0	0	0	0	2.61	0	0	0	1.75	0.52
ES	60.24	0	0	155.68	2.27	0	63.06	11148.12	0	19.01	0	0	4859.85	67.47	266.04
FI	22.45	0	0	0	2.96	0	0	518.99	0	3.59	0	1.14	0	12.05	11.08
FR	197.43	11.83	0	163.62	6.56	0	50.15	5071.64	0.01	68.23	7.31	21.5	31152.22	124.14	129.28
GR	10.98	0	0	18.59	0.22	0	4.64	1753.4	0	2.22	0	0	852.74	11.42	28.11
HR	6.03	0	0	7.19	0.44	0	5.69	1955.8	0	0	0	0	0	6.08	0
HU	0	0	0	0	0.03	0	0	48.33	1.22	0	1.56	0.24	0	5.03	0.53
IE	53.15	0	0	7.7	0.12	0	2.54	0	0	42.67	0.71	1.08	0	9.04	5.32
IT	46.58	0	0	159.5	10.36	0	61.78	1693.37	0	13.93	0.07	0	0	138.3	163.14
LT	0	2.04	0	0	0	0	11.06	23.46	0	0	0	0	0	5	0
LU	0	0	0	6.12	0	0	5.04	0	0	0	0	0	0	1.31	0
LV	0	2.37	0	0.11	0.26	0	0	1472.02	0	0	0	0	0	3.24	0.29
ME	7	0	0	4.25	0	0	0	0	0	1.1	0	0	0	0.45	13.43
MK	1.4	0	0	2.51	0.29	0	0	265.54	0	0	0	0	0	1.54	4.69
NL	41.01	0	0	0	0	0	0	0	0	7.26	7.97	19.99	28861.05	2.9	0
NO	53.81	0	0	0	0.73	0	391.93	79421.13	0	25.57	0	0	0	8.5	0
PL	19.44	24.35	0	46.69	0.4	0	8.32	119.15	0	10.39	2.36	10.82	15020.31	18.49	11.5
PT	10.38	0	0	10.14	2.66	0	66.67	686.82	0	0.96	0	0	280.37	13.46	4.05
RO	2.04	6.48	0	6.97	0	0	18.55	10913.39	0	0	0	0	1634.42	8.13	0.31
RS	0	0	0	0	1.98	0	4.32	424.6	0	0	0	0	0	6.92	0
SE	34.21	3.93	0	0	1.88	0	158.68	29036.31	0	1.97	0	0	0	4.71	2.39
SI	0.25	0	0	3.17	0.19	0	0.54	1491.62	0	0	0	0	0	4.05	3.04
SK	3.98	0	0	8.06	1.1	0	3.94	277.62	2.75	0	0	0.09	0	3.33	0.51
UK	91.86	0	0	75.23	1.2	0	26.64	143.74	0	39.31	14.13	24.98	43901.28	84.01	55.3

Table A-13. Capacity distribution for Model Run 11 (3 Groups per VRES technology)

Country	Onshore	Offshore	PV /out	PV / Tracking	Run-of-river	Rooftop PV	PHS	Reservoir	Biomass CHP	PEM Electrolyzer	H2 OCGT	H2 CCGT	Salt Cavern	Vessel	Li-ion Battery
AL	4.27	0	0	2.02	0.03	0	0	1470.55	0	0.23	0	0	559.28	0.88	0.44
AT	53.71	0	0	30.3	4.61	0	114.15	1053.49	0	15.94	0	0	0	25.67	2.47
BA	9.69	0	0	1.05	0.28	0	1.61	1692.83	0	0.91	0	0	277.45	1.09	0.16
BE	6.85	4.72	0	23.28	0.08	0	6.18	13.82	0	0	0	5.27	0	23.67	4.73
BG	0	0	0	10.76	0.61	0	40.59	1964.22	0	0	0	0	0	5.25	4.62
CH	9.18	0	0	7.84	3.74	0	163.81	5031.16	0	0	0	0	0	15.59	0
CZ	15.97	0	0	16.69	0.41	0	5.99	441.86	0	0	1.24	3.59	0	7.41	13.92
DE	25.55	24.57	0	42.5	4.15	0	39.27	5.46	0	0.5	11.21	22.64	30758.59	64.87	10.57
DK	18.61	0	0	2.91	0	0	0	0	0	8.69	2.18	0	7943.76	0.07	0.12
EE	11.55	0	0	0	0	0	0	0	0	4.43	0	0	0	8.06	1.44
ES	63.92	0	0	146.07	2.27	0	63.06	11148.12	0	15.91	0	0	3209.68	55.5	235.18
FI	21.74	0.76	0	0	2.96	0	0	518.99	0	3.93	0	1.5	0	21.56	9.72
FR	143.27	36.77	0	121.23	6.56	0	50.15	5071.64	0	50.28	3.18	8.79	18402.43	115.7	75.72
GR	12.85	0	0	19.86	0.22	0	4.64	1753.4	0	3.95	0	0	880.87	12.05	31.11
HR	4.52	0	0	5.88	0.44	0	5.69	1955.8	0	0	0	0	0	4.78	0.43
HU	0	0	0	13.82	0.03	0	0	48.33	0.42	0	0	0.55	0	6.53	19.01
IE	22.3	0	0	2.68	0.12	0	2.54	0	0	13.07	0.77	1.24	0	9.7	3.94
IT	64.08	0	0	118.01	10.36	0	61.78	1693.37	0	8.15	0	0	0	137.23	138.57
LT	11.16	0	0	0.06	0	0	11.06	23.46	0	1.86	0	0	0	5.62	0.85
LU	0	0	0	5.68	0	0	5.04	0	0	0	0	0	0	1.42	0.21
LV	1.81	0.58	0	1.5	0.26	0	0	1472.02	0	0.01	0	0	0	3.1	1.39
ME	9.73	0	0	1.58	0	0	0	0	0	4.08	0	0	0	4.21	4.89
MK	2.94	0	0	1.19	0.29	0	0	265.54	0	0	0	0	0	1.93	1.27
NL	27.85	38.64	0	1.73	0	0	0	0	0	31.54	0	11.37	16134.7	18.29	0
NO	43.08	0	0	0	0.73	0	391.93	79421.13	0	21.26	0	0	0	8.73	0
PL	20.49	1.82	0	62.07	0.4	0	8.32	119.15	0	0.66	0	14.23	14224.71	26.68	36.69
PT	10.83	0	0	10.55	2.66	0	66.67	686.82	0	0.57	0	0	160.3	10.43	3.24
RO	4.7	0	0	14.17	0	0	18.55	10913.39	0	0	0	0	1377.02	9.36	0.98
RS	1.23	0	0	0	1.98	0	4.32	424.6	0	0	0	0	0	8.02	0
SE	36.31	0	0	0	1.88	0	158.68	29036.31	0	3.4	1.16	1.69	0	15.99	1.18
SI	0.4	0	0	0	0.19	0	0.54	1491.62	0	0	0	0	0	3.78	0.09
SK	5.14	0	0	10.14	1.1	0	3.94	277.62	0.89	0	0	0	0	4.1	0.56
UK	92.41	33.05	0	49.63	1.2	0	26.64	143.74	0	61.04	2.82	14.22	24801.43	159.46	62.38

Table A-14. Capacity distribution for Model Run 12 (4 Groups per VRES technology)

Country	Onshore	Offshore	PV /out	PV / Tracking	Run-of-river	Rooftop PV	PHS	Reservoir	Biomass CHP	PEM Electrolyzer	H2 OCGT	H2 CCGT	Salt Cavern	Vessel	Li-ion Battery
AL	5.58	0	0	0	0.03	0	0	1470.55	0	0.49	0	0	559.09	0.03	1.24
AT	44.93	0	0	29.08	4.61	0	114.15	1053.49	0	14.09	0	0	0	31.26	2.4
BA	9.36	0	0	1.84	0.28	0	1.61	1692.83	0	0.44	0	0	657.18	0.29	0.41
BE	5.17	4.72	0	22.72	0.08	0	6.18	13.82	0	0	0	4.76	0	20.13	3.63
BG	0	0	0	7.38	0.61	0	40.59	1964.22	0	0	0	0	0	6.13	0.89
CH	13.25	0	0	2.16	3.74	0	163.81	5031.16	0	0	0	0	0	16.3	0
CZ	16.2	0	0	16.11	0.41	0	5.99	441.86	0	1.05	0.11	2.76	0	12.06	7.24
DE	41.1	19.76	0	41.76	4.15	0	39.27	5.46	1.42	5.13	16.75	20.78	38909.51	53.63	4.59
DK	25.78	0	0	0.67	0	0	0	0	0	14.46	1.07	0	7559.35	0.14	0.02
EE	5.4	3.93	0	0	0	0	0	0	0	3.72	0	0	0	25.14	0.8
ES	57.23	0	0	149.24	2.27	0	63.06	11148.12	0	13.76	0	0	3268.09	67.3	238.49
FI	15.77	0.63	0	0	2.96	0	0	518.99	0	1.01	0	2.37	0	21.44	9.35
FR	157.11	21.08	0	119.34	6.56	0	50.15	5071.64	0	56.77	4	13.31	23810.15	124.69	63.71
GR	13.36	0	0	11.94	0.22	0	4.64	1753.4	0	2.58	0	0	839.02	11.47	17.03
HR	5.48	0	0	4.08	0.44	0	5.69	1955.8	0	0	0	0	0	2.69	0
HU	0	0	0	13.59	0.03	0	0	48.33	0	0	0	1.54	0	6.63	4.4
IE	31.53	0	0	0.37	0.12	0	2.54	0	0	20.42	0.6	1.25	0	9.06	6.33
IT	65.28	0	0	107.25	10.36	0	61.78	1693.37	0	6.05	0	0	0	145.81	122.73
LT	12.12	0	0	0	0	0	11.06	23.46	0	2.3	0	0	0	4.89	1.26
LU	0	0	0	4.44	0	0	5.04	0	0	0	0	0	0	1.45	0
LV	1.1	1.02	0	1.58	0.26	0	0	1472.02	0	0.27	0	0	0	3.22	0.39
ME	10.25	0	0	2.64	0	0	0	0	0	3.93	0	0	0	6.07	1.95
MK	2.85	0	0	1.3	0.29	0	0	265.54	0	0	0	0	0	1.8	1.24
NL	21.11	37.6	0	0	0	0	0	0	0	19.26	0.44	13.83	14492.25	19.84	1.71
NO	39.62	0	0	0	0.73	0	391.93	79421.13	0	18.14	0	0	0	9.47	0
PL	22.72	11.39	0	41.06	0.4	0	8.32	119.15	0	7.56	1.21	7.74	14472.34	6.49	9.73
PT	12.93	0	0	16	2.66	0	66.67	686.82	0	2.96	0	0	266.96	11.52	12.32
RO	15.22	0	0	4.25	0	0	18.55	10913.39	0	0	0	0	1702.02	13.24	0.57
RS	0	0	0	0.96	1.98	0	4.32	424.6	0	0	0	0	0	5.83	0
SE	33.56	0	0	0	1.88	0	158.68	29036.31	0	1.79	0.01	2.6	0	24.14	1.06
SI	0.98	0	0	0	0.19	0	0.54	1491.62	0	0	0.16	0	0	3.92	0.02
SK	7.33	0	0	0.48	1.1	0	3.94	277.62	0	0	0	3.25	0	1.45	0.66
UK	112.95	22.07	0	19.1	1.2	0	26.64	143.74	0	58.39	11.27	13.35	28332.3	277.76	16.93

Table A-15. Capacity distribution for Model Run 13 (5 Groups per VRES technology)

Country	Onshore	Offshore	PV /out	PV / Tracking	Run-of-river	Rooftop PV	PHS	Reservoir	Biomass CHP	PEM Electrolyzer	H2 OCGT	H2 CCGT	Salt Cavern	Vessel	Li-ion Battery
AL	4.39	0	0	0.11	0.03	0	0	1470.55	0	0	0	0	511.09	0.89	2.65
AT	40.99	0	0	23.52	4.61	0	114.15	1053.49	0	11.23	0	0	0	25.77	1.45
BA	8.93	0	0	2.97	0.28	0	1.61	1692.83	0	1.57	0	0	718.44	0.01	1.93
BE	4.15	4.72	0	25.34	0.08	0	6.18	13.82	0	0	0.73	2.3	0	16.65	4.32
BG	0	0	0	6.85	0.61	0	40.59	1964.22	0	0	0	0	0	5.64	0.22
CH	14.04	0	0	2.26	3.74	0	163.81	5031.16	0	0.12	0	0	0	15.5	0
CZ	18.54	0	0	14.3	0.41	0	5.99	441.86	0	3.35	3.33	1.32	0	0.03	3.73
DE	47.17	19.75	0	38.46	4.15	0	39.27	5.46	0.94	2.94	7.5	21.1	24771.8	44.26	2.05
DK	23.99	0	0	3.27	0	0	0	0	0	14.99	3.38	0	11207.51	0.02	0.04
EE	12.09	0	0	0.86	0	0	0	0	0	4.88	0	0	0	5.93	0.76
ES	65.23	0	0	127.12	2.27	0	63.06	11148.12	0	13.07	0	0	3126.27	60.45	187.19
FI	22.54	0	0	0	2.96	0	0	518.99	0	4.36	0.16	1.01	0	17.94	10.74
FR	161.74	19	0	122.5	6.56	0	50.15	5071.64	0	56.44	6.86	13.12	24246.56	116.53	62.59
GR	17.52	0	0	11.44	0.22	0	4.64	1753.4	0	3.72	0	0	735.4	13.44	12.68
HR	5.51	0	0	5.87	0.44	0	5.69	1955.8	0	0.49	0	0	0	6.23	0.35
HU	1.41	0	0	18.38	0.03	0	0	48.33	0	0	0	1.41	0	6.5	5.01
IE	28.37	0	0	4.81	0.12	0	2.54	0	0	15.98	0.67	1.32	0	6.62	2.38
IT	56.77	0	0	126.15	10.36	0	61.78	1693.37	0	6.72	0	0	0	140.32	127
LT	9.36	0	0	0	0	0	11.06	23.46	0	1.7	0	0	0	4.36	0.02
LU	0	0	0	4.42	0	0	5.04	0	0	0	0	0	0	1.23	0
LV	0.45	1.32	0	0.78	0.26	0	0	1472.02	0	0	0	0	0	4.38	0.02
ME	8.65	0	0	3.66	0	0	0	0	0	3.75	0	0	0	2.38	3.59
MK	2.16	0	0	2.91	0.29	0	0	265.54	0	0	0	0	0	1.91	2.74
NL	33.16	31.14	0	4.87	0	0	0	0	0	21.71	3.18	9.44	15207.78	11.33	5.71
NO	43.39	0	0	0	0.73	0	391.93	79421.13	0	22.46	0	0	0	7.67	0
PL	30.61	0	0	54.92	0.4	0	8.32	119.15	0	9.36	0	11.28	16256.84	1.71	11.52
PT	12.39	0	0	13.05	2.66	0	66.67	686.82	0	1.68	0	0	263.11	11.06	7.56
RO	8.68	0	0	7.84	0	0	18.55	10913.39	0	0	0	0	1713.71	9.15	3.03
RS	0	0	0	3.18	1.98	0	4.32	424.6	0	0	0	0	0	7.01	0
SE	35.03	0	0	0	1.88	0	158.68	29036.31	0	4.09	2.08	0.07	0	9.37	1.42
SI	2.42	0	0	0	0.19	0	0.54	1491.62	0	0	0	0	0	5.63	0.56
SK	6.93	0	0	0	1.1	0	3.94	277.62	0	0	0	2.22	0	0.64	0.04
UK	110.6	21.47	0	31.34	1.2	0	26.64	143.74	0	59.49	6.82	15.51	31188.08	60	49.84

Table A-16. Capacity distribution for Model Run 14 (6 Groups per VRES technology)

Country	Onshore	Offshore	PV /out	PV / Tracking	Run-of-river	Rooftop PV	PHS	Reservoir	Biomass CHP	PEM Electrolyzer	H2 OCGT	H2 CCGT	Salt Cavern	Vessel	Li-ion Battery
AL	4.47	0	0	1.11	0.03	0	0	1470.55	0	1.03	0	0	787.91	0.51	1.46
AT	38.22	0	0	25.68	4.61	0	114.15	1053.49	0	9.71	0	0	0	25.13	2.35
BA	8.01	0	0	5.97	0.28	0	1.61	1692.83	0	1.74	0	0	647.38	0.01	0.99
BE	3.78	4.72	0	24.8	0.08	0	6.18	13.82	0	0	0	4.34	0	16.95	1.45
BG	0	0	0	7.64	0.61	0	40.59	1964.22	0	0	0	0	0	7.07	0
CH	11.72	0	0	4.3	3.74	0	163.81	5031.16	0	0	0	0	0	16.33	0
CZ	16.91	0	0	13.76	0.41	0	5.99	441.86	0	2.43	1.86	0.94	0	5.47	3.47
DE	36.12	19.7	0	43.24	4.15	0	39.27	5.46	0	0	10.39	26.18	33279.15	28.54	0.68
DK	26.5	0	0	1.14	0	0	0	0	0	15.45	3.43	0	12958.64	0.01	0.21
EE	13.08	0	0	2.1	0	0	0	0	0	5.48	0	0	0	9.28	0.24
ES	56.38	0	0	147.78	2.27	0	63.06	11148.12	0	16.91	0.22	0	3425.81	53.33	239.59
FI	22.55	0	0	0	2.96	0	0	518.99	0	4.25	0.01	1.23	0	13.42	11.32
FR	148.87	14.84	0	147.31	6.56	0	50.15	5071.64	0	49.75	13.15	8.67	28277.97	120.16	90.35
GR	19.01	0	0	9.74	0.22	0	4.64	1753.4	0	4.07	0	0	776.39	15.52	11.68
HR	5.19	0	0	5.14	0.44	0	5.69	1955.8	0	1.2	0	0	0	6.12	0.46
HU	0	0	0	15.43	0.03	0	0	48.33	0	0	0.22	0.85	0	7.63	6.98
IE	25.98	0	0	6.82	0.12	0	2.54	0	0	16.53	0.72	1.27	0	0.01	4.01
IT	53.62	0	0	127.58	10.36	0	61.78	1693.37	0	10.55	0	0	0	143.22	144.92
LT	9.54	0	0	0	0	0	11.06	23.46	0	1.45	0	0	0	4.72	4.11
LU	0	0	0	2.94	0	0	5.04	0	0	0	0	0	0	1.25	0
LV	1.92	0	0	0.25	0.26	0	0	1472.02	0	0	0	0	0	2.51	0.21
ME	8.08	0	0	3.13	0	0	0	0	0	3.47	0	0	0	0.95	2.41
MK	2.26	0	0	1.68	0.29	0	0	265.54	0	0	0	0	0	2.31	1.6
NL	27.85	34.82	0	0	0	0	0	0	0	20.96	4.69	9.8	16640.84	0.02	1.45
NO	44.66	0	0	0	0.73	0	391.93	79421.13	0	24.43	0	0	0	8.4	0
PL	32.98	0	0	64.35	0.4	0	8.32	119.15	0	10.34	0.04	9.73	13566.03	6.04	17.96
PT	14.83	0	0	15.17	2.66	0	66.67	686.82	0	1.94	0	0	491.97	4.39	2.58
RO	10.88	0	0	7.89	0	0	18.55	10913.39	0	0	0	0	1420.58	9.58	3.08
RS	0.58	0	0	1.41	1.98	0	4.32	424.6	0	0	0	0	0	6.36	0
SE	36.67	0	0	0	1.88	0	158.68	29036.31	0	5.23	2.39	0	0	1.72	0.47
SI	4.48	0	0	0	0.19	0	0.54	1491.62	0	0	0	0	0	5.21	0.13
SK	6.29	0	0	0.4	1.1	0	3.94	277.62	0.47	0	0	2.29	0	4.11	0
UK	102.77	22.18	0	26.01	1.2	0	26.64	143.74	0	57.58	0.73	16.84	29854.05	32.75	40.64

Table A-17. Capacity distribution for Model Run 15 (10 Groups per VRES technology)

Country	Onshore	Offshore	PV /out	PV / Tracking	Run-of-river	Rooftop PV	PHS	Reservoir	Biomass CHP	PEM Electrolyzer	H2 OCGT	H2 CCGT	Salt Cavern	Vessel	Li-ion Battery
AL	5.33	0	0	0	0.03	0	0	1470.55	0	1.32	0	0	244.7	0.01	0.32
AT	39.16	0	0	25.37	4.61	0	114.15	1053.49	0	10.93	2.33	0	0	0.09	12.13
BA	13.59	0	0	0	0.28	0	1.61	1692.83	0	5.09	0	0	2018.94	0.01	0.01
BE	4.15	4.72	0	21.15	0.08	0	6.18	13.82	0	0	0.15	2.27	0	0	2.46
BG	0	0	0	7.35	0.61	0	40.59	1964.22	0	0	0	0	0	7.4	0.93
CH	8.63	0	0	1.94	3.74	0	163.81	5031.16	0	0	0	0	0	0.76	0
CZ	18.17	0	0	17.97	0.41	0	5.99	441.86	0	3.87	0.02	3.16	0	0.01	7.47
DE	38.35	25.35	0	33.72	4.15	0	39.27	5.46	2.65	0	7.4	21.88	22041.07	0.01	1.74
DK	17.58	0	0	0	0	0	0	0	0	10.12	0.14	1.09	6189.73	0	0
EE	11.05	0	0	0	0	0	0	0	0	4.58	0	0	0	1.58	0
ES	53.86	0	0	147.08	2.27	0	63.06	11148.12	0	15.63	9.88	3.28	10489.77	41.72	218.58
FI	19.27	0	0	0	2.96	0	0	518.99	0	3.3	0.16	1.14	0	17.42	10.16
FR	158.86	9.91	0	104.75	6.56	0	50.15	5071.64	0	45.07	7.4	26.03	26050.62	40.88	78.08
GR	16.6	0	0	7.3	0.22	0	4.64	1753.4	0	2.76	0	0	534.68	14.16	1.14
HR	5.75	0	0	5.59	0.44	0	5.69	1955.8	0	1.31	0	0	0	4.29	0.15
HU	0	0	0	15.33	0.03	0	0	48.33	0	0	0	1.19	0	3.13	1.59
IE	32.35	0	0	4	0.12	0	2.54	0	0	21.51	0.96	1.01	0	5.94	3.5
IT	49.63	0	0	119.15	10.36	0	61.78	1693.37	0	6.94	1.46	2.42	0	103.75	110.55
LT	11.23	0	0	0	0	0	11.06	23.46	0	1.95	0	0	0	4.46	0
LU	0	0	0	4.06	0	0	5.04	0	0	0	0	0	0	0	0
LV	2.41	0	0	0	0.26	0	0	1472.02	0	0	0	0	0	2.68	0
ME	5.81	0	0	1.56	0	0	0	0	0	1.63	0	0	0	1.85	0.01
MK	2.23	0	0	2.15	0.29	0	0	265.54	0	0	0	0	0	2.13	2.73
NL	25.16	26.69	0	0	0	0	0	0	0	10.32	3.77	17.19	16817.3	0	3.31
NO	58.36	0	0	0	0.73	0	391.93	79421.13	0	31.4	0	0	0	7.58	0
PL	41.77	0.71	0	35.53	0.4	0	8.32	119.15	0	13.1	0.22	11.62	19107.19	0.01	18.33
PT	12.32	0	0	13.69	2.66	0	66.67	686.82	0	1.5	0.24	0	441.77	9.29	15.43
RO	11.6	0	0	3.42	0	0	18.55	10913.39	0	0	0	0	1553.37	5.85	1.04
RS	0	0	0	3.57	1.98	0	4.32	424.6	0	0	0	0	0	5.51	0
SE	35.5	0	0	0	1.88	0	158.68	29036.31	0	4.89	0.14	1.21	0	1.29	0
SI	3	0	0	0	0.19	0	0.54	1491.62	0	0	0.03	0.98	0	0.03	0.38
SK	8.95	0	0	0	1.1	0	3.94	277.62	0	0.53	0.15	3.16	0	0.03	0
UK	135.45	8.53	0	16.95	1.2	0	26.64	143.74	0	61.58	11.56	21.12	37838.52	5.79	17.5

Table A-18. Capacity distribution for Model Run 16 (10 Groups per VRES technology)

Country	Onshore	Offshore	PV /out	PV / Tracking	Run-of-river	Rooftop PV	PHS	Reservoir	Biomass CHP	PEM Electrolyzer	H2 OCGT	H2 CCGT	Salt Cavern	Vessel	Li-ion Battery
AL	5.08	0	0	0	0.03	0	0	1470.55	0	0.98	0	0	216.59	0.99	0.2
AT	38.61	0	0	27.22	4.61	0	114.15	1053.49	0	11.21	0.64	0.47	0	10.34	15.8
BA	16.4	0	0	2.91	0.28	0	1.61	1692.83	0	7.22	0	0	1740.93	11.55	0.85
BE	3.46	4.72	0	22.28	0.08	0	6.18	13.82	0	0	0	2.87	0	4.67	10.21
BG	0	0	0	6.69	0.61	0	40.59	1964.22	0	0	0	0	0	5.73	0.15
CH	8.5	0	0	1.58	3.74	0	163.81	5031.16	0	0	0	0	0	13.36	0
CZ	19.66	0	0	16.24	0.41	0	5.99	441.86	0	4.2	0	2.27	0	7.25	8.9
DE	40.81	21.99	0	33.02	4.15	0	39.27	5.46	0	0	5.81	30.34	26219.45	9.89	1.79
DK	23.57	0	0	0.46	0	0	0	0	0	14.27	0.17	1.19	7213.22	0.01	0.01
EE	12.74	0	0	0	0	0	0	0	0	5.46	0	0	0	1.7	0
ES	54.19	0	0	169.11	2.27	0	63.06	11148.12	0	18.46	8.42	0.44	6262.46	70.64	280.58
FI	20.36	0	0	0	2.96	0	0	518.99	0	4.16	1.01	1.18	0	32.27	8.68
FR	149.05	14.01	0	115.76	6.56	0	50.15	5071.64	0	47.64	3.11	22.15	20961.71	115.6	95.38
GR	17.08	0	0	3.87	0.22	0	4.64	1753.4	0	2.44	0	0	488.02	17.45	1.01
HR	5.97	0	0	4.88	0.44	0	5.69	1955.8	0	1.49	0	0	0	4.62	0.09
HU	0	0	0	18.14	0.03	0	0	48.33	0	0	0	1.47	0	8.71	4.89
IE	26.93	0	0	3.63	0.12	0	2.54	0	0	19.03	1.28	0.68	0	8.54	2.73
IT	50.33	0	0	124.59	10.36	0	61.78	1693.37	0	8.53	0.07	3.05	0	125.64	124.87
LT	11.8	0	0	0	0	0	11.06	23.46	0	2.49	0	0	0	4.66	0
LU	0	0	0	2.3	0	0	5.04	0	0	0	0	0	0	0.94	0
LV	2.55	0	0	0	0.26	0	0	1472.02	0	0.15	0	0	0	2.85	0
ME	4.85	0	0	2.75	0	0	0	0	0	1.16	0	0	0	2.21	0.34
MK	3.22	0	0	0.12	0.29	0	0	265.54	0	0	0	0	0	1.76	2.25
NL	21.11	27.61	0	0	0	0	0	0	0	11.72	2.88	18.53	17711.07	0	11.65
NO	56.15	0	0	0	0.73	0	391.93	79421.13	0	30.23	0	0	0	8.26	0
PL	38.01	4.75	0	35.7	0.4	0	8.32	119.15	0	14.06	1.21	9.24	16131	0.98	20.29
PT	16.95	0	0	15.44	2.66	0	66.67	686.82	0	4.38	0.01	0	399.42	7.93	15.02
RO	13.38	0	0	0.79	0	0	18.55	10913.39	0	0	0	0	1502.78	11.95	0.86
RS	0	0	0	1.62	1.98	0	4.32	424.6	0	0	0	0	0	5.39	0
SE	37.84	0	0	0	1.88	0	158.68	29036.31	0	6.14	0.17	1.2	0	1.96	0
SI	2.51	0	0	0	0.19	0	0.54	1491.62	0	0	0	0.75	0	3.85	1.24
SK	7.42	0	0	0.97	1.1	0	3.94	277.62	0	0.84	0	3.63	0	2.46	0.03
UK	105.62	11.26	0	25.93	1.2	0	26.64	143.74	0	54.72	13.08	18.61	31407.1	68.78	31.61

Table A-19. Capacity distribution for Model Run 17 (12 Groups per VRES technology)

Country	Onshore	Offshore	PV /out	PV / Tracking	Run-of-river	Rooftop PV	PHS	Reservoir	Biomass CHP	PEM Electrolyzer	H2 OCGT	H2 CCGT	Salt Cavern	Vessel	Li-ion Battery
AL	5.08	0	0	0	0.03	0	0	1470.55	0	0.98	0	0	216.59	0.99	0.2
AT	38.61	0	0	27.22	4.61	0	114.15	1053.49	0	11.21	0.64	0.47	0	10.34	15.8
BA	16.4	0	0	2.91	0.28	0	1.61	1692.83	0	7.22	0	0	1740.93	11.55	0.85
BE	3.46	4.72	0	22.28	0.08	0	6.18	13.82	0	0	0	2.87	0	4.67	10.21
BG	0	0	0	6.69	0.61	0	40.59	1964.22	0	0	0	0	0	5.73	0.15
CH	8.5	0	0	1.58	3.74	0	163.81	5031.16	0	0	0	0	0	13.36	0
CZ	19.66	0	0	16.24	0.41	0	5.99	441.86	0	4.2	0	2.27	0	7.25	8.9
DE	40.81	21.99	0	33.02	4.15	0	39.27	5.46	0	0	5.81	30.34	26219.45	9.89	1.79
DK	23.57	0	0	0.46	0	0	0	0	0	14.27	0.17	1.19	7213.22	0.01	0.01
EE	12.74	0	0	0	0	0	0	0	0	5.46	0	0	0	1.7	0
ES	54.19	0	0	169.11	2.27	0	63.06	11148.12	0	18.46	8.42	0.44	6262.46	70.64	280.58
FI	20.36	0	0	0	2.96	0	0	518.99	0	4.16	1.01	1.18	0	32.27	8.68
FR	149.05	14.01	0	115.76	6.56	0	50.15	5071.64	0	47.64	3.11	22.15	20961.71	115.6	95.38
GR	17.08	0	0	3.87	0.22	0	4.64	1753.4	0	2.44	0	0	488.02	17.45	1.01
HR	5.97	0	0	4.88	0.44	0	5.69	1955.8	0	1.49	0	0	0	4.62	0.09
HU	0	0	0	18.14	0.03	0	0	48.33	0	0	0	1.47	0	8.71	4.89
IE	26.93	0	0	3.63	0.12	0	2.54	0	0	19.03	1.28	0.68	0	8.54	2.73
IT	50.33	0	0	124.59	10.36	0	61.78	1693.37	0	8.53	0.07	3.05	0	125.64	124.87
LT	11.8	0	0	0	0	0	11.06	23.46	0	2.49	0	0	0	4.66	0
LU	0	0	0	2.3	0	0	5.04	0	0	0	0	0	0	0.94	0
LV	2.55	0	0	0	0.26	0	0	1472.02	0	0.15	0	0	0	2.85	0
ME	4.85	0	0	2.75	0	0	0	0	0	1.16	0	0	0	2.21	0.34
MK	3.22	0	0	0.12	0.29	0	0	265.54	0	0	0	0	0	1.76	2.25
NL	21.11	27.61	0	0	0	0	0	0	0	11.72	2.88	18.53	17711.07	0	11.65
NO	56.15	0	0	0	0.73	0	391.93	79421.13	0	30.23	0	0	0	8.26	0
PL	38.01	4.75	0	35.7	0.4	0	8.32	119.15	0	14.06	1.21	9.24	16131	0.98	20.29
PT	16.95	0	0	15.44	2.66	0	66.67	686.82	0	4.38	0.01	0	399.42	7.93	15.02
RO	13.38	0	0	0.79	0	0	18.55	10913.39	0	0	0	0	1502.78	11.95	0.86
RS	0	0	0	1.62	1.98	0	4.32	424.6	0	0	0	0	0	5.39	0
SE	37.84	0	0	0	1.88	0	158.68	29036.31	0	6.14	0.17	1.2	0	1.96	0
SI	2.51	0	0	0	0.19	0	0.54	1491.62	0	0	0	0.75	0	3.85	1.24
SK	7.42	0	0	0.97	1.1	0	3.94	277.62	0	0.84	0	3.63	0	2.46	0.03
UK	105.62	11.26	0	25.93	1.2	0	26.64	143.74	0	54.72	13.08	18.61	31407.1	68.78	31.61

Table A-20. Capacity distribution for Model Run 18 (15 Groups per VRES technology)

Country	Onshore	Offshore	PV /out	PV / Tracking	Run-of-river	Rooftop PV	PHS	Reservoir	Biomass CHP	PEM Electrolyzer	H2 OCGT	H2 CCGT	Salt Cavern	Vessel	Li-ion Battery
AL	4.09	0	0	0	0.03	0	0	1470.55	0	0.88	0	0	229.3	0.83	0.77
AT	39.42	0	0	23.38	4.61	0	114.15	1053.49	0	11.63	2.06	0.39	0	5.21	9.53
BA	14.7	0	0	3.18	0.28	0	1.61	1692.83	0	6.84	0	0	2075.75	6.98	0.28
BE	4.15	4.72	0	21.28	0.08	0	6.18	13.82	0	0	0	1.58	0	0.01	3.78
BG	0.27	0	0	7.42	0.61	0	40.59	1964.22	0	0	0	0	0	5.9	1.19
CH	10.44	0	0	1.84	3.74	0	163.81	5031.16	0	0	0	0	0	1.9	0
CZ	19.48	0	0	14.32	0.41	0	5.99	441.86	0	3.14	0	2.94	0	0.07	5.73
DE	32.94	23.75	0	35.46	4.15	0	39.27	5.46	0.53	0	8.48	25.76	23878	0.06	2.38
DK	21.31	0	0	0	0	0	0	0	0	12.98	0.49	0.93	6176.1	0.01	0.18
EE	9.93	0	0	1.34	0	0	0	0	0	4.26	0	0	0	1.59	0.35
ES	53.49	0	0	145.85	2.27	0	63.06	11148.12	0	14.42	7.84	5.14	8376.4	79.61	222.49
FI	18.85	0	0	0	2.96	0	0	518.99	0	3.34	0.32	1.09	0	17.17	9.54
FR	152.62	19.74	0	107.35	6.56	0	50.15	5071.64	0	47.3	6.4	23.07	24684.78	83	70.82
GR	16.18	0	0	5.67	0.22	0	4.64	1753.4	0	2.2	0	0	477.32	18.98	1.36
HR	7.98	0	0	4.06	0.44	0	5.69	1955.8	0	2.51	0	0	0	4.72	0.35
HU	0.29	0	0	15.93	0.03	0	0	48.33	0	0	0	0.94	0	2.76	4.05
IE	25.11	0	0	7.63	0.12	0	2.54	0	0	17.82	0.74	0.67	0	9.47	5.12
IT	54.46	0	0	119.7	10.36	0	61.78	1693.37	0	7.72	0.86	3.17	0	113.24	121.55
LT	11.16	0	0	0	0	0	11.06	23.46	0	2.37	0	0	0	4.57	0
LU	0	0	0	2.74	0	0	5.04	0	0	0	0	0.07	0	0.01	0
LV	2.24	0	0	0	0.26	0	0	1472.02	0	0	0	0	0	2.66	0.06
ME	4.92	0	0	0.62	0	0	0	0	0	0.88	0	0	0	1.13	0.01
MK	3.17	0	0	0	0.29	0	0	265.54	0	0.34	0	0	0	1.84	2.14
NL	22.47	25.73	0	0	0	0	0	0	0	9.81	3.83	18.37	18022.98	0	8.99
NO	55.51	0	0	0	0.73	0	391.93	79421.13	0	29.82	0	0	0	7.38	0
PL	40.75	3.77	0	32.55	0.4	0	8.32	119.15	0	13.44	1.52	8.25	16414.95	0.02	27.7
PT	12.37	0	0	17.95	2.66	0	66.67	686.82	0	1.92	0.34	0	422.18	9.73	26.78
RO	12.18	0	0	3.89	0	0	18.55	10913.39	0	0	0	0	1507.92	11.35	0.57
RS	0	0	0	4.76	1.98	0	4.32	424.6	0	0	0	0	0	6.08	0
SE	40.34	0	0	0	1.88	0	158.68	29036.31	0	8.05	0.5	0.7	0	2.2	0.02
SI	2.01	0	0	0	0.19	0	0.54	1491.62	0	0	0	1.03	0	0.04	1.09
SK	5.9	0	0	0.2	1.1	0	3.94	277.62	0	0	0	4.36	0	4.15	0
UK	106.77	22.01	0	22.95	1.2	0	26.64	143.74	0	59.05	15.65	15.79	32364.62	61.44	25.09

Table A-21. Capacity distribution for Model Run 19 (20 Groups per VRES technology)

Country	Onshore	Offshore	PV /out	PV / Tracking	Run-of-river	Rooftop PV	PHS	Reservoir	Biomass CHP	PEM Electrolyzer	H2 OCGT	H2 CCGT	Salt Cavern	Vessel	Li-ion Battery
AL	3.82	0	0	0.01	0.03	0	0	1470.55	0	0.13	0	0	219.78	0.45	1.24
AT	32.95	0	0	30.63	4.61	0	114.15	1053.49	0	10.13	0	0	0	20.82	11.46
BA	11.05	0	0	0	0.28	0	1.61	1692.83	0	2.93	0	0	1247.37	1.23	0.98
BE	2.09	4.72	0	31.58	0.08	0	6.18	13.82	0	0	0.46	2.47	0	14.06	6.54
BG	0	0	0	7.29	0.61	0	40.59	1964.22	0	0	0	0	0	6.41	2.92
CH	8.63	0	0	5.02	3.74	0	163.81	5031.16	0	0	0	0	0	15.7	0
CZ	14.61	0	0	20.47	0.41	0	5.99	441.86	0	0.92	0.64	1.97	0	6.66	7.95
DE	29.21	26.46	0	37.53	4.15	0	39.27	5.46	0	0	7.42	38.03	33684.37	17.93	1.32
DK	19.05	0	0	0	0	0	0	0	0	10.52	0.59	1.18	9223.62	0.02	0.01
EE	9.51	0.83	0	0.67	0	0	0	0	0	4.68	0	0	0	3.56	1.44
ES	60.33	0	0	130.95	2.27	0	63.06	11148.12	0	15.43	0	0	3129.61	68.54	193.93
FI	18.43	0	0	0	2.96	0	0	518.99	0	2.8	0.61	2.1	0	30.67	4.53
FR	129.44	26.64	0	116.39	6.56	0	50.15	5071.64	0	38.17	4.65	11.97	18946.3	109.75	91.81
GR	14.96	0	0	9.57	0.22	0	4.64	1753.4	0	3.7	0	0	396.68	21.37	7.2
HR	6.95	0	0	4.08	0.44	0	5.69	1955.8	0	1.84	0	0	0	6.25	0.38
HU	0	0	0	18.2	0.03	0	0	48.33	0	0	0	2.05	0	12	22.06
IE	26.56	0	0	5.37	0.12	0	2.54	0	0	18.16	1.1	0.84	0	8.26	2.77
IT	47.7	0	0	130.34	10.36	0	61.78	1693.37	0	10.52	0	0	0	145.19	131.83
LT	11.66	0	0	0	0	0	11.06	23.46	0	2.96	0	0	0	4.56	3.38
LU	0	0	0	4.81	0	0	5.04	0	0	0	0	0	0	1.35	0
LV	2.5	0	0	3.29	0.26	0	0	1472.02	0	0.31	0	0	0	2.91	0.59
ME	2.92	0	0	5.73	0	0	0	0	0	1.23	0	0	0	1.37	0.89
MK	2.86	0	0	0	0.29	0	0	265.54	0	0.02	0	0	0	2.93	0.97
NL	21.11	32.12	0	0	0	0	0	0	0	12.71	0.52	12.62	12499.56	0.01	0.15
NO	61.33	0	0	0	0.73	0	391.93	79421.13	0	33.97	0	0	0	8.49	0
PL	32.06	3.14	0	42.73	0.4	0	8.32	119.15	0	8.69	1.6	11.47	15958.2	0.1	11.89
PT	16.21	0	0	10.12	2.66	0	66.67	686.82	0	2.84	0	0	232.65	16.49	1.26
RO	12.34	0	0	4.4	0	0	18.55	10913.39	0	0	0	0	1652.98	11.01	0.01
RS	4.38	0	0	0	1.98	0	4.32	424.6	0	0.73	0	0	0	7.44	0
SE	46.95	0	0	0	1.88	0	158.68	29036.31	0	16.06	0.44	1.12	0	13.15	1.18
SI	1.51	0	0	0.35	0.19	0	0.54	1491.62	0	0	0	0	0	6.94	2.15
SK	4.4	0	0	1.75	1.1	0	3.94	277.62	0	0	0	2.39	0	2.34	2.01
UK	87.88	29.54	0	22.53	1.2	0	26.64	143.74	0	49.59	2.98	17.15	27235.64	105.24	40.96

Table A-22. Capacity distribution for Model Run 20 (30 Groups per VRES technology)

Country	Onshore	Offshore	PV /out Tracking	PV / Tracking	Run-of-river	Rooftop PV	PHS	Reservoir	Biomass CHP	PEM Electrolyzer	H2 OCGT	H2 CCGT	Salt Cavern	Vessel	Li-ion Battery
AL	3.91	0	0	0	0.03	0	0	1470.55	0	0.26	0	0	203.13	0.65	0
AT	37.92	0	0	31.9	4.61	0	114.15	1053.49	0	10.59	0	0	0	20.44	3.49
BA	11.99	0	0	0	0.28	0	1.61	1692.83	0	3.89	0	0	1548.74	2.72	0.32
BE	4.22	4.72	0	21.61	0.08	0	6.18	13.82	0	0	0	4.02	0	9.67	3.74
BG	0.22	0	0	6.06	0.61	0	40.59	1964.22	0	0	0	0	0	6.43	1
CH	9.15	0	0	2.34	3.74	0	163.81	5031.16	0	0	0	0	0	14.81	0
CZ	15.49	0	0	23.08	0.41	0	5.99	441.86	0	2.18	1.48	1.24	0	2.76	6.69
DE	39.03	20.62	0	37.61	4.15	0	39.27	5.46	0.17	1.08	3.52	24.75	23007.24	47.04	1.27
DK	18.47	0	0	0.32	0	0	0	0	0	9.85	2.96	0.85	9244.3	0.02	0
EE	10.15	0	0	0	0	0	0	0	0	4.43	0	0	0	7.12	1.03
ES	68.97	0	0.01	121.03	2.27	0	63.06	11148.12	0	14.52	0	0	2883.06	68	174.43
FI	21.08	0	0	0	2.96	0	0	518.99	0	4.49	0.21	0.03	0	33.04	9.01
FR	152.24	23.02	0	88.16	6.56	0	50.15	5071.64	0	41.73	3.58	13.18	19221.35	129.93	58.73
GR	15.58	0	0	9.21	0.22	0	4.64	1753.4	0	3.88	0	0	461.44	21.11	1.15
HR	7.98	0	0	4.58	0.44	0	5.69	1955.8	0	2.88	0	0	0	5.34	0.62
HU	3.36	0	0	13.86	0.03	0	0	48.33	0	0	0.17	2.35	0	12.01	9.01
IE	25.92	0	0	4.67	0.12	0	2.54	0	0	18.05	0.84	1.32	0	7.7	5.03
IT	50.84	0	0	113.84	10.36	0	61.78	1693.37	0	8.06	0	0	0	146.29	111.98
LT	9.16	0	0	0	0	0	11.06	23.46	0	2.23	0	0	0	5.17	0.52
LU	0	0	0	5.96	0	0	5.04	0	0	0	0	0.03	0	0.79	0.01
LV	2.58	0	0	0.36	0.26	0	0	1472.02	0	0	0	0	0	2.93	0.02
ME	3.88	0	0	3.94	0	0	0	0	0	1.17	0	0	0	1.94	0
MK	1.92	0	0	1.49	0.29	0	0	265.54	0	0.18	0	0	0	2.97	0.89
NL	19.75	37.53	0	7.41	0	0	0	0	0	20.14	0.18	11.28	13277.75	3.39	4.89
NO	49.43	0	0	0	0.73	0	391.93	79421.13	0	26.52	0	0	0	7.35	0
PL	34.5	1.85	0	47.46	0.4	0	8.32	119.15	0	13.09	0	11.01	15831.74	15.79	10.55
PT	15.03	0	0	6.39	2.66	0	66.67	686.82	0	2.07	0	0	225.56	11.73	0
RO	10.88	0	0	4.33	0	0	18.55	10913.39	0	0	0	0	1526.26	12.16	0.2
RS	4.42	0	0	0	1.98	0	4.32	424.6	0	1.5	0	0	0	11.46	0
SE	43.38	0	0	0	1.88	0	158.68	29036.31	0	13.38	1.73	0.23	0	1.99	0.14
SI	3	0	0	0	0.19	0	0.54	1491.62	0	0	0	0	0	5.42	1.1
SK	5.9	0	0	0.07	1.1	0	3.94	277.62	0	0	0.12	3.05	0	1.39	0.01
UK	97.73	21.73	0	21	1.2	0	26.64	143.74	0	50.44	7.6	17.77	29483.96	97.72	27.9

Table A-23. Capacity distribution for Model Run 21 (60 Groups per VRES technology)

Country	Onshore	Offshore	PV /out Tracking	PV / Tracking	Run-of-river	Rooftop PV	PHS	Reservoir	Biomass CHP	PEM Electrolyzer	H2 OCGT	H2 CCGT	Salt Cavern	Vessel	Li-ion Battery
AL	3.08	0	0	0	0.03	0	0	1470.55	0	0.22	0	0	66.96	1.58	0
AT	36.45	0	0	27.94	4.61	0	114.15	1053.49	0	10.69	0	0	0	20.28	4.43
BA	11.05	0	0	4.31	0.28	0	1.61	1692.83	0	5.06	0	0	1617.66	4.41	1.69
BE	4.83	4.72	0	20.96	0.08	0	6.18	13.82	0	0	0	3.67	0	2.24	3.43
BG	3.4	0	0	4.24	0.61	0	40.59	1964.22	0	0	0	0	0	6.59	0
CH	9.34	0	0	4.22	3.74	0	163.81	5031.16	0	0	0	0	0	14.85	0
CZ	13.16	0	0	20.35	0.41	0	5.99	441.86	0	0.82	0.32	2.75	0	9.47	8.52
DE	36.18	22.23	0	36.83	4.15	0	39.27	5.46	0.52	0	3.21	23.28	21418.15	37.72	2.65
DK	17.96	0	0	0.14	0	0	0	0	0	12.08	1.09	0.98	8267.45	0.03	0.97
EE	10.17	0	0	2.91	0	0	0	0	0	4.6	0	0	0	2.51	0.01
ES	66.11	0	0.01	114.85	2.27	0	63.06	11148.12	0	13.65	0	0	3321.93	66.86	139.62
FI	24.06	0	0	0	2.96	0	0	518.99	0	7.04	0.44	0.34	0	41.09	7.49
FR	149.41	21.61	0	114.78	6.56	0	50.15	5071.64	0	47.38	1.57	13.3	18889.91	154.19	77.13
GR	14.35	0	0	9.4	0.22	0	4.64	1753.4	0	3.16	0	0	419.67	18.3	0.22
HR	6.64	0	0	4.32	0.44	0	5.69	1955.8	0	2.33	0	0	0	4.93	0.52
HU	3.89	0	0	14.89	0.03	0	0	48.33	0	0	0	3.02	0	12.44	4.96
IE	33.4	0	0	2.62	0.12	0	2.54	0	0	21.9	0.87	1.54	0	7.62	0.99
IT	55.16	0	0	114.43	10.36	0	61.78	1693.37	0	10.08	0	0	0	147.76	97.48
LT	9.39	0	0	0	0	0	11.06	23.46	0	2.16	0	0	0	5.04	0
LU	0.04	0	0	5.6	0	0	5.04	0	0	0	0	0	0	1.15	0.12
LV	2.6	0	0	0.27	0.26	0	0	1472.02	0	0.2	0	0	0	2.86	0
ME	2.92	0	0	1.12	0	0	0	0	0	0.7	0	0	0	1.62	0
MK	0.96	0	0	2.12	0.29	0	0	265.54	0	0.12	0	0	0	3.53	0.65
NL	23.82	32.61	0	0	0	0	0	0	0	16.07	0.68	14.45	16065.17	6.56	2.72
NO	43.56	0	0	0	0.73	0	391.93	79421.13	0	23.52	0	0	0	7.62	0
PL	31.02	2.01	0	52.78	0.4	0	8.32	119.15	0	10.2	1.17	11.59	16146.51	1.54	19.87
PT	16.12	0	0	8.6	2.66	0	66.67	686.82	0	2.35	0	0	188.83	11.95	0.01
RO	9.3	0	0	1.77	0	0	18.55	10913.39	0	0	0	0	1602.19	11.27	0
RS	5.06	0	0	0	1.98	0	4.32	424.6	0	1.81	0	0	0	8.1	0
SE	40.22	0	0	0	1.88	0	158.68	29036.31	0	9.42	1.12	0.49	0	3.17	0.22
SI	2.01	0	0	0	0.19	0	0.54	1491.62	0	0	0	0	0	3.13	1.31
SK	4.4	0	0	1.64	1.1	0	3.94	277.62	0.06	0	0	1.61	0	2.18	0
UK	94.93	27.42	0	13.1	1.2	0	26.64	143.74	0	48.46	8.94	18.58	31118.6	50.12	31.77

Table A-24. Capacity distribution for Model Run 22 (72 Groups per VRES technology)

Country	Onshore	Offshore	PV /out Tracking	PV / Tracking	Run-of-river	Rooftop PV	PHS	Reservoir	Biomass CHP	PEM Electrolyzer	H2 OCGT	H2 CCGT	Salt Cavern	Vessel	Li-ion Battery
AL	3.42	0	0	0	0.03	0	0	1470.55	0	0.13	0	0	45.76	0.71	0
AT	34.88	0	0	27.35	4.61	0	114.15	1053.49	0	9.08	0	0	0	16.75	3.79
BA	9.88	0	0	5.74	0.28	0	1.61	1692.83	0	4.3	0	0	1620.57	0.49	1.87
BE	4.03	4.74	0	25.69	0.08	0	6.18	13.82	0	0	0	3.34	0	11.42	8.17
BG	3.21	0	0	4.88	0.61	0	40.59	1964.22	0	0	0	0	0	6.01	0
CH	10.01	0	0	3.85	3.74	0	163.81	5031.16	0	0	0	0	0	14.61	0
CZ	15.03	0	0	17.53	0.41	0	5.99	441.86	0	1.77	0.16	1.98	0	11.68	6.94
DE	35.73	22.99	0	42.47	4.15	0	39.27	5.46	0.13	0	3.39	21.43	20403.4	30.75	9.38
DK	18.58	0	0	0.75	0	0	0	0	0	12.01	1.65	0.81	9396.35	0.01	0.31
EE	10.14	0.31	0	1.24	0	0	0	0	0	4.51	0	0	0	1.49	0
ES	63.88	0	0.01	116.1	2.27	0	63.06	11148.12	0	12.33	0	0	3517.33	59.3	160.42
FI	22.99	0	0	0	2.96	0	0	518.99	0	5.98	0.41	0.58	0	21.22	6.6
FR	151.47	19.6	0	134.07	6.56	0	50.15	5071.64	0	50.62	1.29	12.57	17838.53	123.91	87
GR	13.44	0	0	9	0.22	0	4.64	1753.4	0	2.83	0	0	480.23	15.5	0.61
HR	5.99	0	0	4.48	0.44	0	5.69	1955.8	0	1.94	0	0	0	5.39	0.63
HU	2.03	0	0	17.65	0.03	0	0	48.33	0	0	0.47	2.86	0	16.75	7.73
IE	27.21	0	0	7.11	0.12	0	2.54	0	0	17.06	0.8	1.44	0	6	0.48
IT	53.5	0	0	115.18	10.36	0	61.78	1693.37	0	9.33	0	0	0	145.17	98.88
LT	8.71	0	0	0	0	0	11.06	23.46	0	1.73	0	0	0	4.82	0.31
LU	0.04	0	0	5.05	0	0	5.04	0	0	0	0	0	0	1.16	0.31
LV	2.47	0	0	2.14	0.26	0	0	1472.02	0	0.13	0	0	0	2.78	0.22
ME	3.24	0	0	1.71	0	0	0	0	0	0.9	0	0	0	2.37	0
MK	0.8	0	0	2.18	0.29	0	0	265.54	0	0.06	0	0	0	3.11	0.18
NL	23.37	29.52	0	5.55	0	0	0	0	0	14.65	1.42	13.99	15110.68	0.01	0.62
NO	50.83	0	0	0	0.73	0	391.93	79421.13	0	28.06	0	0	0	7.06	0
PL	29.55	1.62	0	51.39	0.4	0	8.32	119.15	0	9.11	1.1	10.7	14543.46	4.86	13
PT	16.41	0	0	8.57	2.66	0	66.67	686.82	0	2.34	0	0	236.78	11.11	0
RO	10.2	0	0	4.52	0	0	18.55	10913.39	0	0	0	0	1874.8	12.38	0.72
RS	4.23	0	0	0	1.98	0	4.32	424.6	0	1.79	0	0	0	6.82	0
SE	40.18	0	0	0	1.88	0	158.68	29036.31	0	10.83	1.58	0.36	0	1.78	0
SI	2.08	0	0	0	0.19	0	0.54	1491.62	0	0	0	0	0	3	0.42
SK	4.3	0	0	1.63	1.1	0	3.94	277.62	0	0	0	1.37	0	3.16	0.02
UK	85.71	27.94	0	25.16	1.2	0	26.64	143.74	0	47.01	8.76	17.91	32617.77	6.88	49.95

Table A-25. Capacity distribution for Model Run 23 (90 Groups per VRES technology)

Country	Onshore	Offshore	PV /out Tracking	PV / Tracking	Run-of-river	Roof-top PV	PHS	Reservoir	Biomass CHP	PEM Electrolyzer	H2 OCGT	H2 CCGT	Salt Cavern	Vessel	Li-ion Battery
AL	2.92	0	0	0.26	0.03	0	0	1470.55	0	0.23	0	0	192.23	0.31	0
AT	35.03	0	0	24.35	4.61	0	114.15	1053.49	0	8.12	0	0	0	17.68	5.02
BA	10.47	0	0	3.93	0.28	0	1.61	1692.83	0	4.81	0	0	1527.88	3.34	0.85
BE	3.69	4.74	0	27.14	0.08	0	6.18	13.82	0	0	0	2.51	0	12.16	16.76
BG	2.56	0	0	4.28	0.61	0	40.59	1964.22	0	0	0	0	0	6.4	0.04
CH	9.7	0	0	2.17	3.74	0	163.81	5031.16	0	0	0	0	0	14.6	0
CZ	13.44	0	0	11.95	0.41	0	5.99	441.86	0	0	0	1.53	0	13.44	4.49
DE	29.06	25.27	0	39.19	4.15	0	39.27	5.46	0	2.15	4.43	29.91	25595.22	47.34	4.48
DK	21.03	0	0	0.46	0	0	0	0	0	12.78	1.05	1.05	9613.64	0.03	0.2
EE	9.34	0.68	0	0	0	0	0	0	0	4.26	0	0	0	4.73	0.97
ES	66.35	0	0.01	118.64	2.27	0	63.06	11148.12	0	15.39	0	0	2567.11	65.2	158.57
FI	22.28	0	0	0	2.96	0	0	518.99	0	5.69	1.22	0.84	0	28.97	6.23
FR	143.58	20.99	0	122	6.56	0	50.15	5071.64	0	39.76	2.97	17.01	21639.98	109.39	83.64
GR	13.06	0	0	12.44	0.22	0	4.64	1753.4	0	4.06	0	0	455.88	19.08	3.64
HR	6.11	0	0	4.23	0.44	0	5.69	1955.8	0	1.64	0	0	0	4.73	0.43
HU	3.17	0	0	19.58	0.03	0	0	48.33	0	0	0.3	2.51	0	7.34	7.25
IE	32.35	0	0	4.75	0.12	0	2.54	0	0	21.24	0.94	1.34	0	7.28	1.71
IT	50.19	0	0	125.31	10.36	0	61.78	1693.37	0	12.41	0	0	0	140.08	121.81
LT	11.02	0	0	0	0	0	11.06	23.46	0	3.05	0	0	0	4.65	5.66
LU	0.03	0	0	5.69	0	0	5.04	0	0	0	0	0	0	0.95	0.16
LV	2.82	0	0	4.47	0.26	0	0	1472.02	0	0.8	0	0	0	3.89	0.77
ME	3.24	0	0	3.17	0	0	0	0	0	0.84	0	0	0	0.91	0
MK	1.28	0	0	1.75	0.29	0	0	265.54	0	0.06	0	0	0	3.08	0.98
NL	23.16	24.84	0	0	0	0	0	0	0	9.61	0	16.79	14963.77	0.42	3.53
NO	49.51	0	0	0	0.73	0	391.93	79421.13	0	26.94	0	0	0	8.11	0
PL	30.56	5.09	0	39.32	0.4	0	8.32	119.15	0	9.16	0.47	11.12	14289.44	21.56	14.53
PT	15.9	0	0	9.31	2.66	0	66.67	686.82	0	2.5	0	0	140.88	12.41	0.11
RO	11.66	0	0	2.23	0	0	18.55	10913.39	0	0	0	0	1511.45	9.85	3.59
RS	3.39	0	0	0	1.98	0	4.32	424.6	0	1.65	0	0	0	10.99	0
SE	44.27	0	0	0	1.88	0	158.68	29036.31	0	13.76	1	1.24	0	4.71	1.17
SI	1.68	0	0	0	0.19	0	0.54	1491.62	0	0	0	0	0	3.9	1.72
SK	3.9	0	0	0.01	1.1	0	3.94	277.62	0	0	0	2.23	0	3.01	0
UK	97.9	26.07	0	20.35	1.2	0	26.64	143.74	0	54.52	7.32	20.56	31953.85	65.15	36.83

Table A-26. Capacity distribution for Model Run 24 (Value of onshore wind energy)

Country	Onshore	Offshore	PV fount Tracking	PV / Tracking	Run-of-river	Rooftop PV	PHS	Reservoir	Biomass CHP	PEM Electrolyzer	H2 OCGT	H2 CCGT	Salt Cavern	Vessel	Li-ion Battery
AL	0	0	0	9.2	0.03	0	0	1470.55	0	1.16	0	0	355.44	0.01	21.01
AT	0	0	0	25.66	4.61	0	114.15	1053.49	3.5	0	0	0.01	0	21.12	4.28
BA	0	0	0	24.76	0.28	0	1.61	1692.83	0	4.26	0	0	969.07	0.01	55.94
BE	0	4.72	0	15.82	0.08	0	6.18	13.82	4.75	0	0	2.29	0	6.73	2.38
BG	0	1.81	0	6.17	0.61	0	40.59	1964.22	0	0	0	0	0	5.08	0.33
CH	0	0	0	8.49	3.74	0	163.81	5031.16	1.25	0	0	0	0	12.47	0.01
CZ	0	0	0	11.2	0.41	0	5.99	441.86	5	0	0	1.25	0	6.12	0.01
DE	0	50.43	0	24.5	4.15	0	39.27	5.46	19	0	0	21.52	19607.61	2.25	1.34
DK	0	41.11	0	1.37	0	0	0	0	0	25.62	0	0	1180.65	0.01	0.13
EE	0	12.12	0	0	0	0	0	0	0	5.45	0	0	0	6.59	1.81
ES	0	6.6	0.02	271.58	2.27	0	63.06	11148.12	0	26.49	0	0	6763.94	32.07	570.65
FI	0	12.29	0	0	2.96	0	0	518.99	1.26	1.17	0	1.5	0	32.09	7.02
FR	0	86.78	2.25	126.43	6.56	0	50.15	5071.64	9.65	22.14	1.27	13.59	13580.92	50.33	137.24
GR	0	5.26	0	29.02	0.22	0	4.64	1753.4	0	4.85	0	0	999.14	11.87	51.52
HR	0	2.52	0	9.26	0.44	0	5.69	1955.8	0	0	0	0	0	8.6	15.97
HU	0	0	0	6.28	0.03	0	0	48.33	3.66	0	0	0	0	6.26	1.29
IE	0	19.57	0	8.49	0.12	0	2.54	0	0	11.55	0.19	1.79	0	7.29	1.81
IT	0	16.2	0.01	220.48	10.36	0	61.78	1693.37	3.85	22.79	0	0	0	181.51	307.02
LT	0	6.86	0	6.95	0	0	11.06	23.46	0	0	0	0.1	0	4.75	0
LU	0	0	0	1.86	0	0	5.04	0	0	0	0	0.54	0	0.07	0
LV	0	2.48	0	3.62	0.26	0	0	1472.02	0	0.41	0	0	0	2.8	0.3
ME	0	0	0	12.23	0	0	0	0	0	1.08	0	0	0	1.24	21
MK	0	0	0	1.64	0.29	0	0	265.54	0	0	0	0	0	1.46	1.2
NL	0	52.17	0	0.04	0	0	0	0	0	11.87	0	6.36	8076.49	0.01	16.52
NO	0	0	0	0.37	0.73	0	391.93	79421.13	0	0.02	0	0	0	9.58	0
PL	0	21.36	0	22.73	0.4	0	8.32	119.15	5.71	4.44	0	8.32	8785.3	0.07	0.95
PT	0	9.1	0	7.74	2.66	0	66.67	686.82	0	0.83	0	0	818.31	0.02	1.79
RO	0	9.44	0	2.02	0	0	18.55	10913.39	0	0	0	0	1010.9	6.76	0.36
RS	0	0	0	0	1.98	0	4.32	424.6	0	0	0	0	0	4.2	0
SE	0	19	0	3.2	1.88	0	158.68	29036.31	0	0	0	0	0	0.43	0
SI	0	0	0	0.2	0.19	0	0.54	1491.62	0	0	0	0	0	3.56	0.01
SK	0	0	0	6	1.1	0	3.94	277.62	2.75	0	0	0.09	0	5.32	0.02
UK	0	148.21	0	45.64	1.2	0	26.64	143.74	0	86.69	5.64	16.3	14009.39	24.26	31.72

Table A-27. Capacity distribution for Model Run 25 (Value of offshore wind energy)

Country	Onshore	Offshore	PV /out Tracking	PV / Tracking	Run-of-river	Rooftop PV	PHS	Reservoir	Biomass CHP	PEM Electrolyzer	H2 OCGT	H2 CCGT	Salt Cavern	Vessel	Li-ion Battery
AL	3.08	0	0	0.89	0.03	0	0	1470.55	0	0.44	0	0	207.27	0.02	0
AT	38.42	0	0	31.89	4.61	0	114.15	1053.49	0	8.46	0	0	0	16.16	6.58
BA	11.05	0	0	0	0.28	0	1.61	1692.83	0	3.76	0	0	1381.05	2.71	0
BE	6.38	0	0	28.14	0.08	0	6.18	13.82	4.75	0	0	1.28	0	0.08	9.14
BG	2.93	0	0	2.91	0.61	0	40.59	1964.22	0	0	0	0	0	5.18	0.68
CH	10.44	0	0	5.98	3.74	0	163.81	5031.16	0	0	0	0	0	14.77	0
CZ	12.86	0	0	18.68	0.41	0	5.99	441.86	0	0	0.02	3.96	0	11.55	14.91
DE	57.56	0	0	37.47	4.15	0	39.27	5.46	5.09	0	5.27	25.28	23484.17	24.01	2.15
DK	22.81	0	0	2.43	0	0	0	0	13.83	1.35	0.36	0.36	8771.25	0.02	0.14
EE	9.51	0	0	0	0	0	0	0	4.05	0	0	0	0	5.28	0
ES	61.38	0	0.01	128.53	2.27	0	63.06	11148.12	0	11.13	0	0	3628.13	71.61	183.52
FI	19.42	0	0	0	2.96	0	0	518.99	0	3.58	0.87	0.15	0	22.23	11.16
FR	174.23	0	0.01	140.72	6.56	0	50.15	5071.64	0	46.4	0	10.76	16399.89	106.1	93.72
GR	13.72	0	0	5.44	0.22	0	4.64	1753.4	0	0.93	0	0	477.57	12.9	0.09
HR	6.59	0	0	4.88	0.44	0	5.69	1955.8	0	1.64	0	0	0	1.95	0.18
HU	4.06	0	0	13.2	0.03	0	0	48.33	0	0	1.74	0	0	5.1	3.31
IE	39.3	0	0	7.69	0.12	0	2.54	0	0	31.11	1.47	0.32	0	12.04	6.96
IT	54.19	0	0	114.14	10.36	0	61.78	1693.37	0	8.95	0	0	0	145.49	102.5
LT	11.11	0	0	0.01	0	0	11.06	23.46	0	2.14	0	0	0	6.29	1.01
LU	0.04	0	0	6.22	0	0	5.04	0	0	0	0	0.24	0	0.14	1.36
LV	2.82	0	0	1.69	0.26	0	0	1472.02	0	0	0	0	0	3.72	0.46
ME	3.12	0	0	4.11	0	0	0	0	0	1.28	0	0	0	5.26	0
MK	0.96	0	0	1.53	0.29	0	0	265.54	0	0	0	0	0	2.02	0.22
NL	39.72	0	0	0	0	0	0	0	0.53	2.38	1.51	22.13	19460.78	0.06	5.11
NO	56.44	0	0	0	0.73	0	391.93	79421.13	0	30.78	0	0	0	7.11	0
PL	35.99	0	0	45.33	0.4	0	8.32	119.15	0	9.62	0.48	12.04	17269.7	0.72	16.35
PT	16.51	0	0	11.62	2.66	0	66.67	686.82	0	3.74	0	0	267.3	10.93	2.45
RO	11.78	0	0	3.26	0	0	18.55	10913.39	0	0	0	0	1589.91	9.44	0.99
RS	4.62	0	0	0	1.98	0	4.32	424.6	0	1.54	0	0	0	7.96	0
SE	40.75	0	0	1.14	1.88	0	158.68	29036.31	0	11.26	1.28	1.56	0	4.95	0.23
SI	2.01	0	0	0.01	0.19	0	0.54	1491.62	0	0	0	0	0	3.49	0.29
SK	4.4	0	0	2.97	1.1	0	3.94	277.62	0	0	0	2.55	0	0.03	3.48
UK	125.03	0	0	16.52	1.2	0	26.64	143.74	0	56.3	13.02	15.51	30839.74	140.41	33.25

Table A-28. Capacity distribution for Model Run 26 (Value of PV without tracking)

Country	Onshore	Offshore	PV /out	PV / Tracking	Run-of-river	Rooftop PV	PHS	Reservoir	Biomass CHP	PEM Electrolyzer	H2 OCGT	H2 CCGT	Salt Cavern	Vessel	Li-ion Battery
AL	3.08	0	0	3.18	0.03	0	0	1470.55	0	1.17	0	0	23.67	1.3	0
AT	35.17	0	0	3.77	4.61	0	114.15	1053.49	0	0	0.01	0.66	0	18.05	6.25
BA	11.86	0	0	2.97	0.28	0	1.61	1692.83	0	4.45	0	0	1077.1	0.01	0
BE	3.8	4.72	0	3.15	0.08	0	6.18	13.82	4.54	0	0	0	0	15.19	1.05
BG	3.86	0	0	4.93	0.61	0	40.59	1964.22	0	0	0	0	0	9.61	0
CH	9.15	0	0	0.29	3.74	0	163.81	5031.16	0	0	0.08	0	0	14.52	0
CZ	9.24	0	0	4.19	0.41	0	5.99	441.86	3.03	0	0.05	0.82	0	11.32	0
DE	28.51	24.38	0	2.33	4.15	0	39.27	5.46	14.59	0	6.62	52.71	40825.69	19.66	0.24
DK	25.91	0	0	0.14	0	0	0	0	0	14.76	0.61	0	5789.57	1.88	1.04
EE	9.5	0	0	0.42	0	0	0	0	0	3.98	0.01	0	0	10.58	0.23
ES	73.75	0	0	74.09	2.27	0	63.06	11148.12	0	18.11	0.01	4.17	9787.29	60.03	123.79
FI	20.89	0	0	0	2.96	0	0	518.99	0	4.58	1.21	0.32	0	29.07	9.27
FR	172.84	12.25	0	53.67	6.56	0	50.15	5071.64	1.35	39.72	4.62	35.94	28410.65	169.12	33.94
GR	13.22	0	0	7.31	0.22	0	4.64	1753.4	0	3.35	0	0	258.21	12.73	0.63
HR	5.39	0	0	8.85	0.44	0	5.69	1955.8	0	1.57	0	0	0	5.15	3.79
HU	6.58	0	0	4.98	0.03	0	0	48.33	0	0	0	0.84	0	7.65	1.37
IE	43.14	0	0	1.88	0.12	0	2.54	0	0	31.88	0.87	0.82	0	11.94	4.36
IT	51.4	0	0	31.48	10.36	0	61.78	1693.37	4.08	1.39	0.49	3.57	0	152.91	10.85
LT	7.54	0	0	9.05	0	0	11.06	23.46	0	0.07	0.12	0.04	0	6.14	0.97
LU	0	0	0	0.31	0	0	5.04	0	0	0	0	0	0	0.81	0
LV	3.62	0	0	7.41	0.26	0	0	1472.02	0	1.77	0.01	0	0	3.37	4.24
ME	2.99	0	0	2.09	0	0	0	0	0	0.23	0	0	0	0.77	0
MK	0.96	0	0	1.46	0.29	0	0	265.54	0	0.2	0	0	0	3.22	0
NL	23.41	14.49	0	8.57	0	0	0	0	0	0.38	0.82	26.89	22789.42	1.27	6.38
NO	68.68	0	0	0	0.73	0	391.93	79421.13	0	41.66	0	0	0	13.26	0
PL	31.76	16.9	0	22.26	0.4	0	8.32	119.15	0	15.5	1.1	7.27	13784.88	9.53	7.04
PT	14.67	0	0	12.45	2.66	0	66.67	686.82	0	4.23	0	0	218.9	21.36	6.93
RO	9.31	0	0	6.28	0	0	18.55	10913.39	0	0	0	0	1320.72	7.17	0
RS	4.96	0	0	0	1.98	0	4.32	424.6	0	2.31	0	0	0	8.07	0
SE	48.88	0	0	0.59	1.88	0	158.68	29036.31	0	12.45	0.47	0	0	10.88	4.38
SI	2.01	0	0	1.9	0.19	0	0.54	1491.62	0	0	0	0.27	0	5.58	1.21
SK	4.4	0	0	1.88	1.1	0	3.94	277.62	0	0	0	5.63	0	15.08	0
UK	105.09	23.92	0	4.24	1.2	0	26.64	143.74	0	60.51	19.96	25.54	50248.18	226.14	14.48

Table A-29. Capacity distribution for Model Run 27 (Value of PV with tracking)

Country	Onshore	Offshore	PV /out Tracking	PV / Tracking	Run-of-river	Rooftop PV	PHS	Reservoir	Biomass CHP	PEM Electrolyzer	H2 OCGT	H2 CCGT	Salt Cavern	Vessel	Li-ion Battery
AL	4	0	1.16	0	0.03	0	0	1470.55	0	0.47	0	0	50.5	1.01	0.08
AT	31.31	0	6.13	0	4.61	0	114.15	1053.49	0.27	0.02	0.11	0.47	0	16.63	0.62
BA	11.05	0	7.84	0	0.28	0	1.61	1692.83	0	5.46	0	0	1080.68	4.09	0.65
BE	4.14	4.72	4.95	0	0.08	0	6.18	13.82	4.75	0	0	0.78	0	19.99	1.74
BG	3.86	0	5.45	0	0.61	0	40.59	1964.22	0	0	0	0	0	10.07	0.16
CH	11.72	0	0.48	0	3.74	0	163.81	5031.16	0	0	0	0	0	15.84	0
CZ	10.34	0	6.25	0	0.41	0	5.99	441.86	2.28	0	0	3.51	0	12.69	0.01
DE	33.49	25.62	3.14	0	4.15	0	39.27	5.46	11.13	0	13.17	44.06	46254.39	35.03	0
DK	25.41	0	0.87	0	0	0	0	0	0	14.24	0.66	0	5145.06	0.09	0.55
EE	9.98	0	0	0	0	0	0	0	0	3.45	0.05	0	0	5.84	4.47
ES	70.6	0	98.52	0	2.27	0	63.06	11148.12	0	13.7	0	0.99	5345.88	59.77	141.16
FI	22.98	0	0	0	2.96	0	0	518.99	0	6	0.98	0.07	0	42.44	13.81
FR	173.21	11.06	92.76	0	6.56	0	50.15	5071.64	0.96	45.55	18.35	18.83	41208.63	174.72	33.34
GR	15.58	0	9.5	0	0.22	0	4.64	1753.4	0	4.57	0	0	385.54	12.65	1.38
HR	5.36	0	7.88	0	0.44	0	5.69	1955.8	0	0.77	0	0	0	5.75	4.85
HU	3.39	0	9.66	0	0.03	0	0	48.33	0	0	0	2.01	0	26.66	4.66
IE	37.74	0	3.7	0	0.12	0	2.54	0	0	30.64	0.59	0.62	0	8.13	4.52
IT	46.03	0	51.57	0	10.36	0	61.78	1693.37	3.23	1.55	0	9.67	0	142.94	15.63
LT	9.17	0	14.16	0	0	0	11.06	23.46	0	2.79	0.05	0.87	0	9.65	2.76
LU	0	0	0.39	0	0	0	5.04	0	0	0	0	0	0	0.97	0
LV	3.3	0	3.48	0	0.26	0	0	1472.02	0	1.1	0.05	0	0	4.42	1.81
ME	2.92	0	3.71	0	0	0	0	0	0	0.47	0	0	0	1.17	0.01
MK	0.96	0	0.95	0	0.29	0	0	265.54	0	0	0	0	0	2.7	0.32
NL	22.36	14.07	11.08	0	0	0	0	0	0.89	0	4.24	20.84	23128.91	8.77	7.58
NO	61.81	0	0	0	0.73	0	391.93	79421.13	0	34.55	0	0	0	7.89	0
PL	41.22	13.66	32.15	0	0.4	0	8.32	119.15	0	17.45	0.49	6.78	15031.44	11.03	6.03
PT	15.55	0	13.72	0	2.66	0	66.67	686.82	0	3.7	0	0	326.21	23.86	13.69
RO	9.31	0	8.88	0	0	0	18.55	10913.39	0	0	0	0	1491.78	8.21	0.03
RS	2.24	0	0	0	1.98	0	4.32	424.6	0	2.13	0	0	0	8.63	0
SE	41.51	0.02	2.28	0	1.88	0	158.68	29036.31	0	7.44	0.34	0	0	2.51	4.86
SI	2.24	0	2.95	0	0.19	0	0.54	1491.62	0	0	0	0.08	0	5.39	1.1
SK	4.4	0	3.52	0	1.1	0	3.94	277.62	0.2	0	0	4.49	0	4.34	0.26
UK	106.47	21.59	9.37	0	1.2	0	26.64	143.74	0	60.97	31.46	13.5	55254.22	162.87	24.04

Table A-30. Capacity distribution for Model Run 28 (Value of Hydro Run-of-river)

Country	Onshore	Offshore	PV /out Tracking	PV / Tracking	Run-of-river	Rooftop PV	PHS	Reservoir	Biomass CHP	PEM Electrolyzer	H2 OCGT	H2 CCGT	Salt Cavern	Vessel	Li-ion Battery
AL	3.08	0	0	0	0	0	0	1470.55	0	0.23	0	0	51.93	1.19	0.01
AT	38.9	0	0	36.52	0	0	114.15	1053.49	0	9.58	0	0	0	16.51	13.23
BA	11.05	0	0	3.83	0	0	1.61	1692.83	0	4.89	0	0	1566.06	5.51	1.51
BE	4.83	4.72	0	19.23	0	0	6.18	13.82	0	0	0	3.92	0	38.21	2.39
BG	3.86	0	0	3.83	0	0	40.59	1964.22	0	0	0	0	0	6.67	0.01
CH	10.44	0	0	7.77	0	0	163.81	5031.16	0	0	0	0	0	16.2	0
CZ	14.68	0	0	22.66	0	0	5.99	441.86	0	1.44	0	2.81	0	14.79	10.82
DE	35.47	23.08	0	38.71	0	0	39.27	5.46	3.65	0	3.09	24.18	21351.98	60.2	4.32
DK	19.12	0	0	0.45	0	0	0	0	0	11.83	2.77	0.27	10710.28	0.07	0.2
EE	9.72	0	0	0	0	0	0	0	0	4.12	0	0	0	4.39	0
ES	66.46	0	0.01	122.3	0	0	63.06	11148.12	0	15.09	0	0	2782.4	71.23	172.65
FI	24.56	0	0	0	0	0	0	518.99	0	6.09	0	1.75	0	30.1	8.94
FR	150.86	23.37	0	120.34	0	0	50.15	5071.64	0	42.37	3.21	15.4	21359.48	154.17	74.09
GR	14.34	0	0	8.99	0	0	4.64	1753.4	0	2.92	0	0	411.69	19.11	0.64
HR	6.95	0	0	5.3	0	0	5.69	1955.8	0	2.48	0	0	0	4.88	0.36
HU	4.75	0	0	17.98	0	0	0	48.33	0	0	0	2.36	0	16.03	8.65
IE	24.9	0	0	7.26	0	0	2.54	0	0	16.54	1.02	1.35	0	8.03	0.86
IT	58.29	0	0	135.05	0	0	61.78	1693.37	0	11.12	0	0	0	146.08	128.95
LT	11.24	0	0	0	0	0	11.06	23.46	0	2.86	0	0	0	4.79	0.01
LU	0.04	0	0	5.99	0	0	5.04	0	0	0	0	0	0	1.14	0.19
LV	2.56	0	0	2.36	0	0	0	1472.02	0	0.46	0	0	0	3.06	0.32
ME	3.88	0	0	1.65	0	0	0	0	0	1.05	0	0	0	3.17	0
MK	0.96	0	0	3.06	0	0	0	265.54	0	0.03	0	0	0	3.07	0.95
NL	22.59	31.16	0	0	0	0	0	0	0	14.66	0.06	14.78	15115.72	1.41	3.06
NO	52.28	0	0	0	0	0	391.93	79421.13	0	27.44	0	0	0	9.54	0
PL	35.4	3.31	0	45.1	0	0	8.32	119.15	0	13.1	1.03	12.24	16778.52	16.81	13.87
PT	17.9	0	0	9.02	0	0	66.67	686.82	0	2.28	0	0	193.83	11.34	1.88
RO	9.92	0	0	2.65	0	0	18.55	10913.39	0	0	0	0	1397.94	10.26	1.47
RS	5.06	0	0	0	0	0	4.32	424.6	0	1.31	0	0	0	9.61	0
SE	46.42	0	0	0	0	0	158.68	29036.31	0	10.73	2.24	0.02	0	14.19	0
SI	2.01	0	0	0.98	0	0	0.54	1491.62	0	0	0	0	0	3.98	2.72
SK	4.4	0	0	1.64	0	0	3.94	277.62	0.22	0	0	2.06	0	2.04	1.24
UK	92.38	30	0	32.09	0	0	26.64	143.74	0	55.57	11.88	14.82	29152.2	133.1	33.78

Table A-31. Capacity distribution for Model Run 29 (Value of Rooftop PV)

Country	Onshore	Offshore	PV /out	PV / Tracking	Run-of-river	Rooftop PV	PHS	Reservoir	Biomass CHP	PEM Electrolyzer	H2 OCGT	H2 CCGT	Salt Cavern	Vessel	Li-ion Battery
AL	3.08	0	0	0	0.03	0	0	1470.55	0	0.22	0	0	67.95	1.58	0
AT	36.45	0	0	27.93	4.61	0	114.15	1053.49	0	10.69	0	0	0	20.27	4.42
BA	11.05	0	0	4.3	0.28	0	1.61	1692.83	0	5.06	0	0	1616.64	4.44	1.69
BE	4.83	4.72	0	20.95	0.08	0	6.18	13.82	0	0	0	3.67	0	2.37	3.41
BG	3.4	0	0	4.24	0.61	0	40.59	1964.22	0	0	0	0	0	6.57	0
CH	9.33	0	0	4.24	3.74	0	163.81	5031.16	0	0	0	0	0	14.86	0
CZ	13.16	0	0	20.34	0.41	0	5.99	441.86	0	0.83	0.33	2.75	0	9.39	8.51
DE	36.19	22.22	0	36.84	4.15	0	39.27	5.46	0.52	0	3.21	23.26	21405.5	37.73	2.69
DK	17.96	0	0	0.14	0	0	0	0	12.08	1.09	0.98	8267.08	0.02	0.97	0
EE	10.17	0	0	2.93	0	0	0	0	4.6	0	0	0	0	2.46	0.01
ES	66.1	0	0	114.87	2.27	0	63.06	11148.12	0	13.65	0	0	3321.53	66.92	139.63
FI	24.06	0	0	0	2.96	0	0	518.99	0	7.04	0.44	0.34	0	41.06	7.48
FR	149.41	21.61	0	114.78	6.56	0	50.15	5071.64	0	47.39	1.57	13.3	18893.31	153.12	77.13
GR	14.35	0	0	9.39	0.22	0	4.64	1753.4	0	3.16	0	0	420.03	18.31	0.22
HR	6.64	0	0	4.32	0.44	0	5.69	1955.8	0	2.33	0	0	0	4.93	0.52
HU	3.89	0	0	14.89	0.03	0	0	48.33	0	0	0	3.02	0	12.42	4.96
IE	33.4	0	0	2.62	0.12	0	2.54	0	0	21.89	0.87	1.54	0	7.63	0.98
IT	55.16	0	0	114.43	10.36	0	61.78	1693.37	0	10.08	0	0	0	147.76	97.47
LT	9.39	0	0	0	0	0	11.06	23.46	0	2.17	0	0	0	5.04	0
LU	0.04	0	0	5.61	0	0	5.04	0	0	0	0	0	0	1.16	0.13
LV	2.6	0	0	0.26	0.26	0	0	1472.02	0	0.19	0	0	0	2.86	0
ME	2.92	0	0	1.12	0	0	0	0	0	0.7	0	0	0	1.62	0
MK	0.96	0	0	2.12	0.29	0	0	265.54	0	0.12	0	0	0	3.53	0.65
NL	23.82	32.62	0	0	0	0	0	0	0	16.07	0.68	14.45	16061.13	6.49	2.73
NO	43.55	0	0	0	0.73	0	391.93	79421.13	0	23.51	0	0	0	7.61	0
PL	31.01	2.01	0	52.79	0.4	0	8.32	119.15	0	10.18	1.16	11.61	16154.31	1.81	19.86
PT	16.12	0	0	8.6	2.66	0	66.67	686.82	0	2.35	0	0	189.03	11.95	0.01
RO	9.3	0	0	1.77	0	0	18.55	10913.39	0	0	0	0	1602.45	11.23	0
RS	5.06	0	0	0	1.98	0	4.32	424.6	0	1.81	0	0	0	8.09	0
SE	40.22	0	0	0	1.88	0	158.68	29036.31	0	9.42	1.12	0.49	0	3.34	0.22
SI	2.01	0	0	0	0.19	0	0.54	1491.62	0	0	0	0	0	3.13	1.32
SK	4.4	0	0	1.64	1.1	0	3.94	277.62	0.06	0	0	1.61	0	2.22	0
UK	94.92	27.43	0	13.1	1.2	0	26.64	143.74	0	48.45	8.94	18.58	31120.96	51.01	31.78

Table A-32. Capacity distribution for Model Run 30 (Value of Pumped Hydro Storage)

Country	Onshore	Offshore	PV /out Tracking	PV / Tracking	Run-of-river	Rooftop PV	PHS	Reservoir	Biomass CHP	PEM Electrolyzer	H2 OCGT	H2 CCGT	Salt Cavern	Vessel	Li-ion Battery
AL	3.08	0	0	0	0.03	0	0	1470.55	0	0.2	0	0	87.08	1.52	0.13
AT	37.15	0	0	26.89	4.61	0	0	1053.49	0	11.87	0	0	0	23.01	9.33
BA	11.05	0	0	5.2	0.28	0	0	1692.83	0	5.54	0	0	1659.89	6.58	2.98
BE	5.17	4.72	0	19.06	0.08	0	0	13.82	0	0	0	4.41	0	19.37	4.94
BG	3.86	0	0	3.61	0.61	0	0	1964.22	0	0	0	0	0	6.59	0.7
CH	9.8	0	0	3.08	3.74	0	0	5031.16	0	0	0	0	0	14.86	2.94
CZ	13.2	0	0	19.34	0.41	0	0	441.86	0	0.09	0	3.06	0	13.19	15.76
DE	33.41	22.77	0	34.6	4.15	0	0	5.46	3.06	0	2.32	27.96	24033.62	42.62	18.29
DK	18.3	0	0	0	0	0	0	0	0	12.74	1	1	8473.64	0.08	1.5
EE	10.49	0	0	2.82	0	0	0	0	0	4.85	0	0	0	3.93	0.51
ES	65.75	0	0.01	129.27	2.27	0	0	11148.12	0	14.12	0	0	2988.55	67.01	225.62
FI	24.35	0	0	0	2.96	0	0	518.99	0	6.85	0.35	0.38	0	37.97	7.58
FR	148.69	23.37	0.01	112.57	6.56	0	0	5071.64	0	47.95	1.42	12.95	18513.68	151.28	100.34
GR	15.58	0	0	8.06	0.22	0	0	1753.4	0	3.27	0	0	453.57	21.63	2.56
HR	6.95	0	0	3.87	0.44	0	0	1955.8	0	2.42	0	0	0	4.91	2.06
HU	3.17	0	0	13.16	0.03	0	0	48.33	0	0	0	2.65	0	15.38	7.51
IE	32.35	0	0	2.21	0.12	0	0	0	0	20.71	0.83	1.65	0	9.29	1.2
IT	55.36	0	0.01	123.4	10.36	0	0	1693.37	0	11.24	0	0	0	148.44	180.02
LT	9.68	0	0	0	0	0	0	23.46	0	2.37	0	0	0	4.7	1.13
LU	0.08	0	0	4.8	0	0	0	0	0	0	0	0	0	1.12	4.8
LV	2.72	0	0	0.61	0.26	0	0	1472.02	0	0.27	0	0	0	2.84	0.04
ME	3.25	0	0	0.17	0	0	0	0	0	1.32	0	0	0	5.91	0.02
MK	0.96	0	0	1.95	0.29	0	0	265.54	0	0.09	0	0	0	2.46	1.23
NL	23.82	33.6	0	0	0	0	0	0	0	16.68	1.2	12.55	15108.73	4.49	6.21
NO	43.48	0	0	0	0.73	0	0	79421.13	0	23.44	0	0	0	8.47	0
PL	33.03	2.23	0	51.51	0.4	0	0	119.15	0	10.29	1.05	11.83	16098.76	7.06	35.77
PT	18.31	0	0	8.03	2.66	0	0	686.82	0	3.37	0	0	266.11	9.9	2.83
RO	9.73	0	0	2.11	0	0	0	10913.39	0	0	0	0	1362.12	13.8	1.66
RS	5.06	0	0	0	1.98	0	0	424.6	0	1.36	0	0	0	8.35	0.17
SE	40.71	0	0	0	1.88	0	0	29036.31	0	9.81	0.99	0.88	0	2.53	0.04
SI	2.01	0	0	0.12	0.19	0	0	1491.62	0	0	0	0	0	3.36	1.83
SK	4.4	0	0	1.64	1.1	0	0	277.62	1.02	0	0	1.79	0	3.43	2.11
UK	94.99	28.41	0	10.84	1.2	0	0	143.74	0	48.64	8.73	19.99	32018.5	59.73	42.95

Table A-33. Capacity distribution for Model Run 31 (Value of Hydro Reservoir)

Country	Onshore	Offshore	PV /out Tracking	PV / Tracking	Run-of-river	Rooftop PV	PHS	Reservoir	Biomass CHP	PEM Electrolyzer	H2 OCGT	H2 CCGT	Salt Cavern	Vessel	Li-ion Battery
AL	4.96	0	0	0.01	0.03	0	0	0	0	1.04	0	0	540.43	0.01	0.71
AT	36.75	0	0	36.28	4.61	0	114.15	0	0	12.32	0	0	0	20.82	9.6
BA	12.65	0	0	8.6	0.28	0	1.61	0	0	8.88	0	0	3925.01	0.07	11.36
BE	5.17	4.72	0	21.71	0.08	0	6.18	0	0	0	0	4.1	0	24.47	2.42
BG	3.86	0	0	8.08	0.61	0	40.59	0	0	0.05	0	0	0	6.17	3.12
CH	10.14	0	0	7.31	3.74	0	163.81	0	0	0	0	2.96	0	15.97	0.44
CZ	13.7	0	0	20.5	0.41	0	5.99	0	0	1.04	0	4.34	0	12.54	8.59
DE	28.48	25.06	0	39.09	4.15	0	39.27	0	4.81	0	2.17	31.89	28187.29	30.54	3.16
DK	19.2	0	0	0.76	0	0	0	0	0	11.49	0.57	0.88	16686.71	0.01	0.07
EE	10.59	0	0	0	0	0	0	0	0	4.42	0	0	0	4.02	1.26
ES	61.54	0	0.01	161.48	2.27	0	63.06	0	0	17.06	0	0	4181.39	58.84	324.37
FI	25.35	0	0	0	2.96	0	0	0	0	8.05	0.16	0.81	0	16	8.5
FR	153.76	22.86	0.01	136.6	6.56	0	50.15	0	0	55.74	3.77	18.34	26417.23	117.91	96.03
GR	15.58	0	0	14.73	0.22	0	4.64	0	0	5.65	0	0	1067.28	16.18	20.72
HR	9.25	0	0	8.64	0.44	0	5.69	0	0	4.53	0	0.53	0	6.58	2.3
HU	3.38	0	0	15.42	0.03	0	0	0	0	0	0	3.76	0	20.69	5.66
IE	20.7	0	0	8.73	0.12	0	2.54	0	0	12.26	0.97	1.59	0	5.88	1.09
IT	51.94	0	0.01	141.82	10.36	0	61.78	0	0	12.78	0	0.35	0	146.11	180.2
LT	9.42	0	0	0	0	0	11.06	0	0	1.63	0	0	0	5.14	0.32
LU	0.04	0	0	5.67	0	0	5.04	0	0	0	0	0	0	1.36	0
LV	3.29	0	0	4.06	0.26	0	0	0	0	1.21	0	0	0	2.83	1.29
ME	4.85	0	0	0.78	0	0	0	0	0	1.48	0	0	0	0.76	0.43
MK	1.92	0	0	1.54	0.29	0	0	0	0	0.49	0	0	0	1.81	1.2
NL	25.24	33.6	0	2.39	0	0	0	0	0	17.83	0.76	9.66	12902.77	0.02	0.6
NO	48.97	0	0	0.28	0.73	0	391.93	0	0	19.42	0	0	0	6.89	0.6
PL	34.18	1.85	0	54.57	0.4	0	8.32	0	0	13.33	0.36	12.05	18437	6.05	11.49
PT	17.8	0	0	9.51	2.66	0	66.67	0	0	3.19	0	0	607.21	7.29	0.65
RO	15.87	0	0	10.87	0	0	18.55	0	0	4	0	1.31	2733.56	11.55	4.2
RS	5.12	0	0	3.96	1.98	0	4.32	0	0	2.12	0	0	0	8.59	0.01
SE	55.96	0	0	3.42	1.88	0	158.68	0	0	20.25	0	3.86	0	1.38	0.57
SI	2.09	0	0	0.58	0.19	0	0.54	0	0	0	0	1.69	0	5.21	4.41
SK	4.4	0	0	1.64	1.1	0	3.94	0	0	0	0	3.85	0	3.3	1.78
UK	89.25	27.07	0	41.67	1.2	0	26.64	0	0	52.74	6.3	19.05	32220.61	36.72	50.22

Table A-34. Capacity distribution for Model Run 32 (Value of Biomass)

Country	Onshore	Offshore	PV /out Tracking	PV / Tracking	Run-of-river	Roof-top PV	PHS	Reservoir	Biomass CHP	PEM Electrolyzer	H2 OCGT	H2 CCGT	Salt Cavern	Vessel	Li-ion Battery
AL	3.08	0	0	0	0.03	0	0	1470.55	0	0.22	0	0	69.32	1.49	0
AT	36.47	0	0	27.9	4.61	0	114.15	1053.49	0	10.81	0	0	0	20.56	4.41
BA	11.05	0	0	4.31	0.28	0	1.61	1692.83	0	5.08	0	0	1624.13	4.38	1.66
BE	4.83	4.72	0	20.96	0.08	0	6.18	13.82	0	0	0	3.67	0	2.38	3.15
BG	3.4	0	0	4.26	0.61	0	40.59	1964.22	0	0	0	0	0	6.59	0
CH	9.4	0	0	4.31	3.74	0	163.81	5031.16	0	0	0	0	0	14.86	0
CZ	13.16	0	0	20.55	0.41	0	5.99	441.86	0	0.87	0.35	2.72	0	9.08	8.47
DE	36.54	22.35	0	37.07	4.15	0	39.27	5.46	0	0	3.29	23.71	21727.33	36.83	2.86
DK	17.97	0	0	0.14	0	0	0	0	0	12.12	11.06	0.96	8260.16	0.01	1.03
EE	10.17	0	0	2.85	0	0	0	0	0	4.59	0	0	0	2.29	0.03
ES	66.16	0	0.02	114.85	2.27	0	63.06	11148.12	0	13.68	0	0	3290.38	67.36	139.7
FI	24.1	0	0	0	2.96	0	0	518.99	0	7.06	0.43	0.33	0	40.72	7.54
FR	149.39	21.63	0.01	115.02	6.56	0	50.15	5071.64	0	47.49	1.49	13.26	18807.43	153.69	77.53
GR	14.35	0	0	9.41	0.22	0	4.64	1753.4	0	3.17	0	0	421.93	18.25	0.21
HR	6.68	0	0	4.32	0.44	0	5.69	1955.8	0	2.36	0	0	0	4.81	0.51
HU	3.95	0	0	14.92	0.03	0	0	48.33	0	0	0	3.01	0	11.94	5.04
IE	33.27	0	0	2.57	0.12	0	2.54	0	0	21.77	0.88	1.61	0	7.61	0.97
IT	55.23	0	0.01	114.54	10.36	0	61.78	1693.37	0	10.11	0	0	0	147.76	97.63
LT	9.39	0	0	0	0	0	11.06	23.46	0	2.17	0	0	0	5.04	0
LU	0.04	0	0	5.61	0	0	5.04	0	0	0	0	0	0	1.13	0.15
LV	2.6	0	0	0.36	0.26	0	0	1472.02	0	0.2	0	0	0	2.85	0
ME	2.92	0	0	1.1	0	0	0	0	0	0.69	0	0	0	1.63	0
MK	0.96	0	0	2.13	0.29	0	0	265.54	0	0.12	0	0	0	3.52	0.65
NL	23.82	32.64	0	0	0	0	0	0	0	16.05	0.68	14.46	16083.07	5.9	2.91
NO	43.57	0	0	0	0.73	0	391.93	79421.13	0	23.54	0	0	0	7.59	0
PL	31.1	2.02	0	52.78	0.4	0	8.32	119.15	0	10.31	1.17	11.6	16223.69	1.09	19.86
PT	16.14	0	0	8.62	2.66	0	66.67	686.82	0	2.35	0	0	199.83	11.73	0.01
RO	9.31	0	0	1.81	0	0	18.55	10913.39	0	0	0	0	1597.37	11.18	0
RS	5.06	0	0	0	1.98	0	4.32	424.6	0	1.8	0	0	0	8.16	0
SE	40.22	0	0	0	1.88	0	158.68	29036.31	0	9.51	1.09	0.51	0	3.19	0.22
SI	2.01	0	0	0	0.19	0	0.54	1491.62	0	0	0	0	0	3.07	1.31
SK	4.4	0	0	1.64	1.1	0	3.94	277.62	0	0	0	1.66	0	2.31	0.01
UK	94.95	27.43	0	13	1.2	0	26.64	143.74	0	48.46	8.93	18.53	31153.59	51.77	31.64

Table A-35. Capacity distribution for Model Run 33 (Value of SOFC)

Country	Onshore	Offshore	PV /out Tracking	PV / Tracking	Run-of-river	Rooftop PV	PHS	Reservoir	Biomass CHP	PEM Electrolyzer	H2 OCGT	H2 CCGT	Salt Cavern	Vessel	Li-ion Battery
AL	3.08	0	0	0	0.03	0	0	1470.55	0	0.23	0	0	69.54	1.56	0
AT	36.46	0	0	27.92	4.61	0	114.15	1053.49	0	10.7	0	0	0	20.39	4.4
BA	11.05	0	0	4.31	0.28	0	1.61	1692.83	0	5.06	0	0	1614.97	4.45	1.69
BE	4.83	4.72	0	20.94	0.08	0	6.18	13.82	0	0	0	3.67	0	2.42	3.4
BG	3.4	0	0	4.24	0.61	0	40.59	1964.22	0	0	0	0	0	6.57	0
CH	9.32	0	0	4.28	3.74	0	163.81	5031.16	0	0	0	0	0	14.84	0
CZ	13.16	0	0	20.35	0.41	0	5.99	441.86	0	0.82	0.32	2.75	0	9.47	8.5
DE	36.19	22.22	0	36.87	4.15	0	39.27	5.46	0.51	0	3.21	23.28	21420.14	37.44	2.79
DK	17.96	0	0	0.14	0	0	0	0	0	12.08	1.09	0.97	8261.77	0.02	0.97
EE	10.17	0	0	2.89	0	0	0	0	0	4.59	0	0	0	2.49	0.02
ES	66.11	0	0.01	114.86	2.27	0	63.06	11148.12	0	13.65	0	0	3322.35	66.98	139.59
FI	24.05	0	0	0	2.96	0	0	518.99	0	7.04	0.44	0.34	0	41.16	7.47
FR	149.39	21.63	0.01	114.75	6.56	0	50.15	5071.64	0	47.37	1.56	13.29	18895.84	150.88	77.17
GR	14.34	0	0	9.38	0.22	0	4.64	1753.4	0	3.16	0	0	420.31	18.28	0.22
HR	6.63	0	0	4.31	0.44	0	5.69	1955.8	0	2.33	0	0	0	4.93	0.53
HU	3.89	0	0	14.89	0.03	0	0	48.33	0	0	0	3.02	0	12.32	4.99
IE	33.42	0	0	2.62	0.12	0	2.54	0	0	21.91	0.89	1.6	0	7.64	0.89
IT	55.18	0	0.01	114.43	10.36	0	61.78	1693.37	0	10.08	0	0	0	147.75	97.47
LT	9.39	0	0	0	0	0	11.06	23.46	0	2.17	0	0	0	5.04	0
LU	0.04	0	0	5.63	0	0	5.04	0	0	0	0	0	0	1.15	0.14
LV	2.6	0	0	0.31	0.26	0	0	1472.02	0	0.2	0	0	0	2.86	0.01
ME	2.92	0	0	1.14	0	0	0	0	0	0.7	0	0	0	1.63	0
MK	0.96	0	0	2.11	0.29	0	0	265.54	0	0.12	0	0	0	3.54	0.64
NL	23.82	32.6	0	0	0	0	0	0	0	16.06	0.68	14.46	16062.92	6.45	2.74
NO	43.56	0	0	0	0.73	0	391.93	79421.13	0	23.52	0	0	0	7.6	0
PL	31.01	2.02	0	52.75	0.4	0	8.32	119.15	0	10.2	1.17	11.6	16141.77	1.73	19.82
PT	16.11	0	0	8.61	2.66	0	66.67	686.82	0	2.35	0	0	188.39	11.95	0.01
RO	9.31	0	0	1.77	0	0	18.55	10913.39	0	0	0	0	1603.7	11.17	0
RS	5.06	0	0	0	1.98	0	4.32	424.6	0	1.81	0	0	0	8.11	0
SE	40.22	0	0	0	1.88	0	158.68	29036.31	0	9.41	1.12	0.5	0	3.49	0.22
SI	2.01	0	0	0	0.19	0	0.54	1491.62	0	0	0	0	0	3.13	1.33
SK	4.4	0	0	1.64	1.1	0	3.94	277.62	0.07	0	0	1.6	0	2.29	0.01
UK	94.92	27.41	0	13.09	1.2	0	26.64	143.74	0	48.44	8.92	18.52	31111.94	53.28	31.86

Table A-36. Capacity distribution for Model Run 34 (Value of PEMFC)

Country	Onshore	Offshore	PV /out Tracking	PV / Tracking	Run-of-river	Rooftop PV	PHS	Reservoir	Biomass CHP	PEM Electrolyzer	H2 OCGT	H2 CCGT	Salt Cavern	Vessel	Li-ion Battery
AL	3.08	0	0	0.01	0.03	0	0	1470.55	0	0.23	0	0	71.52	1.58	0
AT	36.46	0	0	27.91	4.61	0	114.15	1053.49	0	10.7	0	0	0	20.35	4.41
BA	11.05	0	0	4.3	0.28	0	1.61	1692.83	0	5.06	0	0	1614.67	4.47	1.69
BE	4.83	4.72	0	20.92	0.08	0	6.18	13.82	0	0	0	3.67	0	3.19	3.4
BG	3.4	0	0	4.24	0.61	0	40.59	1964.22	0	0	0	0	0	6.53	0
CH	9.32	0	0	4.3	3.74	0	163.81	5031.16	0	0	0	0	0	14.84	0
CZ	13.16	0	0	20.37	0.41	0	5.99	441.86	0	0.82	0.32	2.75	0	9.46	8.47
DE	36.18	22.22	0.01	36.88	4.15	0	39.27	5.46	0.51	0	3.2	23.28	21412.35	37.45	2.84
DK	17.96	0	0	0.14	0	0	0	0	0	12.08	1.09	0.93	8261.12	0.05	0.97
EE	10.17	0	0	2.9	0	0	0	0	0	4.59	0	0	0	2.5	0.02
ES	66.11	0	0.02	114.84	2.27	0	63.06	11148.12	0	13.65	0	0	3317.8	67.21	139.51
FI	24.05	0	0	0	2.96	0	0	518.99	0	7.04	0.44	0.35	0	41.06	7.47
FR	149.4	21.63	0.01	114.75	6.56	0	50.15	5071.64	0	47.38	1.55	13.29	18900.2	149.31	77.23
GR	14.34	0	0	9.38	0.22	0	4.64	1753.4	0	3.16	0	0	421.25	18.31	0.22
HR	6.63	0	0	4.31	0.44	0	5.69	1955.8	0	2.33	0	0	0	4.93	0.52
HU	3.89	0	0	14.89	0.03	0	0	48.33	0	0	0	3.02	0	12.2	5.01
IE	33.41	0	0	2.62	0.12	0	2.54	0	0	21.9	0.88	1.57	0	7.65	0.83
IT	55.19	0	0.01	114.41	10.36	0	61.78	1693.37	0	10.08	0	0	0	147.74	97.47
LT	9.39	0	0	0	0	0	11.06	23.46	0	2.17	0	0	0	5.04	0
LU	0.04	0	0	5.65	0	0	5.04	0	0	0	0	0	0	1.16	0.16
LV	2.6	0	0	0.31	0.26	0	0	1472.02	0	0.19	0	0	0	2.86	0.01
ME	2.92	0	0	1.15	0	0	0	0	0	0.7	0	0	0	1.61	0
MK	0.96	0	0	2.11	0.29	0	0	265.54	0	0.12	0	0	0	3.54	0.64
NL	23.82	32.6	0	0	0	0	0	0	0	16.05	0.68	14.46	16044.52	6.2	2.73
NO	43.57	0	0	0	0.73	0	391.93	79421.13	0	23.52	0	0	0	7.61	0
PL	31.01	2.02	0	52.76	0.4	0	8.32	119.15	0	10.2	1.16	11.62	16138.09	2.4	19.79
PT	16.11	0	0	8.61	2.66	0	66.67	686.82	0	2.35	0	0	190.38	11.93	0.02
RO	9.31	0	0	1.75	0	0	18.55	10913.39	0	0	0	0	1600.13	11.21	0.01
RS	5.06	0	0	0	1.98	0	4.32	424.6	0	1.81	0	0	0	8.1	0
SE	40.22	0	0	0	1.88	0	158.68	29036.31	0	9.42	1.12	0.54	0	3.86	0.22
SI	2.01	0	0	0	0.19	0	0.54	1491.62	0	0	0	0	0	3.13	1.33
SK	4.4	0	0	1.64	1.1	0	3.94	277.62	0.07	0	0	1.6	0	2.41	0.01
UK	94.89	27.42	0	13.1	1.2	0	26.64	143.74	0	48.43	8.93	18.55	31115.84	54.42	31.93

Table A-37. Capacity distribution for Model Run 35 (Value of H₂ OCGT)

Country	Onshore	Offshore	PV /out Tracking	PV / Tracking	Run-of-river	Rooftop PV	PHS	Reservoir	Biomass CHP	PEM Electrolyzer	H2 OCGT	H2 CCGT	Salt Cavern	Vessel	Li-ion Battery
AL	3.08	0	0	0	0.03	0	0	1470.55	0	0.25	0	0	82.54	1.39	0
AT	36.22	0	0	28.04	4.61	0	114.15	1053.49	0	10.55	0	0	0	19.23	4.5
BA	11.05	0	0	4.56	0.28	0	1.61	1692.83	0	5.29	0	0	1740.57	0.05	1.76
BE	4.83	4.72	0	21.71	0.08	0	6.18	13.82	0	0	0	3.39	0	40.05	4.01
BG	3.3	0	0	4.37	0.61	0	40.59	1964.22	0	0	0	0	0	6.34	0
CH	9.15	0	0	4.08	3.74	0	163.81	5031.16	0	0	0	0	0	17.56	0
CZ	12.99	0	0	21.06	0.41	0	5.99	441.86	0	0.81	0	3.14	0	14.26	8.85
DE	35.92	22.43	0	37.14	4.15	0	39.27	5.46	0.54	0	0	25.98	19892.88	82.58	3.8
DK	17.9	0	0	0.14	0	0	0	0	0	11.79	0	1.67	7480.69	0.02	0.48
EE	10.17	0	0	3.2	0	0	0	0	0	4.63	0	0	0	5.15	0.01
ES	66.27	0	0.01	116.34	2.27	0	63.06	11148.12	0	14.36	0	0	3442.01	61.27	136.94
FI	24.01	0	0	0	2.96	0	0	518.99	0	6.94	0	0.45	0	44.61	9.43
FR	150.79	21.59	0.01	115.31	6.56	0	50.15	5071.64	0	48.48	0	13.33	17064.9	182.4	81.08
GR	14.17	0	0	9.34	0.22	0	4.64	1753.4	0	3.09	0	0	399.59	19.57	0.35
HR	6.85	0	0	4.29	0.44	0	5.69	1955.8	0	2.5	0	0	0	4.51	0.39
HU	3.91	0	0	15.38	0.03	0	0	48.33	0	0	0	2.87	0	14.24	5.62
IE	34.42	0	0	3.32	0.12	0	2.54	0	0	22.81	0	2.4	0	6.29	1.1
IT	56.11	0	0.01	113.98	10.36	0	61.78	1693.37	0	10.2	0	0	0	149.44	97.32
LT	9.36	0	0	0	0	0	11.06	23.46	0	2.16	0	0	0	5.22	0
LU	0.04	0	0	5.65	0	0	5.04	0	0	0	0	0	0	1.53	0.16
LV	2.61	0	0	0.02	0.26	0	0	1472.02	0	0.18	0	0	0	2.86	0
ME	2.92	0	0	1.06	0	0	0	0	0	0.57	0	0	0	1.68	0
MK	0.96	0	0	2.02	0.29	0	0	265.54	0	0.09	0	0	0	3.46	0.57
NL	23.82	32.93	0	0	0	0	0	0	0	16.23	0	15.26	15315.09	11.25	2.04
NO	43.53	0	0	0	0.73	0	391.93	79421.13	0	23.37	0	0	0	7.56	0
PL	31.01	2.02	0	54.59	0.4	0	8.32	119.15	0	10.17	0	12.61	15600.11	17.14	22.06
PT	16.08	0	0	8.32	2.66	0	66.67	686.82	0	2.25	0	0	249.31	10.7	0.01
RO	9.3	0	0	1.62	0	0	18.55	10913.39	0	0	0	0	1467.91	13.87	0
RS	5.06	0	0	0	1.98	0	4.32	424.6	0	1.72	0	0	0	8.63	0
SE	40.04	0	0	0	1.88	0	158.68	29036.31	0	9.2	0	1.82	0	3.24	0.14
SI	2.01	0	0	0	0.19	0	0.54	1491.62	0	0	0	0	0	5.97	0.83
SK	4.4	0	0	1.64	1.1	0	3.94	277.62	0	0	0	1.83	0	3.94	0
UK	93.63	24.05	0	12.89	1.2	0	26.64	143.74	0	45.16	0	27.69	31794.76	83.23	31.72

Table A-38. Capacity distribution for Model Run 36 (Value of H₂ CCGT)

Country	Onshore	Offshore	PV /out Tracking	PV / Tracking	Run-of-river	Roof-top PV	PHS	Reservoir	Biomass CHP	PEM Electrolyzer	H2 OCGT	H2 CCGT	Salt Cavern	Vessel	Li-ion Battery
AL	3.08	0	0	0	0.03	0	0	1470.55	0	0.17	0	0	83.86	0.64	0.13
AT	36.87	0	0	28.62	4.61	0	114.15	1053.49	0	9.26	0	0	0	16.93	1.6
BA	9.88	0	0	4.25	0.28	0	1.61	1692.83	0	4.21	0	0	1111.4	5.7	2.2
BE	5.17	4.72	0	23.45	0.08	0	6.18	13.82	0	0	0	0	0	22	7.97
BG	2.59	0	0	4.4	0.61	0	40.59	1964.22	0	0	0	0	0	6.17	0.01
CH	9.16	0	0	5.21	3.74	0	163.81	5031.16	0	0	0	0	0	15.93	0
CZ	12.8	0	0	19.87	0.41	0	5.99	441.86	1.41	0	0.71	0	0	10.25	7.81
DE	33.46	22.32	0.01	35.99	4.15	0	39.27	5.46	9.68	0	6.28	0	18860.86	53.94	11.27
DK	17.14	0	0	0	0	0	0	0	0	11.23	2.45	0	9657.85	0.09	0.74
EE	10.36	0	0	0.94	0	0	0	0	0	4.68	0	0	0	6.04	0.32
ES	65.48	0	0.02	112.7	2.27	0	63.06	11148.12	0	12.41	0	0	3177.39	75.5	138.24
FI	24.55	0	0	0	2.96	0	0	518.99	0	6.94	0.66	0	0	52.75	7.29
FR	148.19	22.78	0.01	113.77	6.56	0	50.15	5071.64	0	45.63	4.98	0	19409.67	116.44	83.51
GR	13.48	0	0	8.45	0.22	0	4.64	1753.4	0	2.25	0	0	589.4	15.18	0.54
HR	5.83	0	0	3.8	0.44	0	5.69	1955.8	0	1.37	0	0	0	4.26	0.33
HU	0.53	0	0	12.09	0.03	0	0	48.33	0.58	0	1.63	0	0	7.42	3.74
IE	32.35	0	0	5.02	0.12	0	2.54	0	0	21.3	1.48	0	0	11.43	0.76
IT	55.78	0	0.01	115.96	10.36	0	61.78	1693.37	0	10.1	0	0	0	145.74	109.54
LT	9.36	0	0	0	0	0	11.06	23.46	0	1.94	0	0	0	5.22	0.2
LU	0.04	0	0	6	0	0	5.04	0	0	0	0	0	0	1.3	0.57
LV	2.55	0	0	0.01	0.26	0	0	1472.02	0	0.12	0	0	0	4.65	0.12
ME	2.92	0	0	0.01	0	0	0	0	0	0.37	0	0	0	2.57	0.01
MK	0.96	0	0	2.01	0.29	0	0	265.54	0	0.02	0	0	0	2.24	1.44
NL	23.82	31.6	0	0.01	0	0	0	0	0	15.7	8.74	0	20176.72	5.87	0.7
NO	40.03	0	0	0	0.73	0	391.93	79421.13	0	21.63	0	0	0	8.35	0
PL	28.23	0.91	0	50.53	0.4	0	8.32	119.15	3.5	6.92	3.49	0	12736.17	17.73	20.86
PT	15.02	0	0	8.1	2.66	0	66.67	686.82	0	1.99	0	0	145.85	13.03	0.07
RO	9.54	0	0	0.75	0	0	18.55	10913.39	0	0	0	0	1617.6	13.55	0.15
RS	5.06	0	0	0	1.98	0	4.32	424.6	0	1.54	0	0	0	10.18	0
SE	40.21	0	0	0	1.88	0	158.68	29036.31	0	8.98	2.4	0	0	4.23	0.1
SI	2.01	0	0	0	0.19	0	0.54	1491.62	0	0	0	0	0	2.71	0.34
SK	4.1	0	0	1.64	1.1	0	3.94	277.62	2.61	0	0.01	0	0	4.44	1.07
UK	94.96	30.18	0	14.63	1.2	0	26.64	143.74	0	50.32	12.56	0	33397.74	122.45	37.49

Table A-39. Capacity distribution for Model Run 37 (Value of Salt Cavern)

Country	Onshore	Offshore	PV /out Tracking	PV / Tracking	Run-of-river	Rooftop PV	PHS	Reservoir	Biomass CHP	PEM Electrolyzer	H2 OCGT	H2 CCGT	Salt Cavern	Vessel	Li-ion Battery
AL	4.38	0	0	0.01	0.03	0	0	1470.55	0	1.3	0	0	0	4.44	0
AT	33.98	0	0	34.59	4.61	0	114.15	1053.49	0	2.01	0	0	0	64.03	2.05
BA	7.4	0	0	0.01	0.28	0	1.61	1692.83	0	2.32	0	0	0	2.48	0.01
BE	1.75	4.72	0	13.17	0.08	0	6.18	13.82	4.75	0	0	3.86	0	345.16	10.82
BG	2.05	0	0	5.67	0.61	0	40.59	1964.22	0	0	0	0	0	9.69	0
CH	10.19	0	0	5.13	3.74	0	163.81	5031.16	0	0	0	0	0	68.48	0
CZ	9.43	0	0	22.67	0.41	0	5.99	441.86	3.86	0	0	0	0	18.96	5.98
DE	35.51	15.99	0.01	34.8	4.15	0	39.27	5.46	26.71	0	0	7.32	0	203.79	2.05
DK	6.09	0	0	0	0	0	0	0	0	0	0	0	0	46.83	0.07
EE	10.17	0	0	0	0	0	0	0	0	2.27	0	0	0	10.09	0.02
ES	88.94	0	0.02	106.53	2.27	0	63.06	11148.12	0	31.69	1.34	0	0	426.44	87.34
FI	24.12	0	0	0	2.96	0	0	518.99	0	5.73	0.44	0.39	0	104.93	6.41
FR	136.95	25.03	0.01	113.53	6.56	0	50.15	5071.64	8.9	31.42	0	2.3	0	1546.44	75.42
GR	15.23	0	0	10.93	0.22	0	4.64	1753.4	0	4.75	0	0	0	91.76	0.45
HR	5.2	0	0	6.89	0.44	0	5.69	1955.8	0	0.71	0	0	0	11.35	0.08
HU	0	0	0	11.87	0.03	0	0	48.33	3.97	0	0	1.88	0	42.84	2.55
IE	17.26	0	0	6.76	0.12	0	2.54	0	0.25	5.81	0.53	3.44	0	552.64	3.13
IT	58.14	0	0.01	91.18	10.36	0	61.78	1693.37	0	7.12	0	0	0	640.44	89.57
LT	8.66	0	0	0	0	0	11.06	23.46	0	0	0	0	0	11.48	0.24
LU	0.04	0	0	6.22	0	0	5.04	0	0	0	0	0	0	14.81	1.41
LV	2.34	0	0	0	0.26	0	0	1472.02	0	0	0	0	0	17.3	0.05
ME	3.88	0	0	2.02	0	0	0	0	0	0.11	0	0	0	1.26	0
MK	1.92	0	0	1.5	0.29	0	0	265.54	0	0.23	0	0	0	5.76	0.4
NL	15.62	29.64	0	0	0	0	0	0	4	1.71	0	2.68	0	311.05	7.88
NO	66.77	0	0	0	0.73	0	391.93	79421.13	0	48.92	0	0	0	56.58	0
PL	14.89	0	0	36.41	0.4	0	8.32	119.15	14.25	0	0	0.62	0	133.44	15.87
PT	17.5	0	0	9.6	2.66	0	66.67	686.82	0	4.74	0	0	0	39.24	0.01
RO	10.08	0	0	0.75	0	0	18.55	10913.39	0	0	0	0	0	44.27	1.06
RS	5.06	0	0	2.25	1.98	0	4.32	424.6	0	2.61	0	0	0	16.12	0
SE	44.49	0	0	0	1.88	0	158.68	29036.31	0	11.83	0	0	0	62.49	0.2
SI	2.01	0	0	1.08	0.19	0	0.54	1491.62	0	0	0	0	0	5.55	0
SK	2.91	0	0	1.64	1.1	0	3.94	277.62	0.11	0	0	0	0	14.59	0
UK	62.7	37.02	0	10.99	1.2	0	26.64	143.74	11	26.4	8.23	6.44	0	3262.45	35.68

Table A-40. Capacity distribution for Model Run 38 (Value of Vessel)

Country	Onshore	Offshore	PV /out Tracking	PV / Tracking	Run-of-river	Rooftop PV	PHS	Reservoir	Biomass CHP	PEM Electrolyzer	H2 OCGT	H2 CCGT	Salt Cavern	Vessel	Li-ion Battery
AL	3.08	0	0	0	0.03	0	0	1470.55	0	0.22	0	0	230.5	0	0.01
AT	37.2	0	0	27.04	4.61	0	114.15	1053.49	0	11.18	0	0	0	0	2.67
BA	10.98	0	0	4.4	0.28	0	1.61	1692.83	0	4.95	0	0	1734.5	0	1.91
BE	4.83	4.72	0	20.65	0.08	0	6.18	13.82	0	0	0.04	3.82	0	0	3.31
BG	3.06	0	0	4.55	0.61	0	40.59	1964.22	0	0	0	0	0	0	0
CH	9.8	0	0	4.25	3.74	0	163.81	5031.16	0	0	0	0	0	0	0
CZ	13.16	0	0	19.06	0.41	0	5.99	441.86	0	0.17	1.68	1.61	0	0	8.07
DE	36.77	21.76	0	36.72	4.15	0	39.27	5.46	0	0	4.98	23.05	22062.6	0	2.4
DK	17.77	0	0	0.04	0	0	0	0	0	12.05	1.01	0.99	8371.89	0	0.92
EE	10.74	0	0	1.73	0	0	0	0	0	5.06	0	0	0	0	0.29
ES	65.31	0	0.01	115.05	2.27	0	63.06	11148.12	0	12.52	0	0	6209.45	0	145.53
FI	23.8	0	0	0	2.96	0	0	518.99	0	6.93	0.56	0.31	0	0	7.1
FR	148.36	21.32	0.01	110.68	6.56	0	50.15	5071.64	0	45.83	5.07	12.78	25527.96	0	69.81
GR	14.46	0	0	8.51	0.22	0	4.64	1753.4	0	2.67	0	0	1338.92	0	0.82
HR	6.44	0	0	4.2	0.44	0	5.69	1955.8	0	2	0	0	0	0	0.52
HU	3.06	0	0	13.96	0.03	0	0	48.33	0	0	0.32	2.17	0	0	4.47
IE	37.74	0	0	3.38	0.12	0	2.54	0	0	25.83	0.87	1.44	0	0	1.06
IT	54.39	0	0	115.12	10.36	0	61.78	1693.37	0	10.15	0	0	0	0	99.24
LT	9.59	0	0	0	0	0	11.06	23.46	0	2.38	0	0	0	0	0.01
LU	0.04	0	0	5.46	0	0	5.04	0	0	0	0	0	0	0	0
LV	2.62	0	0	1.15	0.26	0	0	1472.02	0	0.19	0	0	0	0	0.01
ME	2.92	0	0	0.47	0	0	0	0	0	0.37	0	0	0	0	0
MK	0.96	0	0	2.07	0.29	0	0	265.54	0	0.15	0	0	0	0	0.62
NL	23.82	32.7	0	0	0	0	0	0	0	16.45	1.08	13.69	16251.44	0	2.96
NO	44.08	0	0	0	0.73	0	391.93	79421.13	0	23.85	0	0	0	0	0
PL	31.02	2	0	49.44	0.4	0	8.32	119.15	0	9.9	1.31	11.45	17036.79	0	17.19
PT	16.18	0	0	8.2	2.66	0	66.67	686.82	0	2.25	0	0	918.83	0	0.02
RO	9.35	0	0	1.92	0	0	18.55	10913.39	0	0	0	0	2370.22	0	0
RS	5.06	0	0	0	1.98	0	4.32	424.6	0	1.77	0	0	0	0	0
SE	40.22	0	0	0	1.88	0	158.68	29036.31	0	9.44	0.98	0.83	0	0	0.21
SI	2.01	0	0	0	0.19	0	0.54	1491.62	0	0	0	0	0	0	1.59
SK	4.4	0	0	1.64	1.1	0	3.94	277.62	0.72	0	0	1.98	0	0	0.04
UK	93.52	29.47	0	13.42	1.2	0	26.64	143.74	0	49.43	9.34	17.98	33800.47	0	33.68

Table A-41. Capacity distribution for Model Run 39 (Value of Lithium-ion Battery)

Country	Onshore	Offshore	PV /out Tracking	PV / Tracking	Run-of-river	Rooftop PV	PHS	Reservoir	Biomass CHP	PEM Electrolyzer	H2 OCGT	H2 CCGT	Salt Cavern	Vessel	Li-ion Battery
AL	3.08	0	0	0	0.03	0	0	1470.55	0	0.22	0	0	107.18	0.06	0
AT	34.51	0	0	22.68	4.61	0	114.15	1053.49	0	7.39	0.2	0	0	8.56	0
BA	11.05	0	0	6.05	0.28	0	1.61	1692.83	0	5.83	0	0	1588.92	0	0
BE	5.51	4.72	0	18.9	0.08	0	6.18	13.82	0	0	3.25	5.46	0	34.95	0
BG	3.8	0	0	4.26	0.61	0	40.59	1964.22	0	0	0	0	0	5.84	0
CH	9.8	0	0	3	3.74	0	163.81	5031.16	0	0	0	0	0	8.33	0
CZ	12.09	0	0	10.72	0.41	0	5.99	441.86	0.67	0	0.91	2.09	0	5.05	0
DE	29.14	22.83	0	34.62	4.15	0	39.27	5.46	3.71	0	12.88	23.99	23389.79	0.05	0
DK	17.27	0	0	0.04	0	0	0	0	0	10.58	3.77	0.53	9098.62	0	0
EE	9.69	0	0	3.6	0	0	0	0	0	4.33	0	0	0	2.47	0
ES	94.76	0.72	7.47	83.05	2.27	0	63.06	11148.12	0	24.22	10.75	2.78	9203.14	83.14	0
FI	24.16	0	0	0	2.96	0	0	518.99	0	6.82	1.66	1.05	0	46.54	0
FR	161.81	25.29	0.15	98.19	6.56	0	50.15	5071.64	0.01	56.63	21.06	17.86	17840.62	360	0
GR	15.18	0	0	9.73	0.22	0	4.64	1753.4	0	3.95	0	0	489.06	14.45	0
HR	6.95	0	0	3.99	0.44	0	5.69	1955.8	0	3	0.02	0	0	0.33	0
HU	3.81	0	0	11.36	0.03	0	0	48.33	0	0	4.03	2.44	0	56.5	0
IE	37.08	0	0	1.88	0.12	0	2.54	0	0	25.04	1.58	1.57	0	7.24	0
IT	56.37	0	24.51	57.56	10.36	0	61.78	1693.37	1.42	7.67	8.13	2.95	0	189.15	0
LT	8.28	0	0	0	0	0	11.06	23.46	0	1.4	0	0	0	4.36	0
LU	0.04	0	0	4.52	0	0	5.04	0	0	0	0	0	0	1.94	0
LV	2.74	0	0	0.01	0.26	0	0	1472.02	0	0.25	0	0	0	2.83	0
ME	2.92	0	0	0.89	0	0	0	0	0	0.32	0	0	0	0.71	0
MK	0.96	0	0	2.59	0.29	0	0	265.54	0	0.23	0	0	0	0.78	0
NL	22.47	34.96	0	0	0	0	0	0	0	17.47	1.35	11.97	16735.82	0	0
NO	43.7	0	0	0	0.73	0	391.93	79421.13	0	23.33	0	0	0	2.2	0
PL	31.79	3.83	0	48.04	0.4	0	8.32	119.15	0	10.33	3.15	10.17	14651.35	0.04	0
PT	17.02	0	0	9.04	2.66	0	66.67	686.82	0	3.39	0	0	443.49	14.33	0
RO	9.64	0	0	5.59	0	0	18.55	10913.39	0	0	0	0	835.74	6.13	0
RS	5.06	0	0	0	1.98	0	4.32	424.6	0	1.71	0	0	0	0	0
SE	38.59	0	0	0	1.88	0	158.68	29036.31	0	8.13	3.31	0.35	0	5.11	0
SI	2.76	0	0	0	0.19	0	0.54	1491.62	0	0	0.07	0	0	4.32	0
SK	4.4	0	0	2.12	1.1	0	3.94	277.62	0.93	0	0.07	2.44	0	0.89	0
UK	100.82	24.61	0	8.7	1.2	0	26.64	143.74	0	51.93	16.39	20.83	26212	70.83	0

Table A-42. Capacity distribution for Model Run 40 (Value of Pipeline)

Country	Onshore	Offshore	PV /out Tracking	PV / Tracking	Run-of-river	Roof-top PV	PHS	Reservoir	Biomass CHP	PEM Electrolyzer	H2 OCGT	H2 CCGT	Salt Cavern	Vessel	Li-ion Battery
AL	3.08	0	0	0	0.03	0	0	1470.55	0	0.27	0	0	162.4	0	0.13
AT	35.63	0	0	26.57	4.61	0	114.15	1053.49	0	4.09	0	0	0	262.04	6.26
BA	7.4	0	0	3.08	0.28	0	1.61	1692.83	0	0.57	0	0	320.48	0	0.83
BE	6.52	4.72	0	32.91	0.08	0	6.18	13.82	1.17	6.02	0	0	0	391.98	14.13
BG	3.86	0	0	6.07	0.61	0	40.59	1964.22	0	1.13	0	0	0	15.41	0
CH	10.43	0	0	8.18	3.74	0	163.81	5031.16	0	3.25	0	0	0	183.52	0
CZ	15.48	0	0	22.87	0.41	0	5.99	441.86	2.44	3.66	0	0	0	236.1	4.56
DE	48.79	30.63	0	41.78	4.15	0	39.27	5.46	8.55	34.68	2.49	10.61	23785.7	87.3	4.98
DK	13.19	0	0	0.14	0	0	0	0	0	5.05	0.41	4.16	4480.69	0.01	0.03
EE	8.62	0	0	0	0	0	0	0	0	0.37	0	0	0	20.39	0
ES	67.51	0	0.01	119.16	2.27	0	63.06	11148.12	0	21.78	0.1	0	5232.73	105.48	139.8
FI	19.14	0.04	0	0	2.96	0	0	518.99	0.71	2.67	0.06	0.22	0	178.22	7.89
FR	140.95	25.93	0	128.13	6.56	0	50.15	5071.64	5.38	36.4	0.69	3.16	7044.73	1359.47	127.9
GR	14.48	0	0	11.46	0.22	0	4.64	1753.4	0	4.26	0	0	901.56	36.42	1.42
HR	5.88	0	0	7.77	0.44	0	5.69	1955.8	0	1.6	0	0	0	68.82	0.01
HU	3.48	0	0	16.22	0.03	0	0	48.33	2.3	1.57	0	0	0	105.89	5.67
IE	11.27	0	0	5.8	0.12	0	2.54	0	0.11	1.94	0	0	0	159.07	3.41
IT	65.71	0	0	150.17	10.36	0	61.78	1693.37	0	30.23	0	0	0	1580.48	88.65
LT	9.23	0	0	0	0	0	11.06	23.46	0	1.13	0	0	0	78.06	0
LU	0.13	0	0	6.22	0	0	5.04	0	0	0.29	0	0	0	20.86	0.73
LV	3.16	0	0	0	0.26	0	0	1472.02	0	0.75	0	0	0	35.29	0
ME	2.92	0	0	0.06	0	0	0	0	0	0.1	0	0	0	2.71	0
MK	1.53	0	0	1.97	0.29	0	0	265.54	0	0.41	0	0	0	18.95	0.64
NL	26.12	31.4	0	1.22	0	0	0	0	0	15.57	0.03	17.4	16335.46	0	1.96
NO	4.1	0	0	0	0.73	0	391.93	79421.13	0	1.2	0	0	0	9.85	0
PL	41.74	2.09	0	63.54	0.4	0	8.32	119.15	0	18.32	1.27	12.62	14798.76	0	20.44
PT	15.88	0	0	9.53	2.66	0	66.67	686.82	0	3.48	0	0	1157.4	2.84	0.06
RO	10.85	0	0	8.76	0	0	18.55	10913.39	0	4.01	0	0	1667.24	24.01	0.09
RS	5.06	0	0	0	1.98	0	4.32	424.6	0	1.43	0	0	0	33.91	0
SE	26.86	0	0	0	1.88	0	158.68	29036.31	0	0.38	0	0	0	20.5	0
SI	2.93	0	0	1.74	0.19	0	0.54	1491.62	0	0.9	0	0	0	44.67	0.38
SK	4.4	0	0	1.64	1.1	0	3.94	277.62	2.22	1.06	0	0	0	73.56	2.73
UK	96.54	20.87	0	21.5	1.2	0	26.64	143.74	0	50.39	7.7	25.04	35272.66	720.07	20.59

Table A-43. Capacity distribution for Model Run 41 (Value of HVAC Connections)

Country	Onshore	Offshore	PV /out Tracking	PV / Tracking	Run-of-river	Rooftop PV	PHS	Reservoir	Biomass CHP	PEM Electrolyzer	H2 OCGT	H2 CCGT	Salt Cavern	Vessel	Li-ion Battery
AL	3.08	0	0	2.04	0.03	0	0	1470.55	0	0.39	0.2	0.26	342.91	0	0.84
AT	16.04	0	0	10.42	4.61	0	114.1	1053.49	0.68	8.65	1.1	3.38	0	0	8.82
BA	3.73	0	0	2.58	0.28	0	1.61	1692.83	0	2.72	0	0	1232.74	0	0
BE	9.47	4.72	0	19.13	0.08	0	6.18	13.82	4.75	0	0	7.69	0	0	17.8
BG	3.88	0	0	7.88	0.61	0	40.59	1964.22	0	1.02	0.3	0.22	0	0	6.93
CH	10.37	0	1.5	6.72	3.74	0	163.8	5031.16	1	3.97	1.4	5.13	0	0	6.21
CZ	7.19	0	0	11.03	0.41	0	5.99	441.86	4.48	0.01	0.5	2.09	0	0	8.51
DE	60.99	12.6	1.4	52.73	4.15	13.5	39.27	5.46	25.5	7.93	5.2	32.2	21256.1	0.01	51.09
DK	15.42	0	0	1.14	0	0	0	0	0	11.1	0.5	0.59	14475.9	0	1.05
EE	3.22	1.01	0	4.06	0	0	0	0	0	2.95	0.3	0.62	0	1.16	1.89
ES	48.76	0	0.9	200.6	2.27	0	63.06	11148.1	0.74	30.6	6.0	13.0	15869.5	0.01	417.7
FI	29.38	0	0	0	2.96	0	0	518.99	0	12.2	0.7	4.02	0	26.9	7.13
FR	130.4	2.02	0.0	148.4	6.56	0	50.15	5071.64	8.99	54.6	7.1	37.0	40644.4	3.96	171.0
G	13.94	0	0	15.83	0.22	0	4.64	1753.4	0	5.84	0.4	1	2045.48	0.01	26.93
HR	4.79	0	0	3.86	0.44	0	5.69	1955.8	0	2.03	0.1	0.6	0	0	1.43
HU	4.92	0	0	9.43	0.03	0	0	48.33	4.17	0	0.4	2.24	0	0	8.74
IE	59.3	0	0	3.11	0.12	0	2.54	0	0	48.5	1.7	2.03	0	0	0.69
IT	36.43	0	0.0	122.3	10.3	0	61.78	1693.37	8.26	9.09	1.1	10.4	0	47.5	184.9
LT	5.11	0	0	6.48	0	0	11.06	23.46	0.56	1.79	0	1.43	0	0	0.94
LU	0.15	0	0	2.93	0	0	5.04	0	0	0	0	0.31	0	0	1.93
LV	4.21	0	0	4.31	0.26	0	0	1472.02	0.74	1.76	0	0.21	0	0.09	2.99
M	3.31	0	0	2.12	0	0	0	0	0	2.03	0	0	0	0	1.93
M	0.96	0	0	0.33	0.29	0	0	265.54	0	0.15	0.0	0.39	0	0	0.22
NL	22.47	11.6	0	22.72	0	0	0	0	0.61	11.9	3.7	10.9	14035.0	0	14.82
N	57.75	0	0	0	0.73	0	391.9	79421.1	0	37.4	0.6	0.83	0	7.32	1.58
PL	22.23	1.78	0	30.76	0.4	0	8.32	119.15	7.1	3.93	2.1	9.84	12690.3	0	19.21
PT	10.58	0	0	22.1	2.66	0	66.67	686.82	0	4.72	0.5	0.21	1182.02	0	30.29
R	7.91	0.3	0	11.3	0	0	18.55	10913.3	0.33	1.35	0.0	1.51	3327.19	0	9.02
RS	5.06	0	0	5.13	1.98	0	4.32	424.6	0	2.39	0.8	0.7	0	0	1.43
SE	50.4	0	0	7.14	1.88	0	158.6	29036.3	0	23.4	3.4	10.4	0	0.01	5.02
SI	2.18	0	0	2.31	0.19	0	0.54	1491.62	0	0	0.4	0.73	0	0	1.41
SK	2.91	0	0	3.82	1.1	0	3.94	277.62	1.29	0.32	0.1	1.21	0	0	0
UK	117.0	10.0	0	35.35	1.2	0	26.64	143.74	2.89	60.4	7.5	29.7	46152.1	0.01	48.88

Table A-44. Capacity distribution for Model Run 42 (Value of HVDC Connections)

Country	Onshore	Offshore	PV /out Tracking	PV / Tracking	Run-of-river	Roof-top PV	PHS	Reservoir	Biomass CHP	PEM Electrolyzer	H2 OCGT	H2 CCGT	Salt Cavern	Vessel	Li-ion Battery
AL	2.07	0	0	0.18	0.03	0	0	1470.55	0	0	0	0	22.14	0.7	0
AT	37.11	0	0	26.89	4.61	0	114.15	1053.49	0	9.4	0	0	0	15.17	4.71
BA	9.2	0	0	5.05	0.28	0	1.61	1692.83	0	3.9	0	0	1273.41	0.09	0.61
BE	4.52	4.72	0	25.3	0.08	0	6.18	13.82	0	0	0	5.36	0	0.01	12.43
BG	3.63	0	0	3.63	0.61	0	40.59	1964.22	0	0	0	0	0	7.35	0.01
CH	9.8	0	0	5.01	3.74	0	163.81	5031.16	0	0	0	0	0	10.75	0
CZ	12.43	0	0	16.51	0.41	0	5.99	441.86	0.87	0	1.52	2.35	0	0.1	5.39
DE	39.04	25.85	0	40.75	4.15	0	39.27	5.46	10.1	2.57	4.51	28.51	24875.67	24.16	3.42
DK	17.4	0	0	0.11	0	0	0	0	0	10.63	0	0	5531.08	0.01	1.28
EE	10.97	0	0	1.98	0	0	0	0	0	4.57	0	0	0	3.66	0.44
ES	65.58	0	0.01	121.75	2.27	0	63.06	11148.12	0	14.91	0	0	3114.07	68.14	149.58
FI	23.29	0	0	0	2.96	0	0	518.99	0	7.65	0.51	2.68	0	26.6	7.44
FR	145.78	21.68	0.01	119.2	6.56	0	50.15	5071.64	0.15	51.75	2.35	16.25	21662.97	97.05	93.99
GR	14.1	0	0	8.95	0.22	0	4.64	1753.4	0	3.07	0	0	406.66	15.12	1.67
HR	4.65	0	0	1.99	0.44	0	5.69	1955.8	0	0.84	0	0	0	7.51	0.18
HU	2.22	0	0	16.6	0.03	0	0	48.33	0	0	0.15	2.47	0	9.44	6.84
IE	26.94	0	0	3.45	0.12	0	2.54	0	0	16.72	0.72	2.57	0	6.81	1.64
IT	57.24	0	0	129.32	10.36	0	61.78	1693.37	0	14.18	0.11	0.17	0	146.53	125.02
LT	10.68	0	0	0	0	0	11.06	23.46	0	2.85	0	0	0	4.39	0
LU	0.04	0	0	5.42	0	0	5.04	0	0	0	0	0	0	0.4	0
LV	2.6	0	0	0.01	0.26	0	0	1472.02	0	0.36	0	0	0	2.84	0
ME	2.83	0	0	2.49	0	0	0	0	0	1.09	0	0	0	1.97	0
MK	0.96	0	0	3	0.29	0	0	265.54	0	0.46	0	0	0	3.86	0.77
NL	22.47	33.07	0	0	0	0	0	0	0	15.52	0	14.61	15852.3	0.01	1.51
NO	48.79	0	0	0	0.73	0	391.93	79421.13	0	31.01	0	0	0	9	0
PL	31.23	2.77	0	53.48	0.4	0	8.32	119.15	0.25	10.3	0.29	12.1	15666.57	0.39	22.29
PT	16.6	0	0	7.48	2.66	0	66.67	686.82	0	2.46	0	0	245.64	10.66	0.01
RO	9.3	0	0	2.54	0	0	18.55	10913.39	0	0	0	0	1666.27	10.42	0
RS	5.06	0	0	0	1.98	0	4.32	424.6	0	1.97	0	0	0	4.94	0
SE	22.65	0	0	0	1.88	0	158.68	29036.31	0	7.24	0	0	0	4.59	0
SI	1.76	0	0	0	0.19	0	0.54	1491.62	0	0	0	0	0	4.35	2.26
SK	4.4	0	0	1.23	1.1	0	3.94	277.62	1.81	0	0	1.68	0	1.19	0.09
UK	101.32	27.23	0	20.71	1.2	0	26.64	143.74	0	59.85	9.46	27.38	36126.83	64.25	45.27

Table A-45. Capacity distribution for Model Run 43 (Value of Wind Energy)

Country	Onshore	Offshore	PV /out Tracking	PV / Tracking	Run-of-river	Rooftop PV	PHS	Reservoir	Biomass CHP	PEM Electrolyzer	H2 OCGT	H2 CCGT	Salt Cavern	Vessel	Li-ion Battery
AL	0	0	0	27.78	0.03	0	0	1470.55	0	9.71	0	0	3590.51	0	46.51
AT	0	0	0	76.46	4.61	0	114.15	1053.49	3.5	1.78	0	4.14	0	0.01	109.51
BA	0	0	0	42.59	0.28	0	1.61	1692.83	0	13.57	0	0	9824.44	0	59.31
BE	0	0	0	67.13	0.08	0	6.18	13.82	4.75	0	0	10.62	0	0	83.69
BG	0	0	0	23.72	0.61	0	40.59	1964.22	0	4.41	0	0	0	0	27.6
CH	0	0	0.03	8.84	3.74	0	163.81	5031.16	1.25	0	0	0.02	0	0	0.97
CZ	0	0	0	40.98	0.41	0	5.99	441.86	5	0	0	0	0	0	48.59
DE	0	0	0.01	54.27	4.15	0	39.27	5.46	27.75	0	0	25.46	49063.77	0.01	0.01
DK	0	0	0	5.99	0	0	0	0	3.75	0	0	0	1762.28	0	0.23
EE	0	0	0	0	0	0	0	0	1	0	0	0	0	1.8	0.01
ES	0	0	36.91	622.74	2.27	0	63.06	11148.12	0	268.07	0	0	70639.32	0.02	721.95
FI	0	0	0	0	2.96	0	0	518.99	3.75	0	0	1.9	0	10.58	1.26
FR	0	0	1.07	428.01	6.56	0	50.15	5071.64	26.87	62.02	0	17	67120.65	1.73	624.29
GR	0	0	0.01	61.49	0.22	0	4.64	1753.4	0	15.47	0	0	5979.38	0	100.72
HR	0	0	0	35	0.44	0	5.69	1955.8	0	10.68	0	0	0	0	44.89
HU	0	0	0	0.01	0.03	0	0	48.33	7.25	0	0	0	0	0	0
IE	0	0	0	38.79	0.12	0	2.54	0	0.25	0	0	0.03	0	0	45.99
IT	0	0	0.01	301.91	10.36	0	61.78	1693.37	14.75	44.66	0	0	0	149.88	506.31
LT	0	0	0	0.01	0	0	11.06	23.46	1.75	0	0	0	0	0.01	0.01
LU	0	0	0	6.22	0	0	5.04	0	0	0	0	0.69	0	0	0.01
LV	0	0	0	0.77	0.26	0	0	1472.02	1.75	0	0	0	0	3.31	0.01
ME	0	0	0	8.08	0	0	0	0	0	0.01	0	0	0	0	15.41
MK	0	0	0	4.12	0.29	0	0	265.54	0	0	0	0	0	0	7.2
NL	0	0	0	33.58	0	0	0	0	4	0	0	5.63	29514.74	0	0.02
NO	0	0	0	0.06	0.73	0	391.93	79421.13	0	1.73	0	0	0	7.39	0
PL	0	0	0.01	100.94	0.4	0	8.32	119.15	14.25	0	0	0.68	8608.83	0.01	105.21
PT	0	0	0.01	107.55	2.66	0	66.67	686.82	0	42.77	0	0	22358.05	0	134.06
RO	0	0	0	8.43	0	0	18.55	10913.39	5.07	0	0	0	1719.6	0	0.01
RS	0	0	0	0	1.98	0	4.32	424.6	0	0	0	0	0	0	0
SE	0	0	0	23.11	1.88	0	158.68	29036.31	5.5	0	0	0	0	0.16	0
SI	0	0	0	0.66	0.19	0	0.54	1491.62	0.75	0	0	0	0	0	0.01
SK	0	0	0	8.69	1.1	0	3.94	277.62	2.75	0	0	0	0	0	0
UK	0	0	0.01	99.96	1.2	0	26.64	143.74	12.5	0	0	30.63	100493.35	0.01	60

Table A-46. Capacity distribution for Model Run 44 (Value of Solar Energy)

Country	Onshore	Offshore	PV /out Tracking	PV / Tracking	Run-of-river	Rooftop PV	PHS	Reservoir	Biomass CHP	PEM Electrolyzer	H2 OCGT	H2 CCGT	Salt Cavern	Vessel	Li-ion Battery
AL	3.46	0	0	0	0.03	0	0	1470.55	0	0.19	0	0	70.8	0	0
AT	33.12	0	0	0	4.61	0	114.15	1053.49	0	1.66	0.59	1.17	0	0.01	4.43
BA	11.05	0	0	0	0.28	0	1.61	1692.83	0	2.78	0	0	1273.11	0	0
BE	1.83	3.67	0	0	0.08	0	6.18	13.82	4.75	0	0	3.37	0	0	7.41
BG	3.86	0	0	0	0.61	0	40.59	1964.22	0	0	0	0	0	2.88	0
CH	10.02	0	0	0	3.74	0	163.81	5031.16	0	0	0	0	0	0	0
CZ	17.39	0	0	0	0.41	0	5.99	441.86	2.43	0	0	2.21	0	0	0.64
DE	27.27	31.69	0	0	4.15	0	39.27	5.46	17.66	0	0	18.53	17358.24	0.01	24.03
DK	34.69	0.21	0	0	0	0	0	0	0	20.58	1.41	0	8584.43	0	1.66
EE	8.08	0	0	0	0	0	0	0	0	2.33	0	0	0	1.68	2.27
ES	82.44	0	0	0	2.27	0	63.06	11148.12	16.38	3.62	0	1.77	5189.2	11.61	30.57
FI	19.05	0	0	0	2.96	0	0	518.99	0	3.86	0.58	0.71	0	22.67	12.32
FR	127.67	27.37	0	0	6.56	0	50.15	5071.64	18.5	24.7	10.8	6.57	15435.21	13.09	51.49
GR	18.71	0	0	0	0.22	0	4.64	1753.4	0	2.05	1.25	0	1238.77	9.39	5.09
HR	6.49	0	0	0	0.44	0	5.69	1955.8	0	0	0	0	0	0	2.19
HU	3.51	0	0	0	0.03	0	0	48.33	1.32	0	0	0.66	0	0.01	0.47
IE	63.47	0	0	0	0.12	0	2.54	0	0	44.67	0.54	0.28	0	0	0.46
IT	57.43	0	0	0	10.36	0	61.78	1693.37	13.52	0	0	2.12	0	112.14	18.56
LT	4.6	4.08	0	0	0	0	11.06	23.46	0	1.48	0	0.65	0	3.88	0
LU	0	0	0	0	0	0	5.04	0	0	0	0	0.43	0	0	0
LV	4.21	1.06	0	0	0.26	0	0	1472.02	0	1.79	0	0	0	2.68	0.51
ME	2.92	0	0	0	0	0	0	0	0	0.4	0	0	0	0	0
MK	1.92	0	0	0	0.29	0	0	265.54	0	0.49	0	0	0	0.7	0.05
NL	12.84	24.82	0	0	0	0	0	0	4	0	1.93	8.09	9664.12	0	11.47
NO	52.56	0	0	0	0.73	0	391.93	79421.13	0	31.93	0	0	0	6.21	0
PL	35.98	1.85	0	0	0.4	0	8.32	119.15	5.4	1.34	0	3.06	6710.59	0.01	18.69
PT	15.77	4.32	0	0	2.66	0	66.67	686.82	1.25	1.18	0	0	694.81	0	4.46
RO	14.97	0	0	0	0	0	18.55	10913.39	0	0	0	0	1125.99	2.49	0
RS	5.06	0	0	0	1.98	0	4.32	424.6	0	0.06	0	0	0	0.01	0
SE	46.7	0	0	0	1.88	0	158.68	29036.31	0	12.79	1.65	0	0	0.03	3.93
SI	2.34	0	0	0	0.19	0	0.54	1491.62	0	0	0	0.33	0	1.03	0.23
SK	4.4	0	0	0	1.1	0	3.94	277.62	2.75	0	0	1.92	0	0	0
UK	131.55	19.2	0	0	1.2	0	26.64	143.74	0	66.16	0.74	17.68	40063.19	0	48.64

Table A-47. Capacity distribution for Model Run 45 (Weather Year 1980)

Country	Onshore	Offshore	PV /out Tracking	PV / Tracking	Run-of-river	Rooftop PV	PHS	Reservoir	Biomass CHP	PEM Electrolyzer	H2 OCGT	H2 CCGT	Salt Cavern	Vessel	Li-ion Battery
AL	2.07	0	0	2.34	0.03	0	0	1470.55	0	0.51	0	0	74.5	0	0
AT	40.42	0	0	30.46	4.61	0	114.15	1053.49	0	15.22	0	0.42	0	35.55	8.97
BA	11.05	0	0	0	0.28	0	1.61	1692.83	0	3.63	0	0	1123.73	0	0
BE	5.51	3.13	0	15.2	0.08	0	6.18	13.82	3.38	0	0	1.11	0	18.58	4.12
BG	1.94	0	0	4.47	0.61	0	40.59	1964.22	0	0	0	0	0	7.33	0
CH	8.24	0	0	3.89	3.74	0	163.81	5031.16	0	0	0	0	0	13.37	0
CZ	14.15	0	0	3.65	0.41	0	5.99	441.86	0.57	0.69	0.25	1.55	0	10.36	3.76
DE	38.99	23.02	0.01	51.23	4.15	0	39.27	5.46	0.01	0	2.09	35.09	38335.96	8.53	7.36
DK	13.86	0	0	1.07	0	0	0	0	0	5.34	0.64	0	2437.09	0.03	0.67
EE	6.38	0	0	0.13	0	0	0	0	0	0.56	0	0	0	4.61	1.83
ES	76.68	0	0.04	123.08	2.27	0	63.06	11148.12	0	25.38	3.92	0	10285.93	26.83	173.98
FI	20.19	0	0	0	2.96	0	0	518.99	0	2.44	0.21	1.39	0	22.99	4.58
FR	172.3	10.44	0.01	123.9	6.56	0	50.15	5071.64	0	58.63	8.15	21.33	20751.99	89.85	92.88
GR	11.95	0	0	9.9	0.22	0	4.64	1753.4	0	2.25	0	0	668.12	11.94	3.55
HR	6.51	0	0	3.88	0.44	0	5.69	1955.8	0	2.35	0	0	0	0.05	0.34
HU	4.75	0	0	16.84	0.03	0	0	48.33	0	0	0.53	0.01	0	21.42	12.94
IE	59.64	0	0	0.38	0.12	0	2.54	0	0	42.98	0.88	0	0	9.58	3.25
IT	58.87	0	0.02	115.55	10.36	0	61.78	1693.37	0	16.06	0	0	0	190.91	112.71
LT	14.14	0	0	4.39	0	0	11.06	23.46	0	2.83	0.55	0	0	5.52	6.04
LU	0.13	0	0	5.89	0	0	5.04	0	0	0	0	0	0	1.05	0.01
LV	3.38	0	0	0.01	0.26	0	0	1472.02	0	0.68	0	0	0	2.87	0.12
ME	2.92	0	0	0.59	0	0	0	0	0	0.26	0	0	0	0	0
MK	0.96	0	0	2.49	0.29	0	0	265.54	0	0.13	0	0	0	0.08	0
NL	21.12	20.59	0	2.54	0	0	0	0	1.65	5.93	5.91	17.74	27620.16	0.02	0.92
NO	39.93	0	0	0	0.73	0	391.93	79421.13	0	17.89	0	0	0	17.1	0
PL	38.3	0.93	0	34.8	0.4	0	8.32	119.15	0	7	5.84	6.86	16174.7	0.11	5.78
PT	12.54	0	0	4.15	2.66	0	66.67	686.82	0	0.71	0	0	1656.08	0.03	3.6
RO	13.76	0	0	0.71	0	0	18.55	10913.39	0	0	0	0	912.68	6.87	0
RS	5.06	0	0	0	1.98	0	4.32	424.6	0	2.13	0	0	0	0.01	0
SE	27.29	0.98	0	4.71	1.88	0	158.68	29036.31	0	0	0.44	0	0	4.06	1.05
SI	2.77	0	0	0.01	0.19	0	0.54	1491.62	0	0	0	0	0	6.28	0.51
SK	2.91	0	0	4.57	1.1	0	3.94	277.62	0	0	0	1.73	0	7.65	5.65
UK	99.02	18.74	0	28.8	1.2	0	26.64	143.74	0	50.18	15.24	17.42	43264.15	89.6	16.57

Table A-48. Capacity distribution for Model Run 45 (Weather Year 1981)

Country	Onshore	Offshore	PV /out Tracking	PV / Tracking	Run-of-river	Rooftop PV	PHS	Reservoir	Biomass CHP	PEM Electrolyzer	H2 OCGT	H2 CCGT	Salt Cavern	Vessel	Li-ion Battery
AL	2.07	0	0	2.33	0.03	0	0	1470.55	0	0.53	0	0	156.85	0.02	0
AT	38.95	0	0	23.13	4.61	0	114.15	1053.49	0	13.84	0	0	0	16.77	4.39
BA	11.05	0	0	3.4	0.28	0	1.61	1692.83	0	4.91	0	0	1000.48	0	0
BE	5.17	4.72	0	8.01	0.08	0	6.18	13.82	4.75	0	0	2.97	0	0	0.01
BG	3.86	0	0	3.09	0.61	0	40.59	1964.22	0	0	0	0	0	6.07	0
CH	7.97	0	0	0.71	3.74	0	163.81	5031.16	0	0	0	0	0	7.53	0
CZ	16.12	0	0	9.98	0.41	0	5.99	441.86	0	1.38	0	2.22	0	24.61	3.45
DE	34.99	19.99	0	40.4	4.15	0	39.27	5.46	3.53	0	0	11.71	9343.14	25.37	1.57
DK	13	0	0	1.83	0	0	0	0	0	3.24	0	0	503.19	6.4	1.41
EE	9.51	0	0	2.03	0	0	0	0	0	2.81	0	0	0	1.48	1.2
ES	76.11	1.08	0.01	135.05	2.27	0	63.06	11148.12	0	26.5	0.07	0	4421.94	38.53	201.88
FI	19.94	0	0	0	2.96	0	0	518.99	0	3.69	0	2.37	0	36.83	6.59
FR	160.66	0.23	0	128.74	6.56	0	50.15	5071.64	0	43.46	7.19	22.12	15223.55	70.65	111.71
GR	14.14	0	1.61	6.93	0.22	0	4.64	1753.4	0	3.28	0	0	742.03	10.41	0.79
HR	4.65	0	0	2.73	0.44	0	5.69	1955.8	0	0.82	0	0	0	1.43	0
HU	4.99	0	0	5.15	0.03	0	0	48.33	0	0	0.48	0.26	0	14.2	6.38
IE	53.89	0	0	0	0.12	0	2.54	0	0	37.58	0.96	0	0	10.05	6.28
IT	52.74	0	0	124.13	10.36	0	61.78	1693.37	0	10.8	0.15	0.02	0	152.9	146.05
LT	15.42	0	0	9.49	0	0	11.06	23.46	0	6.45	0	0	0	3.89	2.65
LU	0.04	0	0	4.19	0	0	5.04	0	0	0	0	0.38	0	0.01	0
LV	3.57	0	0	0.01	0.26	0	0	1472.02	0	0.46	0	0	0	2.22	0.02
ME	2.92	0	0	0	0	0	0	0	0	0.08	0	0	0	0.03	0
MK	1.85	0	0	1.56	0.29	0	0	265.54	0	0.25	0	0	0	1.39	0
NL	25.26	15.18	0	0	0	0	0	0	3.89	2.92	0	10.55	9630.75	0	2
NO	39.8	0	0	0	0.73	0	391.93	79421.13	0	17.57	0	0	0	5.49	0
PL	28.11	11.92	0	25.48	0.4	0	8.32	119.15	0	5.51	0	4.69	6539.8	8.46	9.19
PT	10.68	0	0	5.69	2.66	0	66.67	686.82	0	0.03	0	0	1674.58	2.54	0
RO	14.49	0	0	7.46	0	0	18.55	10913.39	0	2.22	0	0	843.01	7.47	0.72
RS	5.06	0	0	0	1.98	0	4.32	424.6	0	2.27	0	0	0	1.02	0
SE	35.84	0	0	3.95	1.88	0	158.68	29036.31	0	3.34	0	0	0	0.81	5.85
SI	1.51	0	0	0	0.19	0	0.54	1491.62	0	0	0	0	0	7.8	0.08
SK	5.68	0	0	6.94	1.1	0	3.94	277.62	0	0	0	0.28	0	9.27	3.96
UK	120.92	11.01	0	15.41	1.2	0	26.64	143.74	0	50.7	6.63	20	22285.11	27.65	15.24

Table A-49. Capacity distribution for Model Run 47 (Weather Year 1982)

Country	Onshore	Offshore	PV /out	PV / Tracking	Run-of-river	Rooftop PV	PHS	Reservoir	Biomass CHP	PEM Electrolyzer	H2 OCGT	H2 CCGT	Salt Cavern	Vessel	Li-ion Battery
AL	4.09	0	0	0	0.03	0	0	1470.55	0	0.56	0	0	124.71	0.19	0
AT	33.43	0	0	30.49	4.61	0	114.15	1053.49	0	5.75	0	3.49	0	14.5	13.15
BA	11.05	0	0	5.34	0.28	0	1.61	1692.83	0	4.91	0	0	1555.8	1.72	0.01
BE	3.12	4.48	0	6.63	0.08	0	6.18	13.82	4.75	0	0	0.55	0	0.01	1.26
BG	3.86	0	0	4.82	0.61	0	40.59	1964.22	0	0	0	0	0	6.24	0
CH	5.12	0	0	2.92	3.74	0	163.81	5031.16	0	0	0	0.13	0	6.17	0
CZ	16.6	0	0	9.61	0.41	0	5.99	441.86	1.14	0.38	0	3.48	0	7.95	2.77
DE	19.84	20.46	0	29.91	4.15	0	39.27	5.46	12.11	0	0	36.63	23969.64	16.87	0
DK	13.81	1.09	0	0.77	0	0	0	0	0	5.71	0	2.96	6735.54	0	0
EE	9.51	2	0	0	0	0	0	0	0	5.87	0	0	0	17.81	1.51
ES	73.04	0	0	142.05	2.27	0	63.06	11148.12	0	27.42	3.48	0	5831.72	79.69	221.84
FI	19.86	0	0	0	2.96	0	0	518.99	0	4.73	0	3.96	0	11.63	2.65
FR	137.16	16.21	0	92.3	6.56	0	50.15	5071.64	3.13	33.92	6.14	24.66	20862.98	129.7	116.66
GR	14.88	0	0	4.9	0.22	0	4.64	1753.4	0	2.05	0	0	309.19	17.56	0
HR	6.95	0	0	4.13	0.44	0	5.69	1955.8	0	2.38	0	0	0	9.32	1.38
HU	4.32	0	0	18.74	0.03	0	0	48.33	0	0	0	0.01	0	7.45	13.13
IE	53.89	0	0	1.72	0.12	0	2.54	0	0	42.46	0.41	0.43	0	12.21	7.83
IT	45.08	0	0	152.02	10.36	0	61.78	1693.37	0	12.72	0	5.05	0	108.33	153.92
LT	15.19	0	0	0.92	0	0	11.06	23.46	0	4.03	0	0	0	5.78	0.59
LU	0	0	0	2.37	0	0	5.04	0	0	0	0	0	0	0.01	0
LV	4.21	0	0	0.93	0.26	0	0	1472.02	0	1.11	0	0	0	4.5	1.27
ME	3.88	0	0	2.68	0	0	0	0	0	1.24	0	0	0	2.2	0.21
MK	0.96	0	0	1.93	0.29	0	0	265.54	0	0.25	0	0	0	1.9	1.74
NL	17	22.54	0	0	0	0	0	0	2.86	3.27	0	9.96	11292.35	0	2.99
NO	72.4	0	0	0	0.73	0	391.93	79421.13	0	38.76	0	0	0	8.64	0
PL	47.41	0	0	69.11	0.4	0	8.32	119.15	0	12.46	0	5.3	12114.62	9.37	18.17
PT	4.01	0	0	32.42	2.66	0	66.67	686.82	0	3.3	0.7	0	1237.73	8.15	56.05
RO	10.65	0	0	5.93	0	0	18.55	10913.39	0	0	0	0	1361.89	11.95	0.71
RS	5.1	0	0	0	1.98	0	4.32	424.6	0	3	0	0	0	8.18	0
SE	31.8	0	0	3.73	1.88	0	158.68	29036.31	0	0.93	0	3.19	0	7.91	0.24
SI	2.76	0	0	1.83	0.19	0	0.54	1491.62	0	0.6	0	0	0	1.48	0.9
SK	5.9	0	0	0	1.1	0	3.94	277.62	0	0	0	2.62	0	0.05	5.18
UK	110.68	10.21	0	35.15	1.2	0	26.64	143.74	0	49.9	9.76	13.79	5415.9	135.11	16.68

Table A-50. Capacity distribution for Model Run 48 (Weather Year 1983)

Country	Onshore	Offshore	PV /out Tracking	PV / Tracking	Run-of-river	Rooftop PV	PHS	Reservoir	Biomass CHP	PEM Electrolyzer	H2 OCGT	H2 CCGT	Salt Cavern	Vessel	Li-ion Battery
AL	3.08	0	0	1.82	0.03	0	0	1470.55	0	0.53	0	0	189.74	0	0
AT	32.97	0	0	26.94	4.61	0	114.15	1053.49	0	6.15	0.49	0.48	0	20.32	15.1
BA	7.59	0	0	0	0.28	0	1.61	1692.83	0	1.61	0	0	805.68	0	0
BE	3.81	3.76	0	29.83	0.08	0	6.18	13.82	0	0	0.02	7.76	0	0.01	19.08
BG	3.86	0	0	3.08	0.61	0	40.59	1964.22	0	0	0	0	0	7.32	0
CH	6.8	0	0	0.36	3.74	0	163.81	5031.16	0	0	0	0	0	9.65	0
CZ	16.76	0	0	6.19	0.41	0	5.99	441.86	0	1.45	0.55	5.42	0	31.8	3.43
DE	36.05	17.59	0	29.82	4.15	0	39.27	5.46	0	0	0	29.13	24529.63	6.8	3.85
DK	16.06	0	0	0.47	0	0	0	0	0	6.87	0	0	1859.1	0	1.98
EE	7.8	0	0	3.1	0	0	0	0	0	2.34	0	0	0	1.61	0
ES	45.55	0	0.01	170.86	2.27	0	63.06	11148.12	0	18.58	1.13	0	7221.98	22.71	300.92
FI	18.37	0	0	0	2.96	0	0	518.99	0	3.48	0.59	1.16	0	22.72	8.7
FR	171.46	29.5	2.21	90.05	6.56	0	50.15	5071.64	0	65.71	0.13	8.27	17671.1	94.12	57.47
GR	12.38	0	0	8.19	0.22	0	4.64	1753.4	0	2.49	0	0	426.23	12.94	2.92
HR	4.65	0	0	4.1	0.44	0	5.69	1955.8	0	0.46	0	0	0	6.06	2.95
HU	1.08	0	0	17.25	0.03	0	0	48.33	0	0	0	0	0	7.8	10.94
IE	37.74	0	0	0.95	0.12	0	2.54	0	0	23.68	0.64	0.01	0	0	9.29
IT	46.06	0	0	123.86	10.36	0	61.78	1693.37	0	11.89	0.48	0	0	152.99	154.52
LT	7.86	0	0	7.44	0	0	11.06	23.46	0	0	0	0	0	4.7	1.47
LU	0.13	0	0	5.56	0	0	5.04	0	0	0	0	0	0	0.1	0.56
LV	4.21	0	0	1.8	0.26	0	0	1472.02	0	1.62	0	0	0	2.65	0.46
ME	2.92	0	0	0.03	0	0	0	0	0	0.1	0	0	0	0.01	0
MK	0.96	0	0	1.96	0.29	0	0	265.54	0	0.24	0	0	0	1.26	0
NL	31.84	16.57	0	15.46	0	0	0	0	0	9.59	0	3.89	6366.53	0	36.34
NO	52.94	0	0	0	0.73	0	391.93	79421.13	0	28.91	0	0	0	7.86	0
PL	54.77	0	0	34.89	0.4	0	8.32	119.15	0	16.37	2.24	0.45	5581.83	0.01	16.06
PT	9.04	0	0	12.41	2.66	0	66.67	686.82	0	1.22	0	0	1875.93	0.01	2.47
RO	12.41	0	0	0	0	0	18.55	10913.39	0	0	0	0	1849.92	6.84	0
RS	4.57	0	0	0	1.98	0	4.32	424.6	0	0.78	0	0	0	8.88	0
SE	40.83	0	0	0.54	1.88	0	158.68	29036.31	0	7.23	0	0	0	0.87	1.95
SI	2.51	0	0	0.11	0.19	0	0.54	1491.62	0	0	0	0	0	5.19	0.78
SK	5.9	0	0	0.77	1.1	0	3.94	277.62	0	0	0.59	2.42	0	2.25	8.39
UK	81.84	7.95	0	45.79	1.2	0	26.64	143.74	0	27.04	9.03	15.19	20668.72	0.07	86.4

Table A-51. Capacity distribution for Model Run 49 (Weather Year 1984)

Country	Onshore	Offshore	PV /out Tracking	PV / Tracking	Run-of-river	Rooftop PV	PHS	Reservoir	Biomass CHP	PEM Electrolyzer	H2 OCGT	H2 CCGT	Salt Cavern	Vessel	Li-ion Battery
AL	3.58	0	0	0.35	0.03	0	0	1470.55	0	0.8	0	0	198.65	0.01	0.12
AT	31.11	0	0	17.44	4.61	0	114.15	1053.49	0	3.65	0	0	0	26.97	7.26
BA	14.7	0	0	7.5	0.28	0	1.61	1692.83	0	9.09	0	0	807.06	0.05	0.61
BE	3.47	2.17	0	36.62	0.08	0	6.18	13.82	2.23	0	0.02	3.01	0	32	23.24
BG	2.47	0	0	4.1	0.61	0	40.59	1964.22	0	0	0	0	0	5.74	0.05
CH	9.06	0	0	0.83	3.74	0	163.81	5031.16	0	0	0	0	0	11.55	0
CZ	16.58	0	0	12.56	0.41	0	5.99	441.86	0	0	0	2.57	0	9.65	12.66
DE	28.63	28.98	0.01	39.71	4.15	0	39.27	5.46	0	0	0.03	10.48	5561.04	35.04	27.07
DK	19.14	3.5	0	2.8	0	0	0	0	0	10.82	0	0	2375.69	3.29	2.71
EE	6.38	0	0	0.01	0	0	0	0	0	0.28	0	0	0	1.86	1.8
ES	83.09	0	0.04	112.15	2.27	0	63.06	11148.12	0	26.62	0	2.9	3823.09	69.2	135.41
FI	19.54	0	0	0	2.96	0	0	518.99	0	2.52	0.31	2.05	0	30.19	9.6
FR	169.03	0.95	0.02	115.81	6.56	0	50.15	5071.64	0	37.04	0.61	10.99	8681.82	131.92	124.38
GR	13.45	0	0	16.18	0.22	0	4.64	1753.4	0	4.54	0.08	0	526.58	15.19	19.75
HR	4.65	0	0	6.82	0.44	0	5.69	1955.8	0	2.11	0	0	0	1.97	1.77
HU	5.76	0	0	9.24	0.03	0	0	48.33	0	0	1.31	0.09	0	13.41	8.35
IE	14.62	0	0	10.31	0.12	0	2.54	0	0	6.84	0	1.4	0	7.1	11.86
IT	41.5	0	0.01	132.74	10.36	0	61.78	1693.37	0	11.16	0.52	0.15	0	143.39	139.81
LT	16.41	0	0	7.47	0	0	11.06	23.46	0	4.91	0	0	0	3.93	1.37
LU	0.17	0	0	5.43	0	0	5.04	0	0	0	0	0.42	0	6.58	0.02
LV	4.21	0	0	3.9	0.26	0	0	1472.02	0	0.94	0	0	0	1.65	1.81
ME	3.88	0	0	3.98	0	0	0	0	0	2.2	0	0	0	0.4	1.12
MK	0.96	0	0	2.34	0.29	0	0	265.54	0	0.29	0	0	0	2.51	1.81
NL	22.35	19.17	0	12.31	0	0	0	0	0	3.65	3.93	3.12	2409.62	0.04	45.67
NO	71.45	0	0	0	0.73	0	391.93	79421.13	0	38.73	0	0	0	7.25	0
PL	54.54	0.01	0	36.54	0.4	0	8.32	119.15	0	12.35	3.51	3.08	5898.04	11.32	30.45
PT	12.13	0	0.01	21.31	2.66	0	66.67	686.82	0	4.08	0.85	0	1395.66	11.19	24.58
RO	12.22	0	0	2.73	0	0	18.55	10913.39	0	0	0	0	329.04	10.41	0.17
RS	5.06	0	0	0.01	1.98	0	4.32	424.6	0	1.7	0	0	0	3.31	0
SE	35.3	0	0	3.31	1.88	0	158.68	29036.31	0	1.49	0	0	0	1.37	1.71
SI	2.48	0	0	0	0.19	0	0.54	1491.62	0	0	0	0	0	0.05	0.42
SK	5.92	0	0	2.29	1.1	0	3.94	277.62	0	0	0	2.96	0	24.24	0.52
UK	96.05	13.74	0.01	66.27	1.2	0	26.64	143.74	0	39.09	6.26	10.1	14804.17	111.66	73.49

Table A-52. Capacity distribution for Model Run 50 (Weather Year 1985)

Country	Onshore	Offshore	PV /out Tracking	PV / Tracking	Run-of-river	Rooftop PV	PHS	Reservoir	Biomass CHP	PEM Electrolyzer	H2 OCGT	H2 CCGT	Salt Cavern	Vessel	Li-ion Battery
AL	5.08	0	0	4.67	0.03	0	0	1470.55	0	2.13	0	0	758.17	0	0
AT	42.12	0	0	20.97	4.61	0	114.1	1053.49	0	11.9	0	0	0	5.94	3.22
BA	11.05	0	0	6.13	0.28	0	1.61	1692.83	0	5.43	0	0	2393.67	0	0
BE	3.8	3.57	0	26.04	0.08	0	6.18	13.82	4.75	0	0	0.74	0	0.01	15.89
BG	3.24	0	0	4.79	0.61	0	40.59	1964.22	0	0	0	0	0	5	0
CH	8.73	0	0	3.64	3.74	0	163.8	5031.16	0	0	0	0	0	0.57	0.08
CZ	19.93	0	0	5.04	0.41	0	5.99	441.86	0.73	4	0	1.14	0	0.01	2.56
DE	27.21	11.6	0	33.04	4.15	0	39.27	5.46	19.8	0	0	16.6	14662.0	0.02	0
DK	13.67	0	0	0.61	0	0	0	0	0	2.98	0	0.81	2241.13	0	1.35
EE	9.51	0.32	0	0	0	0	0	0	0	1.91	0	0.01	0	1.14	1.18
ES	79.1	0	0.0	116.6	2.27	0	63.06	11148.1	0	23.7	0	0	6123.04	16.51	156.7
FI	20.35	0	0	0	2.96	0	0	518.99	0	2.87	0.5	0.76	0	18.55	4.8
FR	176.6	11.2	0	139.1	6.56	0	50.15	5071.64	1.76	51.7	0	8.3	12606.0	74.26	128.1
G	15.58	0	0	8.75	0.22	0	4.64	1753.4	0	3.85	0	0	658.03	7.33	1.55
HR	6.95	0	0	2.5	0.44	0	5.69	1955.8	0	2.54	0	0	0	0.07	0
HU	14.2	0	0	10.07	0.03	0	0	48.33	0	1.47	0	0	0	3.93	3.75
IE	50.15	0	0	1.09	0.12	0	2.54	0	0	34.2	0.4	0	0	0.19	6.11
IT	53.34	0	0	117.7	10.3	0	61.78	1693.37	0	7.48	0	0.88	0	131.6	86.33
LT	9.16	0	0	0.21	0	0	11.06	23.46	0	0	0	0.25	0	3.2	4.42
LU	0.25	0	0	6.22	0	0	5.04	0	0	0	0	0	0	0.01	0
LV	4.21	1.12	0	0	0.26	0	0	1472.02	0	2.01	0	0.01	0	1.95	0.9
M	3.88	0	0	2.95	0	0	0	0	0	1.3	0	0	0	0.01	0
M	1.32	0	0	1.89	0.29	0	0	265.54	0	0.2	0	0	0	0.01	0.17
NL	23.82	11.3	0	0	0	0	0	0	4	0	0	14.9	13029.9	0	16.53
N	53.5	0	0	0	0.73	0	391.9	79421.1	0	30.0	0	0	0	7.74	0
PL	27.15	7	0	17.69	0.4	0	8.32	119.15	5.37	2.83	0	11.0	14859.9	0.01	3.49
PT	13.3	0	0	14.98	2.66	0	66.67	686.82	0	2.58	0	0	2413.13	0	8.97
R	9.3	0	0	4.42	0	0	18.55	10913.3	0	1.22	0	0	1063.12	3.82	0
RS	5.06	0	0	0	1.98	0	4.32	424.6	0	2.03	0	0	0	0.08	0
SE	33	0	0	5.51	1.88	0	158.6	29036.3	0	0.86	0	0.6	0	1.25	3.7
SI	2.35	0	0	0	0.19	0	0.54	1491.62	0	0	0	0	0	3.08	0.17
SK	8.95	0	0	0	1.1	0	3.94	277.62	0	2.45	0	0	0	0.02	3.03
UK	104.6	26.3	0	6.02	1.2	0	26.64	143.74	0	46.9	7.7	15.6	20309.8	73.72	51.64

Table A-53. Capacity distribution for Model Run 51 (Weather Year 1986)

Country	Onshore	Offshore	PV /out Tracking	PV / Tracking	Run-of-river	Rooftop PV	PHS	Reservoir	Biomass CHP	PEM Electrolyzer	H2 OCGT	H2 CCGT	Salt Cavern	Vessel	Li-ion Battery
AL	3.01	0	0	0.27	0.03	0	0	1470.55	0	0.39	0	0	247.2	0	0.08
AT	31.95	0	0	23.33	4.61	0	114.15	1053.49	0	3.28	0.57	0.65	0	3.14	22.82
BA	7.4	0	0	0	0.28	0	1.61	1692.83	0	1.43	0	0	1410.22	0	0
BE	5.51	4.35	0	25.27	0.08	0	6.18	13.82	3.23	0	0	2.24	0	0	7.73
BG	3.84	0	0	2.87	0.61	0	40.59	1964.22	0	0	0	0	0	0.03	0
CH	6.31	0	0.01	4.98	3.74	0	163.81	5031.16	0	0	0.04	0	0	0.01	0
CZ	13.43	0	0	9.73	0.41	0	5.99	441.86	0	0	0.26	3.71	0	0.01	3.04
DE	29.23	19.99	0	25.38	4.15	0	39.27	5.46	0	0	1.46	24.36	23389.06	0.02	0.36
DK	18.11	0	0	0.49	0	0	0	0	0	6.42	0	0	1680.04	0	0.33
EE	4.11	0	0	0	0	0	0	0	0	0.27	0	0	0	1.94	0.32
ES	60.28	0	0.04	129.88	2.27	0	63.06	11148.12	0	16.07	1.7	0	7838.39	17.93	211.45
FI	16.99	0	0	0	2.96	0	0	518.99	0	2.11	0.32	2.41	0	14.17	7.93
FR	159.2	7.67	2.23	111.12	6.56	0	50.15	5071.64	0	42.47	5.12	8.32	21023.08	23.92	128.65
GR	14.67	0	0	9.87	0.22	0	4.64	1753.4	0	3.71	0	0	1036.14	14.24	1.99
HR	5.43	0	0	3.93	0.44	0	5.69	1955.8	0	1.45	0	0	0	0.01	0.28
HU	4.75	0	0	6.24	0.03	0	0	48.33	0	0	0	0	0	0.01	3.95
IE	35.51	0	0	5.11	0.12	0	2.54	0	0	24.36	0.78	0	0	0	5.25
IT	37.05	0	0.01	151.15	10.36	0	61.78	1693.37	0	10.63	0.71	0.2	0	144.82	183.47
LT	9.16	0	0	0	0	0	11.06	23.46	0	0.99	0	0	0	2.77	0.08
LU	0.13	0	0	5.09	0	0	5.04	0	0	0	0	0.01	0	0	0
LV	4.21	0	0	1.55	0.26	0	0	1472.02	0	1.44	0	0	0	1.61	0.32
ME	2.92	0	0	0	0	0	0	0	0	0.28	0	0	0	0	0
MK	0.34	0	0	2.71	0.29	0	0	265.54	0	0	0	0	0	0.04	1.46
NL	23.82	16.67	0	0	0	0	0	0	0	8.16	1.94	10.44	12460.82	0	2.33
NO	44.08	0	0	0	0.73	0	391.93	79421.13	0	25.01	0	0	0	5.5	0
PL	72.65	2.69	0	37.4	0.4	0	8.32	119.15	0	23.51	0	0	11034.57	0.01	21.39
PT	12.61	0	0	23.31	2.66	0	66.67	686.82	0	4.74	0.02	0	2026.43	0.01	37.67
RO	14.19	0	0	0	0	0	18.55	10913.39	0	0	0	0	2569.22	0.01	2.19
RS	5.06	0	0	0	1.98	0	4.32	424.6	0	1.34	0	0	0	0.01	0
SE	31.11	0	0	3.68	1.88	0	158.68	29036.31	0	3.12	0	0	0	0.39	2.37
SI	3	0	0	0	0.19	0	0.54	1491.62	0	0	0	0	0	0.81	1.07
SK	5.9	0	0	10.66	1.1	0	3.94	277.62	0	0	0.82	3.06	0	0	6.69
UK	104.48	12.86	0	44.81	1.2	0	26.64	143.74	0	56.3	6.7	12.83	28639.42	0.01	49.28

Table A-54. Capacity distribution for Model Run 52 (Weather Year 1987)

Country	Onshore	Offshore	PV /out	PV / Tracking	Run-of-river	Rooftop PV	PHS	Reservoir	Biomass CHP	PEM Electrolyzer	H2 OCGT	H2 CCGT	Salt Cavern	Vessel	Li-ion Battery
AL	4.39	0	0	0	0.03	0	0	1470.55	0	0.67	0	0	257.54	0	0
AT	40.16	0	0	32.51	4.61	0	114.15	1053.49	0	12.47	0	0	0	0.01	9.91
BA	11.05	0	0	0	0.28	0	1.61	1692.83	0	4.09	0	0	1777.27	0	0
BE	2.09	0.8	0	14.65	0.08	0	6.18	13.82	4.75	0	0	1.38	0	0	0
BG	3.86	0	0	0.42	0.61	0	40.59	1964.22	0	0	0	0	0	0	0
CH	7.32	0	0	5.66	3.74	0	163.81	5031.16	0	0	0	0	0	0	0
CZ	22.44	0	0	11.51	0.41	0	5.99	441.86	0	5.26	0	0.89	0	0	6.94
DE	27.2	14.39	0	18.01	4.15	0	39.27	5.46	24.57	0	0	12.27	12090.97	0	0
DK	12.84	0	0	0.71	0	0	0	0	0	2.88	0	2.64	4102.1	0	1.36
EE	9.78	0	0	0	0	0	0	0	0	2.76	0	0	0	1.06	2.71
ES	91.93	0	0	95.18	2.27	0	63.06	11148.12	0	23.54	0	0	7342.42	0.44	78.18
FI	19.86	0	0	0	2.96	0	0	518.99	0	3.58	0.37	1.97	0	14.95	10.47
FR	155.93	4.15	0	125.38	6.56	0	50.15	5071.64	12.97	39.53	0.43	10.58	14031.03	22.27	72.74
GR	16.57	0	0	8.46	0.22	0	4.64	1753.4	0	4.14	0	0	889.16	5.95	0
HR	6.05	0	0	0.48	0.44	0	5.69	1955.8	0	0.9	0	0	0	0	0.01
HU	4.75	0	0	11.3	0.03	0	0	48.33	0	0	0	1.88	0	0.01	4.07
IE	36.7	0	0	5.86	0.12	0	2.54	0	0	27.5	0.41	0.27	0	0	1.78
IT	58.26	0	0	105.56	10.36	0	61.78	1693.37	2.05	12.04	0.49	0.28	0	139.49	65.39
LT	17.02	0	0	0	0	0	11.06	23.46	0	5.45	0	0	0	2.7	2.62
LU	0	0	0	6.22	0	0	5.04	0	0	0	0	0	0	0	0
LV	4.21	0	0	0	0.26	0	0	1472.02	0	1.6	0	0	0	2.01	1.92
ME	4.85	0	0	0	0	0	0	0	0	0.65	0	0	0	0	0
MK	1.15	0	0	0.99	0.29	0	0	265.54	0	0	0	0	0	0	0
NL	23.82	22.71	0	0	0	0	0	0	4	0	0	11.55	9412.72	0	0.72
NO	71.44	0	0	0	0.73	0	391.93	79421.13	0	44	0	0	0	5.91	0
PL	57.75	1.07	0	41.81	0.4	0	8.32	119.15	0	12.42	0	6.29	10938.51	0	24.43
PT	16.11	0	0	8.91	2.66	0	66.67	686.82	0	4.11	0	0	3071.88	0	0.72
RO	9.3	0	0	0	0	0	18.55	10913.39	0	0	0	0	1543.36	0	0
RS	5.06	0	0	0	1.98	0	4.32	424.6	0	3.61	0	0	0	0	0
SE	36.77	0	0	0	1.88	0	158.68	29036.31	0	5.09	0	1.47	0	0.51	5.41
SI	2.01	0	0	0.71	0.19	0	0.54	1491.62	0	0	0	0	0	0	1.43
SK	8.95	0	0	6.01	1.1	0	3.94	277.62	0	0	0	0.08	0	0	6.48
UK	100.6	12.09	0	28.54	1.2	0	26.64	143.74	7.03	36.9	1.28	15.27	23401	0	30.97

Table A-55. Capacity distribution for Model Run 53 (Weather Year 1988)

Country	Onshore	Offshore	PV /out Tracking	PV / Tracking	Run-of-river	Roof-top PV	PHS	Reservoir	Biomass CHP	PEM Electrolyzer	H2 OCGT	H2 CCGT	Salt Cavern	Vessel	Li-ion Battery
AL	2.55	0	0	0.48	0.03	0	0	1470.55	0	0	0	0	162.05	0	0
AT	37.33	0	0	27.84	4.61	0	114.15	1053.49	0	10.76	0	0	0	0.87	11.02
BA	14.7	0	0	5.9	0.28	0	1.61	1692.83	0	8.29	0	0	3525.6	0	0
BE	5.51	3.64	0	30.05	0.08	0	6.18	13.82	0	0	0	7.78	0	0	14.88
BG	3.86	0	0	4.93	0.61	0	40.59	1964.22	0	0.52	0	0	0	2.83	0.65
CH	6.17	0	0	1.05	3.74	0	163.81	5031.16	0	0	0	0	0	0	0
CZ	14.88	0	0	4.09	0.41	0	5.99	441.86	0	0.31	0	0	0	0.01	5.34
DE	39.17	16.86	0	23.31	4.15	0	39.27	5.46	0	0	0	16.47	15071.74	0.01	18.69
DK	21.96	0	0	5.73	0	0	0	0	0	11.11	0	0	3155.96	0	1.9
EE	6.38	0	0	1.36	0	0	0	0	0	0.96	0	0	0	1.95	0.87
ES	72.71	0	0.01	126.05	2.27	0	63.06	11148.12	0	21.64	0	0	6714.61	2.96	140.46
FI	19.86	0	0	0	2.96	0	0	518.99	0	3.4	0.08	0.52	0	12.39	6.09
FR	145	6.41	0	110.64	6.56	0	50.15	5071.64	0	35.76	0.44	3.98	12998.9	33.03	85.93
GR	17.72	0	0	10.67	0.22	0	4.64	1753.4	0	6.45	0	0	1481.61	10.99	5.76
HR	6.76	0	0	1.97	0.44	0	5.69	1955.8	0	1.46	0	0	0	0.01	1.7
HU	4.75	0	0	17.73	0.03	0	0	48.33	0	0	0	0	0	3.82	13.37
IE	38.05	0	0	2.28	0.12	0	2.54	0	0	23.63	0.29	0.96	0	0	2.12
IT	36.95	0	0	119.84	10.36	0	61.78	1693.37	0	9.15	0	0	0	143.97	106.97
LT	10.57	0	0	17.4	0	0	11.06	23.46	0	2.8	0	0	0	3.44	10.34
LU	0.04	0	0	5.08	0	0	5.04	0	0	0	0	0	0	0	0
LV	2.53	0	0	0	0.26	0	0	1472.02	0	0.53	0	0	0	2.5	0.18
ME	3.88	0	0	1.05	0	0	0	0	0	1.96	0	0	0	0	0
MK	0.96	0	0	2.97	0.29	0	0	265.54	0	0.63	0	0	0	0.79	0.21
NL	30.51	22.71	0	2.52	0	0	0	0	0	12.83	0	0	4887.97	0	5.91
NO	41.23	0	0	0	0.73	0	391.93	79421.13	0	21.72	0	0	0	7.72	0
PL	55.35	0	0	44.91	0.4	0	8.32	119.15	0	15.1	0	0.78	6009.6	0.01	37.72
PT	18.16	0	0	8.93	2.66	0	66.67	686.82	0	3.63	0	0	2804.24	0	1.54
RO	13.05	0	0	4.22	0	0	18.55	10913.39	0	0.46	0	0	1518.41	3.46	0
RS	5.06	0	0	1.13	1.98	0	4.32	424.6	0	1.28	0	0	0	2.04	0
SE	31.22	0	0	9.48	1.88	0	158.68	29036.31	0	1.33	0	0	0	0.86	8.09
SI	1.51	0	0	0.87	0.19	0	0.54	1491.62	0	0	0	0	0	0.01	0.26
SK	5.9	0	0	0	1.1	0	3.94	277.62	0	0	0	0	0	0.01	1.97
UK	72.04	19.88	0	54.19	1.2	0	26.64	143.74	0	27.23	3.47	10.32	20470.31	0.01	31.55

Table A-56. Capacity distribution for Model Run 54 (Weather Year 1989)

Country	Onshore	Offshore	PV /out	PV / Tracking	Run-of-river	Rooftop PV	PHS	Reservoir	Biomass CHP	PEM Electrolyzer	H2 OCGT	H2 CCGT	Salt Cavern	Vessel	Li-ion Battery
AL	3.3	0	0	3.9	0.03	0	0	1470.55	0	1.64	0	0	518.64	0	1.62
AT	28.69	0	0	26.16	4.61	0	114.15	1053.49	0	3.39	1.43	1.51	0	0.01	3.96
BA	7.4	0	0	0.17	0.28	0	1.61	1692.83	0	2.54	0.01	0	1492.35	0	0
BE	2.78	1.33	0	21.14	0.08	0	6.18	13.82	4.75	0	0	3.71	0	0	9.34
BG	3.86	0	0	3.97	0.61	0	40.59	1964.22	0	0	0	0	0	0	0.33
CH	3.68	0	0	6.24	3.74	0	163.81	5031.16	0	0	0	0	0	0	0
CZ	14.4	0	0	6.91	0.41	0	5.99	441.86	0	0	0.36	5.36	0	0	1.51
DE	29.51	31.25	0	23.55	4.15	0	39.27	5.46	6.03	0	3.02	13.33	12877.24	0	18.8
DK	19.63	0	0	0.52	0	0	0	0	0	11.01	0	0	1372.33	0	0.01
EE	9.52	0	0	0	0	0	0	0	0	2.82	0	0	0	1.46	0.51
ES	74.44	1.69	0	115.07	2.27	0	63.06	11148.12	0	16.2	8.23	2.81	20905.46	0.01	147.35
FI	20.87	0	0	0	2.96	0	0	518.99	0	4.86	1.79	0.8	0	38.73	2.52
FR	140.16	1.65	0	150.19	6.56	0	50.15	5071.64	6.15	33.33	24.46	21.56	45097.59	13.95	141.45
GR	15.96	0	0	5.35	0.22	0	4.64	1753.4	0	2.97	0	0	1649.04	0.02	1.33
HR	4.65	0	0	6.25	0.44	0	5.69	1955.8	0	1.05	0	0	0	0	1.45
HU	9.26	0	0	12.18	0.03	0	0	48.33	0	0	0	0	0	0	1.19
IE	43.13	0	0	2.41	0.12	0	2.54	0	0	33.21	0.76	0.43	0	0	3.01
IT	24.25	0	0	167.33	10.36	0	61.78	1693.37	0.5	11	0	0.22	0	81.1	281.83
LT	6.04	0	0	0	0	0	11.06	23.46	0	0	0	0	0	0	0
LU	0	0	0	6.14	0	0	5.04	0	0	0	0	0	0	0	0
LV	2.3	0	0	0	0.26	0	0	1472.02	0	0	0	0	0	2	1.8
ME	2.92	0	0	1.98	0	0	0	0	0	0.11	0	0	0	0	0.03
MK	0.96	0	0	2.88	0.29	0	0	265.54	0	0.06	0	0.42	0	0	3.28
NL	19.75	23.6	0	0	0	0	0	0	0	1.73	0	6.05	7471.55	0	14.15
NO	72.18	0	0	0	0.73	0	391.93	79421.13	0	40.64	0	0	0	5.71	0
PL	60.61	2.4	0	34.08	0.4	0	8.32	119.15	0	19.05	6.69	0	11583.35	0	17.84
PT	15.61	0	0	8.38	2.66	0	66.67	686.82	0	1.82	0	0	2322.25	0	0.67
RO	15.76	0	0	4.5	0	0	18.55	10913.39	0	3.25	0	0	2253.23	0	3.07
RS	0.7	0	0	1.65	1.98	0	4.32	424.6	0	0.76	0	0	0	0	1.25
SE	31.39	0	0	0	1.88	0	158.68	29036.31	0	4.59	0	0	0	0.02	0
SI	1.51	0	0	1.57	0.19	0	0.54	1491.62	0	0	0	0	0	0	4.16
SK	4.4	0	0	0	1.1	0	3.94	277.62	0	0	0.45	4.28	0	0	2.71
UK	96.91	17.64	0	29.06	1.2	0	26.64	143.74	0.19	44.2	4.06	14.87	17136.67	0	47.45

Table A-57. Capacity distribution for Model Run 55 (Weather Year 1990)

Country	Onshore	Offshore	PV /out Tracking	PV / Tracking	Run-of-river	Rooftop PV	PHS	Reservoir	Biomass CHP	PEM Electrolyzer	H2 OCGT	H2 CCGT	Salt Cavern	Vessel	Li-ion Battery
AL	2.24	0	0	3.5	0.03	0	0	1470.55	0	0.24	0	0	385.45	0.01	0.9
AT	28.11	0	0	30.94	4.61	0	114.15	1053.49	0	5.52	0.3	0	0	19.99	28.66
BA	7.4	0	0	3.12	0.28	0	1.61	1692.83	0	3.36	0.34	0	1444.9	0.01	0.01
BE	5.17	2.33	0	13.08	0.08	0	6.18	13.82	4.75	0	0	0	0	0.2	6.47
BG	1.61	0	0	4.93	0.61	0	40.59	1964.22	0	0	0.07	0	0	5.07	1.88
CH	6.42	0	0	3.42	3.74	0	163.81	5031.16	0	0	0	0	0	6.36	0
CZ	19.03	0	0	13.56	0.41	0	5.99	441.86	0	3.58	1.49	0.24	0	0.02	12.88
DE	35.59	16.4	0	34.32	4.15	0	39.27	5.46	4.43	0	4.13	27.39	24734.52	2.89	23.68
DK	12.87	0	0	4.01	0	0	0	0	0	4.94	0	0	605.61	0.01	0.78
EE	3.22	0	0	2.92	0	0	0	0	0	0.25	0	0	0	2.14	0.95
ES	61.07	0	0.02	143.42	2.27	0	63.06	11148.12	0	18.93	2.75	1.06	7367.19	27.29	237.72
FI	18.61	0	0	0	2.96	0	0	518.99	0	3.95	0.54	1.1	0	14.05	6.41
FR	159.14	2.14	0.01	120.5	6.56	0	50.15	5071.64	0	38.57	8.66	3.77	13884.38	90.7	96.91
GR	11.04	0	2.12	10.46	0.22	0	4.64	1753.4	0	2.96	2.13	0	2465.38	12.27	15.53
HR	4.54	0	0	2.86	0.44	0	5.69	1955.8	0	0.79	0	0	0	2.6	0.5
HU	3.71	0	0	18.71	0.03	0	0	48.33	0	0	0	0	0	4.88	19.52
IE	32.97	0	0	5.99	0.12	0	2.54	0	0	19.1	0.68	0	0	0.02	4.23
IT	32.61	0	0.01	135.39	10.36	0	61.78	1693.37	0	4.04	0	0	0	139.83	186.02
LT	16.45	0	0	13.52	0	0	11.06	23.46	0	7.12	0	0	0	3.54	0.95
LU	0.04	0	0	1.96	0	0	5.04	0	0	0	0	0.14	0	0.05	0.01
LV	4.21	0	0	8.58	0.26	0	0	1472.02	0	1.35	0	0	0	1.45	0.97
ME	2.92	0	0	4.05	0	0	0	0	0	1.99	0	0	0	0.71	0
MK	0.96	0	0	2.52	0.29	0	0	265.54	0	0.21	0	0	0	1.4	1.5
NL	23.82	8.35	0	0	0	0	0	0	3.13	0	3.33	8.5	11463.71	0	9.41
NO	61.96	0	0	0	0.73	0	391.93	79421.13	0	35.85	0	0	0	6.5	0
PL	42.06	0.01	0	39.16	0.4	0	8.32	119.15	0	10.49	0	0	5288.95	0.01	26
PT	6.98	0	0	32.36	2.66	0	66.67	686.82	0	3.75	0.09	0	2556.42	0.01	69.81
RO	13.69	0	0	8.03	0	0	18.55	10913.39	0	0.85	0	0	1767.06	6.18	1.03
RS	4.66	0	0	0	1.98	0	4.32	424.6	0	0.24	0	0	0	4.02	0
SE	34.12	0	0	4.16	1.88	0	158.68	29036.31	0	5.91	0	0	0	0.43	3.31
SI	1.51	0	0	1.53	0.19	0	0.54	1491.62	0	0	0	0	0	3.24	4.59
SK	4.4	0	0	0.54	1.1	0	3.94	277.62	0	0	3.35	0.68	0	0.01	3.18
UK	94.85	15.85	0	40.28	1.2	0	26.64	143.74	0	40.79	6.77	8.86	11408.49	0.14	40.08

Table A-58. Capacity distribution for Model Run 56 (Weather Year 1991)

Country	Onshore	Offshore	PV /out Tracking	PV / Tracking	Run-of-river	Roof-top PV	PHS	Reservoir	Biomass CHP	PEM Electrolyzer	H2 OCGT	H2 CCGT	Salt Cavern	Vessel	Li-ion Battery
AL	3.41	0	0	0.84	0.03	0	0	1470.55	0	0.49	0	0	246.14	0	0.13
AT	29.48	0	0	37.52	4.61	0	114.15	1053.49	0	7.42	0.39	1.68	0	23.61	42.09
BA	18.06	0	0	6.27	0.28	0	1.61	1692.83	0	11.49	0	0	2241.76	0	0.43
BE	2.09	1.47	0	32.31	0.08	0	6.18	13.82	4.75	0	9.79	3.52	0	0	13.03
BG	2.19	0	0	4.58	0.61	0	40.59	1964.22	0	0	0	0	0	1.73	0
CH	6.03	0	0	4.39	3.74	0	163.81	5031.16	0	0	0	0	0	0.31	0
CZ	12.21	0	0	15.12	0.41	0	5.99	441.86	0	0	0	5.38	0	0	11.08
DE	24.1	26	0	37.47	4.15	0	39.27	5.46	9.39	0	0	19.67	12400.78	0.01	3.32
DK	18.99	0	0	0	0	0	0	0	0	9.05	0	0	2666.8	0	1.42
EE	9.5	0	0	5.33	0	0	0	0	0	5.24	0	0	0	1.12	0.67
ES	68.29	0	0.01	119.51	2.27	0	63.06	11148.12	0	21.33	25.23	0.78	33350	14.81	136.92
FI	19.86	0	0	0	2.96	0	0	518.99	0	3.13	1.1	1.47	0	16.41	5.42
FR	177.31	1.34	0	166.1	6.56	0	50.15	5071.64	0.72	61.96	13.91	12.67	16873.49	18.29	189.99
GR	15.04	0	0	10.72	0.22	0	4.64	1753.4	0	4.2	0.34	0	813.53	11.72	10.18
HR	7.35	0	0	1.9	0.44	0	5.69	1955.8	0	1.57	0	0	0	0	0.25
HU	4.24	0	0	19.02	0.03	0	0	48.33	0	0	0	0.53	0	2.87	15.99
IE	32.35	0	0	1.06	0.12	0	2.54	0	0	24.35	0.44	1.28	0	0	0.44
IT	42.44	0	0	158.22	10.36	0	61.78	1693.37	0	13.82	0.61	1.26	0	100.94	188.89
LT	21.53	0	0	0	0	0	11.06	23.46	0	7.82	0	0	0	3.01	1.11
LU	0	0	0	6.22	0	0	5.04	0	0	0	0.14	0.01	0	0	0.32
LV	5.16	0	0	0	0.26	0	0	1472.02	0	0.42	0	0	0	1.92	0.18
ME	4.85	0	0	2.37	0	0	0	0	0	1.95	0	0	0	0	1
MK	0.96	0	0	0	0.29	0	0	265.54	0	0	0	0	0	0.02	1.21
NL	21.11	14.5	0	10.94	0	0	0	0	4	0	0	1.75	5540.67	0	10.1
NO	59.59	0	0	0	0.73	0	391.93	79421.13	0	34.14	0	0	0	7.04	0
PL	41.73	4.54	0	27.83	0.4	0	8.32	119.15	0	7.27	0	5.05	9545.93	0	23.77
PT	11.42	0	0	18.3	2.66	0	66.67	686.82	0	4.21	2.25	0	2956.35	0.01	21.83
RO	9.58	0	0	2.86	0	0	18.55	10913.39	0	0	0	0	974.67	3.11	1.38
RS	5.06	0	0	0	1.98	0	4.32	424.6	0	2.52	0	0	0	0	0
SE	32.63	0	0	0	1.88	0	158.68	29036.31	0	1.43	0	0	0	1.02	1.61
SI	2.74	0	0	0	0.19	0	0.54	1491.62	0	0	0	0	0	0	1.46
SK	5.67	0	0	1.12	1.1	0	3.94	277.62	0	0	0	2.7	0	0.01	3.54
UK	86.73	6.58	0	34.55	1.2	0	26.64	143.74	6.93	31.6	1.29	17.16	24320.33	4.62	16.95

Table A-59. Capacity distribution for Model Run 57 (Weather Year 1992)

Country	Onshore	Offshore	PV /out	PV / Tracking	Run-of-river	Rooftop PV	PHS	Reservoir	Biomass CHP	PEM Electrolyzer	H2 OCGT	H2 CCGT	Salt Cavern	Vessel	Li-ion Battery
AL	2.07	0	0	1.38	0.03	0	0	1470.55	0	0.27	0	0	181.43	0	0
AT	45.04	0	0	25.73	4.61	0	114.15	1053.49	0	14.93	0	0	0	18.94	3.81
BA	11.05	0	0	0	0.28	0	1.61	1692.83	0	4.43	0	0	1672.98	0	0
BE	3.8	2.58	0	17.21	0.08	0	6.18	13.82	4.75	0	0	3.94	0	0.01	5
BG	3.86	0	0	4.31	0.61	0	40.59	1964.22	0	0.05	0	0	0	5.35	3.53
CH	7.97	0	0	3.27	3.74	0	163.81	5031.16	0	0	0	0	0	0.3	0
CZ	19.48	0	0	9.4	0.41	0	5.99	441.86	0	4.98	0	2.27	0	0.4	0.57
DE	25.94	29.82	0	21.46	4.15	0	39.27	5.46	4.11	0	0	14.02	8741.34	0.02	1.1
DK	16.5	0.54	0	0	0	0	0	0	0	7.57	0	0	1726.13	0.01	2.13
EE	9.51	0	0	0	0	0	0	0	0	2.88	0	0	0	1.12	0
ES	84.67	0.36	0	121.22	2.27	0	63.06	11148.12	0	23.76	0	0	5119.94	24.1	151.23
FI	19.86	0	0	0	2.96	0	0	518.99	0	4.72	1.42	0.25	0	17.63	6.91
FR	141.05	16.6	0	100.73	6.56	0	50.15	5071.64	4.33	30.52	8.71	7.9	11905.46	34.64	104.24
GR	13.01	0	0	8.61	0.22	0	4.64	1753.4	0	3.86	0.68	0	1064.03	13.65	4.68
HR	4.65	0	0	0	0.44	0	5.69	1955.8	0	0.8	0	0	0	0.62	0
HU	6.06	0	0	13.22	0.03	0	0	48.33	0	0	0	0.85	0	5.29	12.45
IE	53.89	0	0	0	0.12	0	2.54	0	0	38.8	1.56	0.61	0	1.82	0.44
IT	42.12	0	0	109.03	10.36	0	61.78	1693.37	0	4.37	0.36	3.93	0	120.74	95.17
LT	18.22	0	0	0	0	0	11.06	23.46	0	6.26	0	0	0	3.2	3.26
LU	0	0	0	3.06	0	0	5.04	0	0	0	0	0.07	0	0.01	0
LV	3.33	0	0	1.57	0.26	0	0	1472.02	0	0.53	0	0	0	2.16	1.17
ME	1.95	0	0	3.75	0	0	0	0	0	0.73	0	0	0	0.01	0
MK	0	0	0	3.3	0.29	0	0	265.54	0	0.25	0	0	0	0.69	0.07
NL	21.11	12.69	0	0	0	0	0	0	4	0	0	11.68	8795.62	0	15.95
NO	49.99	0	0	0	0.73	0	391.93	79421.13	0	26.7	0	0	0	5.91	0
PL	29.8	3.91	0	55.26	0.4	0	8.32	119.15	0	4.15	0	3.15	6001.46	0.02	30.67
PT	11.28	0	0	10.45	2.66	0	66.67	686.82	0	1.68	0	0	2572.01	0	6.58
RO	15.7	0	0	0.17	0	0	18.55	10913.39	0	2.03	0	0	1121.75	5.38	0.75
RS	5.06	0	0	0	1.98	0	4.32	424.6	0	1.56	0	0	0	1.54	0
SE	30.64	0	0	0	1.88	0	158.68	29036.31	0	3.17	0	0	0	0.84	0.16
SI	2.96	0	0	0	0.19	0	0.54	1491.62	0	0	0	0	0	0.14	0.61
SK	4.4	0	0	7.47	1.1	0	3.94	277.62	0	0.38	0	0.08	0	2.04	2.21
UK	92.12	27.88	0	14.44	1.2	0	26.64	143.74	0	46.1	13.47	14.08	30478.33	1.65	5.19

Table A-60. Capacity distribution for Model Run 58 (Weather Year 1993)

Country	Onshore	Offshore	PV /out Tracking	PV / Tracking	Run-of-river	Roof-top PV	PHS	Reservoir	Biomass CHP	PEM Electrolyzer	H2 OCGT	H2 CCGT	Salt Cavern	Vessel	Li-ion Battery
AL	4.09	0	0	1.73	0.03	0	0	1470.55	0	1.23	0.61	0	1064.38	5.79	0.11
AT	48.71	0	0	20.76	4.61	0	114.15	1053.49	0	18.13	0	2.76	0	39.94	5.38
BA	11.05	0	0	4.57	0.28	0	1.61	1692.83	0	8.29	0.22	0	3015.04	0.08	0.12
BE	1.06	0.92	0	32.35	0.08	0	6.18	13.82	4.44	0	0	0.03	0	36.37	7.27
BG	3.86	0	0	4.51	0.61	0	40.59	1964.22	0	0.27	0	0	0	3.41	0.92
CH	8.89	0	0	8.56	3.74	0	163.81	5031.16	0	0	0.29	0	0	13.12	0.01
CZ	16.08	0	0	7.04	0.41	0	5.99	441.86	0	0.69	0.42	5.36	0	10.27	4.09
DE	33.84	13.95	0.01	44.11	4.15	0	39.27	5.46	3.27	0	3.02	23.97	22363.89	58.99	0
DK	17.63	0.63	0	3.17	0	0	0	0	0	8.33	1.04	0.81	4096.09	0.82	0.59
EE	8.86	0	0	0.01	0	0	0	0	0	3.08	0	0	0	1.54	0.24
ES	57.31	0	0.04	150.94	2.27	0	63.06	11148.12	0	25.17	2.98	0	6998.36	46.81	239.32
FI	17.98	0.14	0	0	2.96	0	0	518.99	0	4.22	1.33	1.02	0	14.97	6.27
FR	183.16	0	0.01	108.44	6.56	0	50.15	5071.64	1.05	49.07	7.41	31.55	33313.87	186.26	83.11
GR	13.76	0	2.05	5.41	0.22	0	4.64	1753.4	0	2.83	0	0	433.73	19.61	0.01
HR	6.95	0	0	2.19	0.44	0	5.69	1955.8	0	2.12	0.49	0	0	2.98	0.8
HU	4.75	0	0	20.94	0.03	0	0	48.33	0	0	0	0	0	8.19	20.93
IE	37.74	0	0	3.69	0.12	0	2.54	0	0	25.09	1.36	0.13	0	12.94	3.05
IT	55.31	0	0.02	118.49	10.36	0	61.78	1693.37	0	11.63	0.7	3.15	0	136.06	129.76
LT	19.89	0	0	0.29	0	0	11.06	23.46	0	7.58	0	0	0	45.92	0.52
LU	0	0	0	6.22	0	0	5.04	0	0	0	0	0	0	1.61	0
LV	2.81	0	0	0.51	0.26	0	0	1472.02	0	0.16	0	0	0	3.4	0.19
ME	2.92	0	0	2.2	0	0	0	0	0	1.22	0	0	0	4.15	0.11
MK	0	0	0	4.91	0.29	0	0	265.54	0	0.49	0.96	0	0	13.4	7.62
NL	19.75	19.39	0	0.01	0	0	0	0	0	0.9	0.6	17.21	12919.93	4.48	0.47
NO	48.41	0	0	0	0.73	0	391.93	79421.13	0	25.37	0	0	0	5.74	0
PL	59.63	0.91	0	35.45	0.4	0	8.32	119.15	0	21.17	4.18	10.47	20645.78	14.78	10.92
PT	14.67	0	0	10.79	2.66	0	66.67	686.82	0	2.58	0	0	1162.45	8.1	6.88
RO	12.18	0	0	7.24	0	0	18.55	10913.39	0	1.36	0.18	0	1276.05	9.74	0.41
RS	7.75	0	0	0.01	1.98	0	4.32	424.6	0	2.95	0.01	0	0	4.32	0
SE	31.32	0	0	0.54	1.88	0	158.68	29036.31	0	3.18	0.98	0.43	0	18.1	2.3
SI	4	0	0	0.09	0.19	0	0.54	1491.62	0	0.74	0.01	0	0	3.51	4.1
SK	3.55	0	0	0.02	1.1	0	3.94	277.62	0	0	1.45	1.92	0	2.78	1.88
UK	87.6	21.43	0	20.46	1.2	0	26.64	143.74	0	36.48	2.45	23.22	29652.18	116.12	20.67

Table A-61. Capacity distribution for Model Run 59 (Weather Year 1994)

Country	Onshore	Offshore	PV /out Tracking	PV / Tracking	Run-of-river	Roof-top PV	PHS	Reservoir	Biomass CHP	PEM Electrolyzer	H2 OCGT	H2 CCGT	Salt Cavern	Vessel	Li-ion Battery
AL	3.31	0	0	2.67	0.03	0	0	1470.55	0	1.15	0	0	622.93	0	0
AT	31.25	0	0	30.1	4.61	0	114.15	1053.49	0	3.48	0	0	0	0	21.91
BA	11.05	0	0	0	0.28	0	1.61	1692.83	0	4.26	0	0	2851.5	0	0
BE	3.12	0.73	0	45.37	0.08	0	6.18	13.82	4.75	0	0	1.17	0	0	32.96
BG	3.86	0	0	2.23	0.61	0	40.59	1964.22	0	0.12	0	0	0	0	0
CH	6.68	0	0	4.07	3.74	0	163.81	5031.16	0	0	0	0	0	0	0
CZ	12.65	0	0	8.28	0.41	0	5.99	441.86	0	0	0	3.99	0	0	4.93
DE	26.15	24.72	0	41.67	4.15	0	39.27	5.46	7.21	0	0	8.59	14682.44	0	31.53
DK	19.73	0	0	0.89	0	0	0	0	0	9.25	0	0	9522.64	0	2.49
EE	6.38	0	0	0	0	0	0	0	0	0.79	0	0	0	1.55	0.35
ES	58.1	0	0.01	139.43	2.27	0	63.06	11148.12	0	18.45	0	0	8760.02	0	257.6
FI	18.02	0	0	0	2.96	0	0	518.99	0	2.97	0.65	1.19	0	14.08	10.76
FR	150.79	0	0	135.89	6.56	0	50.15	5071.64	1.5	32.02	0	13.53	23399.4	4.27	108.38
GR	14.26	0	0	8.6	0.22	0	4.64	1753.4	0	3.21	0	0	1771.11	0	1.03
HR	5.57	0	0	1.86	0.44	0	5.69	1955.8	0	0	0	0	0	0	0
HU	0.39	0	0	20.75	0.03	0	0	48.33	0	0	0	0	0	0	15.97
IE	43.12	0	0	0.16	0.12	0	2.54	0	0	28.82	0.94	0	0	0	5.04
IT	40.48	0	0	129.71	10.36	0	61.78	1693.37	0	7.67	0	0	0	77.74	136.86
LT	13.18	0	0	9.52	0	0	11.06	23.46	0	4.25	0	0	0	0	1.68
LU	0	0	0	4.61	0	0	5.04	0	0	0	0	0.15	0	0	0.43
LV	3.59	0	0	1.16	0.26	0	0	1472.02	0	1.38	0	0	0	1.84	5.87
ME	3.88	0	0	1.99	0	0	0	0	0	1.83	0	0	0	0	0
MK	0.96	0	0	2.81	0.29	0	0	265.54	0	0.34	0	0	0	0	0.21
NL	22.47	12.24	0	5.19	0	0	0	0	4	0	0	3.56	4489.76	0	15.58
NO	51.59	0	0	0	0.73	0	391.93	79421.13	0	30.4	0	0	0	5.82	0
PL	42.97	0	0	50.29	0.4	0	8.32	119.15	0	12	0	0	7508.2	0	44.23
PT	16.09	0	0	16.9	2.66	0	66.67	686.82	0	6.4	0	0	5229.17	0	9.22
RO	10.27	0	0	8.06	0	0	18.55	10913.39	0	0.48	0	0	2357.35	0	1.82
RS	5.06	0	0	0	1.98	0	4.32	424.6	0	2.18	0	0	0	0	0
SE	25.3	0	0	0.54	1.88	0	158.68	29036.31	0	0	0	0	0	0	0.98
SI	2.96	0	0	0	0.19	0	0.54	1491.62	0	0	0	0	0	0	0.58
SK	5.67	0	0	2.13	1.1	0	3.94	277.62	0	0	0	0	0	0	3.21
UK	97.01	14.51	0	22.32	1.2	0	26.64	143.74	0	42.89	8.08	7.32	27491.52	0	43.19

Table A-62. Capacity distribution for Model Run 60 (Weather Year 1995)

Country	Onshore	Offshore	PV /out Tracking	PV / Tracking	Run-of-river	Rooftop PV	PHS	Reservoir	Biomass CHP	PEM Electrolyzer	H2 OCGT	H2 CCGT	Salt Cavern	Vessel	Li-ion Battery
AL	3.2	0	0	1.25	0.03	0	0	1470.55	0	0.73	0	0	281.56	0	0
AT	29.81	0	0	29.64	4.61	0	114.15	1053.49	0	4.46	0	0	0	0.01	15.72
BA	9.72	0	0	4.08	0.28	0	1.61	1692.83	0	4.65	0	0	1865.61	0	0
BE	6.21	3.89	0	26	0.08	0	6.18	13.82	4.75	0	0	1.27	0	0	6.07
BG	3.86	0	0	4.67	0.61	0	40.59	1964.22	0	0.34	0	0	0	0	0.72
CH	6.08	0	0	6.38	3.74	0	163.81	5031.16	0	0	0	0	0	0	0
CZ	11.32	0	0	12.17	0.41	0	5.99	441.86	1.08	0	0	2.6	0	0	4.91
DE	29.5	13.78	0	34.33	4.15	0	39.27	5.46	6.68	0	2.96	17.47	23587.28	0	11.13
DK	12.03	0	0	0.63	0	0	0	0	0	2.94	0.26	1.99	3985.03	0	0.1
EE	9.96	0	0	0	0	0	0	0	0	4.52	0	0	0	1.52	0.45
ES	86.53	0	0.01	109.1	2.27	0	63.06	11148.12	0	23.92	1.74	0	7886.72	0.01	128.82
FI	20.23	0	0	0	2.96	0	0	518.99	0	4.45	0.93	0.84	0	22.43	7.94
FR	169.74	10.74	0	102.64	6.56	0	50.15	5071.64	0	46.03	0	10.08	22871.56	17.67	66.33
GR	14.96	0	0	12.56	0.22	0	4.64	1753.4	0	4.68	0	0	1706.2	0	4.24
HR	5.54	0	0	0.01	0.44	0	5.69	1955.8	0	1	0	0	0	0	0.27
HU	4.73	0	0	22.21	0.03	0	0	48.33	0	0	0	1.48	0	0	18.64
IE	34.15	0	0	2.24	0.12	0	2.54	0	0	21.56	0.94	0.63	0	0	2.89
IT	47.22	0	0	115.18	10.36	0	61.78	1693.37	0	9.67	0	0	0	88.44	112.03
LT	22.17	0	0	0	0	0	11.06	23.46	0	7.66	0	0	0	0.01	3.74
LU	0.04	0	0	6.22	0	0	5.04	0	0	0	0.01	0.06	0	0	0.29
LV	4.21	0	0	0.04	0.26	0	0	1472.02	0	1.41	0	0	0	2.57	1.93
ME	2.92	0	0	1.93	0	0	0	0	0	0.09	0	0	0	0	0
MK	0.96	0	0	3.93	0.29	0	0	265.54	0	0.27	0	0	0	0	2.64
NL	19.75	13.38	0	0	0	0	0	0	0	0	0	24.48	24126.46	0	5.1
NO	48.1	0	0	0	0.73	0	391.93	79421.13	0	28.71	0	0	0	6.79	0
PL	37.12	0	0	34.51	0.4	0	8.32	119.15	0	1.39	0.06	5.76	11385.86	0	16.36
PT	16.78	0	0	10.76	2.66	0	66.67	686.82	0	5.87	1.18	0	4418.94	0	3.59
RO	9.69	0	0	8.35	0	0	18.55	10913.39	0	0	0	0	2285.69	0	2.35
RS	5.06	0	0	0	1.98	0	4.32	424.6	0	3.41	0	0	0	0	0
SE	35.21	0	0	0	1.88	0	158.68	29036.31	0	7.31	0	1.24	0	0.59	3.68
SI	2.01	0	0	0	0.19	0	0.54	1491.62	0	0	0	0	0	0	0.41
SK	4.2	0	0	1.53	1.1	0	3.94	277.62	0	0	0	1.03	0	0	0
UK	102.57	12.91	0	28.23	1.2	0	26.64	143.74	0	43.97	14.03	9.98	29635.96	0	25.68

Table A-63. Capacity distribution for Model Run 61 (Weather Year 1996)

Country	Onshore	Offshore	PV /out Tracking	PV / Tracking	Run-of-river	Roof-top PV	PHS	Reservoir	Biomass CHP	PEM Electrolyzer	H2 OCGT	H2 CCGT	Salt Cavern	Vessel	Li-ion Battery
AL	3.08	0	0	1.22	0.03	0	0	1470.55	0	0.13	0	0	106.44	0.01	0.52
AT	32.8	0	0	19.65	4.61	0	114.15	1053.49	0	8.83	0	0	0	17.27	2.73
BA	11.05	0	0	0	0.28	0	1.61	1692.83	0	3.61	0	0	898.48	0	0
BE	4.49	3.17	0	25.71	0.08	0	6.18	13.82	3.54	0	0.96	1.18	0	18.78	4.51
BG	3.86	0	0	3.49	0.61	0	40.59	1964.22	0	0	0	0	0	5.34	0
CH	8.76	0	0	1.48	3.74	0	163.81	5031.16	0	0	0	0	0	8.31	0
CZ	14.05	0	0	15.4	0.41	0	5.99	441.86	0	1.59	0	1.65	0	19.15	7.17
DE	35.76	26.86	0	43.58	4.15	0	39.27	5.46	1.18	0	5.16	10.23	11932.74	5.71	37.07
DK	15.69	0	0	1.07	0	0	0	0	0	5.72	0	0	2167.91	0.01	0.9
EE	10.49	0	0	6.03	0	0	0	0	0	4	0	0	0	1.71	5.47
ES	81.68	0	0.01	102.78	2.27	0	63.06	11148.12	0	21.82	0	0	4429.37	30.77	47.57
FI	19.86	0	0	0	2.96	0	0	518.99	0	3.47	0.39	2.87	0	32.81	2.89
FR	169.62	13.12	0.01	154.53	6.56	0	50.15	5071.64	0	56.59	5.83	6.77	12190.8	118.34	186.92
GR	17.48	0	0	8.71	0.22	0	4.64	1753.4	0	4.13	0	0	778.07	12.5	0.57
HR	4.65	0	0	1.85	0.44	0	5.69	1955.8	0	0.11	0	0	0	3.74	0
HU	4.75	0	0	18.8	0.03	0	0	48.33	0	0	0	0	0	12.65	11.47
IE	34.83	0	0	0.04	0.12	0	2.54	0	0	23.21	10.36	0	0	0.01	2.24
IT	53.52	0	0.01	112.19	10.36	0	61.78	1693.37	0	8.39	0	0	0	135.37	60.71
LT	14.51	0	0	10.4	0	0	11.06	23.46	0	1.36	0	0	0	3.38	2.69
LU	0	0	0	2.76	0	0	5.04	0	0	0	0	0.32	0	0.14	0.02
LV	3.67	0	0	3.76	0.26	0	0	1472.02	0	0.23	0	0	0	2.14	0.2
ME	2.92	0	0	0.42	0	0	0	0	0	0.13	0	0	0	0.03	0
MK	0.96	0	0	3.54	0.29	0	0	265.54	0	0.28	0	0	0	1.38	0.35
NL	22.47	11.81	0	5.21	0	0	0	0	1.29	0	1.44	13.18	12930.63	0	41.85
NO	51.2	0	0	0	0.73	0	391.93	79421.13	0	27.56	0	0	0	5.77	0
PL	55.2	0	0	35.1	0.4	0	8.32	119.15	0	7.18	3.09	1.8	6044.7	0.01	27.94
PT	17.31	0	0	13.8	2.66	0	66.67	686.82	0	6.53	0	0	2661.74	0.03	1.13
RO	9.3	0	0	4	0	0	18.55	10913.39	0	0	0	0	776.43	6.58	0
RS	5.06	0	0	0	1.98	0	4.32	424.6	0	2.6	0	0	0	0.8	0
SE	27.98	0	0	1.15	1.88	0	158.68	29036.31	0	0	0	0	0	1.22	1.43
SI	2.01	0	0	0	0.19	0	0.54	1491.62	0	0	0	0	0	2.88	0.91
SK	4.4	0	0	9.01	1.1	0	3.94	277.62	0	0.05	0	0.07	0	4.27	13.36
UK	108.44	10.28	0	42.68	1.2	0	26.64	143.74	0	48.31	5.96	16.21	29418.96	0.04	34.91

Table A-64. Capacity distribution for Model Run 62 (Weather Year 1997)

Country	Onshore	Offshore	PV /out Tracking	PV / Tracking	Run-of-river	Roof-top PV	PHS	Reservoir	Biomass CHP	PEM Electrolyzer	H2 OCGT	H2 CCGT	Salt Cavern	Vessel	Li-Ion Battery
AL	3.08	0	0	1.44	0.03	0	0	1470.55	0	0.58	0	0	428.19	0	0
AT	37.44	0	0	35.95	4.61	0	114.1	1053.49	0	9.82	0	0.78	0	27.78	13.65
BA	13.04	0	0	0	0.28	0	1.61	1692.83	0	5.59	0	0	1309.41	0	0
BE	7.16	2.32	0	23.4	0.08	0	6.18	13.82	4.75	0	0	0	0	18	3.97
BG	3.86	0	0	2.49	0.61	0	40.59	1964.22	0	0	0	0	0	4.52	0
CH	8.89	0	0	5.29	3.74	0	163.8	5031.16	0	0	0	0	0	14.32	0
CZ	9.74	0	0	10.28	0.41	0	5.99	441.86	3.56	0	0	2.31	0	8.97	0.55
DE	37.23	14.6	0	27.66	4.15	0	39.27	5.46	20.3	0	9.8	12.1	21869.7	30.13	0.62
DK	18.14	0.78	0	0.51	0	0	0	0	0	9.54	0.3	0	1818.42	0.45	1.35
EE	9.51	0.63	0	0	0	0	0	0	0	4.12	0	0	0	1.54	0.12
ES	113.0	0.87	0	105.2	2.27	0	63.06	11148.1	0	28.4	0.5	0	6488.21	42.21	98.74
FI	21.68	0	0	0	2.96	0	0	518.99	0	4.79	0.5	0	0	17.3	15.03
FR	155.4	13.7	0.1	100.4	6.56	0	50.15	5071.64	5.96	46.9	4.2	9.02	16739.3	120.0	111.6
G	14.76	0	0	13.55	0.22	0	4.64	1753.4	0	6.32	0	1.05	1561.43	11.85	9.19
HR	6.03	0	0	1.06	0.44	0	5.69	1955.8	0	1.04	0	0	0	4.72	1.13
HU	4.75	0	0	8.67	0.03	0	0	48.33	0	0	0	0	0	8.72	2.29
IE	23.91	0	0	1.82	0.12	0	2.54	0	0	14.6	0.2	1.18	0	8.14	3.11
IT	51.17	0	0	105.5	10.3	0	61.78	1693.37	4.14	13.4	0	0.97	0	148.6	61.22
LT	11.78	0	0	0	0	0	11.06	23.46	0	3.51	0	0	0	4.92	0.29
LU	0.08	0	0	2.28	0	0	5.04	0	0	0	0	0.31	0	0.92	0
LV	4.21	0	0	0	0.26	0	0	1472.02	0	1.48	0	0	0	2.72	0.15
M	4.85	0	0	0.48	0	0	0	0	0	1.35	0	0	0	0.05	0
M	0.96	0	0	2.39	0.29	0	0	265.54	0	0.19	0	0	0	0.01	0
NL	22.47	13.1	0	2.52	0	0	0	0	4	0	1.2	15.4	14480.9	0.03	0.45
N	59.66	0	0	0	0.73	0	391.9	79421.1	0	33.2	0	0	0	7.18	0
PL	36.92	7.38	0	40.43	0.4	0	8.32	119.15	0.44	12.5	0.6	6.73	9983.1	0.02	4.28
PT	6.98	0	0	15.15	2.66	0	66.67	686.82	0	1.82	1.1	0	1694.43	12.39	11.73
R	14.05	0	0	5.02	0	0	18.55	10913.3	0	1.92	0	0	1210.36	6.72	1.21
RS	5.06	0	0	0	1.98	0	4.32	424.6	0	1.79	0	0	0	2.22	0
SE	31.65	0	0	1.08	1.88	0	158.6	29036.3	0	4	0.0	0	0	1.27	0.86
SI	2.51	0	0	0	0.19	0	0.54	1491.62	0	0	0	0	0	3.61	0.95
SK	6.15	0	0	9.75	1.1	0	3.94	277.62	0.04	0	0.0	2.75	0	0.02	0.41
UK	95.31	28.2	0	27.24	1.2	0	26.64	143.74	0	42.7	4.1	13.2	21373.6	60.23	19.16

Table A-65. Capacity distribution for Model Run 63 (Weather Year 1998)

Country	Onshore	Offshore	PV /out Tracking	PV / Tracking	Run-of-river	Rooftop PV	PHS	Reservoir	Biomass CHP	PEM Electrolyzer	H2 OCGT	H2 CCGT	Salt Cavern	Vessel	Li-ion Battery
AL	2.38	0	0	1.95	0.03	0	0	1470.55	0	0.75	0	0	0.73	0.32	0
AT	32.24	0	0	19.72	4.61	0	114.15	1053.49	0	7.23	2.28	0	0	26.61	11.62
BA	11.05	0	0	0.13	0.28	0	1.61	1692.83	0	4.2	0	0	237.56	0.01	0
BE	4.08	4.72	0	25.16	0.08	0	6.18	13.82	0	0	0.22	5.01	0	84.36	17.33
BG	3.86	0	0	3	0.61	0	40.59	1964.22	0	0	0	0	0	4.66	0.01
CH	7.16	0	0	1.46	3.74	0	163.81	5031.16	0	0	0	0	0	24.6	0
CZ	12.87	0	0	4.49	0.41	0	5.99	441.86	0	0	0	2.39	0	5.92	6.68
DE	42.61	20.07	0	34.14	4.15	0	39.27	5.46	0	0	10.2	19.04	15781.45	55.94	0.56
DK	16.51	3.03	0	0.04	0	0	0	0	0	9.41	0.84	0	3568.18	0.02	1.35
EE	9.51	1.22	0	3.22	0	0	0	0	0	3.42	0	0	0	1.24	1.06
ES	61.79	0	0.01	114.07	2.27	0	63.06	11148.12	0	10.6	2.47	0	2753.94	91.42	164.63
FI	18.82	0	0	0	2.96	0	0	518.99	0	3.47	0.11	2.39	0	23.44	1.53
FR	164.82	9.14	0.01	95.47	6.56	0	50.15	5071.64	0	50.16	2.54	8.6	7279.81	95.19	60.33
GR	13.68	0	0	8.31	0.22	0	4.64	1753.4	0	3.18	2.25	0	1734.01	17.63	2.59
HR	4.75	0	0	2.6	0.44	0	5.69	1955.8	0	1.17	0	0	0	1.43	0
HU	4.75	0	0	10.34	0.03	0	0	48.33	0	0	0.75	1.76	0	22.22	6.24
IE	32.86	0	0	3.63	0.12	0	2.54	0	0	23.56	0.56	1.03	0	8.3	5.71
IT	46.28	0	0.01	108.61	10.36	0	61.78	1693.37	0	12.03	0	0.22	0	148.08	68.17
LT	13.71	0	0	7.46	0	0	11.06	23.46	0	6.24	0.14	0	0	3.89	0.95
LU	0.04	0	0	4.24	0	0	5.04	0	0	0	0	0.11	0	1.89	0
LV	4.21	0	0	2.85	0.26	0	0	1472.02	0	1.72	0	0	0	2.23	0.27
ME	3.74	0	0	3.95	0	0	0	0	0	2.1	0	0	0	0.01	0
MK	0	0	0	1.86	0.29	0	0	265.54	0	0.02	0	0	0	1.98	0
NL	23.82	25.4	0	7.97	0	0	0	0	0	10.22	0.02	2.96	3329.1	14.49	30.7
NO	38.7	0	0	0	0.73	0	391.93	79421.13	0	19.8	0	0	0	6.15	0
PL	46.79	6.52	0	20.65	0.4	0	8.32	119.15	0	14.48	0.45	6.38	10748.27	6.42	4.21
PT	12.61	0	0	5.33	2.66	0	66.67	686.82	0	0.96	0	0	391.44	12.13	2.12
RO	12.36	0	0	6.94	0	0	18.55	10913.39	0	0.64	0	0	624.04	10.08	0
RS	5.06	0	0	0	1.98	0	4.32	424.6	0	2.62	0	0	0	0.01	0
SE	30.04	0	0	0	1.88	0	158.68	29036.31	0	0.18	0.75	0.07	0	1.99	2.54
SI	2.01	0	0	0	0.19	0	0.54	1491.62	0	0	0	0	0	0.02	0.74
SK	2.91	0	0	6.3	1.1	0	3.94	277.62	0	0	0	1.08	0	1.79	4.94
UK	120.34	14.99	0	28.72	1.2	0	26.64	143.74	0	56.67	6.81	13.66	10585.29	76.96	18.58

Table A-66. Capacity distribution for Model Run 64 (Weather Year 1999)

Country	Onshore	Offshore	PV /out Tracking	PV / Tracking	Run-of-river	Rooftop PV	PHS	Reservoir	Biomass CHP	PEM Electrolyzer	H2 OCGT	H2 CCGT	Salt Cavern	Vessel	Li-ion Battery
AL	2.07	0	0	2.3	0.03	0	0	1470.55	0	0	0	0	244.59	0	0
AT	32.21	0	0	22.13	4.61	0	114.15	1053.49	0	7.17	0	0	0	24.01	4.71
BA	10.9	0	0	5.12	0.28	0	1.61	1692.83	0	5.54	0	0	1627.26	0	0
BE	4.91	0.54	0	42.53	0.08	0	6.18	13.82	0.85	0	2.52	6.78	0	0.02	45.59
BG	2.07	0	0	5.79	0.61	0	40.59	1964.22	0	0	0	0	0	5.19	0.54
CH	8.11	0	0	1.65	3.74	0	163.81	5031.16	0	0	0	0	0	1.08	0
CZ	16.85	0	0	16.56	0.41	0	5.99	441.86	0	1.37	2.76	0	0	4.95	21.43
DE	56.37	19.48	0	49.71	4.15	0	39.27	5.46	0	0	0	7.55	7864.04	0.03	68.54
DK	11.12	0	0	1.58	0	0	0	0	0	2.48	0	0	594.56	0.01	0.25
EE	5.93	0	0	0	0	0	0	0	0	0.44	0	0	0	2.13	1.81
ES	46.35	0	0.02	151.01	2.27	0	63.06	11148.12	0	14.48	0	0	4720.1	15.1	224.24
FI	19.66	0	0	0	2.96	0	0	518.99	0	2.45	0.02	0.57	0	12.03	13.14
FR	159.88	0.4	0.01	105.43	6.56	0	50.15	5071.64	0	35.96	1.07	1.48	9559.05	43.73	149.18
GR	12.82	0	1.11	11.69	0.22	0	4.64	1753.4	0	3.96	0	0	995	11.17	12.59
HR	5.17	0	0	5.1	0.44	0	5.69	1955.8	0	1.82	0	0	0	0.18	0.59
HU	4.75	0	0	14.29	0.03	0	0	48.33	0	0	0	0	0	8.51	11.69
IE	64.63	0	0	2.87	0.12	0	2.54	0	0	43.43	1.02	0	0	0	2.39
IT	22.95	0	0.01	136.26	10.36	0	61.78	1693.37	0	6.35	0	0	0	144.69	191.48
LT	9.88	0	0	7.18	0	0	11.06	23.46	0	1.09	0	0	0	4.19	4.34
LU	0.08	0	0	5.67	0	0	5.04	0	0	0	0	1.11	0	0.01	2.49
LV	2.57	0	0	3.06	0.26	0	0	1472.02	0	0.76	0	0	0	3.57	1.88
ME	1.95	0	0	2.75	0	0	0	0	0	0.88	0	0	0	0.01	0
MK	0.48	0	0	2.3	0.29	0	0	265.54	0	0.37	0	0	0	0.05	0.23
NL	27.86	11.16	0	9.21	0	0	0	0	0	1.37	1.05	5.44	7528.32	0	20.81
NO	47.2	0	0	0	0.73	0	391.93	79421.13	0	27.56	0	0	0	6.74	0
PL	43.07	0	0	32.68	0.4	0	8.32	119.15	0	6.3	0.46	0	4196.81	0.01	27.55
PT	17.16	0	0.12	13.09	2.66	0	66.67	686.82	0	5.32	0	0	2653.81	0.01	1.21
RO	13.05	0	0	11.39	0	0	18.55	10913.39	0	2.14	0	0	1140.72	5.19	1.68
RS	5.06	0	0	0	1.98	0	4.32	424.6	0	0.24	0	0	0	0.4	0
SE	25.83	0	0	6.84	1.88	0	158.68	29036.31	0	1.49	0	0	0	2.91	0.04
SI	3	0	0	0.09	0.19	0	0.54	1491.62	0	0.2	0	0	0	3.02	0.55
SK	5.9	0	0	0.01	1.1	0	3.94	277.62	0	0	0	0	0	4.74	7.24
UK	91.94	18.48	0	33.62	1.2	0	26.64	143.74	0	40.86	2.33	8.02	22616.49	0.02	43.66

Table A-67. Capacity distribution for Model Run 65 (Weather Year 2000)

Country	Onshore	Offshore	PV /out Tracking	PV / Tracking	Run-of-river	Rooftop PV	PHS	Reservoir	Biomass CHP	PEM Electrolyzer	H2 OCGT	H2 CCGT	Salt Cavern	Vessel	Li-ion Battery
AL	2.81	0	0	2.32	0.03	0	0	1470.55	0	0.29	0	0	50.96	0.94	0
AT	32.23	0	0	19.65	4.61	0	114.15	1053.49	0	5.51	0	0	0	13.98	1.46
BA	11.05	0	0	1.94	0.28	0	1.61	1692.83	0	4.14	0	0	124.57	0.02	0
BE	5.5	4.03	0	30.04	0.08	0	6.18	13.82	0.36	0	0.17	7.47	0	0.34	13.88
BG	3.86	0	0	3.92	0.61	0	40.59	1964.22	0	0	0	0	0	6.22	0.53
CH	8.89	0	0	1.9	3.74	0	163.81	5031.16	0	0	0	0	0	15.11	0
CZ	11.62	0	0	16.59	0.41	0	5.99	441.86	0	0.94	0	0	0	12.19	11.18
DE	33.65	29.84	0	43.59	4.15	0	39.27	5.46	0	0	2.64	7.33	5246.01	15.66	29.46
DK	16.08	0.78	0	1.71	0	0	0	0	0	7.89	0	0	2033.94	0.02	4.14
EE	10.45	0	0	0	0	0	0	0	0	2.62	0	0	0	1.49	2.8
ES	65.02	0	0.03	131.55	2.27	0	63.06	11148.12	0	21.34	0	0	4754.1	46.58	197.17
FI	18.38	0	0	0	2.96	0	0	518.99	0	2.99	0.76	0.27	0	19.24	6.54
FR	152.56	19.81	0.01	98.47	6.56	0	50.15	5071.64	0	48.87	0	4.88	8588.93	132.32	77.68
GR	14.31	0	0	5.78	0.22	0	4.64	1753.4	0	2.83	0	0	214.02	15.49	0.92
HR	4.65	0	0	4.13	0.44	0	5.69	1955.8	0	1.38	0	0	0	5.95	0
HU	7.52	0	0	13.61	0.03	0	0	48.33	0	0.21	0.09	0	0	8.73	10.42
IE	32.35	0	0	8	0.12	0	2.54	0	0	21	1.19	0.84	0	10.66	0.02
IT	47.81	0	0.01	102.49	10.36	0	61.78	1693.37	0	9.62	0	0	0	141.85	86.23
LT	13.71	0	0	0	0	0	11.06	23.46	0	1.13	0.21	0.01	0	4.72	4.31
LU	0.13	0	0	5.48	0	0	5.04	0	0	0	0.05	0	0	1.12	0.03
LV	4	0	0	0	0.26	0	0	1472.02	0	0.77	0	0	0	2.72	0.86
ME	3.88	0	0	2.23	0	0	0	0	0	1.47	0	0	0	0.6	0
MK	0.96	0	0	1.85	0.29	0	0	265.54	0	0.44	0	0	0	3.71	0.04
NL	23.82	21.13	0	2.63	0	0	0	0	0	10.34	1.04	7	7987.88	0.01	14.02
NO	60.25	0	0	0	0.73	0	391.93	79421.13	0	33.72	0	0	0	7.36	0
PL	45.21	1.06	0	35.02	0.4	0	8.32	119.15	0	11.3	3.3	1.24	4955.91	2.92	28.02
PT	17.48	0	0	7.86	2.66	0	66.67	686.82	0	4.49	0	0	1298.03	6.72	0.07
RO	13.1	0	0	5.33	0	0	18.55	10913.39	0	1.25	0	0	281.7	15.6	0.66
RS	5.06	0	0	0	1.98	0	4.32	424.6	0	2.5	0	0	0	7.25	0
SE	36.15	0	0	5.7	1.88	0	158.68	29036.31	0	6.63	0	0	0	1.63	8.42
SI	2.01	0	0	0	0.19	0	0.54	1491.62	0	0	0	0	0	4.93	0
SK	5.9	0	0	0	1.1	0	3.94	277.62	0	0.24	1.03	0	0	4.74	0.44
UK	92.24	4.29	0	48.32	1.2	0	26.64	143.74	0	34.12	4.57	17.5	13654.95	307.54	22.75

Table A-68. Capacity distribution for Model Run 66 (Weather Year 2001)

Country	Onshore	Offshore	PV /out Tracking	PV / Tracking	Run-of-river	Rooftop PV	PHS	Reservoir	Biomass CHP	PEM Electrolyzer	H2 OCGT	H2 CCGT	Salt Cavern	Vessel	Li-ion Battery
AL	3.34	0	0	2.55	0.03	0	0	1470.55	0	1.01	0	0	268.5	0.02	0
AT	44.92	0	0	22.17	4.61	0	114.15	1053.49	0	13.58	0	0	0	31.01	8.72
BA	14.7	0	0	3.67	0.28	0	1.61	1692.83	0	8.51	0	0	2448.97	0.01	0
BE	3.12	2.27	0	16.1	0.08	0	6.18	13.82	4.75	0	0	1.18	0	26.83	0.01
BG	4.94	0	0	2.02	0.61	0	40.59	1964.22	0	0	0	0	0	6.11	0.8
CH	10.18	0	0	5.22	3.74	0	163.81	5031.16	0	0	0	0	0	14.02	0
CZ	20.81	0	0	6.68	0.41	0	5.99	441.86	0	2.71	0	0	0	13.4	6.01
DE	44.15	25.11	0	52.36	4.15	0	39.27	5.46	0	0	2.83	14.37	14958.23	20.45	5.42
DK	19.99	1.01	0	1.47	0	0	0	0	0	9.91	0	0	5698.85	0.02	2.85
EE	10.44	0	0	0	0	0	0	0	0	3.05	0	0	0	9.04	0.82
ES	87.78	0	0.05	129.84	2.27	0	63.06	11148.12	0	34.21	0	0	8194	72.06	178.72
FI	19.87	0	0	0	2.96	0	0	518.99	0	5.28	0	2.75	0	42.99	5.1
FR	165.27	7.55	0.01	100.11	6.56	0	50.15	5071.64	0	46.73	8.36	11.33	21179.22	96.4	60.67
GR	12.82	0	0	6.77	0.22	0	4.64	1753.4	0	2.93	0.8	0	739.9	16.26	3.6
HR	5.07	0	0	1.09	0.44	0	5.69	1955.8	0	0.94	0	0	0	2.98	0.12
HU	11.93	0	0	10.84	0.03	0	0	48.33	0	0.73	0	0	0	10.95	8.47
IE	23.22	0	0	2.49	0.12	0	2.54	0	0	12.02	0.37	1.18	0	9.87	1.61
IT	62.41	0	0.01	77.98	10.36	0	61.78	1693.37	0	10.9	0	0	0	145.4	22.93
LT	9.29	0	0	0	0	0	11.06	23.46	0	0.6	0.01	0.04	0	4.67	0.03
LU	0.17	0	0	4.2	0	0	5.04	0	0	0	0	0.43	0	1.38	0
LV	3.2	0	0	0	0.26	0	0	1472.02	0	0.1	0	0	0	3.15	0.17
ME	3.88	0	0	3.49	0	0	0	0	0	2.09	0	0	0	0.63	0
MK	0.87	0	0	2.72	0.29	0	0	265.54	0	0.49	0	0	0	1.78	0.41
NL	22.47	13.87	0	2.54	0	0	0	0	4	0.6	7.16	12.07	16853.58	0.29	3.53
NO	48.78	0	0	0	0.73	0	391.93	79421.13	0	23.71	0	0	0	7.43	0
PL	50.92	0.62	0	45.45	0.4	0	8.32	119.15	0	14.55	1.58	6.41	8961.58	11.92	20.09
PT	15.36	0	0.01	7.2	2.66	0	66.67	686.82	0	2.15	0	0	653.46	5.3	6.47
RO	11.46	0	0	2.42	0	0	18.55	10913.39	0	0	0	0	602.94	6.29	0.19
RS	5.06	0	0	0	1.98	0	4.32	424.6	0	2.31	0	0	0	9.48	0
SE	35.88	0.98	0	0	1.88	0	158.68	29036.31	0	4.45	1.81	0	0	7.01	3.88
SI	1.51	0	0	0	0.19	0	0.54	1491.62	0	0	0	0	0	0.5	0.92
SK	7.43	0	0	3.64	1.1	0	3.94	277.62	0	1.42	0	0	0	4.96	0
UK	86.69	22.01	0	49.4	1.2	0	26.64	143.74	0	41.65	0.69	28.81	29413.71	113.47	19.34

Table A-69. Capacity distribution for Model Run 67 (Weather Year 2002)

Country	Onshore	Offshore	PV /out Tracking	PV / Tracking	Run-of-river	Rooftop PV	PHS	Reservoir	Biomass CHP	PEM Electrolyzer	H2 OCGT	H2 CCGT	Salt Cavern	Vessel	Li-ion Battery
AL	3.08	0	0	1.34	0.03	0	0	1470.55	0	1.04	0	0	688.76	0	0.33
AT	31.19	0	0	12.5	4.61	0	114.1	1053.49	0	2.08	0	0	0	0.03	6.99
BA	14.7	0	0	3.46	0.28	0	1.61	1692.83	0	8.25	0	0	2320.93	0	0
BE	9.79	4.54	0	16.46	0.08	0	6.18	13.82	4.75	0	0.6	4.53	0	0	10.43
BG	3.86	0	0	9.13	0.61	0	40.59	1964.22	0	0.61	0	0	0	0	5.07
CH	7.85	0	0	6.37	3.74	0	163.8	5031.16	0	0	0	0	0	0	0
CZ	7.64	0	0	8.83	0.41	0	5.99	441.86	3.93	0	0	0.69	0	0	1.17
DE	30.88	20.9	0	34.82	4.15	0	39.27	5.46	14.1	0	4.8	0	9068.11	0	0.36
DK	15.83	0	0	0	0	0	0	0	0	5.29	0	0	1546.83	0	0.9
EE	7.71	0	0	5.48	0	0	0	0	0	3.17	0	0	0	1.49	0.6
ES	80.74	0	0.0	121.4	2.27	0	63.06	11148.1	0	29.7	0	0	9643.23	0.01	103.0
FI	17.55	0	0	0	2.96	0	0	518.99	0	2.68	0.3	0.92	0	15.59	7.35
FR	188.0	1.84	0	118.4	6.56	0	50.15	5071.64	0	50.1	1.2	5.09	14515.2	12.29	94.91
G	13.6	0	0	12.41	0.22	0	4.64	1753.4	0	3.67	0	0	1561.41	0	5.82
HR	7.96	0	0	1.35	0.44	0	5.69	1955.8	0	2.96	0	0	0	0	0.71
HU	0.84	0	0	9.22	0.03	0	0	48.33	0	0	0.0	1.14	0	0	3.1
IE	34.62	0	0	9.93	0.12	0	2.54	0	0	27.1	0.4	0	0	0	2.74
IT	42.46	0	0	143.1	10.3	0	61.78	1693.37	0	12.5	0	0.25	0	119.9	153.8
LT	11.77	0	0	4.65	0	0	11.06	23.46	0	0.31	0	0	0	0.19	7.04
LU	0.13	0	0	5.44	0	0	5.04	0	0	0	0.0	0	0	0	0.07
LV	4.21	0	0	2.16	0.26	0	0	1472.02	0	1.09	0	0	0	2.47	1.78
M	2.92	0	0	2.15	0	0	0	0	0	1.86	0	0	0	0	0.24
M	0	0	0	3.71	0.29	0	0	265.54	0	0.45	0	0	0	0	0.53
NL	18.38	20.8	0	0	0	0	0	0	0.22	4.71	3.1	4.41	9045.45	0	6.42
N	40.93	0	0	0	0.73	0	391.9	79421.1	0	22.1	0	0	0	5.47	0
PL	31.24	15.4	0	29.96	0.4	0	8.32	119.15	0	12.3	1.2	3.4	8095.88	0	29.68
PT	12.06	0	0	11.36	2.66	0	66.67	686.82	0	2.12	0	0	2565.88	0	12.87
R	14.15	0	0	7.57	0	0	18.55	10913.3	0	1.89	0	0	2138.51	0	1.87
RS	5.06	0	0	0	1.98	0	4.32	424.6	0	1.53	0	0	0	0	0
SE	29.92	0	0	3.2	1.88	0	158.6	29036.3	0	1.07	0	0	0	0	6.75
SI	3.5	0	0	0	0.19	0	0.54	1491.62	0	0.19	0	0	0	0	2
SK	5.34	0	0	1.8	1.1	0	3.94	277.62	1.86	0	0.0	1.23	0	0	0.29
UK	88.08	10.9	0	44.38	1.2	0	26.64	143.74	0	24.3	8.0	16.2	27181.1	0	35.62

Table A-70. Capacity distribution for Model Run 68 (Weather Year 2003)

Country	Onshore	Offshore	PV /out Tracking	PV / Tracking	Run-of-river	Rooftop PV	PHS	Reservoir	Biomass CHP	PEM Electrolyzer	H2 OCGT	H2 CCGT	Salt Cavern	Vessel	Li-ion Battery
AL	4.68	0	0	3.33	0.03	0	0	1470.55	0	1.7	0	0	758.42	0	0
AT	35.94	0	0	33.05	4.61	0	114.15	1053.49	0	10.19	0	0	0	17.18	28.21
BA	16.77	0	0	8.18	0.28	0	1.61	1692.83	0	10.5	0	0	2620.57	0	0
BE	6.84	4.72	0	45.03	0.08	0	6.18	13.82	0	0	0.89	6.15	0	36.43	63.82
BG	1.77	0	0	3.77	0.61	0	40.59	1964.22	0	0	0	0	0	5.9	0
CH	8.11	0	0	6.4	3.74	0	163.81	5031.16	0	0	0	0	0	12.33	0.09
CZ	15.57	0	0	21.96	0.41	0	5.99	441.86	0	3.57	0	0.48	0	18.19	34.75
DE	35.22	13.48	0	53.91	4.15	0	39.27	5.46	0.47	0	4.61	7.9	6130.44	26.44	30.1
DK	12.55	0	0	4.24	0	0	0	0	0	4.28	1.11	0	2515.85	0	1.77
EE	6.38	1.18	0	0.84	0	0	0	0	0	1.15	0	0	0	2.01	4.49
ES	73.26	0.82	0.01	121.43	2.27	0	63.06	11148.12	0	16.93	1.48	0	3167.5	76.79	123.36
FI	19.03	0	0	0	2.96	0	0	518.99	0	3.96	0.36	1.19	0	18.86	5.06
FR	168.26	4.77	0.01	147.87	6.56	0	50.15	5071.64	0	37.6	0	0	4674.62	88.33	150.16
GR	15.58	0	0.85	7.38	0.22	0	4.64	1753.4	0	3.92	0	0	720.4	12.1	0.57
HR	6.95	0	0	5.54	0.44	0	5.69	1955.8	0	3.16	0	0	0	0.03	0
HU	4.46	0	0	20.46	0.03	0	0	48.33	0	0	0	0	0	7.86	23.23
IE	39	0	0	9.92	0.12	0	2.54	0	0	31.87	1.57	0	0	6.32	2.74
IT	48.81	0	0.01	108.68	10.36	0	61.78	1693.37	0	6.51	0	0	0	159.55	91.28
LT	9.43	0	0	0	0	0	11.06	23.46	0	1.16	0.19	0	0	5.05	1.28
LU	0.26	0	0	6.22	0	0	5.04	0	0	0	0	0.59	0	1.47	6.25
LV	3.44	0	0	0.01	0.26	0	0	1472.02	0	0.85	0	0	0	3.35	0.9
ME	5.81	0	0	2.24	0	0	0	0	0	2.05	0	0	0	0.23	0
MK	0.96	0	0	1.48	0.29	0	0	265.54	0	0	0	0	0	1.3	0
NL	26.51	12.47	0	32.27	0	0	0	0	0	8.74	2.78	1.99	4268.87	0.01	37.31
NO	48.24	0	0	0	0.73	0	391.93	79421.13	0	23.14	0	0	0	6.61	0
PL	38.08	0.47	0	69.23	0.4	0	8.32	119.15	0	8.7	0.94	2.89	4718.33	12.19	70.51
PT	16.55	0	0	19.98	2.66	0	66.67	686.82	0	5.85	0	0	2040.67	9.03	19.27
RO	11.68	0	0	6.34	0	0	18.55	10913.39	0	0	0	0	421.5	9.45	0.97
RS	4.76	0	0	0	1.98	0	4.32	424.6	0	2.38	0	0	0	1.84	0
SE	38.16	0	0	3.19	1.88	0	158.68	29036.31	0	3.54	0.93	0	0	1.84	12.01
SI	2.01	0	0	0.18	0.19	0	0.54	1491.62	0	0.15	0	0	0	1.28	3.06
SK	5.9	0	0	0.52	1.1	0	3.94	277.62	0	0	0	0	0	7.05	6.85
UK	70.18	18.01	0	67.72	1.2	0	26.64	143.74	0	25.57	4.75	18.68	23060.89	50.02	60.81

Table A-71. Capacity distribution for Model Run 69 (Weather Year 2004)

Country	Onshore	Offshore	PV /out Tracking	PV / Tracking	Run-of-river	Roof-top PV	PHS	Reservoir	Biomass CHP	PEM Electrolyzer	H2 OCGT	H2 CCGT	Salt Cavern	Vessel	Li-ion Battery
AL	3.08	0	0	1.69	0.03	0	0	1470.55	0	0.83	0	0	98.82	0	0
AT	37.52	0	0	20.61	4.61	0	114.15	1053.49	0	8.14	0	2.19	0	5.41	9.12
BA	11.05	0	0	0	0.28	0	1.61	1692.83	0	4.54	0	0	358.46	0	0
BE	1.75	4.72	0	15.7	0.08	0	6.18	13.82	4.75	0	0	7.47	0	23.25	4.25
BG	3.86	0	0	3.23	0.61	0	40.59	1964.22	0	0.09	0	0	0	5.8	0
CH	9.28	0	0	1.57	3.74	0	163.81	5031.16	0	0	0	0	0	11.49	0
CZ	14.61	0	0	16.1	0.41	0	5.99	441.86	0.01	1.89	0	1.8	0	3.5	6.82
DE	41.45	13.76	0	34.69	4.15	0	39.27	5.46	7.13	0	0	28.19	18788.79	14.3	3.64
DK	20.24	0	0	0	0	0	0	0	0	8.14	0	1.34	3649.98	0	0
EE	12.61	0	0	0	0	0	0	0	0	3.26	0	0	0	6.64	1.82
ES	66.32	0.59	0.01	173.37	2.27	0	63.06	11148.12	0	28.67	0	0	6007.2	45.26	318.54
FI	20.65	0	0	0	2.96	0	0	518.99	0	3.69	0	1.3	0	35.04	6.63
FR	172.5	3.54	0	132.39	6.56	0	50.15	5071.64	1.63	52.18	0	7.71	12689.66	111.96	101.81
GR	10.8	0	0	9.63	0.22	0	4.64	1753.4	0	2.36	0	0	616.68	10.72	1.4
HR	5.29	0	0	0	0.44	0	5.69	1955.8	0	0.47	0	0	0	4.14	0
HU	4.75	0	0	20.67	0.03	0	0	48.33	0	0	0	2.99	0	15.59	8.58
IE	48.52	0	0	0	0.12	0	2.54	0	0	38.94	0.21	1.24	0	8.85	0.11
IT	56.84	0	0.01	90.3	10.36	0	61.78	1693.37	0	5.83	0	0	0	145.37	79.21
LT	14.91	1.38	0	6.4	0	0	11.06	23.46	0	4.83	0	1.35	0	4.33	0
LU	0.08	0	0	6.22	0	0	5.04	0	0	0	0	0.02	0	1.05	0
LV	4.21	1.06	0	0	0.26	0	0	1472.02	0	1.85	0	0	0	3.05	0.86
ME	3.88	0	0	0	0	0	0	0	0	1.33	0	0	0	0	0
MK	0.55	0	0	4.1	0.29	0	0	265.54	0	0.44	0	0	0	0.41	0
NL	17	17.53	0	0	0	0	0	0	4	0	0	4.52	8454.43	0.01	0.22
NO	51.7	0	0	0	0.73	0	391.93	79421.13	0	26.4	0	0	0	8.6	0
PL	38.4	5.53	0	25.43	0.4	0	8.32	119.15	0	9.35	0	6.78	10940.92	9.06	2.43
PT	16.57	0	0	9.84	2.66	0	66.67	686.82	0	3.17	0	0	1166.33	7.44	6.77
RO	10.63	0	0	5.38	0	0	18.55	10913.39	0	0.18	0	0	1659.99	5.91	1.29
RS	5.06	0	0	3.08	1.98	0	4.32	424.6	0	3.37	0	0	0	0.83	0
SE	33.42	0	0	0	1.88	0	158.68	29036.31	0	2.23	0	1.34	0	2.91	2.9
SI	1.51	0	0	0	0.19	0	0.54	1491.62	0	0	0	0	0	0	0.14
SK	3.54	0	0	0	1.1	0	3.94	277.62	0	0	0	1.45	0	0	0.52
UK	97.22	21	0	24.44	1.2	0	26.64	143.74	4.13	47.74	6.48	16.58	18474.5	88.49	14.27

Table A-72. Capacity distribution for Model Run 70 (Weather Year 2005)

Country	Onshore	Offshore	PV /out Tracking	PV / Tracking	Run-of-river	Roof-top PV	PHS	Reservoir	Biomass CHP	PEM Electrolyzer	H2 OCGT	H2 CCGT	Salt Cavern	Vessel	Li-ion Battery
AL	2.58	0	0	1.21	0.03	0	0	1470.55	0	0.12	0	0	17.77	0.76	0
AT	36.93	0	0	16.25	4.61	0	114.15	1053.49	0	5.58	0	0	0	8.75	17.63
BA	11.05	0	0	0	0.28	0	1.61	1692.83	0	3.42	0	0	95.68	1.29	0
BE	2.44	4.72	0	33.43	0.08	0	6.18	13.82	0	0	7.5	4.16	0	0	22.96
BG	3.86	0	0	4.76	0.61	0	40.59	1964.22	0	0	0	0	0	5.51	0.43
CH	6.03	0	0	6.76	3.74	0	163.81	5031.16	0	0	0	0	0	5.42	0
CZ	16.08	0	0	16.1	0.41	0	5.99	441.86	0	0.78	1.53	0	0	0.03	17.37
DE	30.12	24.33	0	40.49	4.15	0	39.27	5.46	0	0	3.48	19.75	11312.8	0.02	10.04
DK	18.36	0.2	0	0.88	0	0	0	0	0	7.44	0.26	0.63	3198.02	0.01	3.18
EE	12.62	0	0	2.2	0	0	0	0	0	4.85	0.11	0	0	1.37	0.15
ES	64.98	0	0.01	117.24	2.27	0	63.06	11148.12	0	16.96	0	0	738.53	83.93	168.56
FI	20.68	0	0	0	2.96	0	0	518.99	0	5.77	0.19	1.12	0	13.25	8.47
FR	138.18	12.54	0.61	118.35	6.56	0	50.15	5071.64	0	36.08	1.57	3.16	5921.98	94.79	101.68
GR	12.15	0	0	12.93	0.22	0	4.64	1753.4	0	3.34	0	0	487.89	15.12	4.28
HR	4.65	0	0	0	0.44	0	5.69	1955.8	0	0.61	0	0	0	7.34	0
HU	8.64	0	0	9.49	0.03	0	0	48.33	0	0	0	0	0	0.34	3.29
IE	40.56	0	0	5.27	0.12	0	2.54	0	0	27.43	0.04	0	0	9.51	3.01
IT	46.25	0	0	99.05	10.36	0	61.78	1693.37	0	3.71	0	0	0	135.08	73.76
LT	8.79	0	0	0	0	0	11.06	23.46	0	0	0.11	0.12	0	3.66	0.01
LU	0	0	0	6.22	0	0	5.04	0	0	0	0	0	0	0.01	3.86
LV	2.34	0	0	0.85	0.26	0	0	1472.02	0	0.01	0.11	0	0	2.33	1.05
ME	2.92	0	0	0	0	0	0	0	0	0.18	0	0	0	0.4	0
MK	0.96	0	0	3.72	0.29	0	0	265.54	0	0.31	0	0	0	2.21	0.2
NL	18.38	24.39	0	0	0	0	0	0	0	4.08	0.96	7.42	8039.93	0	9.73
NO	61.06	0	0	0	0.73	0	391.93	79421.13	0	33.54	0	0	0	6.23	0
PL	42.05	0	0	54.08	0.4	0	8.32	119.15	0	5.06	1.57	6.97	6302.49	0.01	42.49
PT	16.43	0	0	11.48	2.66	0	66.67	686.82	0	3.86	0	0	2237.23	7.72	4.41
RO	10.92	0	0	2.93	0	0	18.55	10913.39	0	0	0	0	872.47	6.46	0
RS	4.15	0	0	0	1.98	0	4.32	424.6	0	0.95	0	0	0	4.24	0
SE	33.08	0	0	7.91	1.88	0	158.68	29036.31	0	3.16	1.41	0.34	0	1.78	7.25
SI	1.69	0	0	0.98	0.19	0	0.54	1491.62	0	0	0	0	0	3.57	0.13
SK	4.06	0	0	7.03	1.1	0	3.94	277.62	0	0	0	0	0	0.01	7.72
UK	123.31	11.72	0	33.21	1.2	0	26.64	143.74	0	56.14	0.03	14.02	17631.53	55.87	53.3

Table A-73. Capacity distribution for Model Run 71 (Weather Year 2006)

Country	Onshore	Offshore	PV /out Tracking	PV / Tracking	Run-of-river	Roof-top PV	PHS	Reservoir	Biomass CHP	PEM Electrolyzer	H2 OCGT	H2 CCGT	Salt Cavern	Vessel	Li-ion Battery
AL	2.07	0	0	1.69	0.03	0	0	1470.55	0	0.15	0	0	256.41	0.64	0.34
AT	40.05	0	0	21.14	4.61	0	114.15	1053.49	0	10.04	0.16	0	0	35.52	17.9
BA	11.05	0	0	0	0.28	0	1.61	1692.83	0	3.6	0	0	1183.76	1.42	0.83
BE	4.01	3.17	0	29.61	0.08	0	6.18	13.82	4.75	0	0	0	0	9.16	14.36
BG	3.86	0	0	4.41	0.61	0	40.59	1964.22	0	0.87	0	0	0	9.25	1.06
CH	6.03	0	0	6.72	3.74	0	163.81	5031.16	0	0	0.04	0	0	7.84	0.12
CZ	16.4	0	0	10.79	0.41	0	5.99	441.86	0	2.35	0	2.44	0	7.41	6.11
DE	25.07	25.55	0.01	39.71	4.15	0	39.27	5.46	1.27	0	6.88	31.68	29385.31	85.79	11.4
DK	11.15	4.95	0	0.57	0	0	0	0	0	5.33	0.54	0.01	3019.69	0.02	2.19
EE	7.61	1.02	0	0	0	0	0	0	0	1.5	0	0	0	9.78	0.31
ES	63.77	0	0.03	184.74	2.27	0	63.06	11148.12	0	33.65	0	0	6786.41	63.52	336.21
FI	19.56	0	0	0	2.96	0	0	518.99	0	2.81	0.1	2.14	0	23.46	4.25
FR	141.7	5.75	0.1	139.29	6.56	0	50.15	5071.64	0.82	41.89	10.48	26.54	28294.14	168.46	191.51
GR	15.46	0	0	11.76	0.22	0	4.64	1753.4	0	5.08	0.67	0	861.6	20.06	9.46
HR	7.29	0	0	0	0.44	0	5.69	1955.8	0	1.88	0	0	0	5.04	0.8
HU	0	0	0	11.97	0.03	0	0	48.33	0	0	0	0	0	10.59	6.66
IE	49.74	0	0	0	0.12	0	2.54	0	0	34.64	0	0	0	78.56	4.06
IT	35.8	0	0.01	141.49	10.36	0	61.78	1693.37	0	9.2	0.41	0	0	147.7	201.4
LT	13.72	0	0	0	0	0	11.06	23.46	0	1.24	0	0	0	5.54	4.37
LU	0.04	0	0	6.22	0	0	5.04	0	0	0	0	0	0	0.31	2.95
LV	4.21	1.46	0	0	0.26	0	0	1472.02	0	2.36	0	0	0	3.26	0.39
ME	2.32	0	0	2.4	0	0	0	0	0	1.21	0	0	0	0.57	0.57
MK	0	0	0	4.53	0.29	0	0	265.54	0	0.43	0	0	0	2.2	2.87
NL	27.85	12.47	0	3.88	0	0	0	0	0.38	0.56	21.47	8.07	31816.38	53.31	2.03
NO	43.3	0	0	0	0.73	0	391.93	79421.13	0	22.3	0	0	0	9.48	0
PL	59.1	7.02	0	43.81	0.4	0	8.32	119.15	0	16.34	0	0.8	7244.25	17.11	26.09
PT	18.39	0	0	16.89	2.66	0	66.67	686.82	0	6.18	0	0	2906.22	11.41	7.16
RO	13.64	0	0	2.7	0	0	18.55	10913.39	0	0.33	0	0	1035.6	7.93	1.06
RS	5.06	0	0	4.98	1.98	0	4.32	424.6	0	2.84	0	0	0	6.37	0.02
SE	34.41	0	0	10.23	1.88	0	158.68	29036.31	0	2.98	0.59	0.01	0	7.51	2.17
SI	3	0	0	0	0.19	0	0.54	1491.62	0	0	0	0	0	1.33	1.53
SK	4.41	0	0	10.03	1.1	0	3.94	277.62	0	0	0	5.48	0	26.42	12.29
UK	72.45	30.92	0	37.47	1.2	0	26.64	143.74	1.95	43	23.69	16.78	48742.27	131.25	23.04

Table A-74. Capacity distribution for Model Run 72 (Weather Year 2007)

Country	Onshore	Offshore	PV /out	PV / Tracking	Run-of-river	Roof-top PV	PHS	Reservoir	Biomass CHP	PEM Electrolyzer	H2 OCGT	H2 CCGT	Salt Cavern	Vessel	Li-ion Battery
AL	2.07	0	0	3.19	0.03	0	0	1470.55	0	0.29	0	0	72.3	0.21	0.2
AT	41.48	0	0	21.51	4.61	0	114.15	1053.49	0	13.96	0	0	0	13.52	1.74
BA	11.05	0	0	0	0.28	0	1.61	1692.83	0	3.12	0	0	221.36	0.48	0
BE	2.78	1.86	0	21.48	0.08	0	6.18	13.82	3.6	0	0	1.93	0	0	0.12
BG	3.86	0	0	4.67	0.61	0	40.59	1964.22	0	0	0	0	0	8.76	0
CH	11.91	0	0	3.96	3.74	0	163.81	5031.16	0	0	0	0	0	0	0
CZ	22.52	0	0	13.65	0.41	0	5.99	441.86	0	7.93	0	0	0	19.73	1.74
DE	47.52	16.78	0	31.18	4.15	0	39.27	5.46	0	0	0	9.45	5184.62	23.89	20.41
DK	18.12	0	0	1.74	0	0	0	0	0	9.5	0	0	1.65	9.94	1.56
EE	6.38	1.01	0	0	0	0	0	0	0	1.76	0	0	0	2.48	5.04
ES	52.07	0	0	157.67	2.27	0	63.06	11148.12	0	20.94	2.57	14.07	17197.46	29	294.93
FI	19.86	0	0	0	2.96	0	0	518.99	0	4.65	0.29	1.22	0	13.92	6.08
FR	170.1	0	0	113.01	6.56	0	50.15	5071.64	0	42.43	8.38	36.63	28330.35	15.34	115.4
GR	13.3	0	0	8.38	0.22	0	4.64	1753.4	0	3.18	0	0	416.4	11.72	3.76
HR	6.95	0	0	0.91	0.44	0	5.69	1955.8	0	1.91	0	0	0	7.98	0.16
HU	4.75	0	0	11.16	0.03	0	0	48.33	0	0	0	0.75	0	10.12	3.78
IE	19.54	0	0	7.63	0.12	0	2.54	0	0	11.85	0.49	0.61	0	0	3.04
IT	61.79	0	0	98.9	10.36	0	61.78	1693.37	0	14.27	0.04	0	0	142.81	90.09
LT	10.32	0	0	0	0	0	11.06	23.46	0	0	0	0	0	6.01	1.94
LU	0.04	0	0	3.6	0	0	5.04	0	0	0	0	0.56	0	0	0
LV	3.76	0	0	2.04	0.26	0	0	1472.02	0	1.48	0	0	0	3.84	1.08
ME	1.95	0	0	1.87	0	0	0	0	0	0.23	0	0	0	0.95	0
MK	0	0	0	1.88	0.29	0	0	265.54	0	0.01	0	0	0	4.1	0
NL	22.47	16.12	0	2.51	0	0	0	0	0.63	1.3	3.46	20.16	10985.98	42.47	10.78
NO	57.07	0	0	0	0.73	0	391.93	79421.13	0	29.42	0	0	0	6.27	0
PL	58.78	0	0	48.57	0.4	0	8.32	119.15	0	17.44	0.15	4.73	2880.84	21.78	4.33
PT	6.98	0	0	24.58	2.66	0	66.67	686.82	0	3.35	0.63	0.93	2119.07	0.01	45.74
RO	10.87	0	0	2	0	0	18.55	10913.39	0	0	0	0	847.37	7.75	0.26
RS	3.37	0	0	0	1.98	0	4.32	424.6	0	0	0	0	0	7.79	0
SE	37.76	0	0	0.54	1.88	0	158.68	29036.31	0	7.61	0	0	0	2.91	1.69
SI	3.49	0	0	0	0.19	0	0.54	1491.62	0	0	0	0	0	0.38	0.39
SK	6.74	0	0	0.31	1.1	0	3.94	277.62	0	0	0	1.65	0	20.93	1.2
UK	98.89	18.52	0	46.19	1.2	0	26.64	143.74	0	47.13	2.5	21.71	20515.6	10.05	19.61

Table A-75. Capacity distribution for Model Run 73 (Weather Year 2008)

Country	Onshore	Offshore	PV /out Tracking	PV / Tracking	Run-of-river	Rooftop PV	PHS	Reservoir	Biomass CHP	PEM Electrolyzer	H2 OCGT	H2 CCGT	Salt Cavern	Vessel	Li-ion Battery
AL	3.08	0	0	2.96	0.03	0	0	1470.55	0	0.16	0	0	35.72	0.02	0
AT	27.72	0	0	28.4	4.61	0	114.15	1053.49	0	4.58	0.35	0	0	30.46	14.26
BA	13.65	0	0	0	0.28	0	1.61	1692.83	0	5.86	0	0	275.99	0	0
BE	2.09	2.32	0	25.51	0.08	0	6.18	13.82	0	0	0.3	6.97	0	37.49	17.01
BG	0.2	0	0	4.95	0.61	0	40.59	1964.22	0	0	0	0	0	5.68	0
CH	7.59	0	0	2.47	3.74	0	163.81	5031.16	0	0	0	0	0	17.52	0
CZ	12.62	0	0	8.06	0.41	0	5.99	441.86	0	0	1.15	0.86	0	14.39	6.64
DE	40.45	28.93	0	29.13	4.15	0	39.27	5.46	0	1.17	0.6	7.96	8418.25	21.3	16.59
DK	16.98	0	0	0.21	0	0	0	0	0	6.55	0	0	802.71	0.9	2.09
EE	6.38	1.01	0	0	0	0	0	0	0	1.53	0	0	0	1.65	1.7
ES	55.45	0	0.01	137.71	2.27	0	63.06	11148.12	0	15.67	0	0	3743.7	46.25	192.19
FI	19.33	0	0	0	2.96	0	0	518.99	0	3.05	1.08	0.98	0	39.85	6.26
FR	157	3.01	0	120.14	6.56	0	50.15	5071.64	0	32.73	2.31	6.42	8722.38	133.84	110.66
GR	13.03	0	0	10.31	0.22	0	4.64	1753.4	0	3.12	0	0	342.51	11.72	4.8
HR	5.88	0	0	0.43	0.44	0	5.69	1955.8	0	0.93	0	0	0	8.56	0
HU	4.75	0	0	22.88	0.03	0	0	48.33	0	0	0.14	1.01	0	25.75	22.82
IE	51.72	0	0	0.39	0.12	0	2.54	0	0	38.44	1.1	0	0	40.93	2.33
IT	50.17	0	0	98.24	10.36	0	61.78	1693.37	0	6.31	1.6	0	0	164.66	58.52
LT	11.78	0	0	0	0	0	11.06	23.46	0	2.45	0	0	0	4.84	0.36
LU	0.21	0	0	5.28	0	0	5.04	0	0	0	0	0	0	2.59	3.08
LV	4.21	0	0	4.42	0.26	0	0	1472.02	0	2.01	0	0	0	2.91	1.56
ME	2.92	0	0	1.95	0	0	0	0	0	1.02	0	0	0	0.29	0
MK	0.96	0	0	1.56	0.29	0	0	265.54	0	0	0	0	0	2.57	0.21
NL	23.82	27.31	0	2.52	0	0	0	0	0	10.35	1.88	4.79	7267.49	0.01	15.1
NO	33.67	0	0	0	0.73	0	391.93	79421.13	0	16.27	0	0	0	5.74	0
PL	37.03	13.93	0	38.56	0.4	0	8.32	119.15	0	11.93	1.2	1.81	5249.89	1.55	19.79
PT	10.76	0	0	27.78	2.66	0	66.67	686.82	0	4.46	0	0	1714.74	0.03	48.01
RO	12.41	0	0	5.64	0	0	18.55	10913.39	0	0.63	0	0	398.46	13.52	1.13
RS	5.06	0	0	0	1.98	0	4.32	424.6	0	1.25	0	0	0	0.46	0
SE	28.36	0	0	0.54	1.88	0	158.68	29036.31	0	1.43	0	0	0	0.8	0.52
SI	2.01	0	0	0	0.19	0	0.54	1491.62	0	0	0	0	0	7.42	0.17
SK	5.9	0	0	0	1.1	0	3.94	277.62	0	0	0	1.39	0	18.98	0.02
UK	125.84	3.08	0	48	1.2	0	26.64	143.74	0	59.18	8.63	15.01	24556.72	56.88	27.51

Table A-76. Capacity distribution for Model Run 74 (Weather Year 2009)

Country	Onshore	Offshore	PV /out	PV / Tracking	Run-of-river	Rooftop PV	PHS	Reservoir	Biomass CHP	PEM Electrolyzer	H2 OCGT	H2 CCGT	Salt Cavern	Vessel	Li-ion Battery
AL	4.09	0	0	3.19	0.03	0	0	1470.55	0	1.21	0	0	383.25	0.37	0.11
AT	37.44	0	0	26.4	4.61	0	114.15	1053.49	0	5.98	0	0	0	31.48	2.58
BA	11.05	0	0	1.01	0.28	0	1.61	1692.83	0	4.2	0	0	778.49	8.56	0
BE	3.46	2.78	0	22.76	0.08	0	6.18	13.82	3.01	0	0	3.53	0	23.1	36.55
BG	3.86	0	0	2.54	0.61	0	40.59	1964.22	0	0	0	0	0	6.08	0
CH	8.89	0	0	3.44	3.74	0	163.81	5031.16	0	0	0	0	0	13.57	3.51
CZ	17.75	0	0	5.04	0.41	0	5.99	441.86	0	0	0	2.65	0	14.1	1.28
DE	35.12	25.86	0	25.85	4.15	0	39.27	5.46	0	0	0	15.51	7320.09	50.92	13.35
DK	15.63	0.8	0	0.57	0	0	0	0	0	6.38	0	0	1359.01	6.64	4.38
EE	3.22	3.06	0	0	0	0	0	0	0	0.34	0	0	0	1.89	0.22
ES	96.4	0	0	85.4	2.27	0	63.06	11148.12	0	20.37	0	0	2962.04	70.7	52.31
FI	20.41	0	0	0	2.96	0	0	518.99	0	2.53	0.27	1.21	0	19.11	8.48
FR	167.64	4.88	0	136.43	6.56	0	50.15	5071.64	0	40.35	1.24	5.59	5996.41	125.48	120.21
GR	15.58	0	0	9.25	0.22	0	4.64	1753.4	0	3.49	0	0	496.92	17.75	3.4
HR	8.52	0	0	4.4	0.44	0	5.69	1955.8	0	2.68	0	0	0	5.43	0.01
HU	4.75	0	0	10.79	0.03	0	0	48.33	0	0	1.32	0.34	0	10.68	3.02
IE	48.52	0	0	1.88	0.12	0	2.54	0	0	33.72	0.79	0	0	7.42	5.24
IT	59.49	0	0	97.01	10.36	0	61.78	1693.37	0	12.16	0.02	1.96	0	171.59	45.72
LT	9.16	2.76	0	7.08	0	0	11.06	23.46	0	2.22	0	0	0	5.13	2.4
LU	0.13	0	0	6.22	0	0	5.04	0	0	0	0	0.18	0	2.25	0.66
LV	4.21	0	0	0	0.26	0	0	1472.02	0	0.8	0	0	0	3.06	0.21
ME	5.81	0	0	0	0	0	0	0	0	0.97	0	0	0	1.79	0
MK	0.96	0	0	2.64	0.29	0	0	265.54	0	0.29	0	0	0	2.39	1.05
NL	23.82	22.37	0	19.18	0	0	0	0	0	8.23	0	0.91	1711.09	0.02	16.3
NO	56.47	0	0	0	0.73	0	391.93	79421.13	0	28.5	0	0	0	10.15	0
PL	47.49	3.01	0	30.02	0.4	0	8.32	119.15	0	7.51	0	4.91	3880.34	32.36	21.02
PT	13.4	0	0	16.61	2.66	0	66.67	686.82	0	4.28	0	0	2135.16	8.55	7.06
RO	8.78	0	0	11.35	0	0	18.55	10913.39	0	0	0	0	418.33	11.75	0
RS	2.51	0	0	0	1.98	0	4.32	424.6	0	0.9	0	0	0	6.09	0
SE	30.24	0	0	3.62	1.88	0	158.68	29036.31	0	0	0	0	0	2.31	5.64
SI	2.01	0	0	0	0.19	0	0.54	1491.62	0	0	0	0	0	5.24	0.97
SK	7.43	0	0	0.77	1.1	0	3.94	277.62	0	0	0	2.53	0	8.27	0.07
UK	96.46	16.31	0	34.88	1.2	0	26.64	143.74	0	42.43	7.27	16.96	17095.97	89.5	45.2

Table A-77. Capacity distribution for Model Run 75 (Weather Year 2010)

Country	Onshore	Offshore	PV /out Tracking	PV / Tracking	Run-of-river	Rooftop PV	PHS	Reservoir	Biomass CHP	PEM Electrolyzer	H2 OCGT	H2 CCGT	Salt Cavern	Vessel	Li-ion Battery
AL	3.08	0	0	3.2	0.03	0	0	1470.55	0	1.32	0	0	443.04	0.01	0.34
AT	43.27	0	0	32.06	4.61	0	114.15	1053.49	0	11.76	0	0	0	5.06	26.55
BA	14.7	0	0	10.33	0.28	0	1.61	1692.83	0	11.38	0	0	3652.43	0	0.17
BE	0.7	3.64	0	23.73	0.08	0	6.18	13.82	4.75	0	0.36	6.39	0	0.01	19.88
BG	3.86	0	0	0.79	0.61	0	40.59	1964.22	0	0	0	0	0	3.7	0
CH	11.73	0	0	0.62	3.74	0	163.81	5031.16	0	0	0	0	0	6.61	0
CZ	19.47	0	0	17.27	0.41	0	5.99	441.86	0.22	3.65	0	0.62	0	0.02	16.01
DE	34	19.6	0	44.6	4.15	0	39.27	5.46	5.97	0	0.04	12.68	10396.96	0.05	28.7
DK	15.63	0	0	0	0	0	0	0	0	4.74	0	0	955.58	0.01	1.79
EE	7.65	3.05	0	0	0	0	0	0	0	1.97	0	0	0	1.21	0.01
ES	90.11	0	0.01	118.15	2.27	0	63.06	11148.12	0	30.87	0	0	7121.84	35.27	88.49
FI	19.86	1.19	0	0	2.96	0	0	518.99	0	3.35	0.11	0.78	0	17.6	6.72
FR	180.31	18.53	0	88.34	6.56	0	50.15	5071.64	2.91	58.58	0	0.8	12413.09	84.62	64.44
GR	14.7	0	0	11.87	0.22	0	4.64	1753.4	0	5.33	0	0	1181.21	12.6	2.79
HR	5.61	0	0	6.77	0.44	0	5.69	1955.8	0	2.06	0	0	0	0	0.21
HU	9.47	0	0	3.16	0.03	0	0	48.33	0	0	0	0	0	0.92	1.6
IE	18.23	0	0	7.87	0.12	0	2.54	0	0	5.33	0.77	0.11	0	0.96	6.21
IT	59.84	0	0	105.88	10.36	0	61.78	1693.37	0	12.82	0	0	0	152.91	43.23
LT	11.68	0.9	0	19.46	0	0	11.06	23.46	0	3.16	0	0	0	3.35	15.71
LU	0.04	0	0	5.5	0	0	5.04	0	0	0	0.03	0.79	0	0	0
LV	4.21	0	0	0	0.26	0	0	1472.02	0	0.95	0	0	0	2	0
ME	3.88	0	0	0.13	0	0	0	0	0	0.79	0	0	0	0.03	0
MK	0.96	0	0	0.3	0.29	0	0	265.54	0	0	0	0	0	1.25	0.75
NL	15.62	29.29	0	0	0	0	0	0	4	4.17	0	2.8	4949.79	0	25.43
NO	57.06	0	0	0	0.73	0	391.93	79421.13	0	27.47	0	0	0	5.99	0
PL	33.96	1.91	0	35.21	0.4	0	8.32	119.15	2.16	5.03	0	4.2	7082.54	0.01	16.67
PT	15.54	0	0	18.33	2.66	0	66.67	686.82	0	5.8	0	0	3047.85	1.47	6.79
RO	13.41	0	0	2.38	0	0	18.55	10913.39	0	0.34	0	0	794.5	4.96	0
RS	5.06	0	0	0	1.98	0	4.32	424.6	0	1.98	0	0	0	2.67	0
SE	37.53	0	0	0	1.88	0	158.68	29036.31	0	0.8	0	0	0	1.2	4.17
SI	2.08	0	0	2.38	0.19	0	0.54	1491.62	0	0	0	0	0	0.01	0.97
SK	4.97	0	0	10.82	1.1	0	3.94	277.62	0	0.12	0	2.16	0	0.01	14.81
UK	81.95	41.16	0	26	1.2	0	26.64	143.74	0	29.5	2.75	13.92	20610.64	17.67	53.49

Table A-78. Capacity distribution for Model Run 76 (Weather Year 2011)

Country	Onshore	Offshore	PV /out Tracking	PV / Tracking	Run-of-river	Roof-top PV	PHS	Reservoir	Biomass CHP	PEM Electrolyzer	H2 OCGT	H2 CCGT	Salt Cavern	Vessel	Li-ion Battery
AL	2.07	0	0	0.91	0.03	0	0	1470.55	0	0.02	0	0	62.73	0.01	0
AT	38.7	0	0	28.53	4.61	0	114.15	1053.49	0	7.76	5.04	0.27	0	37.62	15.87
BA	11.05	0	0	0.56	0.28	0	1.61	1692.83	0	4.03	0	0	491.57	0.02	0
BE	2.09	2.25	0	30.98	0.08	0	6.18	13.82	4.75	0	0	0	0	0.66	11.41
BG	0	0	0	7.29	0.61	0	40.59	1964.22	0	0	0	0	0	9.98	0.23
CH	7.85	0	0	6.53	3.74	0	163.81	5031.16	0	0	0	0	0	8.96	0
CZ	14.64	0	0	14.93	0.41	0	5.99	441.86	0	0	0.55	3.08	0	1.1	5.43
DE	33.88	26.79	0	41.74	4.15	0	39.27	5.46	2.97	2.73	9.78	12.99	16417.25	14.4	3.73
DK	19.27	0	0	0.57	0	0	0	0	0	8.89	0	0	312.89	11.03	0.66
EE	6.38	1.74	0	0.09	0	0	0	0	0	2.47	0	0	0	1.75	1.01
ES	59.64	0	0.01	145.02	2.27	0	63.06	11148.12	0	16.11	0	0	4049.81	37.41	196.67
FI	19.49	0	0	0	2.96	0	0	518.99	0	4.43	1.2	1.8	0	26.05	5.99
FR	135.6	14.48	0.01	115.69	6.56	0	50.15	5071.64	1.27	32.69	14.1	14.44	24061.77	122.86	135.7
GR	12.97	0	0	11.71	0.22	0	4.64	1753.4	0	4.23	0	0	283.49	11.99	11.93
HR	4.8	0	0	0.01	0.44	0	5.69	1955.8	0	0.11	0	0	0	3.72	0.04
HU	0	0	0	18.38	0.03	0	0	48.33	0	0	0	0.63	0	10.52	34.76
IE	62.26	0	0	4.53	0.12	0	2.54	0	0	45.96	1.29	0	0	17.03	3.61
IT	39.54	0	0	153.71	10.36	0	61.78	1693.37	0	15.28	0.06	0.03	0	122.95	196.4
LT	13.59	0	0	1.45	0	0	11.06	23.46	0	4.24	0	0	0	6.26	9.51
LU	0	0	0	4.81	0	0	5.04	0	0	0	0	0	0	0.66	0.04
LV	4.39	0	0	0	0.26	0	0	1472.02	0	1.55	0	0	0	1.41	0
ME	3.88	0	0	1.95	0	0	0	0	0	0.76	0	0	0	0.02	0
MK	0	0	0	2.52	0.29	0	0	265.54	0	0	0	0	0	1.6	0
NL	19.75	17.44	0	5.43	0	0	0	0	1.32	2.53	9.25	14.59	22197.81	0.02	3.62
NO	63.35	0	0	0	0.73	0	391.93	79421.13	0	34.91	0	0	0	5.81	0
PL	29.52	11.7	0	36.31	0.4	0	8.32	119.15	0	8.95	2.11	6.76	10605.34	4.02	12.67
PT	9.26	0	0	13.29	2.66	0	66.67	686.82	0	1.04	0	0	769.23	4.49	20.3
RO	10	0	0	6.12	0	0	18.55	10913.39	0	0	0	0	1107.46	5.03	1.1
RS	4.01	0	0	1.37	1.98	0	4.32	424.6	0	1.57	0	0	0	0.03	0
SE	30.17	0	0	0	1.88	0	158.68	29036.31	0	1.69	0	0	0	0.23	2.61
SI	3.5	0	0	0.64	0.19	0	0.54	1491.62	0	0	0	0	0	1.44	0.62
SK	4.55	0	0	10.71	1.1	0	3.94	277.62	0	0	0.23	0.43	0	1.38	8.12
UK	94.76	10.66	0	36.8	1.2	0	26.64	143.74	0	37.41	6.4	15.7	18506.42	60.75	42.93

Table A-79. Capacity distribution for Model Run 77 (Weather Year 2012)

Country	Onshore	Offshore	PV /out Tracking	PV / Tracking	Run-of-river	Rooftop PV	PHS	Reservoir	Biomass CHP	PEM Electrolyzer	H2 OCGT	H2 CCGT	Salt Cavern	Vessel	Li-ion Battery
AL	3.03	0	0	2.31	0.03	0	0	1470.55	0	0.4	0	0	79.13	0.02	0.01
AT	36.16	0	0	21.3	4.61	0	114.15	1053.49	0	7.65	0	0	0	11.01	2.99
BA	11.05	0	0	2.64	0.28	0	1.61	1692.83	0	5.48	0	0	837.49	0.01	0
BE	4.49	2.32	0	35.77	0.08	0	6.18	13.82	0	0	0	2.25	0	8.39	26.8
BG	3.86	0	0	4.2	0.61	0	40.59	1964.22	0	0	0	0	0	6.28	0
CH	7.32	0	0	2.02	3.74	0	163.81	5031.16	0	0	0	0	0	6.67	0
CZ	18.49	0	0	6.88	0.41	0	5.99	441.86	0	1.31	0	0	0	1.25	14.81
DE	35.35	24.82	0	36.8	4.15	0	39.27	5.46	0	0	0	5.98	6441.91	0.17	16.72
DK	17.1	0	0	1.2	0	0	0	0	0	7.12	0	0	1797.92	0.04	1.47
EE	9.51	2.16	0	1.95	0	0	0	0	0	3.87	0	0	0	1.82	0.4
ES	71.95	0	0.01	115.02	2.27	0	63.06	11148.12	0	22.91	1.74	0	6652.59	23.94	167.73
FI	21.88	0	0	0	2.96	0	0	518.99	0	4.28	0.47	1.33	0	19.76	5.11
FR	171.85	5.1	0	114.56	6.56	0	50.15	5071.64	0	42.82	0.21	12.34	10523.34	50.64	115.15
GR	14.51	0	0	8.33	0.22	0	4.64	1753.4	0	3.72	0	0	697.48	14.36	0.68
HR	4.65	0	0	1.49	0.44	0	5.69	1955.8	0	0.45	0	0	0	4.62	0
HU	9.67	0	0	11.38	0.03	0	0	48.33	0	0	0	0	0	10.94	4.91
IE	46.33	0	0	1.82	0.12	0	2.54	0	0	28.99	0.54	0.72	0	4.21	2.76
IT	44.19	0	5.14	101.96	10.36	0	61.78	1693.37	0	10.53	0	0	0	155.86	56.55
LT	9.86	0	0	11.54	0	0	11.06	23.46	0	1.48	0	0	0	4.76	3.97
LU	0.21	0	0	6.22	0	0	5.04	0	0	0	0	0	0	0.37	5.67
LV	4.21	0	0	3.36	0.26	0	0	1472.02	0	1.58	0	0	0	2.97	0.04
ME	2.81	0	0	0.07	0	0	0	0	0	0.11	0	0	0	0.2	0
MK	0.96	0	0	1.73	0.29	0	0	265.54	0	0.08	0	0	0	2.03	0
NL	19.75	33.32	0	13.27	0	0	0	0	0	12.24	0	4.81	8075.01	0	35.28
NO	39.5	0	0	0	0.73	0	391.93	79421.13	0	20.92	0	0	0	7.57	0
PL	26.71	6.97	0	45.3	0.4	0	8.32	119.15	0	6.85	0.19	8.71	8430.98	0.33	15.24
PT	11.28	0	0	21.78	2.66	0	66.67	686.82	0	3	0	0	1696.29	0.03	33.57
RO	7.97	0	0	8.47	0	0	18.55	10913.39	0	0.01	0	0	524.37	8.22	0.34
RS	5.06	0	0	0	1.98	0	4.32	424.6	0	2.27	0	0	0	3.7	0
SE	27.67	0	0	1.58	1.88	0	158.68	29036.31	0	0	0	0	0	1.69	4.69
SI	2.7	0	0	0	0.19	0	0.54	1491.62	0	0	0	0	0	1.5	0.01
SK	4.4	0	0	8.34	1.1	0	3.94	277.62	0	1.39	0	0	0	8.56	3.83
UK	106.09	15.21	0	17.84	1.2	0	26.64	143.74	0	39.87	10.55	16.07	20000.39	7.82	33.65

Table A-80. Capacity distribution for Model Run 78 (Weather Year 2013)

Country	Onshore	Offshore	PV /out Tracking	PV / Tracking	Run-of-river	Rooftop PV	PHS	Reservoir	Biomass CHP	PEM Electrolyzer	H2 OCGT	H2 CCGT	Salt Cavern	Vessel	Li-ion Battery
AL	2.6	0	0	1.29	0.03	0	0	1470.55	0	0	0	0	7.81	0.98	0.28
AT	29.96	0	0	20.88	4.61	0	114.15	1053.49	0	2.78	0	0	0	40.15	5.75
BA	11.05	0	0	5.86	0.28	0	1.61	1692.83	0	5.93	0	0	207.27	1.24	0
BE	5.51	4.72	0	15.32	0.08	0	6.18	13.82	4.75	0	0	9.47	0	33.07	9.41
BG	3.86	0	0	3.93	0.61	0	40.59	1964.22	0	0	0	0	0	8.83	0.33
CH	6.03	0	0	1.14	3.74	0	163.81	5031.16	0	0	0	0	0	10.97	0
CZ	14.09	0	0	13.05	0.41	0	5.99	441.86	0	0	0	2.8	0	10.2	3.54
DE	42.7	17.03	0	45.01	4.15	0	39.27	5.46	1.1	0	0	35.76	24805.41	13.44	2.44
DK	14.45	0	0	4.79	0	0	0	0	0	5.52	0.31	1.67	4037.17	0.02	1.73
EE	9.88	0	0	6.18	0	0	0	0	0	3.61	0	0	0	4.18	8.37
ES	87.67	0	0.01	108.92	2.27	0	63.06	11148.12	0	31.48	0	0	1005.95	82.32	65.96
FI	20.18	0	0	0	2.96	0	0	518.99	0	3.17	1.38	0	0	42.15	5.71
FR	153.68	27.33	0	78.99	6.56	0	50.15	5071.64	0	45.3	0	7.63	12477.03	129.45	82.48
GR	16.17	0	0	8.26	0.22	0	4.64	1753.4	0	4.85	0	0	282.84	11.85	1.49
HR	4.65	0	0	4.74	0.44	0	5.69	1955.8	0	1.35	0	0	0	4.91	0
HU	9.47	0	0	8.76	0.03	0	0	48.33	0	0	0	0	0	6.09	4
IE	37.74	0	0	5.06	0.12	0	2.54	0	0	27.45	0.74	0	0	12.1	5.21
IT	55.89	0	0	101.68	10.36	0	61.78	1693.37	0	8.27	0.63	0	0	137.14	107.48
LT	9.4	0	0	7.47	0	0	11.06	23.46	0	0	0.1	0.41	0	5.09	1.23
LU	0.08	0	0	6.22	0	0	5.04	0	0	0	0	1.01	0	0.64	0.83
LV	3.59	0	0	5.23	0.26	0	0	1472.02	0	1.2	0	0	0	4.07	1.37
ME	3.88	0	0	0	0	0	0	0	0	0.68	0	0	0	0.01	0
MK	0.96	0	0	1.87	0.29	0	0	265.54	0	0	0	0	0	3.46	0.08
NL	23.82	15.15	0	10.22	0	0	0	0	0	1.36	0	5.26	8388.45	0	14.01
NO	44.56	0	0	0	0.73	0	391.93	79421.13	0	21.49	0	0	0	9.4	0
PL	33.13	1.95	0	39.34	0.4	0	8.32	119.15	0	2.6	1.59	10.23	11878.29	1.11	29.14
PT	13.93	0	0	5.9	2.66	0	66.67	686.82	0	1.95	0	0	1398.31	11.66	0.46
RO	12.74	0	0	3.12	0	0	18.55	10913.39	0	0	0	0	823.94	11.55	0.64
RS	5.06	0	0	0	1.98	0	4.32	424.6	0	2.69	0	0	0	1.75	0
SE	37.28	0	0	15.65	1.88	0	158.68	29036.31	0	7.04	0.22	0.66	0	2.05	3.61
SI	1.51	0	0	0	0.19	0	0.54	1491.62	0	0.09	0	0	0	4.08	0
SK	5.9	0	0	6.61	1.1	0	3.94	277.62	0	0	0.7	0.22	0	4.04	6.13
UK	119.23	19.45	0	43.42	1.2	0	26.64	143.74	0	59.85	1.52	8.77	16144.89	93.83	53.6

Table A-81. Capacity distribution for Model Run 79 (Weather Year 2014)

Country	Onshore	Offshore	PV /out Tracking	PV / Tracking	Run-of-river	Rooftop PV	PHS	Reservoir	Biomass CHP	PEM Electrolyzer	H2 OCGT	H2 CCGT	Salt Cavern	Vessel	Li-ion Battery
AL	2.6	0	0	3.87	0.03	0	0	1470.55	0	0.47	0	0	338.08	0	1.51
AT	39.82	0	0	23.1	4.61	0	114.15	1053.49	0	4.96	0	0	0	16.54	17.97
BA	10.84	0	0	6.3	0.28	0	1.61	1692.83	0	6.38	0	0	1786.96	0	0
BE	1.4	4.61	0	12.58	0.08	0	6.18	13.82	4.61	0	0	2.77	0	0	8.35
BG	3.56	0	0	4.93	0.61	0	40.59	1964.22	0	0	0	0	0	4.15	0.02
CH	8.24	0	0	3.2	3.74	0	163.81	5031.16	0	0	0	0	0	1.51	0
CZ	18.52	0	0	19.88	0.41	0	5.99	441.86	0	1.18	0	0	0	0.07	24.06
DE	29.45	28.93	0	36.64	4.15	0	39.27	5.46	2.75	1.79	0	7.33	5917.56	0.01	9.66
DK	19.25	0.53	0	6.03	0	0	0	0	0	10.74	0	0	2891.66	0	0.02
EE	6.38	0.81	0	7.84	0	0	0	0	0	2.85	0	0	0	1.7	3.66
ES	69.73	0	0.01	173.15	2.27	0	63.06	11148.12	0	35.57	0	1.86	9187.22	10.87	259.79
FI	18.62	0	0	0	2.96	0	0	518.99	0	3.06	0.66	0.87	0	21.19	7.5
FR	155.28	9.08	0	112.61	6.56	0	50.15	5071.64	1.5	41.87	0	26.34	20566.88	81.68	79.44
GR	17.4	0	0	15.07	0.22	0	4.64	1753.4	0	6.68	0	0	1508.62	12.13	20.68
HR	6.02	0	0	0	0.44	0	5.69	1955.8	0	0.12	0	0	0	0.31	0.09
HU	4.75	0	0	11.16	0.03	0	0	48.33	0	0	0	0.3	0	1.59	3.15
IE	25.38	0	0	10.79	0.12	0	2.54	0	0	14.9	0	1.06	0	0.01	7.92
IT	37.62	0	0	142.23	10.36	0	61.78	1693.37	0	11.39	0	0.78	0	164.52	175.27
LT	9.16	0.12	0	10.34	0	0	11.06	23.46	0	0	0	0	0	5.48	7.18
LU	0	0	0	5.03	0	0	5.04	0	0	0	0	0.99	0	0	0
LV	3.51	0.03	0	0.01	0.26	0	0	1472.02	0	0.89	0	0	0	3.07	0.73
ME	1.95	0	0	3.96	0	0	0	0	0	0.9	0	0	0	0	1.03
MK	0.56	0	0	1.95	0.29	0	0	265.54	0	0.16	0	0	0	0.01	0.94
NL	17	27.13	0	11.48	0	0	0	0	0	6.66	0	7.55	7032.4	0	5.68
NO	52.38	0	0	0.76	0.73	0	391.93	79421.13	0	30.83	0	0	0	6.28	0
PL	38.64	10.9	0	57.49	0.4	0	8.32	119.15	0	12.95	0	2.56	5787.93	0.01	42.57
PT	14.81	0	0	24.42	2.66	0	66.67	686.82	0	6.32	0	0.42	3447.33	0	22.97
RO	13.05	0	0	6.39	0	0	18.55	10913.39	0	1.09	0	0	1288.44	2.32	0.26
RS	5.06	0	0	0	1.98	0	4.32	424.6	0	1.51	0	0	0	0	0
SE	37.54	0.49	0	5.99	1.88	0	158.68	29036.31	0	5.59	0	0	0	0.31	4.52
SI	2.53	0	0	0	0.19	0	0.54	1491.62	0	0	0	0	0	0.37	0.33
SK	7.43	0	0	5.31	1.1	0	3.94	277.62	1	0.23	0	0.65	0	0.01	2.56
UK	70.35	13.77	0	50.07	1.2	0	26.64	143.74	3.05	26.79	0	15.21	21386.38	0.04	41.69

Table A-82. Capacity distribution for Model Run 80 (Weather Year 2015)

Country	Onshore	Offshore	PV /out Tracking	PV / Tracking	Run-of-river	Roof-top PV	PHS	Reservoir	Biomass CHP	PEM Electrolyzer	H2 OCGT	H2 CCGT	Salt Cavern	Vessel	Li-ion Battery
AL	3.08	0	0	0	0.03	0	0	1470.55	0	0.22	0	0	66.96	1.58	0
AT	36.45	0	0	27.94	4.61	0	114.15	1053.49	0	10.69	0	0	0	20.28	4.43
BA	11.05	0	0	4.31	0.28	0	1.61	1692.83	0	5.06	0	0	1617.66	4.41	1.69
BE	4.83	4.72	0	20.96	0.08	0	6.18	13.82	0	0	0	3.67	0	2.24	3.43
BG	3.4	0	0	4.24	0.61	0	40.59	1964.22	0	0	0	0	0	6.59	0
CH	9.34	0	0	4.22	3.74	0	163.81	5031.16	0	0	0	0	0	14.85	0
CZ	13.16	0	0	20.35	0.41	0	5.99	441.86	0	0.82	0.32	2.75	0	9.47	8.52
DE	36.18	22.23	0	36.83	4.15	0	39.27	5.46	0.52	0	3.21	23.28	21418.15	37.72	2.65
DK	17.96	0	0	0.14	0	0	0	0	0	12.08	1.09	0.98	8267.45	0.03	0.97
EE	10.17	0	0	2.91	0	0	0	0	0	4.6	0	0	0	2.51	0.01
ES	66.11	0	0.01	114.85	2.27	0	63.06	11148.12	0	13.65	0	0	3321.93	66.86	139.62
FI	24.06	0	0	0	2.96	0	0	518.99	0	7.04	0.44	0.34	0	41.09	7.49
FR	149.41	21.61	0	114.78	6.56	0	50.15	5071.64	0	47.38	1.57	13.3	18889.91	154.19	77.13
GR	14.35	0	0	9.4	0.22	0	4.64	1753.4	0	3.16	0	0	419.67	18.3	0.22
HR	6.64	0	0	4.32	0.44	0	5.69	1955.8	0	2.33	0	0	0	4.93	0.52
HU	3.89	0	0	14.89	0.03	0	0	48.33	0	0	0	3.02	0	12.44	4.96
IE	33.4	0	0	2.62	0.12	0	2.54	0	0	21.9	0.87	1.54	0	7.62	0.99
IT	55.16	0	0	114.43	10.36	0	61.78	1693.37	0	10.08	0	0	0	147.76	97.48
LT	9.39	0	0	0	0	0	11.06	23.46	0	2.16	0	0	0	5.04	0
LU	0.04	0	0	5.6	0	0	5.04	0	0	0	0	0	0	1.15	0.12
LV	2.6	0	0	0.27	0.26	0	0	1472.02	0	0.2	0	0	0	2.86	0
ME	2.92	0	0	1.12	0	0	0	0	0	0.7	0	0	0	1.62	0
MK	0.96	0	0	2.12	0.29	0	0	265.54	0	0.12	0	0	0	3.53	0.65
NL	23.82	32.61	0	0	0	0	0	0	0	16.07	0.68	14.45	16065.17	6.56	2.72
NO	43.56	0	0	0	0.73	0	391.93	79421.13	0	23.52	0	0	0	7.62	0
PL	31.02	2.01	0	52.78	0.4	0	8.32	119.15	0	10.2	1.17	11.59	16146.51	1.54	19.87
PT	16.12	0	0	8.6	2.66	0	66.67	686.82	0	2.35	0	0	188.83	11.95	0.01
RO	9.3	0	0	1.77	0	0	18.55	10913.39	0	0	0	0	1602.19	11.27	0
RS	5.06	0	0	0	1.98	0	4.32	424.6	0	1.81	0	0	0	8.1	0
SE	40.22	0	0	0	1.88	0	158.68	29036.31	0	9.42	1.12	0.49	0	3.17	0.22
SI	2.01	0	0	0	0.19	0	0.54	1491.62	0	0	0	0	0	3.13	1.31
SK	4.4	0	0	1.64	1.1	0	3.94	277.62	0.06	0	0	1.61	0	2.18	0
UK	94.93	27.42	0	13.1	1.2	0	26.64	143.74	0	48.46	8.94	18.58	31118.6	50.12	31.77

Table A-83. Capacity distribution for Model Run 81 (Weather Year 2016)

Country	Onshore	Offshore	PV /out Tracking	PV / Tracking	Run-of-river	Rooftop PV	PHS	Reservoir	Biomass CHP	PEM Electrolyzer	H2 OCGT	H2 CCGT	Salt Cavern	Vessel	Li-ion Battery
AL	3.08	0	0	1.75	0.03	0	0	1470.55	0	0.65	0	0	163.04	0.01	0
AT	36.24	0	0	19.86	4.61	0	114.1	1053.49	0	8.53	0	0	0	25.73	7.58
BA	11.05	0	0	2.27	0.28	0	1.61	1692.83	0	5.63	0	0	613.65	0	0
BE	4.73	3.24	0	11.84	0.08	0	6.18	13.82	4.75	0	0.4	4.99	0	26.32	7.41
BG	3.86	0	0	3.64	0.61	0	40.59	1964.22	0	0	0	0	0	5.52	0
CH	8.38	0	0	2	3.74	0	163.8	5031.16	0	0	0	0	0	8.62	0
CZ	15.36	0	0	9.95	0.41	0	5.99	441.86	0.39	0	0	1.78	0	11.92	7.43
DE	28.58	23.8	0	44.72	4.15	0	39.27	5.46	10.5	0	0	0.8	4910.54	18.78	17.44
DK	13.02	0	0	1.36	0	0	0	0	0	4.9	0	0	1445.82	0.15	1.97
EE	7.64	0	0	3.23	0	0	0	0	0	1.88	0	0	0	1.57	0.19
ES	51.4	0	0.0	157.2	2.27	0	63.06	11148.1	0	17.0	0	0	3781.31	34.75	259.5
FI	19.06	0	0	0	2.96	0	0	518.99	0	3.02	0.0	2.25	0	27.37	5.08
FR	173.3	2.7	3.0	154.9	6.56	0	50.15	5071.64	4.75	52.9	0	9.31	11323.9	87.56	163.5
G	13.75	0	0	11.56	0.22	0	4.64	1753.4	0	4	0	0	599.87	15.48	3.93
HR	5.1	0	0	0.65	0.44	0	5.69	1955.8	0	0.88	0	0	0	5.39	0.12
HU	7.51	0	0	20.46	0.03	0	0	48.33	0	0	0	0	0	9.57	13.93
IE	48.52	0	0	7.62	0.12	0	2.54	0	0	33.4	0.6	0.42	0	7.82	7.16
IT	57.54	0	0	109.4	10.3	0	61.78	1693.37	0	14.8	0	0	0	163.9	61.56
LT	17.33	0	0	7.46	0	0	11.06	23.46	0	5.04	0	0	0	5.11	4.04
LU	0.04	0	0	6.22	0	0	5.04	0	0	0	0	0.68	0	0.32	3.3
LV	4.21	0	0	2.43	0.26	0	0	1472.02	0	2	0	0	0	2.9	0.23
M	2.92	0	0	2.33	0	0	0	0	0	0.6	0	0	0	0.58	0
M	0.96	0	0	2.37	0.29	0	0	265.54	0	0.25	0	0	0	2.04	0.46
NL	18.87	16.2	0	24.66	0	0	0	0	3.88	0	0	4.25	4094.06	0.01	29.95
N	46.69	0	0	0	0.73	0	391.9	79421.1	0	21.0	0	0	0	6.42	0
PL	46.07	8.24	0	25.81	0.4	0	8.32	119.15	0	9.1	0	11.2	8566.06	4.85	27.95
PT	18.3	0	0	15.34	2.66	0	66.67	686.82	0	7	0	0	2861.91	1.25	9.85
R	12.65	0	0	4.05	0	0	18.55	10913.3	0	1.15	0	0	620.81	6.02	0
RS	5.06	0	0	0	1.98	0	4.32	424.6	0	3.58	0	0	0	5.03	0
SE	37.47	0	0	11.11	1.88	0	158.6	29036.3	0	7.79	0	0	0	1.66	3.01
SI	1.51	0	0	0	0.19	0	0.54	1491.62	0	0	0	0	0	3.51	0.03
SK	5.9	0	0	0	1.1	0	3.94	277.62	0	0	0	0.27	0	3.25	0.6
UK	82.86	15.9	0	37.45	1.2	0	26.64	143.74	6.16	39.2	1.7	16.4	23866.1	55.77	36.58

Table A-84. Capacity distribution for Model Run 82 (Weather Year 2017)

Country	Onshore	Offshore	PV /out Tracking	PV / Tracking	Run-of-river	Rooftop PV	PHS	Reservoir	Biomass CHP	PEM Electrolyzer	H2 OCGT	H2 CCGT	Salt Cavern	Vessel	Li-ion Battery
AL	2.07	0	0	1.33	0.03	0	0	1470.55	0	0	0	0	193.72	0.01	0
AT	40.46	0	0	33.28	4.61	0	114.15	1053.49	0	12.83	0	0	0	19.96	24.36
BA	16.08	0	0	3.7	0.28	0	1.61	1692.83	0	8.05	0	0	1909.4	0.77	0
BE	1.05	0	0	29.65	0.08	0	6.18	13.82	3.14	0	0	1.14	0	28.06	18.33
BG	3.07	0	0	2.75	0.61	0	40.59	1964.22	0	0	0	0	0	6.23	0
CH	10.71	0	0	1.06	3.74	0	163.81	5031.16	0	0	0	0	0	18.42	0
CZ	18.98	0	0	10.8	0.41	0	5.99	441.86	0	4.96	0.07	2.63	0	9.02	6.91
DE	38.68	28.91	0	23.58	4.15	0	39.27	5.46	0	0	2.65	8.74	5330.31	61.33	16.76
DK	21.42	0	0	0.97	0	0	0	0	0	9.69	0	0	994.44	14.2	0.11
EE	10.47	0	0	0	0	0	0	0	0	3.05	0	0	0	1.68	0.08
ES	62.94	0	0.05	120.41	2.27	0	63.06	11148.12	0	15.69	0	0	2747.67	82.09	166.02
FI	19.86	0	0	0	2.96	0	0	518.99	0	4.04	0.81	0.8	0	15.64	7.15
FR	154.48	5.37	0	84.52	6.56	0	50.15	5071.64	2.07	23.51	0	8.78	10603.18	177.65	68.69
GR	10.81	0	0	8.43	0.22	0	4.64	1753.4	0	1.5	0.03	0	451.44	12.86	2.43
HR	6.23	0	0	3.19	0.44	0	5.69	1955.8	0	2.1	0	0	0	4.37	0.43
HU	4.75	0	0	9.73	0.03	0	0	48.33	0	0	0	0	0	7.44	2.33
IE	29.24	0	0	6.71	0.12	0	2.54	0	0	20.17	0.31	0.44	0	8.43	9.33
IT	43.57	0	0	114.03	10.36	0	61.78	1693.37	0	9.81	0.18	0	0	151.79	127.69
LT	13.71	0.48	0	7.27	0	0	11.06	23.46	0	2.85	0	0	0	5.19	7.02
LU	0	0	0	5.42	0	0	5.04	0	0	0	0	0.17	0	1.4	0.25
LV	4.21	0	0	0	0.26	0	0	1472.02	0	1.48	0	0	0	3.01	0.44
ME	1.95	0	0	2.77	0	0	0	0	0	1.47	0.2	0	0	3.39	0
MK	0.27	0	0	2.32	0.29	0	0	265.54	0	0.14	0	0	0	2.3	0.06
NL	21.11	14.54	0	1.04	0	0	0	0	3.34	0	0	17.87	10976.8	4.16	7.84
NO	64.64	0	0	0	0.73	0	391.93	79421.13	0	33.64	0	0	0	6.68	0
PL	52.09	3.85	0	28.11	0.4	0	8.32	119.15	0	16.59	0	2.12	8207.27	13.38	18.51
PT	20.13	0	0.23	10.51	2.66	0	66.67	686.82	0	5.46	0	0	1001.6	12.77	0.62
RO	13.05	0	0	0	0	0	18.55	10913.39	0	0	0	0	1225.79	6.62	0.39
RS	5.06	0	0	0	1.98	0	4.32	424.6	0	0	0	0	0	7.67	0
SE	31.7	0	0	0	1.88	0	158.68	29036.31	0	2.03	0	0	0	1.6	2.77
SI	3.01	0	0	1.22	0.19	0	0.54	1491.62	0	0.64	0	0	0	4.38	0.2
SK	5.9	0	0	2.85	1.1	0	3.94	277.62	0	0.16	0.79	2.55	0	6.02	1.75
UK	103.49	20.02	0	35.92	1.2	0	26.64	143.74	0	53.29	8.44	15.74	18091.42	80.75	26.96

Table A-85. Capacity distribution for "Value of Country Connection"

Country	Onshore	Offshore	PV float Tracking	PV / Tracking	Run-of-river	Rooftop PV	PHS	Reservoir	Biomass CHP	PEM Electrolyzer	H2 OCGT	H2 CCGT	Salt Cavern	Vessel	Li-Ion Battery
AL	1.46	0	0.0	1.65	0.03	0	0	1470.55	0	0.16	0.2	0.26	302.94	5.16	1.07
AT	13.76	0	0.0	9.26	4.61	0	114.1	1053.49	2.75	3.86	0	1.48	0	193.35	9.19
BA	1.37	0	0.0	1.34	0.28	0	1.61	1692.83	0	0.27	0	0	18.95	1.93	0
BE	18.46	4.72	0.0	73.62	0.08	0	6.18	13.82	4.75	14.5	0	6.66	0	3220.6	68.22
B	3.87	0	0.0	8.61	0.61	0	40.59	1964.22	0.54	1.19	0	0	0	44.34	6.44
C	20.01	0	2.8	6.16	3.74	7.68	163.8	5031.16	1.25	6.54	0	3.43	0	599.24	18.36
CZ	11.53	0	0.0	24.22	0.41	0	5.99	441.86	5	3.81	0	0.59	0	303.79	30.04
DE	103.3	35.8	3.3	51.12	4.15	31.6	39.27	5.46	26.8	55.0	6.7	29.0	50558.9	0.23	67.64
DK	7.15	0.01	0.0	3.13	0	0	0	0	0	4.12	0.8	2.14	3436.84	1.59	2.31
EE	2.1	0.01	0.0	2.23	0	0	0	0	1	0.53	0.1	0.37	0	91.76	1.56
ES	50.74	0.01	0.1	191.9	2.27	0	63.06	11148.1	0.91	27.0	4	7.21	15522.2	0.41	382.7
FI	19.23	0.01	0	0	2.96	0	0	518.99	3	5.22	0.3	2.26	0	642.88	10.08
FR	147.2	6.55	0.1	131.9	6.56	0	50.15	5071.64	6.04	60.9	3.0	32.3	36641.8	30.81	122.5
G	12.44	0	0.0	15.27	0.22	0	4.64	1753.4	0	4.14	0.6	0.05	1629.99	9.34	24.84
H	3.17	0	0.0	7.39	0.44	0	5.69	1955.8	0	1.38	0	0.11	0	98.46	9.37
H	6.15	0	0.0	12.8	0.03	0	0	48.33	6.95	1.91	0.0	0.19	0	57.79	11.86
IE	7.54	1.94	0.0	15.69	0.12	0	2.54	0	0.25	3.79	0	2.83	0	1099.8	9.74
IT	54.09	0.01	0.0	180.5	10.3	0	61.78	1693.37	14.6	32.2	0	1.27	0	911.97	245.0
LT	4.63	0	0.0	7.97	0	0	11.06	23.46	1.75	1.67	0	0.8	0	595.31	0.96
LU	1.49	0	0.0	4.95	0	0	5.04	0	0	1.03	0	0.25	0	184.79	2.05
LV	3.11	0.01	0.0	3.64	0.26	0	0	1472.02	1.17	0.68	0	0	0	32.41	1.72
M	0.7	0	0.0	1.53	0	0	0	0	0	0.25	0	0.15	0	32.22	3.22
M	0.96	0	0.0	4.92	0.29	0	0	265.54	0	0.44	0	0.06	0	33.85	12.38
NL	27.75	10.0	0.0	36.49	0	0	0	0	1.79	15.0	3.7	10.5	13915	30.54	33.94
N	1.28	0.01	0	0	0.73	0	391.9	79421.1	0	1.39	0.2	0.25	0	16.92	1.3
PL	34.26	1.04	0.0	41.77	0.4	0	8.32	119.15	5.82	15.5	3.2	9.94	12931.0	1.54	24.78
PT	11.27	0	0.0	18.61	2.66	0	66.67	686.82	0	3.49	0.5	0	1946.88	0.06	22.15
R	9.94	1.57	0.0	14.45	0	0	18.55	10913.3	0	3.8	0.0	0	1385.13	2.63	9.69
RS	4.65	0	0.0	4.76	1.98	0	4.32	424.6	1	1.65	0	0.43	0	128.04	1.93
SE	15.96	0.01	0.0	3.11	1.88	0	158.6	29036.3	1.75	11.1	2.4	7.66	0	723.45	3.17
SI	1.68	0	0.0	3.1	0.19	0	0.54	1491.62	0.47	0.95	0	0	0	41.62	1.99
SK	3	0	0.0	4.29	1.1	0	3.94	277.62	2.56	1.02	0	0.04	0	44.57	0.03
UK	102.5	10.8	0.0	51.46	1.2	0	26.64	143.74	8.4	53.4	9.2	26.8	41618.1	0.27	60.91

Table A-86. Capacity distribution for "Pipeline Investment Cost 145 € kW⁻¹ m⁻¹"

Country	Onshore	Offshore	PV /out	PV / Tracking	Run-of-river	Rooftop PV	PHS	Reservoir	Biomass CHP	PEM Electrolyzer	H2 OCGT	H2 CCGT	Salt Cavern	Vessel	Li-ion Battery
AL	3.08	0	0	0	0.03	0	0	1470.55	0	0.17	0	0	50.83	1.39	0
AT	36.2	0	0	27.7	4.61	0	114.15	1053.49	0	10.43	0	0	0	20.08	3.9
BA	11.05	0	0	4.33	0.28	0	1.61	1692.83	0	5.04	0	0	1612.1	6.73	1.56
BE	4.83	4.72	0	20.98	0.08	0	6.18	13.82	0	0	0	3.69	0	1.99	3.4
BG	3.26	0	0	4.35	0.61	0	40.59	1964.22	0	0	0	0	0	6.43	0
CH	9.3	0	0	4.28	3.74	0	163.81	5031.16	0	0	0	0	0	14.86	0
CZ	13.04	0	0	19.94	0.41	0	5.99	441.86	0	0.47	0.44	2.75	0	8.18	8.9
DE	35.77	22.1	0	37.01	4.15	0	39.27	5.46	0.38	0	3.48	23.73	21355.7	37.24	1.59
DK	17.4	0	0	0.14	0	0	0	0	0	11.54	1.26	0.98	8459.45	0.02	0.77
EE	10.17	0	0	2.58	0	0	0	0	0	4.56	0	0	0	2.59	0
ES	65.83	0	0	115.4	2.27	0	63.06	11148.12	0	13.59	0	0	3372.85	63.21	142.29
FI	25.08	0	0	0	2.96	0	0	518.99	0	7.99	0.59	0.29	0	37.23	6.87
FR	148.09	21.39	0	112.79	6.56	0	50.15	5071.64	0	45.74	1.64	13.45	18681.96	135.17	76.25
GR	14.3	0	0	9.16	0.22	0	4.64	1753.4	0	3	0	0	421.4	17.54	0.26
HR	6.52	0	0	4.26	0.44	0	5.69	1955.8	0	2.28	0	0	0	4.8	0.54
HU	3.89	0	0	14.86	0.03	0	0	48.33	0	0	0	2.98	0	13.6	4.9
IE	36.26	0	0	3.03	0.12	0	2.54	0	0	24.64	0.89	1.47	0	7.44	0.66
IT	54.88	0	0	113.98	10.36	0	61.78	1693.37	0	9.88	0	0	0	144.55	97.16
LT	9.44	0	0	0	0	0	11.06	23.46	0	2.36	0	0	0	5.05	0
LU	0.04	0	0	5.68	0	0	5.04	0	0	0	0	0	0	1.16	0.17
LV	2.6	0	0	0.33	0.26	0	0	1472.02	0	0.11	0	0	0	2.87	0
ME	2.92	0	0	0.93	0	0	0	0	0	0.83	0	0	0	2.02	0
MK	0.96	0	0	2.08	0.29	0	0	265.54	0	0.1	0	0	0	3.45	0.72
NL	23.82	32.42	0	0	0	0	0	0	0	15.86	0.68	14.48	16137.58	4.87	2.98
NO	47.23	0	0	0	0.73	0	391.93	79421.13	0	26.05	0	0	0	7.44	0
PL	30.27	2.07	0	51.45	0.4	0	8.32	119.15	0	9.11	1.2	11.26	15775.06	4.24	20.18
PT	16.33	0	0	8.68	2.66	0	66.67	686.82	0	2.4	0	0	172.52	12.47	0.01
RO	9.3	0	0	1.95	0	0	18.55	10913.39	0	0	0	0	1672.7	10.69	0
RS	5.06	0	0	0	1.98	0	4.32	424.6	0	1.73	0	0	0	6.95	0
SE	40.4	0	0	0	1.88	0	158.68	29036.31	0	9.83	1.12	0.4	0	2.72	0.22
SI	2.01	0	0	0	0.19	0	0.54	1491.62	0	0	0	0	0	2.76	1.36
SK	4.4	0	0	1.64	1.1	0	3.94	277.62	0.01	0	0	1.88	0	1.74	0
UK	92.97	27.51	0	12.27	1.2	0	26.64	143.74	0	46.6	9.11	18.62	31605.61	58.19	31.67

Table A-87. Capacity distribution for "Pipeline Investment Cost 225 € kW⁻¹ m⁻¹"

Country	Onshore	Offshore	PV /out Tracking	PV / Tracking	Run-of-river	Roof-top PV	PHS	Reservoir	Biomass CHP	PEM Electrolyzer	H2 OCGT	H2 CCGT	Salt Cavern	Vessel	Li-ion Battery
AL	3.08	0	0	0	0.03	0	0	1470.55	0	0.31	0	0	93.59	0.73	0
AT	36.72	0	0	27.54	4.61	0	114.15	1053.49	0	10.9	0	0	0	22.06	4.03
BA	11.05	0	0	4.29	0.28	0	1.61	1692.83	0	5.05	0	0	1600.08	3.57	1.69
BE	4.83	4.72	0	21.29	0.08	0	6.18	13.82	0	0	0	3.6	0	4.73	3.49
BG	3.41	0	0	4.22	0.61	0	40.59	1964.22	0	0	0	0	0	6.45	0
CH	9.34	0	0	4.15	3.74	0	163.81	5031.16	0	0	0	0	0	14.86	0
CZ	13.16	0	0	20.9	0.41	0	5.99	441.86	0	0.94	0.33	2.53	0	9.11	9.03
DE	36.65	22.37	0	36.77	4.15	0	39.27	5.46	0.48	0	3.14	23.02	21668.27	36.54	4.1
DK	18.36	0	0	0.14	0	0	0	0	0	12.36	0.97	0.99	8127.27	0.03	0.9
EE	10.17	0	0	3.04	0	0	0	0	0	4.54	0	0	0	2.57	0.01
ES	66.17	0	0.01	115.04	2.27	0	63.06	11148.12	0	14	0	0	3268.5	70.66	137.3
FI	23.63	0	0	0	2.96	0	0	518.99	0	6.33	0.34	0.39	0	46.6	7.87
FR	150.51	21.78	0	115.98	6.56	0	50.15	5071.64	0	48.61	11.39	13.2	18803.95	159.36	78.09
GR	14.31	0	0	9.42	0.22	0	4.64	1753.4	0	3.19	0	0	436.31	18.86	0.23
HR	6.76	0	0	4.27	0.44	0	5.69	1955.8	0	2.4	0	0	0	4.93	0.43
HU	3.83	0	0	14.9	0.03	0	0	48.33	0	0	0	2.89	0	11.94	5.01
IE	32.35	0	0	2.44	0.12	0	2.54	0	0	20.86	0.87	1.56	0	7.65	0.96
IT	55.58	0	0	114.67	10.36	0	61.78	1693.37	0	10.18	0	0	0	148.65	97.98
LT	9.36	0	0	0	0	0	11.06	23.46	0	2.12	0	0	0	5.04	0
LU	0.04	0	0	5.64	0	0	5.04	0	0	0	0	0	0	1.35	0.15
LV	2.6	0	0	0.01	0.26	0	0	1472.02	0	0.17	0	0	0	2.86	0
ME	2.92	0	0	1.22	0	0	0	0	0	0.56	0	0	0	1.78	0
MK	0.96	0	0	2.15	0.29	0	0	265.54	0	0.11	0	0	0	3.3	0.61
NL	23.82	32.9	0	0	0	0	0	0	0	16.41	10.68	14.41	15874.12	9.17	2.34
NO	40.82	0	0	0	0.73	0	391.93	79421.13	0	21.61	0	0	0	8.02	0
PL	31.55	2.01	0	54.2	0.4	0	8.32	119.15	0	10.88	0.98	11.87	16179.2	1.81	19.85
PT	15.98	0	0	8.33	2.66	0	66.67	686.82	0	2.19	0	0	184.41	13.05	0.02
RO	9.3	0	0	1.64	0	0	18.55	10913.39	0	0	0	0	1518.71	12.25	0
RS	5.06	0	0	0	1.98	0	4.32	424.6	0	1.85	0	0	0	8.9	0
SE	40.22	0	0	0	1.88	0	158.68	29036.31	0	9.52	0.97	0.85	0	3.96	0.23
SI	2.01	0	0	0	0.19	0	0.54	1491.62	0	0	0	0	0	3.17	1.36
SK	4.4	0	0	1.64	1.1	0	3.94	277.62	0.23	0	0	1.47	0	2.44	0.01
UK	95.14	27.02	0	13.39	1.2	0	26.64	143.74	0	48.4	8.85	18.65	31225.74	50.33	31.91

Table A-88. Capacity distribution for "Electrolyzer Investment Cost 300 € kW⁻¹"

Country	Onshore	Offshore	PV /out Tracking	PV / Tracking	Run-of-river	Roof-top PV	PHS	Reservoir	Biomass CHP	PEM Electrolyzer	H2 OCGT	H2 CCGT	Salt Cavern	Vessel	Li-ion Battery
AL	3.08	0	0	0	0.03	0	0	1470.55	0	0.17	0	0	87.69	1.44	0
AT	36.32	0	0	25.74	4.61	0	114.15	1053.49	0	12.36	0	0	0	19.94	1.8
BA	11.05	0	0	4.03	0.28	0	1.61	1692.83	0	5.53	0	0	1706.54	2.27	0.3
BE	5.17	4.72	0	17.15	0.08	0	6.18	13.82	0	0	0	3.81	0	4.53	2.99
BG	2.9	0	0	4.93	0.61	0	40.59	1964.22	0	0	0	0	0	6.4	0
CH	9.15	0	0	3.42	3.74	0	163.81	5031.16	0	0	0	0	0	14.55	0
CZ	14.24	0	0	17.66	0.41	0	5.99	441.86	0	2.39	0.72	2.39	0	3.45	6.02
DE	39.37	18.97	0	35.53	4.15	0	39.27	5.46	0	0.32	5.55	24.43	25669.76	13.37	1.64
DK	19.96	0	0	0	0	0	0	0	0	13.42	1.7	0.25	8543.69	0.02	0.67
EE	10.36	0	0	0	0	0	0	0	0	4.58	0	0	0	1.81	0
ES	69.55	0	0.01	118.91	2.27	0	63.06	11148.12	0	22.18	0	0	2298.25	80.11	121.34
FI	23.91	0	0	0	2.96	0	0	518.99	0	7.25	0.44	0.34	0	32.19	7.5
FR	150.23	21.01	0	114.44	6.56	0	50.15	5071.64	0	57.01	1.79	13.54	18643.1	118.39	67.62
GR	15.01	0	0	10.44	0.22	0	4.64	1753.4	0	5.09	0	0	506.45	19.18	0
HR	6.4	0	0	4.23	0.44	0	5.69	1955.8	0	2.72	0	0	0	3.38	0.24
HU	3.77	0	0	13.61	0.03	0	0	48.33	0	0	0	3.29	0	14.65	4.55
IE	37.74	0	0	1.48	0.12	0	2.54	0	0	26.8	0.96	1.54	0	7.93	0.5
IT	52.92	0	0	113.55	10.36	0	61.78	1693.37	0	13.47	0	0	0	145.49	84.9
LT	9.47	0	0	0	0	0	11.06	23.46	0	2.12	0	0	0	4.44	0
LU	0.04	0	0	5.44	0	0	5.04	0	0	0	0	0	0	1.41	0
LV	2.64	0	0	0	0.26	0	0	1472.02	0	0.2	0	0	0	2.75	0
ME	2.92	0	0	1.48	0	0	0	0	0	0.69	0	0	0	1.5	0
MK	0.96	0	0	2.28	0.29	0	0	265.54	0	0.41	0	0	0	3.75	0.84
NL	26.38	29.19	0	0	0	0	0	0	0	17.35	1.7	14.25	15627.25	0.02	3.33
NO	41.46	0	0	0	0.73	0	391.93	79421.13	0	22.07	0	0	0	7.85	0
PL	34.84	0.91	0	48.27	0.4	0	8.32	119.15	0	13.98	1.84	10.63	17306.25	0.47	16.83
PT	15.56	0	0	9.03	2.66	0	66.67	686.82	0	2.17	0	0	119.01	14.59	0.71
RO	9.31	0	0	2.11	0	0	18.55	10913.39	0	0	0	0	1407.32	12.6	0
RS	5.06	0	0	0	1.98	0	4.32	424.6	0	1.95	0	0	0	6.9	0
SE	37.56	0	0	0	1.88	0	158.68	29036.31	0	8.92	1.7	0.15	0	11.78	0.45
SI	2.01	0	0	0	0.19	0	0.54	1491.62	0	0	0	0	0	2.92	0.63
SK	4.4	0	0	1.64	1.1	0	3.94	277.62	0	0	0	2.36	0	2.8	0.01
UK	99.82	21.59	0	8.53	1.2	0	26.64	143.74	0	49.38	9.47	19.82	35444.34	46.55	22.17

A.5. System Design with Different Market Penetration Values of Hydrogen Demand

0% Market Penetration (Weather Year : 2015)

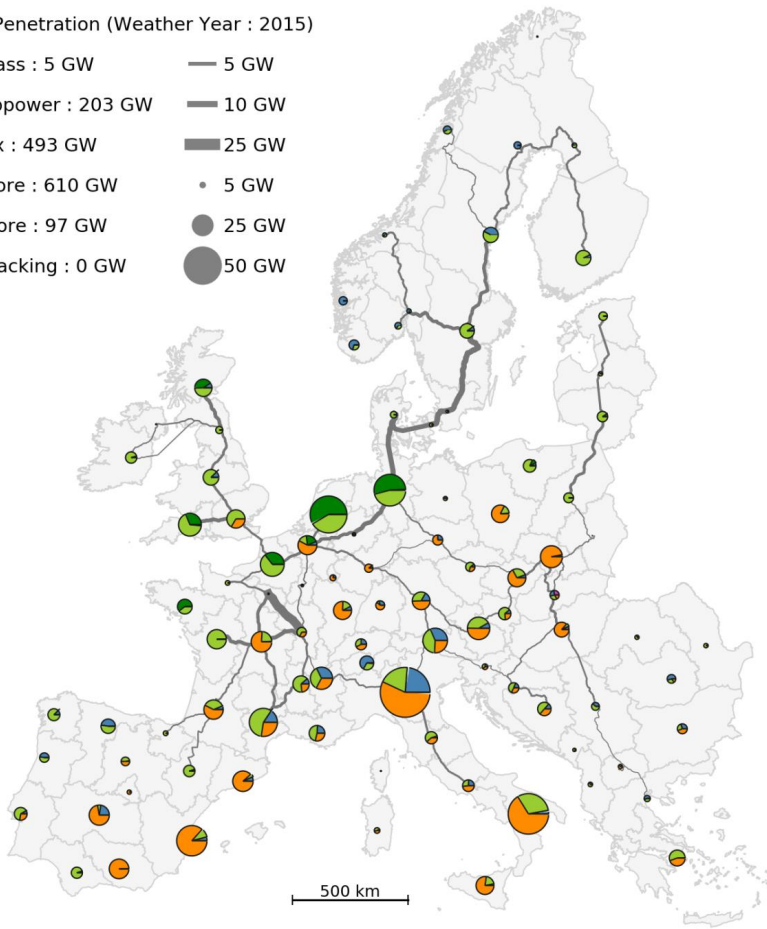
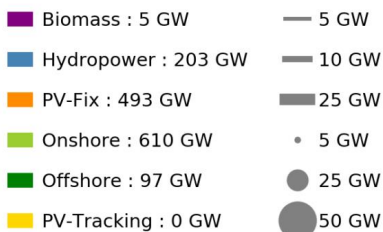


Figure A-2 System design at 0% market penetration

10% Market Penetration (Weather Year : 2015)

- Biomass : 4 GW
- Hydropower : 203 GW
- PV-Fix : 502 GW
- Onshore : 632 GW
- Offshore : 97 GW
- PV-Tracking : 0 GW
- 5 GW
- 10 GW
- 25 GW
- 5 GW
- 25 GW
- 50 GW

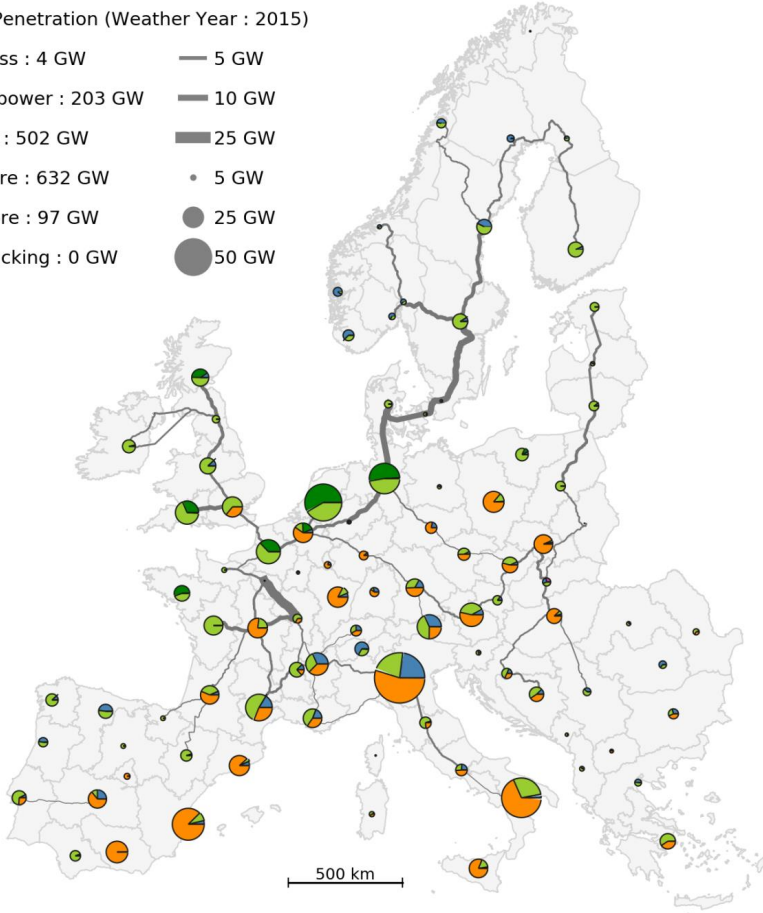


Figure A-3 System design at 10% market penetration

20% Market Penetration (Weather Year : 2015)

- | | |
|--|---------|
| ■ Biomass : 4 GW | — 5 GW |
| ■ Hydropower : 203 GW | — 10 GW |
| ■ PV-Fix : 509 GW | — 25 GW |
| ■ Onshore : 654 GW | ● 5 GW |
| ■ Offshore : 100 GW | ● 25 GW |
| ■ PV-Tracking : 0 GW | ● 50 GW |

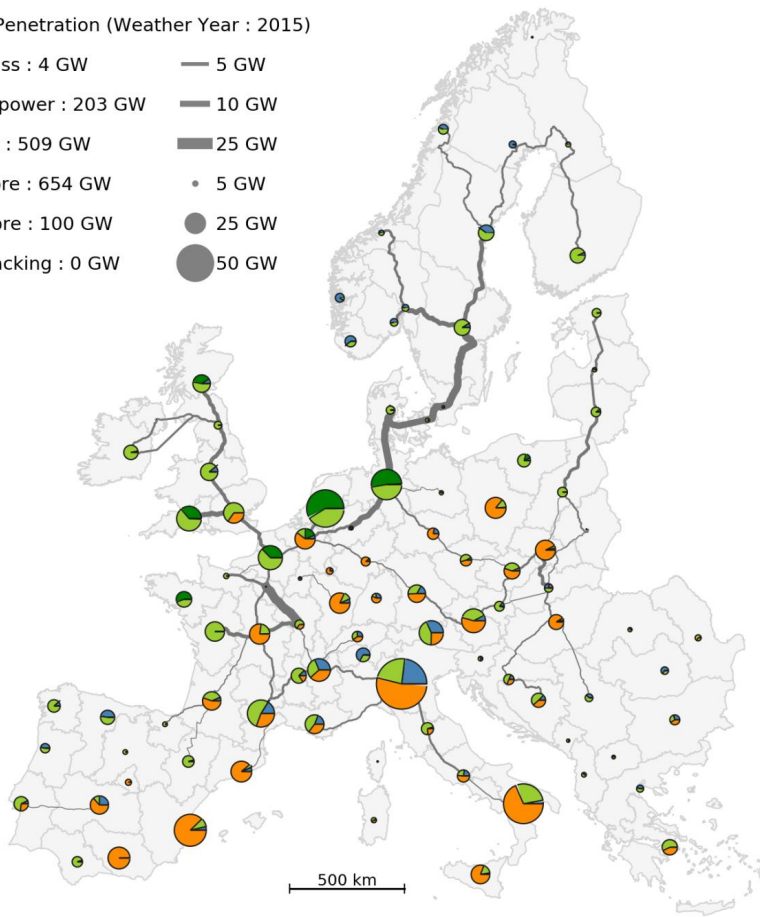


Figure A-4 System design at 20% market penetration

30% Market Penetration (Weather Year : 2015)

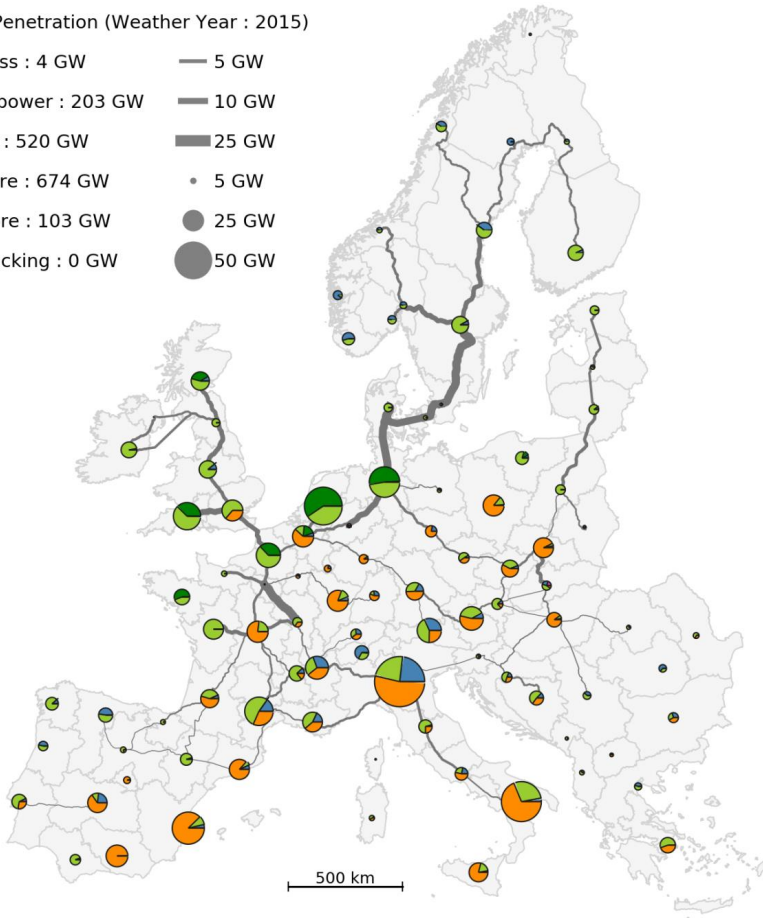


Figure A-5 System design at 30% market penetration

40% Market Penetration (Weather Year : 2015)

- | | |
|--|---------|
| ■ Biomass : 3 GW | — 5 GW |
| ■ Hydropower : 203 GW | — 10 GW |
| ■ PV-Fix : 531 GW | — 25 GW |
| ■ Onshore : 699 GW | ● 5 GW |
| ■ Offshore : 104 GW | ● 25 GW |
| ■ PV-Tracking : 0 GW | ● 50 GW |

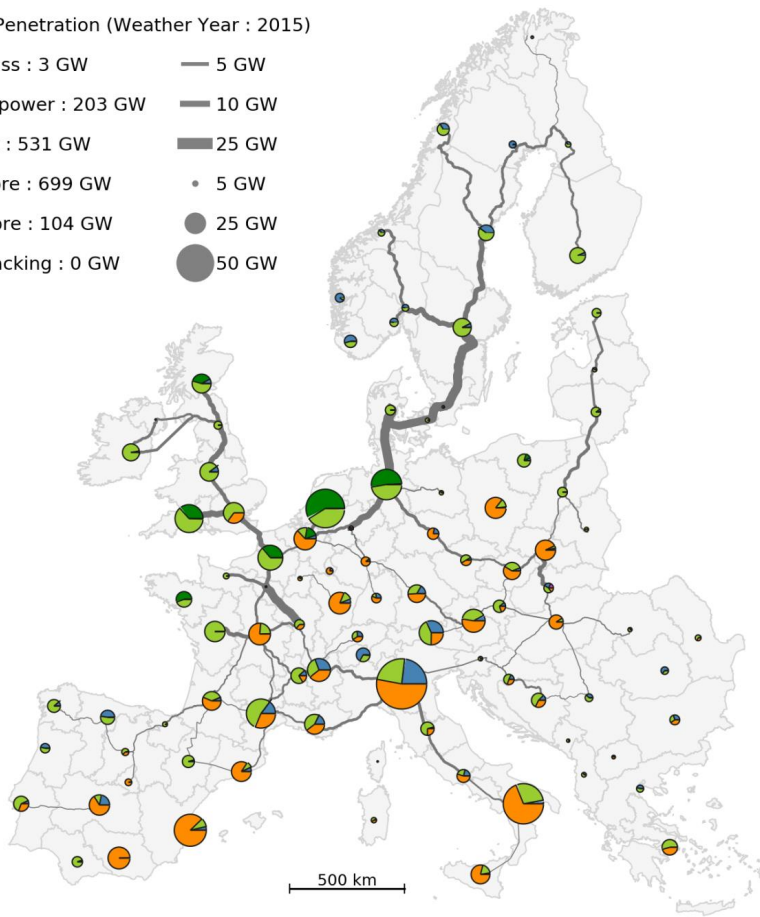


Figure A-6 System design at 40% market penetration

50% Market Penetration (Weather Year : 2015)

- Biomass : 2 GW
- Hydropower : 203 GW
- PV-Fix : 545 GW
- Onshore : 723 GW
- Offshore : 105 GW
- PV-Tracking : 0 GW
- 5 GW
- 10 GW
- 25 GW
- 5 GW
- 25 GW
- 50 GW

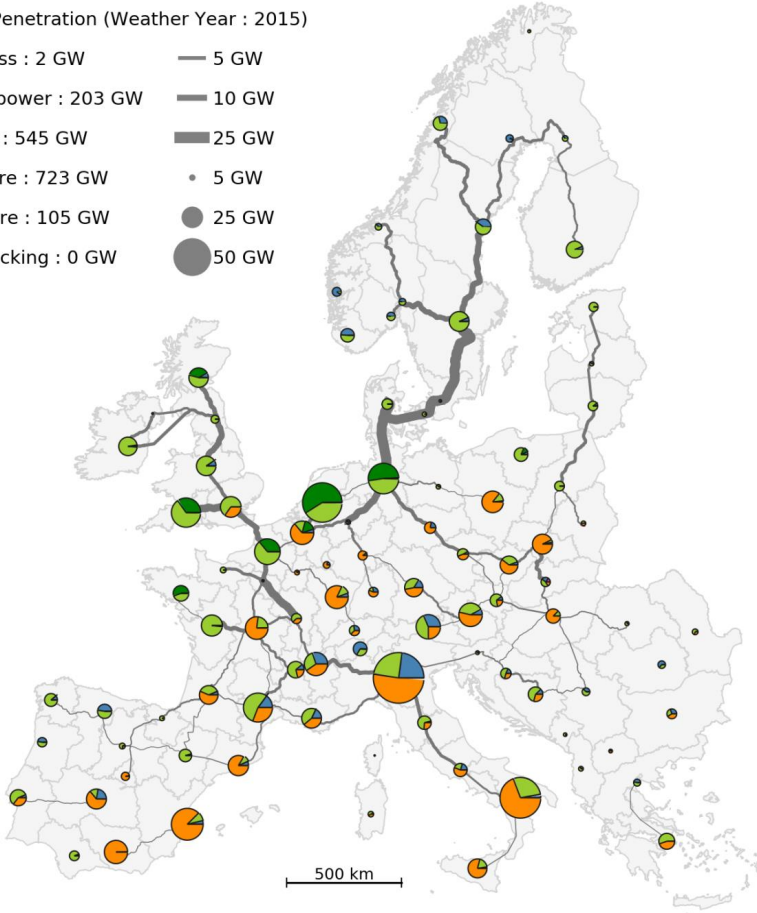


Figure A-7 System design at 50% market penetration

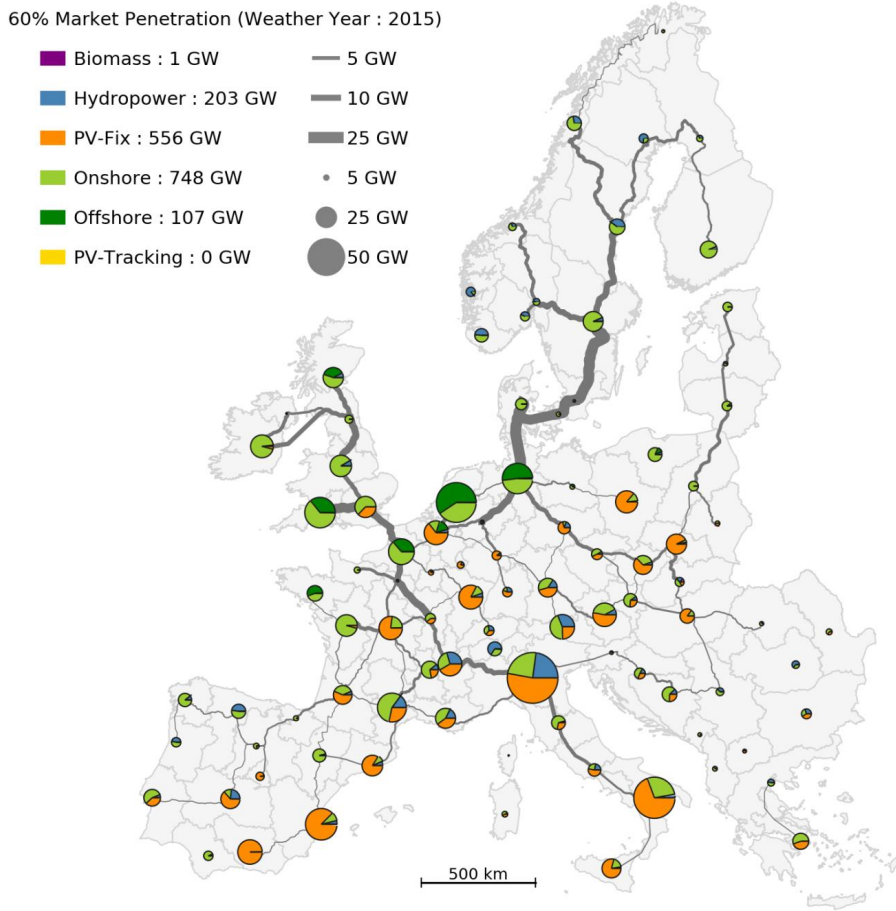


Figure A-8 System design at 60% market penetration

70% Market Penetration (Weather Year : 2015)

- | | |
|--|--|
| ■ Biomass : 1 GW | 5 GW |
| ■ Hydropower : 203 GW | 10 GW |
| ■ PV-Fix : 572 GW | 25 GW |
| ■ Onshore : 773 GW | 5 GW |
| ■ Offshore : 109 GW | 25 GW |
| ■ PV-Tracking : 0 GW | 50 GW |

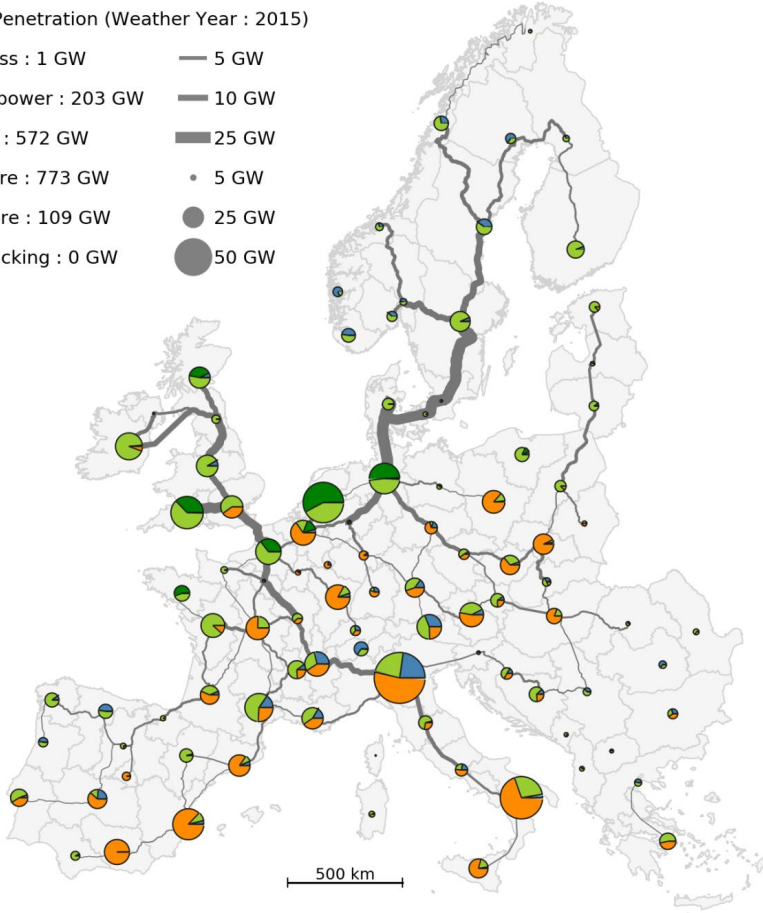


Figure A-9 System design at 70% market penetration

80% Market Penetration (Weather Year : 2015)

- | | |
|--|---------|
| ■ Biomass : 0 GW | — 5 GW |
| ■ Hydropower : 203 GW | — 10 GW |
| ■ PV-Fix : 592 GW | — 25 GW |
| ■ Onshore : 797 GW | ● 5 GW |
| ■ Offshore : 110 GW | ● 25 GW |
| ■ PV-Tracking : 0 GW | ● 50 GW |

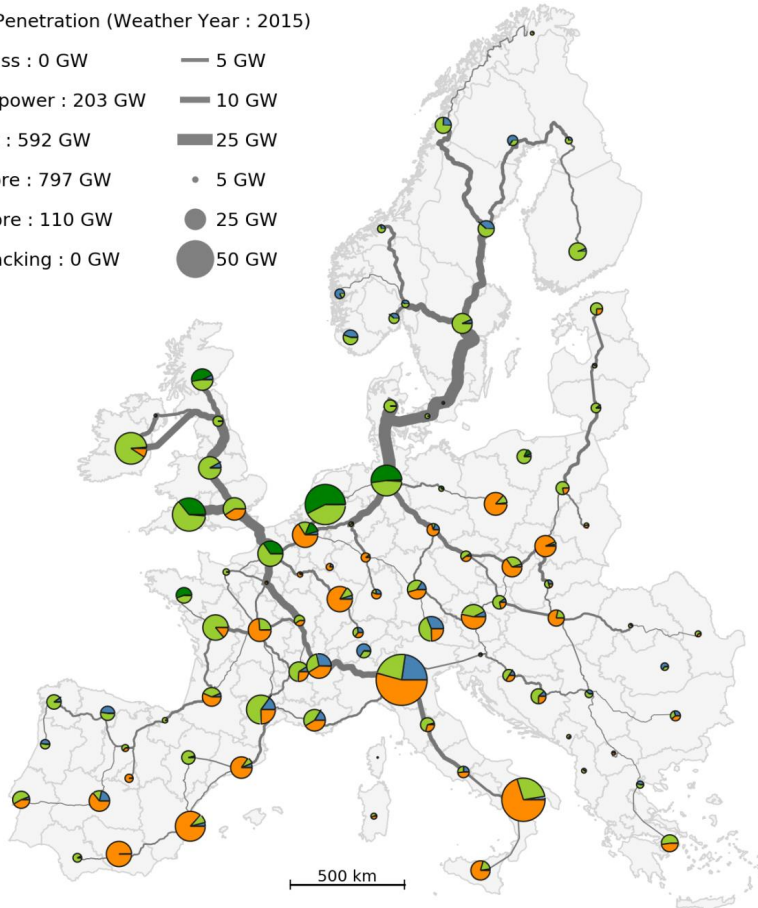


Figure A-10 System design at 80% market penetration

90% Market Penetration (Weather Year : 2015)

- | | |
|-----------------------|---------|
| ■ Biomass : 0 GW | — 5 GW |
| ■ Hydropower : 203 GW | — 10 GW |
| ■ PV-Fix : 612 GW | — 25 GW |
| ■ Onshore : 821 GW | ● 5 GW |
| ■ Offshore : 111 GW | ● 25 GW |
| ■ PV-Tracking : 0 GW | ● 50 GW |

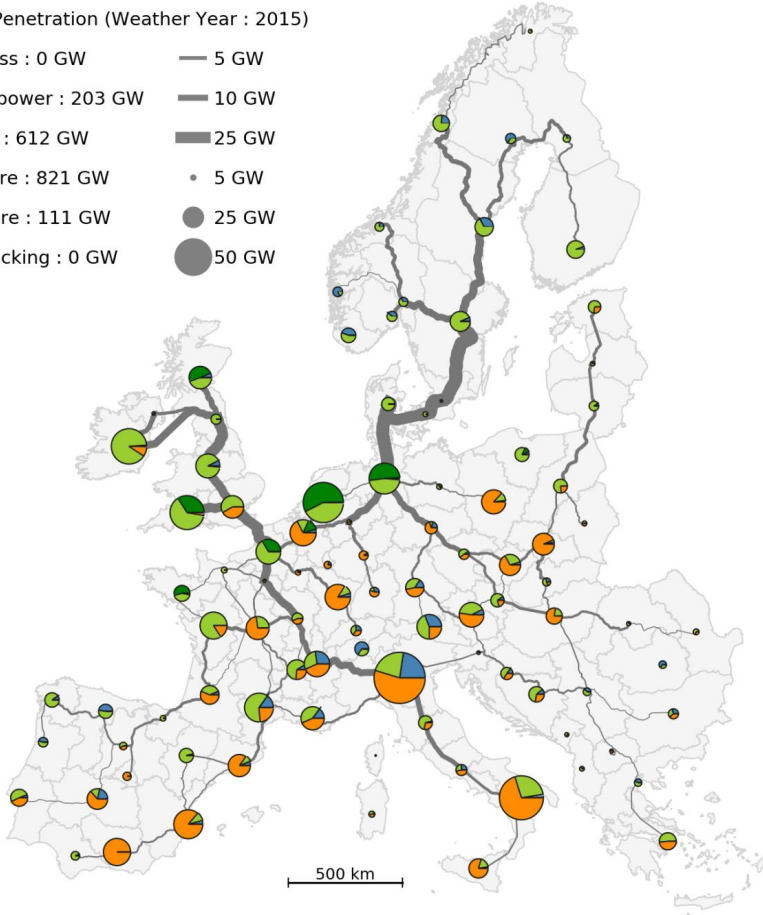


Figure A-11 System design at 90% market penetration

100% Market Penetration (Weather Year : 2015)

- | | |
|--|---------|
| ■ Biomass : 0 GW | — 5 GW |
| ■ Hydropower : 203 GW | — 10 GW |
| ■ PV-Fix : 632 GW | — 25 GW |
| ■ Onshore : 846 GW | ● 5 GW |
| ■ Offshore : 112 GW | ● 25 GW |
| ■ PV-Tracking : 0 GW | ● 50 GW |

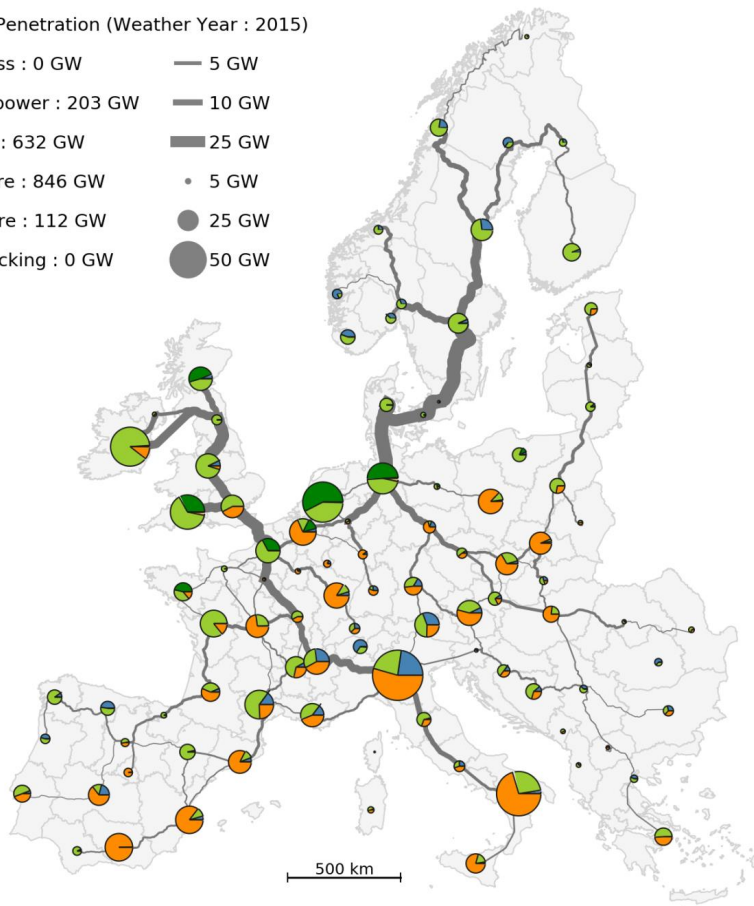


Figure A-12 System design at 100% market penetration

A.6. Top-down Spatial Redistribution of VRES Technologies

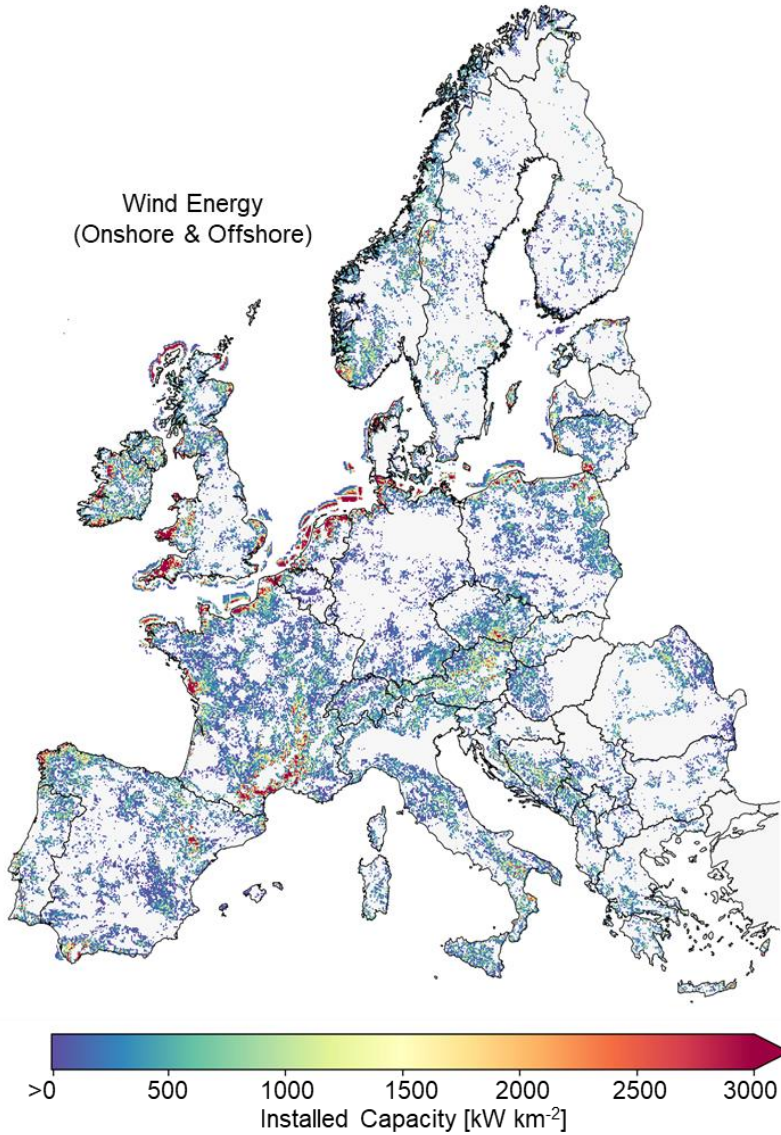


Figure A-13 Top-down spatial distribution of wind energy based on the regional capacities reported in Table A-89 (Resulting system design presented in Chapter 6)

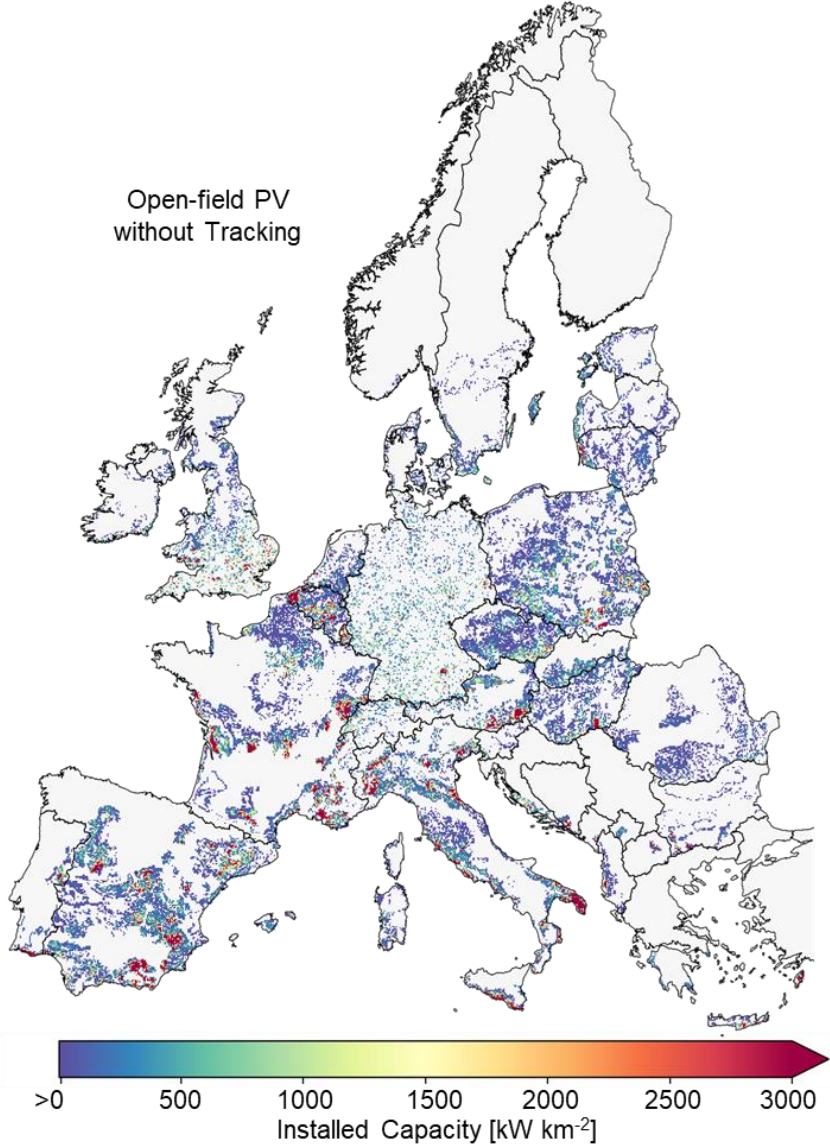


Figure A-14 Top-down spatial distribution of open-field PV based on the regional capacities reported in Table A-89 (Resulting system design presented in Chapter 6)

A.7. Variation in Total Annual Cost by Iterations

Figure A-15 shows the distribution of total annual costs found in each weather year within the corresponding iterative step. In order to provide a single design, which can ensure the security of supply and robust among all the weather years, the iterative approach is implemented. Therefore, there is an increasing trend in the total annual costs from “Iteration 0” until “Iteration 1” because of the additional capacities of various technologies that are installed to obtain a robust system design. Furthermore, a steep increase between “Iteration 3” and “Iteration 4” can be seen, which can be explained by the use of time series aggregation. When the time series aggregation is omitted in the system, the impact of extreme days on the total annual cost can be seen clearly. The meaning of iterative steps can be explained simply:

Iteration 0: Results of impact of different weather years. System is optimized at different weather years independently. These total annual costs and system designs are discussed in Section 5.3.

Iteration 1: At this step, the maximum capacities for each technology from “Iteration 0” are defined as the technical limit in each region. Moreover, the average capacities are set as the minimum capacity that has to be installed. In the case of hydrogen pipeline, minimum capacities are only set for the pipeline connections repeating 50% of the times. For the optimizations, 30 typical days are used.

Iteration 2: At this step, the maximum capacities for each technology from “Iteration 1” are defined as the technical limit in each region. Moreover, the average capacities are set as the minimum capacity that has to be installed. In the case of hydrogen pipeline, minimum capacities are only set for the pipeline connections repeating 50% of the times. For the optimizations, 30 typical days are used.

Iteration 3: At this step, the maximum capacities for each technology from “Iteration 2” are defined as the technical limit in each region. Moreover, the average capacities are set as the minimum capacity that has to be installed. In the case of hydrogen pipeline, minimum capacities are only set for the pipeline connections repeating 50% of the times. For the optimizations, 30 typical days are used.

Iteration 4: The variations in the total annual costs between “iteration 2” and “Iteration 3” are less than 1% for all weather years. Therefore, all the capacities except biomass CHP plants are fixed at “Iteration 4”. The assumed capacities are the maximum optimal capacities of technologies among all the weather years estimated at “Iteration 3”. Optimizations are conducted without time series aggregation since the fixed capacities decreased the complexity and memory requirement. The purpose of this step is to scale the biomass CHP plant capacities to capture extreme periods

(days), which could not be captured with the use of 30 typical days. The main objective of this step is to scale the biomass plant capacity to ensure the security of supply in extreme periods.

Iteration 5: Design results obtained in “Iteration 4” are analyzed to identify the maximum biomass CHP plant capacity in each region among all the weather years. Afterwards, like all the other technologies, biomass CHP plant capacities are set to these maximum values obtained in “Iteration 4”. At this iterative step, the main purpose is to find the optimal operation of technologies with design capacities proposed in Section 6. Therefore, the average results for curtailment, losses and transported commodities are estimated by using all the results indicated at “Iteration 5”.

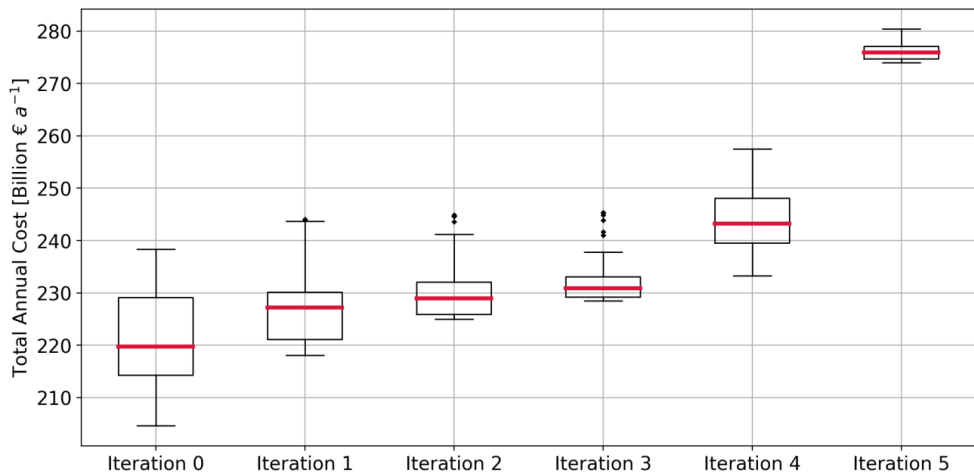


Figure A-15 Total annual cost distribution as a boxplot between Iteration 0 and Iteration 5

A.8. Regional Capacities of System Design Proposed in Section 6

Table A-89. Proposed Capacities of Generation and Conversion Technologies in Section 6

	Generation Technologies [GW]				Conversion Technologies [GW]		
	Biomass CHP	Onshore Wind	Offshore Wind	Open-field PV	PEM Electrolyzer	H ₂ OCGT	H ₂ CCGT
01_es	0.7	16.8	0.0	0.0	5.6	0.1	0.0
02_es	1.7	7.0	0.0	16.0	0.3	0.2	0.0
03_es	2.7	4.4	0.0	7.2	1.5	0.2	0.0
04_es	1.3	5.4	0.0	1.8	1.6	0.7	0.5
05_es	2.0	13.6	0.0	4.6	6.1	0.6	0.2
06_es	1.3	3.3	0.0	14.7	0.4	1.1	0.4
07_es	0.3	0.1	0.0	6.0	0.2	0.0	0.0
08_es	1.5	3.0	0.0	7.4	0.1	0.0	0.0
09_es	1.7	11.3	0.2	9.7	0.5	0.1	0.0
10_es	2.0	2.5	0.0	29.5	5.2	0.4	0.1
11_es	2.0	8.2	0.0	34.3	3.5	0.7	0.5
12_pt	1.2	6.2	0.0	4.3	0.9	0.3	0.1
13_pt	1.5	8.0	0.0	11.2	2.9	0.2	0.1
14_fr	3.5	13.9	0.0	7.4	2.2	1.5	0.8
15_fr	2.0	27.5	0.0	3.3	10.1	0.2	0.1
16_fr	1.5	13.0	0.0	19.8	8.6	0.4	0.0
17_fr	3.3	18.8	0.0	14.5	5.7	0.4	0.4
18_fr	4.0	8.9	0.0	16.9	0.9	1.0	2.8
19_fr	1.0	17.6	0.0	6.5	7.8	0.2	0.6
20_fr	1.0	9.6	0.0	11.6	1.1	0.5	0.5
21_fr	0.8	11.0	4.3	4.0	1.9	0.0	0.0
22_fr	0.5	8.2	0.7	0.2	6.4	0.3	0.6
23_fr	1.5	0.9	0.0	5.6	0.0	0.4	6.6
24_fr	2.5	10.7	0.0	4.1	1.7	1.0	0.9
25_fr	2.0	5.3	0.0	22.2	0.3	0.5	0.6
26_fr	3.3	20.9	4.6	3.6	0.4	1.4	4.1
27_fr	1.3	1.2	0.0	1.4	0.3	0.0	0.1
28_be	4.8	4.1	3.1	24.6	0.0	1.1	4.0
29_lu	0.0	0.1	0.0	5.4	0.0	0.0	0.3
30_nl	4.0	22.5	18.7	5.8	4.1	4.2	10.7
31_de	3.7	20.7	18.2	2.5	0.1	1.8	8.5
32_de	5.0	3.4	4.2	2.6	0.1	0.1	0.2

	Generation Technologies [GW]				Conversion Technologies [GW]		
	Biomass CHP	Onshore Wind	Offshore Wind	Open- field PV	PEM Electrolyzer	H ₂ OCGT	H ₂ CCGT
33_de	3.0	0.8	0.0	1.8	0.0	1.9	8.2
34_de	4.5	1.2	0.0	7.8	0.0	0.5	2.3
35_de	3.8	0.2	0.0	7.3	0.0	0.3	0.5
36_de	3.0	2.4	0.0	5.8	0.0	0.4	1.2
37_de	4.8	6.7	0.0	10.1	0.0	0.3	0.9
38_dk	1.6	11.7	0.4	0.7	5.9	0.1	0.1
39_cz	2.7	4.5	0.0	3.9	0.4	0.1	0.5
40_cz	2.3	12.0	0.0	7.8	1.5	0.1	2.3
41_pl	2.1	16.3	0.0	6.6	2.6	0.4	1.0
42_pl	2.8	7.0	0.0	12.6	4.0	0.2	2.2
43_pl	2.0	2.8	0.0	12.3	1.9	0.6	1.4
44_pl	4.0	6.0	0.7	7.9	0.2	0.4	1.0
45_pl	0.2	14.0	3.2	1.7	3.4	0.1	0.6
46_sk	2.7	5.7	0.0	3.9	0.2	0.4	2.2
47_ch	1.0	4.2	0.0	3.7	0.0	0.0	0.0
48_ch	0.3	4.0	0.0	0.4	0.0	0.0	0.0
49_at	0.8	12.8	0.0	7.4	0.1	0.0	0.0
50_at	1.3	12.9	0.0	16.0	5.4	0.4	0.9
51_at	1.5	11.8	0.0	3.4	3.7	0.1	0.3
52_it	6.8	13.2	0.0	51.4	0.6	0.1	1.2
53_it	2.8	7.8	0.0	7.2	0.8	0.1	0.5
54_it	1.0	2.9	0.0	12.2	2.2	0.1	0.1
55_it	2.5	17.0	0.0	34.9	3.9	0.0	0.0
56_it	1.2	6.6	0.0	15.4	3.4	0.0	0.0
57_si	0.8	2.5	0.0	0.5	0.1	0.0	0.0
58_hu	4.1	5.5	0.0	14.1	0.1	0.2	0.9
59_ro	0.0	2.5	0.0	0.8	0.2	0.0	0.0
60_ro	0.1	2.5	0.0	1.5	0.1	0.0	0.0
61_ro	0.0	7.3	0.0	2.3	0.4	0.0	0.0
62_hr	0.0	5.9	0.0	2.5	1.5	0.0	0.0
63_ba	0.3	11.9	0.0	2.8	5.9	0.0	0.0
64_me	0.0	3.4	0.0	1.7	1.1	0.0	0.0
65_rs	1.0	4.9	0.0	0.3	2.1	0.0	0.0
66_bg	1.2	3.3	0.0	4.0	0.1	0.0	0.0

	Generation Technologies [GW]				Conversion Technologies [GWh]		
	Biomass CHP	Onshore Wind	Offshore Wind	Open- field PV	PEM Electrolyzer	H ₂ OCGT	H ₂ OCGT
67_mk	0.0	0.8	0.0	2.4	0.2	0.0	0.0
68_gr	1.7	4.0	0.0	0.0	2.2	0.6	0.1
69_gr	1.5	10.4	0.0	10.0	1.8	0.0	0.0
70_al	0.0	3.1	0.0	1.9	0.7	0.0	0.0
72_dk	0.0	5.0	0.1	0.8	1.5	0.3	0.3
73_ee	1.0	8.5	0.7	1.6	2.8	0.0	0.0
74_fi	0.0	5.2	0.0	0.0	3.3	0.1	0.0
75_fi	2.5	14.8	0.0	0.0	0.7	0.7	1.6
77_it	1.5	13.2	0.2	4.8	3.4	0.1	0.1
78_lv	0.9	3.9	0.1	1.5	1.1	0.0	0.0
79_no	0.0	13.4	0.0	0.0	2.6	0.0	0.0
80_no	0.0	6.7	0.0	0.0	4.2	0.0	0.0
81_no	0.0	3.5	0.0	0.0	3.5	0.0	0.0
82_no	0.0	4.5	0.0	0.0	2.3	0.0	0.0
83_no	0.0	7.3	0.0	0.0	6.7	0.0	0.0
84_no	0.0	15.5	0.0	0.0	8.6	0.0	0.0
85_no	0.0	3.2	0.0	0.0	2.1	0.0	0.0
86_se	0.0	1.6	0.0	0.0	0.6	0.0	0.0
87_se	0.0	12.0	0.0	0.0	2.4	0.0	0.0
88_se	0.0	16.3	0.0	1.2	1.0	0.0	0.0
89_se	0.0	4.2	0.1	2.3	0.1	0.3	0.3
90_uk	4.8	11.0	2.7	16.0	1.0	1.6	5.2
91_uk	0.5	22.2	4.3	5.4	11.7	2.5	4.1
92_uk	4.0	26.4	0.0	12.1	4.6	2.6	8.2
93_uk	1.8	13.8	0.0	2.5	6.1	1.7	0.6
94_uk	1.5	16.9	11.5	0.8	14.8	0.4	0.0
95_uk	0.0	7.8	0.0	0.8	6.5	1.0	0.6
96_ie	0.3	40.7	0.0	4.5	28.0	0.9	0.5
98_it	0.5	3.0	0.0	3.2	1.2	0.1	0.1
99_fr	0.3	0.8	0.0	0.7	0.2	0.0	0.0

Table A-90. Proposed Capacities of Storage Technologies in Section 6

	Storage Technologies [GWh]				
	Salt Cavern	Vessel	Hydro Reservoir	Pumped Hydro Storage	Lithium-ion Batteries
01_es	0	5	0	4	1.5
02_es	370	2	5760	10	16.8
03_es	905	1	0	1	5.1
04_es	2333	2	0	0	6.4
05_es	1533	2	0	14	10.3
06_es	1838	5	807	2	10.7
07_es	0	9	0	0	3.8
08_es	0	4	4581	2	7.8
09_es	0	10	0	5	23.4
10_es	1505	3	0	0	54.1
11_es	1879	7	0	25	40.3
12_pt	1480	3	582	59	2.5
13_pt	898	3	105	8	12.1
14_fr	0	15	553	0	9.6
15_fr	0	5	1606	19	1.6
16_fr	3876	1	907	0	12.3
17_fr	0	12	0	0	9.5
18_fr	0	5	70	0	27.8
19_fr	3824	1	141	0	5.1
20_fr	4027	0	1721	27	1.1
21_fr	0	14	0	0	1.6
22_fr	0	9	0	0	4.2
23_fr	0	17	0	0	7.4
24_fr	9310	1	0	0	6.9
25_fr	3417	1	0	0	16.2
26_fr	0	13	0	0	4.5
27_fr	0	1	0	4	1.1
28_be	0	13	14	6	14.0
29_lu	0	1	0	5	0.8
30_nl	16706	5	0	0	13.6
31_de	5841	4	0	2	3.7
32_de	853	3	0	0	2.1

	Storage Technologies [GWh]				
	Salt Cavern	Vessel	Hydro Reservoir	Pumped Hydro Storage	Lithium-ion Batteries
33_de	8058	3	0	1	1.9
34_de	3366	2	0	17	0.3
35_de	2778	2	1	3	0.2
36_de	323	7	0	12	1.0
37_de	2047	3	5	4	3.7
38_dk	1472	1	0	0	0.7
39_cz	0	4	442	0	4.0
40_cz	0	4	0	6	3.8
41_pl	3043	1	8	0	3.4
42_pl	2449	1	3	1	8.3
43_pl	4844	1	27	3	5.8
44_pl	1415	2	3	0	3.0
45_pl	1286	2	78	4	1.9
46_sk	0	5	278	4	4.0
47_ch	0	6	350	77	0.1
48_ch	0	2	4681	86	0.0
49_at	0	3	1018	97	0.0
50_at	0	8	36	18	7.9
51_at	0	9	0	0	4.3
52_it	0	54	1328	37	13.2
53_it	0	14	71	0	8.1
54_it	0	29	76	8	9.5
55_it	0	19	172	0	54.4
56_it	0	19	0	4	29.2
57_si	0	3	1492	1	1.0
58_hu	0	9	48	0	9.9
59_ro	860	0	1921	0	0.7
60_ro	540	1	8388	19	0.0
61_ro	0	5	605	0	0.0
62_hr	0	3	1956	6	0.4
63_ba	1870	1	1693	2	0.1
64_me	0	1	0	0	0.1
65_rs	0	4	425	4	0.0
66_bg	0	5	1964	41	0.5

	Storage Technologies [GWh]				
	Salt Cavern	Vessel	Hydro Reservoir	Pumped Hydro Storage	Lithium-ion Batteries
67_mk	0	2	266	0	0.8
68_gr	1189	1	1753	5	2.6
69_gr	0	12	0	0	2.6
70_al	388	0	1471	0	0.2
72_dk	2123	1	0	0	0.8
73_ee	0	4	0	0	1.4
74_fi	0	5	0	0	0.2
75_fi	0	21	519	0	6.6
77_it	0	5	23	11	3.5
78_lv	0	3	1472	0	0.9
79_no	0	1	17956	386	0.0
80_no	0	1	10384	0	0.0
81_no	0	1	22397	6	0.0
82_no	0	3	8711	0	0.0
83_no	0	1	6492	0	0.0
84_no	0	1	12520	0	0.0
85_no	0	0	961	0	0.0
86_se	0	1	14441	0	0.0
87_se	0	1	11894	0	0.1
88_se	0	1	2701	159	1.7
89_se	0	1	0	0	1.7
90_uk	0	32	0	0	13.7
91_uk	9287	4	0	0	9.0
92_uk	9359	12	0	10	7.2
93_uk	6635	3	0	0	3.5
94_uk	0	10	144	17	0.6
95_uk	5599	1	0	0	2.0
96_ie	0	13	0	3	4.1
98_it	0	6	46	13	3.4
99_fr	0	6	75	0	1.1

A.9. Average Losses in the System Design Proposed in Section 6

Table A-91. Average Losses in the System Proposed in Section 6

	Losses [GWh a ⁻¹]				
	Total	Electrolyzer	Biomass CHP	Li-ion Battery	Reelectrification of Hydrogen
01_es	7097.8	6970.1	59.1	62.4	6.2
02_es	1217.2	370.4	165.9	661.5	19.4
03_es	2229.7	1771.6	230.4	212.3	15.4
04_es	2347.3	1813.8	121.6	260.4	151.5
05_es	8073.2	7379.3	200.6	417	76.3
06_es	1162.3	430.3	143.3	428.1	160.6
07_es	353.3	178.2	20.6	152.8	1.7
08_es	594.5	155.3	121.1	317	1.2
09_es	1698.2	619.1	150.2	924.1	4.8
10_es	8567.3	6083.2	154.7	2278.6	50.7
11_es	6244.9	4108.4	242.4	1739.9	154.2
12_pt	1271.4	1046.6	95.6	101.2	28
13_pt	4116.9	3485.9	113.2	486.6	31.3
14_fr	3992.3	2534.5	712.7	387.5	357.5
15_fr	13187.3	12915.9	171.4	65.3	34.7
16_fr	11206.9	10572.8	120.1	489	25
17_fr	7931.3	6785.5	621.7	378.5	145.7
18_fr	5304.3	970.6	1605.6	1109.9	1618.1
19_fr	10365	9675	285	211.9	193.2
20_fr	1915.6	1243.2	371.2	47	254.1
21_fr	2598.3	2386.7	144.1	66.7	0.7
22_fr	8583.4	8102.3	99.2	171.4	210.4
23_fr	5246.7	0	749.4	284.3	4213
24_fr	3714.6	1898.6	997.7	281.7	536.6
25_fr	1920.1	343.1	630.3	611	335.7
26_fr	3306	430.7	816.6	188.1	1870.6
27_fr	760.3	330.7	338.4	46.8	44.4
28_be	8843.4	0	3732.6	526.2	4584.6
29_lu	238.1	0	0	35	203.1
30_nl	16452.3	4261.7	2082	532.4	9576.3
31_de	6879	90.4	1283.8	147.2	5357.6
32_de	1484.4	60.3	1207.3	85.2	131.6

	Losses [GWh a ⁻¹]				
	Total	Electrolyzer	Biomass CHP	Li-ion Battery	Reelectrification of Hydrogen
33_de	7166.4	0	1286.7	74.8	5804.9
34_de	2908.7	0	1534.6	14.6	1359.5
35_de	1618.8	0	1274.5	8	336.2
36_de	2413	0	1474.5	43.9	894.5
37_de	3428.2	0	2647.6	145.4	635.1
38_dk	8826.9	8561.1	197.2	28.5	40.1
39_cz	1555.1	380.8	749.1	168.2	257
40_cz	3866.7	1518.8	891.6	154.9	1301.4
41_pl	3957.1	2841.7	468.9	135.5	510.9
42_pl	6856	4533.6	830.6	339.4	1152.4
43_pl	3750.4	2084.1	640.8	237.9	787.6
44_pl	1760.4	167	980.7	122.6	490.1
45_pl	4244.9	3838.9	54.4	78.8	272.7
46_sk	2014.6	170.2	636.9	161.6	1045.9
47_ch	271.3	0	262.3	3.2	5.8
48_ch	60.6	0	59.3	1.1	0.2
49_at	341.1	119.9	220.6	0.2	0.4
50_at	7952.9	6300.8	734.3	329.6	588.2
51_at	5216	4222.3	659.3	181	153.5
52_it	3040.8	580.4	1473.5	531.6	455.3
53_it	1984.2	830.2	622.3	334.1	197.7
54_it	3041.9	2390.4	237.6	387.5	26.5
55_it	7175.2	4304.3	575.9	2291.4	3.6
56_it	5423.9	3923	275.7	1218.4	6.8
57_si	341	134	164	42.9	0
58_hu	1805.5	62.9	937.6	400.2	404.8
59_ro	235.9	205.9	0	29.4	0.6
60_ro	161	156.6	4.3	0.1	0
61_ro	385.2	383.3	0	1.8	0
62_hr	1847.8	1827.4	0	18.8	1.6
63_ba	8028.2	7996.9	25.3	4.4	1.5
64_me	1423.9	1418.4	0	4.9	0.6
65_rs	2785.9	2659.6	124.8	1.5	0
66_bg	172.9	81.2	71.4	19.3	0.9

	Losses [GWh a ⁻¹]				
	Total	Electrolyzer	Biomass CHP	Li-ion Battery	Reelectrification of Hydrogen
67_mk	296.3	252.3	0	34.9	9.1
68_gr	2882.3	2540.6	155.9	106.8	79
69_gr	2351.1	2100.5	143.7	106	1
70_al	958.4	948.5	0	7.5	2.3
72_dk	2199.4	2069.5	0	33.2	96.7
73_ee	3861.3	3632	167	61.1	1.3
74_fi	5118.5	5105.8	0	9.9	2.9
75_fi	2515.2	973.7	517.4	258.5	765.6
77_lt	4520.9	4011.3	315.4	137.8	56.5
78_lv	1567.7	1372.9	155.8	37.6	1.4
79_no	6147.7	6147.7	0	0	0
80_no	10208.7	10208.7	0	0	0
81_no	8782.3	8782.3	0	0	0
82_no	5323.5	5323.5	0	0	0
83_no	16215.3	16215.3	0	0	0
84_no	19453.5	19453.5	0	0	0
85_no	4322.7	4322.7	0	0	0
86_se	1177.1	1177	0	0	0
87_se	4082.9	4079.2	0	3.7	0
88_se	1652.7	1581.2	0	69.4	2.1
89_se	254.9	99.2	0	71.3	84.4
90_uk	7137.4	1155.4	1802.6	526.1	3653.4
91_uk	18392.5	14952	192.5	355.3	2892.7
92_uk	12622	5558.2	1382.1	285.7	5396
93_uk	9144.2	8151.4	463	131.7	398.2
94_uk	22109.3	21726.4	315.8	26.4	40.7
95_uk	9529.8	8915.5	0	78.8	535.5
96_ie	40898.9	40155.9	117.4	160.5	465.2
98_it	1812.7	1510.2	138.1	138.6	25.7
99_fr	328.1	234	47.4	46.7	0

I hereby declare that I have created this work completely on my own and used no other sources or tools than the ones listed, and that I have marked any citations accordingly.

Hiermit versichere ich, dass ich die vorliegende Arbeit selbstständig verfasst und keine anderen als die angegebenen Quellen und Hilfsmittel benutzt sowie Zitate kenntlich gemacht habe.

Aachen, December 2020
Dilara Gülçin Çağlayan

Band / Volume 509

Electric Field Assisted Sintering of Gadolinium-doped Ceria

T. P. Mishra (2020), x, 195 pp

ISBN: 978-3-95806-496-6

Band / Volume 510

Effect of electric field on the sintering of ceria

C. Cao (2020), xix, 143 pp

ISBN: 978-3-95806-497-3

Band / Volume 511

Techno-ökonomische Bewertung von Verfahren zur Herstellung von Kraftstoffen aus H₂ und CO₂

S. Schemme (2020), 360 pp

ISBN: 978-3-95806-499-7

Band / Volume 512

Enhanced crosshole GPR full-waveform inversion to improve aquifer characterization

Z. Zhou (2020), VIII, 136 pp

ISBN: 978-3-95806-500-0

Band / Volume 513

Time-Resolved Photoluminescence on Perovskite Absorber Materials for Photovoltaic Applications

F. Staub (2020), viii, 198 pp

ISBN: 978-3-95806-503-1

Band / Volume 514

Crystallisation of Oxidic Gasifier Slags

J. P. Schupsky (2020), III, 127, XXII pp

ISBN: 978-3-95806-506-2

Band / Volume 515

Modeling and validation of chemical vapor deposition for tungsten fiber reinforced tungsten

L. Raumann (2020), X, 98, XXXVIII pp

ISBN: 978-3-95806-507-9

Band / Volume 516

Zinc Oxide / Nanocrystalline Silicon Contacts for Silicon Heterojunction Solar Cells

H. Li (2020), VIII, 135 pp

ISBN: 978-3-95806-508-6

Band / Volume 517

Iron isotope fractionation in arable soil and graminaceous crops

Y. Xing (2020), X, 111 pp

ISBN: 978-3-95806-509-3

Band / Volume 518

Geophysics-based soil mapping for improved modelling of spatial variability in crop growth and yield

C. Brogi (2020), xxi, 127 pp

ISBN: 978-3-95806-510-9

Band / Volume 519

Measuring and modelling spatiotemporal changes in hydrological response after partial deforestation

I. Wiekenkamp (2020), xxxvii, 276 pp

ISBN: 978-3-95806-512-3

Band / Volume 520

Characterization of Root System Architectures from Field Root Sampling Methods

S. Morandage (2020), xxii, 157 pp

ISBN: 978-3-95806-511-6

Band / Volume 521

Generation Lulls from the Future Potential of Wind and Solar Energy in Europe

D. S. Ryberg (2020), xxvii, 398 pp

ISBN: 978-3-95806-513-0

Band / Volume 522

Towards a Generalized Framework for the Analysis of Solar Cell Performance based on the Principle of Detailed Balance

B. J. Blank (2020), iv, 142 pp

ISBN: 978-3-95806-514-7

Band / Volume 523

A Robust Design of a Renewable European Energy System Encompassing a Hydrogen Infrastructure

D. G. Çağlayan (2020), xxii, 312 pp

ISBN: 978-3-95806-516-1

Energie & Umwelt / Energy & Environment
Band / Volume 523
ISBN 978-3-95806-516-1